



ESA PSS-03-108 Issue 1
November 1989

Spacecraft thermal control design data

Volume 1

STCDDAT 971

Prepared by:


Thermal Control & Life Support Division
European Space Research and Technology Centre
Noordwijk, The Netherlands

Approved by:

The Inspector General, ESA

european space agency / agence spatiale européenne

8-10, rue Mario-Nikis, 75738 PARIS 15, France



Published by ESA Publications Division,
ESTEC, Noordwijk, The Netherlands

Printed in The Netherlands

ESA price code: E4

ISSN 0379 - 4059

Copyright © 1989 by European Space Agency

ABSTRACT

The aim of the present handbook is to assist the thermal design engineer by presenting him in a single document with all the information relevant to spacecraft thermal-control design.

This handbook has been compiled by the School of Aeronautics of the Polytechnic University of Madrid (ETSI-A) under several ESA contracts.

REVISION PROCEDURE

It is intended to issue revisions and additions to this handbook as they become available. It is hoped that in this way it will remain up-to-date as regards state-of-the-art information and recent developments in the field of spacecraft thermal control.

CONTENTS

	Pages
Part C: View factors	C 0-1 to 0-6 C 1-1 to 1-130 C 2-1 to 2-40 C 3-1 to 3-6
Part D: Holes, grooves and cavities	D 0-1 to 0-4 D 1-1 to 1-18 D 2-1 to 2-6
Part E: Spacecraft surface temperature	E 0-1 to 0-4 E 1-1 to 1-110 E 2-1 to 2-32 E 3-1 to 3-22 E 4-1 to 4-2
Part F: Conductive heat transfer	F 0-1 to 0-4 F 1-1 to 1-32 F 2-1 to 2-50 F 3-1 to 3-6
Part G: Structural materials	G 0-1 to 0-6 G 1-1 to 1-172 G 2-1 to 2-10

PAGE INTENTIONALLY LEFT BLANK

DISCLAIMER

The description in this handbook of thermal-control components and systems is intended to be purely illustrative, and the use of tradenames of specific products, which is essential to a proper understanding of the data presented herein, in no way implies any approval, endorsement or recommendation of these products by the European Space Agency.

PAGE INTENTIONALLY LEFT BLANK

STRUCTURAL MATERIALS

1 METALLIC MATERIALS

G

STRUCTURAL
MATERIALS

STRUCTURAL MATERIALS

Table of Contents

	Page
TABLE OF CONTENTS	0-1
LIST OF SYMBOLS	0-3
1. METALLIC MATERIALS	1-1
1.1. General	1-1
1.1.1. Modifiers of Thermal Radiative Properties	1-3
1.1.2. Cladding Definitions	1-5
1.1.3. Temper Designations for Heat Treatable Aluminium Alloys	1-6
1.2. Aluminium Alloys	1-7
1.3. Aluminium-Copper Alloys	1-59
1.4. Aluminium-Magnesium Alloys	1-79
1.5. Aluminium-Zinc Alloys	1-91
1.6. Magnesium-Zinc-Thorium Alloys	1-111
1.7. Titanium-Aluminium-Tin Alloys	1-115
1.8. Titanium-Aluminium-Tin Alloys	1-129
1.9. Titanium-Aluminium-Vanadium Alloys	1-137
1.10. Nickel-Chrome-Cobalt-Molybdenum Alloys	1-153
1.11. Iron-Nickel Alloys	1-163
REFERENCES	2-1

Rev. 2. 1984

INTENTIONALLY BLANK PAGE

STRUCTURAL MATERIALS

List of Symbols

LIST OF SYMBOLS

- B , Magnetic Induction. [T].
- E , Modulus of Elasticity. [Pa].
- H , Magnetic Field Strength. [A.m⁻¹].
- R , Reflectance Factor.
- c , Specific Heat. [J.kg⁻¹.K⁻¹].
- k , Thermal Conductivity. [W.m⁻¹.K⁻¹].
- $\Delta L/L$, Thermal Expansion.
- α , Thermal Diffusivity. [m².s⁻¹]. $\alpha=k/\rho c$.
- α , Temperature Coefficient of Electrical Resistivity. [K⁻¹].
- α , Hemispherical Total Absorptance.
- $\alpha'(\beta, \theta)$, Directional Total Absorptance.
- α_s , Normal Solar Absorptance.
- $\alpha_\lambda(\lambda)$, Hemispherical Spectral Absorptance.
- $\alpha'_\lambda(\lambda, \beta, \theta)$, Directional Spectral Absorptance.
- β , Mean Coefficient of Linear Thermal Expansion. [K⁻¹].
- β , Angle between Surface Normal and Direction of Incident Flux. [Angular Degrees].
- β' , Angle between Surface Normal and Direction of Emitted, Reflected or Transmitted Flux. [Angular Degrees].
- ϵ , Hemispherical Total Emittance.
- $\epsilon'(\beta', \theta')$, Directional Total Emittance.
- $\epsilon_\lambda(\lambda)$, Hemispherical Spectral Emittance.

STRUCTURAL MATERIALS

List of Symbols

$\epsilon'_\lambda(\lambda, \beta', \theta')$, Directional Spectral Emittance.
θ	, Azimuthal Angle of Incident Flux. [Angular Degrees].
θ'	, Azimuthal Angle of Emitted, Reflected or Transmitted Flux. [Angular Degrees].
λ	, Wavelength. [m].
μ/μ_0	, Relative Magnetic Permeability.
ρ	, Density. [kg.m ⁻³].
ρ	, Hemispherical Total Reflectance.
$\rho_\lambda(\lambda)$, Hemispherical Spectral Reflectance.
$\rho'(\beta, \theta)$, Directional-Hemispherical Total Reflectance.
$\rho'(\beta', \theta')$, Hemispherical-Directional Total Reflectance.
ρ'_s	, Normal-Hemispherical Solar Reflectance.
$\rho'_\lambda(\lambda, \beta, \theta)$, Directional-Hemispherical Spectral Reflectance.
$\rho'_\lambda(\lambda, \beta', \theta')$, Hemispherical-Directional Spectral Reflectance.
$\rho''(\beta, \theta, \beta', \theta')$, Bidirectional Total Reflectance.
$\rho''_\lambda(\lambda, \beta, \theta, \beta', \theta')$, Bidirectional Spectral Reflectance.
$\rho''_s(\beta, \theta, \beta', \theta')$, Bidirectional Solar Reflectance.
σ	, Electrical Conductivity. [$\Omega^{-1}.m$]. σ^{-1} , Electrical Resistivity. [$\Omega.m$].
σ_{ult}	, Ultimate Tensile Strength. [Pa].
$\tau'_\lambda(\lambda, \beta, \theta, \beta', \theta')$, Bidirectional Spectral Transmittance.
ω	, Solid Angle of Incident Radiation Beam. [Steradians].

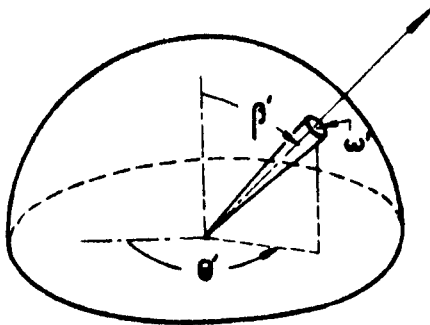
STRUCTURAL MATERIALS

List of Symbols

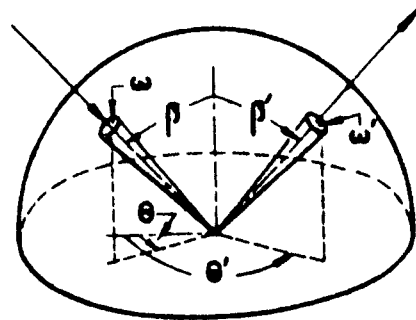
ω' , Solid Angle of Emitted, Reflected or Transmitted Radiation Beam. [Steradians].

The sketches below show the angles used to characterize the radiative fluxes arriving at or leaving a surface element.

Angles used to define directional emittance.



Angles used to define bidirectional reflectance.



INTENTIONALLY BLANK PAGE

METALLIC MATERIALS

General

1. METALLIC MATERIALS1.1. GENERAL

Data for each alloy are arranged as indicated below. When no data on some property are available the heading is omitted.

1. TYPICAL COMPOSITION, PERCENT2. OFFICIAL DESIGNATIONS3. PHYSICAL PROPERTIES3.1. Density3.2. Thermal properties

- 3.2.1. Specific heat
- 3.2.2. Thermal conductivity
- 3.2.3. Thermal diffusivity
- 3.2.4. Thermal expansion
- 3.2.5. Melting range

3.3. Thermal radiation properties3.3.1. Emittance

- 3.3.1.1. Directional spectral emittance
 - 3.3.1.1.1. Normal spectral emittance
 - 3.3.1.1.2. Angular spectral emittance
- 3.3.1.2. Directional total emittance
 - 3.3.1.2.1. Normal total emittance
- 3.3.1.3. Hemispherical spectral emittance
- 3.3.1.4. Hemispherical total emittance

3.3.2. Absorptance

- 3.3.2.1. Directional spectral absorptance
 - 3.3.2.1.1. Normal spectral absorptance
- 3.3.2.2. Directional total absorptance
 - 3.3.2.2.1. Normal total absorptance
- 3.3.2.3. Hemispherical spectral absorptance
- 3.3.2.4. Hemispherical total absorptance
- 3.3.2.5. Solar absorptance
 - 3.3.2.5.1. Normal solar absorptance
 - 3.3.2.5.2. Angular solar absorptance
- 3.3.2.6. Absorptance to emittance ratio

3.3.3. Reflectance

- 3.3.3.1. Bidirectional spectral reflectance
 - 3.3.3.1.1. Normal-normal spectral reflectance
 - 3.3.3.1.2. Angular (non-normal) spectral reflectance
- 3.3.3.2. Directional-hemispherical spectral reflectance
 - 3.3.3.2.1. Normal-hemispherical spectral reflectance
 - 3.3.3.2.2. Angular-hemispherical spectral reflectance

METALLIC MATERIALS

General

- 3.3.3.3. Hemispherical-directional spectral reflectance
 - 3.3.3.3.1. Hemispherical-normal spectral reflectance
- 3.3.3.4. Hemispherical spectral reflectance
- 3.3.3.5. Bidirectional total reflectance
 - 3.3.3.5.1. Normal-normal total reflectance
 - 3.3.3.5.2. Angular (non-normal) total reflectance
- 3.3.3.6. Directional-hemispherical total reflectance
 - 3.3.3.6.1. Normal-hemispherical total reflectance
- 3.3.3.7. Hemispherical-directional total reflectance
 - 3.3.3.7.1. Hemispherical-normal total reflectance
- 3.3.3.8. Bidirectional solar reflectance
 - 3.3.3.8.1. Normal-normal solar reflectance
- 3.3.3.9. Directional-hemispherical solar reflectance
 - 3.3.3.9.1. Normal-hemispherical solar reflectance
- 3.3.4. Transmittance
 - 3.3.4.1. Bidirectional spectral transmittance
 - 3.3.4.1.1. Normal-normal spectral transmittance
 - 3.3.4.1.2. Angular (non-normal) spectral transmittance

3.4. Other physical properties

- 3.4.1. Electrical resistivity
- 3.4.2. Magnetic properties

4. ENVIRONMENTAL BEHAVIOR

- 4.1. Prelaunch
- 4.2. Postlaunch

5. CHEMICAL PROPERTIES

- 5.1. Solution potential
- 5.2. Corrosion resistance

6. FABRICATION

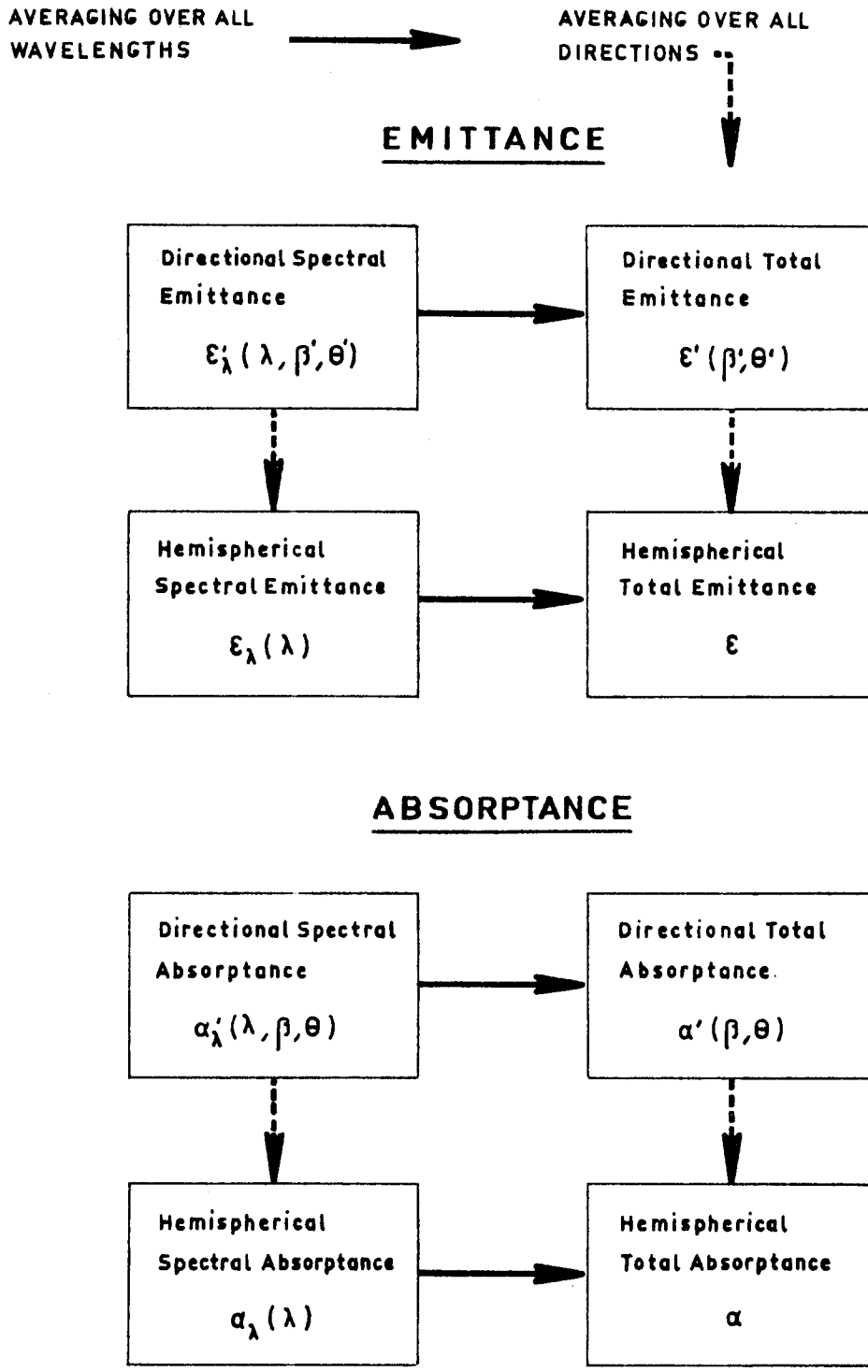
- 6.1. Casting
- 6.2. Forming
- 6.3. Welding
- 6.4. Machining
- 6.5. Heat treatment
- 6.6. Anodizing

7. AVAILABLE FORMS AND CONDITIONS8. USEFUL TEMPERATURE RANGE9. APPLICATIONS

METALLIC MATERIALS

General

1.1.1.1. MODIFIERS OF THERMAL RADIATIVE PROPERTIES



METALLIC MATERIALS

General

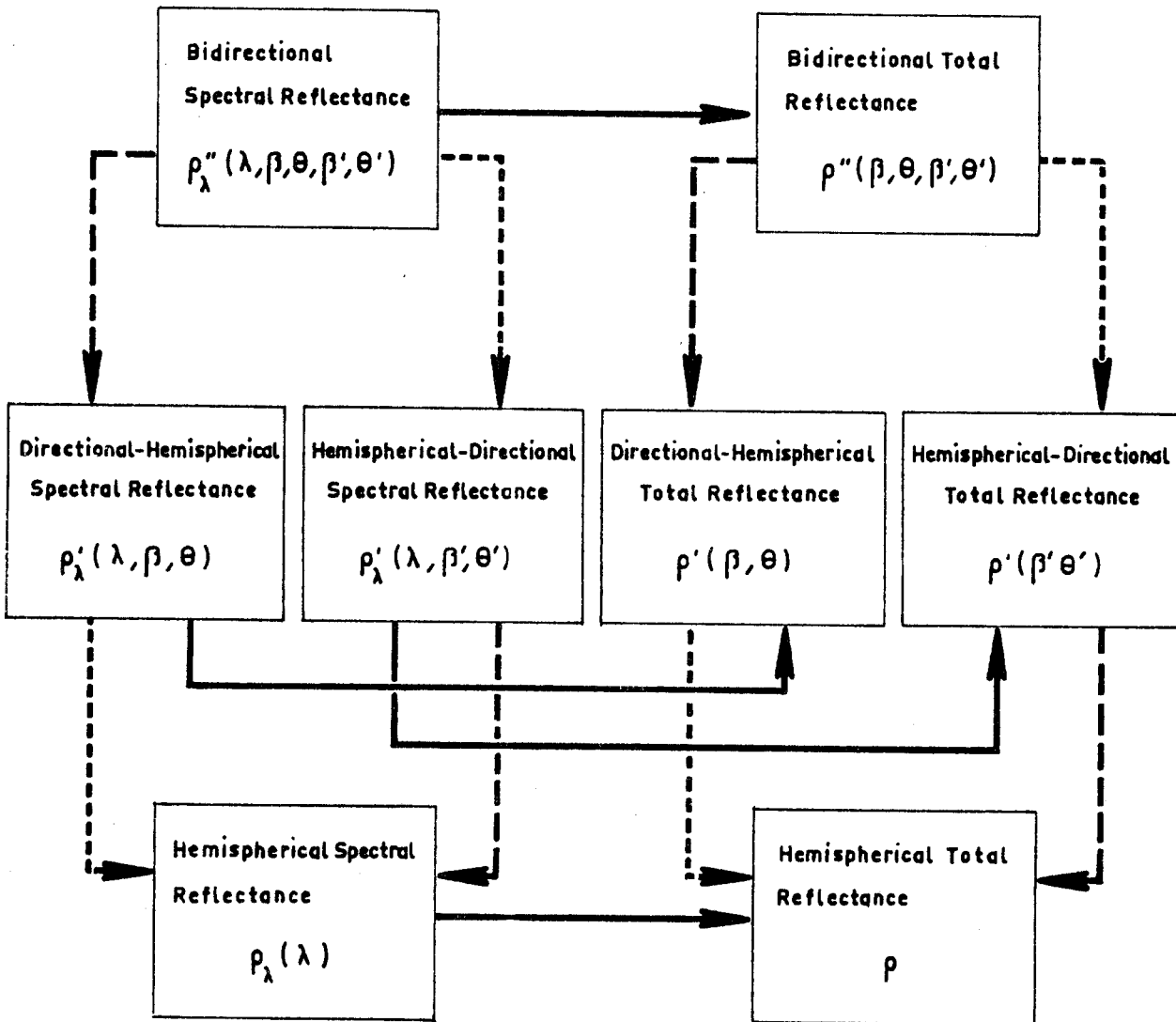
AVERAGING OVER ALL WAVELENGTHS

AVERAGING OVER ALL REFLECTED DIRECTIONS

AVERAGING OVER ALL INCIDENT DIRECTIONS



REFLECTANCE



METALLIC MATERIALS

General

1.1.2. CLADDING DEFINITIONS

- Clad. A composite metallic material containing two or three layers that have been bonded together. Bonding may be achieved by co-rolling, welding, casting, heavy chemical deposition or heavy electroplating.
- Alclad. Clad produced by bonding either a corrosion-resistant aluminium alloy or high purity aluminium to a base of a structurally stronger aluminium alloy.
- Nonclad. Metallic material to which no other alloy has been bonded by cladding.

METALLIC MATERIALS

General

1.1.3. TEMPER DESIGNATIONS FOR HEAT TREATABLE ALUMINIUM ALLOYS

F Condition:

As fabricated.

O Condition:

Annealed (wrought products only).

W Condition:

Solution heat treated.

T1 Condition:

Naturally aged to a stable condition.

T2 Condition:

Annealed (cast products only).

T3 Condition:

Solution heat treated, cold worked, and naturally aged to a substantially stable condition.

T4 Condition:

Solution heat treated and naturally aged to a substantially stable condition.

T5 Condition:

Artificially aged only.

T6 Condition:

Solution heat treated and artificially aged.

T7 Condition:

Solution heat treated and overaged.

T8 Condition:

Solution heat treated, cold worked, and artificially aged. Different amounts of cold working are denoted by a second digit.

T9 Condition:

Solution heat treated, artificially aged, and cold worked.

T10 Condition:

Artificially aged and cold worked.

METALLIC MATERIALS

Aluminium Alloys

1.2. ALUMINIUM ALLOYS

ALLOYS Al - 99.99. Al - 99.9. Al - 99.8. Al - 99.7.
Al - 99.5 . Al - 99.3. Al - 99.

This data item concerns all aluminium alloys whose aluminium content is above 99%.

1. TYPICAL COMPOSITION, PERCENT. Maximum values are given except for Aluminium.

	Al	Cu	Fe	Mn	Si	Zn	Others	
							Each	Total
Al - 99.99	>99.99	-	-	-	-	-	-	.01
Al - 99.9	>99.9	.02	.07	.01	.07	.03	.01	-
Al - 99.8	>99.8	.03	.15	.03	.15	.06	.02	-
Al - 99.7	>99.7	.03	.25	.03	.20	.07	.03	-
Al - 99.5	>99.5	.05	.40	.05	.30	.10	.03	-
Al - 99.3	>99.3	.10	.60	.05	.30	.10	.05	-
Al - 99.0	>99.0	.20	.80	.05	.50	.10	.05	-

METALLIC MATERIALS
Aluminium Alloys

2. OFFICIAL DESIGNATIONS

	AECMA	ISO	AFNOR	AMS	BS	DIN
Al - 99.99					1	Al 99.98R S - Al 99.98R 3.0385
Al - 99.9						Al 99.9 3.0305
Al - 99.8		Al 99.8	A8		1A	Al 99.8 S - Al 99.8 3.0285
Al - 99.7		Al 99.7	A7	~4000		Al 99.7 3.0275
Al - 99.5	Al P99.5	Al 99.5	A5	~4000	1B ~1E	Al 99.5 S - Al 99.5 3.0255 ~E - Al ~3.0257
Al - 99.3			~A45	4040 4041 4042		~S - Al 99.5Ti ~3.0805
Al - 99.0		Al 99.0 ~Al 99.0Cu	A4	~1100 4001 4003 4062 4102 4180 7220	1C	Al 99 3.0205

~ Can be approximately included with those alloys having the indicated aluminium content.

3. PHYSICAL PROPERTIES

3.1. Density. Al-99.99 $\rho = 2\,699 \text{ kg.m}^{-3}$. (Pennington (1961)).

METALLIC MATERIALS

Aluminium Alloys

Al - 99.5 $\rho = 2\,700 \text{ kg.m}^{-3}$. (Kappelt (1961)).

Al - 99.0 $\rho = 2\,710 \text{ kg.m}^{-3}$. (Kappelt (1961)).

3.2. Thermal properties

3.2.1. Specific heat.

Effect of temperature on specific heat: Fig 1-1.

3.2.2. Thermal conductivity.

Effect of temperature on thermal conductivity: Fig 1-2.

Thermal conductivity integrals: Fig 1-3.

3.2.3. Thermal diffusivity.

Effect of temperature on thermal diffusivity: Fig 1-4.

3.2.4. Thermal expansion.

Effect of temperature on thermal expansion: Fig 1-5.

Mean coefficient of linear thermal expansion, β .

The available information concerning thermal expansion coefficients of these alloys seems to indicate that there is no noticeable influence of the aluminium content on β . Values given below correspond to Al - 99.99

T [K]	73- -293	123- -293	173- -293	223- -293	293- -373	293- -473	293- -573	293- -673	293- -773
$\beta \times 10^6$ [K ⁻¹]	18.0	19.9	21.0	21.8	23.6	24.5	25.5	26.4	27.4

From Pennington (1961).

3.2.5. Melting range.

Al - 99.99 : 933 K. (Pennington (1961)).

Al - 99.5 : 919 K - 930 K. (Kappelt (1961)).

Al - 99.0 : 916 K - 930 K. (Kappelt (1961)).

METALLIC MATERIALS
Aluminium Alloys

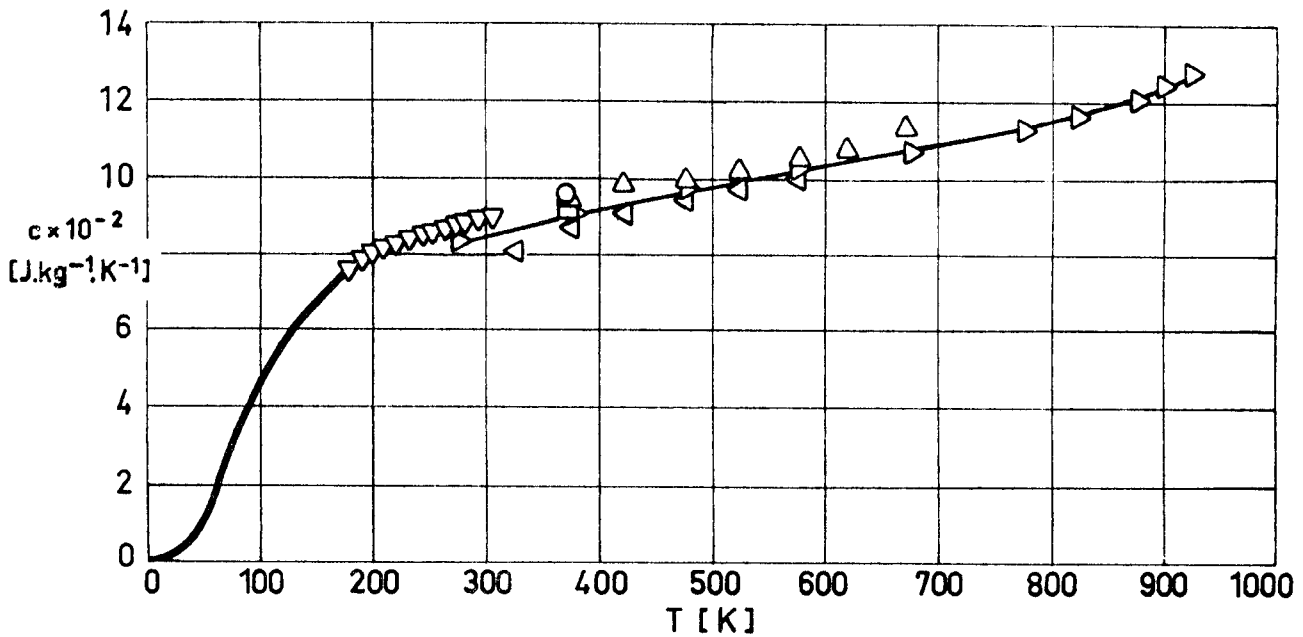


Fig 1-1. Specific heat, c , of Aluminium as a function of temperature, T .

Explanation

Key	Description	Comments	References
○	Al - 99.0		Kappelt (1961).
□	Al - 99.99		Pennington (1961).
△	Al - 99.99 Average of 2 samples 1) Water quenched from 873 K; annealed 100 h at 403 K. 2) Cooled from 873 K at 5 K.min^{-1}	Reported error $\leq 1\%$	Touloukian (1967)a.
▽	Al - 99.9 Single crystal. Melted and cooled 2 d in vacuum.		
▷	Al - 99.9	Reported error $\pm 5\%$	
◁		Reported error 5%	
—			Coston (1967).

METALLIC MATERIALS
Aluminium Alloys

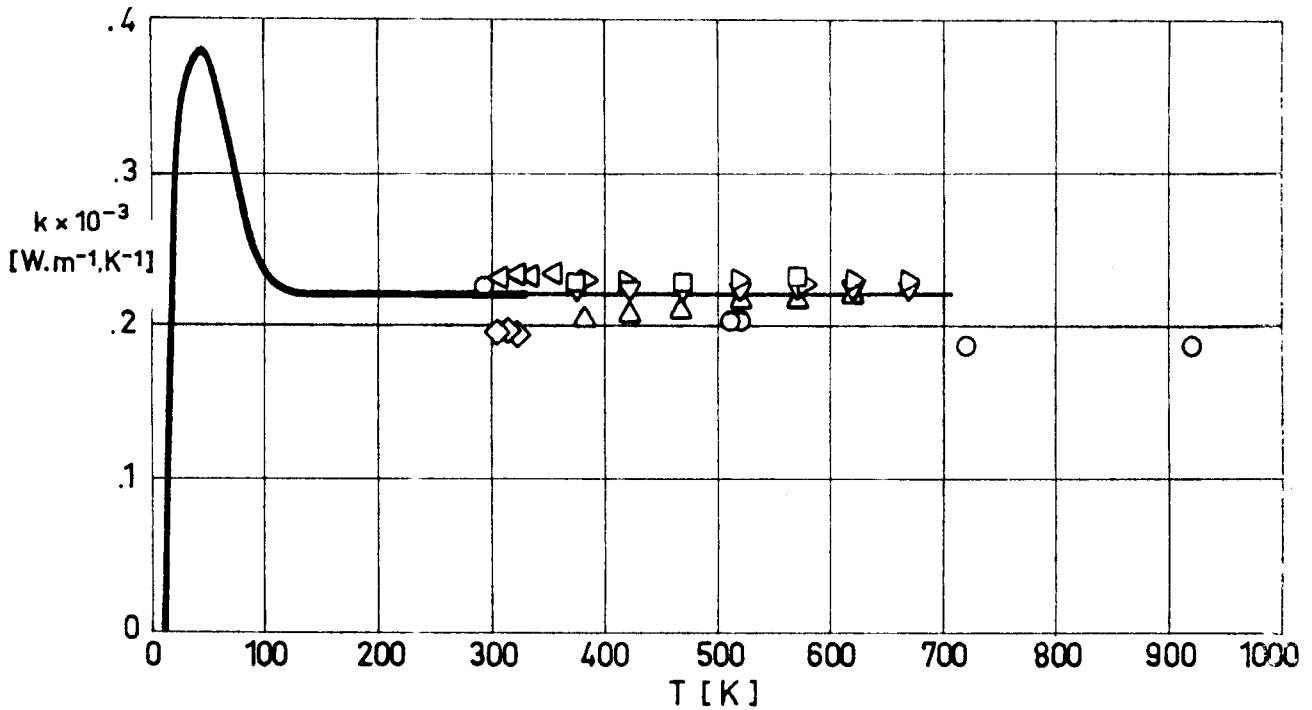


Fig 1-2. Thermal conductivity, k, of Aluminium as a function of temperature, T.

Explanation

Key	Description	Comments	References
○	Al - 99.9	Losses evaluated by measuring unsteady state cooling of rod initially at uniform temperature.	Touloukian (1967)a.
◻	.04 Si - .03 Fe - .006 Cu - .005 Ti, and traces of Mn and Mg. Annealed 1 h at 723 K and cooled slowly.	Reported error ±3%.	
△	Al - 99.5 Cast at 973 K into molds at 473 K; rolled and drawn, then turn into rods.		
▽	Al - 99.9 Same treatment as above.		
▷	Al - 99.99 Same treatment as above.		
◁	Al - 99.99	Reported error 1%.	
◇	Commercially pure. Sample 2×10 ⁻² m in diameter and 1.8×10 ⁻² m length.	Reported error ±3%.	
—			Coston (1967).

METALLIC MATERIALS
Aluminium Alloys

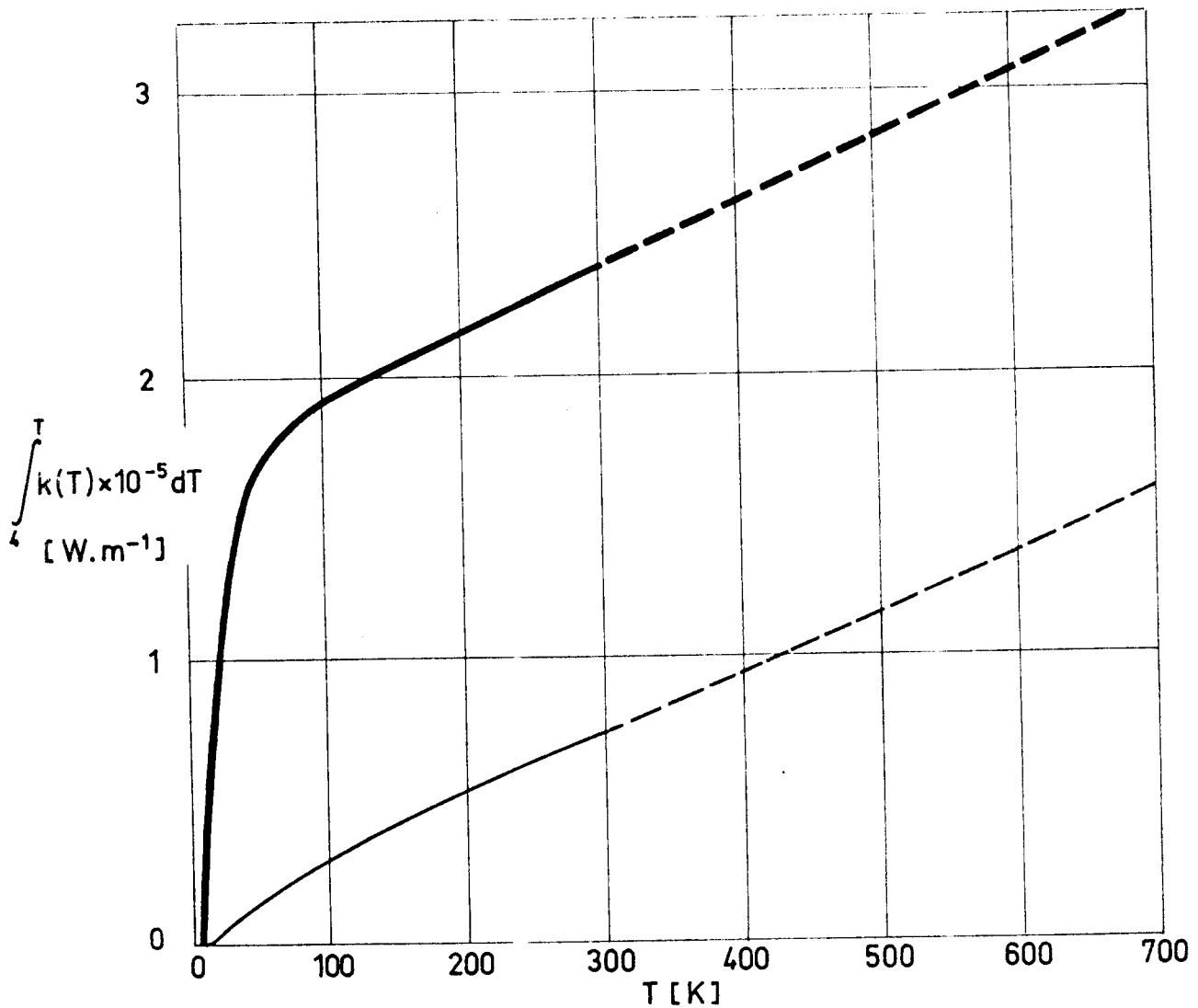


Fig 1-3. Thermal conductivity integrals of Aluminium as a function of temperature, T.

Explanation

- Al - 99.99. From Coston (1967).
- Al - 99.0 From Coston (1967).
- - - Straight line whose slope has been calculated by the compiler by fitting the experimental data points \triangleright and \triangleleft of Fig 1-2 with the least-squares method.
- — — Calculated by the compiler from data points \diamond of Fig 1-2.

METALLIC MATERIALS
Aluminium Alloys

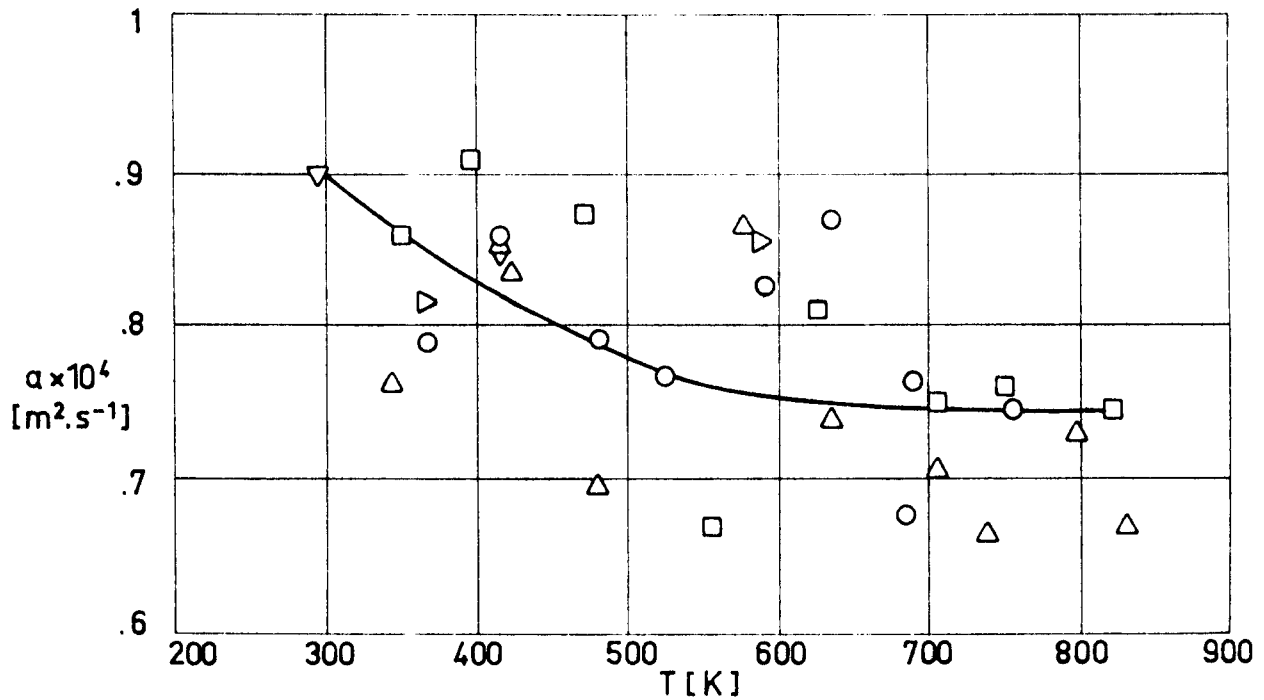


Fig 1-4. Thermal diffusivity, α , of Aluminium as a function of temperature, T.

Explanation

Key	Description	Comments	References
○	Al - 99.9	Reported error 11%.	Touloukian (1967)a.
□	Same as above.	Second run of the above specimen. Reported error 11%.	
△	Same as above.	Third run of the above specimen. Reported error 11%.	
▽	Pure. 1.9×10 ⁻³ m ² square cross-section and 3.52×10 ⁻³ m length.	Reported error ±5%.	
▷	Pure.		

METALLIC MATERIALS
Aluminium Alloys

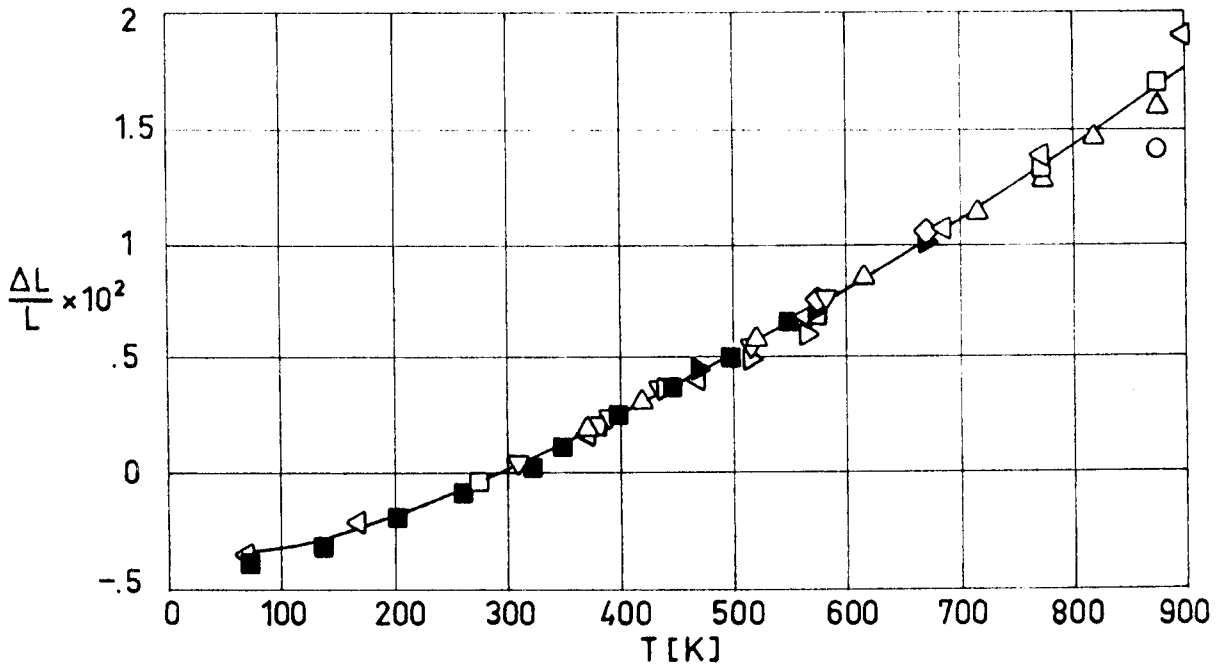


Fig 1-5. Linear thermal expansion, $\Delta L/L$, of Aluminium as a function of temperature, T .

Explanation

Key	Description	Comments	References
○			Touloukian (1967)a.
□	Al - 99.99 Annealed above 873 K.		
□	Al - 99.99		
△	Al - 99.9 Annealed 2 h at 893 K and cooled slowly.		
▽	99.952 Al - .019 Cu - -.015 Fe - .014 Si. Cast in graphite mold.		
▷	Chemically pure.	X-ray diffraction method.	
△	99.989 Al - .004 each Si, Cu - .003 Fe.		
▶	Pure. Pressed rod made of sintered aluminium powder.		
◇	Al - 99.5		

METALLIC MATERIALS

Aluminium Alloys

3.3. Thermal radiation properties

3.3.1. Emittance.

Data concerning emittance have been arranged as indicated in the following Table.

3.3.1.1. Directional spectral emittance.				
Paragraph	Heading	Data presented	Fig.	Table
3.3.1.1.1	Normal $\beta' = 0$	Al - 99.7.	1-6	
		Aluminium conversion coatings.	1-7	
3.3.1.1.2	Angular (non-normal) $\beta' \neq 0$	Al - 99.0.	1-8	
3.3.1.2. Directional total emittance.				
3.3.1.2.1	Normal $\beta' = 0$	Aluminium.		1-1
		Aluminium. Effect of temperature.	1-9	
		Aluminium contact coatings.		1-2 ^a
		Aluminium conversion coatings.		1-3 ^a
		Aluminium conversion coatings. Effect of anodizing thickness.	1-10	
3.3.1.4. Hemispherical total emittance.				
	$\omega' = 2\pi$	Aluminium. Effect of temperature.	1-11	
		Aluminium contact coatings.		1-4
		Aluminium conversion coatings. Effect of temperature.	1-12	

^a Solar absorptance, α_s , has been also included in this Table in order to save space.

METALLIC MATERIALS

Aluminium Alloys

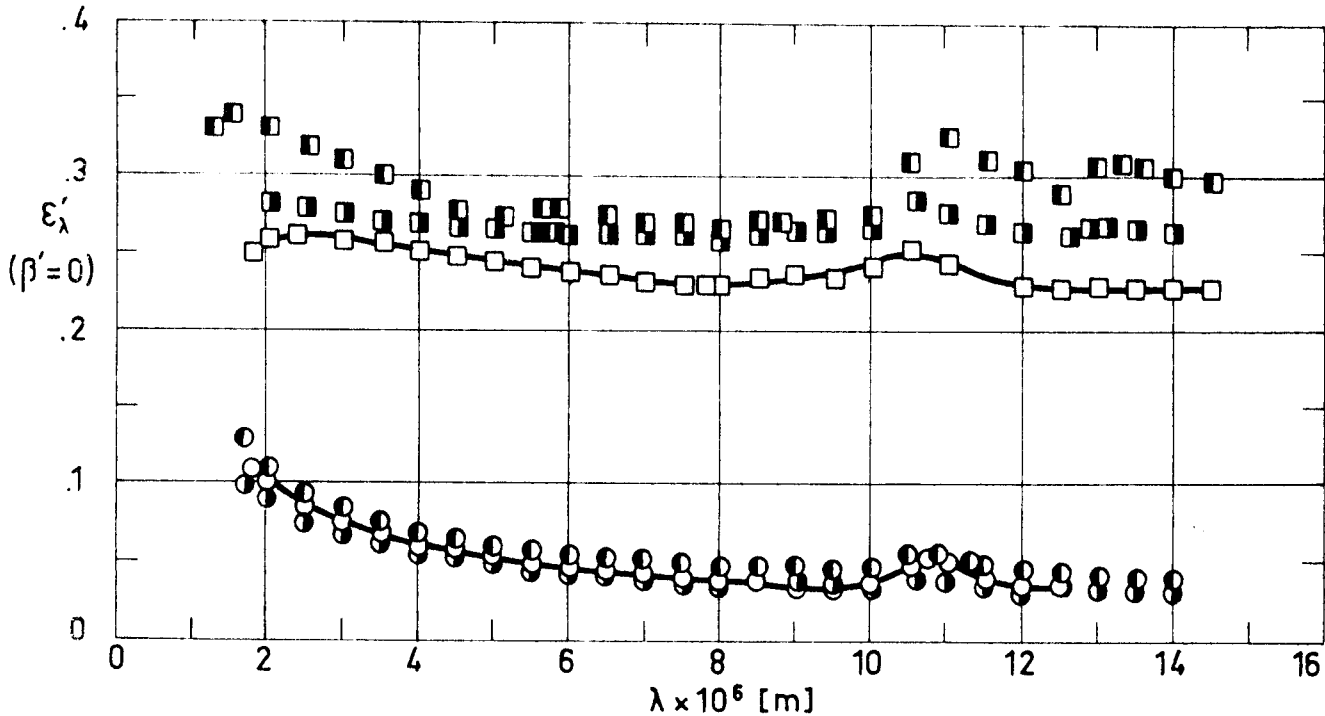


Fig 1-6. Normal spectral emittance, ϵ'_λ , of Aluminium as a function of wavelength, λ .

Explanation

Key	Description	Comments	References
○	99.7 Al - .11 Fe - .11 Si - .01 Cu - .01 Mg - <.01 Mn, Ni, Zn. Cylindrical tube. Heated at 467 K for 15 h. Polished. Surface roughness: 7.62×10^{-8} m (center line average).	Sample temperature: T = 599 K. Data from smooth curve. Reported error $\pm 20\%$ (in the wavelength range 2×10^{-6} to 10^{-5} m).	Touloukian & DeWitt (1970).
●	Same as ○ except heated at 697 K for 20 h.	Same as ○ except T = 697 K.	
◐	Same as ○ except heated at 805 K for 15 h.	Same as ○ except T = 805 K.	
◑	Same specimen as ○ except heated at 462 K for 25 h. Roughened and knurled with grade 180 silicon carbide paper. Surface roughness: 2.92×10^{-6} m (center line average).	T = 462 K. Data from smooth curve. Reported error $\pm 10\%$ (in the wavelength range 2×10^{-6} to 10^{-5} m).	
◒	Same as ◑ except heated at 598 K for 22 h.	Same as ◑ except T = 599 K.	
◓	Same as ◑ except heated at 715 K for 27 h.	Same as ◑ except T = 715 K.	

METALLIC MATERIALS

Aluminium Alloys

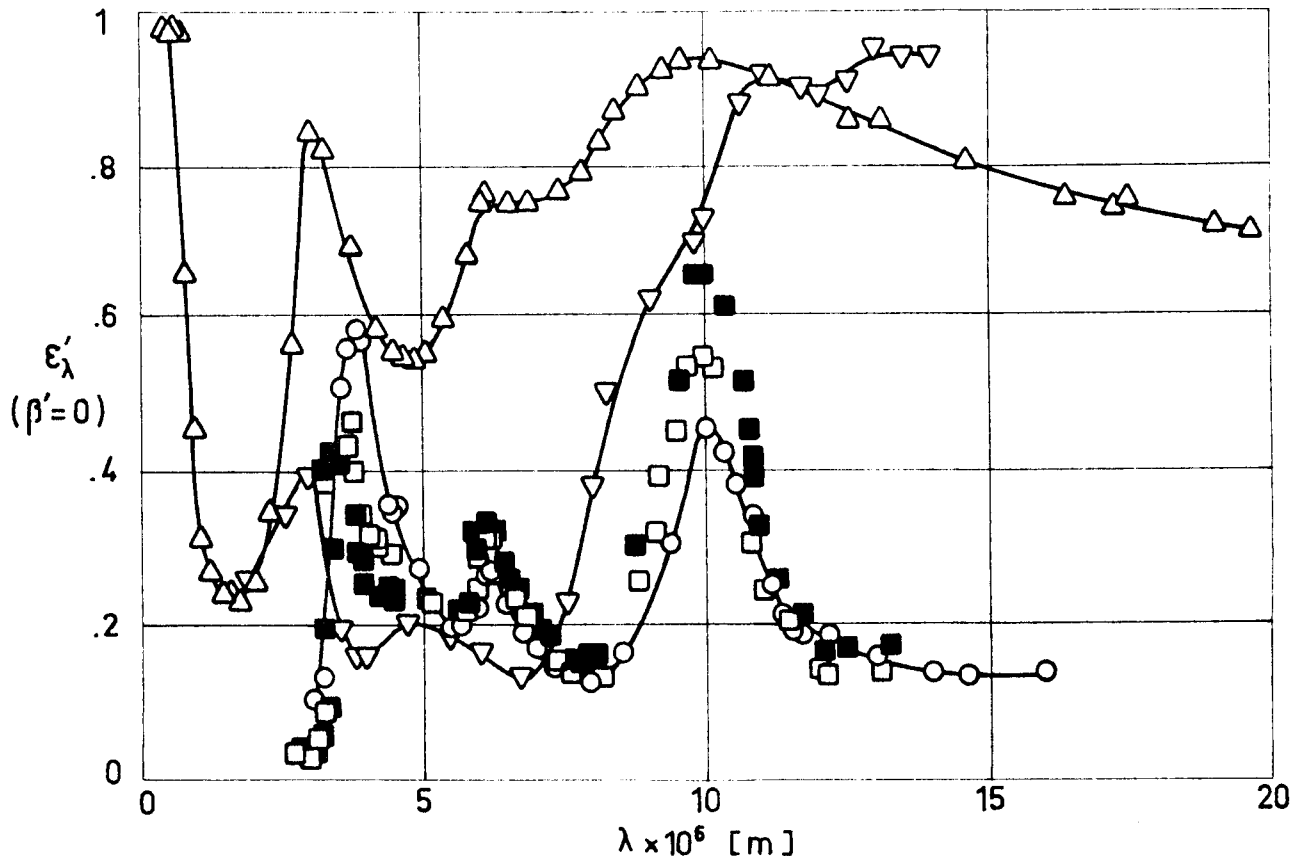


Fig 1-7. Normal spectral emittance, ϵ'_{λ} , of Aluminium conversion coatings as a function of wavelength, λ .

Explanation

Key	Description	Comments	References
○	Alodine 401-45. Reaction of an aluminium surface with an aqueous solution of chromic, phosphoric, and hydrofluoric acid. Substrate: Al - 99.8 (Echo II).	Sample temperature: T=295 K. Data from smooth curve. Converted from R(2π,0).	Touloukian DeWitt & Hernicz (1972).
◻	Same as ○ except reacted for 20 s in a 1 N sodium hydroxide solution at 298 K, then washed in water and dried in air.		
■	Same as ◻. Reacted for 40 s.		
Δ	Black anodized.	T=323 K. Data from smooth curve. Converted from R(2π,0).	
▽	Al - 99.7. Anodized 30 min at 10 ⁻² A.m ⁻² in 4 N analar sulphuric acid at 293K, sealed for 30 min in boiling distilled water. Anodizing thickness 2.54x10 ⁻⁶ m. Heated at 456 K for 15 h.	T=461 K. Data from smooth curve. Reported error ±10%.	

METALLIC MATERIALS
Aluminium Alloys

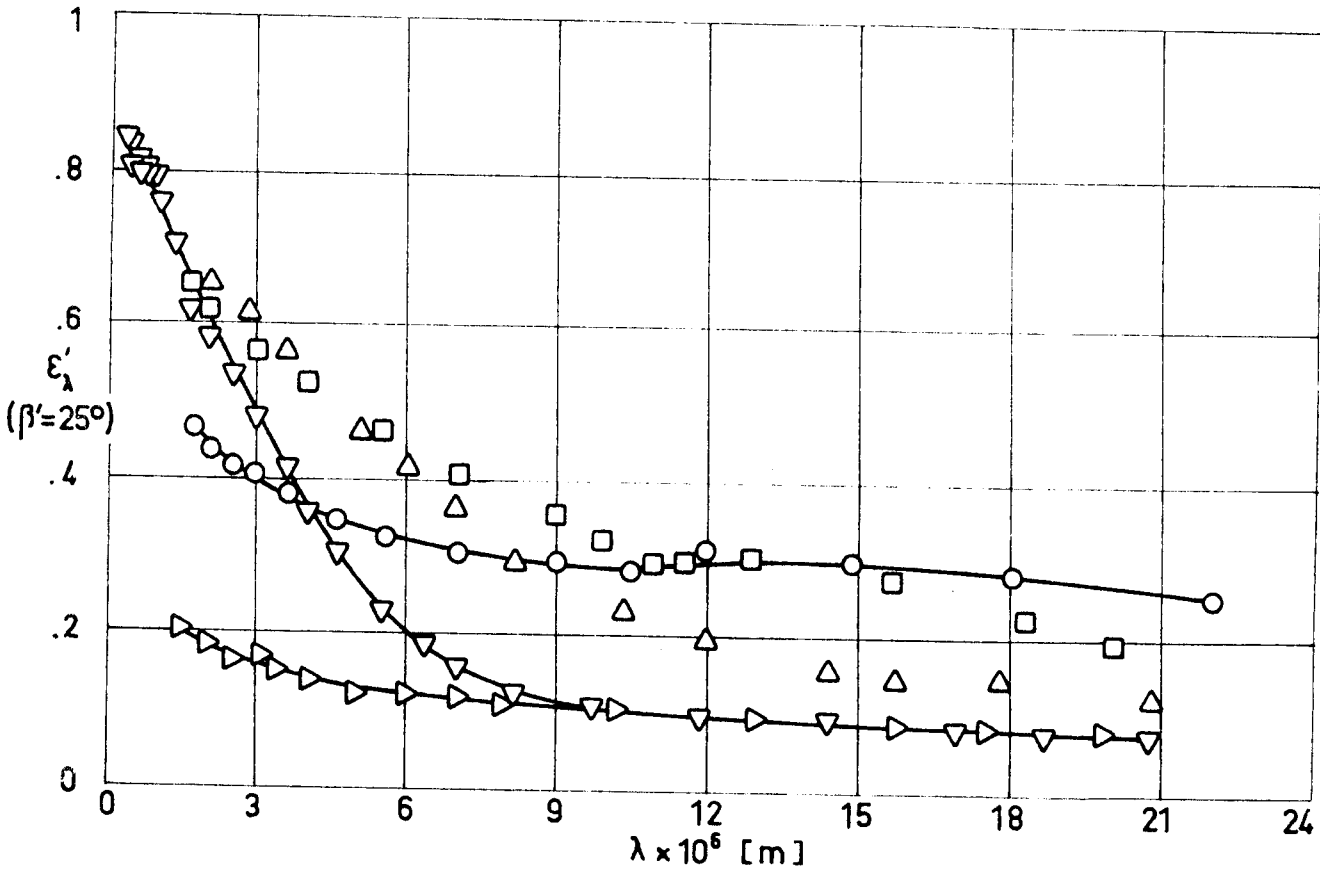


Fig 1-8. Angular spectral emittance, ϵ'_{λ} , of Aluminium as a function of wavelength, λ .

Explanation

Key	Description	Comments	References
○	Al - 99.0. Nominal composition. Sandblasted with 120 mesh alumina (mesh opening 1.25×10^{-4} m).	Sample temperature: $T=306$ K. Authors assumed $\alpha = \epsilon = 1 - \rho$. $\rho(25^\circ, 2\pi)$.	Touloukian & DeWitt (1970).
□	Same as ○ except sandblasted with 320 mesh alumina (mesh opening 4.6×10^{-5} m).		
△	Same as ○ except sandblasted with 600 mesh alumina (mesh opening 2.4×10^{-5} m).		
▽	Same as ○ except sandblasted with 1000 mesh alumina (mesh opening 1.4×10^{-5} m).		
◁	Same as ○ except sanded with 280 mesh silicon carbide paper.		

METALLIC MATERIALS
Aluminium Alloys

Table 1-1
Normal Total Emittance of Aluminium

Alloy	T [K]	ϵ' ($\beta'=0$)	Comments	References
Al - 99.99	298	.03		Pennington (1961).
Al - 99.0		.05	Polished.	Zerlaut, Carrol & Gates (1966).
Al -		.21	Foil, vapor blasted, wet.	
Al - 99.0		.33	Sandblasted.	
Al -	311	.065	Bright foil roughened with abrasive cloth.	Touloukian (1967)a.
Al -	373	.18	Sheet, rough polished.	
Al - 99.99		.02	Foil (1.27×10^{-4} m thick) GMC Bright dip for 10 min at 350 K.	Bevans (1969).
Al -	296	.04	Polished.	TRW (1970).
Al -	298	.055 to .070	Rough plate.	
Al -		.04	Bare metal.	Scollon & Carpitella (1970).
Al - 99.0	370	.022	Polished with MgO and water, measured in vacuum (2.1×10^{-2} Pa).	Touloukian & DeWitt (1970).
Al - 99.99	425.4	.037	Rolled, polished.	
Al - 99.99	647	.045	Same as above.	
Al - 99.99	780	.0497	Same as above.	
Al - 99.99	414	.0486	Highly polished.	
Al - 99.99	610	.0576	Same as above.	
Al - 99.99	733	.065	Same as above.	
Al -	366	.028	Foil.	
Al -	311	.045	Foil, embossed (Pattern No. 1).	
Al -	311	.056	Foil, embossed (Pattern No. 2).	
Al -	311	.047	Foil, embossed (Pattern No. 3).	
Al -	311	.056	Foil, embossed (Pattern No. 4).	
Al -	311	.061	Foil, embossed (Pattern No. 5).	
Al - 99.9	311	.045	.002 Si, .0001 Fe, .001 Cu, .0003 Na, .0003 Ca, .0003 Mg. Electrolytically brightened, density 2.698 kg.m^{-3} at 298 K. aluminium foil reference ($\epsilon=.05$).	
Al -	311	.035 to .050	Foil, bright; etched in hot sodium hydroxide solution .5 to 2 min, and dipped in nitric acid.	
Al -	311	.044	Foil, bright; roughened with abrasive cloth (No. 120 Aloxite cloth).	
Al -	311	.063	Foil, bright; roughened with abrasive cloth (No. 120 Aloxite cloth).	
Al -	311	.066	Foil, bright; roughened with abrasive cloth (No. 120 Aloxite cloth).	
Al -	311	.04	Foil; surface film formed by means of exposure to corrosive attack; foil-covered cardboard taken from foil-insulated dry-ice cabinet exposed to weather on beach during 8 months.	

(Continued onto next page)

METALLIC MATERIALS

Aluminium Alloys

Table 1-1 (Continued)

Normal Total Emittance of Aluminium

Alloy	T [K]	ϵ' ($\beta'=0$)	Comments	References
Al -	311	.05	Foil; suspended vertically in the laboratory for 3 years and measured with the accumulated dust and fume.	Touloukian & DeWitt (1970).
Al -	311	.09	Foil; chemically oxidized by treating with hot solution of sodium carbonate and chromate.	
Al -	311	.10	Foil; lacquer coated; heated to partially decompose lacquer and color it brown.	
Al -	311	.10	Foil after 2 years exposure to salt spray and moisture at seashore.	
Al -	373	.09	Commercial sheet.	
Al -	373	.095	Sheet, polished.	

Table 1-2

Normal Total Emittance and Normal Solar Absorptance of Aluminium Contact Coatings

Alloy	T [K]	ϵ' ($\beta'=0$)	α_s ($\beta=0$)	Comments	References
Al -		.03	.10	Vacuum deposited (opaque thickness) on aluminium sheet with resin undercoat.	Bevans (1969).
Al -		.03	.09	Vacuum deposited (opaque thickness) on aluminium foil, Reynolds Wrapp.	
Al -		.04	.21	Vacuum deposited (opaque thickness) on Beryllium foil.	
Al -		.03	.09	Vacuum deposited (opaque thickness) on Mylar film 2.5×10^{-5} m thick.	
Al -		.014	.08	10^{-7} to 2×10^{-7} m thick aluminium vapor deposited on unspecified surface. Polished surface. Measured in vacuum.	Scollon & Carpitella (1970).
Al -		.051	.15	Same as above. Measured in air.	
Al -		.024	.13	Vapor deposited aluminium on Mylar..	
Al -		$\leq .05$	$\leq .13$	Vapor deposited aluminium on 1.2×10^{-5} m thick Kapton. Data for metallic side. Silicone pressure sensitive adhesive. Schjeldahl.	
Al -		$\leq .06$.10 to .14	Vapor deposited aluminium on Kapton. Data for metallic side. Silicone pressure sensitive tape. Schjeldahl G - 103500 tape.	
Al -		.13 to .17	.12 to .16	Vapor deposited aluminium on 1.2×10^{-5} m thick Kapton plus nylon tulle. Data for metallic surface. Acrylic pressure sensitive adhesive. Second surface reflector. Schjeldahl G - 102000 tape.	
Al -		.025	.11	1.5×10^{-7} m thick evaporated aluminium on Quartz.	

McCargo, Spradley,
Greenberg &
McDonald (1971).

METALLIC MATERIALS

Aluminium Alloys

Table 1-3

Normal Total Emittance and Normal Solar Absorptance of Aluminium Conversion Coatings

Alloy	T [K]	ϵ' ($\beta'=0$)	α_s ($\beta=0$)	Comments	References
Al - 99.99		.77	.20	Hard anodized, 8×10^{-6} m thick, with sulphuric acid electrolyte 11% by weight, at 270 K.	Bevans (1969).
Al - 99.99		.79	.14	Soft anodized, 1.3×10^{-5} m thick, with sulphuric acid electrolyte 15% by weight, at 270 K.	
Al - 99.7		.82	.24	Soft anodized, 1.3×10^{-5} m thick, with sulphuric acid electrolyte 16% by weight, at 294 K.	
Al - 99.7		.74	.40	Anodized, 8×10^{-6} m thick, with chromic acid electrolyte 5% by weight, at 308 K, anodizing voltage 40V DC, 120 min.	
Al - 99.99		.08	.27	Anodized, citric acid electrolyte 1 kg.m^{-3} ammonium citrate, at 295 K, anodizing voltage: 300V DC, 60 min.	
Al - 99.7		.86	.31	Anodized, 2×10^{-5} m thick, oxalic acid solution 3% by weight, at 311 K, anodizing voltage: 30V DC, 60 min.	
Al - 99.99		.39	.33	Anodized, sulphamic acid electrolyte 100 kg.m^{-3} , at 294 K, anodizing voltage: 45V DC, 30 min.	
Al - 99.99		.77	.64	Anodized, sulphamic acid electrolyte 100 kg.m^{-3} , at 294 K, anodizing voltage: 15V DC, 30 min.	
Al - 99.99		.03	.27	Anodized, sulphamic acid electrolyte 100 kg.m^{-3} , at 294 K, anodizing voltage: 5.5V DC, 15 min.	
Al -		.73	.70	Chromic acid anodized. Chemical surface finish. Degradation caused by deposition of outside contaminants (73 h in low earth orbit on board Apollo 9).	Scollon & Carpitella (1970).
Al -		.90		Carbon black impregnated anodized coating. Chemical surface finish.	

METALLIC MATERIALS

Aluminium Alloys

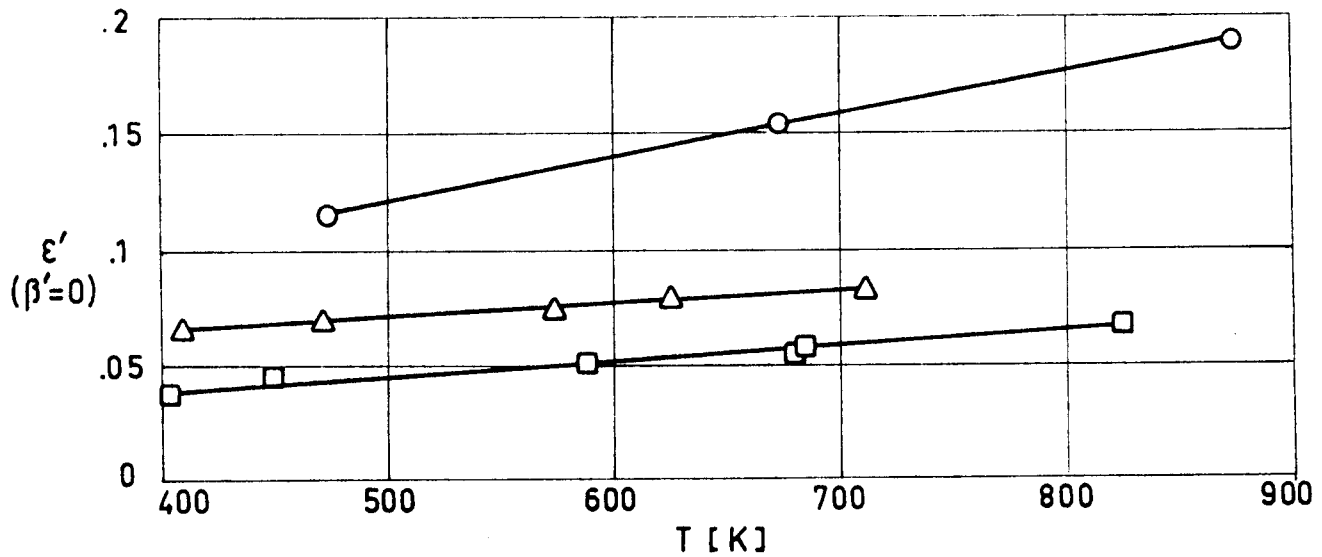


Fig 1-9. Normal total emittance, ϵ' , of Aluminium as a function of temperature, T .

Explanation

Key	Description	Comments	References
○	Cleaned, polished, and oxidized.		Touloukian & DeWitt (1970).
□	Pure. Highly polished.	Reported error 2%	
△	Pure. Rolled, as received.		

METALLIC MATERIALS
Aluminium Alloys

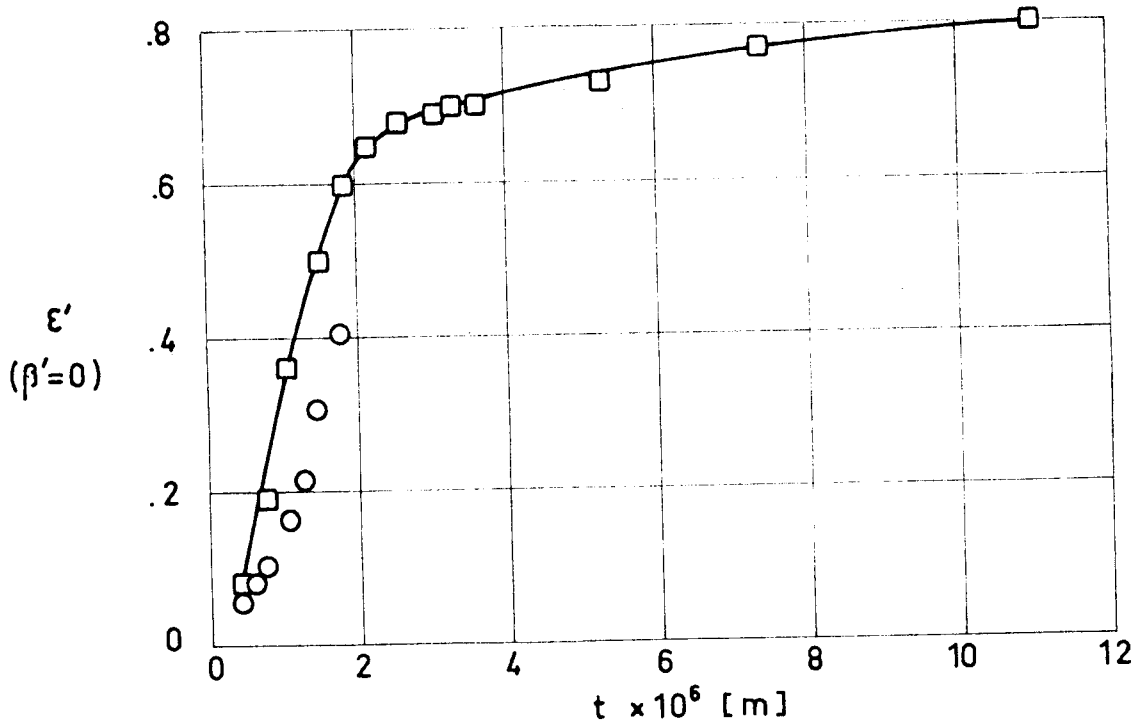


Fig 1-10. Normal total emittance, ϵ' , of Aluminium anodized as a function of anodizing thickness, t_c .

Explanation

Key	Description	Comments	References
○	Barrier-layer anodic coating on a high purity aluminium substrate. Substrate cleaned, electropolished in a fluoboric acid solution, anodized in aqueous ammonium tartrate solution, then immersed in a phosphoric acid solution.	Sample temperature $T \approx 298$ K. Measured in vacuum ($\approx 1.33 \times 10^{-4}$ Pa).	Touloukian, DeWitt & Hernicz (1972).
□	Foil oxidized electrolytically in 15% sulphuric acid.	$T = 311$ K. Measured relative to Aluminium.	

METALLIC MATERIALS
Aluminium Alloys

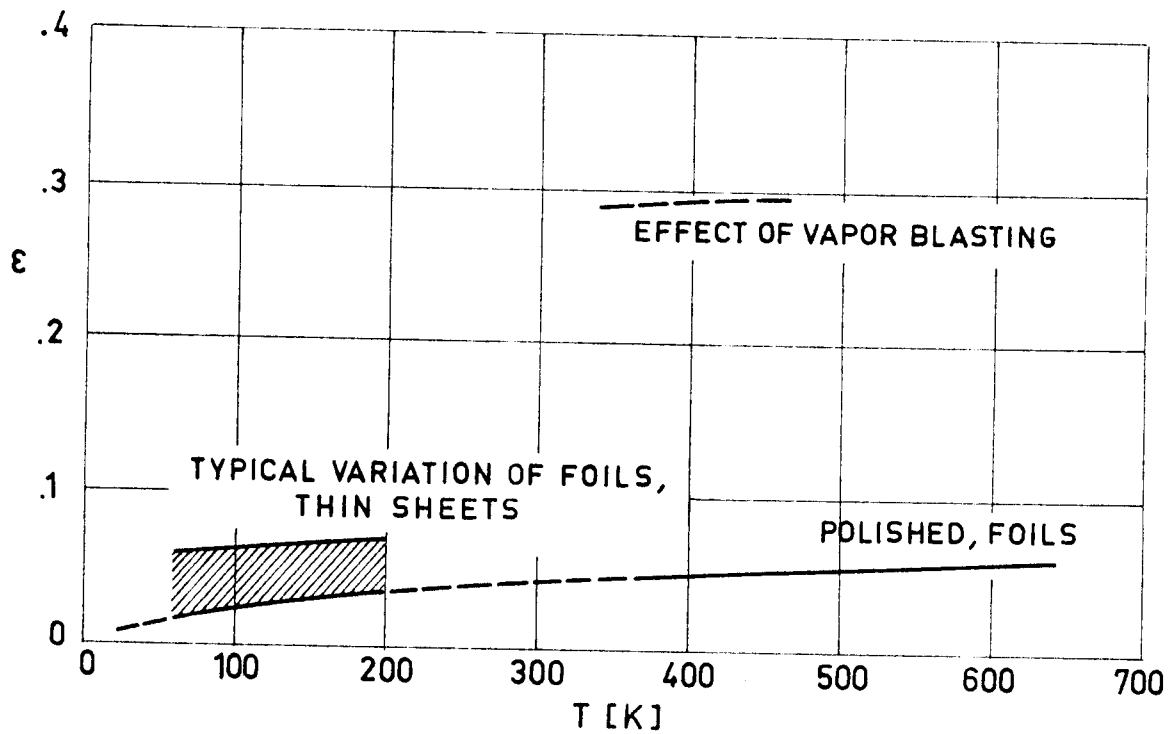


Fig 1-11. Summary of data concerning the hemispherical total emittance, ϵ , of Aluminium as a function of temperature, T . From Touloukian & DeWitt (1970).

METALLIC MATERIALS

Aluminium Alloys

Table 1-4

Hemispherical Total Emittance of Aluminium Contact Coatings

T [K]	ϵ	Comments
76	.04	Aluminium; plastic Mylar (1.27×10^{-5} m thick) and aluminium substrates; produced by vaporizing aluminium on both sides of Mylar. Measured in vacuum (1.3×10^{-4} to 1.3×10^{-5} Pa). Authors assumed $\alpha = \epsilon$ for 300 K blackbody incident radiation. Reported error 5%.
76	.07	Aluminium; stainless steel substrate; Al sprayed on substrate. Measured in vacuum (1.3×10^{-4} to 1.3×10^{-5} Pa). Authors assumed $\alpha = \epsilon$ for 300 K blackbody incident radiation. Reported error 5%.
76	.06	Aluminium; stainless steel substrate; Al sprayed on substrate; wire brushed. Measured in vacuum (1.3×10^{-4} to 1.3×10^{-5} Pa). Authors assumed $\alpha = \epsilon$ for 300 K blackbody incident radiation. Reported error 5%.
76	.04	Aluminium; plastic Mylar (1.27×10^{-5} m thick) and aluminium substrate; Al vapor deposited on both sides of Mylar. Measured in vacuum (1.3×10^{-4} Pa). Authors assumed $\alpha = \epsilon$ for 294 K blackbody radiation.
76	.043	Similar to above specimen and conditions.
773-1273	.69-.78	Aluminium; iron substrate; substrate sandblasted and degreased; coated to a surface density of 75 kg.m^{-2} with aluminium powder suspension; sintered at 1 223 K in vacuum. Measured in vacuum (6.7×10^{-4} Pa). Data extracted from smooth curve. Reported error 2.5%.
378-486	.33-.27	Aluminium (1.27×10^{-4} to 2.03×10^{-4} m thick); Al substrate; sprayed. Measured in vacuum (.13 Pa). Reported error 3%.
333	.047	Aluminium; Mylar substrate. Measured in vacuum (6.7×10^{-4} Pa). Reported error <3.5%.
300-415	.06	Aluminium (10^{-6} m thick); Mylar (1.2×10^{-5} m thick) and stainless steel (2.5×10^{-4} m thick) substrates; Mylar cemented to stainless steel; Al vapor deposited. Measured in vacuum (1.3×10^{-5} Pa). Reported error 5%.
258-348	.0428-.0454	Aluminium (2×10^{-7} m thick); stainless steel substrate; Al vapor deposited on hand-polished substrate; property measured by steady-state calorimetric method. Mentioned below as specimen 1.
248-348	.0293-.0311	Same specimen and conditions as 1 except property measured by transient calorimetric method; property of second side of sample assumed.
303	.024	Same specimen and conditions as 1 except property calculated from $\rho(10^\circ, 10^\circ)$ measured by specular method relative to a front surface aluminized mirror.
300	.0482	Same specimen and conditions as 1 except property calculated from $\rho(7.5^\circ, 2\pi)$ measured by ellipsoid method.
200-400	.0224-.0237	Same specimen and conditions as 1 except property calculated from $R(2\pi-75^\circ, 15^\circ)$. Specimen placed at the center of a heated cavity, so that the angle of viewing can be varied from 15° to 75° . (Millard & Streed (1969))
295	.0279	Same specimen and conditions as 1 except property measured by a portable Quick Emittance Device.
295	.041	Same specimen and conditions as 1 except property measured by a portable emissometer.
~298	.0334	Polyester film (6.35×10^{-6} m thick) double-aluminized. Coating thickness of emitting surface $t_{c1} = 4.55 \times 10^{-8}$ m. Coating thickness of second surface $t_{c2} = 3.78 \times 10^{-8}$ m.
~298	.0335	Similar to above except opposite side measured.
~298	.0335	Similar to above except $t_{c1} = 4.53 \times 10^{-8}$ m. $t_{c2} = 3.95 \times 10^{-8}$ m.
~298	.0378	Similar to above except opposite side measured.
~298	.0300	Similar to above except $t_{c1} = 4.5 \times 10^{-8}$ m. $t_{c2} = 3.95 \times 10^{-8}$ m.
~298	.0331	Similar to above except opposite side measured.

(Continued onto next page)

METALLIC MATERIALS

Aluminium Alloys

Table 1-4 (Continued)

Hemispherical Total Emittance of Aluminium Contact Coatings

T [K]	ϵ	Comments
~298	.0369	Similar to above except $t_{c1}=4.5 \times 10^{-8}$ m. $t_{c2}=4 \times 10^{-8}$ m.
~298	.0358	Similar to above except opposite side measured.
~298	.0335	Similar to above except $t_{c1}=4.56 \times 10^{-8}$ m. $t_{c2}=3.95 \times 10^{-8}$ m.
~298	.0243	Similar to above except opposite side measured.
307	.0246	Aluminium; quartz substrate. Measured in vacuum (1.3×10^{-4} Pa) maintained by diffusion pump.
307	.0143	Polyester film (6.35×10^{-6} m thick) single-aluminized; vacuum deposited. Measured in vacuum as above.
307	.0543	Polyester film (6.35×10^{-6} m thick) double-aluminized; vacuum deposited. Measured in vacuum as above.
307	.0543	Similar to above except opposite side measured.
307	.0613	Polyester film (6.35×10^{-6} m thick) single-aluminized; vacuum deposited. Measured in vacuum as above.
307	.0609	Similar to above specimen and conditions.
307	.0450	Polyester film (6.35×10^{-6} m thick) single-aluminized. $t_{c1}=2.35 \times 10^{-8}$ m. Vacuum deposited. Measured in vacuum as above.
307	.0532	Polyester film (6.35×10^{-6} m thick) double-aluminized; vapor deposited. Measured in vacuum as above.
307	.0773	Polyester film (6.35×10^{-6} m thick) double-aluminized. $t_{c1}=3.34 \times 10^{-8}$ m. $t_{c2}=2.48 \times 10^{-8}$ m. Vapor deposited. Measured in vacuum as above.
307	.0513	Polyester film (6.35×10^{-6} m thick) double-aluminized. $t_{c1}=2.48 \times 10^{-8}$ m. $t_{c2}=3.34 \times 10^{-8}$ m. Vapor deposited. Measured in vacuum as above.
307	.0466	Polyester film (6.35×10^{-6} m thick) single-aluminized; vacuum deposited. Measured in vacuum as above.
307	.0377	Aluminium; Mylar and aluminium substrates; aluminium vacuum deposited on both sides of Mylar. Measured in vacuum as above.
307	.472	Aluminium; reinforced polyester film substrate (aluminized scrim). Measured in vacuum as above.
307	.0248	Aluminium; quartz substrate. Measured in vacuum as above.
307	.0176	Polyester film (6.35×10^{-6} m thick) double-aluminized. Measured in vacuum as above.
307	.041	Polyester film (6.35×10^{-6} m thick) double-aluminized. Measured in vacuum as above.
307	.0416	Polyester film (6.35×10^{-6} m thick) double-aluminized; vapor deposited. Measured in vacuum as above.
307	.0422	Similar to above specimen and conditions.
307	.0398	Similar to above specimen and conditions.
307	.0333	Polyester film (6.35×10^{-6} m thick) double-aluminized. $t_{c1}=4.55 \times 10^{-8}$ m. $t_{c2}=3.78 \times 10^{-8}$ m. Vapor deposited. Measured in vacuum as above.
307	.0334	Polyester film (6.35×10^{-6} m thick) double-aluminized. $t_{c1}=4.53 \times 10^{-8}$ m. $t_{c2}=3.95 \times 10^{-8}$ m. Vapor deposited. Measured in vacuum as above.
307	.0229	Polyester film (6.35×10^{-6} m thick) double-aluminized. $t_{c1}=4.5 \times 10^{-8}$ m. $t_{c2}=3.8 \times 10^{-8}$ m. Vacuum deposited. Measured in vacuum as above.
307	.0369	Polyester film (6.35×10^{-6} m thick) double-aluminized. $t_{c1}=4.5 \times 10^{-8}$ m. $t_{c2}=4 \times 10^{-8}$ m. Vacuum deposited. Measured in vacuum as above.
307	.0334	Polyester film (6.35×10^{-6} m thick) double-aluminized. $t_{c1}=4.56 \times 10^{-8}$ m. $t_{c2}=3.95 \times 10^{-8}$ m. Vapor deposited. Measured in vacuum as above.

(Continued onto next page)

METALLIC MATERIALS

Aluminium Alloys

Table 1-4 (Continued)

Hemispherical Total Emittance of Aluminium Contact Coatings

T [K]	ε	Comments
307	.0335	Polyester film (6.35×10 ⁻⁶ m thick) double-aluminized. t _{c1} =3.78×10 ⁻⁸ m. t _{c2} =4.55×10 ⁻⁸ m. Vapor deposited. Measured in vacuum as above.
307	.0347	Polyester film (6.35×10 ⁻⁶ m thick) double-aluminized. t _{c1} =3.95×10 ⁻⁸ m. t _{c2} =4.53×10 ⁻⁸ m. Vapor deposited. Measured in vacuum as above.
307	.0381	Polyester film (6.35×10 ⁻⁶ m thick) double-aluminized. t _{c1} =3.8×10 ⁻⁸ m. t _{c2} =4.5×10 ⁻⁸ m. Vacuum deposited. Measured in vacuum as above.
307	.0224	Polyester film (6.35×10 ⁻⁶ m thick) double-aluminized. t _{c1} =3.95×10 ⁻⁸ m. t _{c2} =4.56×10 ⁻⁸ m. Vapor deposited. Measured in vacuum as above.
307	.0349	Polyester film (6.35×10 ⁻⁶ m thick) double-aluminized; vapor deposited. Measured in vacuum as above.
307	.0337	Similar to above specimen and conditions.
307	.035	Similar to above specimen and conditions.
307	.0835	Similar to above specimen and conditions.
307	.0306	Similar to above specimen and conditions.
307	.0284	Similar to above specimen and conditions.
307	.0369	Similar to above specimen and conditions.
307	.0369	Similar to above specimen and conditions.
307	.0270	Similar to above specimen and conditions.
307	.0289	Similar to above specimen and conditions.
307	.0326	Polyester film (6.35×10 ⁻⁶ m thick) single-aluminized; vacuum deposited. Measured in vacuum as above.
307	.03	Similar to above specimen and conditions.
307	.0337	Similar to above specimen and conditions.
307	.0231	Polyester film single-aluminized. t _{c1} =2.18×10 ⁻⁸ m. Measured in vacuum as above.
307	.0722	Polyester film single-aluminized. t _{c1} =3×10 ⁻⁹ m. Measured in vacuum as above.
307	.0399	Polyester film single-aluminized. t _{c1} =1.08×10 ⁻⁸ m. Measured in vacuum as above.
333	.038	Polyester film single-aluminized. Measured in vacuum (6.7×10 ⁻⁴ Pa).
77	.043	Aluminium household type foil wrapped loosely; cleaned with acetone. Measured in vacuum (~1.3×10 ⁻³ Pa).

From Touloukian, DeWitt & HERNICZ (1972).

METALLIC MATERIALS
Aluminium Alloys

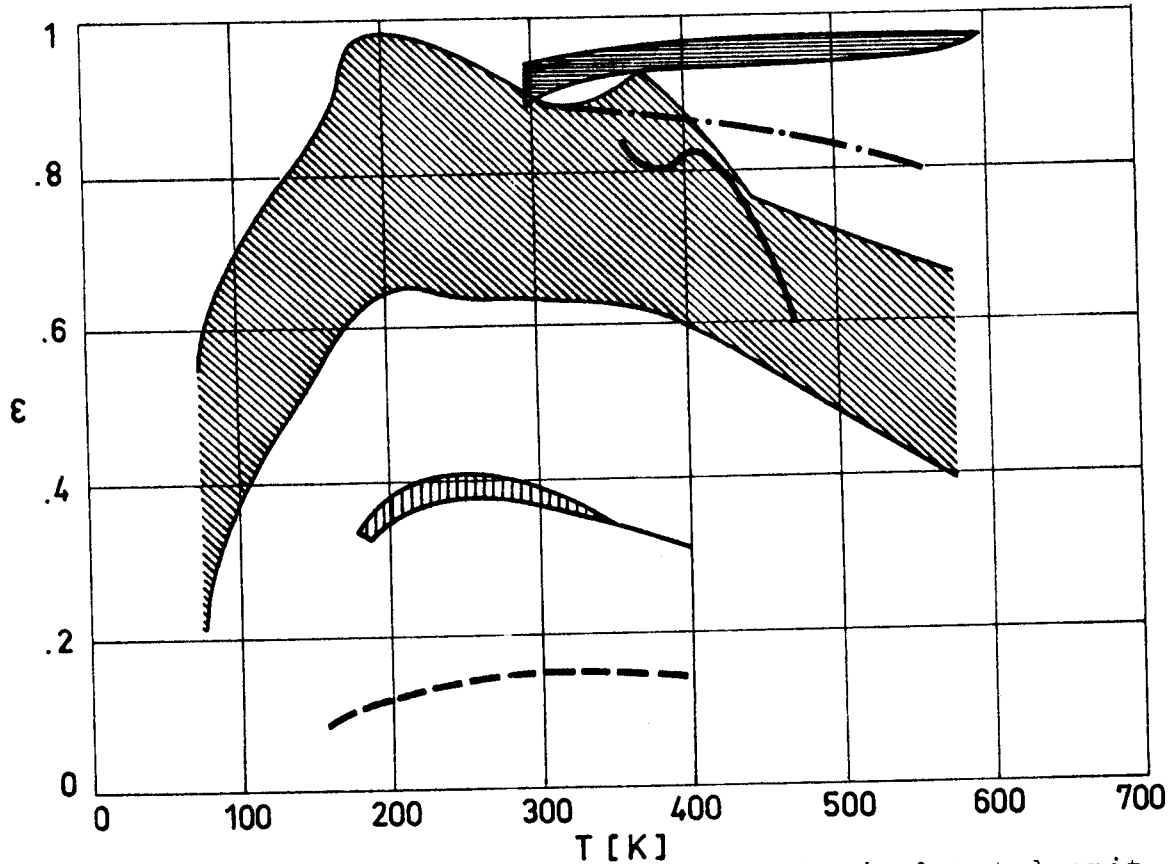








Fig 1-12. Summary of data concerning hemispherical total emissivity, ϵ , of Aluminium conversion coatings vs. temperature, T . From Fouloukian, DeWitt & Hernicz (1972).

Explanation

Key	Description	Comments
	Anodized. Layer of carbon deposited into pores of the surface.	Measured in vacuum (1.33×10^{-5} Pa).
	Al - 99.99, anodized in sulphuric acid. Polished substrate. Coating thickness: 2.54×10^{-6} - 2.54×10^{-5} m.	ϵ increases when coating thickness increases.
	Al - 99.99. Electropolished in fluoboric acid solution, then anodized in ammonium tartrate solution.	
	Anodized. Dull surface.	Measured in vacuum Reported error $\pm 5\%$
	Vapor blasted after anodization.	Measured in vacuum Reported error $\pm 3\%$ Blasting decreases ϵ less than 6%.
	Al - 99.99. Substrate alkaline electropolished (sodium phosphate and sodium carbonate) 15 min at 353 K and 12 V DC, then anodized 15 min at 18 V DC in 10% sulphuric acid.	Measured in vacuum

METALLIC MATERIALS
Aluminium Alloys

3.3.2. Absorptance.

Data concerning absorptance have been arranged as indicated in the following Table.

3.3.2.1. Directional spectral absorptance.				
Paragraph	Heading	Data Presented	Fig.	Table
3.3.2.1.1.	Normal $\beta=0$	Aluminium. A limited amount of information corresponding to $\beta = 25^\circ$ is also presented	1-13	
3.3.2.2. Directional total absorptance.				
3.3.2.2.1.	Normal $\beta=0$	Aluminium. A single value is included in the same Table as the hemispherical total absorptance		1-5
3.3.2.4. Hemispherical total absorptance.				
	$\omega = 2\pi$	Aluminium.		1-5
3.3.2.5. Solar absorptance.				
3.3.2.5.1.	Normal $\beta=0$	Aluminium.		1-6
		Aluminium contact coatings.		1-2
		Aluminium conversion coatings.		1-3,1-7
3.3.2.5.2.	Angular (non-normal) $\beta \neq 0$	Aluminium conversion coatings.		1-8
3.3.2.6. Absorptance to emittance ratio.				
		Aluminium conversion coatings. Degradation effects.	1-14	

METALLIC MATERIALS

Aluminium Alloys

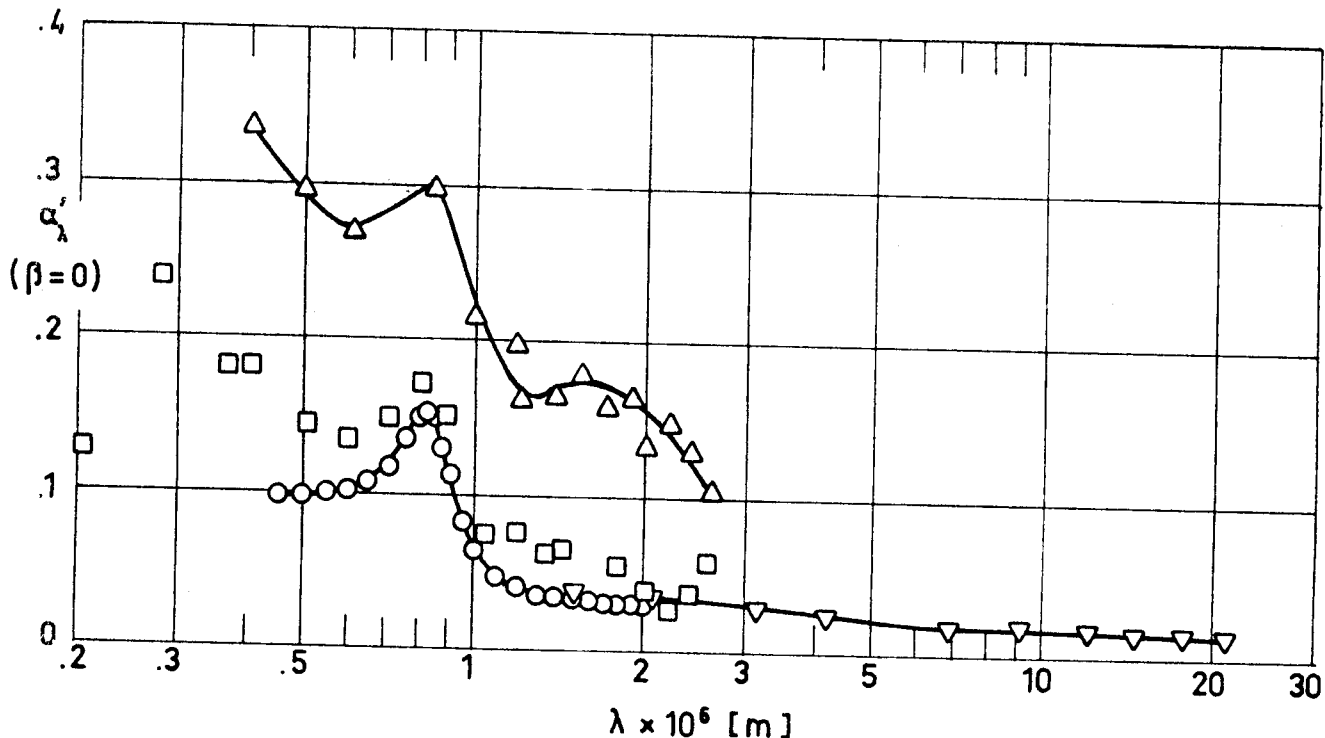


Fig 1-13. Directional spectral absorptance, α'_λ , of Aluminium as a function of wavelength, λ . Data points ∇ correspond to $\beta=25^\circ$.

Explanation

Key	Description	Comments	References
○	Evaporated film; evaporation rate 3×10^{-8} m.s ⁻¹ at 2.66×10^{-3} Pa. Aged 8 d before measurement.	$\beta \sim 10^\circ$ Sample temperature: T=298 K. Measured in vacuum. Reported error $\pm 1.4\%$	Touloukian & DeWitt (1970).
□		T \sim 298 K. Data from smooth curve.	
△	Polished.		
▽	Foil.	$\beta=25^\circ$ T=306 K. Measured in dry nitrogen. Heated cavity at approximately 1056 K with platinum reference. Authors assumed $\alpha=1-R$.	

METALLIC MATERIALS
Aluminium Alloys

Table 1-5
Hemispherical total Absorptance of Aluminium

T [K]	T_b^a [K]	$(\omega=2\pi)$	Comments
2	298	.0111	Normal total absorptance ($\beta \approx 0$) of specimen electropolished. Reported error 1%.
76	300	.018	Kaiser foil (2.54×10^{-5} m thick), unannealed. Measured in vacuum (1.33×10^{-4} to 1.33×10^{-5} Pa). Reported error 5%.
76	300	.018	Cockron home foil (3.81×10^{-5} m thick). Same vacuum and error as above.
76	300	.021	Hurwich home foil (3.81×10^{-5} m thick). Same vacuum and error as above.
76	300	.022	Same as above except measured on bright side.
76	300	.028	Sheet (5.08×10^{-4} m thick). Cold acid cleaned. Same vacuum and error as above.
76	300	.026	Alcoa No. 2 reflector plate (5.08×10^{-4} m thick). Same vacuum and error as above.
76	300	.032	Same as above except sanded with fine emery.
76	300	.035	Same as above except cleaned with alkali.
76	300	.045	Sheet (5.08×10^{-4} m thick). Cleaned with wire brush, emery paper, steel wool and cold acid. Same vacuum and error as above.
76	300	.060	Same as above except wire brush cleaned.
76	300	.140	Same as above except liquid honed.
76	300	.029	Same as above except hot acid cleaned (Alcoa process).
76	294	.0204	Cockron foil (3.81×10^{-5} m thick). Measured in vacuum ($< 1.33 \times 10^{-4}$ Pa).
76	294	.0200	Same as above.
76	294	.0615	Sheet (5.08×10^{-4} m thick). Cleaned with wire brush. Same vacuum as above.
76	294	.0615	Same as above except cleaned with wire brush, emery paper, and steel wool.
76	294	.0452	Same as above except cleaned with wire brush, emery paper, steel wool and cold acid.
76	294	.0356	Same as above except alkali cleaned.
76	294	.0327	Alcoa No. 2 reflector plate (5.08×10^{-4} m thick, $\epsilon = .3$ for visible light at 298 K). Same vacuum as above.
76	294	.0317	Sheet (5.08×10^{-4} m thick). Cold acid cleaned. Same vacuum as above.
76	294	.0283	Same as above.
76	294	.0217	Hurwich home foil (3.81×10^{-5} m thick). Measured on bright side in vacuum ($< 1.33 \times 10^{-4}$ Pa).
76	294	.0212	Same as above except measured on mat side.
76	294	.0204	Cockron home foil (3.81×10^{-5} m thick). Same vacuum as above.
76	294	.0186	Same as above.
76	294	.0213	Kaiser foil (2.54×10^{-5} m thick). Unannealed. Same vacuum as above.
76	294	.0184	Same as above.
76	294	.0186	Kaiser home foil (1.91×10^{-5} m thick). Same vacuum as above.
76	294	.0294	Foil (5.08×10^{-4} m thick). Hot acid cleaned (Alcoa process). Same vacuum as above.

a

T_b is the temperature of the emitting blackbody.

From Touloukian & DeWitt (1970).

METALLIC MATERIALS
Aluminium Alloys

Table 1-6
Normal Solar Absorptance of Aluminium

Alloy	T [K]	α_s ($\beta=0$)	Comments	References
Al - 99.0		.30	Polished.	Zerlaut, Carrol & Gates (1966).
Al - 99.0		.48	Sandblasted.	
Al -		.42	Foil; vapor blasted, wet.	
Al - 99.99		.08	Foil (1.27×10^{-4} m thick) GMC Bright dip for 10 min at 350 K.	Bevans (1969).
Al -		.15	Bare metal.	Scollon & Carpitella (1970).
Al - 99.99	298	.096	Electropolished. Computed from spectral reflectance	Touloukian & DeWitt (1970).
Al - 99.99	298	.104	Same as above except hydrogen ion bombarded ($.25 \times 10^{24}$ ions.m ⁻²).	
Al - 99.99	298	.123	Same as above except hydrogen ion bombarded ($.84 \times 10^{24}$ ions.m ⁻²).	
Al - 99.99	298	.133	Same as above except hydrogen ion bombarded (1.67×10^{24} ions.m ⁻²).	
Al - 99.99	298	.151	Same as above except hydrogen ion bombarded (3.20×10^{24} ions.m ⁻²).	
Al - 99.99	298	.170	Same as above except hydrogen ion bombarded (4.92×10^{24} ions.m ⁻²).	
Al - 99.99	298	.204	Same as above except hydrogen ion bombarded (7.45×10^{24} ions.m ⁻²).	
Al - 99.99	298	.236	Same as above except hydrogen ion bombarded (9.86×10^{24} ions.m ⁻²).	

Table 1-7
Normal Solar Absorptance of Aluminium Conversion Coatings

T [K]	Basic Conditions	Variables Investigated	α_s ($\beta=0$)
~298	Barrier-layer anodic coating on a high-purity aluminium substrate. Coating applied as follows: substrate thoroughly cleaned, electropolished in a fluoboric acid solution, anodized in aqueous ammonium tartrate solution diluted with ethyl alcohol, then immersed in a phosphoric acid solution. Measured in vacuum (1.33×10^{-4} Pa). Computed from spectral reflectance data.	Anodizing voltage. Coating thickness	.129 .122 .142 .129-.136
		361 V 4.7×10^{-7} m	
		1 089 V 1.43×10^{-6} m	
		1 208 V 1.58×10^{-6} m	
		1 360 V 1.78×10^{-6} m	
~298	1199 aluminium anodized in sulphuric acid. Substrate polished in phosphoric/nitric acid bath for 2 min at 364 K. Computed from spectral reflectance data.	Anodizing time. Coating thickness	.12 .14 .16 .17
		10 min 8.36×10^{-6} m	
		15 min 9.38×10^{-6} m	
		20 min 10.96×10^{-6} m	
		25 min 13.21×10^{-6} m	

(Continued onto next page)

METALLIC MATERIALS

Aluminium Alloys

Table 1-7 (Continued)

Normal Solar Absorptance of Aluminium Conversion Coatings

T [K]	Basic Conditions	Variables Investigated	α_s ($\beta=0$)
~298	Al - 99.99 anodized in sulphuric acid. Substrate polished by Alzak process. Computed from spectral reflectance data.	Anodizing time. Coating thickness. Heat treatment	
		15 min 9.38x10 ⁻⁶ m	.16
		Same as above except heat treated 96 h at 589 K in vacuum (6.65x10 ⁻³ Pa).	.18
		25 min 9.38x10 ⁻⁶ m	.18
	Barrier anodized Al - 99.99 (~2.54x10 ⁻⁴ m thick). Data from smooth curve. Absorptance computed from spectral reflectance measured in situ.	Same as above except heat treated 96 h at 589 K in vacuum (6.65x10 ⁻³ Pa).	.22
		Simulated flight time of UV radiation exposure.	
		10 h	.109
		74.6 h	.116
		596 h	.126
		281	Alzak anodized aluminium (3.81x10 ⁻⁶ m thick). Absorptance computed from normal spectral reflectance. Property measured in air.
Unexposed sample (T=298 K).	.13		
20 keV electrons (10 ¹⁴ -5x10 ¹⁵ e.m ⁻² .s ⁻¹); 3x10 ¹⁸ e.m ⁻² , in dark in vacuum (1.33x10 ⁻⁶ Pa), maintained by ion pump.	.14		
10 ¹⁹ e.m ⁻²	.14		
10 ²⁰ e.m ⁻²	.16		
Unexposed sample (T=298 K).	.14		
77	Barrier anodized Al - 99.99 (2.54x10 ⁻⁴ m thick). Exposed to vacuum (6.65x10 ⁻⁷ - 2.66x10 ⁻⁵ Pa), maintained with diffusion pump. Absorptance computed from R(2 π ,0°). Property measured in situ.	80 keV electrons (10 ¹⁴ -5x10 ¹⁵ e.m ⁻² .s ⁻¹); 10 ¹⁹ e.m ⁻² , in dark in vacuum (1.33x10 ⁻⁶ Pa), maintained by ion pump.	.15
		10 ²⁰ e.m ⁻²	.16
		Effect of UV radiation and electron exposure.	
		Unexposed sample.	.17
		6 sun intensity UV radiation; 350 ESH Electron radiation (8.6x10 ¹⁴ -1.6x10 ¹⁶ e.m ⁻² .s ⁻¹); 5.8x10 ¹⁹ e.m ⁻²	.16
		Simultaneous exposure: Electron radiation (3.5x10 ¹⁴ e.m ⁻² .s ⁻¹); 5.8x10 ¹⁹ e.m ⁻² . 8 sun intensity UV radiation; 350 ESH	.20
77	Al - 99.99; sulphuric acid-anodized. Exposed to vacuum (6.65x10 ⁻⁷ - 2.66x10 ⁻⁵ Pa), maintained with diffusion pump. Absorptance computed from R(2 π ,0°). Property measured in situ.	Effect of UV radiation and electron	
		Unexposed sample.	.20
		6 sun intensity UV radiation; 350 ESH	.28
		Electron radiation (8.6x10 ¹⁴ -1.6x10 ¹⁶ e.m ⁻² .s ⁻¹); 5.8x10 ¹⁹ e.m ⁻²	.20
		Simultaneous exposure: Electron radiation (3.5x10 ¹⁴ e.m ⁻² .s ⁻¹); 5.8x10 ¹⁹ e.m ⁻² . 8 sun intensity UV radiation; 350 ESH	.27

From Touloukian, DeWitt & Hernicz (1972).

METALLIC MATERIALS

Aluminium Alloys

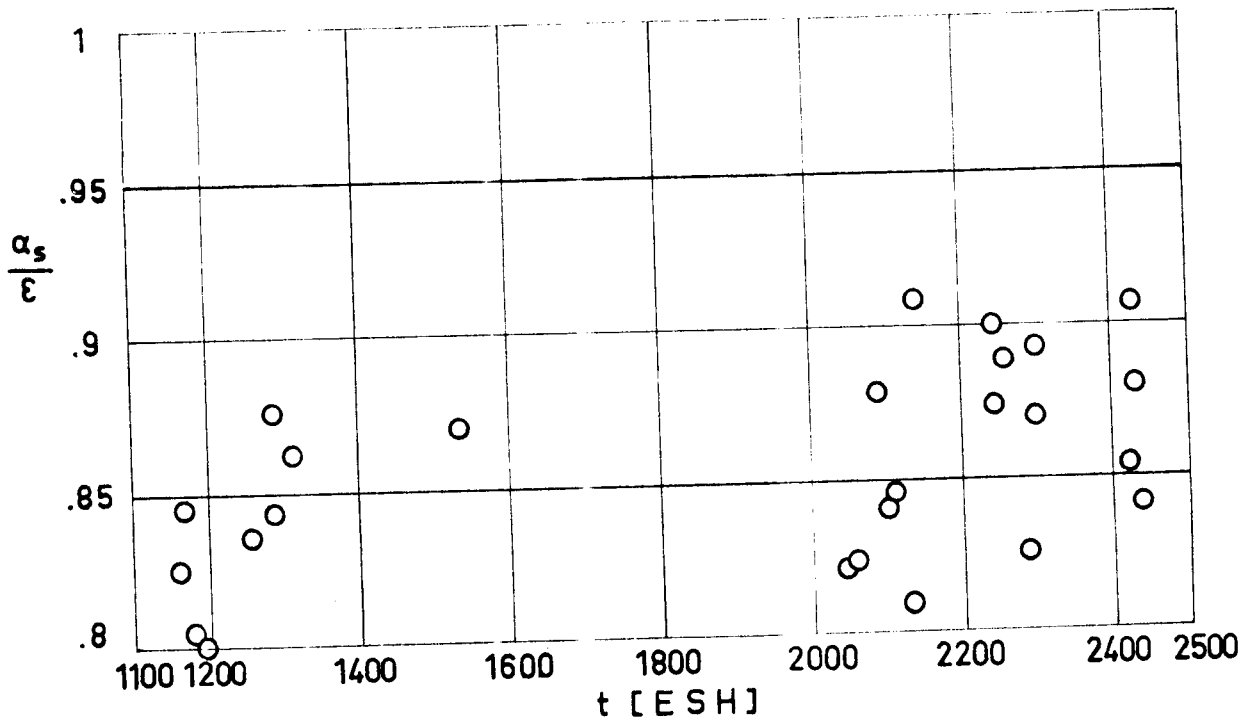


Fig 1-14. Absorptance to emittance ratio, α_s/ϵ , of Aluminium conversion coatings as a function of the exposure time, t .

Explanation

Key	Description	Comments	References
○	Alodine Aluminium.	Deduced from in-flight data concerning the temperature of substrate on board Pegasus II. Initial value, $\alpha_s/\epsilon=0.85$, estimated from Fig. 12 of Schafer & Bannister which deals with Pegasus I flight data.	Schafer & Bannister (1967). Touloukian, DeWitt, HERNICZ (1972).

METALLIC MATERIALS
Aluminium Alloys

Table 1-8

Angular Solar Absorptance of Aluminium

β°	15	30	45	60
α_s	.190	.208	.243	.254
Al-99.99. Foil (5.1×10^{-5} m thick) bright dipped, anodized on both sides (7.6×10^{-6} m thick) in dilute sulphuric acid. Computed from spectral reflectance data for above atm. conditions.				

From Touloukian, DeWitt & Hernicz (1972).

3.3.3. Reflectance.

Data concerning reflectance have been arranged as indicated in the following Table.

3.3.3.1. Bidirectional spectral reflectance.				
Paragraph	Heading	Data Presented	Fig.	Table
3.3.3.1.1.	Normal-normal $\beta = \beta' = 0$	Aluminium.	1-15	
		Aluminium contact coatings.	1-16	
		Aluminium conversion coatings.	1-17	
		Effect of thickness.		
3.3.3.1.2.	Angular (non-normal) $\beta = \beta' \neq 0$	Aluminium contact coatings ($\beta \approx 18^\circ$).	1-18	
		Aluminium conversion coatings. (any β , given λ).	1-19	

(Continued onto next page)

METALLIC MATERIALS

Aluminium Alloys

3.3.3.2. Directional-hemispherical spectral reflectance.				
Paragraph	Heading	Data Presented	Fig.	Table
3.3.3.2.1.	Normal-hemispherical $\beta=0$ $\omega'=2\pi$	Aluminium.	1-20	
		Aluminium conversion coatings. Effect of thickness.	1-21	
		Aluminium conversion coatings. UV exposure effect.	1-22	
		Aluminium conversion coatings. Electron exposure effect.	1-23	
		Aluminium conversion coatings. Simultaneous UV-electron exposure effect.	1-24	
		Aluminium conversion coatings. Proton exposure effect.	1-25	
3.3.3.2.2.	Angular-hemispherical $\beta \neq 0$ $\omega'=2\pi$	Aluminium conversion coatings.	1-26	
3.3.3.3. Hemispherical-directional spectral reflectance.				
3.3.3.3.1.	Hemispherical-normal $\omega=2\pi$ $\beta'=0$	Aluminium contact coatings.	1-27	
3.3.3.5. Bidirectional total reflectance.				
3.3.3.5.2.	Angular (non-normal)	Aluminium.	1-28	
3.3.3.8. Bidirectional solar reflectance.				
3.3.3.8.1.	Normal-normal $\beta=\beta'=0$	Aluminium conversion coatings.		1-9
3.3.3.9. Directional-hemispherical solar reflectance.				
3.3.3.9.1.	Normal-hemispherical $\beta=0$ $\omega'=2\pi$	Aluminium, both bulk and contact coatings.		1-10

METALLIC MATERIALS

Aluminium Alloys

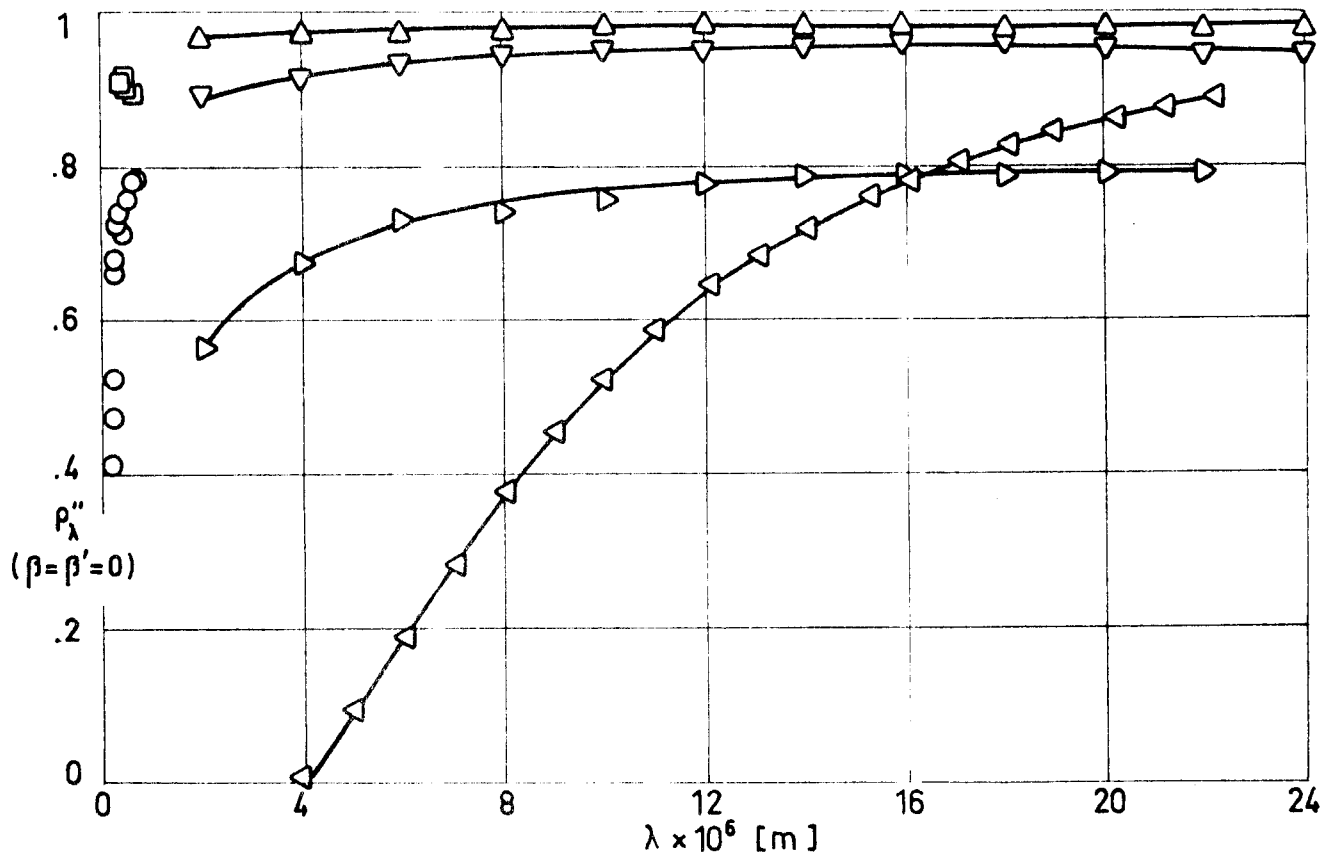


Fig 1-15. Normal-normal spectral reflectance, ρ_{λ}'' , of Aluminium as a function of wavelength, λ .

Explanation

Key	Description	Comments	References
○	Disc. Cold worked, annealed, etch tested, polished, stored in a solution of NaOH+NaF, washed and dried.	Sample temperature: T=298 K. Reported error 2%.	Touloukian & DeWitt (1970).
◻		$\beta = \beta' = 7^\circ$ T=298 K. Measured in air. Reported error <.16%	
◃	Polished.	T=298 K.	
◂	Same as ◃. Cratered. Avg. crater diameter: 1.23×10^{-4} m. Depth: 2.89×10^{-4} m.		
▷	Same as ◃. Cratered. Avg. crater diameter: 5.4×10^{-5} m. Depth: 1.83×10^{-4} m.		
◄	Aluminized dense flint. Flint ground with M 303.5 grinding powder with average particle size of 1.1×10^{-5} m.	$\beta = \beta' \sim 5^\circ$ T=298 K. Al mirror reference, $\omega' = .03$ sr.	

METALLIC MATERIALS
Aluminium Alloys

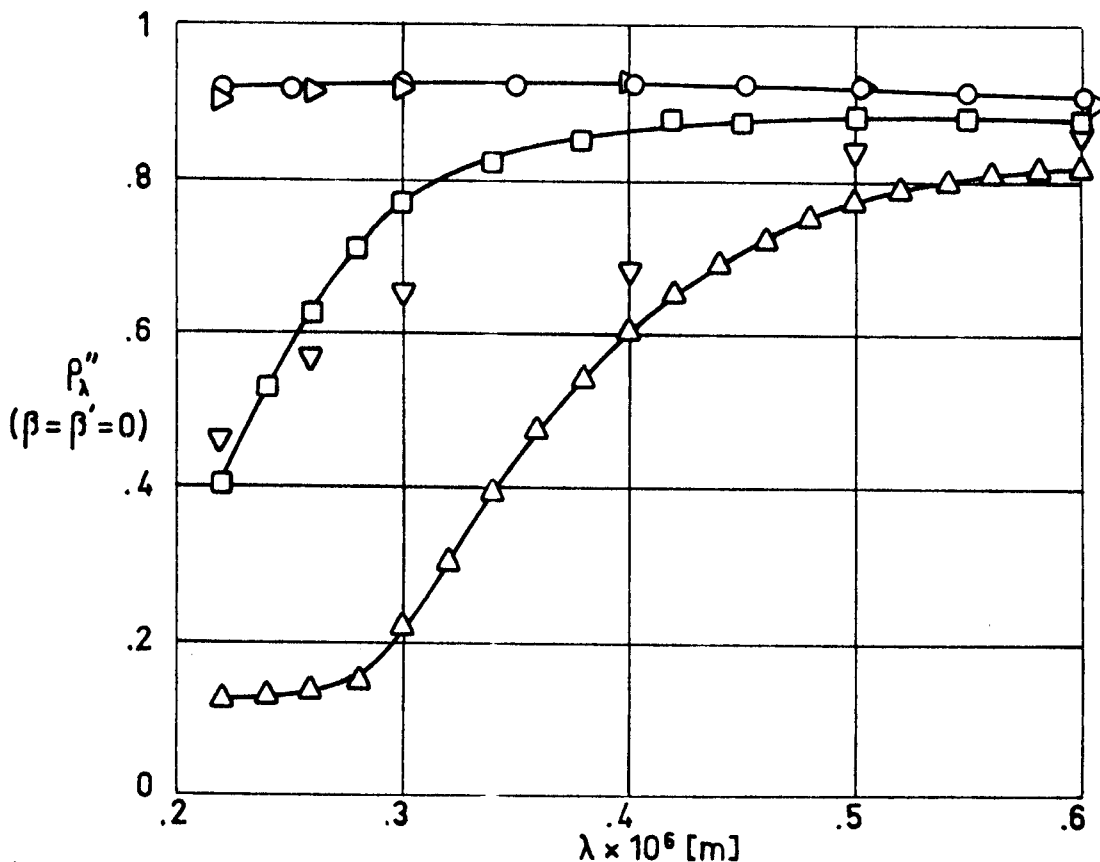


Fig 1-16. Normal-normal spectral reflectance, ρ_{λ}'' , of Aluminium contact coatings as a function of wavelength, λ .

Explanation

Key	Description	Comments	References
○	Al - 99.99 (6×10^{-8} - 7×10^{-8} m thick). Glass substrate. Deposited in vacuum (1.33×10^{-3} - 2.66×10^{-3} Pa) for $t_d = 7$ s.	Sample temperature: $T = 298$ K. Data from smooth curve. Reported error 3%. t_d is the deposition time.	Touloukian, DeWitt & Hernicz (1972).
□	Same as ○ except $t_d = 180$ s.		
△	Same as ○ except $t_d = 145$ s.		
▽	Al - 99.99 ($\sim 7 \times 10^{-8}$ m thick). Glass substrate. Deposited in vacuum (1.33×10^{-3} - 2.66×10^{-3} Pa) at 10^{-9} - 1.5×10^{-9} m.s ⁻¹ with substrate temperature 473 K.		
▽	Al - 99.99 ($\sim 6 \times 10^{-8}$ m thick). Glass substrate. Deposited in vacuum (1.33×10^{-3} Pa) at 3×10^{-8} m.s ⁻¹ with 60° angle of vapor incidence.		

METALLIC MATERIALS

Aluminium Alloys

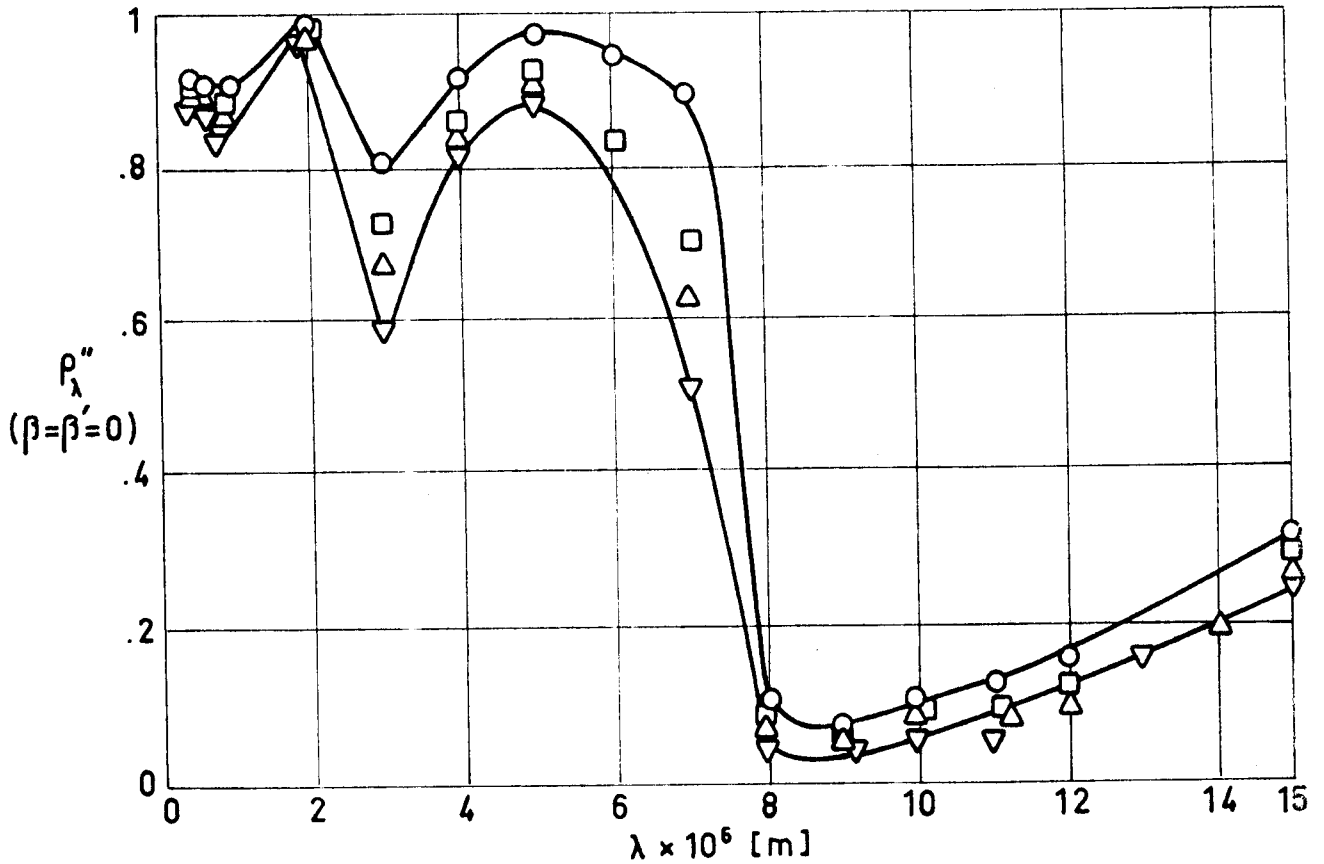


Fig 1-17. Effect of coating thickness on normal-normal spectral reflectance, ρ_{λ}'' , of Aluminium conversion coatings as a function of wavelength, λ .

Explanation

Key	Description	Comments	References
○	Al - 99.99, anodized in sulphuric acid. Polished substrate. Coating thickness, $t_c = 8.4 \times 10^{-6}$ m.	T \approx 298 K.	Touloukian, DeWitt & Hernicz (1972).
□	Same as ○ except $t_c = 9.4 \times 10^{-6}$ m.		
△	Same as ○ except $t_c = 11.4 \times 10^{-6}$ m.		
▽	Same as ○ except $t_c = 13.2 \times 10^{-6}$ m.		

METALLIC MATERIALS
Aluminium Alloys

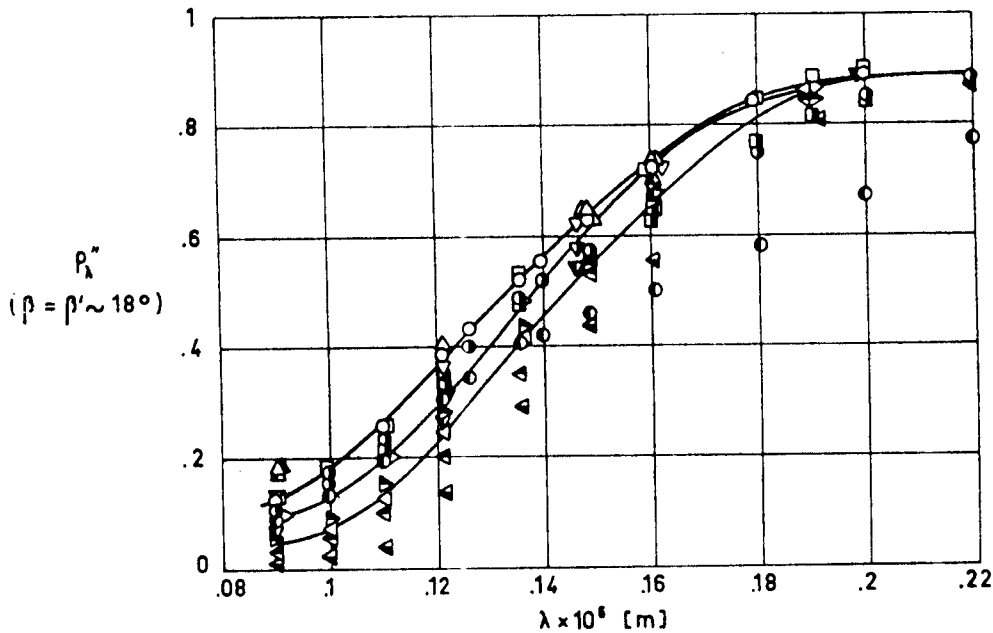


Fig 1-18. Bidirectional reflectance, ρ_{λ}'' , of Aluminium contact coatings as a function of wavelength, λ .

Explanation

Key	Description	Comments	References
○	Evaporated film (8×10^{-8} m thick). Substrate cleaned by a high-voltage DC glow discharge. Evaporated at 1.33×10^{-3} Pa for 2 s. Exposed to air for 24 h.	Sample temperature: $T \sim 298$ K.	Touloukian, DeWitt & HERNICZ (1972).
⊙	Same as ○ except evaporation time 55 s.		
⦿	Same as ○ except evaporation time 130 s.		
□	Evaporated film (9×10^{-8} m thick). Substrate cleaned as ○. Evaporated at 1.33×10^{-3} Pa for 2 s using Al-99.99. Film 24 h old when measurement was made.		
⊠	Same as □. Al-99.5 used for evaporation.		
△	Evaporated film (8×10^{-8} m thick). Substrate cleaned as ○. Substrate temperature at deposition 308 K. Film 2-3 h old.	$T \sim 298$ K.	
▲	Same as △ except substrate at 323 K at time of deposition.		
▴	Same as △ except substrate at 373 K at time of deposition.		
▽	Evaporated film. Substrate cleaned as ○. Aged 10 h before measurement.	$T \sim 298$ K. Data from smooth curve.	
▾	Same as ▽ except aged 100 h.		
▿	Same as ▽ except aged 1000 h.		
▷	Evaporated film. Substrate cleaned as ○. Stored in dry air for 63 d before measurement.		
▸	Same as ▷ except stored in normal air (30-50% humidity) for 63 d before measurement.		
◁	Evaporated film. Substrate cleaned as ○; prepared under optimum conditions. Placed .2 m from a 435-W quartz mercury burner and irradiated for 20 h in dry air.		
◃	Same as ◁ except irradiated for 20 h in normal air (30% humidity).		
◄	Same as ◁ except irradiated for 20 h in moist air (>90% humidity).		

METALLIC MATERIALS
Aluminium Alloys

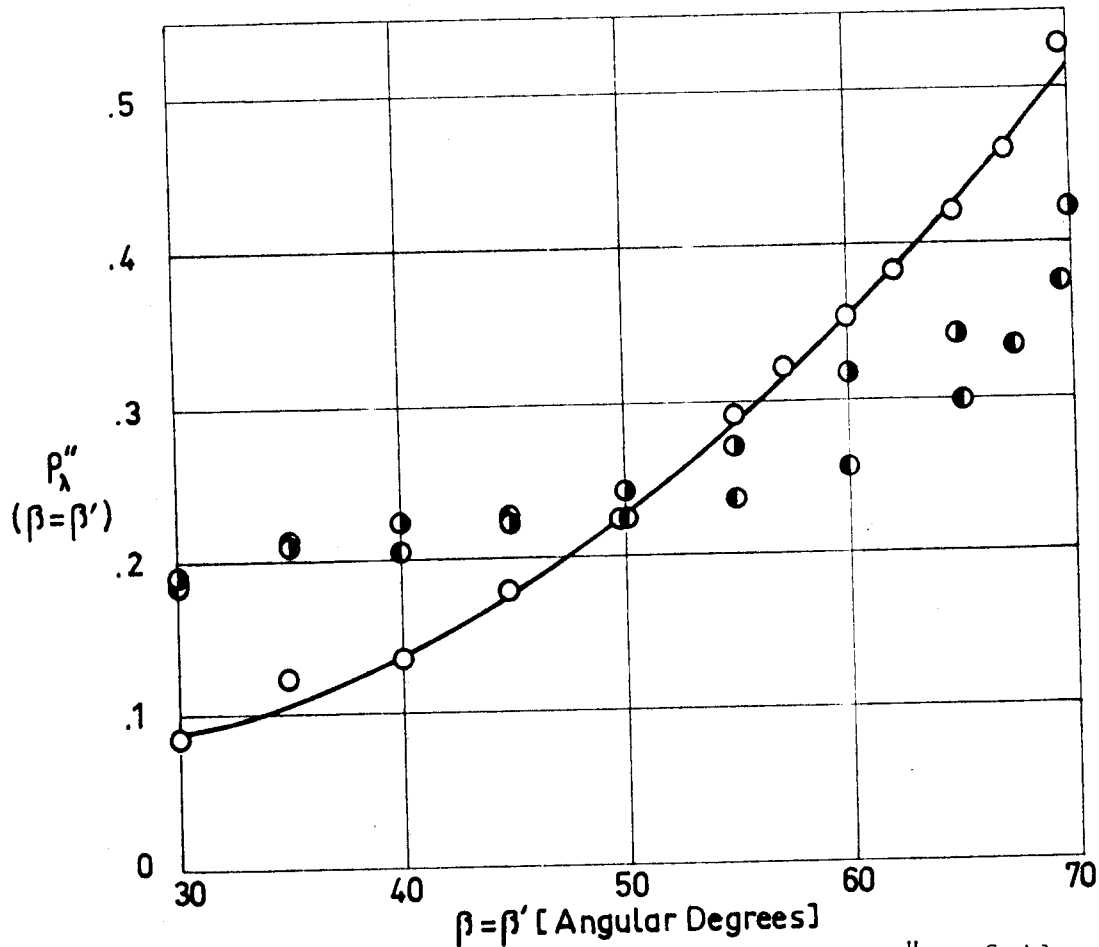


Fig 1-19. Bidirectional spectral reflectance, ρ_{λ}'' , of Aluminium conversion coatings as a function of zenith angles, β and β' , of incident and reflected radiations.

Explanation

Key	Description	Comments	References
○	Aluminium evaporated on Pyrex glass substrate at about 4×10^{-8} m.s ⁻¹ at pressures 1.33×10^{-3} - 2.66×10^{-3} Pa. Coating thickness 3×10^{-7} m. Anodized in a bath of freshly prepared 3% ammonium tartrate solution with a pure Al cathode. Rinsed in distilled water and dried.	T=298 K. $\lambda = 5.07 \times 10^{-8}$ m.	Touloukian, DeWitt & Hernicz (1972).
●	Same as above.	T=298 K. $\lambda = 7.62 \times 10^{-8}$ m.	
●	Same as above.	T=298 K. $\lambda = 1.032 \times 10^{-7}$ m.	

METALLIC MATERIALS
Aluminium Alloys

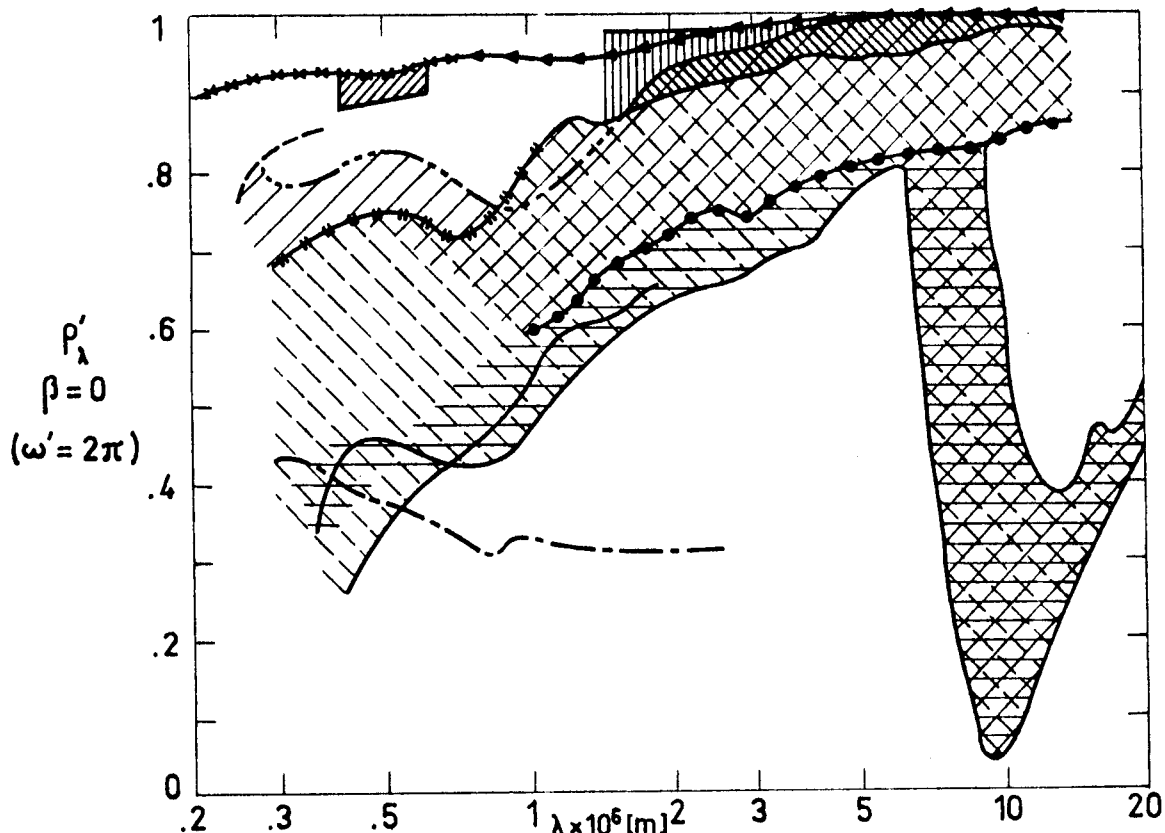


Fig 1-20. Summary of data concerning normal-hemispherical spectral reflectance, ρ'_λ , of Aluminium vs. wavelength, λ . From Touloukian & DeWitt (1970).

Explanation

Key	Description	Comments
	Al - 99.0. Vacuum deposited on glass. Freshly prepared.	$\beta=10^\circ$. $T=298$ K.
	Foil.	
	Mechanically polished, electropolished.	$T=298$ K.
	Mill finished, electropolished.	Measured in vacuum (1.33×10^{-4} Pa).
	Mechanically polished only.	
	Polished.	$T=298$ K.
	Evaporated on Mylar (2×10^{-7} m thick).	$T=298$ K.
	Film vacuum deposited on glass.	$\beta=7^\circ$. $T=298$ K.
	Acid etched.	$\beta \sim 5^\circ$. $T=298$ K.
	Sandblasted.	$T=298$ K.
	Polished, roughened (roughness $\sim 1.27 \times 10^{-8}$ m).	$\beta=5^\circ$. $T=300$ K.
	Foil. Diffuse reflectance.	$T=298$ K.

METALLIC MATERIALS
Aluminium Alloys

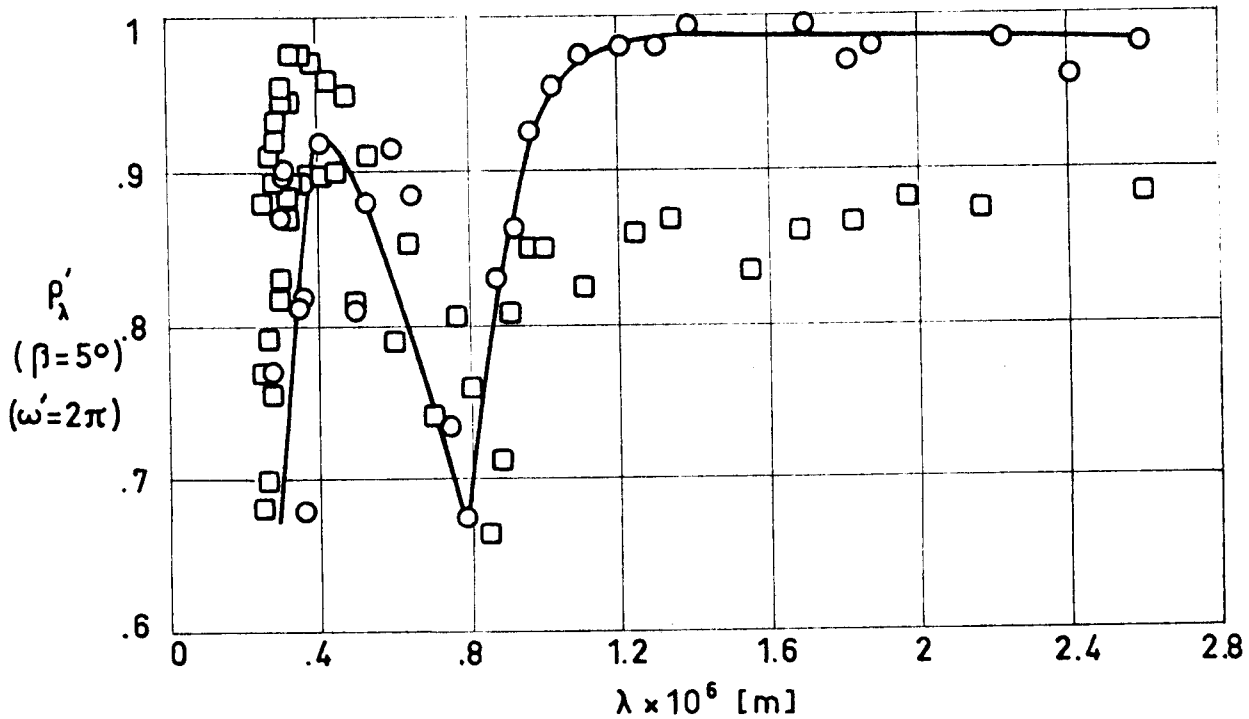


Fig 1-21. Normal-hemispherical spectral reflectance, ρ'_λ , of Aluminium conversion coatings as a function of wavelength, λ .

Explanation

Key	Description	Comments	References
○	Barrier-layer anodic coated Al - 99.99. Coating thickness $3.9 \pm 0.015) \times 10^{-7}$ m.	$T \approx 298$ K. Measured in vacuum (1.33×10^{-4} Pa). Data from smooth curve.	Touloukian, DeWitt & HERNICZ (1972).
□	Same as ○ except coating thickness $1.6 \times 10^{-6} - 1.7 \times 10^{-6}$ m.	Same as ○ except measured relative to MgO.	

METALLIC MATERIALS

Aluminium Alloys

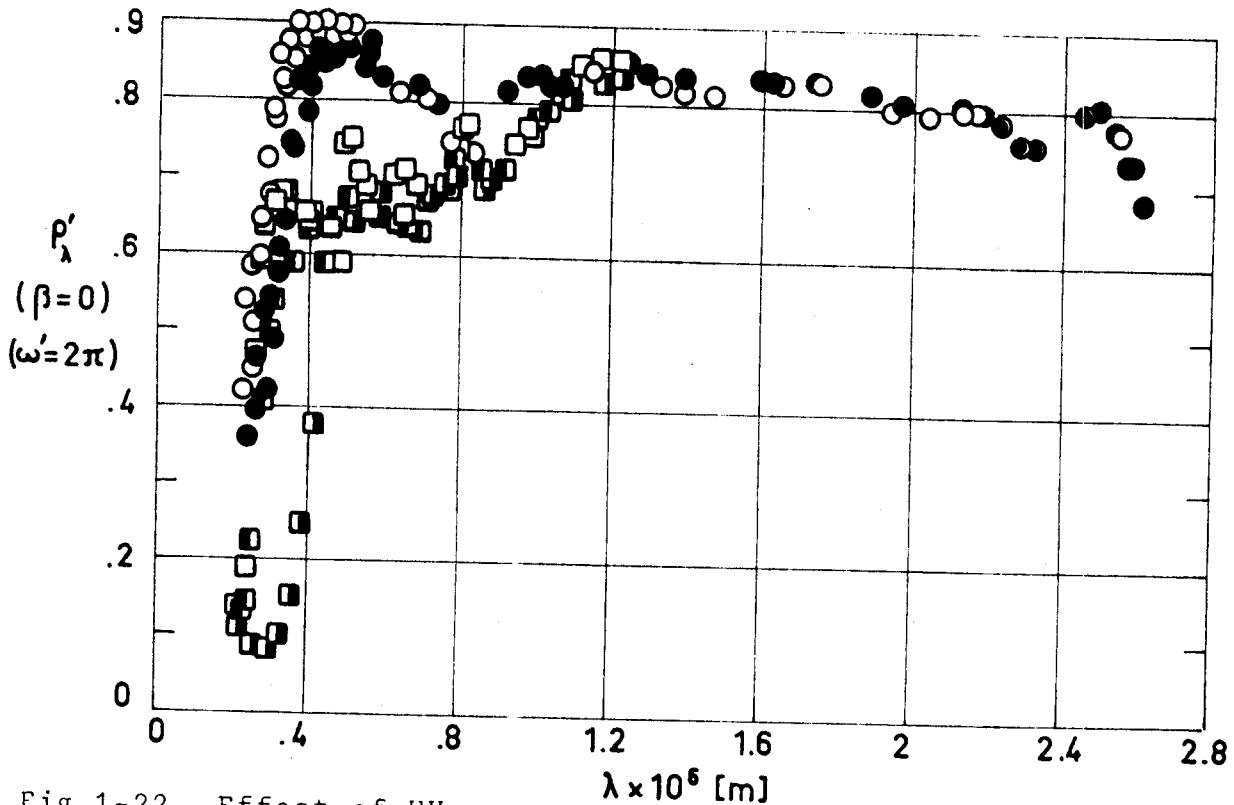


Fig 1-22. Effect of UV exposure on normal-hemispherical spectral reflectance, ρ'_λ , of Aluminium conversion coatings as a function of wavelength, λ .

Explanation

Key	Description	Comments	References
○	Al - 99.99 (2.54×10^{-4} m thick), barrier anodized.	T=77 K. Exposed to vacuum (6.65×10^{-7} - 2.66×10^{-5} Pa). From R($2\pi, 0$) measured in situ. Data from smooth curve.	Touloukian, DeWitt & Hernicz (1972).
●	Same as ○ .	Same as ○ . 350 ESH exposure at 6 sun, in vacuum.	
□	Alodine 401-45. Reaction of Aluminium surface with aqueous solution of chromic, phosphoric, and hydrofluoric acid.	T=300 K. Data from smooth curve.	
◻	Similar to □ .	T=300 K. 353 h exposure at 3-4 suns. Substrate temperature during exposure: $T_s=278$ K.	
◼	Similar to □ .	Same as ◻ except 358 h exposure. $T_s=248$ K.	

METALLIC MATERIALS

Aluminium Alloys

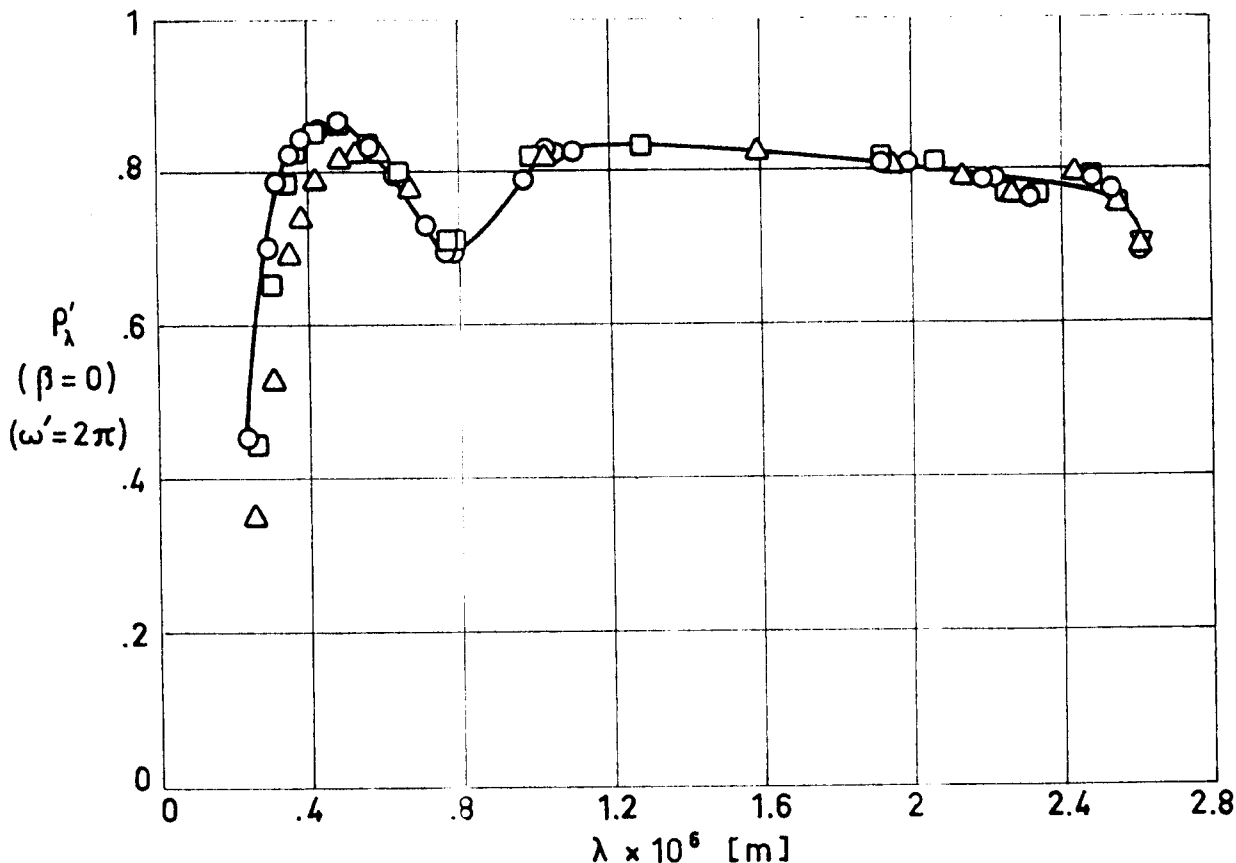


Fig 1-23. Effect of electron exposure on normal-hemispherical spectral reflectance of Aluminium conversion coatings as a function of wavelength, λ .

Explanation

Key	Description	Comments	References
○	Al - 99.99 anodized in sulphuric acid.	T=77 K. Exposed to vacuum (6.65×10^{-7} - 2.66×10^{-5} Pa), maintained by diffusion pump. Calculated from R($2\pi, 0$) measured in situ. Data from smooth curve.	Touloukian, DeWitt & Hernicz (1972).
□	Same as ○ .	Same as ○ except exposed to electron radiation (8.6×10^{14} - 1.6×10^{16} e.m ⁻² .s ⁻¹) in vacuum 5.8×10^{19} e.m ⁻² .	
△	Same as ○ .	Same as □ except total dose 1.2×10^{20} e.m ⁻² .	

METALLIC MATERIALS
Aluminium Alloys

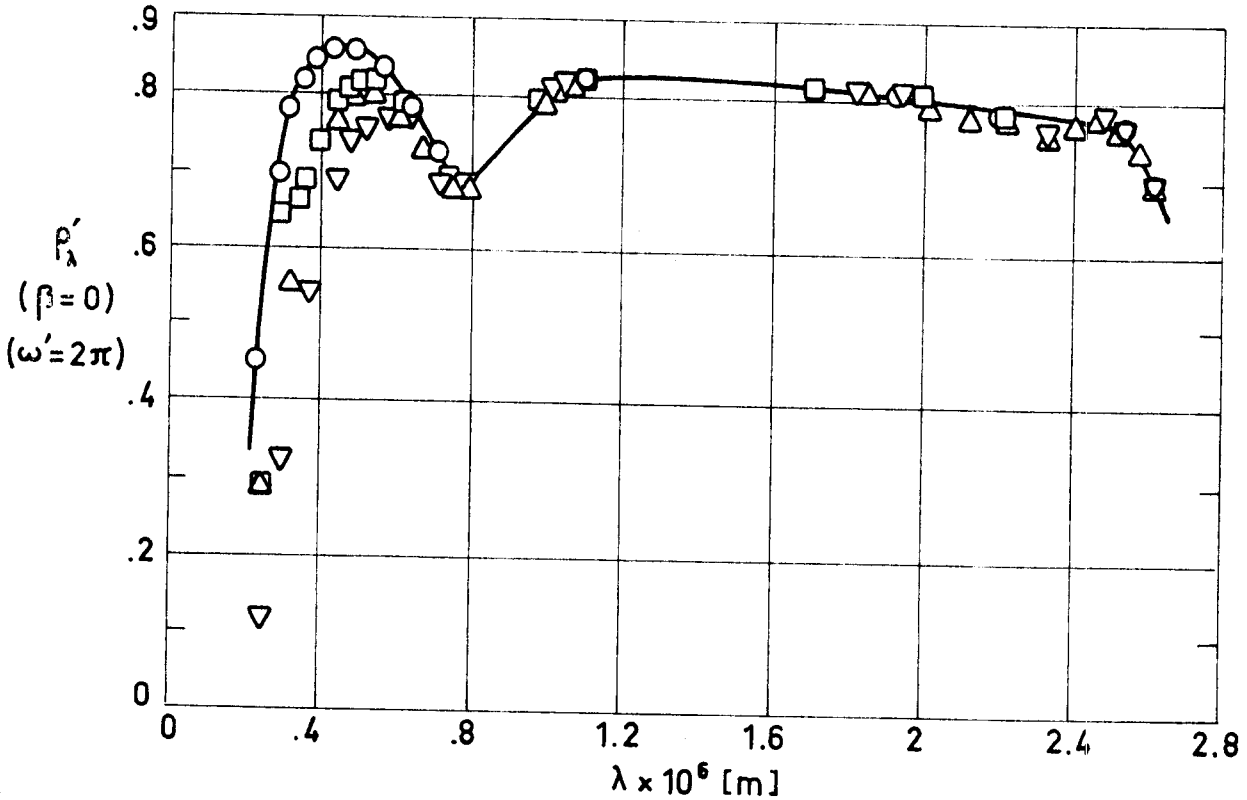


Fig 1-24. Effect of simultaneous UV-electron exposure on normal-hemispherical spectral reflectance, ρ'_λ , of Aluminium conversion coatings as a function of wavelength, λ .

Explanation

Key	Description	Comments	References
○	Al - 99.99 anodized in sulphuric acid.	T = 77 K. Exposed to vacuum (6.65×10^{-7} - 2.66×10^{-5} Pa), maintained by diffusion pump. Calculated from $R(2\pi, 0)$ measured in situ. Data from smooth curve.	Touloukian, DeWitt & Hernicz (1972).
□	Same as ○ .	Same as ○ except: UV 8 sun intensity in vacuum 66 ESH electron 3.5×10^{14} e.m ⁻² .s ⁻¹ ; 1.2×10^{19} e.m ⁻² .	
△	Same as ○ .	Same as ○ except total dose: UV 130 ESH electron 2.3×10^{19} e.m ⁻² .	
▽	Same as ○ .	Same as ○ except total dose: UV 310 ESH electron 5.8×10^{19} e.m ⁻² .	

METALLIC MATERIALS

Aluminium Alloys

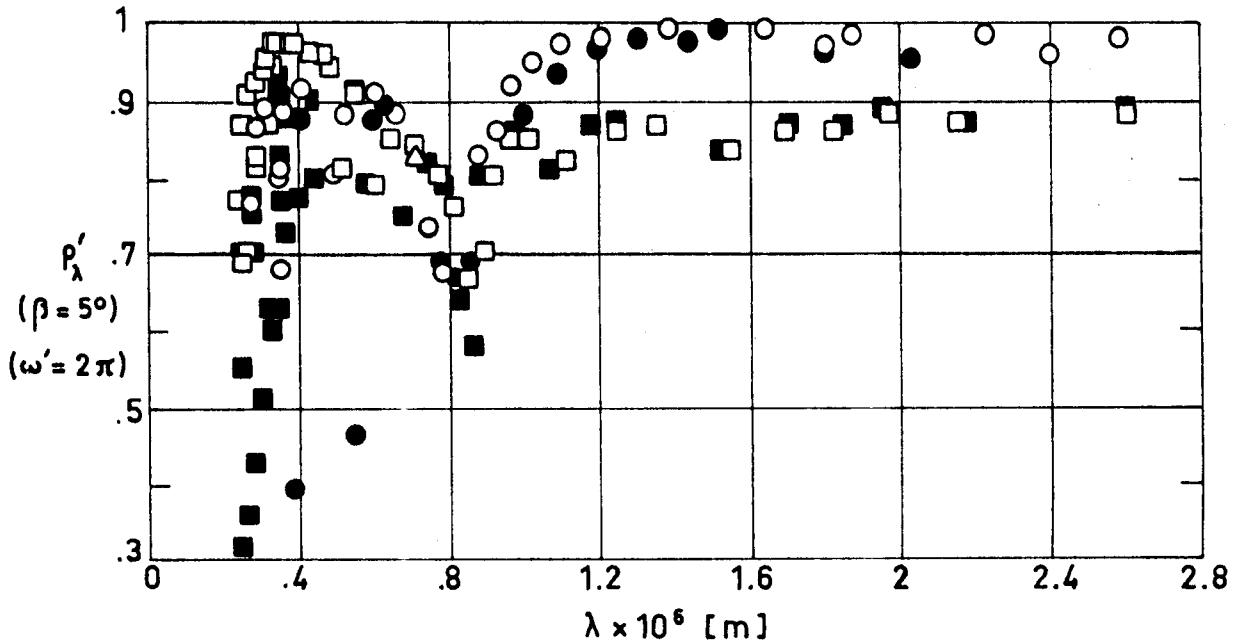


Fig 1-25. Effect of proton exposure on normal-hemispherical spectral reflectance, ρ_{λ}' , of Aluminium conversion coatings as a function of wavelength, λ .

Explanation

Key	Description	Comments	References
○	Al - 99.99, barrier-layer anodic coated. Coating thickness $(3.9 \pm .015) \times 10^{-7}$ m.	T \approx 298 K. Measured in vacuum (1.33×10^{-4} Pa). Data from smooth curve.	Touloukian, DeWitt & Hernicz (1972).
●	Same as ○ .	Same as ○ except irradiated in vacuum at 300 K with 8.7 keV protons to a total dose of 9.25×10^{20} p.m $^{-2}$.	
□	Same as ○ except coating thickness $1.6 \times 10^{-6} - 1.7 \times 10^{-6}$ m.	Same as ○. Measured relative to MgO.	
■	Same as □ .	Same as □ except irradiated in vacuum at 300 K with 8.7 keV protons to a total dose of 10^{20} p.m $^{-2}$.	

METALLIC MATERIALS
Aluminium Alloys

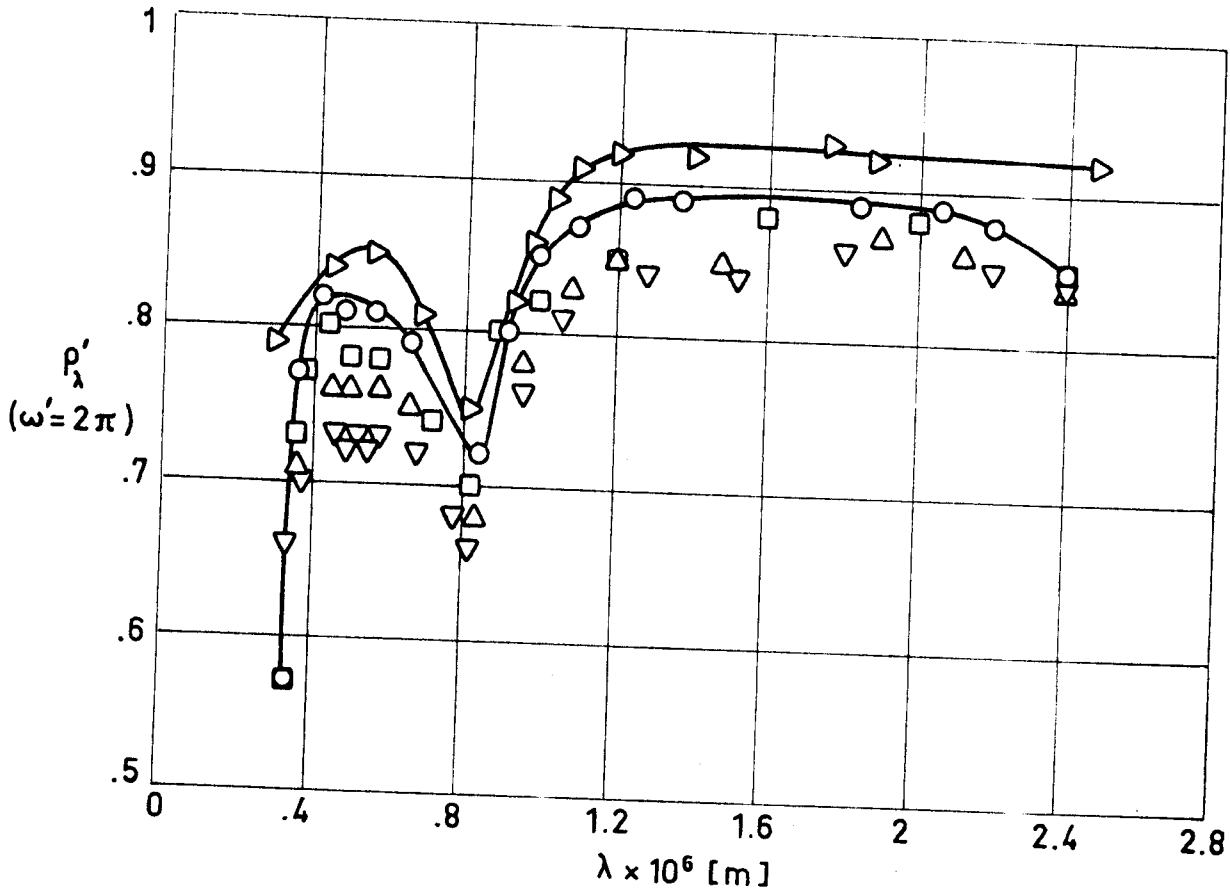


Fig 1-26. Directional-hemispherical spectral reflectance, ρ'_λ , of Aluminium conversion coatings as a function of wavelength, λ .

Explanation

Key	Description	Comments	References
○	Al - 99.99. Foil 5.1×10^{-5} m thick. Bright dipped and anodized on both sides (7.6×10^{-6} m thick) in dilute sulphuric acid.	$\beta = 15^\circ$. $T = 298$ K.	Touloukian, DeWitt & HERNICZ (1972).
□	Same as ○ .	$\beta = 30^\circ$. $T = 298$ K.	
△	Same as ○ .	$\beta = 45^\circ$. $T = 298$ K.	
▽	Same as ○ .	$\beta = 60^\circ$. $T = 298$ K.	
▷	Similar to ○ .	$\beta = 15^\circ$. $T = 298$ K.	

METALLIC MATERIALS
Aluminium Alloys

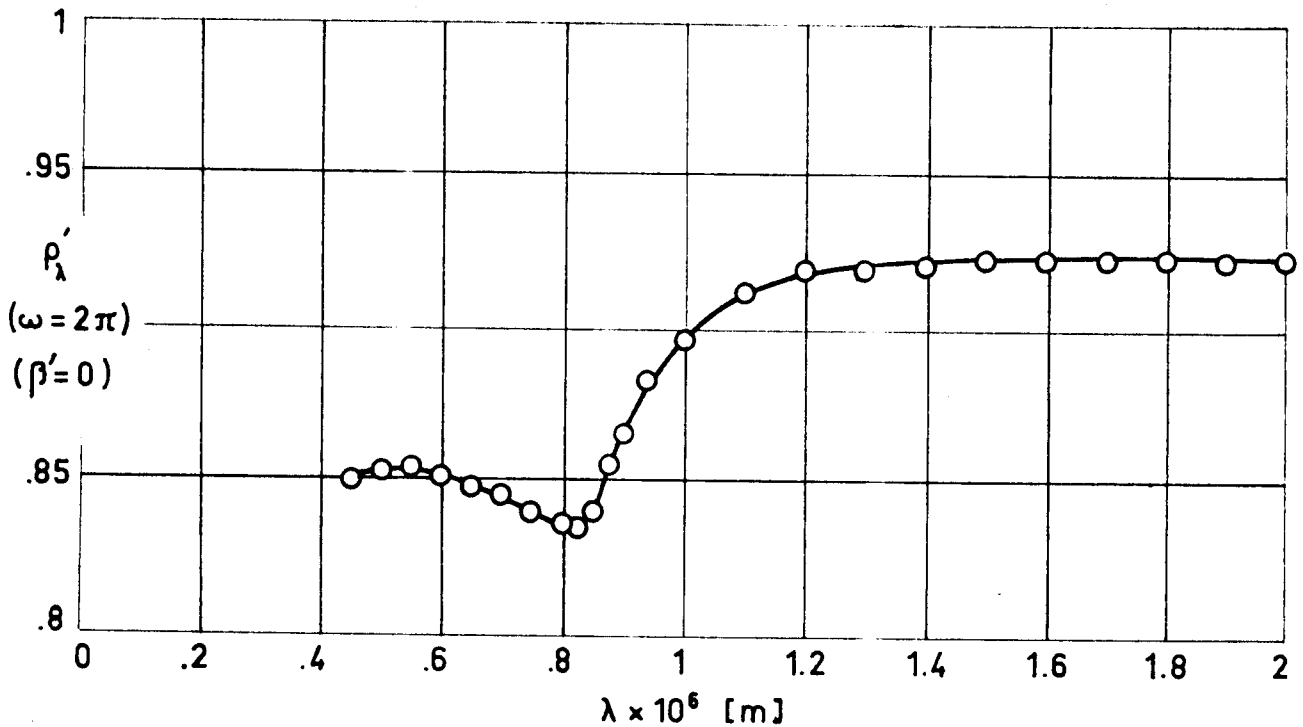


Fig 1-27. Hemispherical-normal spectral reflectance, ρ'_λ , of Aluminium contact coatings as a function of wavelength, λ .

Explanation

Key	Description	Comments	References
○	Evaporated film on mechanically polished and electropolished stainless steel.	T = 298 K.	Touloukian & DeWitt (1970).

METALLIC MATERIALS
Aluminium Alloys

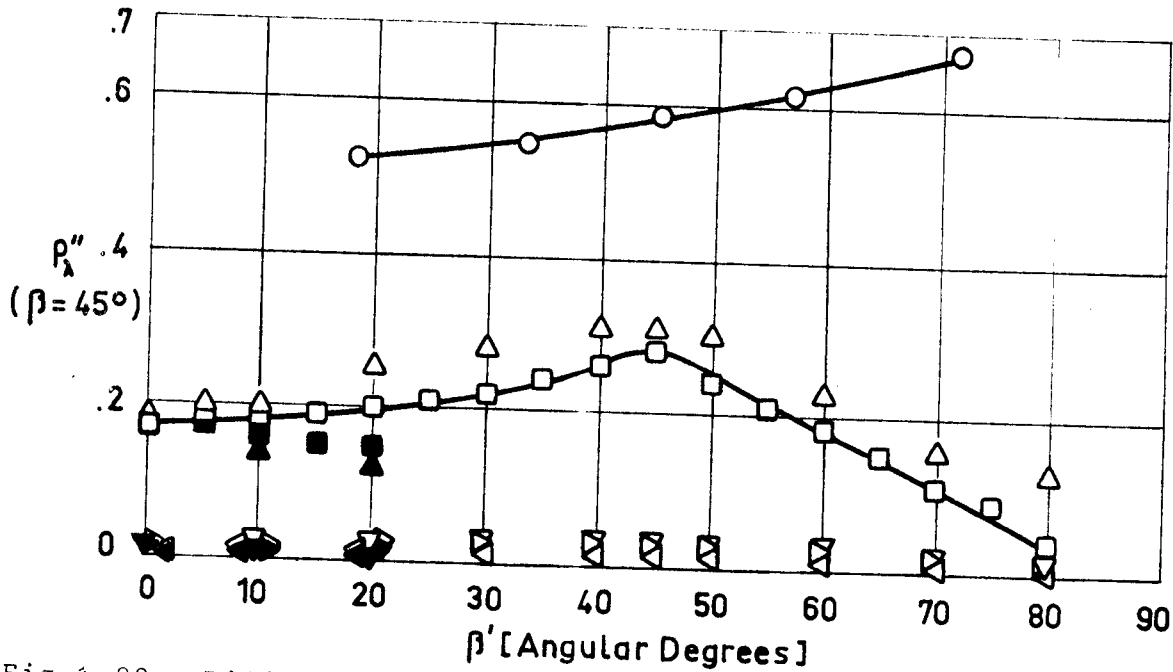


Fig 1-28. Bidirectional total reflectance, ρ'' , of Aluminium as a function of the viewing zenith angle, β' .

Explanation

Key	Description	Comments	References
○		T=298 K. Angle of viewing within 2.5° of angle of specular reflection.	Touloukian & DeWitt (1970).
□	Sandblasted.	T=298 K. $\beta=45^\circ$. $\theta=\theta'=0$. Tungsten filament lamp source.	
■	Same as □ . . .	Same as □ except $\theta'=180^\circ$.	
△	Different sample, same as □ .	Same as □ .	
▲	Same as △ .	Same as □ except $\theta'=180^\circ$.	
▽	Same as △ .	Same as △ except green filter.	
▼	Same as ▽ .	Same as ▽ except $\theta'=180^\circ$.	
▷	Same as △ .	Same as △ except amber filter.	
▶	Same as ▷ .	Same as ▷ except $\theta'=180^\circ$.	
◁	Same as △ .	Same as △ except blue filter.	
◀	Same as ◁ .	Same as ◁ except $\theta'=180^\circ$.	

METALLIC MATERIALS

Aluminium Alloys

Table 1-9

Normal-Normal Solar Reflectance of Aluminium Conversion Coatings

T [K]	ρ''_s ($\beta=\beta'=0$)	Comments
~293	.84	Al-99.99 anodized 15 min in sulphuric acid; coating thickness 9.38×10^{-6} m; substrate polished by Alzak process (electrolytic fluoboric acid bath); calculated from spectral reflectance data.
~298	.82	Similar to above specimen and conditions except heat treated (24 h at 589 K) in vacuum (6.65×10^{-3} Pa).
~298	.81	Similar to above specimen and conditions except heat treated (48 h at 589 K) in vacuum (6.65×10^{-3} Pa).
~298	.82	Similar to above specimen and conditions except heat treated (96 h at 589 K) in vacuum (6.65×10^{-3} Pa).
~298	.82	Similar to above specimen and conditions except anodized 25 min; coating thickness 1.32×10^{-5} m. Mentioned below as specimen 1.
~298	.78	Similar to specimen 1 except heat treated (24 h at 589 K) in vacuum (6.65×10^{-3} Pa).
~298	.77	Similar to specimen 1 except heat treated (48 h at 589 K) in vacuum (6.65×10^{-3} Pa).
~298	.78	Similar to specimen 1 except heat treated (96 h at 589 K) in vacuum (6.65×10^{-3} Pa).
~298	.88	Al-99.99 anodized 10 min in sulphuric acid; coating thickness 8.36×10^{-6} m; substrate polished in phosphoric/nitric acid bath for 2 min at 364 K; calculated from spectral reflectance data.
~298	.86	Similar to above specimen and conditions except anodizing time 15 min; coating thickness 9.38×10^{-6} m.
~298	.84	Similar to above specimen and conditions except anodized 20 min; coating thickness 1.09×10^{-5} m.
~298	.83	Similar to above specimen and conditions except anodized 25 min; coating thickness 1.32×10^{-5} m.

From Touloukian, DeWitt & Hernicz (1972).

METALLIC MATERIALS

Aluminium Alloys

Table 1-10

Normal-Hemispherical Solar Reflectance of Both Bulk Aluminium
and Contact Coatings

T [K]	ρ'_s ($\beta=0$, $(\omega'=2\pi)$)	Comments
298	.90	Pure aluminium on optical flat (2×10^{-7} m thick); measured in air.
298	.88	Aluminium foil Reynolds Wrap-heavy duty; measured in air.
298	.88	Reynolds Wrap-heavy duty foil; measured in air.
298	.90	Pure Al; $.3 \times 10^{-6}$ m thick opaque layer on glass; freshly prepared; MgO reference; computed from spectral data. Mentioned below as specimen 1.
298	.01	Above specimen and conditions; diffuse component only.
298	.91	Different sample, same as 1 specimen and conditions.
298	.01	Above specimen and conditions; diffuse component only.
298	.89	Aluminium film on 6.35×10^{-6} m thick Mylar; measured in air.
298	.88	Aluminium film on 6.35×10^{-6} m thick Mylar; measured in air.

From Touloukian & DeWitt (1970).

3.3.4. Transmittance.

3.3.4.1. Directional spectral transmittance.

3.3.4.1.1. Normal-normal spectral transmittance of Aluminium
($\beta=\beta'=0$): Fig 1-29.3.3.4.1.2. Angular spectral transmittance ($\beta \neq 0$).

Effect of angle β on angular spectral transmittance of
Aluminium: Fig 1-30.

METALLIC MATERIALS
Aluminium Alloys

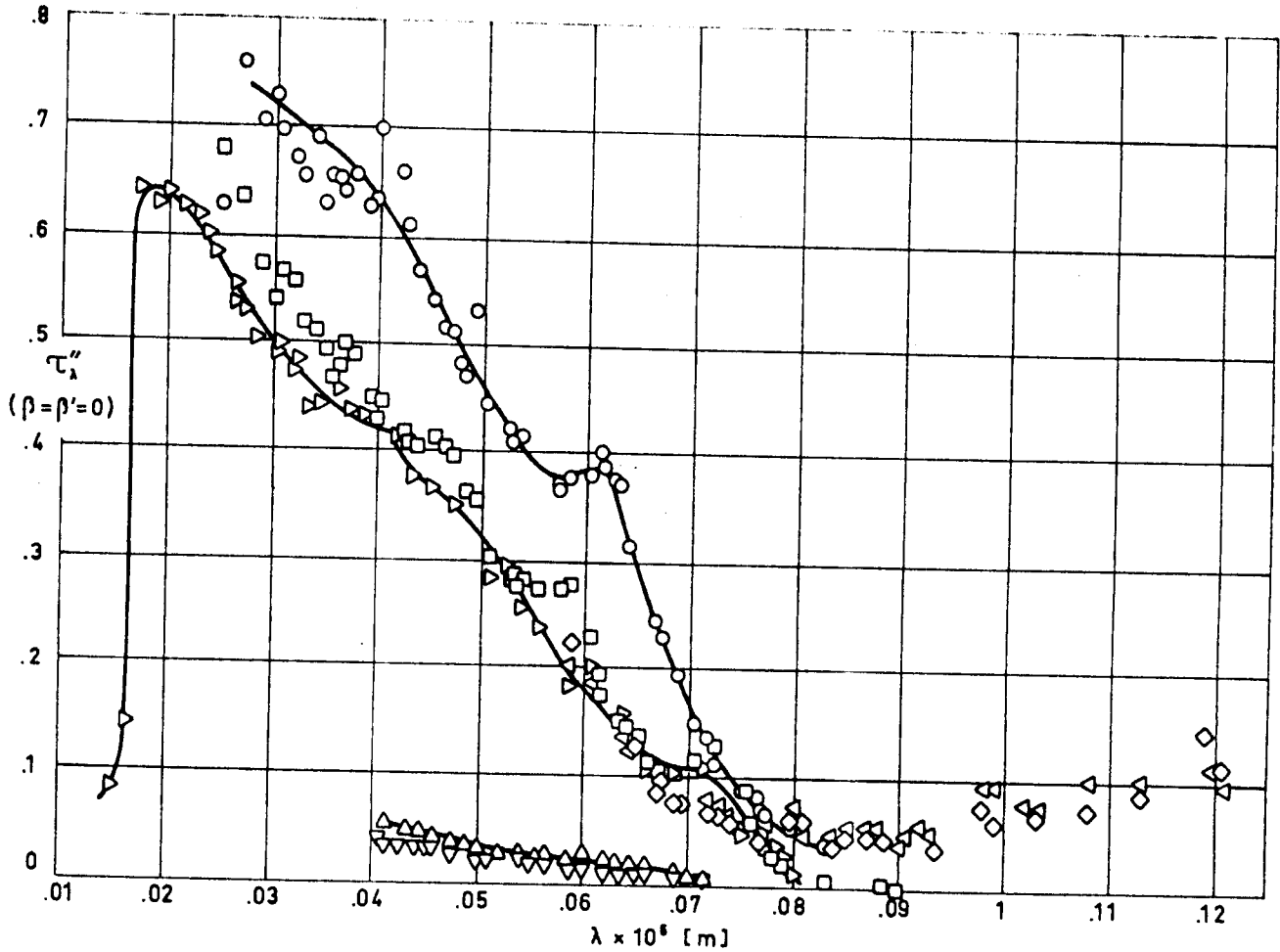


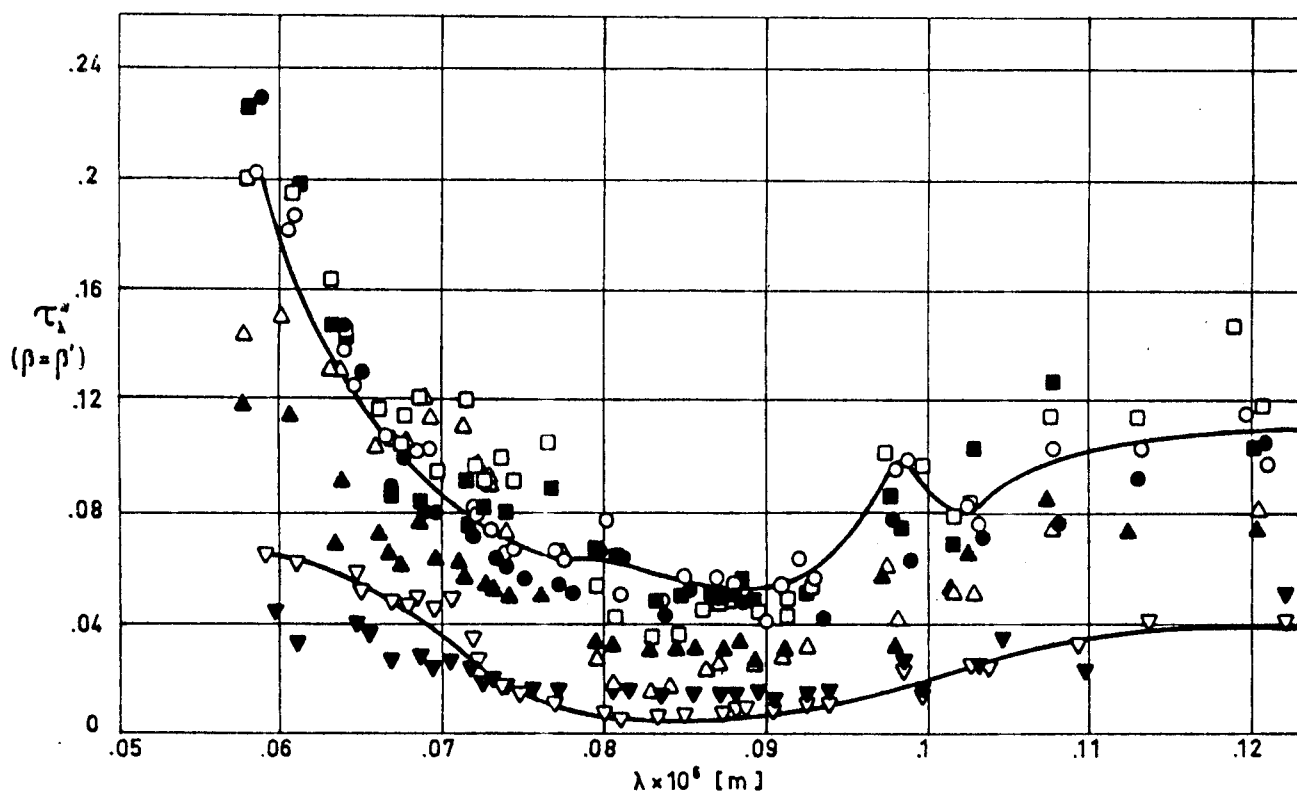
Fig 1-29. Normal-normal spectral transmittance, τ_{λ}'' , of Aluminium as a function of wavelength, λ .

Explanation

Key	Description	Comments	References
○	Evaporated film $(6 \pm 5) \times 10^{-8}$ m thick. Glass slide substrate at room temperature at evaporation. Evaporated at 2.67×10^{-3} Pa in 10-15 s.	Sample temperature: T=298 K. Reported error $\sim 10\%$ at $\lambda > 3.5 \times 10^{-8}$ m $< 25\%$ at $\lambda < 3.5 \times 10^{-8}$ m	Touloukian & DeWitt (1970).
□	Same as ○ except film thickness $(1 \pm 1) \times 10^{-7}$ m.		
△	Evaporated film 4.7×10^{-8} m thick. Unsupported. Exposed to air at atmospheric pressure.	T=298 K.	
▽	Same as △ except film thickness 1.38×10^{-7} m.		
▷	Unbacked film ($\sim 8 \times 10^{-8}$ m thick). Slight oxide layer.	T=298 K. Measured in vacuum ($< 1.33 \times 10^{-3}$ Pa).	
◁	Unbacked foil (3×10^{-8} m thick). Evaporated in vacuum (4×10^{-4} Pa). Exposed to air.	T=298 K. Condensed spark discharge in argon light source. p-polarization dominant. Data uncorrected for partial polarization effects.	
◇	Same as ◁.	Same as ◁ except s-polarization dominant.	

METALLIC MATERIALS

Aluminium Alloys

Fig 1-30. Angular spectral transmittance, τ_{λ}'' , of Aluminium as a function of wavelength, λ .

Explanation

Key	Description	Comments	References
○	Unbacked foil (3×10^{-8} m thick). Evaporated in vacuum (4×10^{-4} Pa). Exposed to air.	$\beta = \beta' = 0$. Sample temperature: $T = 298$ K. Condensed spark discharge in argon light source. p-polarization dominant. Data uncorrected for partial polarization effects.	Touloukian & DeWitt (1970).
●	Same as ○.	Same as ○ except s-polarization dominant.	
□	Same as ○.	Same as ○ except $\beta = \beta' = 20^\circ$.	
■	Same as ○.	Same as □ except s-polarization dominant.	
△	Same as ○.	Same as ○ except $\beta = \beta' = 30^\circ$.	
▲	Same as ○.	Same as △ except s-polarization dominant.	
▽	Same as ○.	Same as ○ except $\beta = \beta' = 45^\circ$.	
▼	Same as ○.	Same as ▽ except s-polarization dominant.	

METALLIC MATERIALS

Aluminium Alloys

3.4. Other physical properties

3.4.1. Electrical resistivity.

Effect of temperature on electrical resistivity: Fig 1-31.

4. ENVIRONMENTAL BEHAVIOR4.1. Prelaunch

Aluminium surface is very susceptible to increases in α_s and ϵ caused by contamination. The surface must be protected from physical abuse, atmospheric exposure and caustic contaminants; cleanliness must be assured.

From Breuch (1967).

4.2. Postlaunch

No known restrictions other than structural.

Adhesive backed bright aluminium foils should not be used externally during ascent nor in areas where the peak ascent temperature is expected to exceed 460 K.

Pressure-sensitive aluminium tapes, if placed externally, should be fastened mechanically on both ends to avoid blistering. These tapes can be used internally where peak temperatures of up to 700 K are anticipated, and externally for temperatures below 670 K.

From Breuch (1967).

METALLIC MATERIALS
Aluminium Alloys

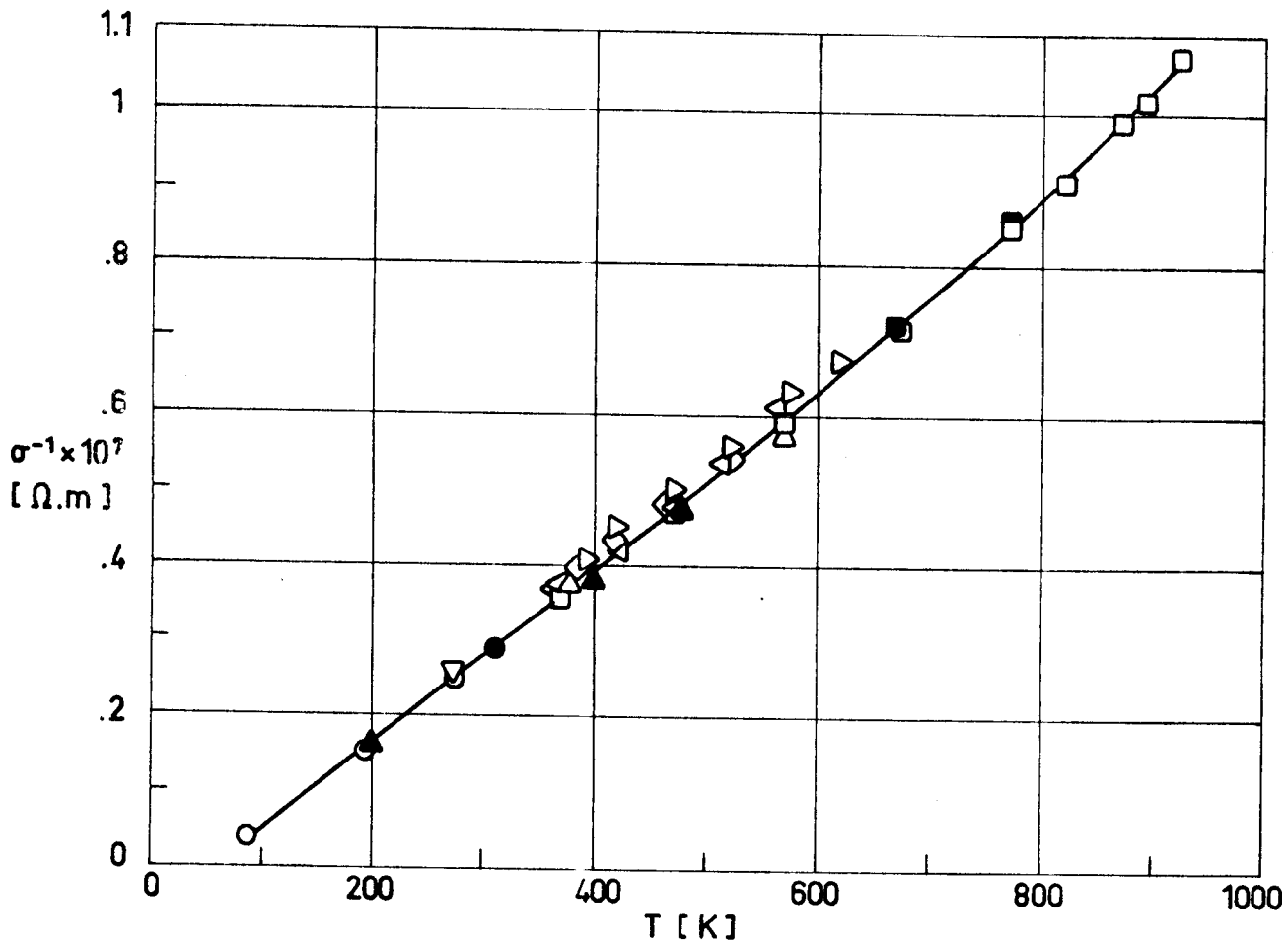


Fig 1-31. Electrical resistivity, σ^{-1} , of Aluminium as a function of temperature, T.

Explanation

Key	Description	Comments	References
○	Traces of Mg, Si, Fe, and Cu.		Touloukian (1967)a.
□	99.9 Al - .05 Si - .03 B.		
△	.04 Si - .03 Fe, traces of Cu, Ti, annealed 1 h at 723 K.	Furnace cooled.	
▽			
▷	Al - 99.5. Cast at 973 K into molds at 473 K, rolled and drawn. Turned into rods.		
◁	Al - 99.9, .038 Fe - .03 Si - .002 Cu. Same treatment as ▷.		
◇	Al - 99.99, .003 Fe - .0027 Si - .0024 Cu. Same treatment as ▷.		
●	SP grade.		
■	Al - 99.6.		
▲	Pure.		

METALLIC MATERIALS

Aluminium Alloys

5. CHEMICAL PROPERTIES5.1. Solution potential (vs. decinormal calomel electrode)

Al - 99.5 : .84 V, any condition.

Al - 99.0 : .83 V, any condition.

From Kappelt (1961).

5.2. Corrosion resistance

These alloys are very stable because they become covered by a thin oxide film which is very resistant and protective. Thicker, more protective oxide coatings can be deposited by chemical or electrolytic treatments.

Corrosion resistance of these alloys is very good in interiors, rural, marine or industrial environments. (Kappelt (1961)).

6. FABRICATION

6.2. Forming. Excellent.

6.3. Welding. Good.

6.4. Machining. Excellent.

6.5. Heat treatment. These alloys are non-heat-treatable.

From Kappelt (1961).

7. AVAILABLE FORMS AND CONDITIONS

These alloys are available in any standard product form such as: sheet, plate, strip, bar, tubing, wire extrusions, and forgings in a wide range of sizes from foils less than 2.5×10^{-5} m thick to big forgings.

METALLIC MATERIALS

Aluminium Alloys

8. USEFUL TEMPERATURE RANGE

Continuous structural use should be limited to temperatures below 400 K.

The temperature range of aluminized plastic films is normally controlled by the linear expansion of the film, which in the case of Mylar is extremely high above 310 K.

9. APPLICATIONS

Structural elements, foils, bushing and gear, tanks, sealing, wires, honeycombs (both cores and faces), thin wall tubing. As coating on Mylar, Teflon, Kapton, To protect aluminium alloys (alclad).

METALLIC MATERIALS
Aluminium-Copper Alloys

1.3. ALUMINIUM-COPPER ALLOYS

ALLOY Al - 4.3 Cu - 1.5 Mg - .6 Mn.

1. TYPICAL COMPOSITION, PERCENT

Cr	Cu	Fe	Mg	Mn	Ni	Si	Ti+Zr	Zn	Others		Al
									Each	Total	
.1	3.8 4.9	.5	1.2 1.8	.3 .9	-	.5	.2	.2	.05	.15	Balance

2. OFFICIAL DESIGNATIONS

AECMA	ISO	AFNOR	AMS	BS	DIN
Al-P13	Al-Cu4Mg1	A-U4G1	2024	2L 65	AlCuMg2 3. 1354

3. PHYSICAL PROPERTIES3.1. Density. $\rho = 2770 \text{ kg.m}^{-3}$. (Kappelt (1961), ASMH (1974)c.)3.2. Thermal properties

3.2.1. Specific heat.

Effect of temperature on specific heat: Fig 1-32.

3.2.2. Thermal conductivity.

Effect of temperature on thermal conductivity: Fig 1-33.

Thermal conductivity integrals: Fig 1-34

3.2.3. Thermal diffusivity.

Effect of temperature on thermal diffusivity: Fig 1-35.

3.2.4. Thermal expansion.

Effect of temperature on thermal expansion: Fig 1-36

3.2.5. Melting range.

773 K - 913 K. (ALCAN (1965)).

METALLIC MATERIALS
Aluminium-Copper Alloys

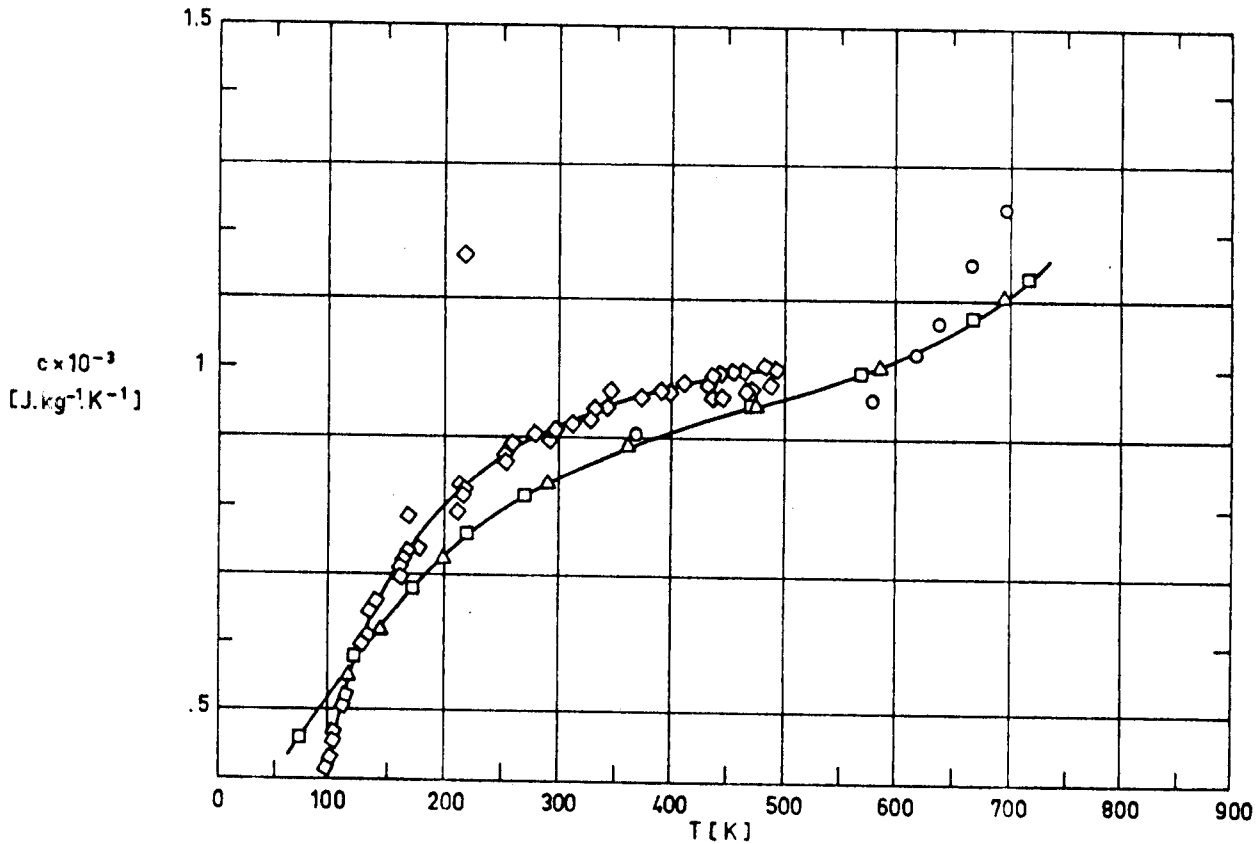


Fig 1-32. Specific heat, c , of Al - 4.3 Cu - 1.5 Mg - .6 Mn as a function of temperature, T .

Explanation

Key	Description	Comments	References
○	4.31 Cu - .29 Si - .14 Fe, and traces of other impurities. Hot worked, annealed several hours at 773 K in vacuum and cooled in 10 d. Heating rate during test 2 K.min ⁻¹ .		Touloukian (1967)b.
□	93.4 Al - 4.5 Cu - 1.5 Mg - .6 Mn. Condition - T4.		
△	Same as □. Condition - T4.	Sealed under helium atmosphere.	
◇	Nominal composition. Hanova liquid platinum was applied on both surfaces of the specimen; on front surface for opaqueness and on rear surface for good conductivity. In addition front surface was undercoated with Parson black to obtain constant absorptance.	Reported error ≤5%.	

METALLIC MATERIALS
Aluminium-Copper Alloys

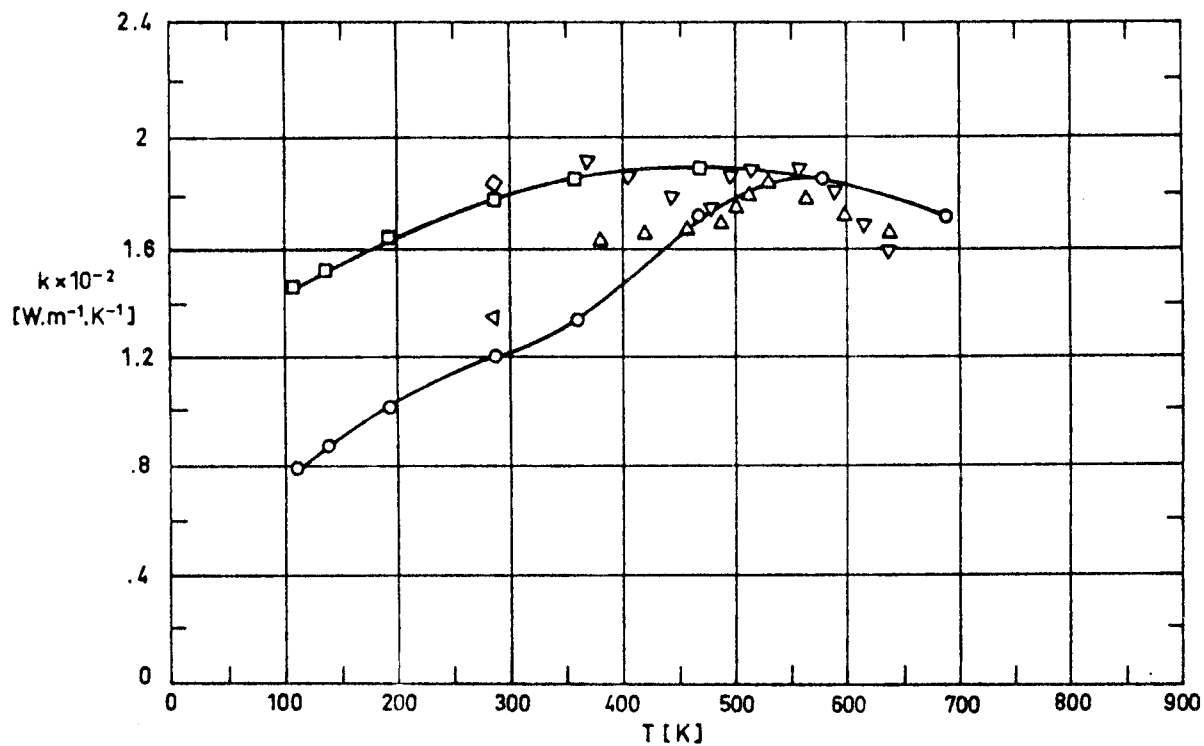


Fig 1-33. Thermal conductivity, k, of Al - 4.3 Cu - 1.5 Mg - .6 Mn as a function of temperature, T.

Explanation

Key	Description	Comments	References
○	Nominal composition. Condition - T4. Density 2 787 Kg.m ⁻³ . As received.		Touloukian (1967)b.
□	Same as ○ . Measured after heating to 575 K.		
△	4.5 Cu - 1.5 Mg - .6 Mn. Heated from virgin conditions to maximum temperature of 648 K.	Reported error ±4%.	
▽	Same as △ . Cooled to room temperature and then repeated the above heat treatment.		
◁	Same as ▽ . Condition - T4-T3.	Reported error ±5%.	
◇	Same as ▽ . Condition - 0 annealed.		

METALLIC MATERIALS
Aluminium-Copper Alloys

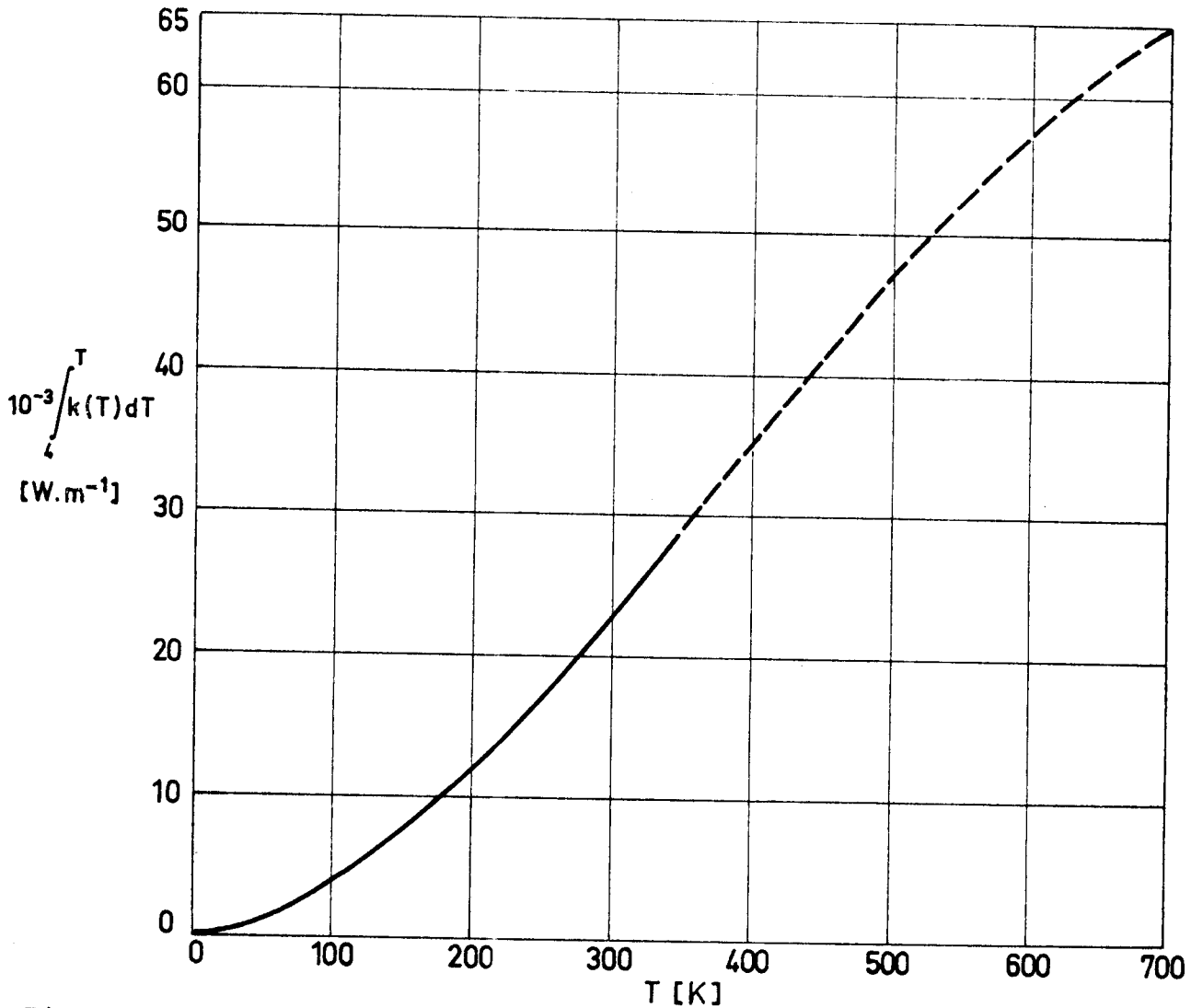


Fig 1-34. Thermal conductivity integrals of Al - 4.3 Cu - 1.5 Mg - .6 Mn as a function of temperature, T.

Explanation

———— From Coston (1967).

----- Calculated, by the compiler, by fitting the experimental data points \circ and \triangleleft of Fig 1-33 with the least-squares method, and integrating the expression, $k(T) = 74.44 - 2.30 \times 10^{-2}T + 9.96 \times 10^{-4}T^2 - 1.09 \times 10^{-6}T^3$ ($r = .977$), which is then obtained; r is the correlation coefficient giving the goodness of the fit.

METALLIC MATERIALS
Aluminium-Copper Alloys

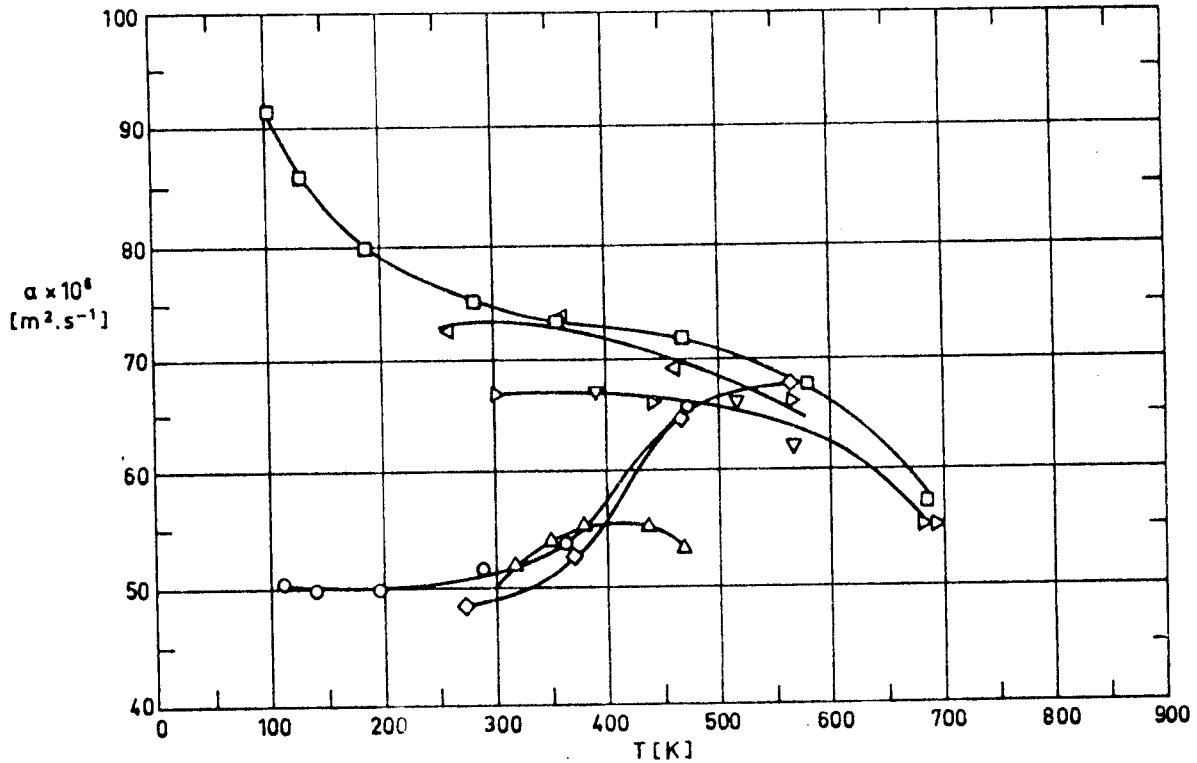


Fig 1-35. Thermal diffusivity, α , of Al-4.3 Cu-1.5 Mg-.6 Mn as a function of temperature, T.

Explanation

Key	Description	Comments	References
○	4.5 Cu - 1.5 Mg - .6 Mn. Condition - T4. As received.		Touloukian (1967)b.
□	Same as ○. Heated above 575 K.		
△	3.8 - 4.9 Cu - 1.2 - 1.8 Mg - .3 - .9 Mn - .5 max Fe - .5 max Si - .25 max Zn - .1 max Cr and .15 max other in total. Condition - T86.	Measured after five exposures to radiation and followed by cooling.	
▽	Same as △.	Measured after eight exposures to radiation and followed by cooling.	
▷	Same as △.	Measured after ten exposures to radiation and followed by cooling.	
◁	4.5 Cu - 1.5 Mg - .6 Mn. Annealed at 723 K.		
◇	4.5 Cu - 1.5 Mg - .6 Mn. Condition - T4.		

METALLIC MATERIALS
Aluminium-Copper Alloys

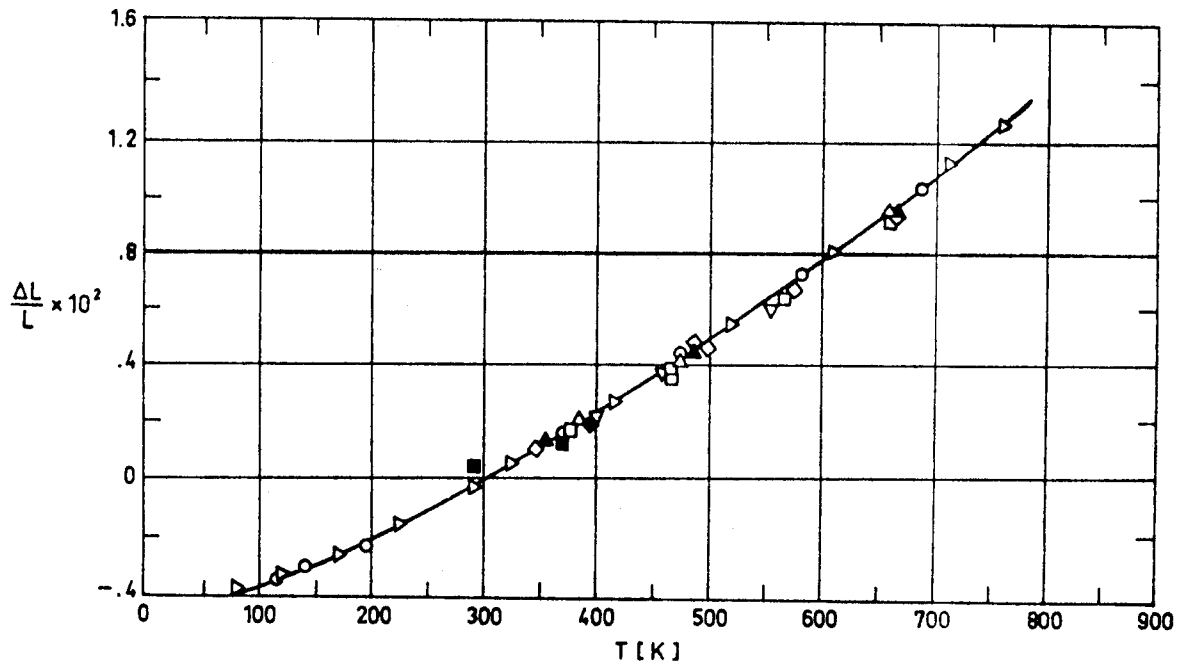


Fig 1-36. Linear thermal expansion, $\Delta L/L$, of Al-4.3 Cu-1.5 Mg-.6 Mn as a function of temperature, T.

Explanation

Key	Description	Comments	References
○	Nominal composition. Condition - T4.	Tested in vacuum.	Touloukian (1967)b.
□	93.09 Al - 4.41 Cu - 1.41 Mg - .67 Mn - .25 Fe - .10 Si - .02 Zn, and .01 Ni, Cr, Pb, Bi each. Solution heat-treated 1 h at 766.5 K, water quenched, and aged at room temperature.	Heating.	
■	Same as □.	Cooling.	
△	Same as □. Aged 100 h at 644 K.	Heating.	
▲	Same as △.	Cooling.	
◇	Same as □. Aged 500 h at 700 K.	Heating.	
◆	Same as ◇.	Cooling.	
▽	2.31 Cu - 1.46 Mg - 1.23 Fe - 1.20 Ni - .88 Si - .07 Ti. Wrought, heated 2 h at 798 K, quenched, aged 16 h at 443 K, quenched.		
▷	4.5 Cu - 1.5 Mg - .6 Mn. Condition - T4.	Tested at 1.5 - 2.5 K.min ⁻¹ rise in argon.	

METALLIC MATERIALS
Aluminium-Copper Alloys

3.3. Thermal radiation properties

3.3.1. Emittance.

3.3.1.1.1. Normal spectral emittance ($\beta'=0$): Fig 1-37

3.3.1.2.1. Normal total emittance ($\beta'=0$).

Effect of temperature on normal total emittance: Fig 1-38

The influence of anodizing is given in Table 1-11

Table 1-11

Normal Total Emittance of Al - 4.3 Cu - 1.5 Mg - .6 Mn, Anodized

T [K]	β'°	ϵ'	Comments
373	~ 0	.55	Anodized in chromic acid. Measured in vacuum ($<1.3 \times 10^{-3}$ Pa).
300	~ 0	.78	1.6×10^{-3} m thick. Anodized in sulphuric acid (coating thickness $\sim 1.3 \times 10^{-5}$ m). Calculated from reflectance measured in air. Mentioned below as specimen 1.
300	~ 0	.78	Similar to 1 except exposed to vacuum (1.3×10^{-6} Pa) for 300 h. Vacuum maintained by ion pump. Measured in air after expo- sure.
300	~ 0	.78	Similar to 1 except exposed to UV radiation in vacuum (1.3×10^{-3} Pa) for 300 h. Vacuum maintained by oil-diffusion pump. H ₂ gas UV source. Measured in air after exposure.
300	~ 0	.78	Similar to above except He gas UV source.

From Touloukian, DeWitt & HERNICZ (1972).

3.3.1.4. Hemispherical total emittance: Table 1-12.

METALLIC MATERIALS
Aluminium-Copper Alloys

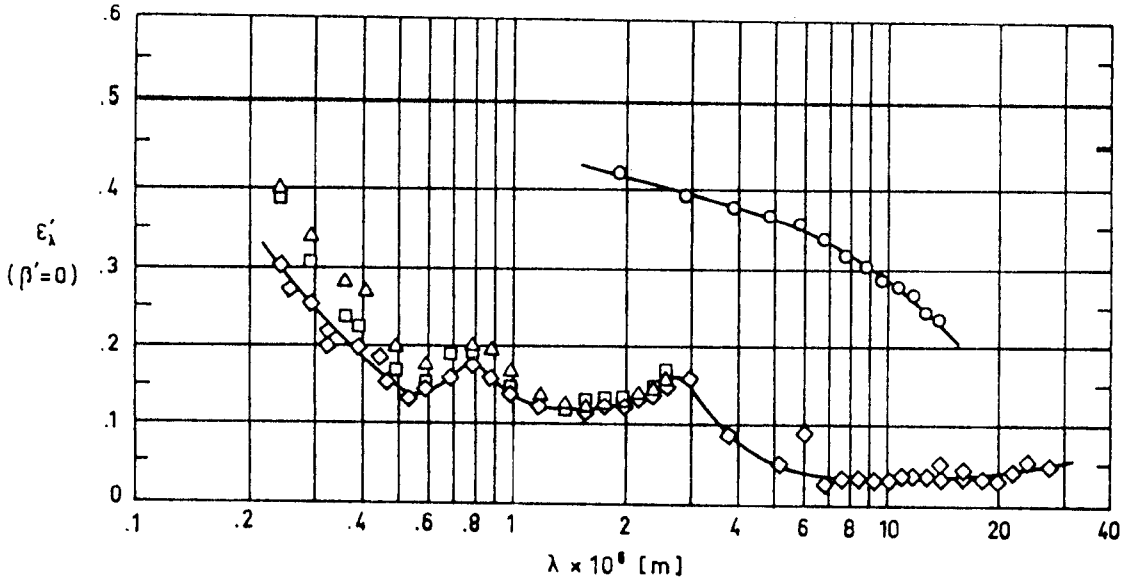


Fig 1-37. Normal spectral emittance, ϵ'_λ , of Al - 4.3 Cu - 1.5 Mg - .6 Mn as a function of wavelength, λ .

Explanation

Key	Description	Comments	References
○	4.5 Cu - 1.5 Mg - .6 Mn. Ultrasonically machined. Oxidized in air at 823 K for 2 h.	Sample temperature: T=823 K. Measured in air. Reported error ±4%.	Touloukian (1967)b.
△	Same as ○. Surface roughness: 9.9×10^{-8} m and 7.1×10^{-8} m in x and y directions respectively.	T=323 K. Measured in nitrogen.	
□	Same as ○. Surface roughness: 4.6×10^{-8} m and 3.8×10^{-8} m in x and y directions respectively.		
◇	Same as ○. Surface roughness: 1.52×10^{-7} m and 1.7×10^{-7} m in x and y directions respectively.		

METALLIC MATERIALS
Aluminium-Copper Alloys

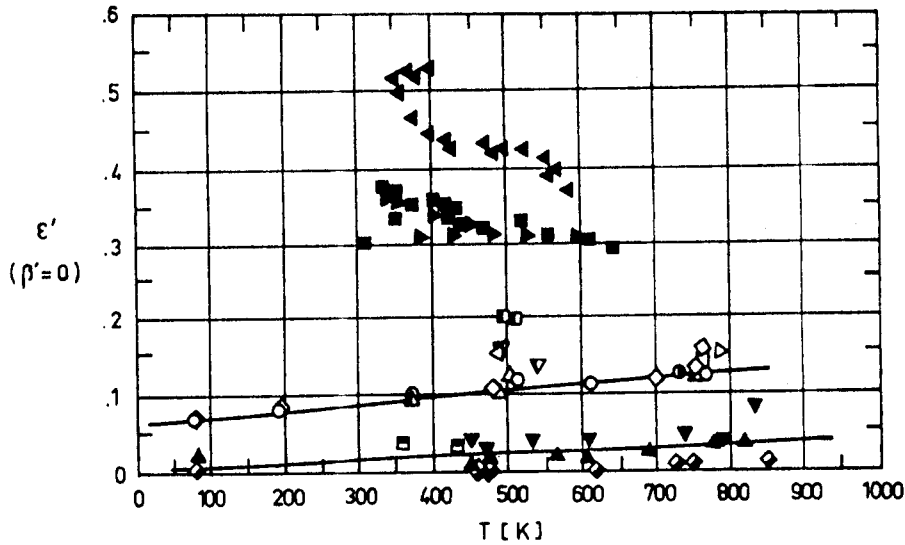


Fig 1-38. Normal total emittance, ϵ' , of Al-4.3 Cu-1.5 Mg-.6 Mn as a function of temperature, T .

Explanation

Key	Description	Comments	References
○	4.5 Cu-1.5 Mg-.6 Mn. As received, wiped.	Measured in helium (1.33×10^{-3} Pa). Cycle 1 heating.	Touloukian (1967)b.
△	Same as ○.	Cycle 1 cooling.	
□	Same as ○.	Cycle 2 heating.	
▽	Same as ○.	Cycle 2 cooling.	
◇	Same as ○. Scrubbed, washed, and wiped.	Same as ○.	
◁	Same as ◇.	Cycle 1 cooling.	
▷	Same as ◇.	Cycle 2 heating.	
◉	Same as ◇.	Cycle 2 cooling.	
▲	Same as ◇. Polished to a mirror like finish and washed.	Same as ○.	
■	Same as ▲.	Cycle 1 cooling.	
◆	Same as ▲.	Cycle 2 heating.	
▼	Same as ▲.	Cycle 2 cooling.	
⊙	Same as ▲.	Cycle 3 heating.	
⊠	Same as ▲.	Cycle 3 cooling.	
◈	4.5 Cu-1.5 Mg-.6 Mn. Alclad. As received.	Measured in vacuum (6.7×10^{-3} Pa). Reported error $\pm 10\%$.	
▲	Same as ◈. Cleaned with liquid detergent or polished with fine polishing compounds on a buffing wheel.		
▼	Same as ▲. Oxidized in air at red heat for 30 min.		
◀	4.5 Cu-1.5 Mg-.6 Mn. Weathered using flat shield.		
▶	Same as ◀. Weathered using conical shield.		
■	Same as ▶.		
▣	Same as ■.	Constant over temperature range 361-433 K. Reported error $\pm 10\%$.	

METALLIC MATERIALS
Aluminium-Copper Alloys

Table 1-12

Hemispherical Total Emittance of Al - 4.3 Cu - 1.5 Mg - .6 Mn

T [K]	ϵ	Comments
303	.052	Measured in air.
303	.26	Different sample, same as above specimen and conditions except weathered.
373	.063	Prefinished with 600 grit aluminium oxide powder on felt; electropolished; measured in vacuum (1.3×10^{-3} Pa).
373	.041	Above specimen and conditions except ion bombarded (3.2×10^{24} ions/m ²).
373	.053	Above specimen and conditions except ion bombarded (6.5×10^{24} ions/m ²).
373	.062	Above specimen and conditions except ion bombarded (9.8×10^{24} ions/m ²).
278	.02	As received.
278	.06	Different sample, same as above specimen and conditions except machine polished and degreased.

From Touloukian & DeWitt (1970).

3.3.2. Absorptance.

3.3.2.5. Solar absorptance.

3.3.2.5.1. Normal solar absorptance: Table 1-13.

METALLIC MATERIALS
Aluminium-Copper Alloys

Table 1-13

Normal Solar Absorptance of Al - 4.3 Cu - 1.5 Mg - 0.6 Mn

T [K]	β°	α_s	Comments
311	~ 0	.45	Heated to 310 K; clean and smooth surface; measured in air at sea level. Mentioned below as sample 1.
311	~ 0	.58	Above specimen and conditions except reheated to 560 K.
311	~ 0	.67	Above specimen and conditions except reheated to 755 K.
311	~ 0	.25	Different sample, same specimen and conditions as 1, except heated to 307 K; polished; surface free from scratches.
311	~ 0	.18	Above specimen and conditions except reheated to 560 K.
311	~ 0	.43	Above specimen and conditions except reheated to 755 K.
311	~ 0	.49	Different sample, same specimen and conditions as 1, except heated to 324 K; cleaned with methyl alcohol.
311	~ 0	.46	Above specimen and conditions except reheated to 603 K.
311	~ 0	.73	Above specimen and conditions except reheated to 755 K.
298	9	.242	As received; computed from spectral reflectance data for sea level conditions. Mentioned below as sample 2.
298	9	.236	Above specimen and conditions except computed for above atmosphere conditions.
298	9	.228	Different sample, same specimen and conditions as 2, except cleaned with liquid detergent.
298	9	.220	Above specimen and conditions except computed for above atmosphere conditions.
298	9	.302	Different sample, same specimen and conditions as 2, except polished.
298	9	.290	Above specimen and conditions except computed for above atmosphere conditions.

(Continued onto next page)

METALLIC MATERIALS
Aluminium-Copper Alloys

Table 1-13 (Continued)

Normal Solar Absorptance of Al - 4.3 Cu - 1.5 Mg - .6 Mn

T [K]	β°	α_s	Comments
298	9	.568	Different sample, same specimen and conditions as 2, except oxidized in air at red heat for .5 h.
298	9	.548	Above specimen and conditions except computed for above atmosphere conditions.
278	~ 0	.27	As received; extraterrestrial. Reported error 10%.
278	~ 0	.31	Different sample, same as above specimen and conditions except machine polished and degreased. Reported error 10%.
297		.20 \pm \pm .05	Alloy sheet (nonclad). Chemically cleaned. From Breuch (1967).
297		.22 \pm \pm .05	Alloy sheet (clad). Chemically cleaned. From Breuch (1967).
323		.16	Alloy sheet (nonclad). Surface roughness $.152 \times 10^{-6}$ m and $.178 \times 10^{-6}$ m in x and y directions respectively. Calculated by the compiler from data of Fig 1-37.

All data are from Touloukian & DeWitt (1970), unless otherwise stated.

The influence of anodizing is given in Table 1-14

Table 1-14

Normal Solar Absorptance of Al - 4.3 Cu - 1.5 Mg - 0.6 Mn, Anodized

T [K]	β°	α_s	Comments
300	~ 0	.15	Anodized in sulphuric acid; coating thickness $\sim 1.27 \times 10^{-5}$ m; absorptance calculated from reflectance measured in air. Mentioned below as sample 1.
300	~ 0	.16	Similar to above specimen and conditions except exposed to vacuum (1.33×10^{-6} Pa) for 300 h; vacuum maintained by ion pump; properly measured in air after vacuum exposure.

(Continued onto next page)

METALLIC MATERIALS
Aluminium-Copper Alloys

Table 1-14 (Continued)

Normal Solar Absorptance of Al - 4.3 Cu - 1.5 Mg - .6 Mn, Anodized

T [K]	β°	α_s	Comments
300	~ 0	.18	Similar specimen and conditions as 1, except exposed to vacuum (1.33×10^{-3} Pa) for 300 h; vacuum maintained by oil-diffusion pump; property measured in air after vacuum exposure.
300	~ 0	.26	Similar to above specimen and conditions except exposed to UV radiation in vacuum for 300 h; H ₂ gas UV source.
300	~ 0	.31	Similar to above specimen and conditions except He gas UV source.

From Touloukian, DeWitt & Hernicz (1972).

3.3.3. Reflectance.

3.3.3.1. Bidirectional spectral reflectance.

3.3.3.1.1. Normal-normal spectral reflectance ($\beta = \beta' = 0$) of alloy anodized: Fig 1-39.

3.3.3.2. Directional-hemispherical spectral reflectance.

Normal-hemispherical spectral reflectance ($\beta = 0, \omega' = 2\pi$):
Fig 1-40.

Normal-hemispherical spectral reflectance ($\beta = 0, \omega' = 2\pi$)
of alloy anodized: Fig 1-41.

3.3.3.6. Normal-hemispherical total reflectance.

3.3.3.9.2. Normal-hemispherical solar reflectance ($\beta = 0, \omega' = 2\pi$) of alloy anodized: Table 1-15.

METALLIC MATERIALS
Aluminium-Copper Alloys

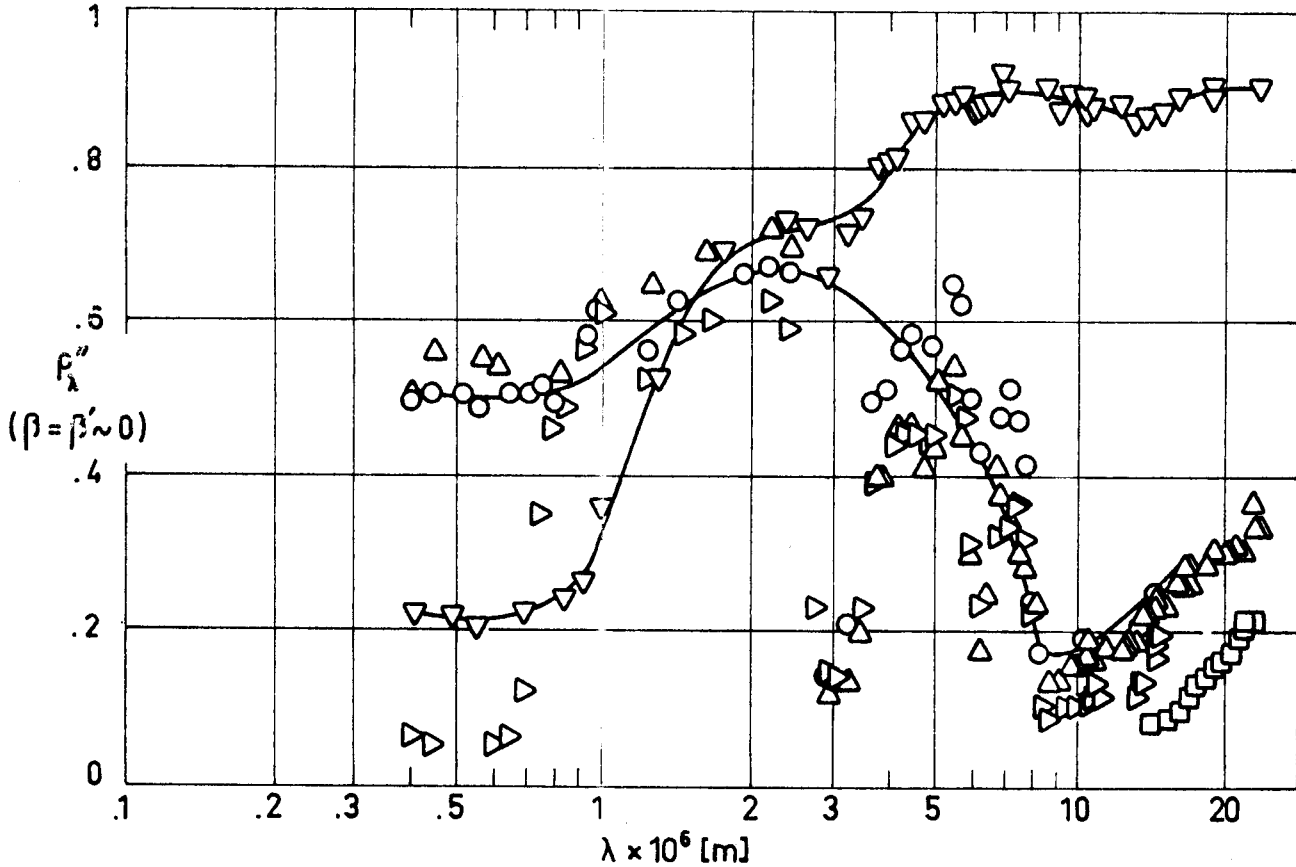


Fig 1-39. Normal-normal spectral reflectance, ρ_{λ}'' , of Al - 4.3 Cu - 1.5 Mg - .6 Mn, anodized, as a function of wavelength, λ .

Explanation

Key	Description	Comments	References
○	Nominal composition. Anodized in sulphuric acid.	Sample temperature: $T=298$ K. Data from smooth curve.	Touloukian, DeWitt & Hernicz (1972).
□	Same as ○.		
△	Same as ○ except substrate chem-milled.		
▽	Same as ○ except anodized in chromic acid.		
▷	Same as ○ except anodized in black chromic acid.		

METALLIC MATERIALS
Aluminium-Copper Alloys

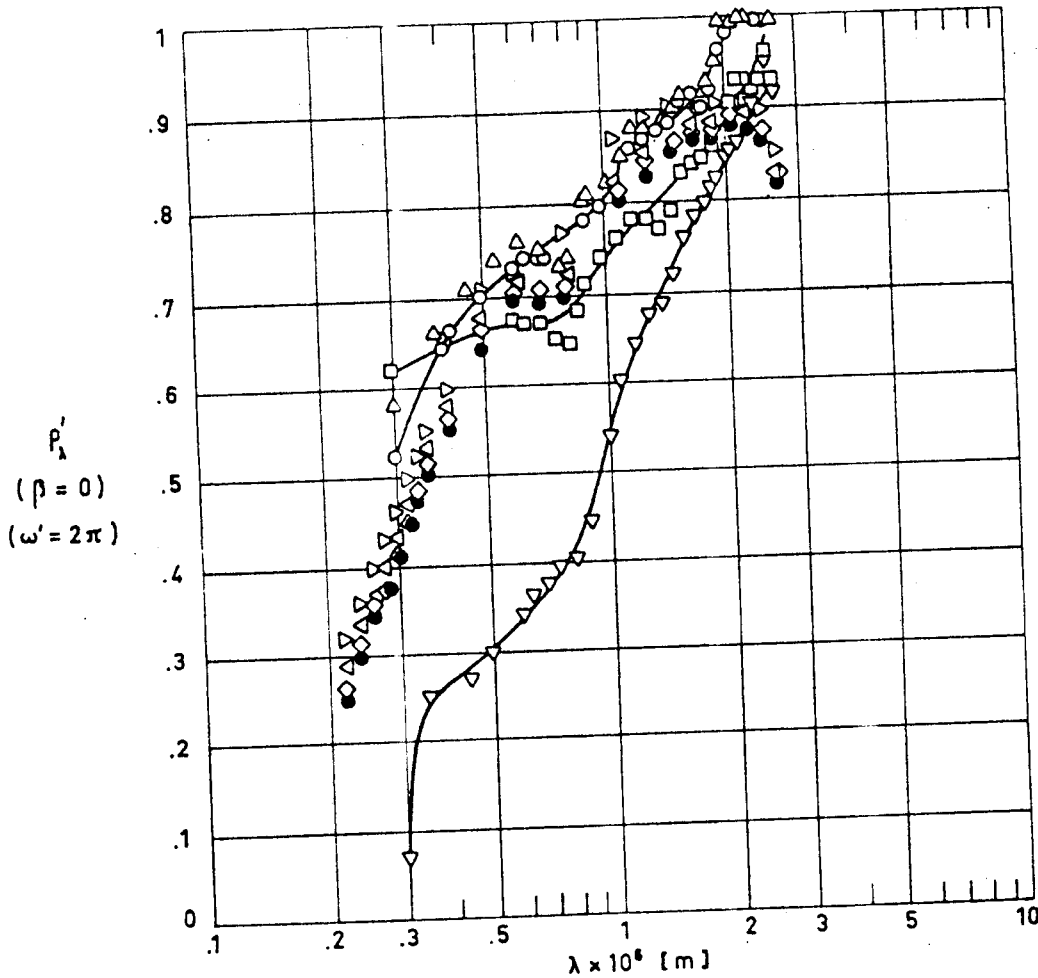


Fig 1-40. Normal-hemispherical spectral reflectance, ρ'_λ , of Al-4.3 Cu-1.5 Mg-.6 Mn as a function of wavelength, λ .

Explanation

Key	Description	Comments	References
○	Nominal composition. As received.	$\beta=9^\circ$ Sample temperature: $T=298$ K. Data from smooth curve. Reported error $\pm 4\%$.	Touloukian & DeWitt (1970).
□	Same as ○ except polished.		
△	Same as ○ except cleaned with liquid detergent.		
▽	Same as ○ except oxidized in air at red heat for 30 min.		
▷	Nominal composition. Cleaned.	$T=378$ K. Measured in vacuum (1.33×10^{-3} Pa). Measured relative to MgO.	
◁	Same as ▷ except exposed to UV radiation for 20 h; G.E. Type UA-3 lamp source.		
◊	Same as ▷ except exposed to UV radiation for 60 h. Same radiation source as ▷.		
●	Same as ▷ except exposed to UV radiation for 100 h. Same radiation source as ▷.		

METALLIC MATERIALS
Aluminium-Copper Alloys

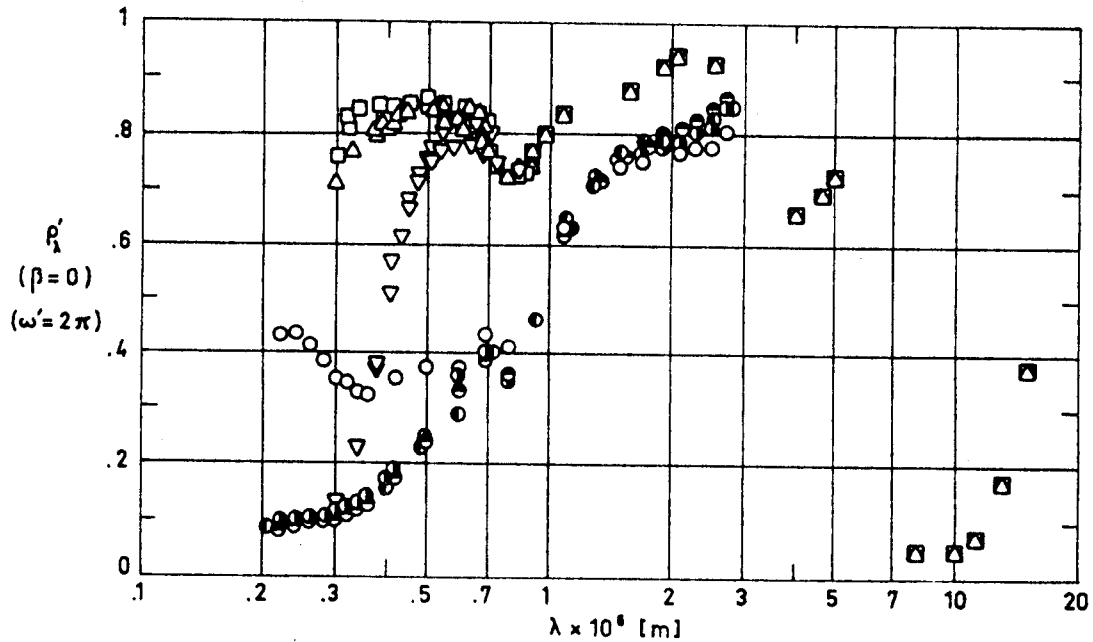


Fig 1-41. Normal-hemispherical spectral reflectance, ρ'_λ , of Al - 4.3 Cu - 1.5 Mg - .6 Mn, anodized, as a function of wavelength, λ .

Explanation

Key	Description	Comments	References
○	Nominal composition. Anodized. Cleaned.	Sample temperature: $T=378$ K. Measured in vacuum (1.33×10^{-3} Pa) relative to MgO.	Touloukian, DeWitt & HERNICZ (1972).
●	Same as ○ .	Same as ○ except exposed to UV radiation for 20 h. Source: GE UA-3 lamp.	
◐	Same as ○ .	Same as ○ except exposed to UV radiation for 60 h.	
◑	Same as ○ .	Same as ○ except exposed to UV radiation for 100 h.	
□	Nominal composition. Sheet $\sim 1.59 \times 10^{-3}$ m thick anodized in sulphuric acid. Coating thickness $\sim 1.27 \times 10^{-5}$ m.	$T=300$ K. Data from smooth curve. The data correspond to two different tests.	
△	Same as □ .	Same as □ except exposed to vacuum (1.33×10^{-6} Pa) for 300 h. Vacuum maintained by ion pump. Measured in air after vacuum exposure.	
▽	Same as □ .	Same as □ except exposed to UV radiation in vacuum for 300 h; H_2 gas UV source.	

METALLIC MATERIALS
Aluminium-Copper Alloys

Table 1-15

Normal Hemispherical Solar Reflectance of
Al - 4.3 Cu - 1.5 Mg - .6 Mn, Anodized

T [K]	β°	ω'	ρ'_s	Comments
298	~ 0	2π	.28	Anodized in chromic acid. Mentioned below as specimen 1.
298	~ 0	2π	.30	Similar to above specimen and conditions except calculated from spectral data.
298	~ 0	2π	.31	Similar to 1 specimen and conditions except anodized in black chromic acid.
298	~ 0	2π	.29	Similar to 1 specimen and conditions except calculated from spectral data.
298	~ 0	2π	.56	Similar to 1 specimen and conditions except anodized in sulphuric acid. Mentioned below as specimen 2.
298	~ 0	2π	.53	Similar to above specimen and conditions except calculated from spectral data.
298	~ 0	2π	.64	Similar to 2 specimen and conditions except substrate was chem-milled.
298	~ 0	2π	.57	Similar to above specimen and conditions except calculated from spectral data.

From Touloukian, DeWitt & HERNICZ (1972).

3.4. Other physical properties

3.4.1. Electrical resistivity (at room temperature).

Condition	0	T3-T4	T6-T81
$\sigma^{-1} \cdot 10^6$ [$\Omega \cdot m$]	.0345 ^{a,b}	.0574 ^{a,b}	.045 ^c

^a Kappelt (1961); ^b ASMH (1974) ^c Aluminium Association (1969).

The coefficient giving the variation of electrical resistivity with temperature is in the range $2 \times 10^{-3} K^{-1}$. (ASMH (1974) ^c)

METALLIC MATERIALS
Aluminium-Copper Alloys

to $2.6 \times 10^{-3} \text{ K}^{-1}$. (Touloukian (1967)b).

4. ENVIRONMENTAL BEHAVIOR

4.1. Prelaunch

Aluminium surface is very susceptible to increases in α_s and ϵ caused by contamination. The surface must be protected from physical abuse, atmospheric exposure, and caustic contaminants; cleanliness must be assured.

4.2. Postlaunch

There are no known restrictions, other than structural. From Breuch (1967).

5. CHEMICAL PROPERTIES

5.1. Solution potential (vs. decinormal calomel electrode)

Condition	T3-T4	T8
Sol. Pot. V	-.68	-.8

From REYNOLDS METALS Co,
(1961).

5.2. Corrosion resistance

It is poor in marine or industrial environments, sufficient in rural and urban environments, and good indoors.

6. FABRICATION

6.2. Forming. Medium.

METALLIC MATERIALS
Aluminium-Copper Alloys

- 6.3. Welding. Poor.
- 6.4. Machining. Good.
- 6.5. Heat treatment. Good.
- 6.6. Anodizing. Poor.

From García-Poggio et al.(1972).

7. AVAILABLE FORMS AND CONDITIONS

This alloy is available in the full commercial range of sizes for sheet, strip, plate, rod, bar, forgings, tubing, wire, extrusions and structural shapes.

8. USEFUL TEMPERATURE RANGE

Some disagreement seems to exist in the literature regarding the maximum operating temperature of this alloy. Although temperatures as high as 425 K are quoted for long term structural purposes (any temper condition), and even higher values for intermittent loading (475 K, T4 condition), it is advisable not to use this alloy (T3, T4 conditions) in a corrosive environment at temperatures above 340 K for several hours, or above 365 K for more than a few minutes.

9. APPLICATIONS

Gear materials in antenna drive, instruments, structural purposes, and thermal control surfaces.

INTENTIONALLY BLANK PAGE

METALLIC MATERIALS
Aluminium-Magnesium Alloys

1.4. ALUMINIUM-MAGNESIUM ALLOYS

ALLOY Al - 1 Mg - .6 Si.

1. TYPICAL COMPOSITION, PERCENT

Cr ^a	Cu	Fe	Mg	Mn	Si	Ti	Zn	Others		Al
								Each	Total	
.15	.15	-	.8	-	.4	-	-	-	-	Balance
.35	.4	.7	1.2	.15	.8	.15	.25	.05	.15	

^a Sometimes this alloy contains Mn (.2% - .8%) instead of Cr.

2. OFFICIAL DESIGNATIONS

AECMA	ISO	AFNOR	AMS	BS	DIN
Al-P34	Al-Mg1SiCu	-	6061	H20	AlMgSi1, 3.2315

3. PHYSICAL PROPERTIES

3.1. Density. $\rho = 2\,700 \text{ kg.m}^{-3}$. (Kappelt (1961)).

3.2. Thermal properties

3.2.1. Specific heat.

From room temperature to 373 K. Conditions 0 and T6.

$$c = 963 \text{ J.kg}^{-1}.\text{K}^{-1}. (\text{ASMH (1974)c}).$$

3.2.2. Thermal conductivity.

At room temperature.

Condition	0	T4	T6
k	180 ^a	155 ^{a,b}	167 ^a
[W.m ⁻¹ .K ⁻¹]	172 ^b	-	155 ^b

^a From ASMH (1974)c.

^b From Kappelt (1961).

METALLIC MATERIALS

Aluminium-Magnesium Alloys

3.2.4. Thermal expansion coefficient

Mean coefficient of linear thermal expansion, β , between 293 K and given temperature.

T [K]	293 ^a	393	493	593
$\beta \times 10^6$ [K ⁻¹]	21.8	23.4	24.3	25.4

^a Lower limit in this case is 213 K:

From Kappelt (1961).

3.2.5. Melting range. 855 K - 922 K. (ASMH 1974)c.

3.3. Thermal radiation properties

3.3.1. Emittance.

3.3.1.2. Normal total emittance ($\beta'=0$): Table 1-16.

Table 1-16

Normal Total Emittance of Al - 1 Mg - .6 Si

T [K]	ϵ'	Comments
	.03	Sheet 3.17×10^{-3} m thick, cleaned and degreased.
	.76	Anodized with chromic acid electrolyte 5% by weight, at 308 K, anodizing voltage: 40V DC, 120 min. Resulting coating thickness: 10^{-5} m.
	.07	Anodized with citric acid electrolyte, 1 kg.m ⁻³ ammonium citrate, at 295 K, anodizing voltage: 200V DC, 45 min.
	.81	Anodized with oxalic acid electrolyte, 3% by weight, at 311 K, anodizing voltage: 30V DC, 60 min. Resulting coating thickness: 10^{-5} m.
	.80	Hard anodized, 7.6×10^{-6} m thick, with sulphuric acid electrolyte 15% by weight, at 269 K.
	.82	Soft anodized, 7.6×10^{-6} m thick, with sulphuric acid electrolyte 17% by weight, at 293 K.

From Bevans (1969).

METALLIC MATERIALS
Aluminium-Magnesium Alloys

3.3.1.4. Hemispherical total emittance: Table 1-17.

Table 1-17

Hemispherical Total Emittance of Al-1Mg-.6Si

T [K]	ϵ	Comments
294	.06±.03 ^a	Nonclad sheet, chemically cleaned.
278	.09±.06 ^a	Forging, chemically cleaned.
323	.10±.06 ^a	Forging, chemically cleaned.
223	.10±.06 ^a	Weld area, chemically cleaned.
278	.10±.06 ^a	Weld area, chemically cleaned.
323	.11±.06 ^a	Weld area, chemically cleaned.
278	.04 ^b	As received.
278	.04 ^b	Different sample, same as above specimen and conditions except machine polished and degreased.
278	.41 ^b	Different sample, same as above specimen and conditions except sandblasted (120 size grit). Reported error: 10%.
302	.0506 ^b	Buffed; measured in vacuum (2.67×10^{-5} Pa). Error below 7.7%.
303	.0500 ^b	Above specimen and conditions; second trial. Error below 7.7%.
302	.0506 ^b	Above specimen and conditions; third trial. Error below 7.7%.
302	.049 ^b	Above specimen and conditions; different analysis of observed data. Error below 7.7%.
302	.0501 ^b	Above specimen and conditions; second trial. Error below 7.7%.

^a From Breuch (1967).

^b From Touloukian & DeWitt (1970).

3.3.2. Absorptance.

3.3.2.5. Solar absorptance.

METALLIC MATERIALS

Aluminium-Magnesium Alloys

3.3.2.5.1. Normal solar absorptance: Table 1-18.

Table 1-18

Normal Solar Absorptance of Al-1Mg-.6Si

T [K]	β°	α_s	Comments
294		.16±.04 ^a	Nonclad sheet, chemically cleaned.
294		.19±.06 ^a	Sheet sanded and chemically cleaned.
		.37 ^b	3.17x10 ⁻³ m thick sheet cleaned and degreased.
		.48 ^b	Hard anodized, 7x10 ⁻⁶ m thick, with sulfuric acid electrolyte, 15% by weight, at 269 K.
		.38 ^b	Soft anodized, 7x10 ⁻⁶ m thick, with sulfuric acid electrolyte, 17% by weight, at 293 K.
		.42 ^b	Anodized with oxalic acid electrolyte, 3% by weight, at 311 K, anodizing voltage: 30V DC, 60 min. Resulting coating thickness: 10 ⁻⁵ m.
		.37 ^b	Anodized with citric acid electrolyte, 1 Kg.m ⁻³ ammonium citrate, at 295 K, anodizing voltage: 200 V DC, 45 min.
		.48 ^b	Anodized with chromic acid electrolyte, 5% by weight, at 308 K, anodizing voltage: 40V DC, 120 min. Resulting coating thickness: 10 ⁻⁵ m.
278	~0	.41 ^c	As received; extraterrestrial. Reported error 10%
278	~0	.35 ^c	Different sample, same as above specimen and conditions except machine polished and degreased. Same reported error as above.
278	~0	.60 ^c	Different sample, same as above specimen and conditions except sandblasted (120 size grit). Same reported error as above.

^a From Breuch (1967).^b From Bevans (1969).^c From Touloukian & DeWitt (1970).

METALLIC MATERIALS
Aluminium-Magnesium Alloys

3.3.3. Reflectance.

3.3.3.1. Bidirectional spectral reflectance.

Normal-hemispherical spectral reflectance ($\beta=0$, $\omega'=2\pi$):

Data concerning different surface conditions are given in the following figures:

As received: Fig 1-42

Grit blasted: Fig 1-43.

Chemically polished: Fig. 1-44.

Chemically milled: Fig 1-45

3.4. Other physical properties

3.4.1. Electrical resistivity.

Condition	0	T4	T6
$\sigma^{-1} \times 10^{-9}$	3.83 a	4.31 a	4.31 a
$[\Omega \cdot m]$	3.71 b	4.29 b	4.11 b

^a From Kappelt (1961).

^b From ASMH (1974)c.

4. ENVIRONMENTAL BEHAVIOR4.1. Prelaunch

Aluminium surface is very susceptible to increases in α_s and ϵ caused by contamination. The surface must be protected from physical abuse, atmospheric exposure and caustic contaminants; cleanliness must be assured. (Breuch (1967)).

4.2. Postlaunch

No known restrictions other than structural. (Breuch (1967)).

METALLIC MATERIALS
Aluminium-Magnesium Alloys

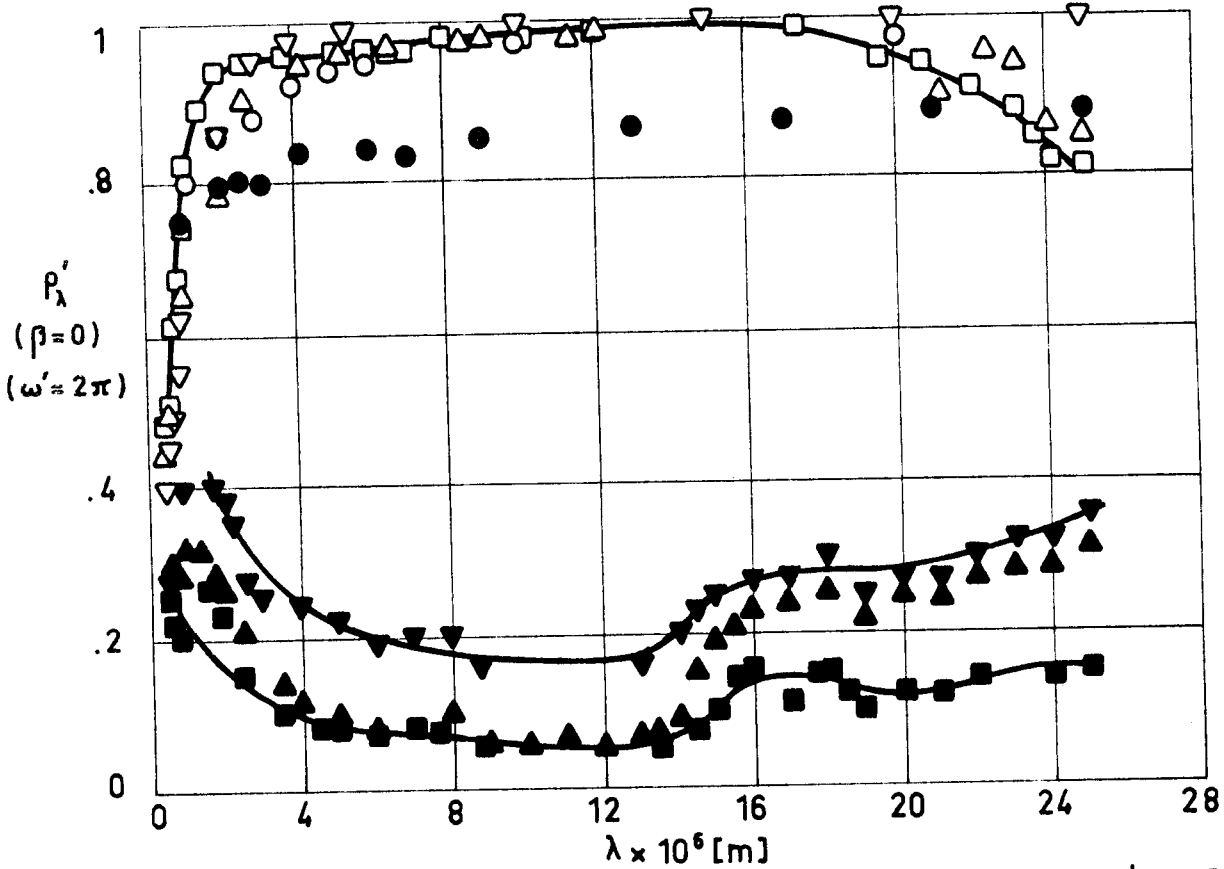


Fig 1-42. Normal-hemispherical spectral reflectance, ρ_{λ}' , of Al-1 Mg - .6 Si, as received, as a function of wavelength, λ .

Explanation

Key	Description	Comments	References
○	Nominal composition. Surface roughness: 1.5×10^{-6} m RMS.	T = 298 K. Converted from $R(2\pi, 0)$.	Touloukian & DeWitt (1970)
●	Same as ○ except surface roughness: 12.5×10^{-6} m RMS.		
□	Nominal composition. Cleaned	T ≈ 322 K.	
■	Same as □. Diffuse component only.	Data from smooth curve.	
△	Same as ○. Exposed to vacuum (5.32×10^{-6} Pa) for 24 h.	Hohlraum at 1 273 K. (Gier & Dunkle). Converted from $R(2\pi, 0)$.	
▲	Same as △. Diffuse component only.	Reported error < 2%.	
▽	Same as ○. X-Ray exposed in vacuum (5.32×10^{-6} Pa) for 24 h.		
▼	Same as ▽. Diffuse component only.		

METALLIC MATERIALS
Aluminium-Magnesium Alloys

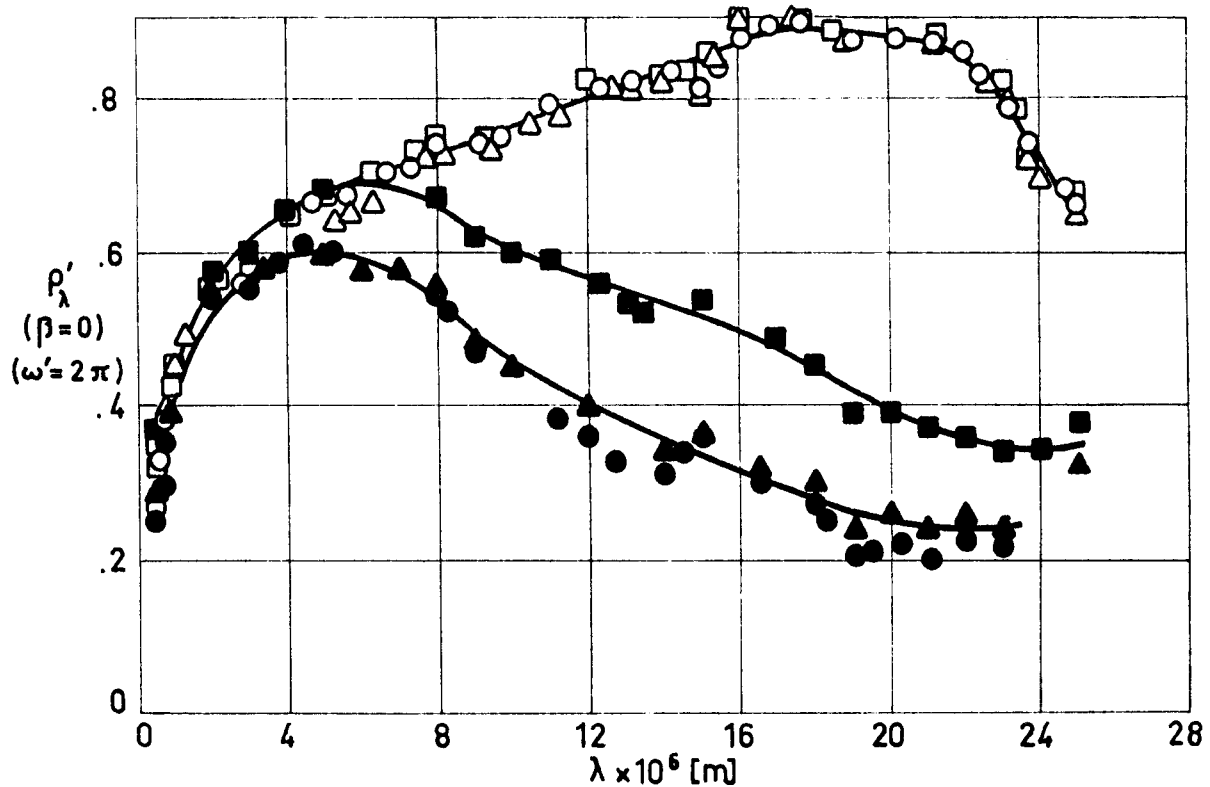


Fig 1-43. Normal-hemispherical spectral reflectance, ρ_{λ}' , of Al - 1 Mg - .6 Si, grit blasted, as a function of wavelength, λ .

Explanation

Key	Description	Comments	References
○	Nominal composition. Blasted using silicon carbide, air pressure $.76 \times 10^6$ to $.83 \times 10^6$ Pa for 30 to 45 s	T \sim 322 K. Data from smooth curve. Hohlraum at 1 273 K. (Gier & Dunkle) Converted from $R(2\pi, 0)$. Reported error <2%	Touloukian & DeWitt (1970)
●	Same as ○. Diffuse component only.		
□	Same as ○ except chem-milled using the Turco 9H process for 3 min; blasted as above.		
■	Same as □. Diffuse component only.		
△	Same as ○ except chem-polished using the Alcoa process with a 2 min immersion at 358 K; blasted as above.		
▲	Same as △. Diffuse component only.		

METALLIC MATERIALS
Aluminium-Magnesium Alloys

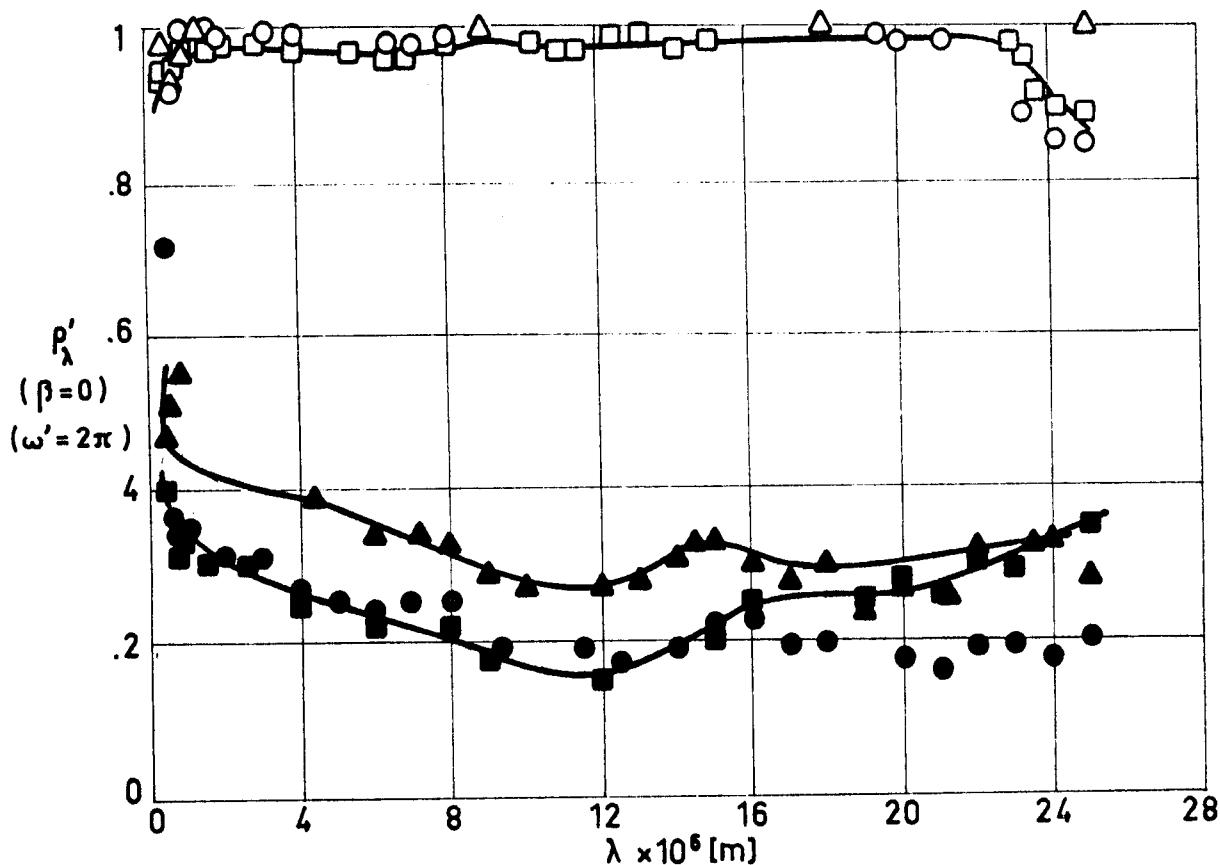


Fig 1-44. Normal-hemispherical spectral reflectance, ρ'_λ , of Al - 1 Mg - .6 Si, chemically polished, as a function of wavelength, λ .

Explanation

Key	Description	Comments	References
○	Nominal composition. Polished using the Alcoa process with a 2 min immersion at 358 K.	$T \sim 322$ K. Data from smooth curve.	Touloukian & DeWitt (1970)
●	Same as ○. Diffuse component only.	Hohlraum at 1 273 K. (Gier & Dunkle) Converted from $R(2\pi, 0)$.	
□	Same as ○. Exposed to vacuum (5.32×10^{-6} Pa) for 24 h.	Reported error <2%	
■	Same as □. Diffuse component only.		
△	Same as ○. X-Ray exposed in vacuum (5.32×10^{-6} Pa) for 24 h.		
▲	Same as △. Diffuse component only.		

METALLIC MATERIALS
Aluminium-Magnesium Alloys

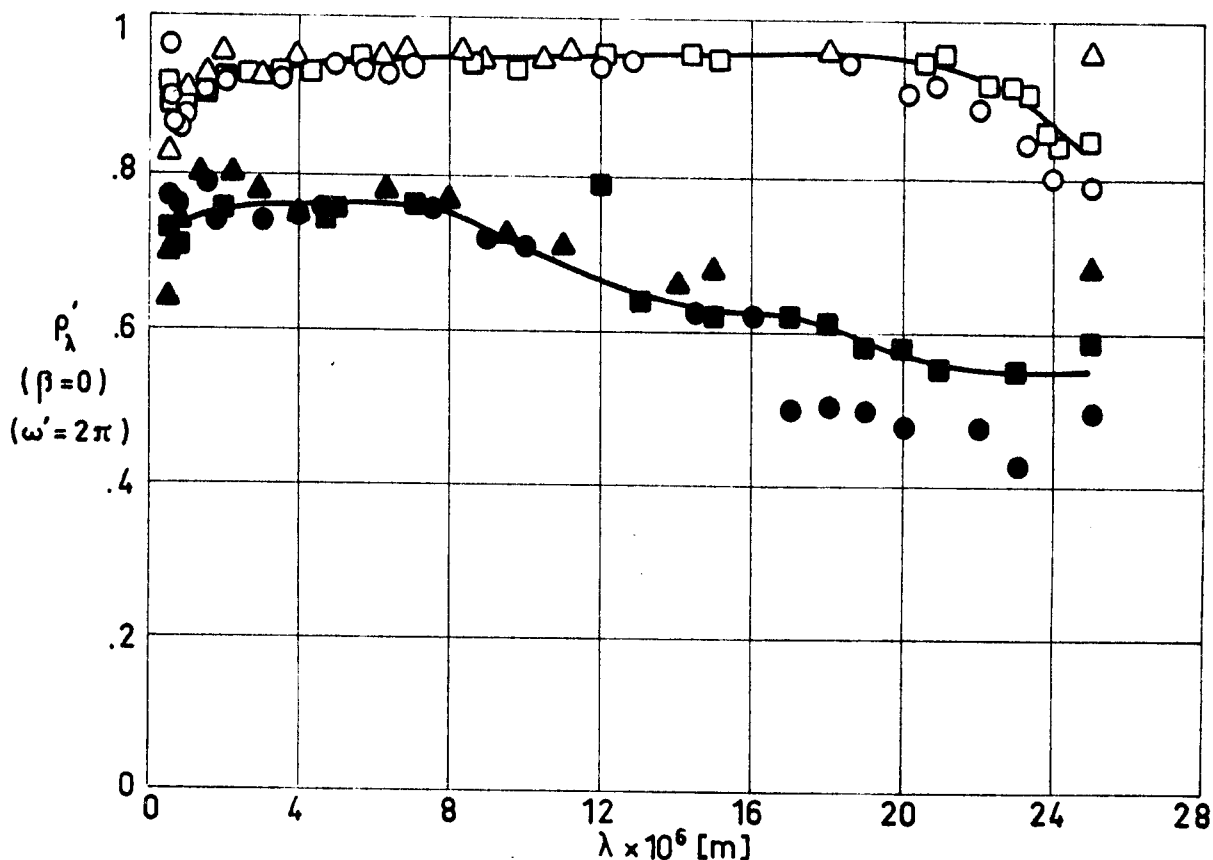


Fig 1-45. Normal-hemispherical spectral reflectance, ρ'_λ , of Al - 1 Mg - .6 Si, chemically milled, as a function of wavelength, λ .

Explanation

Key	Description	Comments	References
○	Nominal composition. Chem-milled using the Turco 9H process for 3 min.	T ~ 322 K. Data from smooth curve. Hohlräum at 1 273 K. (Gier & Dunkle) Converted from R(2 π ,0). Reported error <2%	Touloukian & DeWitt (1970)
●	Same as ○. Diffuse component only.		
□	Same as ○. Exposed to vacuum (5.32×10 ⁻⁶ Pa) for 24 h.		
■	Same as □. Diffuse component only.		
△	Same as ○. X-Ray exposed in vacuum (5.32×10 ⁻⁶ Pa) for 24 h.		
▲	Same as △. Diffuse component only.		

METALLIC MATERIALS
Aluminium-Magnesium Alloys

5. CHEMICAL PROPERTIES

5.1. Solution potential (vs. decinormal calomel electrode)

T4 Condition: -0.80 V.

T6 Condition: -0.83 V.

From Kappelt (1961).

5.2. Corrosion resistance

This alloy is ranked among the best of the heat treatable alloys concerning corrosion resistance. In general, resistance to corrosion is not significantly affected by variations in the heat treatment. (ASMH 1974)c).

6. FABRICATION

6.2. Forming. Good.

6.3. Welding. Good.

6.4. Machining. Good.

6.5. Heat treatment. Good.

6.6. Anodizing. Excellent.

From García-Poggio et al. (1972).

7. AVAILABLE FORMS AND CONDITIONS

This alloy is available in the full commercial range of sizes for sheets, strip, plate, rod, bar, forgings, tubing extrusion and structural shapes. (ASMH (1974)c).

8. USEFUL TEMPERATURE RANGE

Continuous structural use should be limited to temperatures below

METALLIC MATERIALS
Aluminium-Magnesium Alloys

425 K, whatever the temper conditions. Short term utilization temperatures up to 475 K can be achieved using T4 or T6 conditions. (ASMH (1974)c).

9. APPLICATIONS

For electrical power systems, tubing, structural elements, whip antennas, heat pipes, solar absorbers.

INTENTIONALLY BLANK PAGE

METALLIC MATERIALS
Aluminium - Zinc Alloys

1.5. ALUMINIUM-ZINC ALLOYS

ALLOY Al - 5.7 Zn - 2.5 Mg - 1.6 Cu.

1. TYPICAL COMPOSITION, PERCENT

Cr	Cu	Fe	Mg	Mn	Si	Ti	Zn	Others		Al
								Each	Total	
.18	1.2		2.1				5.1			
.40	2.0	.7	2.9	.3	.5	.2	6.1	.05	.15	Balance

2. OFFICIAL DESIGNATIONS

AICMA	ISO	AFNOR	AMS	BS	DIN	UNE
Al-P42		A-Z5GU	7075		AlZnMgCu 1.5 3.4365	Al-5ZnMgCu UNE 38-371

3. PHYSICAL PROPERTIES

3.1. Density. $\rho = 2800 \text{ kg.m}^{-3}$. ASMH (1974)c.

3.2. Thermal properties

3.2.1. Specific heat.

Effect of temperature on specific heat: Fig 1-45.1.

3.2.2. Thermal conductivity.

At 298 K

Condition	k [W.m ⁻¹ .K ⁻¹]
T6	130
T73	155
T76	150

From McCall (1979).

Effect of temperature on thermal conductivity: Fig 1-45.2.

See also p. R 4-113 where k is given in the temperature range 25 K - 300 K.

Rev. 2. 1984

METALLIC MATERIALS
Aluminium - Zinc Alloys

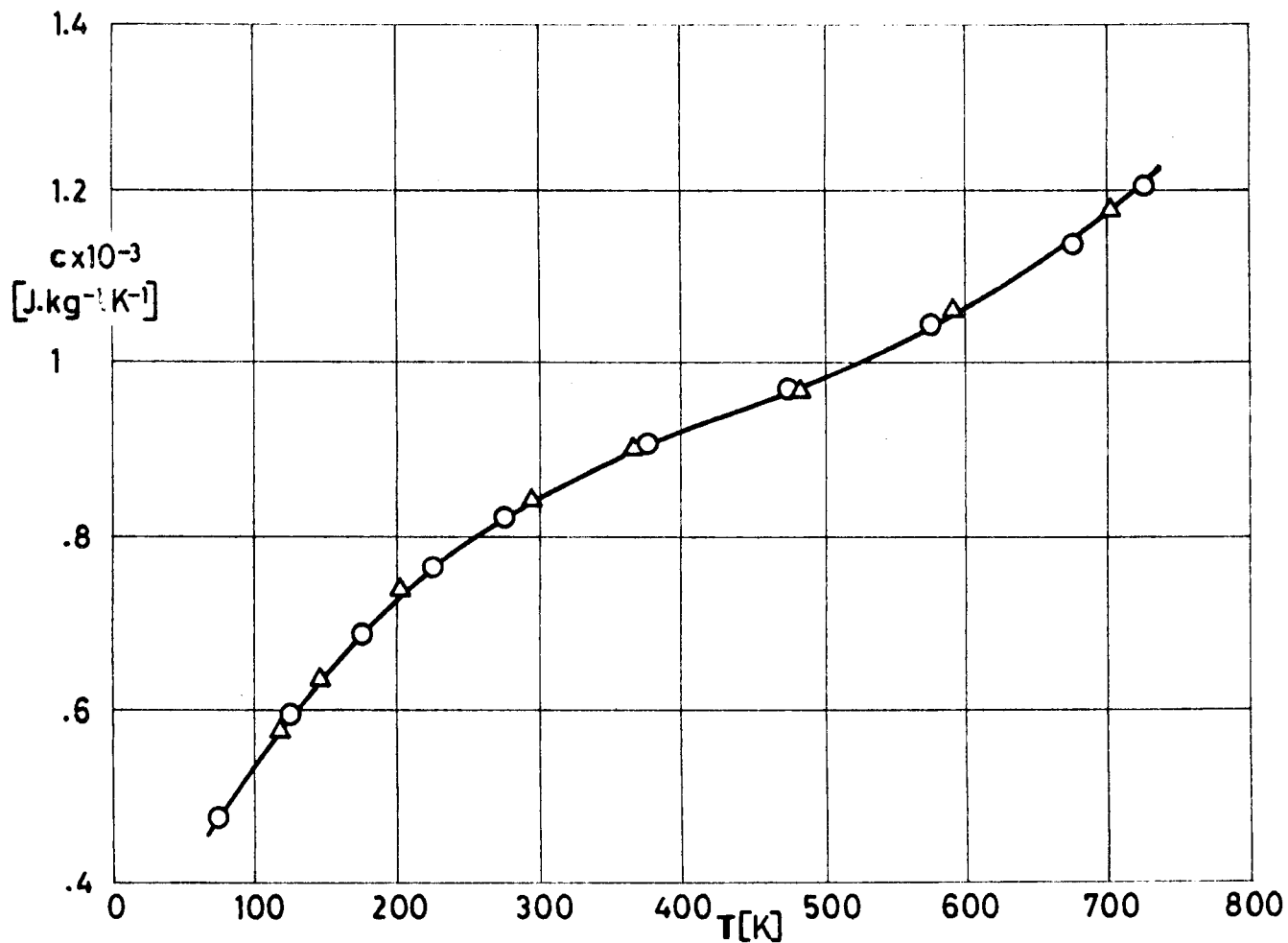


Fig 1-45.1. Specific heat, c , of Al - 5.7 Zn - 2.5 Mg - 1.6 Cu as a function of temperature, T .

Explanation

Key	Description	Comments	References
○	Al alloy 75 S - T6 (Canadian commercial designation). 5.5 Zn, 2.5 Mg, 1.5 Cu, .3 Cr, .2 Mn, Al balance.		Touloukian (1967)c.
△	Al alloy 7075-T6. 5.5 Zn, 2.5 Mg, 1.5 Cu, .3 Cr, Al balance.	Sealed under helium atmosphere.	

METALLIC MATERIALS
Aluminium - Zinc Alloys

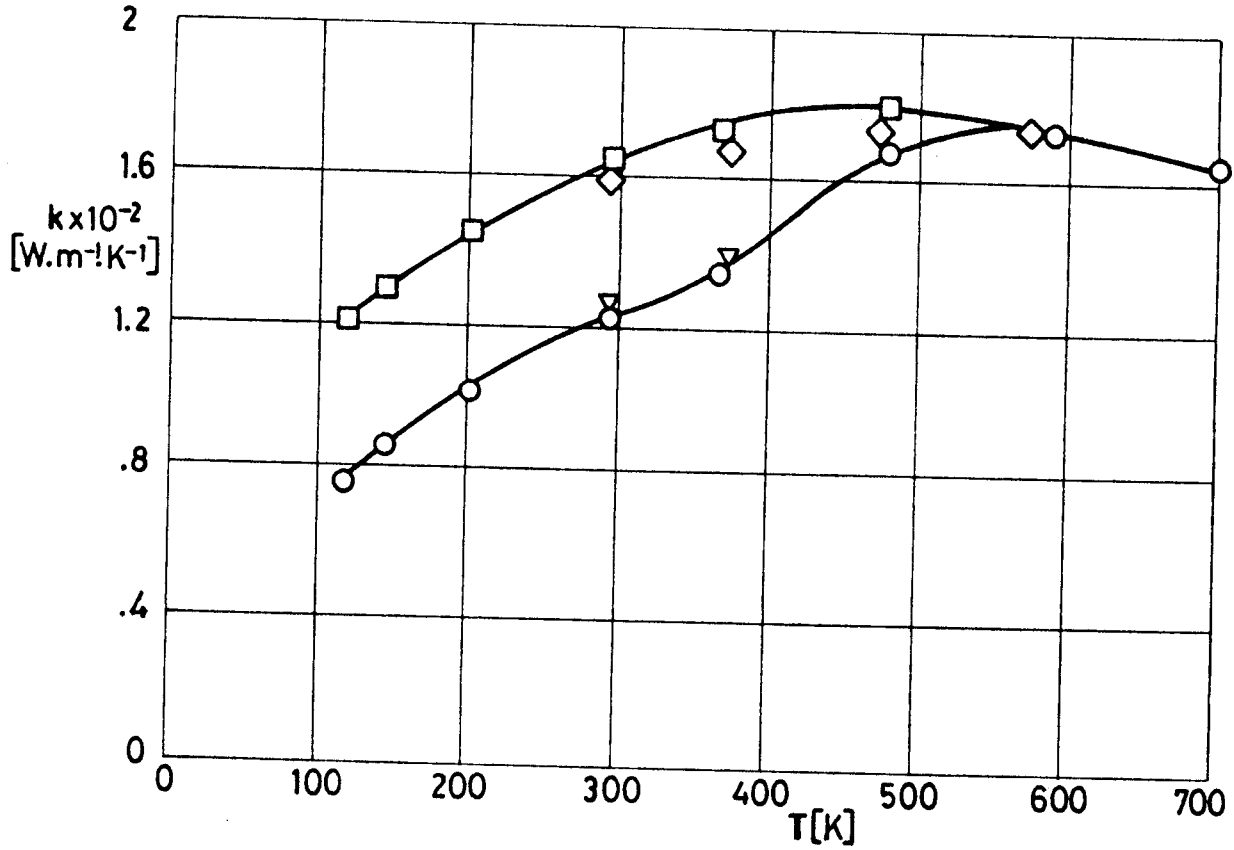


Fig 1-45.2. Thermal conductivity, k , of Al - 5.7 Zn - 2.5 Mg - 1.6 Cu as a function of temperature, T .

Explanation

Key	Description	Comments	References
○	Al alloy 7075-T6 (Alcoa). 5.6 Zn, 2.5 Mg, 1.6 Cu, .3 Cr, Al balance. $\rho = 2800 \text{ kg.m}^{-3}$.	As received.	Touloukian (1967)c.
□	Same as ○.	After heating above 575 K.	
◇	Al alloy RR77 (British designation). 4.96 Zn, 2.54 Mg, 2.2 Cu, .54 Mn, .31 Fe, .26 Si, trace Ti, Al balance.	Wrought, 2 h solution heat treatment at 720 K, quenched in water at 340 K, aged 4 h at 408 K and aircooled.	
▽	Same as ◇.	As received.	

Rev. 2. 1984

METALLIC MATERIALS

Aluminium - Zinc Alloys

Thermal conductivity integral: Fig 1-45.3.

3.2.3. Thermal diffusivity.

Effect of temperature on thermal diffusivity: Fig 1-45.4.

3.2.4. Thermal expansion.

Effect of temperature on thermal expansion: Fig 1-45.5.

3.2.5. Melting range.

750 K - 910 K. ASMH (1974)c.

3.3. Thermal radiation properties

3.3.1. Emittance.

3.3.1.1.1. Normal spectral emittance ($\beta' = 0$): Fig 1-45.6.

3.3.1.1.2. Angular spectral emittance ($\beta' = 25^\circ$): Fig 1-45.7.

3.3.1.2.1. Normal total emittance ($\beta' = 0$).

Effect of temperature on normal total emittance: Fig 1-45.8.

3.3.1.4. Hemispherical total emittance.

75-ST (Alclad) (Canadian commercial designation). Nominal composition (see p. 1-90.1).

Sample temperature: 303 K.

Unpolished surface. Measured in air.

$\epsilon = .02$ (Touloukian (1967)c). See Table 1-19.1, p. 1-90.11.

METALLIC MATERIALS
Aluminium - Zinc Alloys

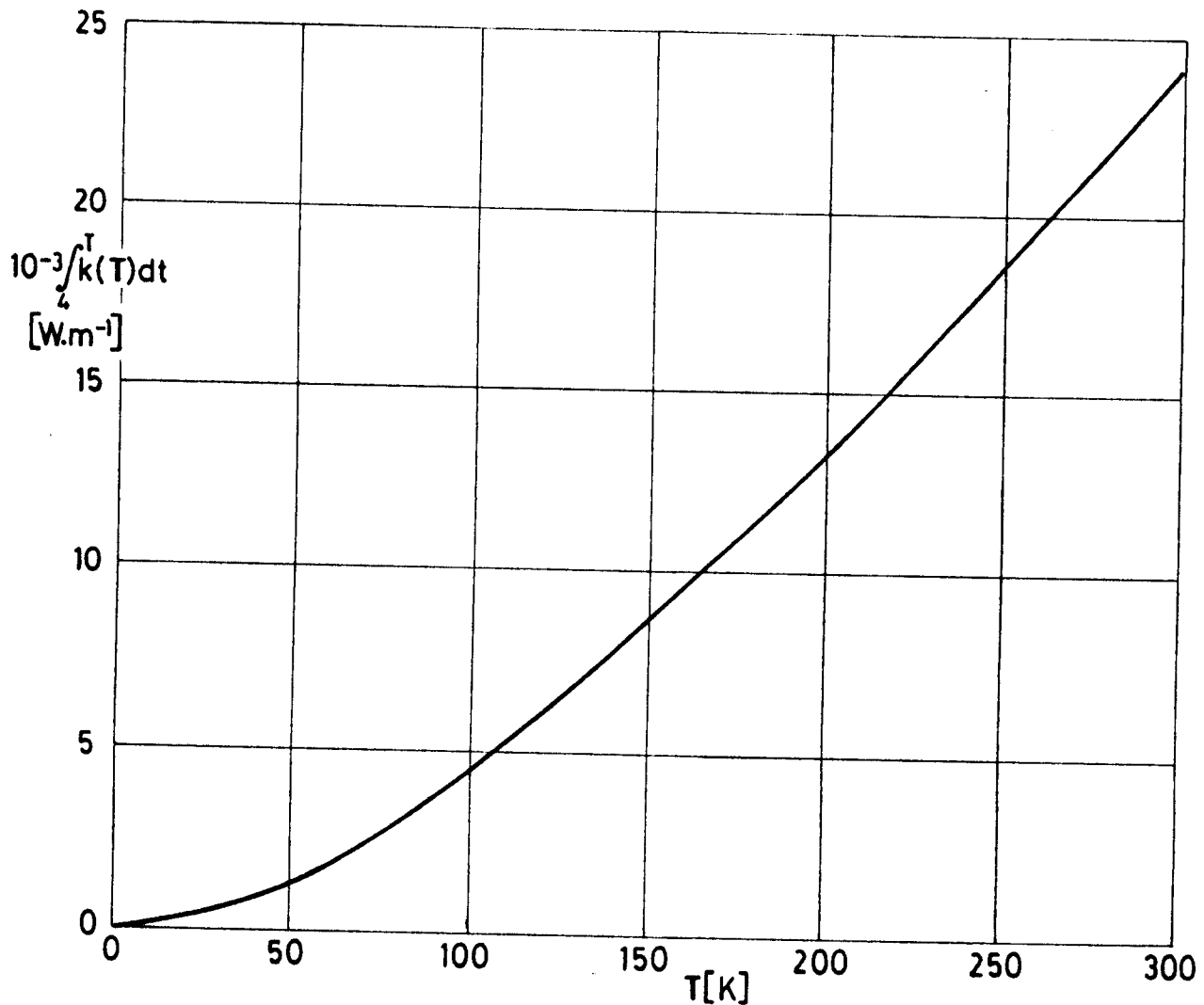


Fig 1-45.3. Thermal conductivity integral of Al - 5.7 Zn - 2.5 Mg - 1.6 Cu as a function of temperature, T.

Explanation

Description	Comments	References
Al alloy 75 S (Canadian commercial designation).		Coston (1967).

METALLIC MATERIALS
Aluminium - Zinc Alloys

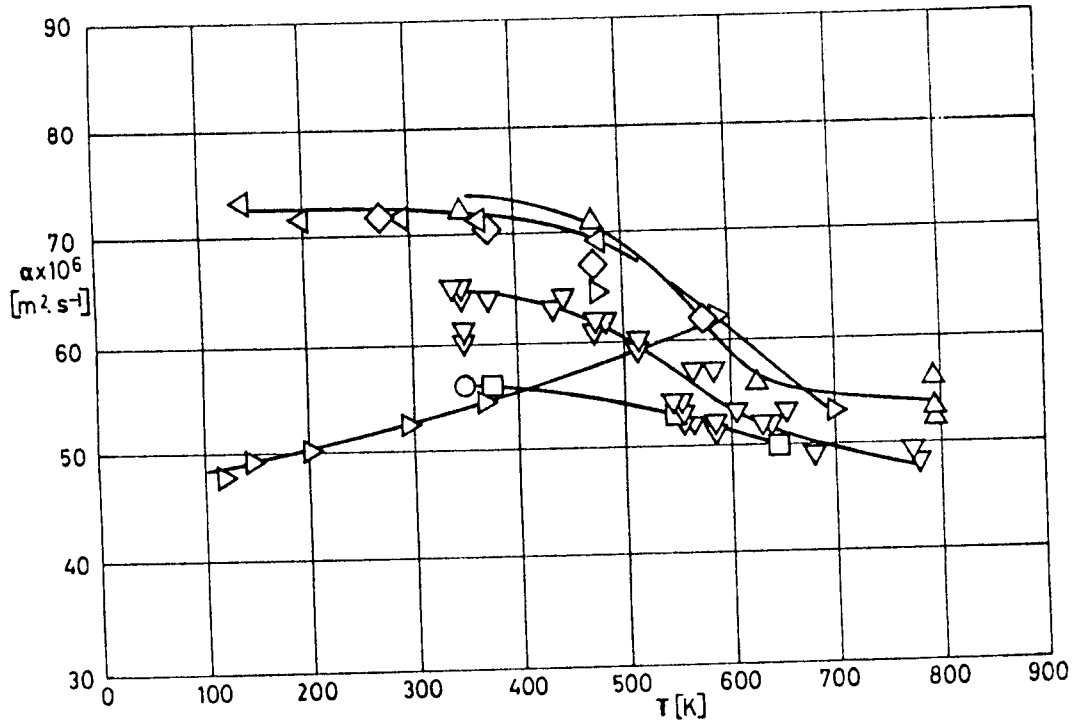


Fig 1-45.4. Thermal diffusivity, α , of Al - 5.7 Zn - 2.5 Mg - 1.6 Cu as a function of temperature, T.

Explanation

Key	Description	Comments	References
○	Al alloy 7075-T6. Nominal composition (see p. 1-90.1).	Measured after exposure to radiation and followed by cooling.	Touloukian (1967)c
◻	Same as ○.	Measured after another exposure to radiation and followed by cooling.	
△	Same as ○.	Measured after the third cycle of exposure.	
▽	Same as ○.	Averaged values on measurements after from 4th to 8th exposure cycles.	
▷	Al alloy 7075-T6. 5.6 Zn, 2.5 Mg, 1.6 Cu, Al balance.	As received.	
◁	Same as ▷.	Heated above 575 K.	
◊	Al alloy 75S (Canadian commercial designation). 5.5 Zn, 2.5 Mg, 1.5 Cu, .3 Cr, .2 Mn.	Annealed at 720 K.	

METALLIC MATERIALS
Aluminium - Zinc Alloys

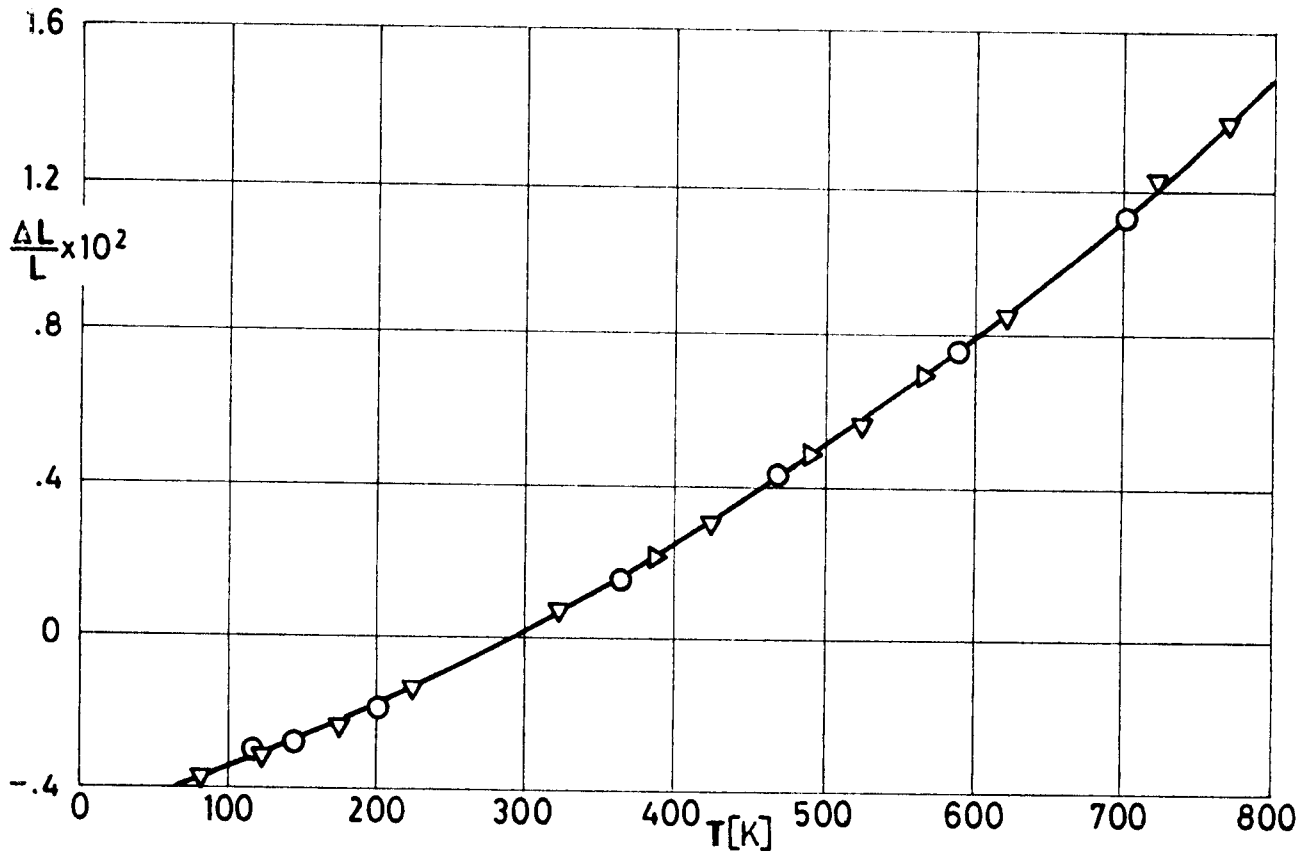


Fig 1-45.5. Linear thermal expansion, $\Delta L/L$, of Al - 5.7 Zn - 2.5 Mg - 1.6 Cu as a function of temperature, T.

Explanation

Key	Description	Comments	References
○	Al alloy 7075-T6 (Alcoa). 5.1-6.1 Zn, 2.1-2.9 Mg, 1.2-2.0 Cu, .7 Fe, .5 Si, Al balance.	Tested in vacuum.	Touloukian (1967)c.
▽	Al alloy 75S-T6 (Canadian commercial designation). 5.6 Zn, 2.5 Mg, 1.6 Cu, .3 Cr, Al balance. $\rho = 2800 \text{ kg.m}^{-3}$.	Tested at 1.5 - 2.5 K/min rise in argon.	
▷	Al alloy RR77 (British designation). 4.96 Zn, 2.54 Mg, 2.20 Cu, .54 Mn, .31 Fe, .26 Si and trace Ti, Al balance.	Wrought, 2 h solution heat treatment at 720 K, quenched in water at 340 K, aged 4 h at 408 K and aircooled.	

Rev. 2. 1984

METALLIC MATERIALS
Aluminium - Zinc Alloys

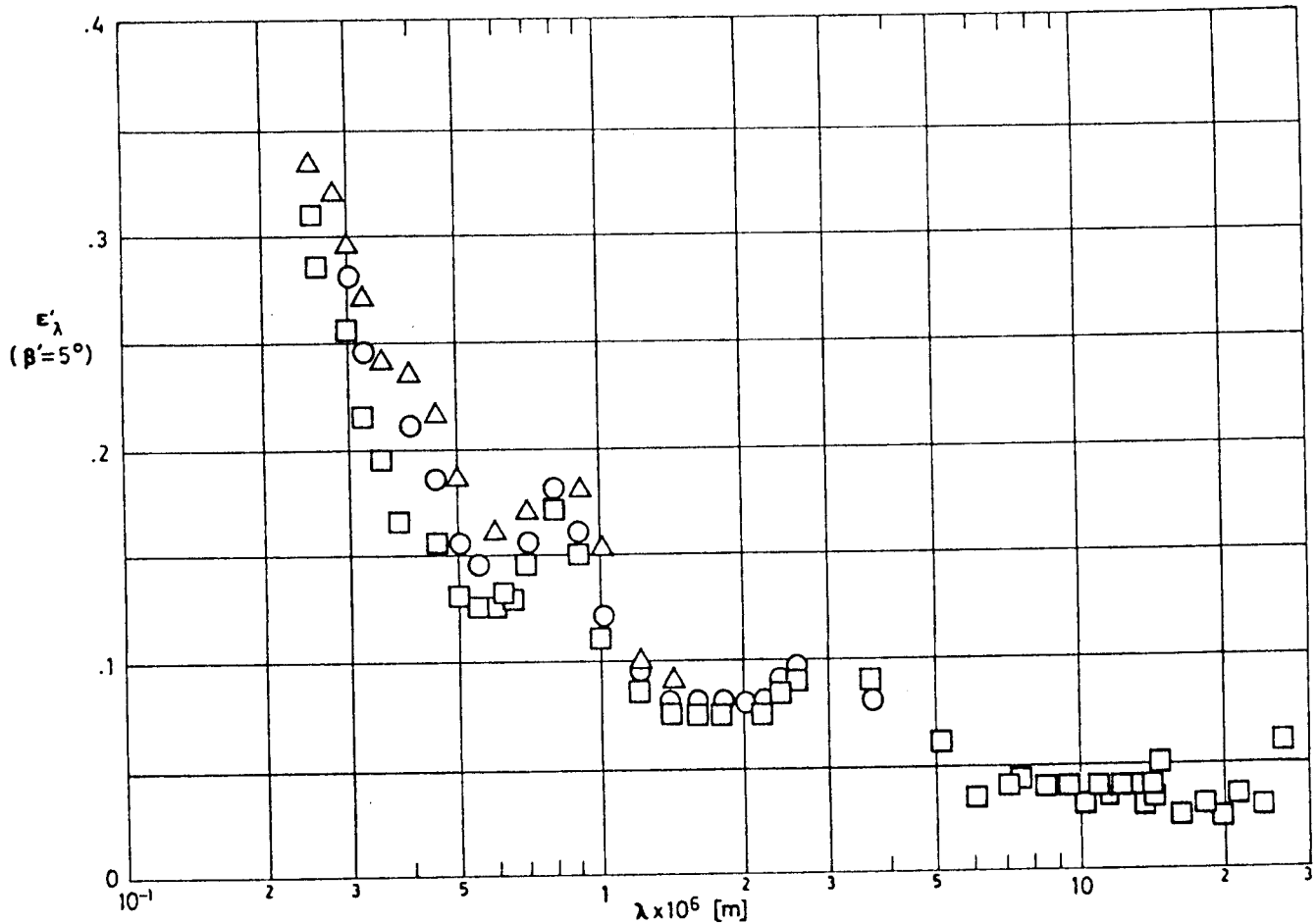


Fig 1-45.6. Normal spectral emittance, ϵ'_λ , of Al-5.7Zn-2.5Mg-1.6Cu as a function of wavelength, λ .

Explanation

Key	Description	Comments	References
○	Al alloy 7075. 5.6 Zn, 2.5 Mg, 1.6 Cu, .3 Cr, Al balance. Surface roughness $.081 \times 10^{-6}$ m - $.112 \times 10^{-6}$ m (center line average).	Sample temperature: T = 323 K. Measured in nitrogen. Computed by $\epsilon = 1-R(2\pi, 5^\circ)$.	Touloukian & DeWitt (1970)
□	Different sample, same as ○ specimen and conditions except surface roughness $.048 \times 10^{-6}$ m - $.064 \times 10^{-6}$ m (center line average).		
△	Different sample, same as ○ specimen and conditions except surface roughness $.081 \times 10^{-6}$ m - $.113 \times 10^{-6}$ m (center line average).		

METALLIC MATERIALS
Aluminium - Zinc Alloys

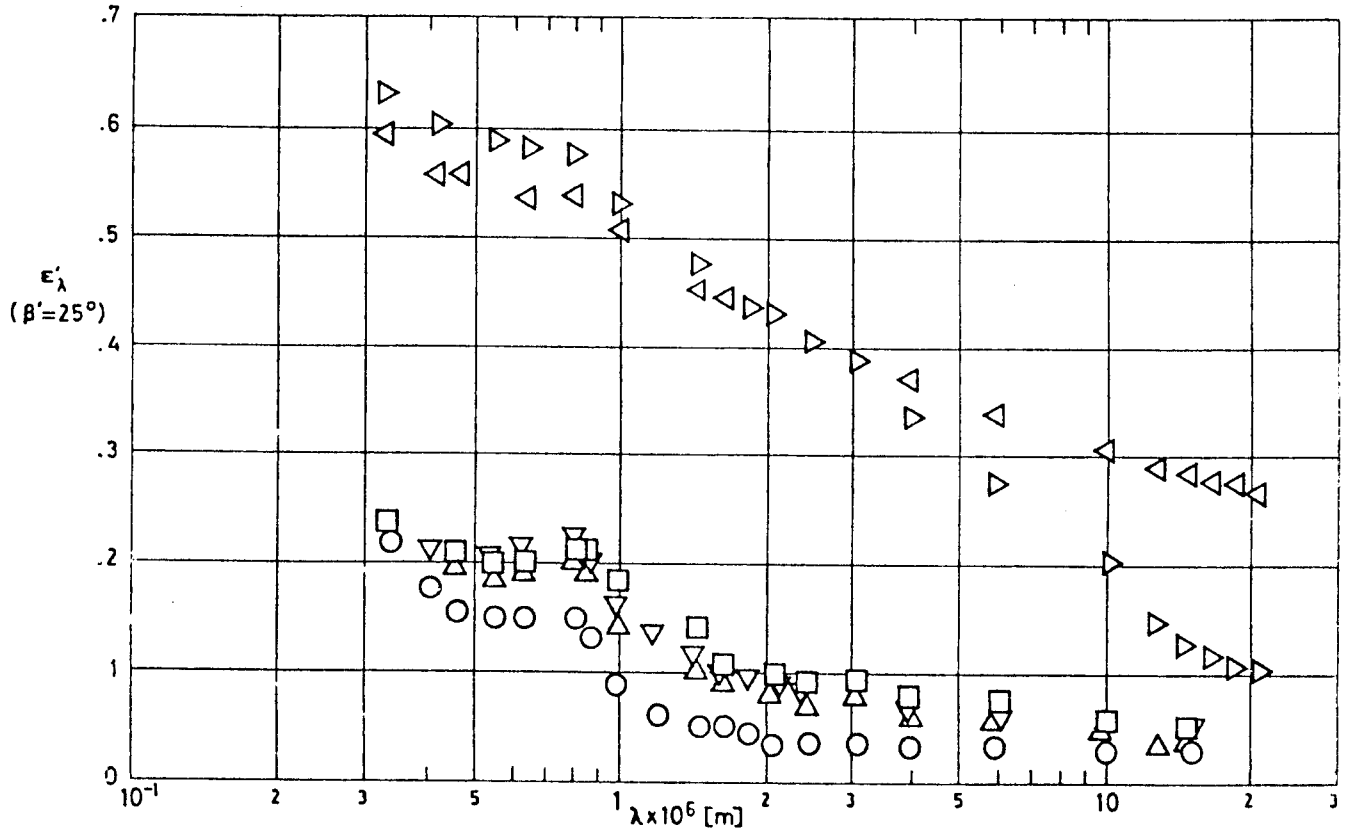


Fig 1-45.7. Angular spectral emittance, ϵ'_λ , of Al - 5.7 Zn - 2.5 Mg - 1.6 Cu as a function of wavelength, λ .

Explanation

Key	Description	Comments	References
○	Al alloy 7075-T6. 5.6 Zn, 2.5 Mg, 1.6 Cu, .3 Cr, Al balance. Polished. Surface roughness $.051 \times 10^{-6}$ m - $.102 \times 10^{-6}$ m (RMS).	Sample temperature: T = 306 K	Touloukian & DeWitt (1970).
□	Al alloy 7075-T6. 5.6 Zn, 2.5 Mg, 1.6 Cu, .3 Cr, Al balance. Sanded with 150 grit paper (grit sieve opening 104×10^{-6} m). Surface roughness: in line $.254 \times 10^{-6}$ m - $.381 \times 10^{-6}$ m, across 1.78×10^{-6} m - 2.29×10^{-6} m (RMS).	Authors assumed $\epsilon = \alpha = 1 - \rho(25^\circ, 2\pi)$	
△	Al alloy 7075-T6. 5.6 Zn, 2.5 Mg, 1.6 Cu, .3 Cr, Al balance. Sanded with 80 grit paper (grit sieve opening 175×10^{-6} m). Surface roughness: in line $.508 \times 10^{-6}$ m - 1.52×10^{-6} m, across 3.81×10^{-6} m - 4.32×10^{-6} m (RMS).		
▽	Al alloy 7075-T6. 5.6 Zn, 2.5 Mg, 1.6 Cu, .3 Cr, Al balance. Sanded with 40 grit paper (grit sieve opening 42×10^{-6} m). Surface roughness: in line 1.27×10^{-6} m - 2.54×10^{-6} m, across 6.86×10^{-6} m - 7.62×10^{-6} m (RMS).		
▷	Al alloy 7075-T6. 5.6 Zn, 2.5 Mg, 1.6 Cu, .3 Cr, Al balance. Sandblasted with 250 mesh silicon carbide (mesh opening 60×10^{-6} m). Surface roughness: $.254 \times 10^{-6}$ m - $.381 \times 10^{-6}$ m (RMS)		
◁	Al alloy 7075-T6. 5.6 Zn, 2.5 Mg, 1.6 Cu, .3 Cr, Al balance. Sandblasted with 60 mesh silicon carbide (mesh opening 250×10^{-6} m). Surface roughness: 6.35×10^{-6} m - 7.62×10^{-6} m (RMS).		

METALLIC MATERIALS
Aluminium - Zinc Alloys

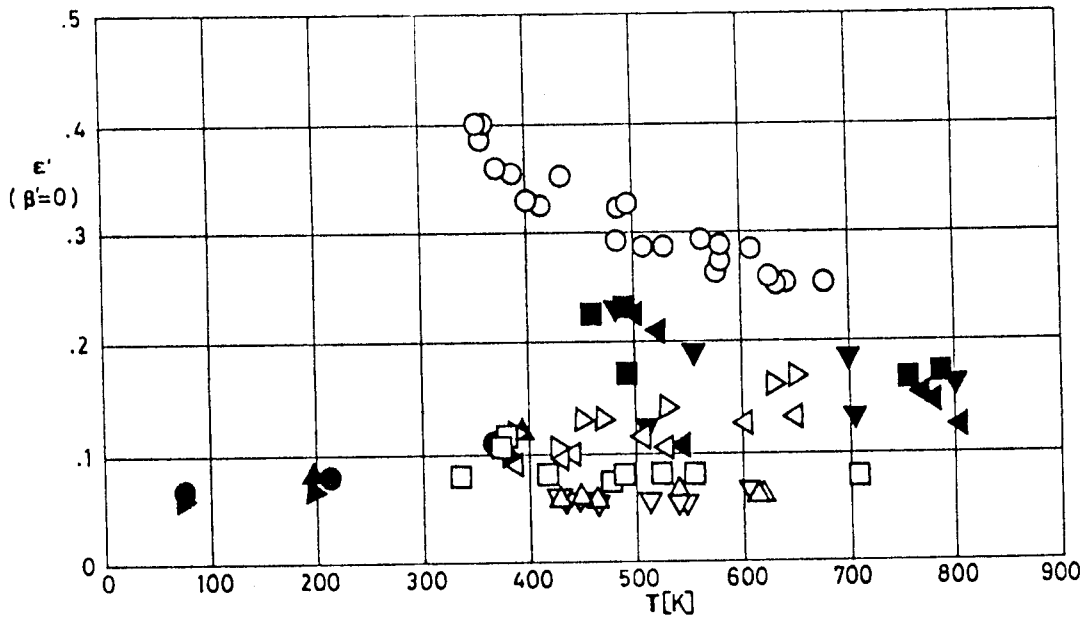


Fig 1-45.8. Normal total emittance, ϵ' , of Al-5.7Zn-2.5Mg-1.6Cu as a function of temperature, T.

Explanation

Key	Description	Comments	References
○	Al alloy 75-ST (alclad) (Canadian commercial designation). 5.6 Zn, 2.5 Mg, 1.6 Cu, .3 Cr, Al balance.	Effect of viewing configuration change was apparent.	Touloukian & DeWitt (1970).
□	Same as ○.	Another change in viewing configuration.	
△	Same as ○.	Another change in viewing configuration.	
▽	Different sample, same as ○ specimen and conditions. Unpolished.		
▷	Different sample, same as ○ specimen and conditions. Polished with aerobright and Bon Ami.		
◁	Same as ▷. Repeated measurement one day later.		
●	Al alloy 75-ST (alclad) (Canadian commercial designation). 5.6 Zn, 2.5 Mg, 1.6 Cu, .3 Cr, Al balance. Cleaned with methyl alcohol.	Heating. Measured in air (.133 Pa).	
■	Different sample, same as ● specimen and conditions.	Measured in argon (.133 Pa).	
▲	Different sample, same as ● specimen and conditions except scrubbed with Bon Ami and a wet cloth, washed and dried, wiped with toluene and alcohol.		
▼	Different sample, same as ▲ specimen and conditions.	Measured in argon (.133 Pa).	
▶	Different sample, same as ● specimen and conditions except polished and then finished with a wool buff and rouge and washed. Surface free from scratches.		
◀	Different sample, same as ▶ specimen and conditions.	Measured in argon (.133 Pa).	

METALLIC MATERIALS
Aluminium - Zinc Alloys

Table 1-19.1

Hemispherical Total Emittance of Al - 5.7 Zn - 2.5 Mg - 1.6 Cu Conversion Coatings.

T [K]	ϵ	Comments
293	.234	Alodined Al alloy 7075-T6, 5.6 Zn, 2.5 Mg, 1.6 Cu, .3 Cr, Al balance. Substrate sandblasted. Measured in vacuum (6.67×10^{-4} Pa).
259	.117	Similar to above specimen and conditions except substrate alclad.
273	.100	Similar to above specimen and conditions except substrate smooth and unclad.
307	.091	
313	.091	
217	.790	Al alloy 7075-T6 Martin Hardcoate anodize. 5.6 Zn, 2.5 Mg, 1.6 Cu, .3 Cr, Al balance. Measured in vacuum (6.67×10^{-4} Pa).
242	.849	
285	.869	
313	.856	

From Touloukian, DeWitt & Hernicz (1972).

3.3.2. Absorptance.

3.3.2.5. Solar absorptance.

3.3.2.5.1. Normal solar absorptance: Table 1-19.2 overleaf.

3.3.3. Reflectance.

3.3.3.2.1. Normal-hemispherical spectral reflectance ($\beta = 0$, $\omega' = 2\pi$): Fig 1-45.9.

3.3.3.9.1. Normal-hemispherical solar reflectance. See Table 1-19.2 overleaf.

Rev. 2. 1984

METALLIC MATERIALS
Aluminium - Zinc Alloys

Table 1-19.2

Normal Solar Absorptance and Normal-Hemispherical Solar Reflectance of Al - 5.6 Zn - 2.5 Mg - 1.6 Cu.

T [K]	β°	α_s	ρ'_s	Comments
311	~ 0	.46	.538	Al alloy 75-ST (Canadian commercial designation). 5.6 Zn, 2.5 Mg, 1.6 Cu, .3 Cr, Al balance. Heated to 324 K. Clean and smooth surface. α_s measured in air at sea level. ρ'_s from α_s .
311	~ 0	.61	.391	Above specimen and conditions except reheated to 559 K.
311	~ 0	.64	.358	Above specimen and conditions except reheated to 795 K.
311	~ 0	.34	.659	Different sample. Same specimen and conditions as in the first case except heated to 314 K. Polished. Surface free from scratches.
311	~ 0	.24	.756	Above specimen and conditions except reheated to 567 K.
311	~ 0	.51	.489	Above specimen and conditions except reheated to 783 K.
311	~ 0	.59	.409	Different sample. Same specimen and conditions as in the first case except heated to 319 K. Cleaned with methyl alcohol.
311	~ 0	.66	.341	Above specimen and conditions except reheated to 617 K.
311	~ 0	.63	.371	Above specimen and conditions except reheated to 755 K.
298	~ 0		.67	Al alloy 75-ST (Canadian commercial designation). 5.6 Zn, 2.5 Mg, 1.6 Cu, .3 Cr, Al balance. Measured in air.

From Touloukian & DeWitt (1970).

METALLIC MATERIALS
Aluminium - Zinc Alloys

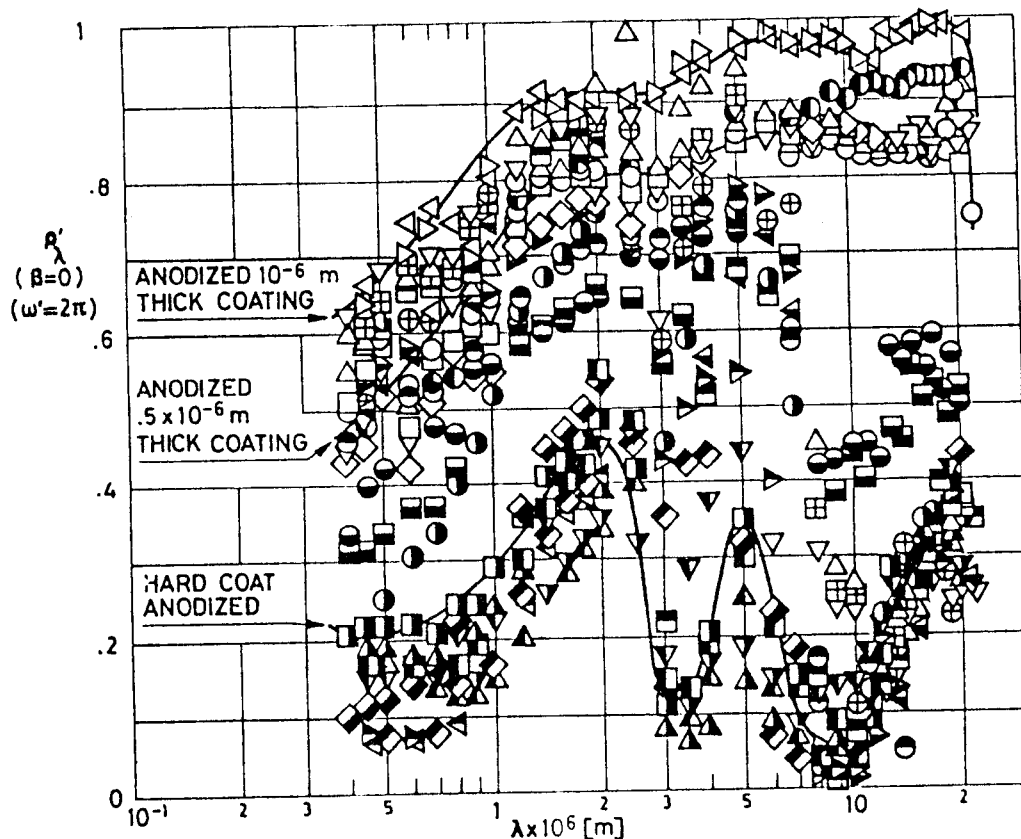


Fig 1-45.9. Normal-hemispherical spectral reflectance, R'_λ , of Al-5.7Zn-2.5Mg-1.6Cu conversion coatings, as a function of wavelength, λ .

Explanation

Key	Description	Comments	References
○	Al alloy 7075. Nominal composition (see p. 1-90.1).	Sample temperature: $T = 298$ K. Mechanically and electropolished, boric acid anodized, 10^{-6} m thick coating. Measured in $\sim 10^{-4}$ Pa vacuum. Converted from $R(2\pi, 0^\circ)$.	Touloukian (1967)c. Touloukian, DeWitt & HERNICZ (1972).
△	Same as ○.	$T = 422$ K. Same specimen and conditions as ○.	
□	Same as ○.	$T = 589$ K. Same specimen and conditions as ○.	
▽	Same as ○.	$T = 714$ K. Same specimen and conditions as ○.	
◇	Same as ○.	$T = 298$ K. Same specimen and conditions as ○ after high temperature runs.	
◁	Same as ○.	$T = 298$ K. Treated as ○, except shorted anodizing time (1/3 standard). $.5 \times 10^{-6}$ m thick coating.	
▷	Same as ○.	$T = 298$ K. Mechanically polished and boric acid anodized. Measured in $\sim 10^{-4}$ Pa vacuum. Converted from $R(2\pi, 0^\circ)$.	
●	Same as ○.	$T = 298$ K. Mill finished, electropolished and boric acid anodized. Measured in 1.33×10^{-1} Pa vacuum.	

Rev. 2. 1984

METALLIC MATERIALS
Aluminium - Zinc Alloys

Key	Description	Comments	References
▲	Al alloy 7075. 5.1-6.1 Zn, 2.1-2.9 Mg, 1.2-2.0 Cu, .7 Fe, .5 Si, .18-.4 Cr, .3 Mn, .2 Ti, Al balance.	T = 298 K. Mechanically polished and electropolished, hard coat anodized. Measured in $\sim 10^{-4}$ Pa vacuum. Converted from $R(2\pi, 0^\circ)$.	Touloukian (1967)c. Touloukian, DeWitt & Hernicz (1972).
■	Same as ▲.	T = 298 K. Treated as ▲ and sealed.	
▼	Same as ▲.	T = 422 K. Same specimen and conditions as ■.	
◆	Same as ▲.	T = 589 K. Same specimen and conditions as ■.	
◀	Same as ▲.	T = 714 K. Same specimen and conditions as ■.	
▶	Same as ▲.	T = 298 K. Same specimen and conditions as ■ after high temperature runs.	
▣	Same as ▲.	T = 298 K. Treated as ▲ and heated in air at 700 K for 30 min.	
●	Same as ▲.	T = 298 K. Mechanically polished and electropolished, hard coat anodizing (1/3 standard time).	
▲	Al alloy 7075.	T = 298 K. Mill finished and electropolished, hard coat anodized, sealed. Measured in $\sim 10^{-4}$ Pa vacuum. Converted from $R(2\pi, 0^\circ)$.	
▼	Al alloy 7075.	T = 298 K. Mechanically polished hard coat anodized. Measured in $\sim 1.33 \times 10^{-4}$ Pa vacuum. Converted from $R(2\pi, 0^\circ)$.	
◆	Al alloy 7075.	T = 298 K. Treated as ▼ except shorter anodizing (1/3 standard) and sealed.	
◀	Al alloy 7075.	T = 298 K. Mechanically and electropolished, sulfuric acid anodized, sealed. Measured in $\sim 10^{-4}$ Pa vacuum. Converted from $R(2\pi, 0^\circ)$.	
▶	Same as ◀.	T = 422 K. Same specimen and conditions as ◀.	
●	Same as ◀.	T = 589 K. Same specimen and conditions as ◀.	
●	Same as ◀.	T = 714 K. Same specimen and conditions as ◀.	
▣	Same as ◀.	T = 298 K. Same specimen and conditions as ◀ after high temperature runs.	
▣	Al alloy 7075.	T = 298 K. Mechanically and electropolished, sulfuric acid anodized, 1.4×10^{-6} m thick coating, sealed. Measured in $\sim 10^{-4}$ Pa vacuum. Converted from $R(2\pi, 0^\circ)$.	
⊕	Al alloy 7075.	T = 298 K. Same as ▣ except not sealed.	
▲	Al alloy 7075.	T = 298 K. Same as ⊕ except shorter anodizing time (1/4 standard).	
▼	Al alloy 7075.	T = 298 K. Same as ▲ and sealed.	
⊕	Al alloy 7075.	T = 298 K. Mechanically polished, sulfuric acid anodized 1/3 standard time, sealed. Measured in $\sim 10^{-4}$ Pa vacuum. Converted from $R(2\pi, 0^\circ)$.	

METALLIC MATERIALS
Aluminium - Zinc Alloys

3.4. Other physical properties

3.4.1. Electrical resistivity (at room temperature).

Condition	T6	T73	T76
$\sigma^{-1} \times 10^6$ [$\Omega \cdot m$]	.052	.043	.045

From McCall (1979).

4. ENVIRONMENTAL BEHAVIOR4.1. Prelaunch

This alloy is normally coated. The surface condition is as important as the material. The production of the coating must be carefully controlled.

4.2. Postlaunch

No known restrictions other than structural.

5. CHEMICAL PROPERTIES5.1. Solution potential (vs. decinormal calomel electrode).

Condition	T6	T73	T76
Sol.Pot. [V] ^a	-.83	-.84	-.84

^a Varies $\pm .02$ V with quenching rate.

From McCall (1979).

5.2. Corrosion resistance

This alloy should be protected at least on faying surfaces.

Rev. 2. 1984

METALLIC MATERIALS
Aluminium - Zinc Alloys

Condition	Stress-Corrosion Cracking
T6, T651, T652, T6510, T6511	Service failures with sustained tension stress acting on short transverse direction relative to grain structure. Limited failures in laboratory tests of long transverse specimens.
T73, T7351	No known instance of failure in service. Limited failures in laboratory tests of short transverse specimens.

From McCall (1979).

Assemblies of this alloy with magnesium alloys require protective insulation (Braun (1979)).

6. FABRICATION

6.2. Forming. Cold workability is poor.

6.3. Welding

Gas. No commonly used methods have been developed.

Arc. Limited weldability because of crack sensitivity or loss in resistance to corrosion and mechanical properties.

Resistance Spot and Seam. Weldable with special techniques or for specific applications which justify trials or development testing.

Brazing. No commonly used methods have been developed.

Soldering. Solderability is poor.

These characteristics do not change significantly with heat treatment.

From McCall (1979).

6.4. Machining. Machinability of this alloy is good (compared to others of the same series) and can be improved through heat treatment.

METALLIC MATERIALS
Aluminium - Zinc Alloys

6.5. Heat treatment

Treatment	Forging	Annealing	Quenching and Aging	
			Quenching	Aging
Usual temperatures and times.	650 K - 720 K	Full annealing: 690 K, followed by 6 h at 500 K for long term storage. Stress relieve annealing: 610 K.	738 K \pm 5 K in water	24 h at 393 K \pm 5 K.

From UNE (1982).

6.6. Anodizing. This alloy can be anodized to increase corrosion resistance, prior to painting or plating, or to increase emittance (see p. 1-90.11). Any of the three principal types of anodizing processes (chromic acid, sulfuric acid or hard anodizing) can be used (Ball (1982)).

7. AVAILABLE FORMS AND CONDITIONS

This alloy is available in the full commercial range of sizes for sheets; plates; extruded rods, bars and wires; extruded shapes; extruded tubes; cold finished rods, bars and wires; drawn tubes and forgings (McCall (1979)).

8. USEFUL TEMPERATURE RANGE

The tensile strength of this alloy (T6) decreases markedly above 400 K (McCall (1979)).

This alloy is not normally used in applications involving cryogenic temperatures. Information on its behavior at low temperatures is scanty. Tensile properties and fracture roughness at temperatures down to 4 K and results of fatigue-life tests are

Rev. 2. 1984

METALLIC MATERIALS

Aluminium - Zinc Alloys

given by Campbell (1980). Other alloys of the Aluminium 7000 series exhibit good behavior at temperatures as low as 20 K (Develay et al. (1967)).

9. APPLICATIONS

Aircraft and other structures, many presently operating commercial jets (Simenz & Guess (1980)).

Aircraft structural parts and other highly stresses structural applications where very high strength and good resistance to corrosion is required.

Caution should be exercised in T6 temper applications where sustained tensile stresses are encountered, either residual or applied, particularly in the transverse grain direction. In such instances the T73 temper should be considered at some sacrifice in tensile strength (McCall (1979)).

10. OTHER QUOTATIONS

These alloys have been explicitly quoted in the following pages of this Handbook.

p. F 2-9 Al alloy 7075-T6

Thermal joint conductance. Bare joints.

p. P 1-14 Al alloy 7075

Used in bellows for louver actuators.

p. R 2-67 Al alloy 7075

Figure of Merit, σ/k , of supporting materials at cryogenic temperatures.

METALLIC MATERIALS

Aluminium - Zinc Alloys

- p. R 4-113 Al alloy 75 S (Canadian commercial designation)
Thermal conductivity in the temperature range
25 K - 300 K.
- p. R 5-23 Al alloy V95 (USSR designation)
Data sources of mechanical properties at cryogenic
temperatures.
- p. R 5-35 Al alloy 7075-T73
Susceptibility to hydrogen embrittlement.

G 1-110

ESA PSS-03-108 Issue 1 (November 1989)

Rev. 2. 1984

INTENTIONALLY BLANK PAGE

METALLIC MATERIALS
Magnesium-Zinc-Thorium Alloys

1.6. MAGNESIUM-ZINC-THORIUM ALLOYS

ALLOY Mg - 5.7 Zn - 1.8 Th - .7 Zr.

1. TYPICAL COMPOSITION, PERCENT

Cu	Ni	Th	Zn	Zr	Others	Mg
-	-	1.4	5.2	.5	-	Balance
.10	.01	2.2	6.2	1	.30	

2. OFFICIAL DESIGNATIONS

AECMA	ISO	AFNOR	AMS	BS	DIN
			4438B		MgZn6Th2Zr, 3.5114

3. PHYSICAL PROPERTIES3.1. Density. $\rho = 1860 \text{ kg.m}^{-3}$. (Rhines (1961)).3.2. Thermal properties

3.2.1. Specific heat.

From 293 K to 373 K, $c = 962 \text{ J.kg}^{-1}.\text{K}^{-1}$. (Rhines (1961)).

3.2.2. Thermal conductivity.

T [K]	293	320	395	445
$[\text{W.m}^{-1}.\text{K}^{-1}]$	109 ^a	113 ^b	123 ^b	127 ^b

^a From Rhines (1961).^b From Touloukian (1967)c.

3.2.4. Thermal expansion.

Mean coefficient of linear thermal expansion, β .

From 293 K to 473 K, $\beta = 27.1 \times 10^{-6} \text{ K}^{-1}$. (Rhines (1961)).

$\beta = 27.6 \times 10^{-6} \text{ K}^{-1}$. (Smithells (1962)).

$\beta = 27.2 \times 10^{-6} \text{ K}^{-1}$. (ASMH (1974)d).

METALLIC MATERIALS

Magnesium-Zinc-Thorium Alloys

3.2.5. Melting range.

773 K - 903 K. (Smithells (1962)).

3.3. Thermal radiation properties

3.3.1. Emittance.

3.3.1.2. Normal total emittance ($\beta'=0$).

No data available. For polished Magnesium: $\epsilon'=.07$. (Scollon & Carpitella (1970)).

3.3.2. Absorptance.

3.3.2.5. Solar absorptance.

3.3.2.5.1. Normal solar absorptance.

No data available. For polished Magnesium: $\alpha_s=.27$.
(Scollon & Carpitella (1970)).

3.4. Other physical properties3.4.1. Electrical resistivity at 293 K. $\sigma^{-1}=6.5 \times 10^{-8} \Omega.m$. (Rhines (1961)).5. CHEMICAL PROPERTIES

5.2. Corrosion resistance.

Although this alloy will corrode in industrial, marine and moist environments, it will perform satisfactorily with suitable surface protection and painting. (ASMH (1974)d).

6. FABRICATION6.1. Casting. Good, even into complicated shapes.6.3. Welding. Good, by argon arc process. Should not be gas-welded.6.4. Machining. Excellent. This alloy can be chemically milled by sulphuric, nitric or hydrochloric acids of 5 percent strength.

METALLIC MATERIALS
Magnesium-Zinc-Thorium Alloys

6.5. Heat treatment. Good in SO₂ atmosphere. This alloy is normally used in T-5 condition.

From ASMH (1974) d.

7. AVAILABLE FORMS AND CONDITIONS

Sand, permanent mold and die castings. Normally used in T-5 condition. (ASMH (1974) d).

8. USEFUL TEMPERATURE RANGE

This alloy shows excellent structural characteristics up to 425 K. Above this temperature the strength drops sharply.

9. APPLICATIONS

This alloy should be considered for any aerospace application requiring a high strength-to-weight ratio at temperatures up to 420 K. In addition, it has excellent dimensional stability at service temperatures up to the quoted value. (ASMH (1974) d).

Safety precautions should be directed to the prevention of fires, burns, and explosions. (ASMH (1974) d).

INTENTIONALLY BLANK PAGE

METALLIC MATERIALS
Titanium-Aluminium-Tin Alloys

1.7. TITANIUM-ALUMINIUM-TIN ALLOYS

ALLOY Ti - 5 Al - 2.5 Sn.

1. TYPICAL COMPOSITION, PERCENT

Al	C	Fe	H	N	O	Sn	Ti
4	-	-	-	-	-	2	Balance
6	.1	.5	.02	.07	.3	3	

2. OFFICIAL DESIGNATIONS

AECMA	ISO	AFNOR	AMS	BS	DIN
			4926		

3. PHYSICAL PROPERTIES3.1. Density. $\rho = 4\,460 \text{ kg.m}^{-3}$. (Stuart Lyman (1961)).3.2. Thermal properties

3.2.1. Specific heat.

Effect of temperature on specific heat: Fig 1-46.

3.2.2. Thermal conductivity.

Effect of temperature on thermal conductivity: Fig 1-47.

3.2.4. Thermal expansion.

Mean coefficient of linear thermal expansion, β , between 293 K and given temperature.

T [K]	366	477	588	700	811	922	1033	1144	1255
$\beta \times 10^6$ [K ⁻¹]	9.4	9.4	9.5	9.5	9.7	9.9	10.1	10.3	10.3

From Stuart Lyman (1961)).

Effect of temperature on thermal expansion: Fig 1-48.

3.2.5. Melting range.

1 822 K - 1922 K. (Stuart Lyman (1961)).

METALLIC MATERIALS

Titanium-Aluminium-Tin Alloys

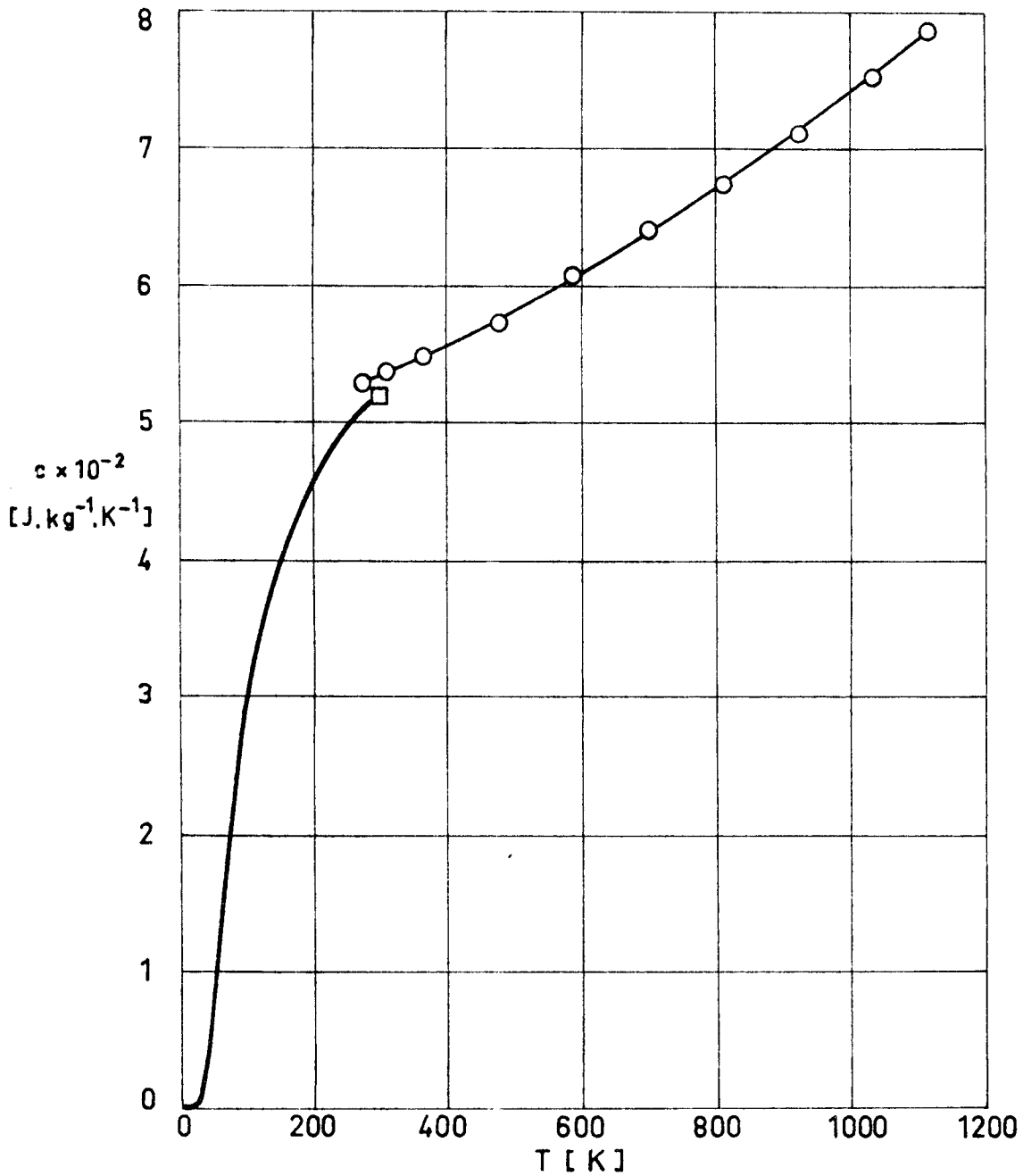


Fig 1-46. Specific heat, c , of Ti - 5 Al - 2.5 Sn as a function of temperature, T .

Explanation

Key	Description	Comments	References
○	Nominal composition.		Stuart Lyman (1961).
□	Nominal composition.		Coston (1967).
—	Titanium.		Coston (1967).

METALLIC MATERIALS
Titanium-Aluminium-Tin Alloys

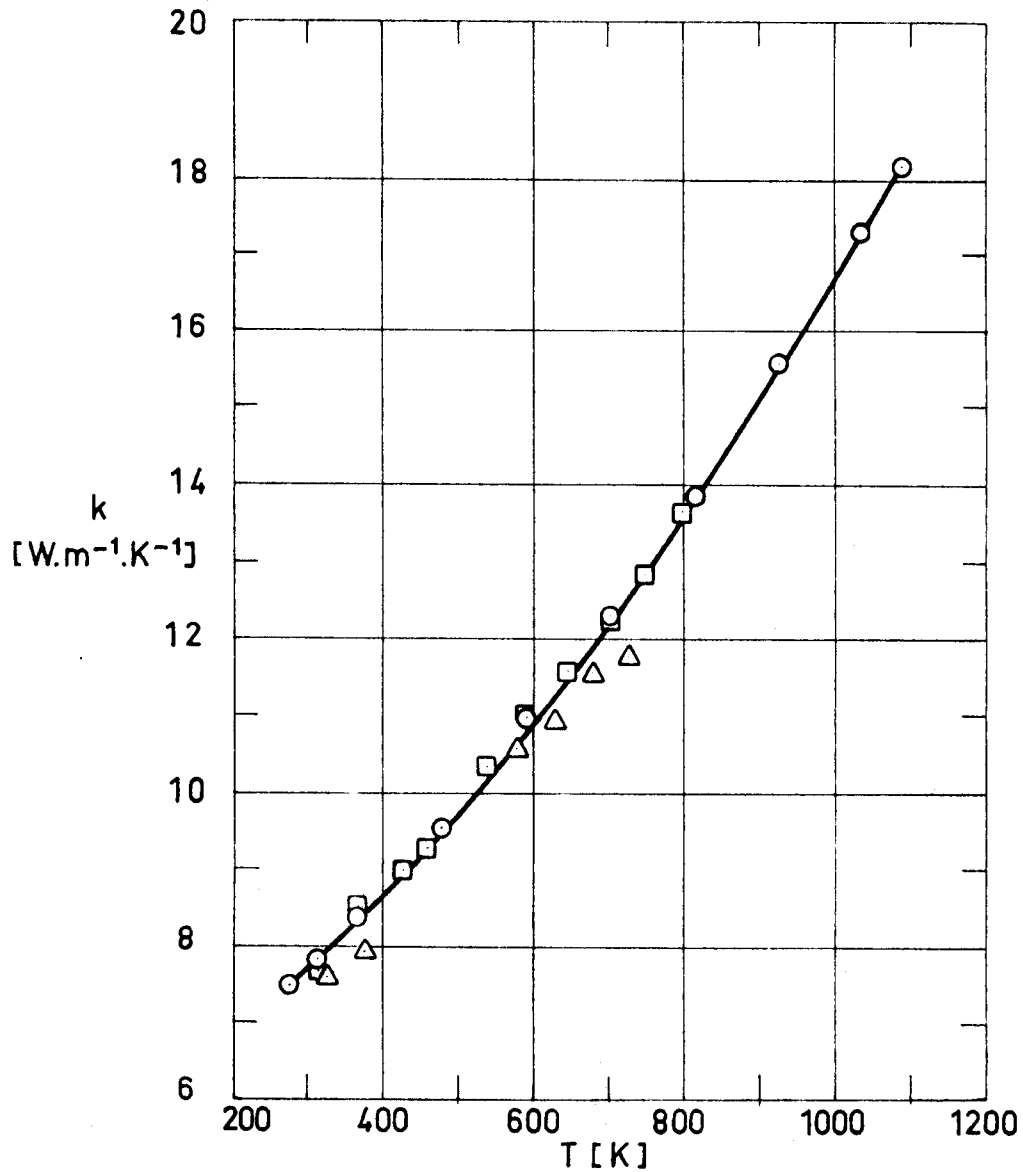


Fig 1-47. Thermal conductivity, k , of Ti - 5 Al - 2.5 Sn as a function of temperature, T .

Explanation

Key	Description	Comments	References
○	Nominal composition		Stuart Lyman (1961).
□	Nominal composition. Mild annealed.	Reported error ±5%.	Touloukian (1967)c.
△	Nominal composition.		

METALLIC MATERIALS
Titanium-Aluminium-Tin Alloys

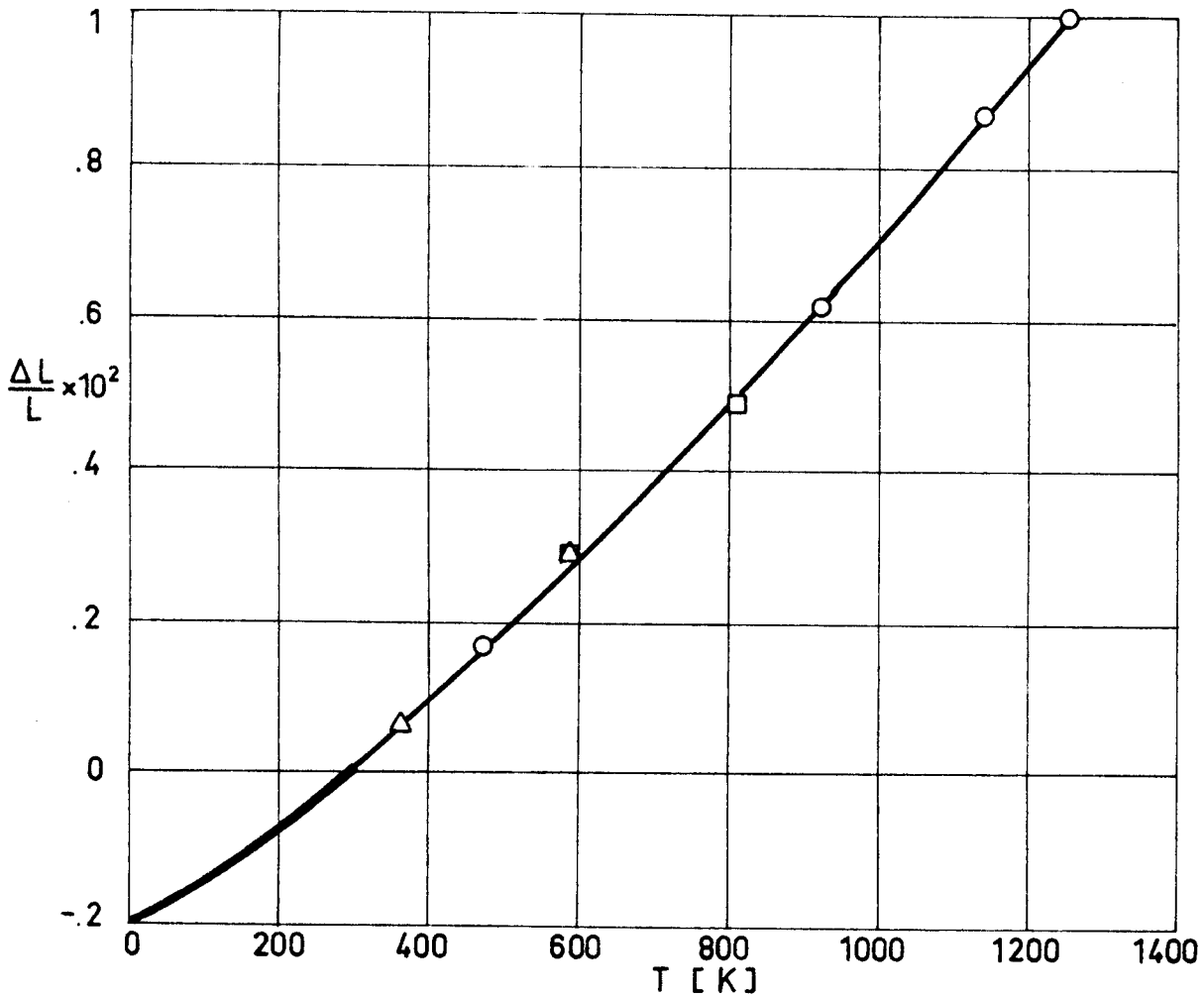


Fig 1-48. Thermal linear expansion, $\Delta L/L$, of Ti - 5 Al - 2.5 Sn as a function of temperature, T.

Explanation

Key	Description	Comments	References
○	Nominal composition.		Touloukian (1967)c.
□	Nominal composition. Density 4 460 - 4 480 kg.m ⁻³ . Alpha phase.		
△	Same as above except low oxygen content.		
—	Nominal composition.		Coston (1967).

METALLIC MATERIALS
Titanium-Aluminium-Tin Alloys

3.3. Thermal radiation properties

3.3.1. Emittance.

3.3.1.1. Normal spectral emittance ($\beta'=0$).

Effect of temperature on normal emittance for a particular wavelength: Fig 1-49.

3.3.1.2. Normal total emittance ($\beta'=0$).

Effect of temperature on normal total emittance: Fig 1-50.

3.3.2. Absorptance.

3.3.2.5. Solar absorptance.

3.3.2.5.1. Normal solar absorptance: Table 1-19.

Table 1-19

Normal Solar Absorptance of Ti - 5 Al - 2.5 Sn

T [K]	β°	α_s	Comments
298	9	.592	As received; computed from spectral reflectance data for sea level conditions. Mentioned below as specimen 1.
298	9	.588	Above specimen and conditions except computed for above atmosphere conditions.
298	9	.489	Different sample, same as 1 specimen and conditions except cleaned.
298	9	.486	Above specimen and conditions except computed for above atmosphere conditions.
298	9	.759	Different sample, same as 1 specimen and conditions except oxidized. Mentioned below as specimen 2.
298	9	.730	Above specimen and conditions except computed for above atmosphere conditions.
298	9	.511	Different sample, same as 2 specimen and conditions except polished.

From Touloukian & DeWitt (1970).

METALLIC MATERIALS

Titanium-Aluminium-Tin Alloys

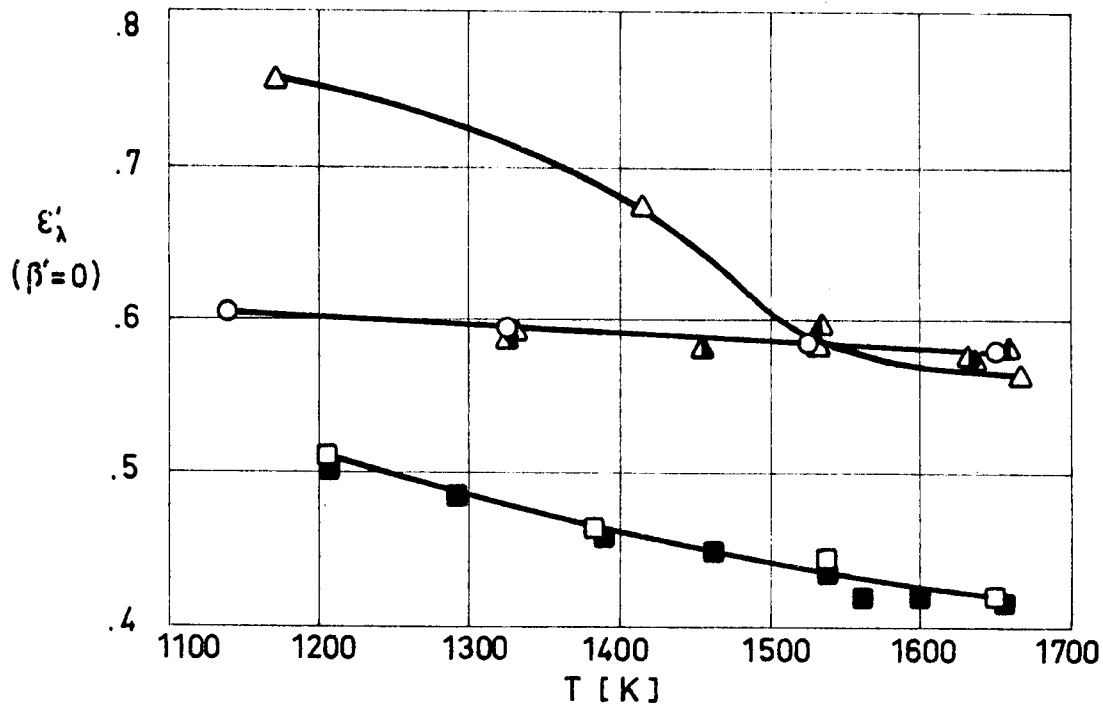


Fig 1-49. Normal spectral emittance, ϵ'_λ , of Ti - 5 Al - 2.5 Sn as a function of temperature, T, for $\lambda=6.65 \times 10^{-7}$ m.

Explanation

Key	Description	Comments	References
○	As received. Cleaned with liquid detergent.	Measured in vacuum (6.65×10^{-2} Pa). Increasing temperature.	Touloukian & DeWitt (1970).
□	Same as ○ except polished.		
■	Same as □ . Cycle 2.		
△	Same as ○ except oxidized in air at red heat for 30 min.		
▲	Same as △ . Cycle 2.		
▲	Same as △ . Cycle 3.		

METALLIC MATERIALS
Titanium-Aluminium-Tin Alloys

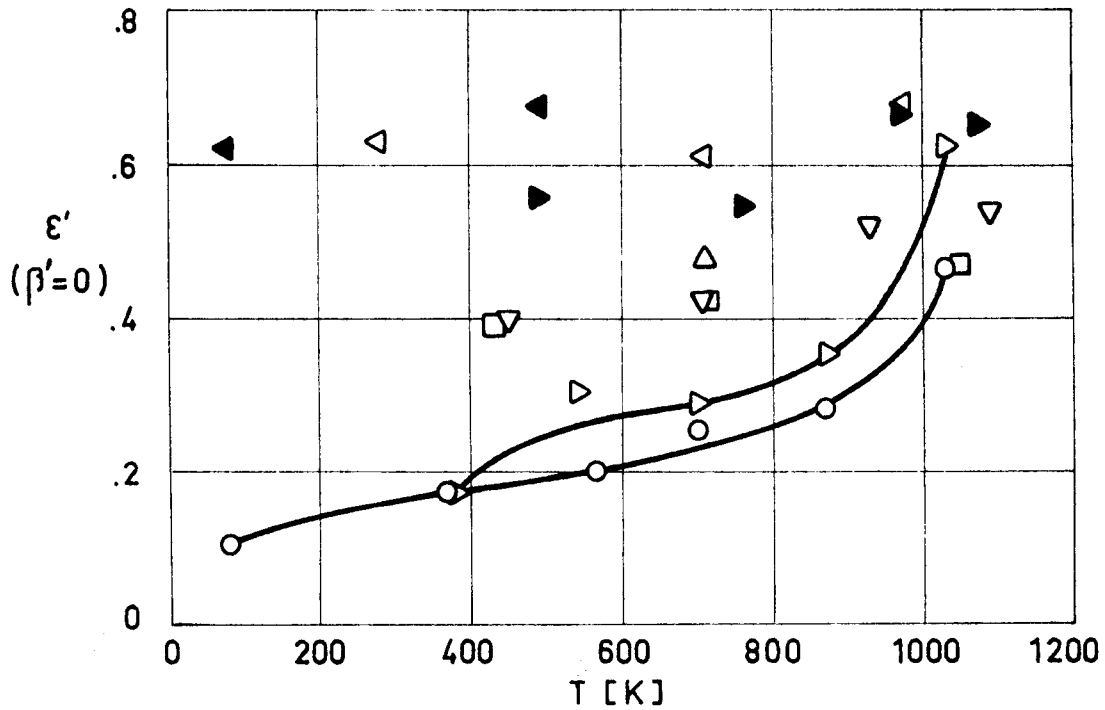


Fig 1-50. Normal total emittance, ϵ' , of Ti - 5 Al - 2.5 Sn as a function of temperature, T.

Explanation

Key	Description	Comments	References
○	Nominal composition. Polished.	Measured in air. Cycle 1.	Touloukian (1967)c.
□	Same as ○ .	Cycle 2 heating.	
△	Same as ○ .	Cycle 2 cooling.	
▽	Same as ○ .	Cycle 3.	
▷	Nominal composition. Oxidized at 922 K for 30 min.	Measured in air. Cycle 1.	
▶	Same as ▷ .	Cycle 2.	
◁	Same as ▷ .	Cycle 3 heating.	
◀	Same as ▷ .	Cycle 3 cooling.	

METALLIC MATERIALS

Titanium-Aluminium-Tin Alloys

3.3.3. Reflectance.

3.3.3.1. Bidirectional spectral reflectance.

Normal-normal spectral reflectance ($\beta=\beta'=0$): Fig 1-51.

3.3.3.2. Directional-hemispherical spectral reflectance.

Normal-hemispherical spectral reflectance ($\beta=0, \omega'=2\pi$):
Fig 1-52.

Effect of anodizing on normal-hemispherical spectral reflectance: Fig 1-53.

3.4. Other physical properties

3.4.1. Electrical resistivity.

Effect of temperature on electrical resistivity: Fig 1-54.

3.4.2. Magnetic properties. This alloy is non-magnetic.

Relative permeability: $\frac{\mu}{\mu_0} = 1.00005$ measured at 1.6×10^3 A.m⁻¹.
(ASMH (1974) e).

5. CHEMICAL PROPERTIES5.1. Solution potential (vs. decinormal calomel electrode)

Data not available. Solution potential of Ti pure is +.20 V
(Ross (1972)).

5.2. Corrosion resistance

This alloy is highly resistant to corrosion. It has excellent resistance to hot oxidation up to 900 K. It resists the attack by normal acids (except fuming nitric) or alkalies at room and even higher temperatures. (Ross (1972)).

METALLIC MATERIALS
 Titanium-Aluminium-Tin Alloys

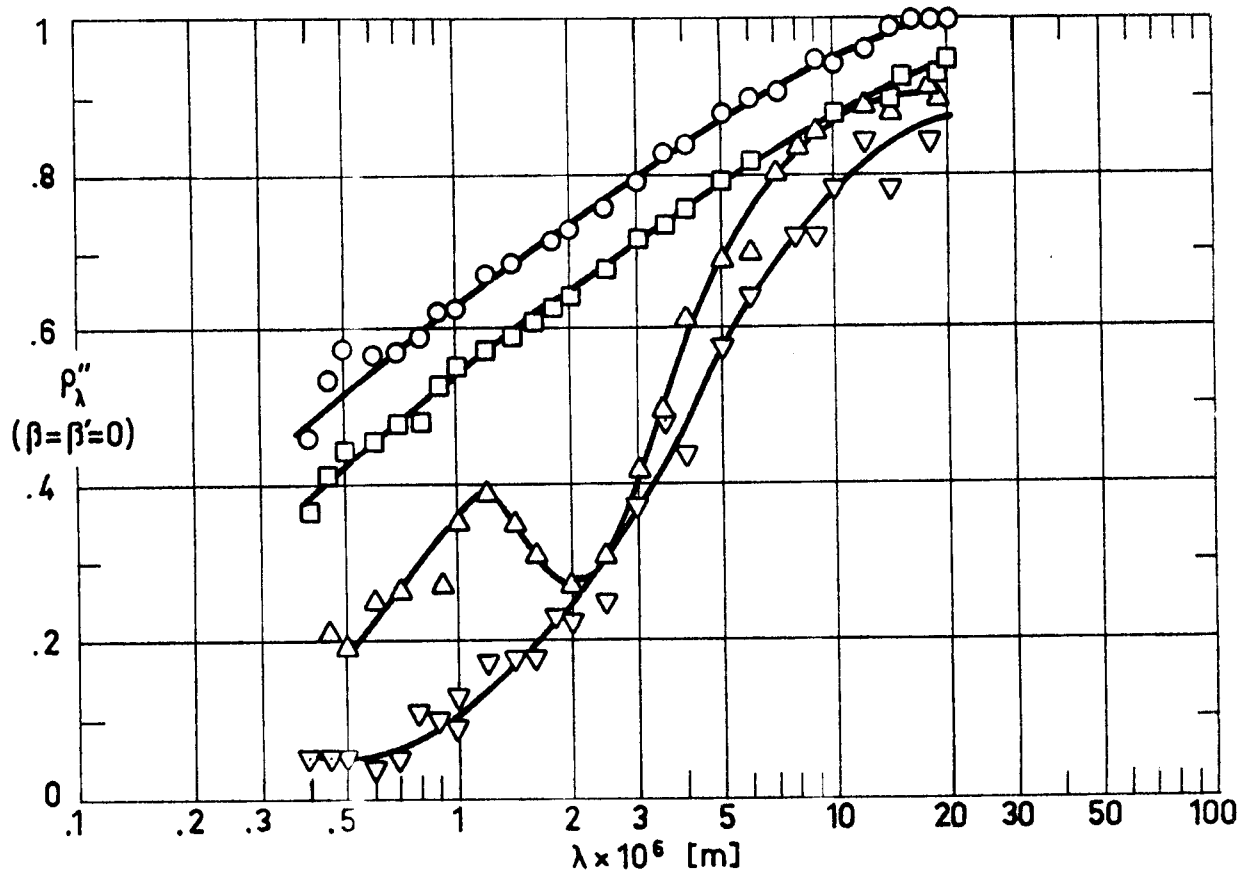


Fig 1-51. Normal-normal spectral reflectance, ρ_{λ}'' , of Ti - 5 Al - 2.5 Sn as a function of wavelength, λ .

Explanation

Key	Description	Comments	References
○	Nominal composition. Mechanically and electropolished.	Measured in vacuum (1.33×10^{-3} Pa). T=298 K.	Touloukian (1967)c.
□	Same as ○ except mechanically polished.		
△	Same as ○ except mechanically polished; pickled, anodized in NaOH, and sealed. 4×10^{-7} m thick coating.		
▽	Same as △ .	Measured in vacuum (1.33×10^{-3} Pa). T=755 K.	

METALLIC MATERIALS

Titanium-Aluminium-Tin Alloys

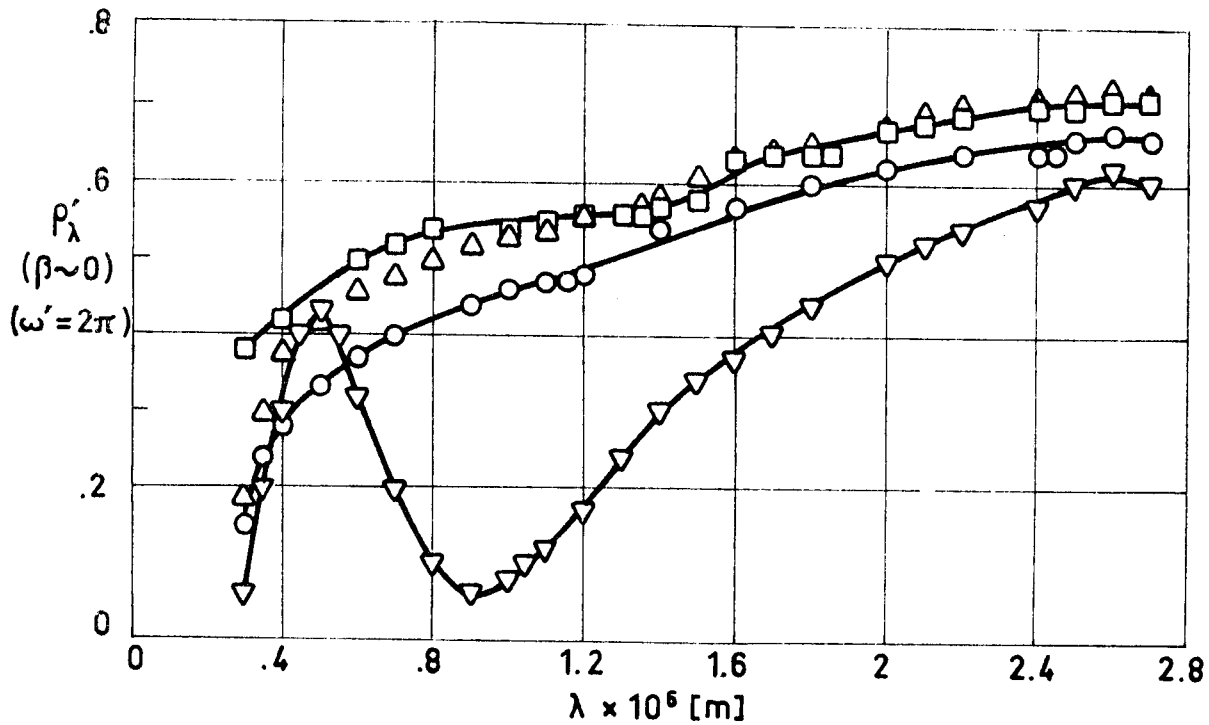


Fig 1-52. Normal-hemispherical spectral reflectance, ρ_{λ}' , of Ti-5 Al-2.5 Sn as a function of wavelength, λ .

Explanation

Key	Description	Comments	References
○	Nominal composition. As received.	$\beta=9^\circ$. $T=298$ K.	Touloukian & DeWitt (1970)
□	Same as ○ except cleaned.		
△	Same as ○ except polished		
▽	Same as ○ except oxidized at 922 K.		

METALLIC MATERIALS
Titanium-Aluminium-Tin Alloys

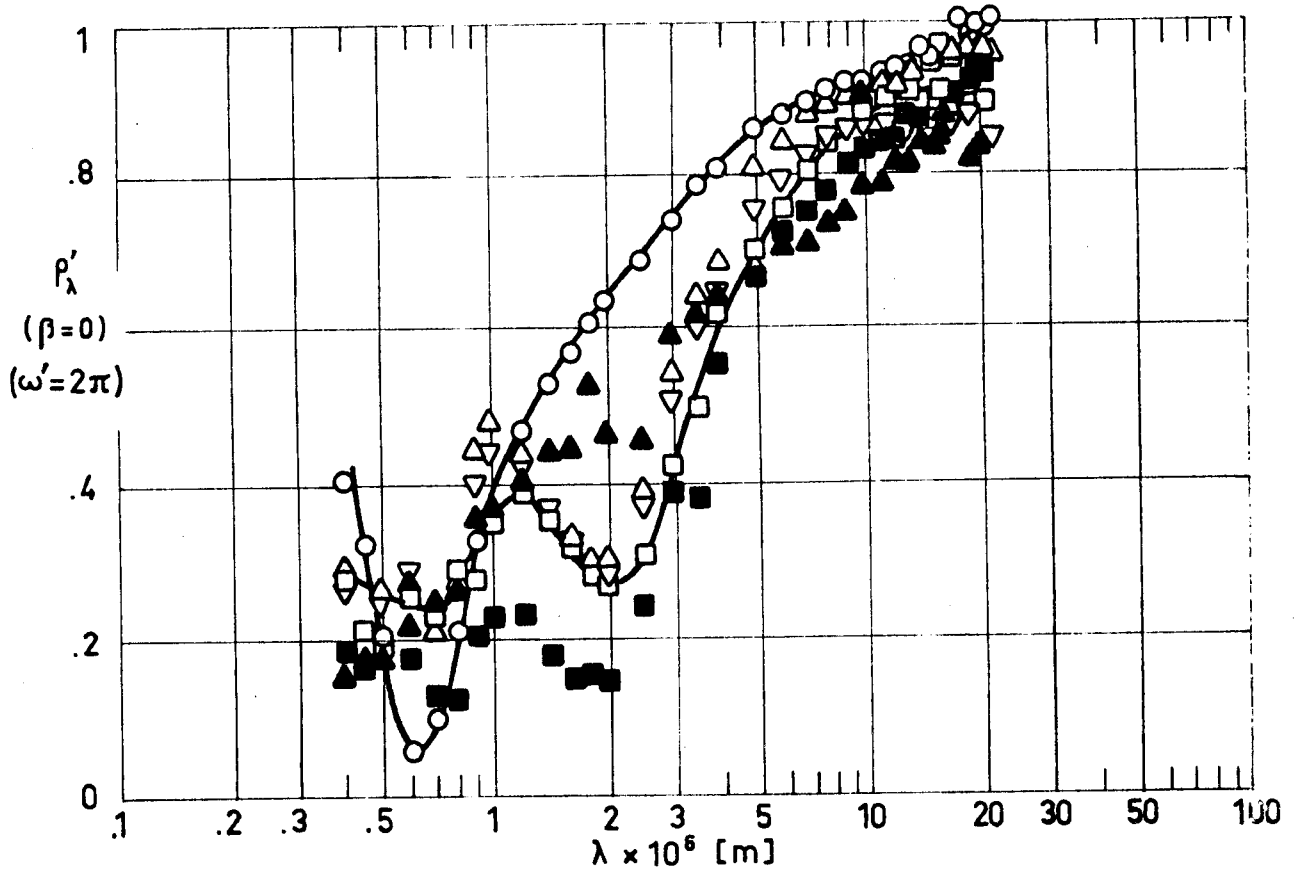


Fig 1-53. Normal-hemispherical spectral reflectance, ρ'_λ , of Ti-5 Al-2.5 Sn, anodized, as a function of wavelength, λ .

Explanation

Key	Description	Comments	References
○	Anodized in sulphuric acid for 20 min. Substrate mechanically and electro-polished.	Measured in vacuum ($\sim 1.33 \times 10^{-4}$ Pa). Converted from $R(2\pi, 0^\circ)$. $T=298$ K.	Touloukian, DeWitt & Hernicz (1972).
□	Anodized in sodium hydroxide for 20 min. Substrate mechanically polished and pickled.		
■	Same as □ .	Same as ○ except $T=589$ K	
△	Same as □ except electro-polished instead of pickled.	Same as ○ .	
▲	Same as △ .	Same as ○ except $T=978$ K	
▽	Same as □ except anodized in sodium hydroxide for 6.7 min.	Same as ○ .	

METALLIC MATERIALS
Titanium-Aluminium-Tin Alloys

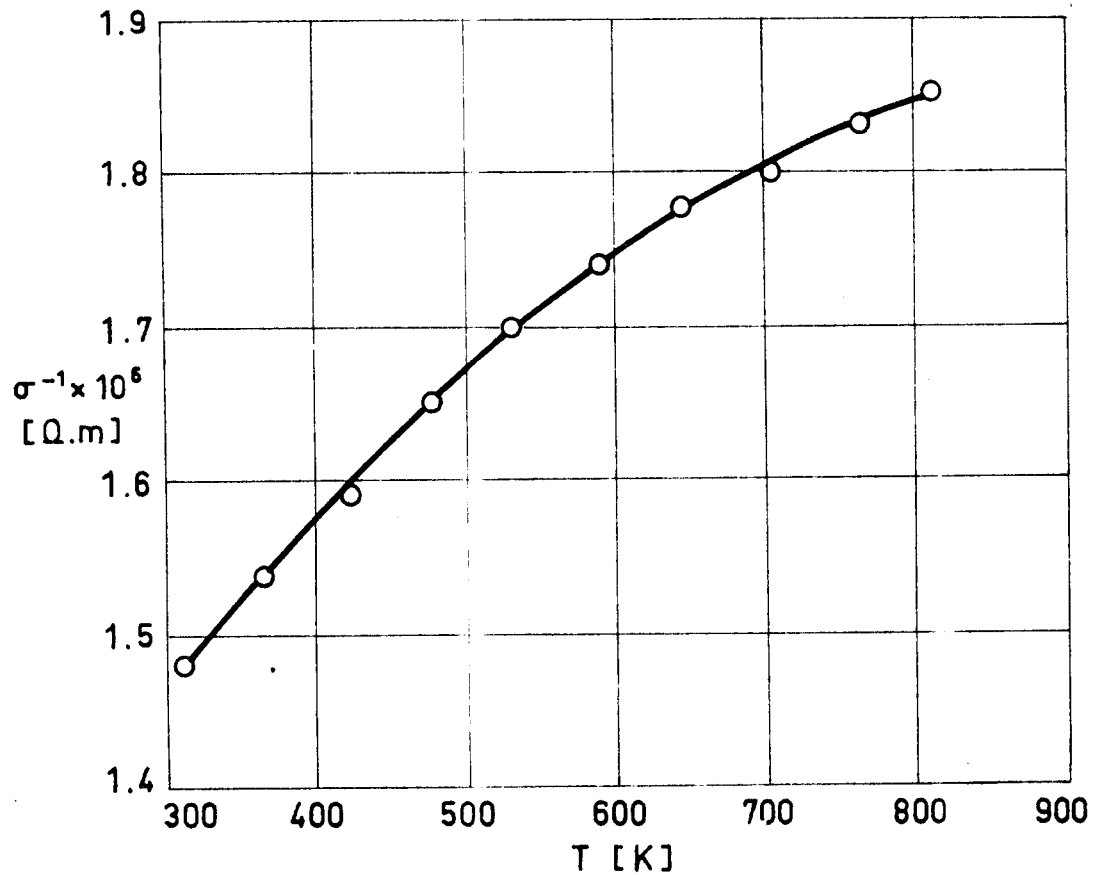


Fig 1-54. Electrical resistivity, σ^{-1} , of Ti - 5 Al - 2.5 Sn as a function of temperature, T.

Explanation

Key	Description	Comments	References
○	Nominal composition. Mild annealed.	Reported error $\pm 5\%$.	Touloukian (1967)c.

METALLIC MATERIALS
Titanium-Aluminium-Tin Alloys

6. FABRICATION

6.2. Forming. Good. In sheet forming the minimum bending radius is 5 times the thickness.

6.3. Welding. Good, using TIG or MIG processes.

6.4. Machining. Possible with slow speeds, coarse feeds, and sharp tools.

6.5. Heat treatment. Good. This alloy can only be annealed.

From ASMH (1974) e.

7. AVAILABLE FORMS AND CONDITIONS

Available in the full range of sizes for sheet, strip, plate, bar, forgings, wire, extrusions and castings. (ASMH (1974)e).

8. USEFUL TEMPERATURE RANGE

The structural use of this alloy should be limited to temperatures below 580 K. The extra-low-interstitial grade (ELI) is recommended for low temperature uses (as low as 20 K). Fresh fracture surfaces of this alloy, when in contact with liquid oxygen, burn expontaneously, and the reaction may spread at a high rate. (ASMH (1974)e).

9. APPLICATIONS

Structural elements, fasteners, bolts and, generally speaking, when high temperature precludes the use of aluminium alloys. Also used in pressure vessels for liquid hydrogen and liquid helium.

INTENTIONALLY BLANK PAGE

METALLIC MATERIALS

Titanium - Aluminium - Tin Alloys

1.8. TITANIUM-ALUMINIUM-TIN ALLOYS

Alloy Ti - 6 Al - 2 Sn - 4 Zr - 2 Mo.

1. TYPICAL COMPOSITION, PERCENT

Al	Mo	Sn	Zr	Fe	O ₂	H ₂	N ₂	C	Others		Al
									Each	Total	
5.5	1.8	1.8	3.6								
6.5	2.2	2.2	4.4	.25	.12	.015	.05	.05	.10	.40	Balance

2. OFFICIAL DESIGNATIONS

AICMA	ISO	AFNOR	AMS	BS	DIN	UNE
			Ti6242			Ti-6Al4ZrMoSn UNE 38-718

3. PHYSICAL PROPERTIES3.1. Density. $\rho = 4\,540 \text{ kg}\cdot\text{m}^{-3}$ (UNE (1984)).3.2. Thermal Properties

3.2.1. Specific heat.

Effect of temperature on specific heat: Fig 1-54.1.

3.2.2. Thermal conductivity.

Effect of temperature on thermal conductivity: Fig 1-54.2.

3.2.3. Thermal diffusivity.

3.2.4. Thermal expansion.

Effect of temperature on thermal expansion: Fig 1-54.3

Rev. 2. 1984

METALLIC MATERIALS

Titanium - Aluminium - Tin Alloys

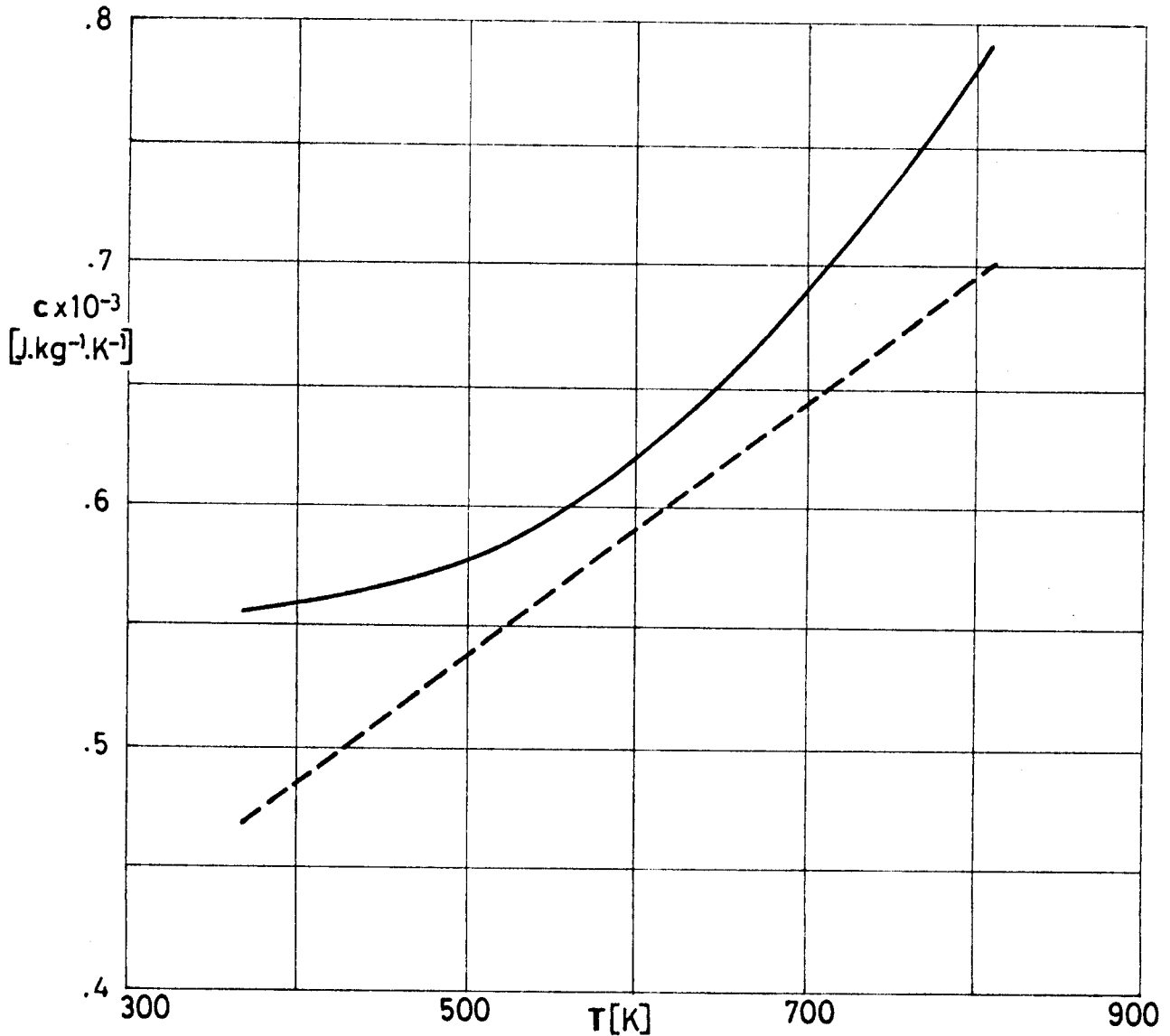


Fig 1-54.1. Specific heat, c, of Ti - 6 Al - 2 Sn - 4 Zr - 2 Mo as a function of temperature, T.

Explanation

Key	Description	Comments	References
—	Nominal Composition. Sheet. 10 ⁻³ m thick. Duplex annealed: 1 170 K, 30 min, air cool + 1 060 K, 15 min, air cool.		ASMH (1978).
- - -	Nominal composition. Bar. .0286 m in diameter. Duplex annealed: 1 170 K, 1 h, air cool + 870 K, 8 h, air cool.		

METALLIC MATERIALS

Titanium - Aluminium - Tin Alloys

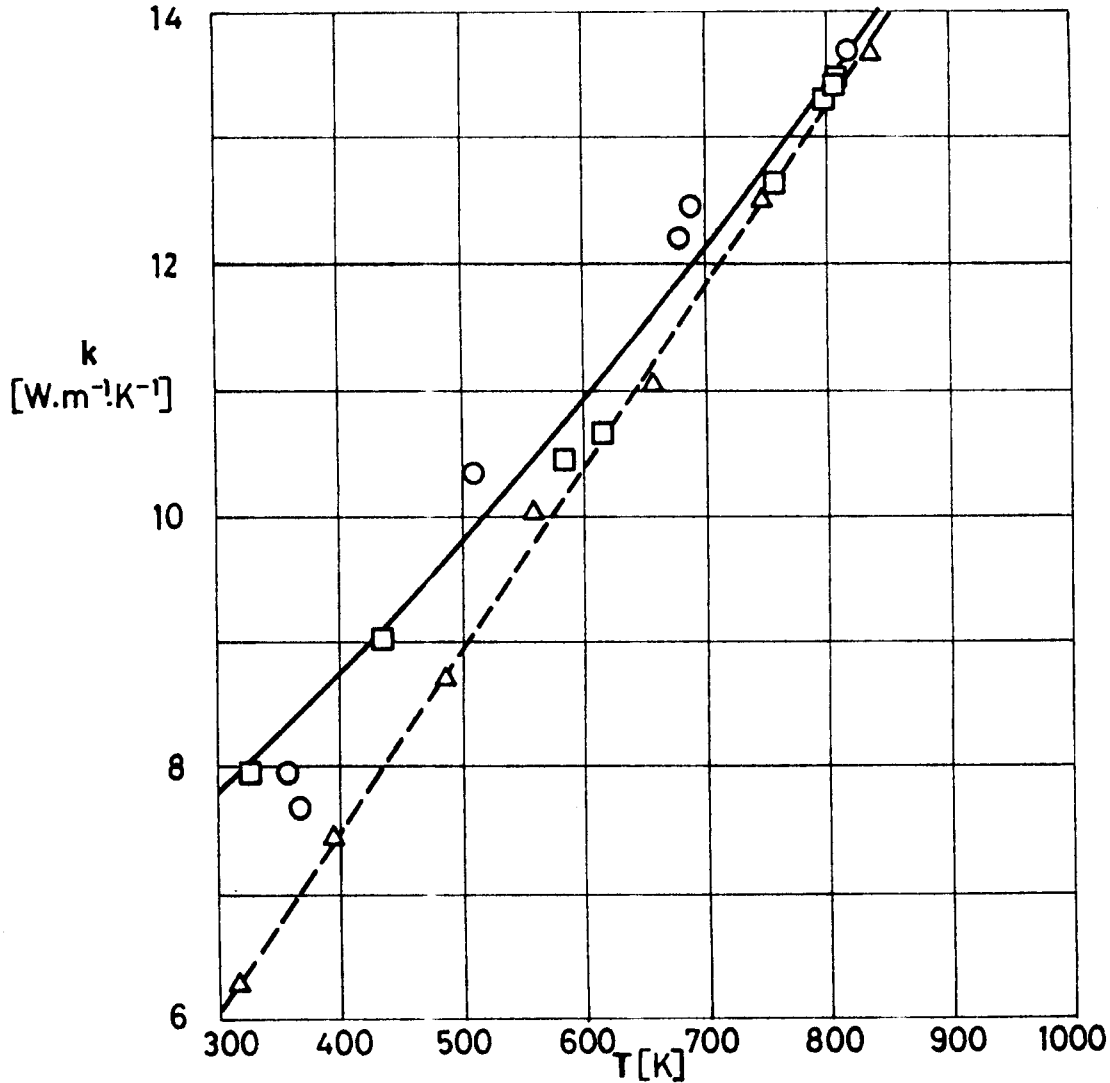


Fig 1-54.2. Thermal conductivity, k , of Ti - 6 Al - 2 Sn - 4 Zr - 2 Mo as a function of temperature, T .

Explanation

Key	Description	Comments	References
○	Nominal composition. Sheet. 10 ⁻³ m thick.	Measured parallel to rolling direction.	ASMH (1978).
□	Duplex annealed: 1 170 K, 30 min, air cool + 1 060 K, 15 min, air cool.		
□	Same as above specimen and conditions.		
△	Nominal composition. Bar. .108 m in diameter.	Measured parallel to long direction.	
---	Duplex annealed: 1 170 K, 1 h, air cool + 870 K, 8 h, air cool.		

METALLIC MATERIALS

Titanium - Aluminium - Tin Alloys

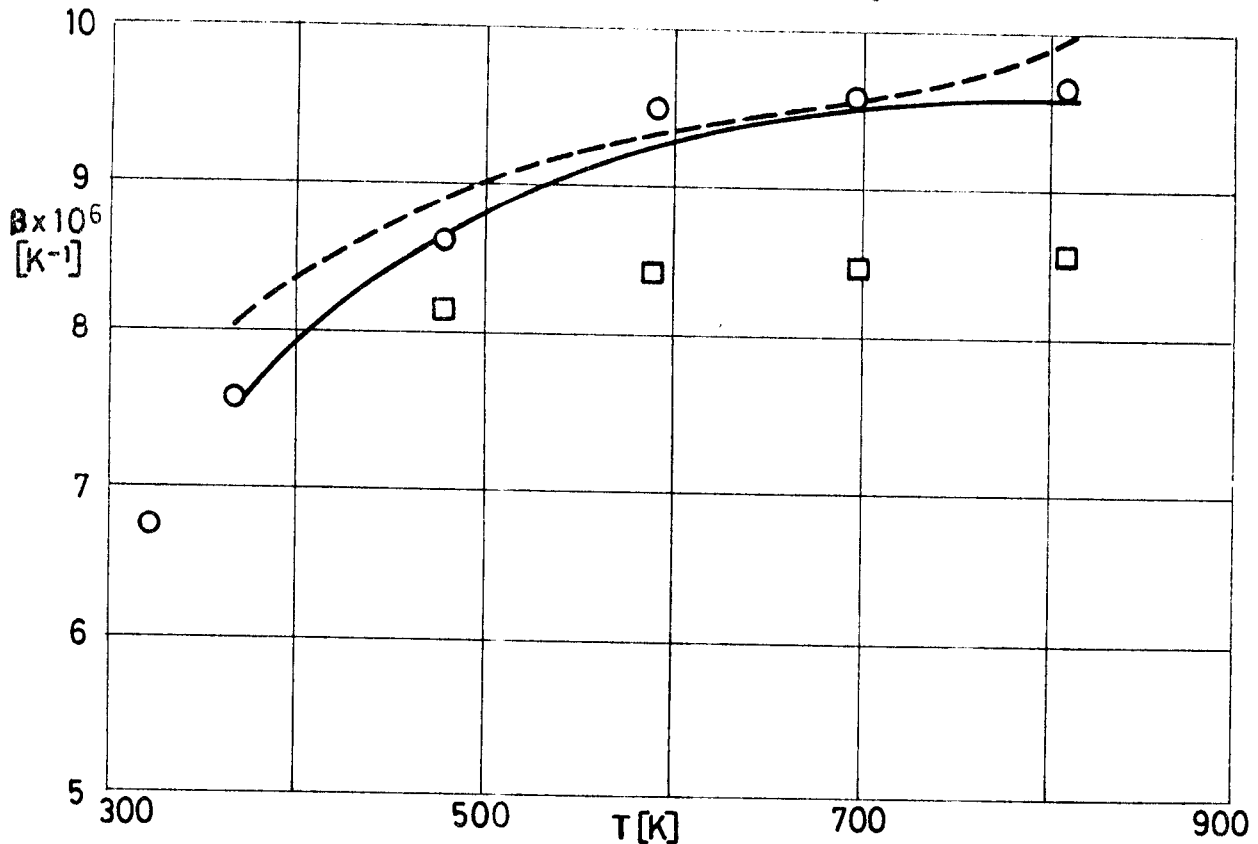


Fig 1-54.3. Mean coefficient of linear thermal expansion, β , of Ti - 6 Al - 2 Sn - 4 Zr - 2 Mo from room temperature to temperature T.

Explanation

Key	Description	Comments	References
—	Nominal composition. Sheet. 10^{-3} m thick. Duplex annealed: 1 170 K, 30 min, air cool + 1 060 K, 15 min, air cool.	Measured in longitudinal and transverse direction.	ASMH (1978).
- - -	Nominal composition. Bar. .0286 m in diameter. Duplex annealed: 1 170 K, 1 h, air cool + 870 K, 8 h air cool.	Measured in longitudinal direction. Average ascending-descending temperatures.	
○	Nominal composition. Cast compressor casing. As cast.		
□	Nominal composition. Pancake forging. Duplex annealed: 1 230 K, 1 h, air cool + 870 K, 8 h air cool.		

METALLIC MATERIALS

Titanium - Aluminium - Tin Alloys

3.2.5. Melting range.

Alloy 6.2 Al, 2 Sn, 4.2 Zr, 1.8 Mo, .06 Fe, .124 O, .008 N, .0052 H, .02 C, Ti balance.

T K	Solidus ^{a,c}	Liquidus ^{b,c}
Range	1845-1890	1970-2010
Average	1860	1920

^a Four determinations.

^b Two determinations.

^c Temperature measurement accuracy ± 19 K. Some diffusion of support tray material (Nb) into sample may have caused slight elevation of solidus and liquidus temperatures.

From ASMH (1978).

3.4. Other physical properties

3.4.1. Electrical resistivity.

Effect of temperature on electrical resistivity: Fig 1.54-4.

3.4.2. Magnetic properties.

This alloy is non-magnetic.

5.2. Corrosion resistance

This alloy is susceptible to solid salt stress corrosion at elevated temperatures and exhibits delayed failure of cracked specimens at room temperature in aqueous salt environments. Stress corrosion characteristics can depend on alloy processing and heat treatment (ASMH (1978)).

The application of a nickel-base protective coating to this alloy yielded limited results because of formation and growth of intermetallic Ni₃Ti and NiTi phases (Tien et al. (1973)).

METALLIC MATERIALS

Titanium - Aluminium - Tin Alloys

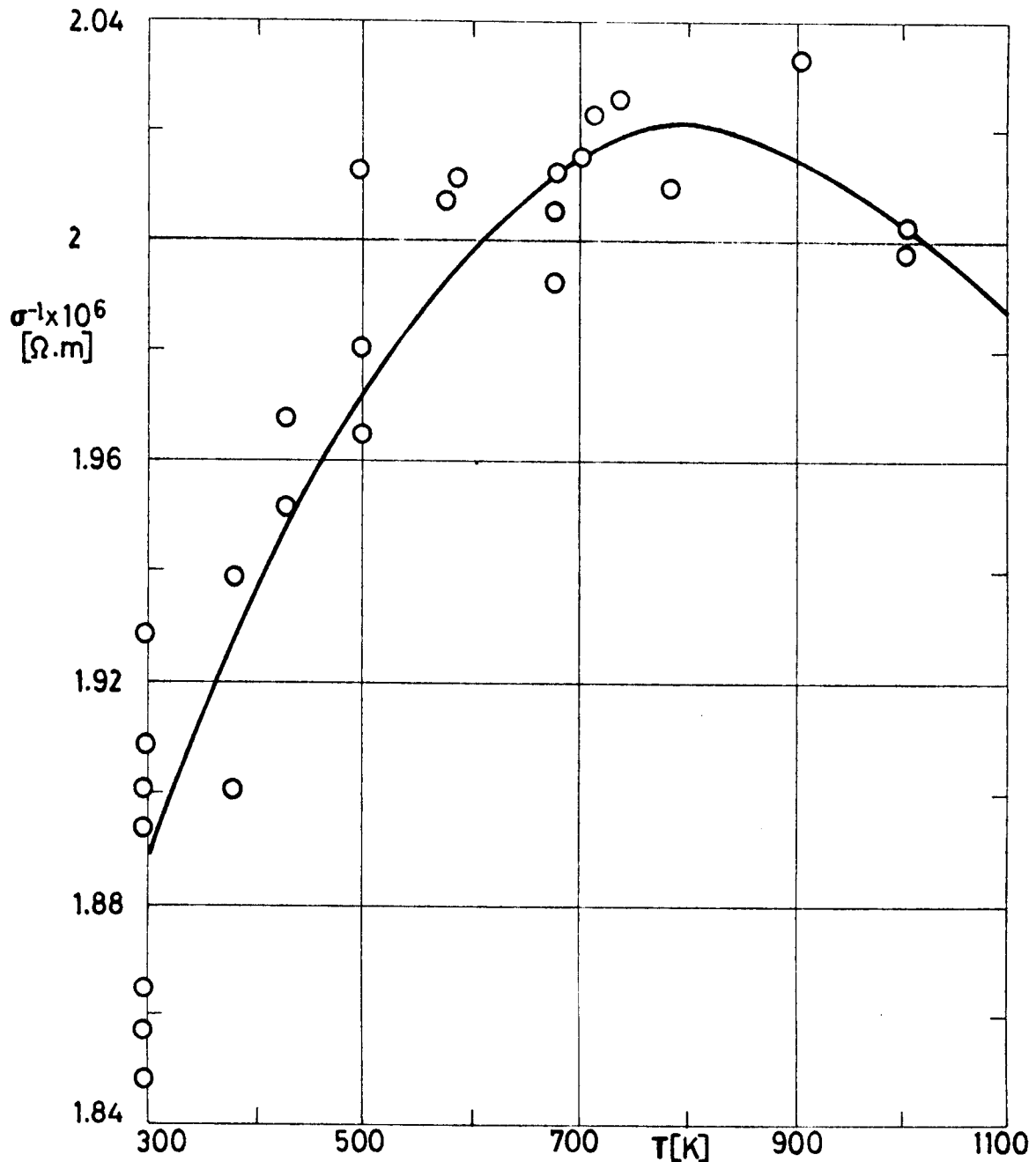


Fig 1-54.4. Electrical resistivity, σ^{-1} , of Ti - 6 Al - 2 Sn - 4 Zr - 2 Mo as a function of temperature, T.

Explanation

Key	Description	Comments	References
○	Nominal composition. Sheet. 10^{-3} m thick. Duplex annealed: 1 170 K, 30 min, air cool + 1 060 K, 15 min, air cool.	Two heatings, two specimens each heating. Measurement parallel to rolling direction.	ASMH (1978).

METALLIC MATERIALS

Titanium - Aluminium - Tin Alloys

6. FABRICATION6.1. Casting

Acceptable castings by the induction melting technique can not be obtained with the use of graphite crucibles and molds due to surface reaction with the mold. This problem is at present circumvented by multiple consumable electrode arc melting under vacuum in water-cooled copper crucibles. A skin of solid titanium, the "skull", is formed providing a non reactive wall between the melt and the crucible.

(ASMH (1978)).

6.2. Forming

Bending. Bend properties are equivalent to those for similar alloys.

Forging. Forgeability of this alloy is similar to Ti - 6 Al - 4 V (see pp. 1-109 to 1-124).

(ASMH (1978)).

6.3. Welding

Fusion welding by either TIG or MIG process can be performed on any of the heat treated conditions of this alloy. Weldment properties are inferior to those of Ti - 6 Al - 4 V (Betner (1980)).

This alloy produces a weld the properties of which are difficult to predict and markedly different from the unwelded metal. Tests seem to indicate that weld properties may vary with ingot source, gage of material welded, weld cooling rate and, possibly, prior heat treatment.

Rev. 2. 1984

METALLIC MATERIALS

Titanium - Aluminium - Tin Alloys

(ASMH (1978)).

6.4. Machining

Good, within the group of Ti alloys (UNE (1984)).

6.5. Heat treatment

This alloy is used in either a duplex or triplex annealed conditions. The heating cycles of duplex annealing for sheets are specified in the Explanations of Figs 1-54.1 to 1-54.4. A final 870 K heating cycle for triplex annealed sheet and duplex annealed bar and forges, followed by 8 h air cool is sometimes referred as stabilization age. (ASMH (1978)).

7. AVAILABLE FORMS AND CONDITIONS

Ingot, bloom bar, billet, sheet, plate, wire (ASMH (1978)).

8. USEFUL TEMPERATURE RANGE

This alloy possesses good strength properties up to 800 K and appears metallurgically stable up to 700 K. These are disappointingly low values relative to the melting point of titanium (1900 K to 1950 K).

No service experience of this alloy at temperatures below 273 K has been gained.

9. APPLICATIONS

Blades and discs of the compressor section of jet engines, and air-frame applications requiring good strength, fracture toughness, erosion properties and improved creep resistance at temperatures up to 800 K.

METALLIC MATERIALS

Titanium-Aluminium-Vanadium Alloys

1.9. TITANIUM-ALUMINIUM-VANADIUM ALLOYS

ALLOY Ti - 6 Al - 4 V.

1. TYPICAL COMPOSITION, PERCENT

Al	C	Fe	H	N	O	V	Ti
5.5	-	-	-	-	-	3.5	Balance
6.75	.1	.4	.015	.07	.3	4.5	

2. OFFICIAL DESIGNATIONS

AECMA	ISO	AFNOR	AMS	BS	DIN
Ti - P63			4911 4928	TA 10	TiAl6V4, 3.7164

3. PHYSICAL PROPERTIES3.1. Density. $\rho = 4\,430 \text{ kg.m}^{-3}$. (Stuart Lyman (1961)).3.2. Thermal properties

3.2.1. Specific heat.

Effect of temperature on specific heat: Fig 1-55.

3.2.2. Thermal conductivity.

Effect of temperature on thermal conductivity: Fig 1-56.

Thermal conductivity integrals: Fig 1-57.

3.2.3. Thermal diffusivity.

Effect of temperature on thermal diffusivity: Fig 1-58.

3.2.4. Thermal expansion.

Mean coefficient of linear thermal expansion, β , between 294 K and given temperature.

T [K]	366	477	588	700	811
$\beta \times 10^6 \text{ [K}^{-1}\text{]}$	9.1	10.2	10.2	10.2	10.2

From Stuart Lyman (1961).

METALLIC MATERIALS
Titanium-Aluminium-Vanadium Alloys

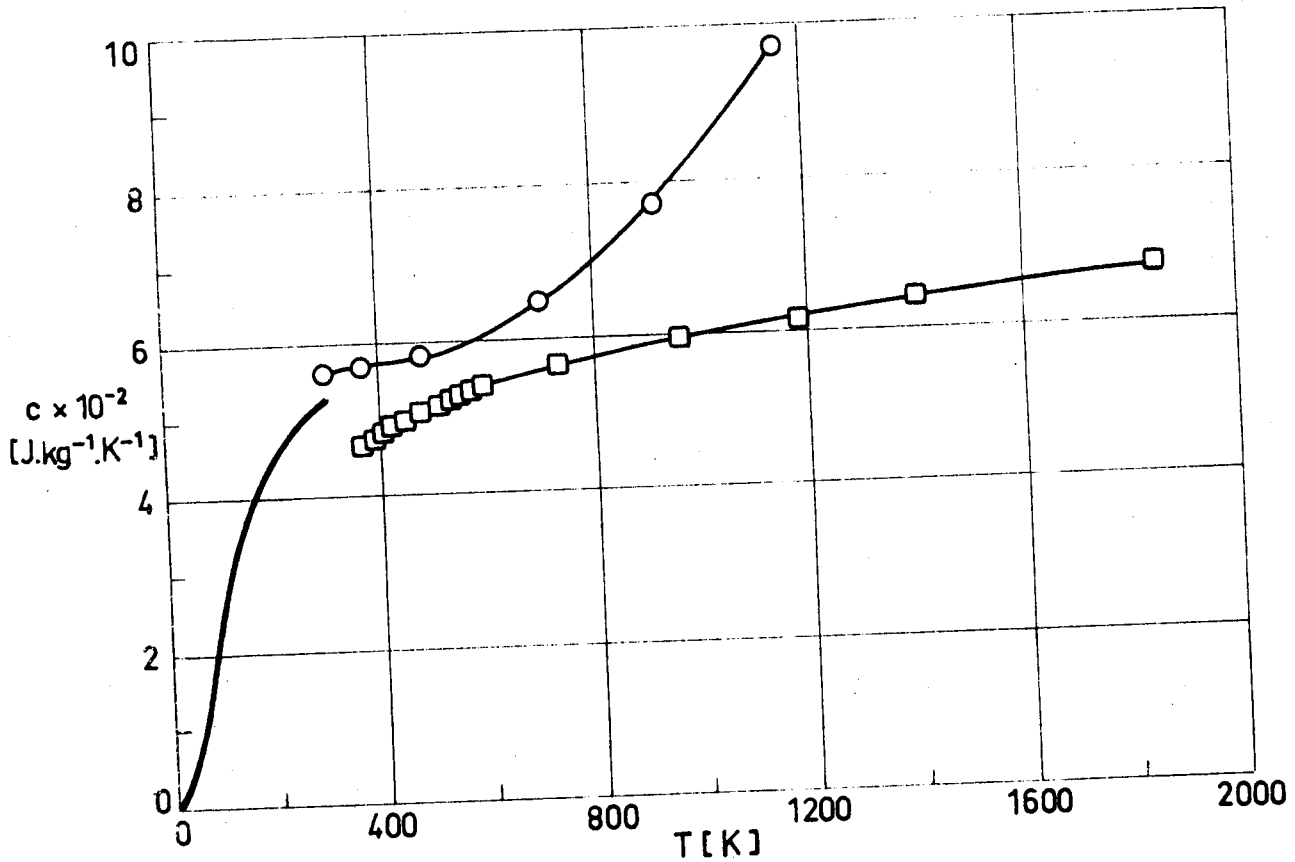


Fig 1-55. Specific heat, c , of Ti - 6 Al - 4 V as a function of temperature, T .

Explanation

Key	Description	Comments	References
○	Nominal composition.		Stuart Lyman (1961).
□	Nominal composition. Solution heat treated at 1200 K for 20 min, oil-quenched and aged at 755 K for 4 h, and then cooled in air.	Reported error <2%.	Touloukian (1967)c.
—	Nominal composition.	Data from smooth curve.	Coston (1967).

METALLIC MATERIALS
Titanium-Aluminium-Vanadium Alloys

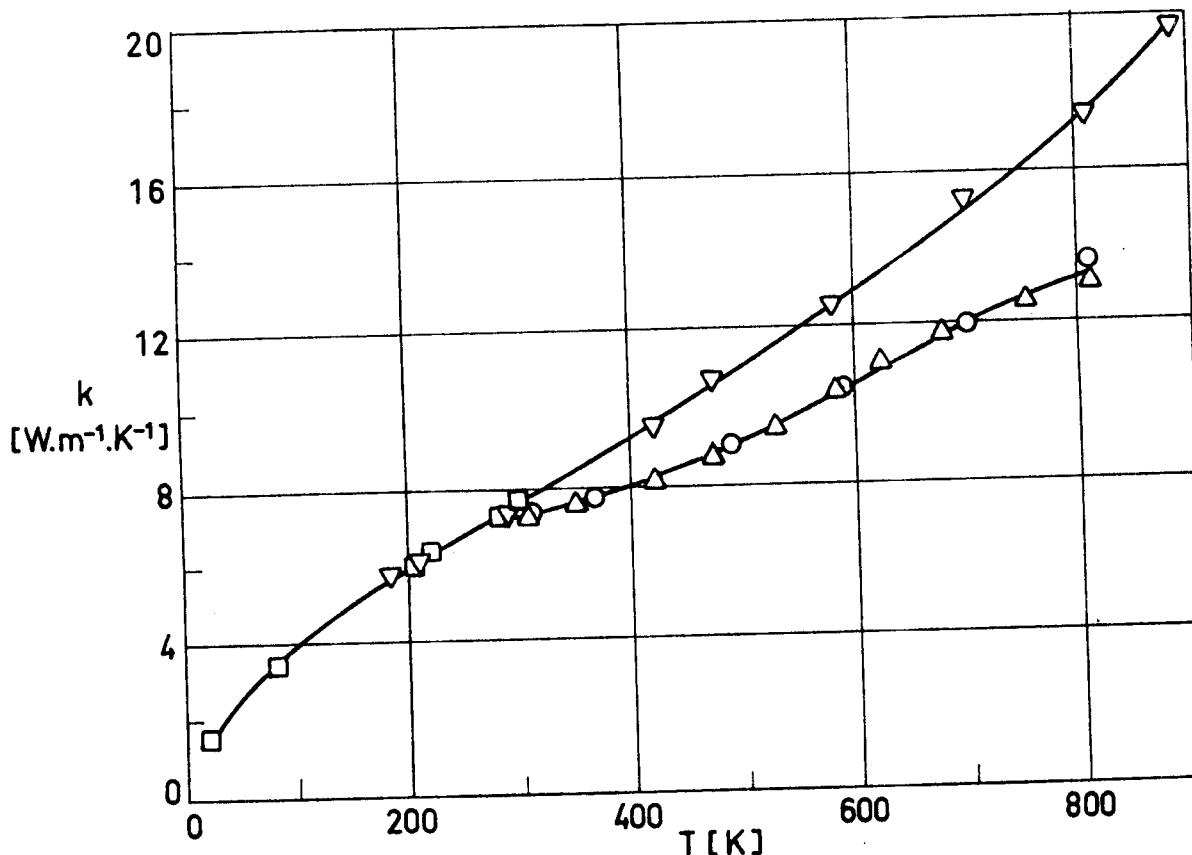


Fig 1-56. Thermal conductivity, k, of Ti - 6 Al - 4 V as a function of temperature, T.

Explanation

Key	Description	Comments	References
○	Nominal composition.		Stuart Lyman (1961).
□	Nominal composition.		Coston (1967).
△	In a mild annealed condition.	Reported error ±5%.	Touloukian (1967)c.
▽	Nominal composition. Sheet no. 1777 A-1.		

METALLIC MATERIALS

Titanium-Aluminium-Vanadium Alloys

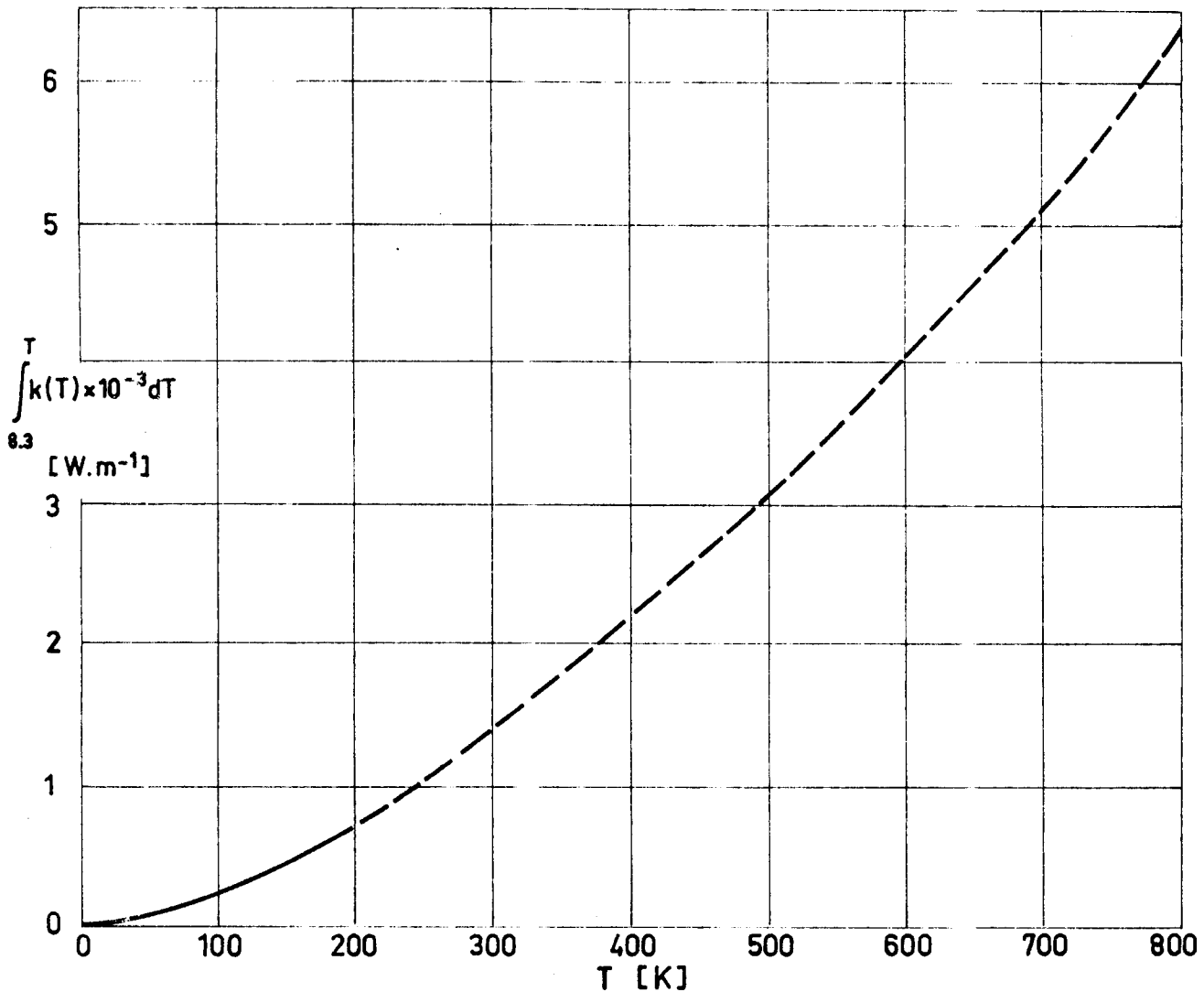


Fig 1-57. Thermal conductivity integrals of Ti - 6 Al - 4 V as a function of temperature, T .

Explanation

———— From Coston (1967).

----- Calculated, by the compiler, by fitting the experimental data points \circ , \square and \triangle of Fig 1-56 with the least-squares method, and integrating the expression, $k(T) = 6.33 + 3.67 \times 10^{-6} T^2$ ($r = .995$), which is then obtained; r is the correlation coefficient giving the goodness of the fit.

METALLIC MATERIALS
Titanium-Aluminium-Vanadium Alloys

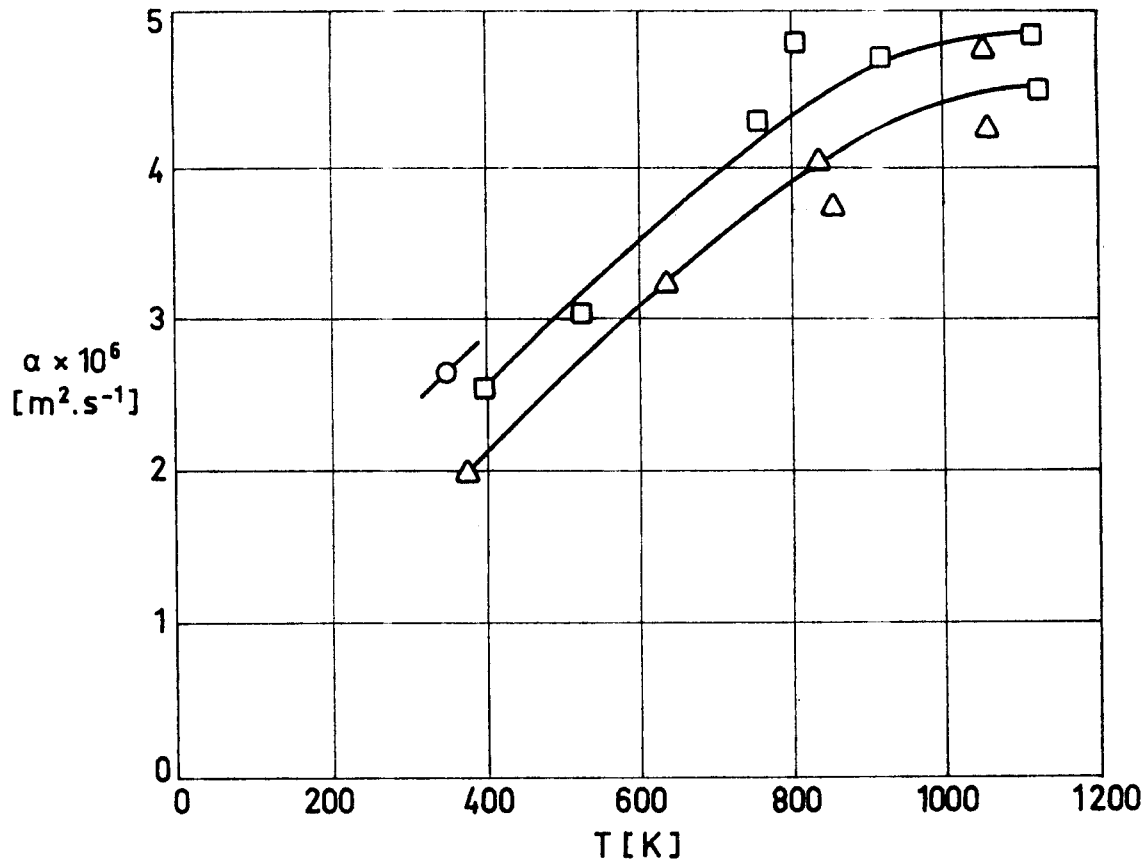


Fig 1-58. Thermal diffusivity, α , of Ti - 6 Al - 4 V as a function of temperature, T.

Explanation

Key	Description	Comments	References
○	Nominal composition.	Exposed to radiation and followed by cooling.	Touloukian (1967)c.
□	Nominal composition.	Measured after three exposures to radiation.	
△	Nominal composition.	Measured after five exposures to radiation.	

METALLIC MATERIALS

Titanium-Aluminium-Vanadium Alloys

Effect of temperature on thermal expansion: Fig 1-59.

3.2.5. Melting range.

1877 K - 1933 K. (Stuart Lyman (1961)).

3.3. Thermal radiation properties

3.3.1. Emittance.

3.3.1.1. Normal spectral emittance ($\beta'=0$).

Effect of temperature on normal spectral emittance: Fig 1-60.

3.3.1.2. Normal total emittance ($\beta'=0$).

Effect of temperature on normal total emittance: Fig 1-61.

3.3.1.4. Hemispherical total emittance.

Effect of temperature on hemispherical total emittance:

Fig 1-62.

3.3.2. Absorptance.

3.3.2.5. Solar absorptance.

3.3.2.5.1. Normal solar absorptance: Table 1-20.

Table 1-20

Normal Solar Absorptance of Ti - 6 Al - 4 V

T [K]	β°	α_s	Comments
298	9	.568	As received; computed from spectral reflectance data for sea level conditions. Mentioned below as specimen 1.
298	9	.563	Above specimen and conditions except computed for above atmosphere conditions.
298	9	.509	Different sample, same specimen and conditions as 1, except cleaned.

(Continued onto next page)

METALLIC MATERIALS

Titanium-Aluminium-Vanadium Alloys

Table 1-20 (Continued)

Normal Solar Absorptance of Ti - 6 Al - 4 V

T [K]	β°	α_s	Comments
298	9	.508	Above specimen and conditions except computed for above atmosphere conditions.
298	9	.515	Different sample, same specimen and conditions as 1, except polished.
298	9	.511	Above specimen and conditions except computed for above atmosphere conditions.
298	9	.878	Different sample, same specimen and conditions as 1, except oxidized.
298	9	.869	Above specimen and conditions except computed for above atmosphere conditions.
298	~ 0	.444	Computed from spectral reflectance.
298	~ 0	.474	Above specimen and conditions except hydrogen ion bombarded (1.10×10^{23} ions. m^{-2}).
298	~ 0	.507	Above specimen and conditions except hydrogen ion bombarded (4.70×10^{23} ions. m^{-2}).
298	~ 0	.515	Above specimen and conditions except hydrogen ion bombarded (1.27×10^{24} ions. m^{-2}).
298	~ 0	.512	Above specimen and conditions except hydrogen ion bombarded (3.07×10^{24} ions. m^{-2}).
298	~ 0	.512	Above specimen and conditions except hydrogen ion bombarded (7.70×10^{24} ions. m^{-2}).
298	~ 0	.511	Above specimen and conditions except hydrogen ion bombarded (9.87×10^{24} ions. m^{-2}).

From Touloukian, D. Witt & HERNICZ (1972).

3.3.3. Reflectance.

3.3.3.2. Directional-hemispherical spectral reflectance.

Normal-hemispherical spectral reflectance ($\beta \sim 0$, $\omega' = 2\pi$):

Fig 1-63.

3.4. Other physical properties

METALLIC MATERIALS

Titanium-Aluminium-Vanadium Alloys

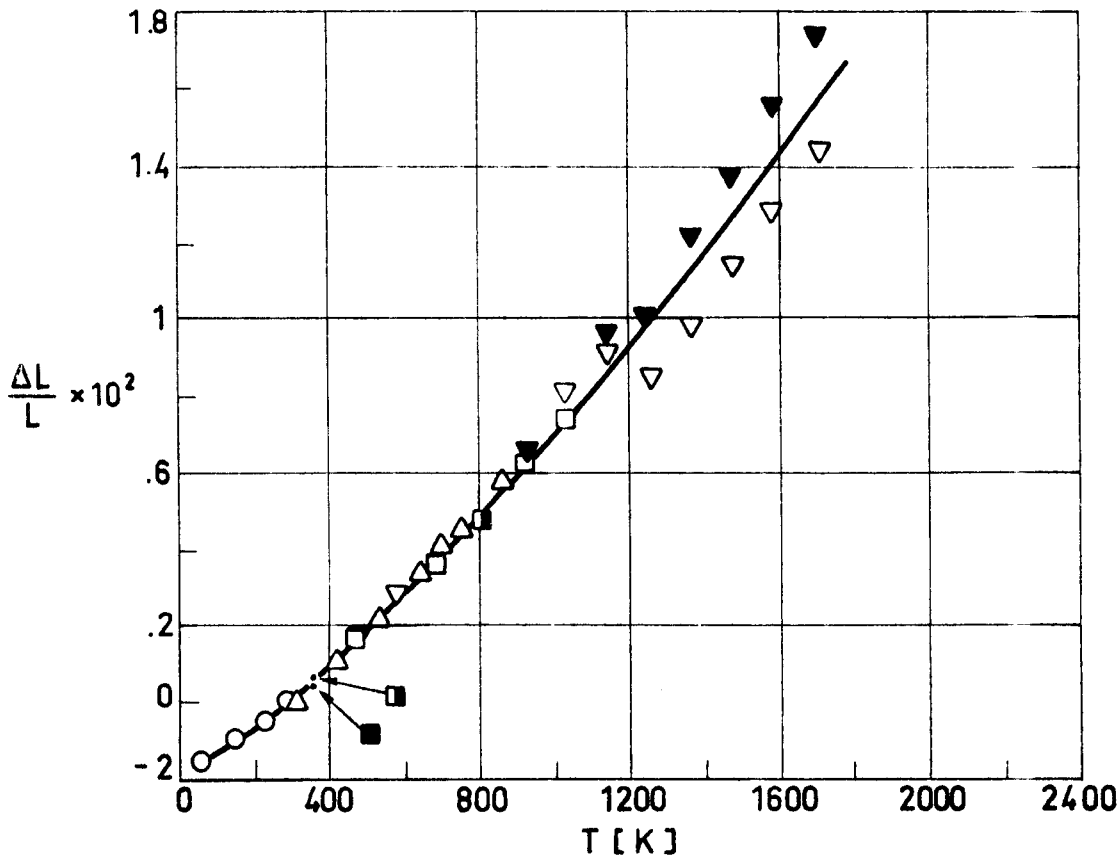


Fig 1-59. Thermal linear expansion, $\Delta L/L$, of Ti - 6 Al - 4 V as a function of temperature, T.

Explanation

Key	Description	Comments	References
○		From smooth curve.	Coston (1967).
□	Nominal composition. Density $4\,430\text{ kg}\cdot\text{m}^{-3}$		Touloukian (1967)c.
■	Same as □. Alpha-beta alloy.		
◻	Same as ■. Low C content		
△	Machined; solution treated, 1 200 K, 20 min; oil-quenched; aged 755 K, 4 h, and air-cooled. Sample 2.54×10^{-3} m in diameter and 5×10^{-2} m length.	Average data of three samples with permanent expansion from .011 to .025 percent.	
▽	Prepared from sponge. Sample 1.59×10^{-2} m in diameter. Annealed.	Measured in vacuum ($\approx 4 \times 10^{-2}$ Pa). Beta-transus temperature 1 270 K. Heating data.	
▼	Same as ▽.	Cooling data.	

METALLIC MATERIALS

Titanium-Aluminium-Vanadium Alloys

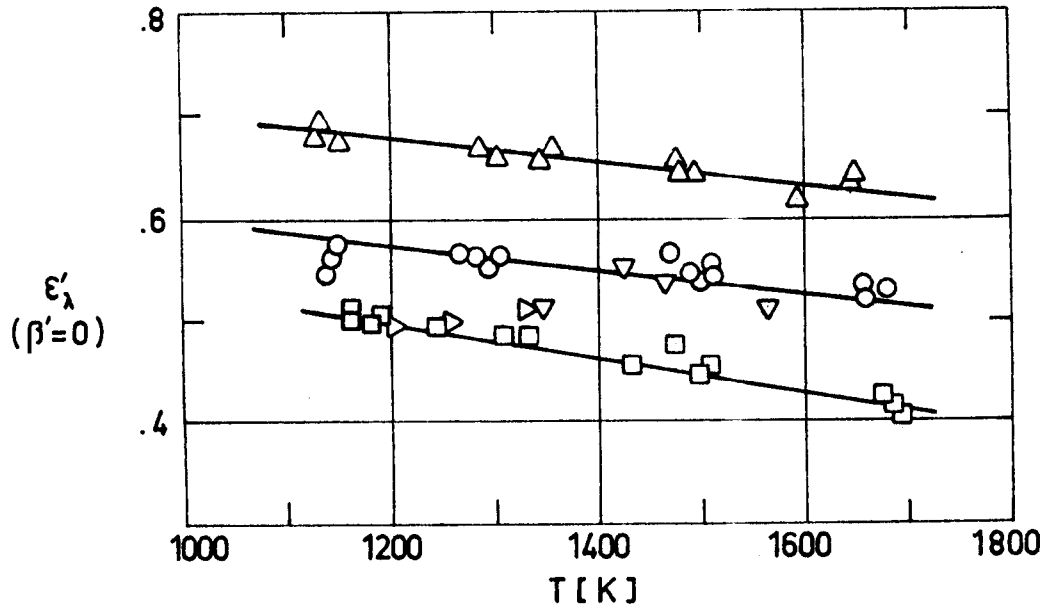


Fig 1-60. Normal spectral emittance, ϵ'_λ , of Ti - 6 Al - 4 V as a function of temperature, T.

Explanation

Key	Description	Comments	References
○	Nominal composition.	Measured in vacuum. Same data for as received and cleaned (with a liquid detergent). $\lambda = 6.65 \times 10^{-7}$ m.	Touloukian (1967)c.
□	Same composition as above. Polished with fine polishing compounds.	Measured in vacuum. $\lambda = 6.65 \times 10^{-7}$ m.	
△	Same composition as above. Oxidized in air at red heat for 30 min.	Measured in vacuum. $\lambda = 6.65 \times 10^{-7}$ m.	
▽	Nominal composition. Surface roughness: 2×10^{-6} - 3×10^{-6} m RMS. Polished.	Measured in vacuum (.4 - .53 Pa). Heating. $\lambda = 6.5 \times 10^{-7}$ m.	
▷	Same as above.	Same as above. Cooling. $\lambda = 6.5 \times 10^{-7}$ m.	

METALLIC MATERIALS

Titanium-Aluminium-Vanadium Alloys

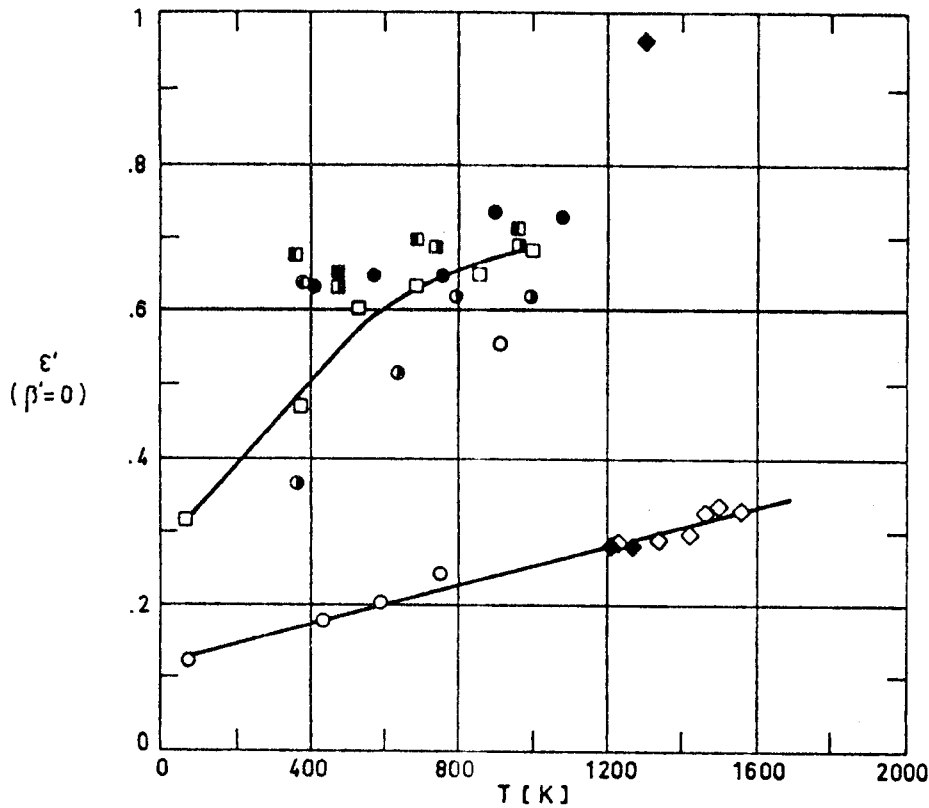


Fig 1-61. Normal total emittance, ϵ' , of Ti-6Al-4V as a function of temperature, T .

Explanation

Key	Description	Comments	References
○	Nominal composition. Polished.	Measured in air. Cycle 1.	Touloukian (1967)c.
◐	Same as above.	Cycle 2 heating.	
◑	Same as above.	Cycle 2 cooling.	
●	Same as above.	Cycle 3.	
□	Nominal composition. Oxidized at 922 K for 30 min.	Measured in air. Cycle 1.	
◻	Same as above.	Cycle 2.	
◼	Same as above.	Cycle 3 heating.	
◽	Same as above.	Cycle 3 cooling.	
◇	Nominal composition. Surface roughness: $2 \times 10^{-6} - 3 \times 10^{-6}$ m RMS. Polished.	Measured in vacuum ($.4 - 1.53$ Pa) Heating.	
◆	Same as above.	Cooling.	

METALLIC MATERIALS

Titanium-Aluminium-Vanadium Alloys

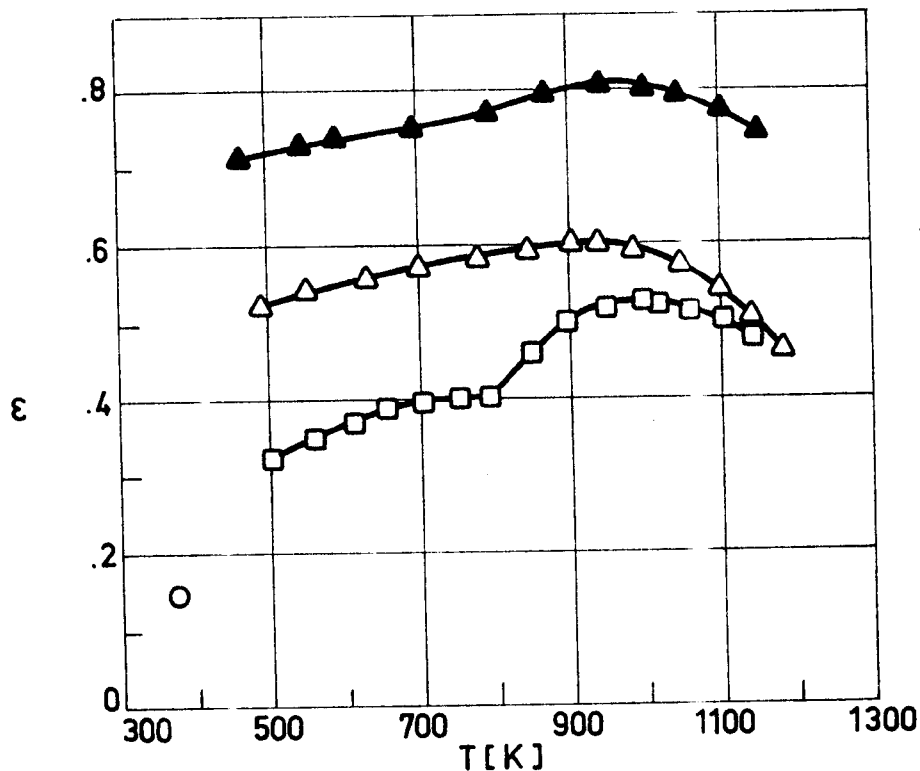


Fig 1-62. Hemispherical total emittance, ϵ , of Ti - 6 Al - 4 V as a function of temperature, T.

Explanation

Key	Description	Comments	References
○	Nominal composition. Pre-finished with 600 grit silicon carbide paper, electropolished.	Measured in vacuum (1.33×10^{-3} Pa). The effect of ion bombardment, quoted in the source, is too small to be distinguishable in the figure.	Touloukian & DeWitt (1970).
□	Nominal composition. Rough surface, as received.	Data from smooth curve. Reported error >6%.	
△	Same as above except preheated at 1150 K in air.	Reported error >6%.	
▲	Rough surface, as received.	Data from smooth curve. Reported error >6%.	

METALLIC MATERIALS

Titanium-Aluminium-Vanadium Alloys

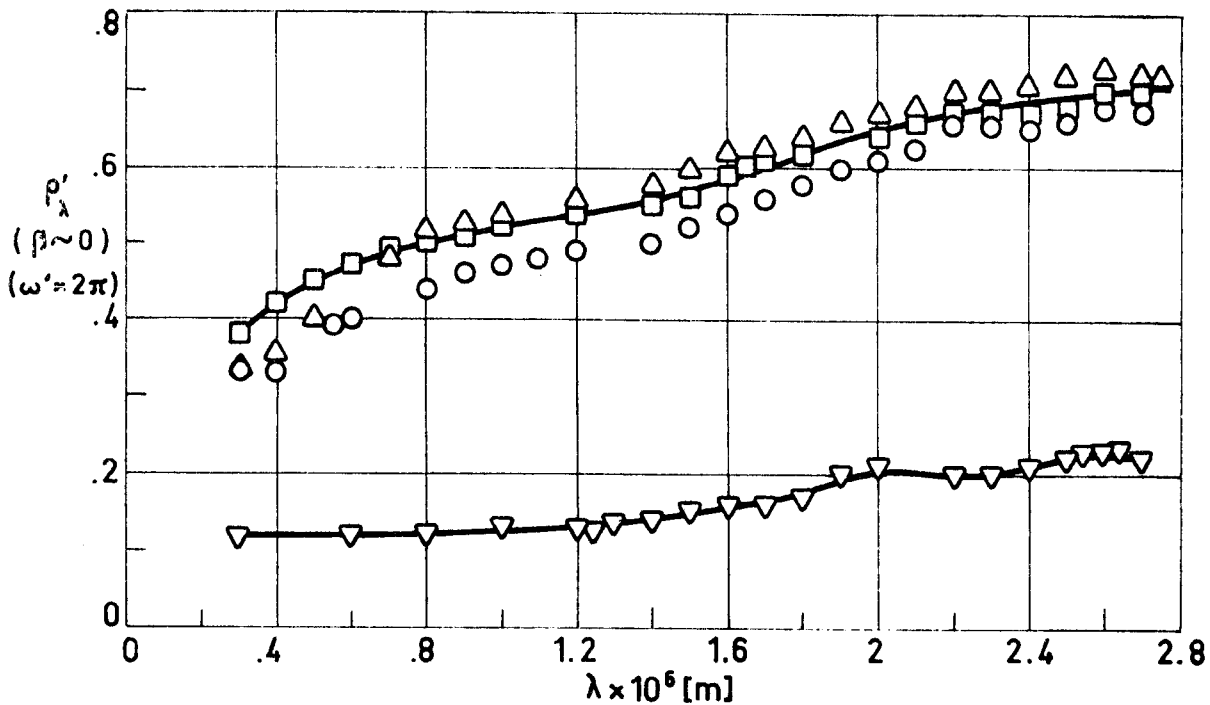


Fig 1-63. Normal-hemispherical spectral reflectance, ρ'_λ , of Ti-6Al-4V as a function of wavelength, λ .

Explanation

Key	Description	Comments	References
○	Nominal composition, as received.	$\beta = 9^\circ$. T = 298 K.	Touloukian & DeWitt (1970).
□	Same as ○ except cleaned.		
△	Same as ○ except polished.		
▽	Same as ○ except oxidized at 922 K for 30 min.		

METALLIC MATERIALS

Titanium-Aluminium-Vanadium Alloys

3.4.1. Electrical resistivity.

Effect of temperature on electrical resistivity: Fig 1-64.

3.4.2. Magnetic properties. This alloy is non-magnetic.

Relative Permeability: $\frac{\mu}{\mu_0} = 1.00005$ measured at 1.6×10^3 A.m⁻¹.

(ASMH (1974)e).

5. CHEMICAL PROPERTIES5.1. Solution potential (vs. decinormal calomel electrode)

Data not available. Solution potential of Ti pure is +.20 V.
(Ross (1972)).

5.2. Corrosion resistance

This alloy is highly resistant to corrosion. It has excellent resistance to hot oxidation up to 800 K. It can not be attacked by normal acids (except fuming nitric) and alkalies at room temperature, and has considerable resistance to many acids at high temperature. (Ross (1972)).

6. FABRICATION

6.2. Forming. Good. In sheet forming the minimum bending radius is 6 times the thickness.

6.3. Welding. Good, using TIG or MIG processes.

6.4. Machining. Possible with slow speeds, coarse feeds, and sharp tools.

6.5. Heat treatment. Good.

METALLIC MATERIALS
Titanium-Aluminium-Vanadium Alloys

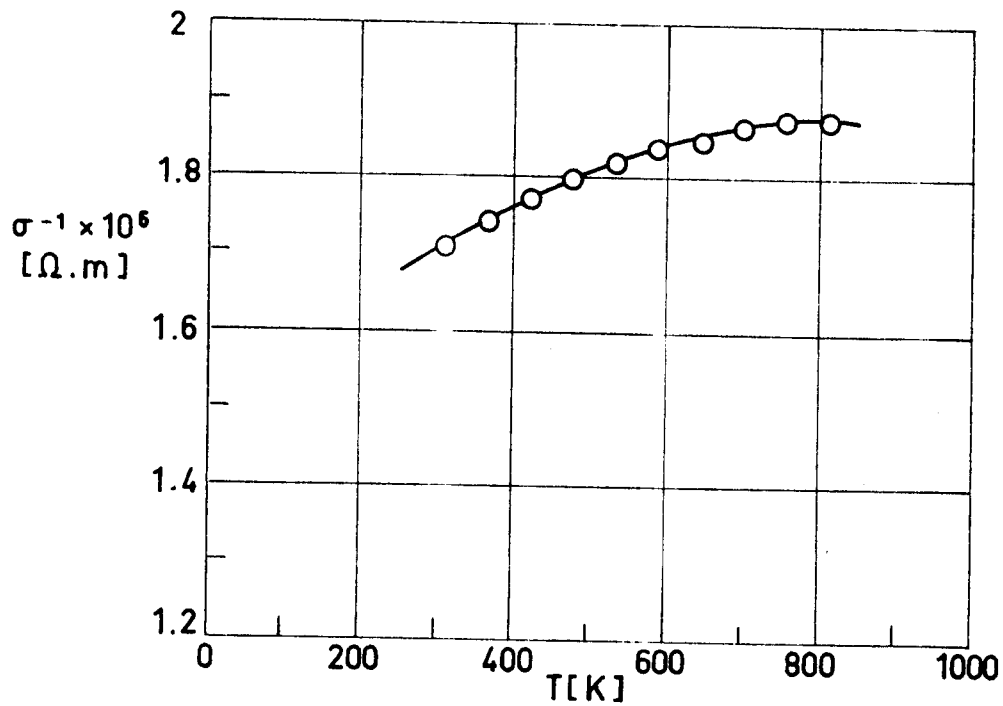


Fig 1-64. Electrical resistivity, σ^{-1} , of Ti - 6 Al - 4 V as a function of temperature, T.

Explanation

Key	Description	Comments	References
○	Nominal composition. Mild annealed.		Touloukian (1967)c.

METALLIC MATERIALS

Titanium-Aluminium-Vanadium Alloys

7. AVAILABLE FORMS AND CONDITIONS

It is available in the full commercial range of sizes for sheet, plate, bar, forgings, wire, extrusions, and castings in the annealed and solution treated conditions. (ASMH (1974)e).

8. USEFUL TEMPERATURE RANGE

The structural use of this alloy should be limited to the temperature range 116 K - 670 K. The extra-low-interstitial grade (ELI) is recommended for low temperature uses. Fresh fracture surfaces of this alloy, when in contact with liquid oxygen, burn expontaneously, and the reaction may spread at a high rate. (ASMH (1974)e).

9. APPLICATIONS

Structural elements, fasteners, bolts and, generally speaking, those applications where high temperature precludes the use of aluminium alloys.

Representative cost of this alloy (sheet stock) is compared with those of other typical metals in Table 1-21 overleaf. Structural data are also included as a guide to cost effectiveness estimation.

METALLIC MATERIALS

Titanium-Aluminium-Vanadium Alloys

Table 1-21

Cost of Ti - 6 Al - 4 V compared with those of other structural metallic materials.

Material	ρ [kg.m ⁻³]	$\sigma_{ult} \times 10^{-8}$ ^a [Pa]	$E \times 10^{-10}$ ^b [Pa]	$\sigma_{ult} \cdot \rho^{-1} \times 10^{-6}$ [m ² .s ⁻²]	$E \cdot \rho^{-1} \times 10^{-8}$ [m ² .s ⁻²]	Cost US \$.kg ⁻¹
Al Alloy 2024-T6	2 770	3.93	7.24	.142	.262	1.3
Mg Alloy HK 31A	1 800	2.25	4.48	.126	.250	12.4
Ti Alloy Ti - 6 Al - 4 V	4 430	8.94	10.90	.202	.246	26.5
Stainless Steel 301 XHSR	8 030	17.30	20.70	.216	.258	2.5
Beryllium hct rolled	1 860	4.83	30.30	.262	1.64	772.0

^a σ_{ult} , Ultimate tensile strength.

^b E, Modulus of Elasticity.

From Adams (1974).

METALLIC MATERIALS

Nickel-Chrome-Cobalt-Molybdenum Alloys

1.10. NICKEL-CHROME-COBALT-MOLYBDENUM ALLOYS

ALLOY Ni - 19 Cr - 11 Co - 10 Mo - 3 Ti.

1. TYPICAL COMPOSITION, PERCENT

Al	B	C	Cr	Co	Fe	Mn	Mo	Si	S	Ti	Ni
1.4	.003	-	18	10	-	-	9	-	-	3	Balance
1.6	.010	.12	20	12	5	.1	10.5	.5	.015	3.5	

2. OFFICIAL DESIGNATIONS

AECMA	ISO	AFNOR	ASM	BS	DIN

This alloy is known as René 41, which is a trade mark.

3. PHYSICAL PROPERTIES

3.1. Density. $\rho = 8\ 190\ \text{kg}\cdot\text{m}^{-3}$. (room temp.)(Alloy Digest (1958)).

3.2. Thermal properties

3.2.1. Specific heat.

Effect of temperature on specific heat: Fig 1-65.

3.2.2. Thermal conductivity.

Effect of temperature on thermal conductivity: Fig 1-66

3.2.4. Thermal expansion.

Mean coefficient of linear thermal expansion, β , between 293 K and given temperature.

T [K]	422	644	866	1033	1200	1311
$\beta \times 10^6$ [K ⁻¹]	12.15	12.82	13.72	14.78	16.2	17.28

From Harris (1961).

Effect of temperature on thermal expansion: Fig 1-67.

METALLIC MATERIALS

Nickel-Chrome-Cobalt-Molybdenum Alloys

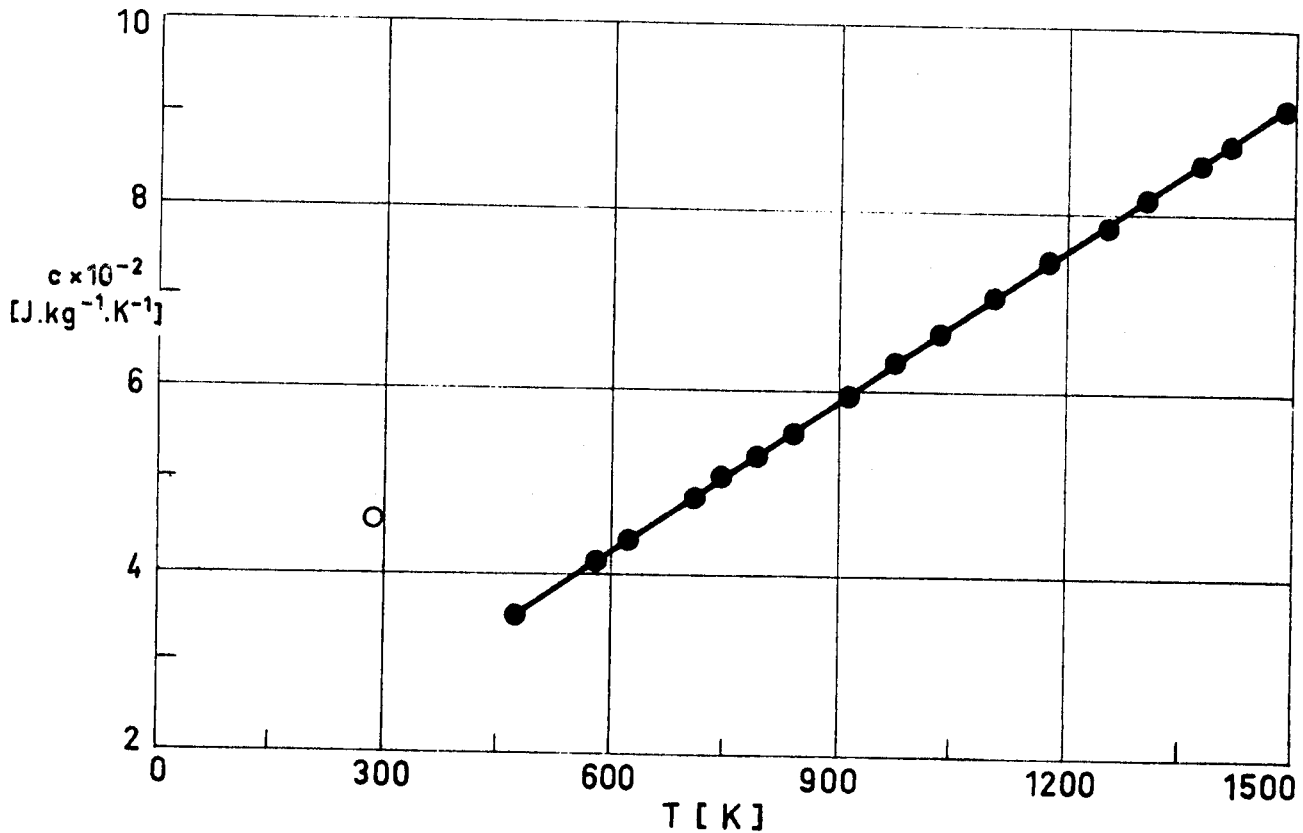


Fig 1-65. Specific heat, c , of Ni - 19 Cr - 11 Co - 10 Mo - 3 Ti as a function of temperature, T .

Explanation

Key	Description	Comments	References
○			Alloy Digest (1958).
●	Nominal composition. Solution heat treated at 1 350 K and water quenched.	Under helium atmosphere. Reported error 3%	Touloukian (1967)c.

METALLIC MATERIALS
 Nickel-Chrome-Cobalt-Molybdenum Alloys

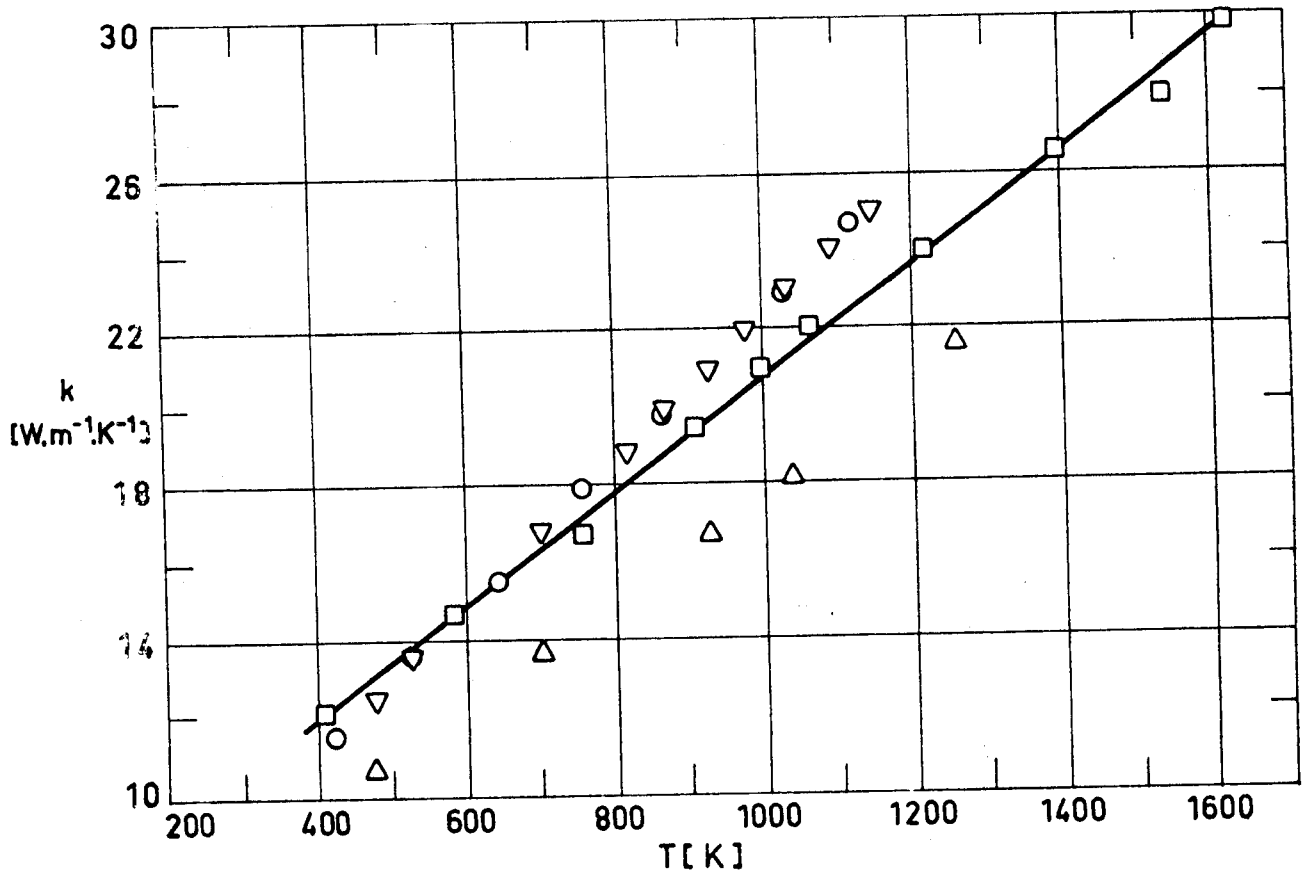


Fig 1-66. Thermal conductivity, k , of Ni - 19 Cr - 11 Co - 10 Mo - 3 Ti as a function of temperature, T .

Explanation

Key	Description	Comments	References
○			Harris (1961).
□	Nominal composition.	Sample contained in five disks of 2.54×10^{-2} m diameter. Reported error <5%.	Touloukian (1967)c.
△	Nominal composition.		
▽			

METALLIC MATERIALS

Nickel-Chrome-Cobalt-Molybdenum Alloys

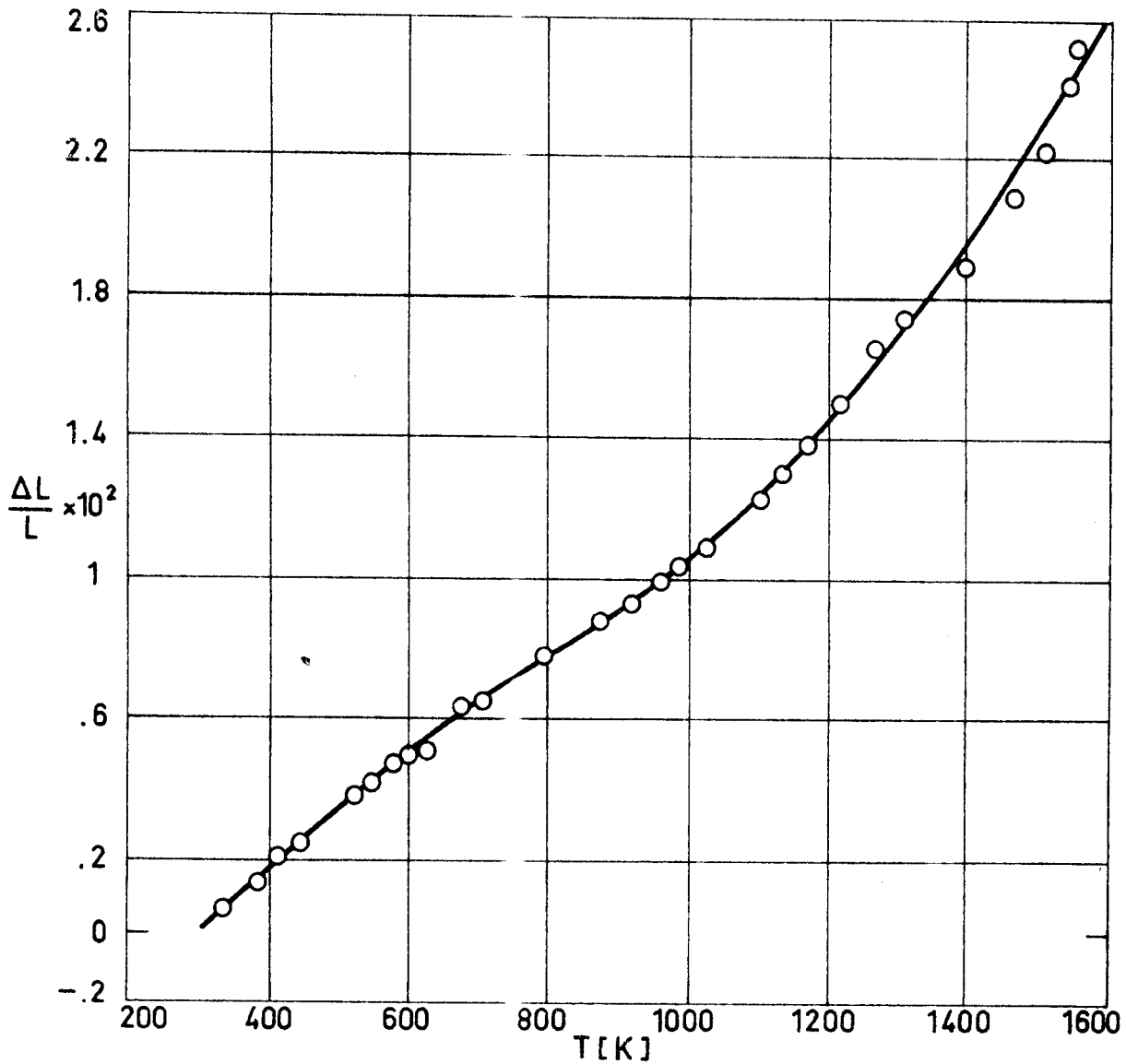


Fig 1-67. Thermal linear expansion, $\Delta L/L$, of Ni - 19 Cr - 11 Co - 10 Mo - 3 Ti as a function of temperature, T.

Explanation

Key	Description	Comments	References
○	Nominal composition. Solution-treated at 1350 K and water-quenched.		Touloukian (1967)c.

METALLIC MATERIALS

Nickel-Chrome-Cobalt-Molybdenum Alloys

3.2.5. Melting range.

1580 K - 1616 F. (ASMH (1974) f).

3.3. Thermal radiation properties

3.3.1. Emittance.

3.3.1.1. Normal spectral emittance ($\beta'=0$): Fig 1-68.

3.3.1.2. Normal total emittance ($\beta'=0$).

Effect of temperature on normal total emittance: Fig 1-69.

3.3.3. Reflectance.

3.3.3.1. Bidirectional spectral reflectance.

Normal-normal spectral reflectance ($\beta=\beta'=0$): Fig 1-70.

3.4. Other physical properties

3.4.1. Electrical resistivity. Table 1-22.

Table 1-22

Electrical Resistivity of Ni - 19Cr - 11Co - 10Mo - 3Ti ^a

T [K]	Condition	$\sigma^{-1} \times 10^6$ [$\Omega \cdot m$.]
19	Solution treated.	1.18
77	Solution treated.	1.20
194	Solution treated.	1.23
273	Solution treated.	1.27
293 ^b	Solution treated.	1.31
293 ^b	Solution treated. Heat treated at 1340 K during 4 h. Air cooled.	1.25
293 ^b	Heat treated at 1030 K during 16 h. Air cooled.	1.26
293 ^b	Heat treated at 1450 K during 30 min. Air cooled.	1.33
293 ^b	Heat treated at 1170 K during 4 h. Air cooled.	1.34

^a A sheet 1.9×10^{-2} m thick was used in any case.

^b It appears in the source as "room temperature".
From ASMH (1974) f.

METALLIC MATERIALS

Nickel-Chrome-Cobalt-Molybdenum Alloys

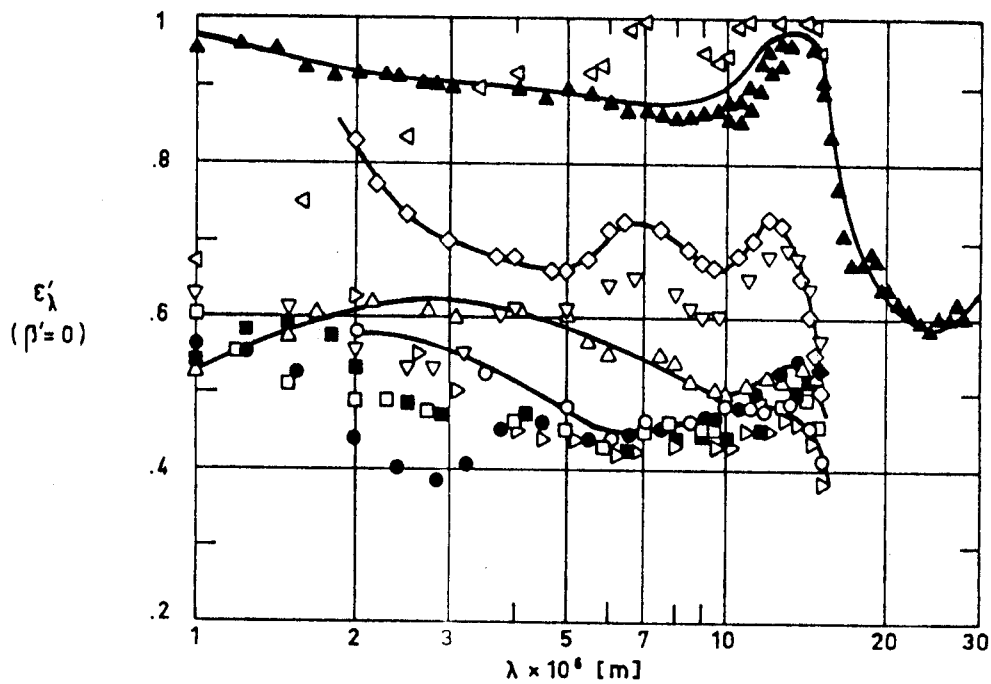


Fig 1-68. Normal spectral emittance, ϵ'_λ , of Ni - 19 Cr - 11 Co - 10 Mo - 3 Ti as a function of wavelength, λ .

Explanation

Key	Description	Comments	References
○	Nominal composition. As received.	Sample temperature: T = 523.2 K.	Touloukian (1967)c.
□	Same as ○ .	T = 773.2 K.	
△	Same as ○ .	T = 1 023 K.	
◇	Nominal composition. Heated in air at 1 255 K for 30 min.	T = 523.2 K.	
▽	Same as ◇ .	T = 773.2 K.	
◁	Same as ◇ .	T = 1 023 K.	
▷	Nominal composition. Heated in vacuum (1.01×10^{-2} Pa) at 1 255 K for 30 min.	T = 523.2 K.	
●	Same as ▷ .	T = 773.2 K.	
■	Same as ▷ .	T = 1 023 K.	
▲	Nominal composition. Well oxidized.	T = 1 041.5 K.	

METALLIC MATERIALS

Nickel-Chrome-Cobalt-Molybdenum Alloys

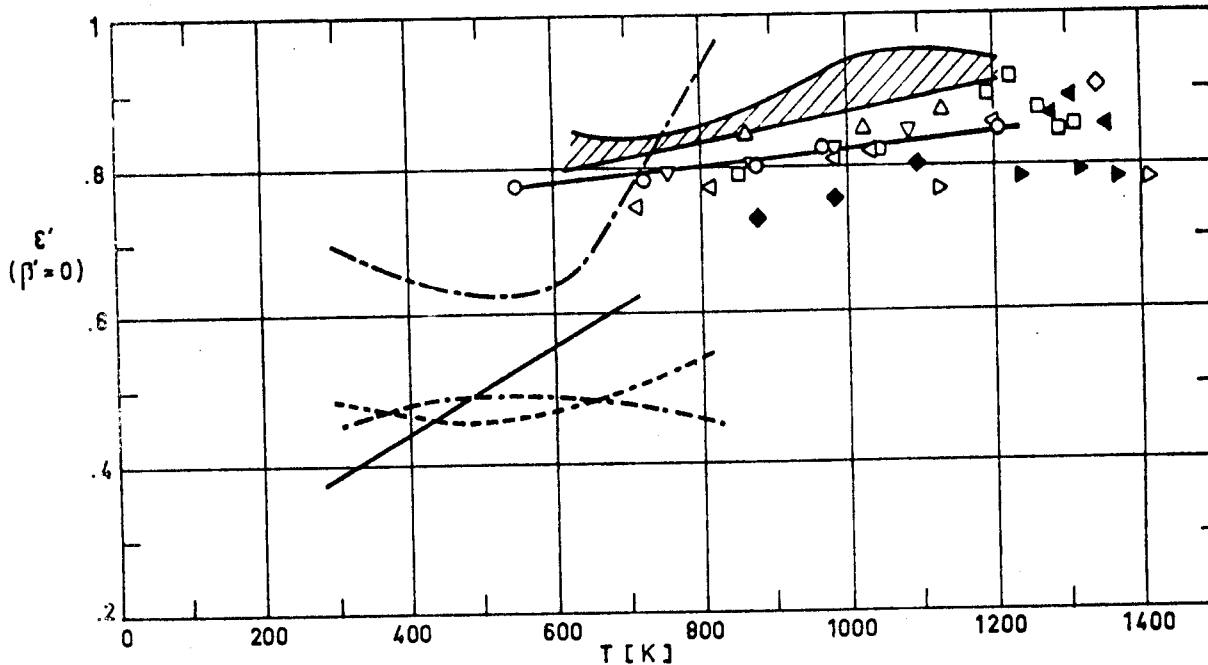


Fig 1-69. Normal total emittance, ϵ' , of Ni - 19 Cr - 11 Co - 10 Mo - 3 Ti as a function of temperature, T.

Explanation

Key	Description	Comments	References
○	Nominal composition. Surface roughness (fully aged): 1) fine structure 2×10^{-6} m high. 2) coarse structure 5×10^{-6} m high at 2×10^{-4} m intervals. Cleaned in 1 to 1 water-diluted HF solution for 1 h, oxidized 1 h at 1 200 K in air.	Measured in decreasing temperatures.	Touloukian (1967)c.
□	Same as ○.	Measured in increasing temperatures. The specimen was heated by gas for temperatures higher than 1 227.6 K.	
△	Same as ○.	Above specimen measured in decreasing temperatures.	
▽	Nominal composition.	Chromel-Alumel thermocouple mounted off center on the face. Electrically heated specimen.	
▷	Same as ▽.	Same as ▽. Gas fired stand.	
▶	Same as ▽.	Same as ▽. Electrically heated stand.	
◁	Same as ▽.	Same as ▽. Gas fired stand.	
◀	Same as ▽.	Same as ▽. Gas fired stand.	
◇	Same as ▽.	Same as ▽. Gas fired stand. Based on optical pyrometer.	
◆	Similar specimen.	Same as ▽. Electrically heated stand.	
—	As received.	Averaged over the wavelength range 2×10^{-6} m - 15×10^{-6} m.	ASMH (1974) f.
—	Heated in air 30 min at 1 255 K.		
—	Heated in vacuum 30 min at 1 255 K.		
—	Oxidized in air 30 min at 1 340 K and 16 h at 1 030 K.		
—	Solution treated in argon atmosphere 30 min at 1 340 K. Air cooled, aged in argon 16 h at 1 030 K, oxidized.		

METALLIC MATERIALS

Nickel-Chrome-Cobalt-Molybdenum Alloys

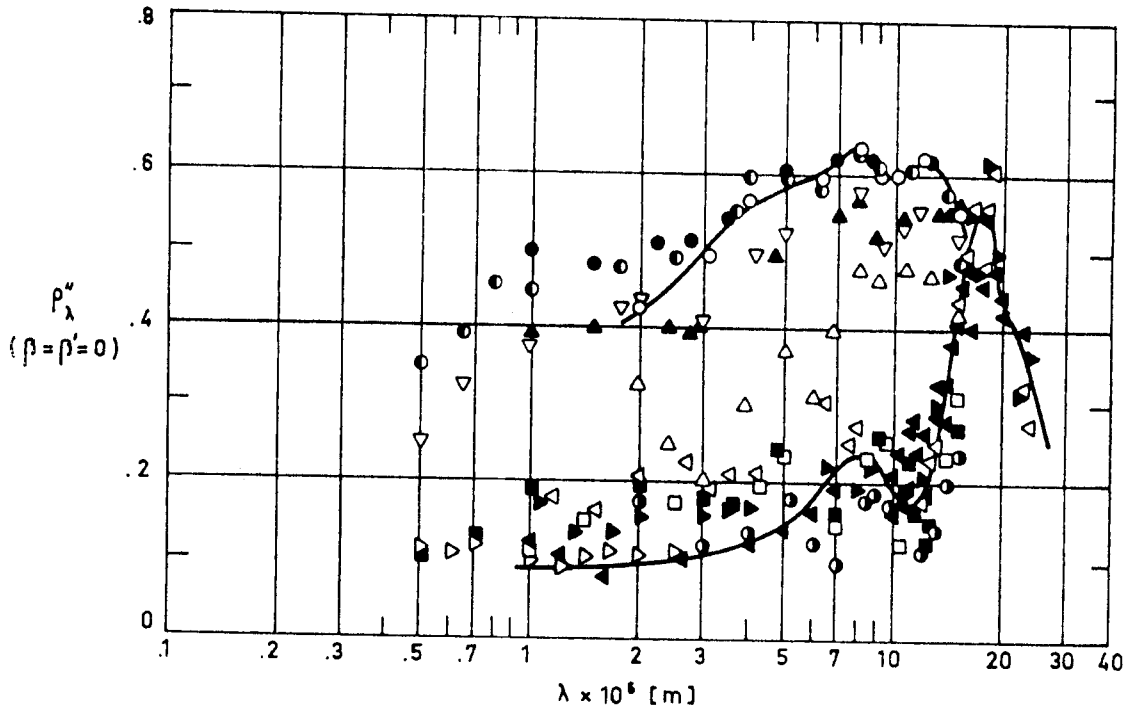


Fig 1-70. Normal-normal spectral reflectance, ρ_{λ}'' , of Ni-19 Cr-11 Co-10 Mo-3 Ti as a function of wavelength, λ . Data points \triangleright correspond to normal-hemispherical reflectance while \blacktriangleright , \triangleleft , \blacktriangleleft correspond to hemispherical-normal reflectance.

Explanation

Key	Description	Comments	References
○	Nominal composition, as received.	523.2 K source.	Touloukian (1967)c.
●	Same as ○	Sample temperature below 322 K. 773.2 K source.	
⊙	Same as ○. Heated in air at 1 250 K for 30 min.	Sample temperature below 322 K. 523.2 K source.	
⊗	Same as ⊙	Sample temperature below 322 K. 1 273 K source.	
□	Same as ⊙	Sample temperature below 322 K. 773.2 K source.	
■	Same as ⊙	Sample temperature below 322 K. 1 273 K source.	
△	Same as ⊙. Heated in vacuum (10^{-2} Pa) at 1 255 K for 30 min.	Sample temperature below 322 K. 523.2 K source.	
▲	Same as △	Sample temperature below 322 K. 773.2 K source.	
▽	Same as △	Sample temperature below 322 K. 1 273 K source.	
▷	Nominal composition. Surface roughness: 1) fine structure 2×10^{-6} m high. 2) coarse structure 5×10^{-6} m high at 2×10^{-4} m intervals. Cleaned in 1 to 1 water-diluted HCl solution for 1 h and oxidized 3 h at 1 200 K in air.	$\beta = 4^\circ$ $\omega' = 2\pi$ Sample temperature: 294.3 K.	
▷	Same as ▷	$\omega = 2\pi$ $\beta' = 7^\circ$ Sample temperature: 294.3 K.	
△	Same as ▷	Same as ▷ although sample temperature is 828.1 K.	
◁	Same as ▷. Well oxidized.	$\omega = 2\pi$ $\beta' = 7^\circ$	

METALLIC MATERIALS

Nickel-Chrome-Cobalt-Molybdenum Alloys

3.4.2. Magnetic properties.

Relative Permeability: $\mu/\mu_0 < 1.002$ measured at 1.6×10^{-3} A.m⁻¹ and room temperature. (ASMH (1974) f).

4. ENVIRONMENTAL BEHAVIOR4.1. Prelaunch

Highly polished surfaces of this alloy are very susceptible to increases in α_s and ϵ , by fingerprinting and surface oxidation. Permanent damage may be caused unless contamination is immediately removed and the surface is protected.

4.2. Postlaunch

Ascent heating is very likely to increase α_s and ϵ .
(From Breuch (1967)).

5. CHEMICAL PROPERTIES5.2. Corrosion resistance

This alloy is highly corrosion and oxidation resistant (Alloy Digest (1958)).

6. FABRICATION

6.2. Forming. Good in the annealed condition. Bad in the age hardening condition. (ASMH (1974) f).

6.3. Welding. Good in inert gas shielded arc (ASMH (1974) f) for electron beam with preheating. (Harris (1961)). Sections thicker than 1.3×10^{-2} m are recommended in the last case.

6.4. Machining. Good with tungsten carbide tools in age hardening condition. (Alloy Digest (1958)).

6. . Heat treatment. Good. (ASMH (1974) f).

METALLIC MATERIALS

Nickel-Chrome-Cobalt-Molybdenum Alloys

7. AVAILABLE FORMS AND CONDITIONS

Bar, sheet, plate, flats and billets.

8. USEFUL TEMPERATURE RANGE

This alloy has excellent properties even at temperature as high as 1250 K. Nevertheless, structural use should be limited to temperatures below 1150 K, and even below 950 when thin sheets are used.

9. APPLICATIONS

For structural elements (high speed airframes) and antennas.

METALLIC MATERIALS

Iron-Nickel Alloys

1.11. IRON-NICKEL ALLOYS

ALLOY Fe - 36 Ni.

1. TYPICAL COMPOSITION, PERCENT

C	Mn	Ni	Si	Fe
-	-	34.5	-	Balance
.12	.5	36	.5	

2. OFFICIAL DESIGNATIONS

AECMA	ISO	AFNOR	AMS	BS	DIN
					Ni 36 1.3912

This alloy is often known as Invar, which is a trade mark.

3. PHYSICAL PROPERTIES

3.1. Density. $\rho = 8\ 082\ \text{kg.m}^{-3}$. (Alloy Digest (1964)).

3.2. Thermal properties

3.2.1. Specific heat.

Effect of temperature on specific heat: Fig 1-71.

3.2.2. Thermal conductivity.

293 K - 373 K, $k=10.96\ \text{W.m}^{-1}.\text{K}^{-1}$. (Hunter (1961)).

$k=10.47\ \text{W.m}^{-1}.\text{K}^{-1}$. (Alloy Digest (1964)).

$k=13.50\ \text{W.m}^{-1}.\text{K}^{-1}$. (Anon.(1973)).

3.2.4. Thermal expansion.

Effect of temperature on thermal expansion: Fig 1-72.

3.2.4.1. Effect of alloying elements on thermal expansion coeffi-

METALLIC MATERIALS
Iron-Nickel Alloys

cient: Fig 1-73.

3.2.4.2. Effect of heat treatment on linear thermal expansion coefficient: Table 1-23

Table 1-23

Linear thermal expansion coefficient of Fe - 36 Ni
under different temper conditions

Condition	Temp. range [K]	$\beta \times 10^6$ [K ⁻¹]
After forging	290-373	1.56
	290-523	3.11
Quenched from 1100 K	291-373	.64
	291-523	2.53
Quenched from 1100 K, tempered.	288-373	1.02
	288-523	2.43
Cooled from 1100 K to room temperature in 19 h.	288-373	2.01
	288-523	2.89

From Hunter (1961).

3.2.5. Melting range.

Solidus temperature: 1 698 K.(Hunter (1961)).

3.3. Thermal radiation properties

3.3.1. Emittance.

3.3.1.1. Normal spectral emittance ($\beta'=0$).

Effect of temperature on normal emittance for a particular wavelength: Fig 1-74.

METALLIC MATERIALS
Iron-Nickel Alloys

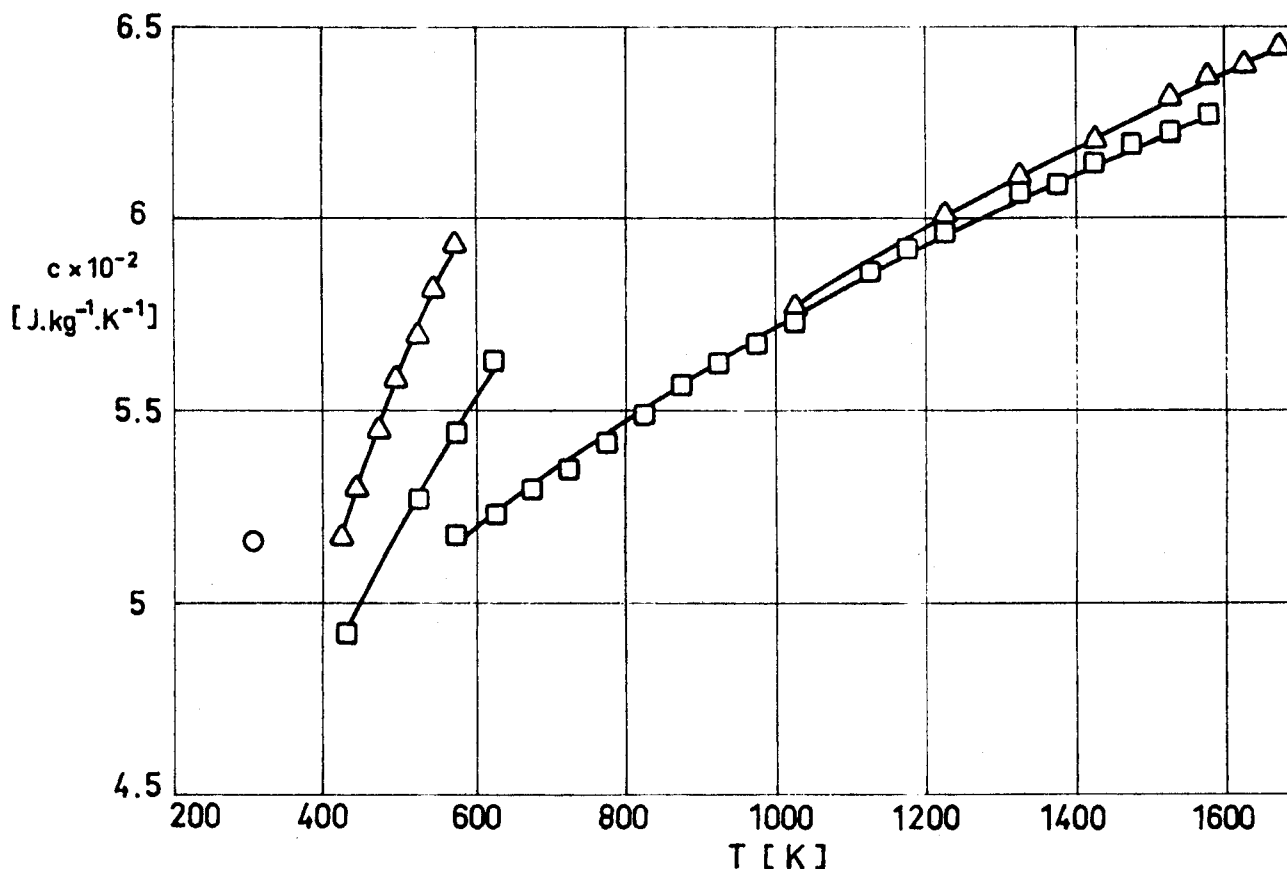


Fig 1-71. Specific heat, c , of Fe - 36 Ni (Invar) as a function of temperature, T .

Explanation

Key	Description	Comments	References
○			Hunter (1961)
□	Fe - 29.5 Ni, prepared from electrolytically deposited pure iron and pure nickel.	Vacuum melted.	Touloukian (1967)d.
△	Fe - 39 Ni, prepared from electrolytically deposited pure iron and pure nickel.		

METALLIC MATERIALS

Iron-Nickel Alloys

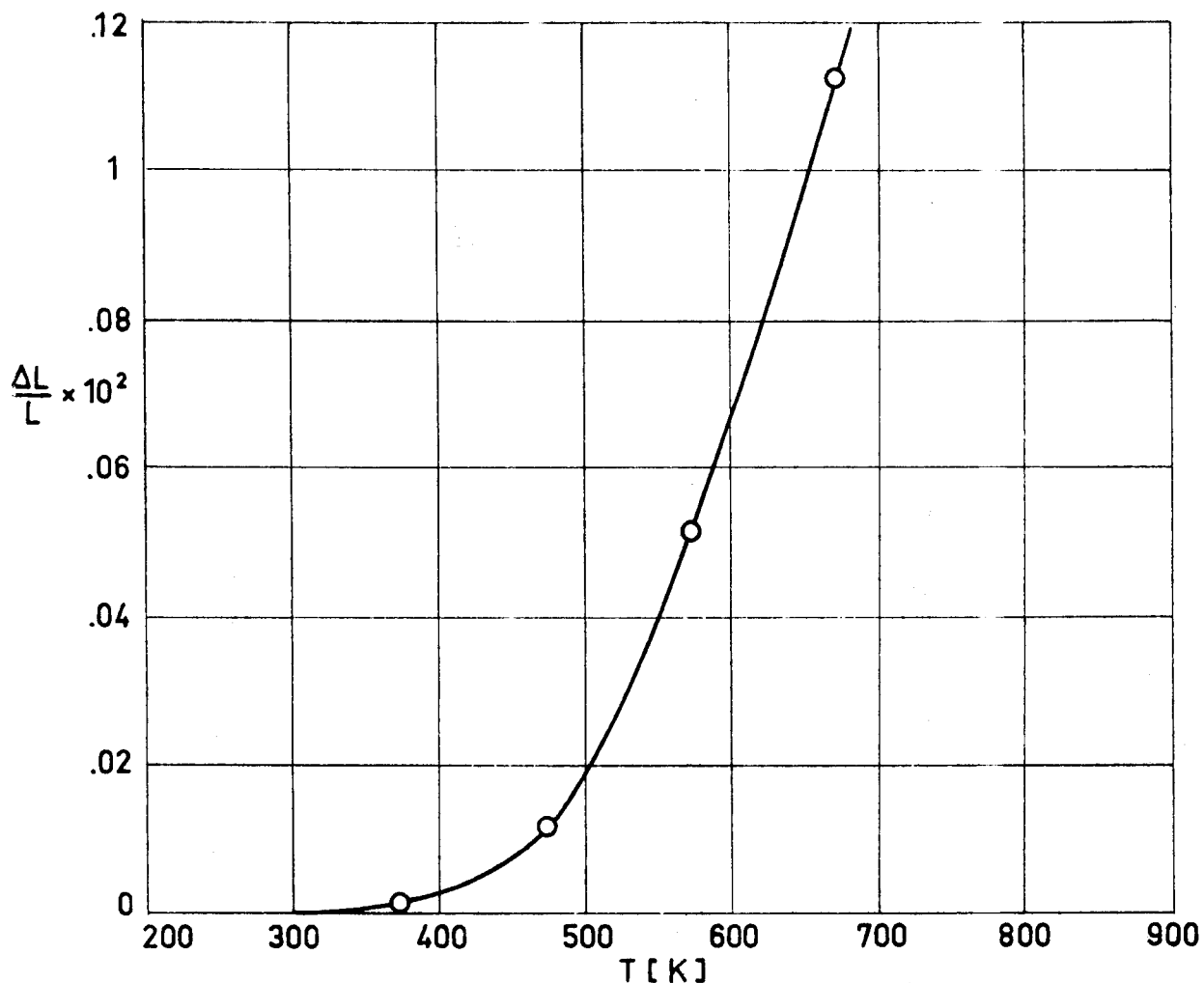


Fig 1-72. Linear thermal expansion, $\Delta L/L$, of Fe - 36 Ni (Invar) as a function of temperature, T .

Explanation

Key	Description	Comments	References
○	Nominal composition. Vacuum-melted, hot-rolled at 1 470 K from 7.5×10^{-2} to 2×10^{-2} m, reheated to 1 270 K, water-quenched, cold-rolled to 10^{-3} m, aged 8 h at 370 K, and cooled slowly.		Touloukian (1967)d.

METALLIC MATERIALS
Iron-Nickel Alloys

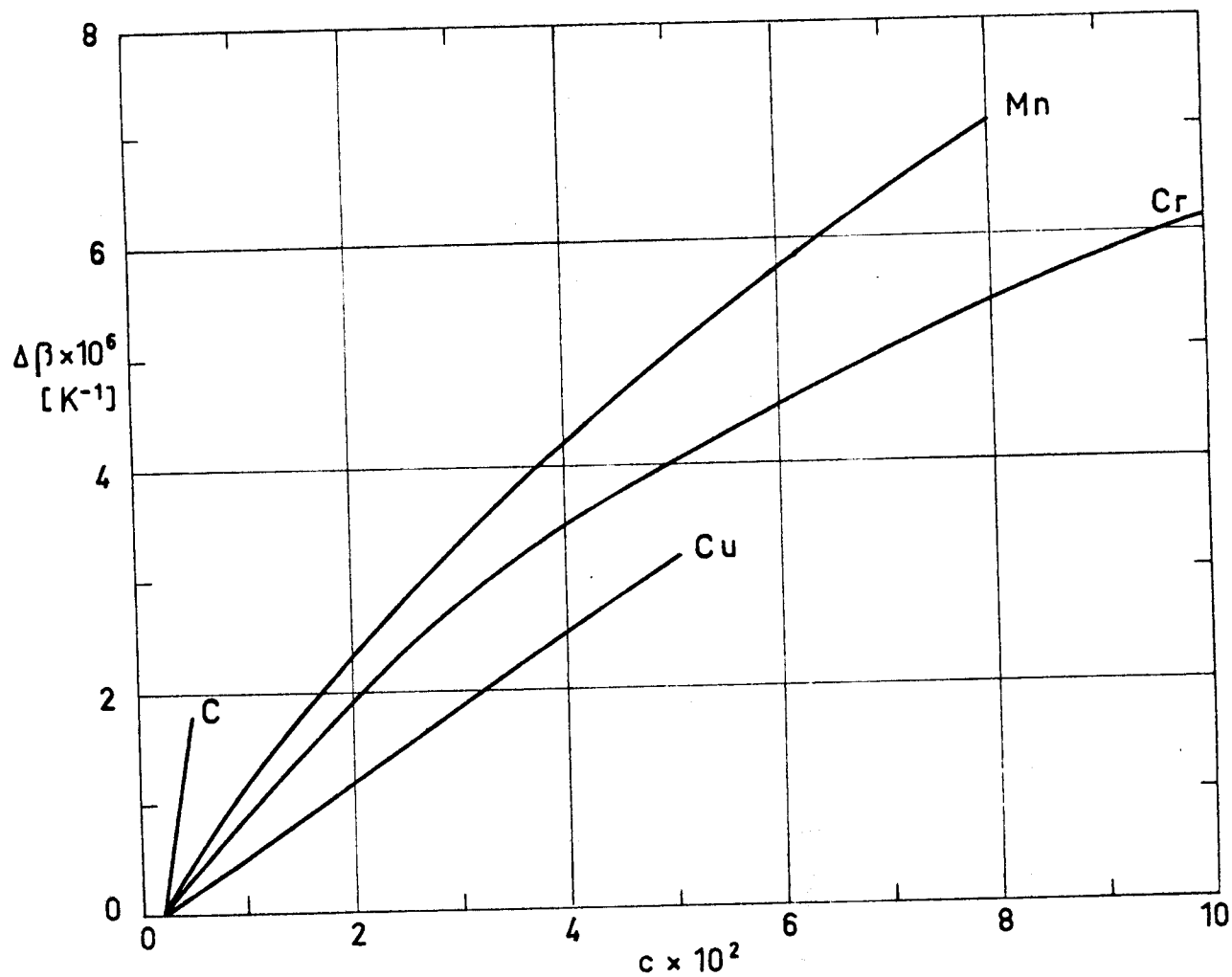


Fig 1-73. Effect of the concentration of alloying elements, c , on the value of the coefficient of linear expansion, β . From MOND NICKEL Co.

METALLIC MATERIALS
Iron-Nickel Alloys

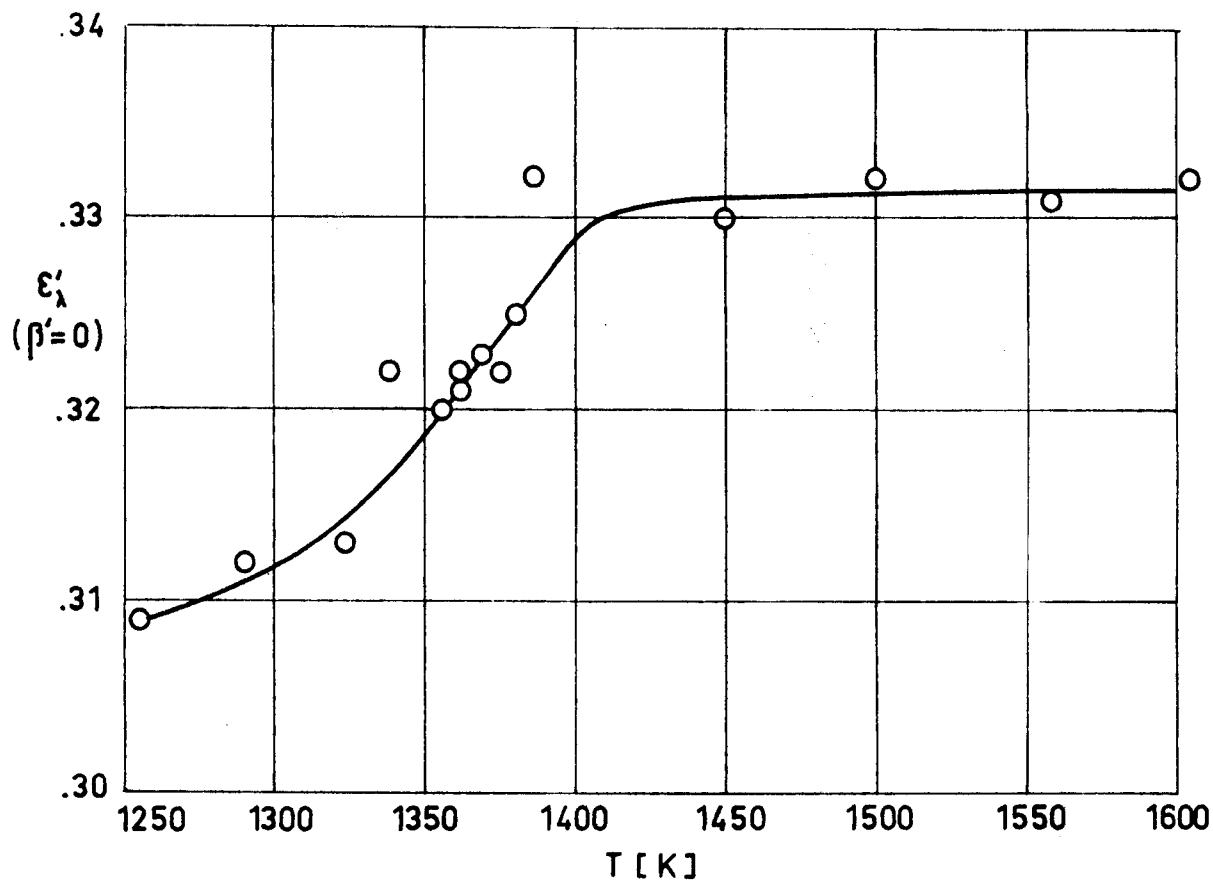


Fig 1-74. Normal emittance, ϵ'_λ , of Fe - 36 Ni (Invar), for $\lambda = 6.7 \times 10^{-7}$ m, as a function of temperature, T .

Explanation

Key	Description	Comments	References
○	Nominal composition. Powders were mixed in desired proportions, compressed at 4.8×10^8 Pa and 298 K, heated at 1 373 K in flowing hydrogen; cold rolled, then heated in hydrogen at 1 273 K.		Touloukian (1967)d.

METALLIC MATERIALS

Iron-Nickel Alloys

3.4. Other physical properties

3.4.1. Electrical resistivity.

$$\sigma^{-1} = (.80 \pm .05) \times 10^{-6} \Omega.m . (Hunter (1961)).$$

Temperature coefficient of electrical resistivity:

$$\alpha = 1.2 \times 10^{-3} K^{-1} . (Hunter (1961)).$$

3.4.2. Magnetic properties. Tables 1-24 and 1-25.

Table 1-24

Magnetic Properties of Fe - 36 Ni under different temper conditions

Condition	Field Strength H [A.m ⁻¹]	Normal Induction B [T]	Relative Permeability (μ/μ_0) $\times 10^{-3}$
Annealed	8	.020	1
	32	.950	2.2
	64	.310	3.7
	95	.440	3.5
	103	.445	3.4
Hard drawn	160	.030	1.7
	320	.160	2.9
	480	.400	4.4
	640	.560	4.5
	800	.650	4.3

From Alloy Digest (1964).

Table 1-25

Relative Permeability of Fe - 36 Ni, measured at 400 A.m⁻¹

T [K]	(μ/μ_0) $\times 10^{-3}$
255	1.800
283	1.715
311	1.630
339	1.545
367	1.450
389	1.360

From Alloy Digest (1964).

METALLIC MATERIALS
Iron-Nickel Alloys

3.4.2.1. Loss of magnetism

Condition	T_i^a [K]	T_f^a [K]
Annealed	435	544
Quenched	478	544

^a T_i initial temperature.

T_f minimum temperature of complete loss.
From Hunter (1961).

5. CHEMICAL PROPERTIES

5.2. Corrosion resistance. This alloy resists the atmospheric corrosion and those produced by fresh water and by salt water. (Anon. (1973)).

6. FABRICATION

6.2. Forming. This alloy has almost unlimited capacity for plastic deformation, either hot or cold. (Alloy Digest (1964)).

6.2.1. Hot working can be performed below 1 530 K, (Alloy Digest (1964)), however, as has been reported by Hunter (1961), careful handling is required to avoid cracking and breaking up.

6.2.2. Invar which has been subjected to cold working or machining may require a stress-relieving heat treatment for stabilization. (Alloy Digest (1964)).

6.3. Welding. May be successfully welded by any of the commonly used methods. (Alloy Digest (1964)).

6.4. Machining. Is somewhat difficult. (Alloy Digest (1964)).

METALLIC MATERIALS

Iron-Nickel Alloys

6.5. Heat treatment. A reducing atmosphere should be used. (Hunter (1961)).

7. AVAILABLE FORMS AND CONDITIONS

Hot rolled and cold drawn bars, wires, strips, and forgings.

8. USEFUL TEMPERATURE RANGE

This alloy retains its characteristic low expansiveness provided that the temperature is maintained below 475 K. For applications at temperatures above this value, higher nickel alloys are recommended. (Alloy Digest (1964)).

9. APPLICATIONS

Because Invar has unusually low thermal expansion, it is used for instruments requiring constant distances between points, glass to metal seals, thermostatic and other temperature control or indicating devices, bimetals, etc.

Invar has positive thermoelastic coefficients over a large temperature range. This anomaly is useful in developing alloys with nearly temperature-invariant elastic constants.

Invar is also a candidate low-temperature material. Its elastic properties between room temperature and liquid helium temperature have been reported by Ledbetter, Naimon & Weston (1977).

INTENTIONALLY BLANK PAGE

STRUCTURAL MATERIALS

References

- Alloy Digest 1958 "G-E Alloy René 41",
in "Data on World Wide Metals and Alloys",
Engineering Alloy Digest, Inc., Upper
Montclair, New Jersey, Nov. 1958, Filing
Code: Ni-47.
- Harris, Jr., W.J. 1961 "Wrought Heat-Resisting Alloys",
in "Metals Handbook, Vol. 1, Properties
and Selection of Metals", 8th ed., T.
Lyman, Ed., American Society for Metals
(ASM), Cleveland, Ohio, 1961, pp. 487-
490.
- Hunter, M.A. 1961 "Low-Expansion Alloys",
in "Metals Handbook, Vol. 1, Properties
and Selection of Metals", 8th ed., T.
Lyman, Ed., American Society for Metals
(ASM), Cleveland, Ohio, 1961, pp. 816-
819.
- Kappelt, G.F. 1961 "Properties of Aluminum and Aluminum Al-
loys",
in "Metals Handbook, Vol. 1, Properties
and Selection of Metals", 8th ed., T.
Lyman, Ed., American Society for Metals
(ASM), Cleveland, Ohio, 1961, pp. 935-
958.
- Pennington, Wm.A. 1961 "Pure Metals",
in "Metals Handbook, Vol. 1, Properties
and Selection of Metals", 8th ed., T.
Lyman, Ed., American Society for Metals
(ASM), Cleveland, Ohio, 1961, p. 1197.

Rev. 2. 1984

STRUCTURAL MATERIALS

References

- Stuart Lyman, W. 1961 "Properties of Titanium and Titanium Alloys",
in "Metals Handbook, Vol. 1, Properties and Selection of Metals", 8th ed.,
T. Lyman, Ed., American Society for Metals (ASM), Cleveland, Ohio, 1961, pp.
537-542 and 1153-1156.
- REYNOLDS METALS Co. 1961 "The Aluminum Data Book",
Reynolds Metals Company, Richmond, Virginia, 1961, p. 49.
- Smithells, C.J. 1962 "Metals Reference Book",
Vol. II, 3rd ed., Butterworths, London,
1962, p. 701.
- Alloy Digest 1964 "Invar",
in "Data on World Wide Metals and Alloys", Engineering Alloy Digest, Inc.,
Upper Montclair, New Jersey, March 1964,
Filing Code: Fe-24.
- ALCAN 1965 "Heat-Treatable Al-Cu-Mg Wrought Alloy
24 S",
in "Aluminum Alloy Tables", 4th ed.,
Alcan S.A., Zürich, Switzerland, Feb.
1965.
- Zerlaut, G.A.,
Carroll, W.F.,
Gates, D.W. 1966 "Spacecraft Temperature-Control Coat-
ings: Selection, Utilization and Problems Related to the Space Environment",
in "Proceedings of the XVth International Astronautical Congress, Athens
1965", Gauthier-Villars, Dunod, Paris,
1966, pp. 259-313.

STRUCTURAL MATERIALS

References

- Breuch, R.A. 1967 "Handbook of Optical Properties for Thermal Control Surfaces", LMSC-A847882, Vol. III, (NAS 8-20353), Lockheed Missiles & Space Company, Sunnyvale, California, 1967.
- Coston, R.M. 1967 "Handbook of Thermal Design Data for Multilayer Insulation Systems", LMSC-A847882, Vol. II, (NAS 8-20353), Lockheed Missiles & Space Company, Sunnyvale, California, 1967.
- Develay, R.,
Faure, A.,
Lehongre, S.,
Mugnier, D.,
Schroeter, D. 1967 "A Versatile Aluminum Alloy for Cryogenic Applications", in "Advances in Cryogenic Engineering", Vol. 12, K.D. Timmerhaus, Ed., Plenum Press, New York, 1967, pp. 484-495.
- Schafer, G.F.,
Bannister, T.C. 1967 "Thermal Control Coating Degradation Data from the Pegasus Experiment Packages", in "Progress in Astronautics and Aeronautics", Vol. 20, G.B. Heller, Ed., Academic Press, New York, 1967, pp. 457-473.
- Touloukian, Y.S. 1967a "Thermophysical Properties of High Temperature Solid Materials", Vol. 1: Elements, The MacMillan Company, New York, 1967.
- Touloukian, Y.S. 1967b "Thermophysical Properties of High Temperature Solid Materials", Vol. 2: "Nonferrous Alloys", Part I: "Nonferrous Binary Alloys", The MacMillan Company, New York, 1967.

Rev. 2. 1984

STRUCTURAL MATERIALS

References

- Touloukian, Y.S. 1967c "Thermophysical Properties of High Temperature Solid Materials",
Vol. 2: "Nonferrous Alloys", Part II:
"Nonferrous Multiple Alloys", the Mac-
Millan Company, New York, 1967.
- Touloukian, Y.S. 1967d "Thermophysical Properties of High Temperature Solid Materials",
Vol. 3: "Ferrous Alloys", The MacMillan
Company, New York, 1967.
- ALUMINUM ASSOCIATION 1969 "Aluminum Standards & Data 1970-71",
2nd ed., The Aluminum Association, New
York, Dec. 1969, p. 35.
- Bevans, J.T. 1969 "Aerospace Coatings for Thermal Control",
Preliminary Report, Space Technology
Laboratories, Inc., Redondo Beach, Cali-
fornia, 1969.
- Millard, J.P., 1969 "A Comparison on Infrared-Emissance Mea-
Streed, E.R. surements and Measurement Techniques",
Applied Optics, Vol. 8, No. 7, July
1969, pp. 1485-1492.
- Scollon, T.R., 1970 "Long Life High Reliability Thermal Con-
Carpitella, M.J. trol Systems Study Data Handbook",
Prepared under Contract NAS 8-26252 by
Space Systems Organization, General Elec-
tric Company, Valley Forge Space Technolo-
gy Center, Pennsylvania, 1970.

STRUCTURAL MATERIALS

References

- Touloukian, Y.S., 1970 "Thermal Radiative Properties. Metallic Elements and Alloys", Thermophysical Properties of Matter, Vol. 7, IFI/Plenum, New York, 1970.
- DeWitt, D.P.
- TRW 1970 "Aerospace Fluid Component Designers' Handbook, Emissivity", Technical Documentary Report No. RPL-TOR-64-25, Feb. 1970, TRW Systems Group, Redondo Beach, California.
- McCargo, M., 1971 "Review of the Transient Degradation/Contamination of Thermal Coatings", LMSC-D1778, (NAS 8-26004), Lockheed Missiles & Space Company, Sunnyvale, California, 1971.
- Spradley, L.W.,
Greenberg, S.A.,
McDonald, S.L.
- García-Poggio, J.A., 1972 "Aleaciones Industriales de Aluminio", Instituto Nacional de Técnica Aeroespacial Esteban Terradas, Madrid, 1972.
- Ramírez, F.,
Torre, J.M. de la,
Vázquez, M.,
Asensi, E.,
Marín, C.,
Ciria, J.
- Touloukian, Y.S., 1972 "Thermal Radiative Properties. Coatings", Thermophysical Properties of Matter, Vol. 9, IFI/Plenum, New York, 1972.
- DeWitt, D.P.,
Hernicz, R.S.
- Ross, R.B. 1972 "Metallic Materials. Specification Handbook", E & F.N. Spon Ltd., London 1972, pp. 676-692.
- Anon. 1973 "1974 Materials Selector, Nonferrous Metals", Materials Engineering, Reinhold Publishing Company, Inc., Mid-Sep. 1973, p. 130.

Rev. 2. 1984

STRUCTURAL MATERIALS

References

- Tien, J.K.,
Chesnutt, J.C.,
Boone, D.H.,
Goward, G.W.
- 1973 "Metallurgy of Nickel-Base Coatings on Titanium Alloys",
in "Titanium Science and Technology",
Vol. 4, R.I. Jaffee & H.M. Burte, Eds.,
Plenum Press, New York & London, 1973,
pp. 2517-2525.
- Adams, D.F.
- 1974 "High-Performance Composite Material Airframe Weight and Cost Estimating Relations",
Journal of Aircraft, Vol. 11, No. 12,
Dec. 1974, pp. 751-757.
- ASMH
- 1974c "Aluminum Alloys; Wrought, Heat Treatable (AIWT)",
in "Aerospace Structural Metals Handbook", AFML-TR-68-115, J. Wolf, Ed.,
Mechanical Properties Data Center,
Watertown, Mass., 1974, Codes 3203 & 3206.
- ASMH
- 1974d "Magnesium Alloys, Cast (MgWT)",
in "Aerospace Structural Metals Handbook", AFML-TR-68-115, J. Wolf, Ed.,
Mechanical Properties Data Center,
Watertown, Mass., 1974, Code 3407.
- ASMH
- 1974e "Titanium Alloys (Ti)",
in "Aerospace Structural Metals Handbook", AFML-TR-68-115, J. Wolf, Ed.,
Mechanical Properties Data Center,
Watertown, Mass., 1974, Codes 3706 & 3707.

STRUCTURAL MATERIALS

Rev. 2. 1984

References

- ASMH 1974f "Nickel Base Alloys (>5% Co)(NiCo)",
in "Aerospace Structural Metals Hand-
book", AFML-TR-68-115, J. Wolf, Ed.,
Mechanical Properties Data Center,
Watertown, Mass., 1974, Code 4205.
- Ledbetter, H.M., 1977 "Low-Temperature Elastic Properties
Naimon, E.R., of Invar",
Weston, W.F. in "Advances in Cryogenic Engineer-
ing", Vol. 22, K.D. Timmerhaus, R.P.
Reed and A.F. Clark, Eds., Plenum
Press, New York, 1977, pp. 174-181.
- ASMH 1978 "Titanium Alloys (Ti-3700)",
in "Aerospace Structural Metals Hand-
book", AFML-TR-68-115, J. Wolf, Ed.,
Mechanical Properties Data Center,
Watertown, Mass., 1974, Code 3718.
- Braun, A.H. 1979 "Selection and Applications of Magne-
sium and Magnesium Alloys",
in "Metals Handbook, Vol. 2, Proper-
ties and Selection: Non Ferrous Al-
loys and Pure Metals", 9th ed., W.H.
Cubberley et al., Eds., American Soc-
iety for Metals (ASM), Metals Park,
Ohio 44073, 1979, pp. 525-679.
- McCall, J.L. 1979 "Introduction to Aluminum and Alumi-
num Alloys",
in "Metals Handbook, Vol. 2, Proper-
ties and Selection: Non Ferrous Al-
loys and Pure Metals", 9th ed., W.H.
Cubberley et al., Eds., American Soc-
iety for Metals (ASM), Metals Park,
Ohio 44073, 1979, pp. 3-236.

Rev. 2. 1984

STRUCTURAL MATERIALS

References

- Betner, D.R. 1980 "Properties of Titanium and Titanium Alloys",
in "Metals Handbook, Vol. 3, Properties and Selection: Stainless Steels, Tool Materials and Special-Purpose Metals", 9th ed., W.H. Cubberley et al., Eds., American Society for Metals (ASM), Metals Park, Ohio 44703, 1980, pp. 372-412.
- Campbell, J.E. 1980 "Alloys for Structural Applications at Subzero Temperatures",
in "Metals Handbook, Vol. 3, Properties and Selection: Stainless Steels, Tool Materials and Special-Purpose Metals", 9th ed., W.H. Cubberley et al., Eds., American Society for Metals (ASM), Metals Park, Ohio 44073, 1980, pp. 723-746.
- Simenz, R.F.,
Guess, M.K. 1980 "Structural Aluminum Materials for the 1980's",
J. Aircraft, Vol. 17, No. 17, July 1980, pp. 514-520.
- Ball, K. 1982 "Cleaning and Finishing of Aluminum and Aluminum Alloys",
in "Metals Handbook, Vol. 5, Surface Cleaning, Finishing, and Coating", 9th ed., W.H. Cubberley et al., Eds., American Society for Metals (ASM), Metals Park, Ohio 44073, 1982, pp. 585-610.

STRUCTURAL MATERIALS

References

- UNE 1982 "Aluminio y Aleaciones de Aluminio para Forja",
UNE 38-371-82, Madrid, Dec. 1982.
- UNE 1984 "Titanio y Aleaciones de Titanio para Forja",
PNE 38-718-84, Madrid, 1984.
- MOND NICKEL Co. "The Physical Properties of the Nickel-Iron Alloys",
The Mond Nickel Company Ltd., London.

G 2-10

ESA PSS-03-108 Issue 1 (November 1989)

Rev. 2. 1984

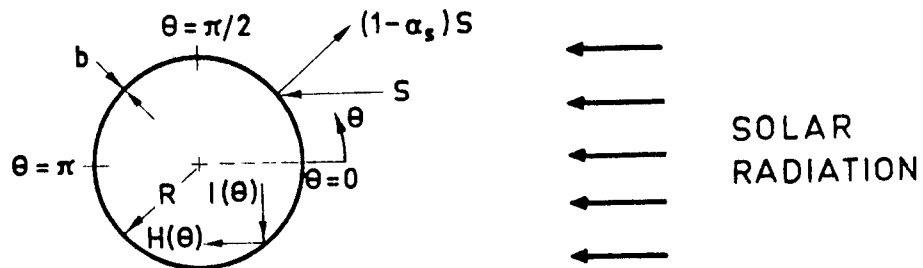
INTENTIONALLY BLANK PAGE

SOLAR RADIATION

Thin-Walled Spherical Bodies. Finite Conductivity

1.10.2. NON-SPINNING SPHERE. INCLUDING INTERNAL RADIATION

Sketch:



$H(\theta)$, Radiation Flux Density Leaving Inside of Sphere.

$I(\theta)$, Radiation Flux Density Impinging on Inside of Sphere.

Dimensionless Parameters:

$$\tau(\theta) = \frac{T(\theta)}{T_R} \quad , , \quad \mu = \frac{kb}{\epsilon\sigma T_R^3 R^2}$$

Differential Equations:

$$\frac{\mu}{\sin\theta} \frac{d}{d\theta} \left[\sin\theta \frac{d\tau}{d\theta} \right] = \begin{cases} 2\tau^4 - 4\cos\theta - 1 & , , \quad \text{when } 0 \leq \theta \leq \frac{\pi}{2} \\ 2\tau^4 - 1 & , , \quad \text{when } \frac{\pi}{2} \leq \theta \leq \pi \end{cases}$$

Boundary Conditions:

$$\frac{d\tau}{d\theta} \Big|_{\theta=0} = \frac{d\tau}{d\theta} \Big|_{\theta=\pi} = 0 \quad , , \quad \tau \Big|_{\theta=\frac{\pi}{2}} \text{ and } \frac{d\tau}{d\theta} \Big|_{\theta=\frac{\pi}{2}} \text{ continuous.}$$

Comments:

The results obtained by numerically solving this problem are given in the following two pages.

Reference: Nichols (1961).

SOLAR RADIATION

Thin-Walled Spherical Bodies. Finite Conductivity

θ°	T/T _R					
	$\mu = 10$	$\mu = 5$	$\mu = 1$	$\mu = .1$	$\mu = .01$	$\mu = 0$
0	1.08461	1.13025	1.22229	1.25422	1.25680	1.25743
5	1.08418	1.12959	1.22127	1.25327	1.25616	1.25648
10	1.08291	1.12716	1.21820	1.25036	1.25328	1.25360
15	1.08081	1.12434	1.21309	1.24549	1.24845	1.24878
20	1.07791	1.11981	1.20592	1.23862	1.24165	1.24198
25	1.04442	1.11405	1.19669	1.22971	1.23284	1.23318
30	1.06981	1.10713	1.18539	1.21868	1.22194	1.22229
35	1.06470	1.09912	1.17204	1.20546	1.20888	1.20925
40	1.05898	1.09010	1.15665	1.18990	1.19355	1.19395
45	1.05270	1.08018	1.13928	1.17186	1.17582	1.17624
50	1.04595	1.06949	1.12002	1.15144	1.15550	1.15596
55	1.03882	1.05815	1.09901	1.12741	1.13236	1.13288
60	1.03139	1.04632	1.07648	1.10062	1.10459	1.10668
65	1.02378	1.03481	1.05272	1.06906	1.07624	1.07696
70	1.01611	1.02192	1.02818	1.03264	1.04224	1.04314
75	1.00851	1.00978	1.00343	1.00307	1.00319	1.00438
80	1.00111	.99798	.97922	.95687	.95702	.95942
85	.99405	.98680	.95649	.91324	.90306	.90618
90	.98752	.97656	.93644	.88491	.85776	.84090
95	.98162	.96746	.92005	.87420	.85522	.84090
100	.97634	.95944	.90687	.85278	.84115	.84090
105	.97161	.95238	.89622	.84870	.84097	.84090
110	.96736	.94614	.88756	.84677	.84095	.84090
115	.96357	.94060	.88049	.84291	.84092	.84090
120	.96018	.93579	.87472	.84217	.84090	.84090
125	.95715	.93152	.86998	.84193	.84090	.84090
130	.95448	.92778	.86609	.84170	.84090	.84090
135	.95212	.92452	.86291	.84146	.84090	.84090
140	.95006	.92170	.86030	.84123	.84090	.84090
145	.94828	.91928	.85818	.84099	.84090	.84090
150	.94676	.91723	.85647	.84093	.84090	.84090
155	.94550	.91554	.85511	.84092	.84090	.84090
160	.94448	.91418	.85405	.84091	.84090	.84090
165	.94370	.91314	.85326	.84090	.84090	.84090
170	.94314	.91240	.85272	.84090	.84090	.84090
175	.94281	.91196	.85240	.84090	.84090	.84090
180	.94270	.91182	.85229	.84090	.84090	.84090

Table 1-2. Temperature distribution on sphere for several μ values, considering internal radiation. No spin. Calculated by the compiler.

SOLAR RADIATION
Thin-Walled Spherical Bodies. Finite Conductivity

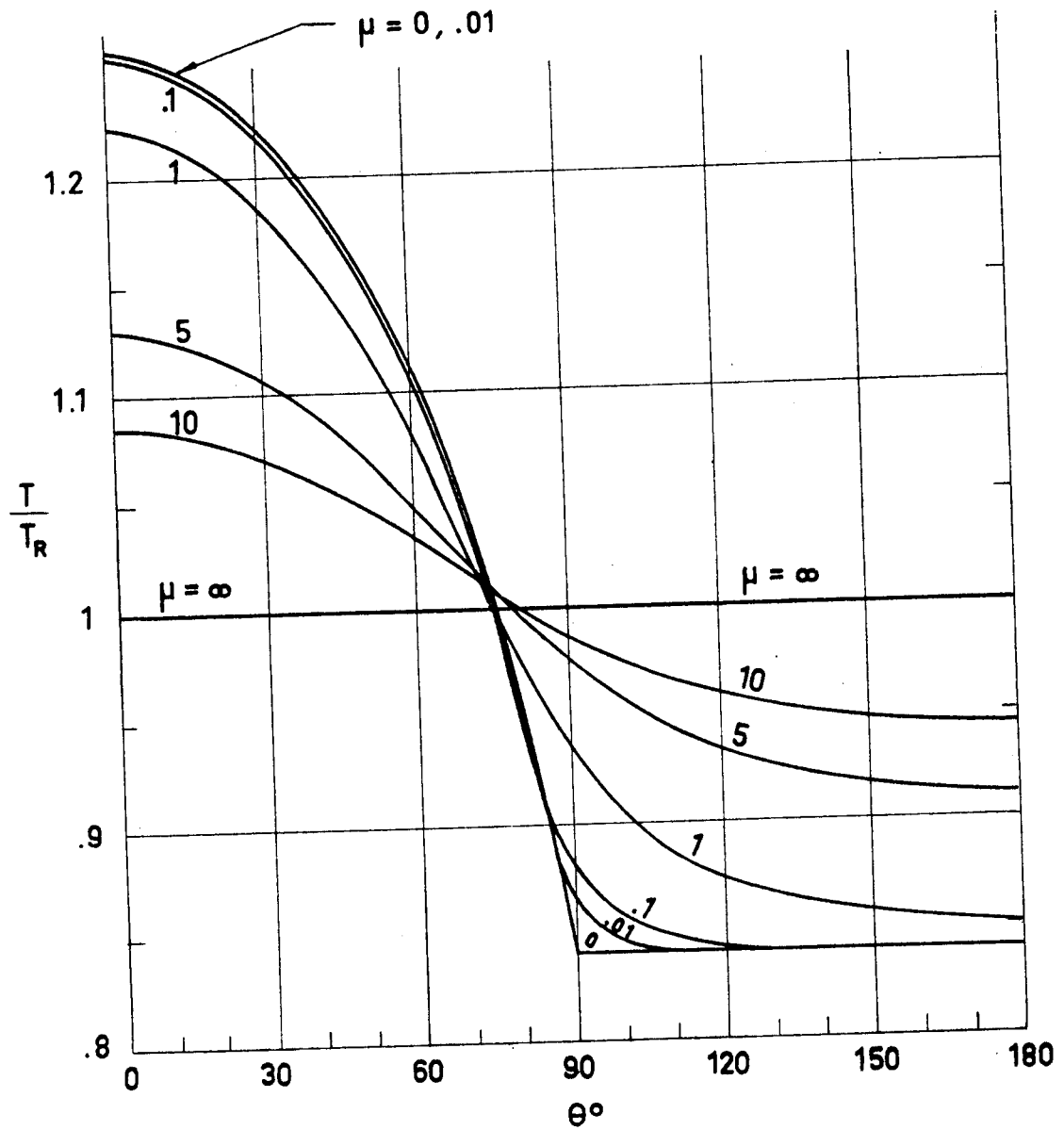


Fig 1-57. Temperature distribution on sphere including internal radiation. No spin. Calculated by the compiler.

INTENTIONALLY BLANK PAGE

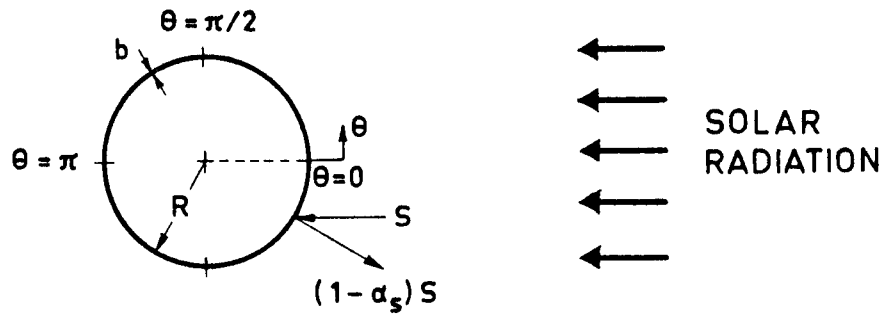
SOLAR RADIATION

Thin-Walled Cylindrical Bodies. Finite Conductivity

1.11. THIN-WALLED CYLINDRICAL BODIES. FINITE CONDUCTIVITY

1.11.1. NON-SPINNING TWO-DIMENSIONAL CIRCULAR CYLINDER

Sketch:



Dimensionless Parameters:

$$\tau(\theta) = \frac{T(\theta)}{T_R} \quad , , \quad \mu = \frac{kb}{\epsilon\sigma T_R^3 R^2}$$

Differential Equations:

$$\mu \frac{d^2\tau}{d\theta^2} = \begin{cases} \tau^4 - \pi \cos\theta & , , \quad \text{when } 0 \leq \theta \leq \pi/2 \\ \tau^4 & , , \quad \text{when } \pi/2 \leq \theta \leq \pi \end{cases}$$

Boundary Conditions:

$$\left. \frac{d\tau}{d\theta} \right|_{\theta=0} = \left. \frac{d\tau}{d\theta} \right|_{\theta=\pi} = 0 \quad , , \quad \tau \Big|_{\theta=\pi/2} \text{ and } \left. \frac{d\tau}{d\theta} \right|_{\theta=\pi/2} \text{ continuous.}$$

Comments:

Assumption concerning axial-symmetry is, obviously, not applicable in this case.

The results presented in the following two pages involve a linearization of the radiative transfer term.

Reference: Charnes & Raynor (1960).

SOLAR RADIATION

Thin-Walled Cylindrical Bodies. Finite Conductivity

θ°	T/T_R			
	$\mu = 50$	$\mu = 10$	$\mu = 5$	$\mu = 0$
0	1.0108	1.0493	1.0892	1.3313
5	1.0107	1.0490	1.0888	1.3301
10	1.0106	1.0483	1.0875	1.3262
15	1.0103	1.0472	1.0854	1.3198
20	1.0100	1.0456	1.0824	1.3108
25	1.0095	1.0435	1.0787	1.2990
30	1.0090	1.0411	1.0742	1.2843
35	1.0084	1.0382	1.0690	1.2666
40	1.0077	1.0351	1.0632	1.2455
45	1.0069	1.0316	1.0569	1.2208
50	1.0061	1.0279	1.0500	1.1921
55	1.0053	1.0239	1.0428	1.1586
60	1.0044	1.0198	1.0352	1.1195
65	1.0035	1.0115	1.0275	1.0734
70	1.0025	1.0112	1.0196	1.0181
75	1.0016	1.0069	1.0118	.9496
80	1.0007	1.0026	1.0040	.8594
85	.9997	.9985	.9965	.7234
90	.9989	.9945	.8993	0
95	.9980	.9908	.9826	0
100	.9973	.9872	.9763	0
105	.9965	.9840	.9705	0
110	.9959	.9809	.9651	0
115	.9952	.9781	.9601	0
120	.9946	.9754	.9555	0
125	.9941	.9730	.9513	0
130	.9936	.9709	.9475	0
135	.9932	.9689	.9441	0
140	.9928	.9671	.9411	0
145	.9924	.9656	.9384	0
150	.9921	.9643	.9361	0
155	.9918	.9631	.9342	0
160	.9916	.9622	.9326	0
165	.9915	.9615	.9314	0
170	.9914	.9610	.9305	0
175	.9913	.9607	.9300	0
180	.9913	.9606	.9298	0

Values for $\mu = 0$ are obtained by exactly solving the problem.

Table 1-3. Temperature distribution on a two-dimensional cylinder for several μ values. No spin. No internal radiation. Calculated by the compiler.

SOLAR RADIATION
Thin-Walled Cylindrical Bodies. Finite Conductivity

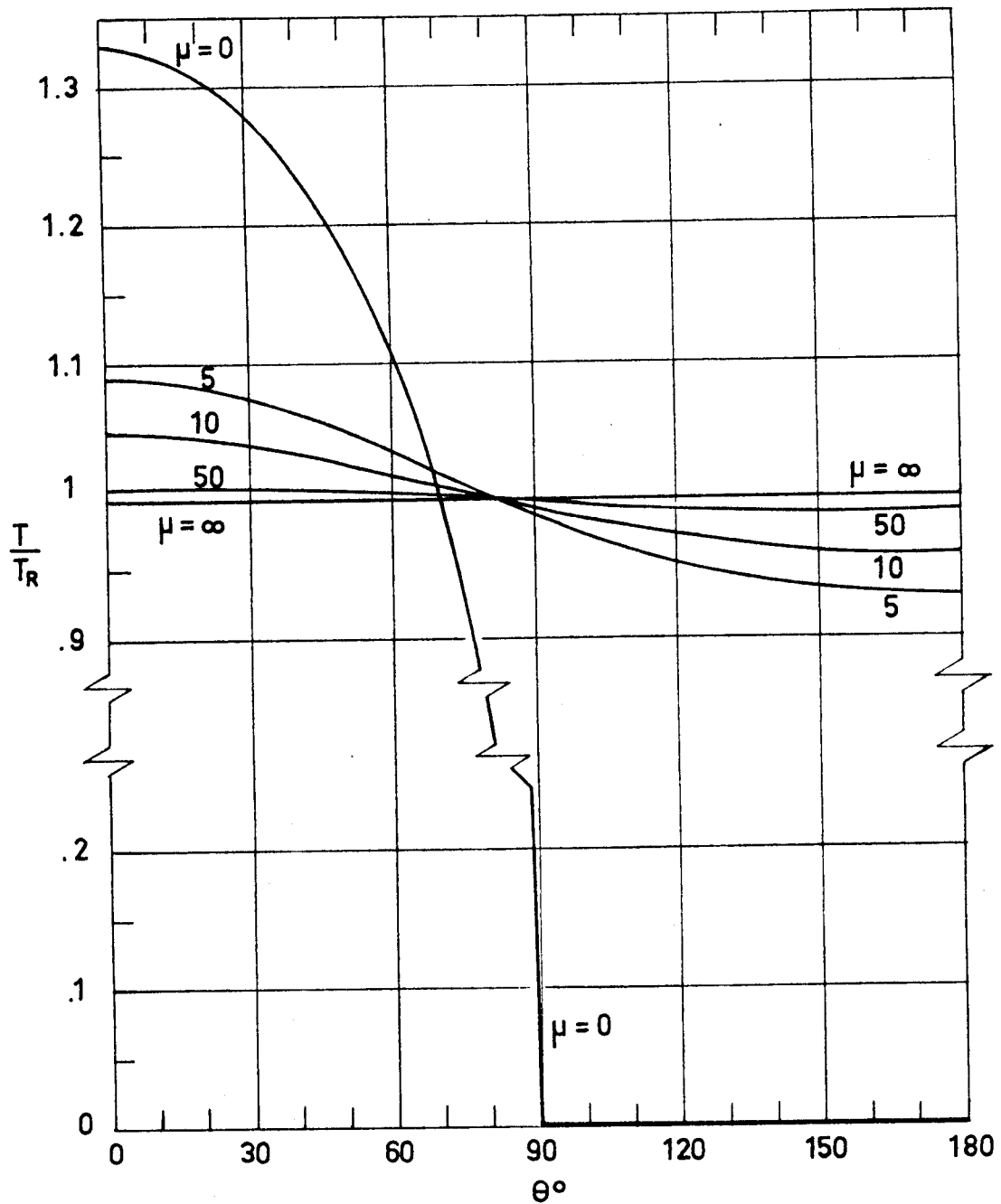


Fig 1-58. Temperature distribution on a two-dimensional cylinder. No spin. No internal radiation. Calculated by the compiler.

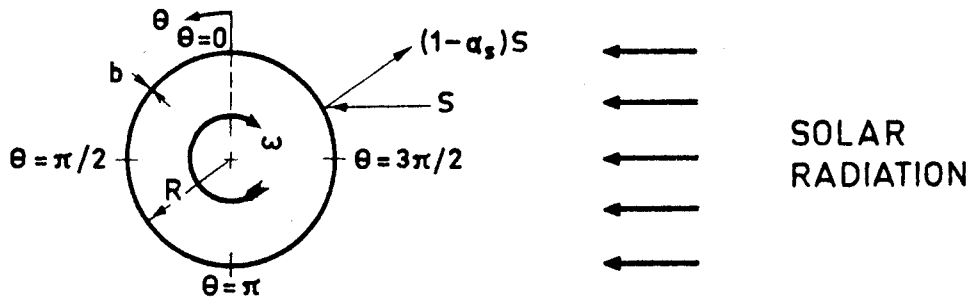
INTENTIONALLY BLANK PAGE

SOLAR RADIATION

Thin-Walled Cylindrical Bodies. Finite Conductivity

1.11.2. SPINNING TWO-DIMENSIONAL CIRCULAR CYLINDER

Sketch:



Dimensionless Parameters:

$$\tau(\theta) = \frac{T(\theta)}{T_R} \quad , , \quad \mu = \frac{kb}{\epsilon\sigma T_R^3 R^2} \quad , , \quad \gamma = \frac{\rho b c \omega}{\epsilon\sigma T_R^3}$$

where:

ω , Angular Velocity. [sec⁻¹].

c , Specific Heat of the Material. [J.kg⁻¹.K⁻¹].

ρ , Density of the Material. [kg.m⁻³].

Differential Equations:

$$\mu \frac{d^2\tau}{d\theta^2} + \gamma \frac{d\tau}{d\theta} = \begin{cases} \tau^4 & , , \quad \text{when } 0 \leq \theta \leq \pi \\ \tau^4 + \pi \sin\theta & , , \quad \text{when } \pi \leq \theta \leq 2\pi \end{cases}$$

Boundary Conditions:

$$\frac{d\tau}{d\theta} \Big|_{\theta=0} = \frac{d\tau}{d\theta} \Big|_{\theta=2\pi} \quad , , \quad \tau \Big|_{\theta=\pi} \quad \text{and} \quad \frac{d\tau}{d\theta} \Big|_{\theta=\pi} \quad \text{continuous.}$$

Comments:

The results presented have been obtained linearizing the equations, either assuming $\mu/\gamma \ll 2\pi$, Fig 1-59, or $|\tau-1| \ll 1$, Fig 1-60. In the last case terms of order $(\tau-1)^2$ have been neglected, so that $\tau^4 = 1 + 4(\tau-1)$. This approximation is valid when $\mu/\gamma \sim 1$.

SOLAR RADIATION

Thin-Walled Cylindrical Bodies. Finite Conductivity

$$0 \leq \frac{\mu}{\gamma} \leq \frac{1}{2}$$

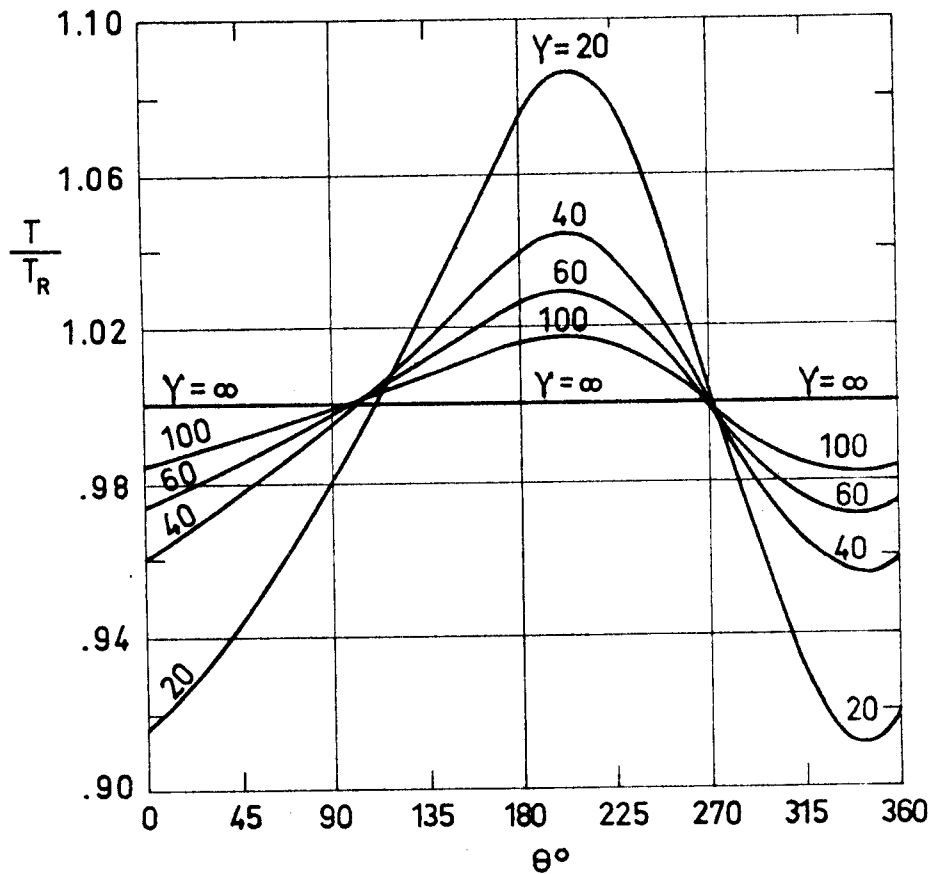


Fig 1-59. Temperature distribution on a two-dimensional spinning cylinder for several μ and γ values. No internal radiation. Calculated by the compiler.

SOLAR RADIATION

Thin-Walled Cylindrical Bodies. Finite Conductivity

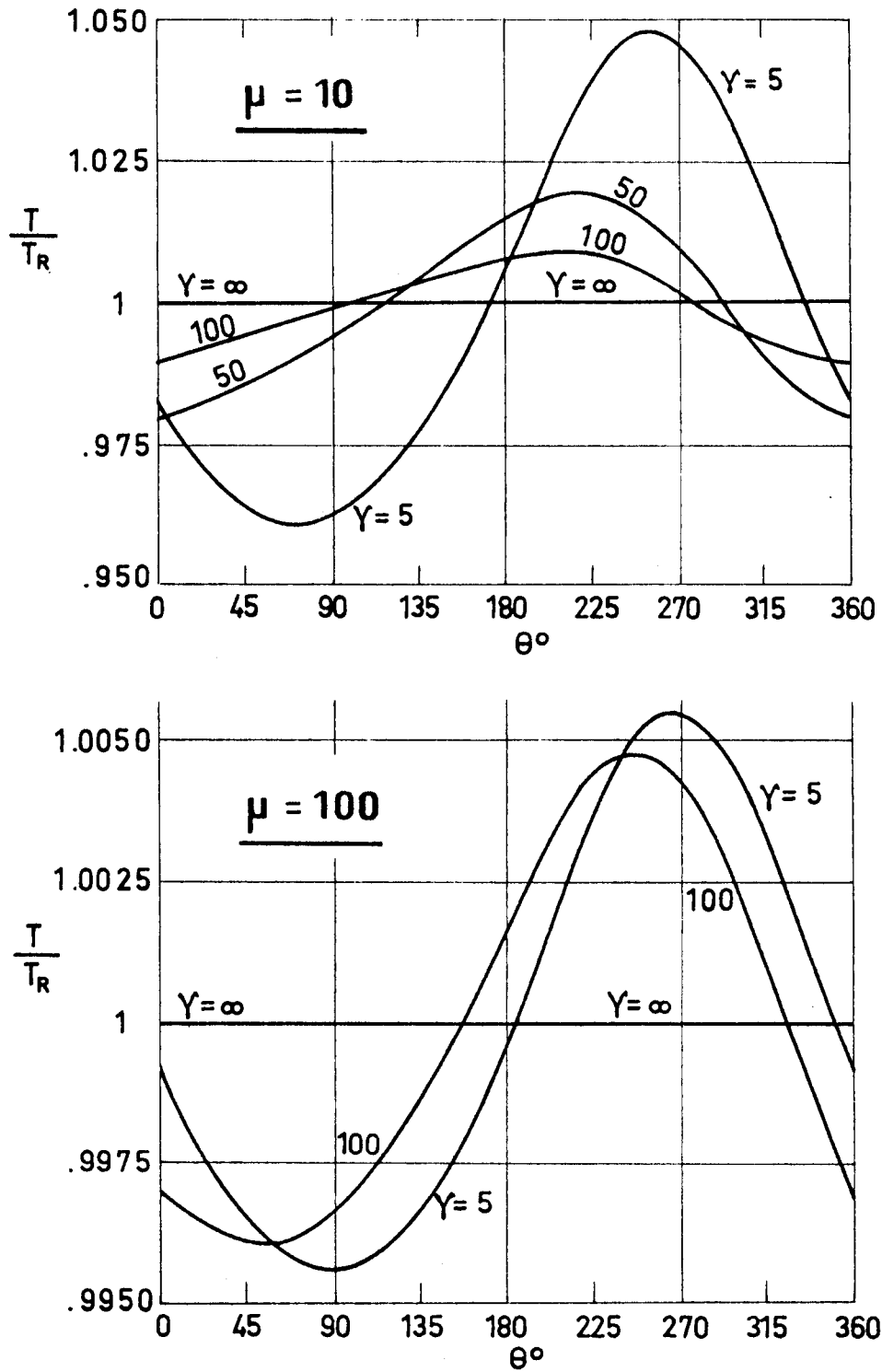


Fig 1-60. Temperature distribution on a two-dimensional spinning cylinder for several μ and γ values. No internal radiation. Calculated by the compiler.

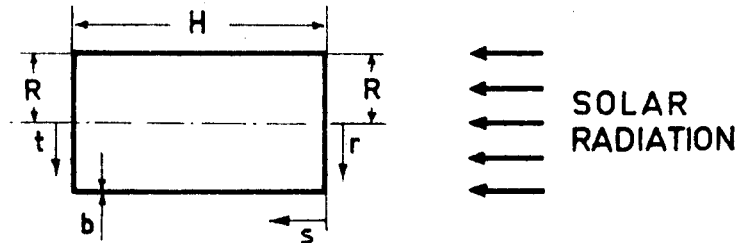
INTENTIONALLY BLANK PAGE

SOLAR RADIATION

Thin-Walled Cylindrical Bodies. Finite Conductivity

1.11.3. CIRCULAR CYLINDER. SOLAR RADIATION PARALLEL TO AXIS OF SYMMETRY

Sketch:



Dimensionless Parameters:

$$x = \frac{r}{R}, \text{ for } 0 \leq x \leq 1 \quad , \quad x = 1 + \frac{s}{H}, \text{ for } 1 \leq x \leq 2 \quad , \quad x = 3 - \frac{t}{R}, \text{ for } 2 \leq x \leq 3$$

$$\tau = \frac{T}{T_R} \quad , \quad \lambda = \frac{H}{R} \quad , \quad \mu = \frac{kb}{\epsilon \sigma T_R^3 R^2}$$

Differential Equations:

$$\frac{\mu}{x} \frac{d}{dx} \left(x \frac{d\tau_1}{dx} \right) = \tau_1^4 - 2(\lambda + 1) \quad , \quad \text{when } 0 \leq x \leq 1$$

$$\frac{\mu}{\lambda^2} \frac{d^2\tau_2}{dx^2} = \tau_2^4 \quad , \quad \text{when } 1 \leq x \leq 2$$

$$\frac{\mu}{3-x} \frac{d}{dx} \left[(3-x) \frac{d\tau_3}{dx} \right] = \tau_3^4 \quad , \quad \text{when } 2 \leq x \leq 3$$

Boundary Conditions:

$$\left. \frac{d\tau_1}{dx} \right|_{x=0} = \left. \frac{d\tau_3}{dx} \right|_{x=3} = 0 \quad , \quad \tau_1 \Big|_{x=1} = \tau_2 \Big|_{x=1} \quad , \quad \tau_2 \Big|_{x=2} = \tau_3 \Big|_{x=2}$$

$$\lambda \left. \frac{d\tau_1}{dx} \right|_{x=1} = \left. \frac{d\tau_2}{dx} \right|_{x=1} \quad , \quad \left. \frac{d\tau_2}{dx} \right|_{x=2} = \lambda \left. \frac{d\tau_3}{dx} \right|_{x=2}$$

Comments:

To obtain the results presented in the following two pages, the 4th power temperature terms, which appear in the above equations, have been linearized according to the expression $\tau^4 = 4\tau - 3$. Note that this linearization will give results with increased accuracy as the parameter μ gets larger.

Reference: Nichols (1961).

SOLAR RADIATION

Thin-Walled Cylindrical Bodies. Finite Conductivity

x	T/T _R					
	H/R = 1				H/R = 3	
	$\mu = 4$	$\mu = 9$	$\mu = 16$	$\mu = 36$	$\mu = 16$	$\mu = 36$
0	1.2218	1.1165	1.0700	1.0326	1.2547	1.1280
.2	1.2165	1.1137	1.0683	1.0318	1.2510	1.1262
.4	1.2004	1.1052	1.0632	1.0294	1.2397	1.1209
.6	1.1732	1.0909	1.0546	1.0254	1.2209	1.1118
.8	1.1338	1.0707	1.0425	1.0197	1.1943	1.0990
1.0	1.0812	1.0441	1.0268	1.0125	1.1597	1.0827
1.2	1.0277	1.0165	1.0106	1.0050	1.0609	1.0344
1.4	.9854	.9940	.9971	.9986	.9901	.9971
1.6	.9525	.9758	.9859	.9934	.9413	.9701
1.8	.9278	.9616	.9772	.9892	.9098	.9518
2.0	.9101	.9512	.9707	.9861	.8927	.9416
2.2	.8976	.9441	.9659	.9838	.8897	.9398
2.4	.8881	.9384	.9622	.9820	.8873	.9383
2.6	.8816	.9343	.9596	.9807	.8857	.9373
2.8	.8778	.9319	.9581	.9800	.8846	.9367
3.0	.8765	.9311	.9575	.9797	.8843	.9365

Table 1-4. Temperature distribution on cylinder for several μ and H/R values. No spin. No internal radiation. From Nichols (1961).

SOLAR RADIATION

Thin-Walled Cylindrical Bodies. Finite Conductivity

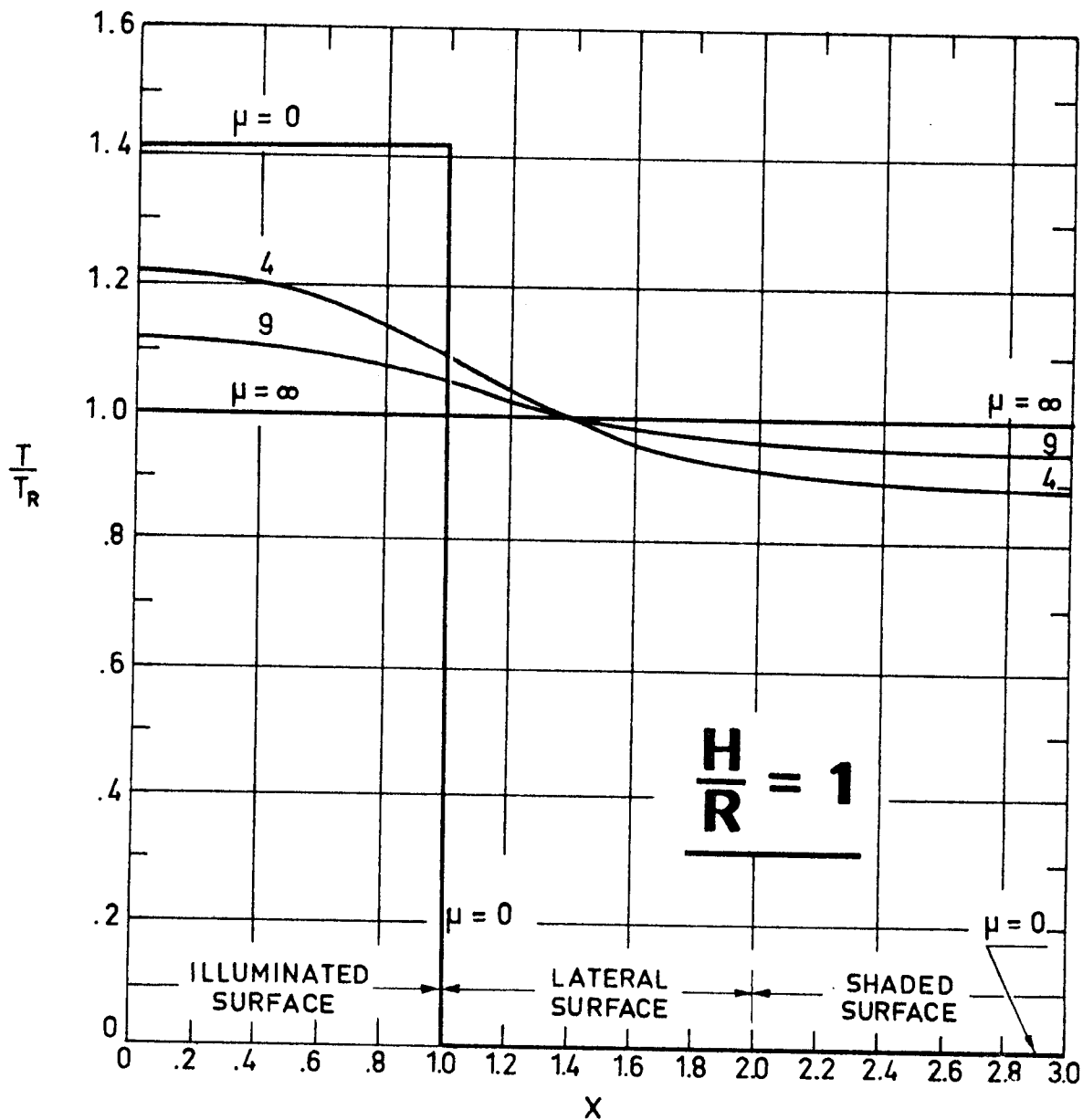


Fig 1-61. Temperature distribution on cylinder. No spin. No internal radiation. From Nichols (1961).

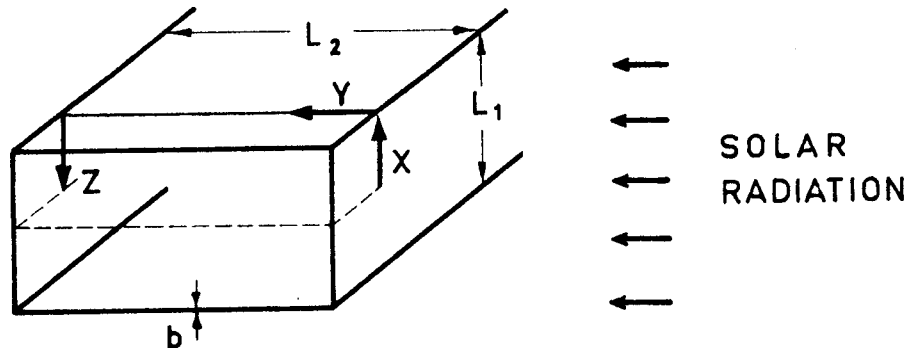
INTENTIONALLY BLANK PAGE

SOLAR RADIATION

Thin-Walled Cylindrical Bodies. Finite Conductivity

1.11.4. CYLINDRICAL SURFACE OF RECTANGULAR CROSS SECTION. SOLAR RADIATION NORMAL TO A FACE

Sketch:



Dimensionless Parameters:

$$x = \frac{2X}{L_1}, \text{ for } 0 \leq x \leq 1 \quad , \quad x = 1 + \frac{2Y}{L_1}, \text{ for } 1 \leq x \leq 1 + 2\lambda$$

$$x = 1 + 2\lambda + \frac{2Z}{L_1}, \text{ for } 1 + 2\lambda \leq x \leq 2(1 + \lambda)$$

$$\tau = \frac{T}{T_R} \quad , \quad \lambda = \frac{L_2}{L_1} \quad , \quad \mu = \frac{4kb}{\epsilon\sigma T_R^3 L_1^2}$$

Differential Equations:

$$\mu \frac{d^2\tau_1}{dx^2} = \tau_1^4 - 4 \quad , \quad \text{when } 0 \leq x \leq 1$$

$$\mu \frac{d^2\tau_2}{dx^2} = \tau_2^4 \quad , \quad \text{when } 1 \leq x \leq 2(1 + \lambda)$$

Boundary Conditions:

$$\frac{d\tau_1}{dx} \Big|_{x=0} = \frac{d\tau_2}{dx} \Big|_{x=2(1+\lambda)} = 0 \quad , \quad \tau_1 \Big|_{x=1} = \tau_2 \Big|_{x=1}$$

$$\frac{d\tau_1}{dx} \Big|_{x=1} = \frac{d\tau_2}{dx} \Big|_{x=1}$$

Comments:

The results obtained by numerically solving this problem are given in the following six pages.

Reference: Compiler.

SOLAR RADIATION

Thin-Walled Cylindrical Bodies. Finite Conductivity

$$\lambda = .5$$

x	T/T _R					
	$\mu = 10$	$\mu = 5$	$\mu = 1$	$\mu = .5$	$\mu = .1$	$\mu = 0$
.0	1.2163	1.2812	1.3928	1.4089	1.4142	1.4142
.2	1.2126	1.2759	1.3879	1.4063	1.4141	1.4142
.4	1.2016	1.2598	1.3710	1.3960	1.4137	1.4142
.6	1.1829	1.2317	1.3346	1.3684	1.4098	1.4142
.8	1.1560	1.1901	1.2644	1.2988	1.3774	1.4142
1.0	1.1203	1.1324	1.1355	1.1331	1.1317	-
1.2	1.0829	1.0719	.9942	.9430	.7880	0
1.4	1.0510	1.0221	.8931	.8193	.6257	0
1.6	1.0240	.9811	.8179	.7328	.5293	0
1.8	1.0013	.9475	.7608	.6699	.4657	0
2.0	.9828	.9203	.7173	.6232	.4214	0
2.2	.9679	.8990	.6845	.5888	.3899	0
2.4	.9566	.8829	.6605	.5642	.3679	0
2.6	.9487	.8716	.6442	.5476	.3532	0
2.8	.9439	.8649	.6348	.5382	.3447	0
3.0	.9424	.8627	.6318	.5356	.3420	0

Table 1-5. Temperature distribution on a cylindrical surface whose cross section is a rectangle of aspect-ratio $\lambda = .5$. No internal radiation. Calculated by the compiler.

SOLAR RADIATION
Thin-Walled Cylindrical Bodies. Finite Conductivity

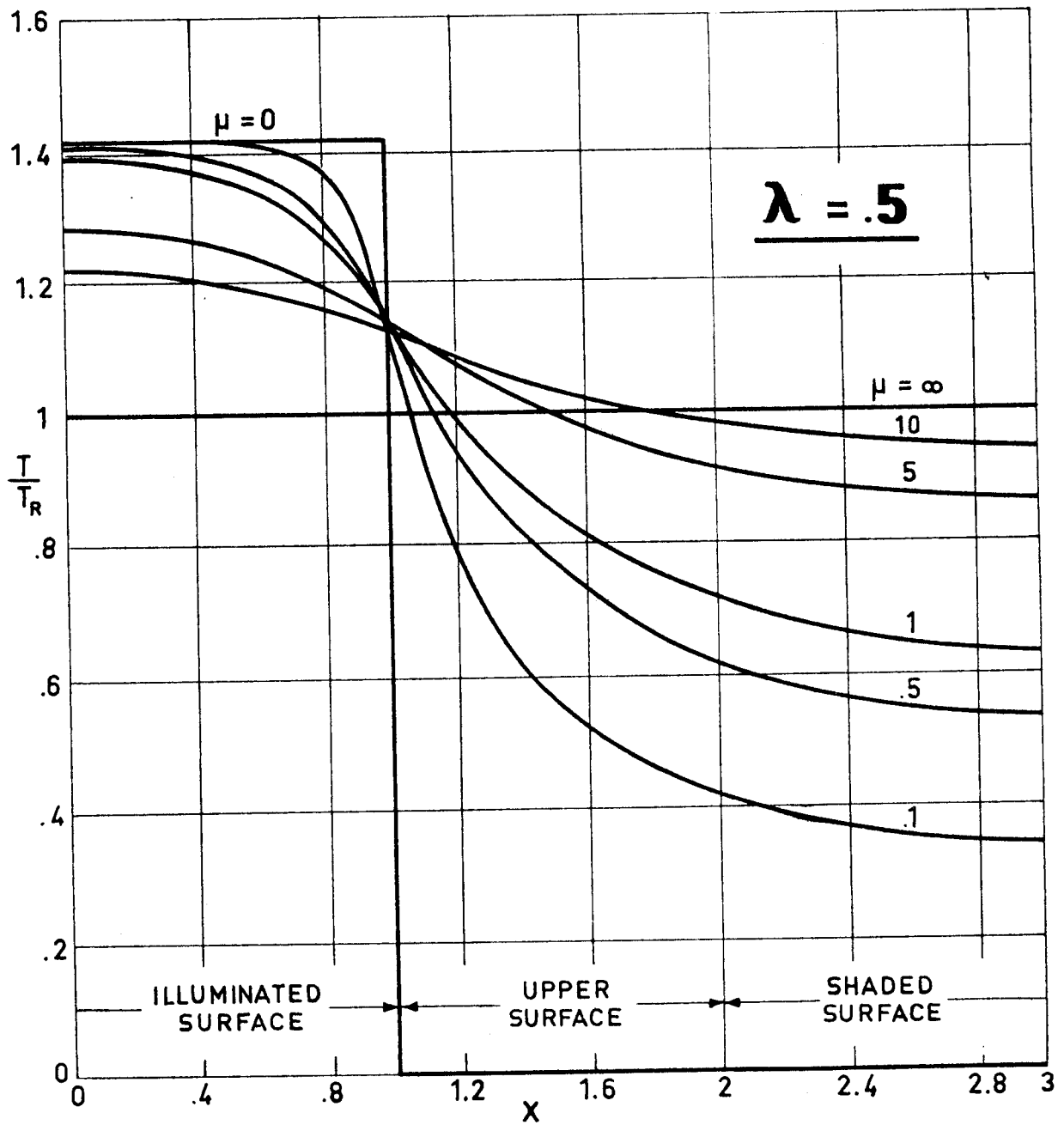


Fig 1-62. Temperature distribution on a cylindrical surface whose cross section is a rectangle of aspect-ratio $\lambda=0.5$. No internal radiation. Calculated by the compiler.

SOLAR RADIATION

Thin-Walled Cylindrical Bodies. Finite Conductivity

$$\lambda = 1$$

x	T/T _R					
	$\mu = 10$	$\mu = 5$	$\mu = 1$	$\mu = .5$	$\mu = .1$	$\mu = 0$
.0	1.1968	1.2732	1.3925	1.4088	1.4142	1.4142
.2	1.1929	1.2676	1.3875	1.4062	1.4141	1.4142
.4	1.1811	1.2507	1.3704	1.3959	1.4137	1.4142
.6	1.1610	1.2212	1.3337	1.3681	1.4098	1.4142
.8	1.1321	1.1775	1.2627	1.2982	1.3774	1.4142
1.0	1.0939	1.1172	1.1324	1.1318	1.1314	-
1.2	1.0534	1.0534	.9890	.9402	.7878	0
1.4	1.0178	.9995	.8850	.8142	.6242	0
1.6	.9865	.9536	.8059	.7244	.5261	0
1.8	.9591	.9144	.7441	.6572	.4600	0
2.0	.9350	.8808	.6946	.6050	.4122	0
2.2	.9140	.8520	.6545	.5638	.3764	0
2.4	.8958	.8275	.6219	.5307	.3486	0
2.6	.8801	.8066	.5952	.5041	.3268	0
2.8	.8669	.7893	.5735	.4826	.3096	0
3.0	.8559	.7749	.5562	.4654	.2961	0
3.2	.8471	.7635	.5427	.4520	.2857	0
3.4	.8403	.7548	.5327	.4420	.2779	0
3.6	.8356	.7487	.5260	.4350	.2726	0
3.8	.8327	.7451	.5222	.4309	.2694	0
4.0	.8318	.7440	.5215	.4295	.2684	0

Table 1-6. Temperature distribution on a cylindrical surface whose cross section is a rectangle of aspect-ratio $\lambda = 1$. No internal radiation. Calculated by the compiler.

SOLAR RADIATION
Thin-Walled Cylindrical Bodies. Finite Conductivity

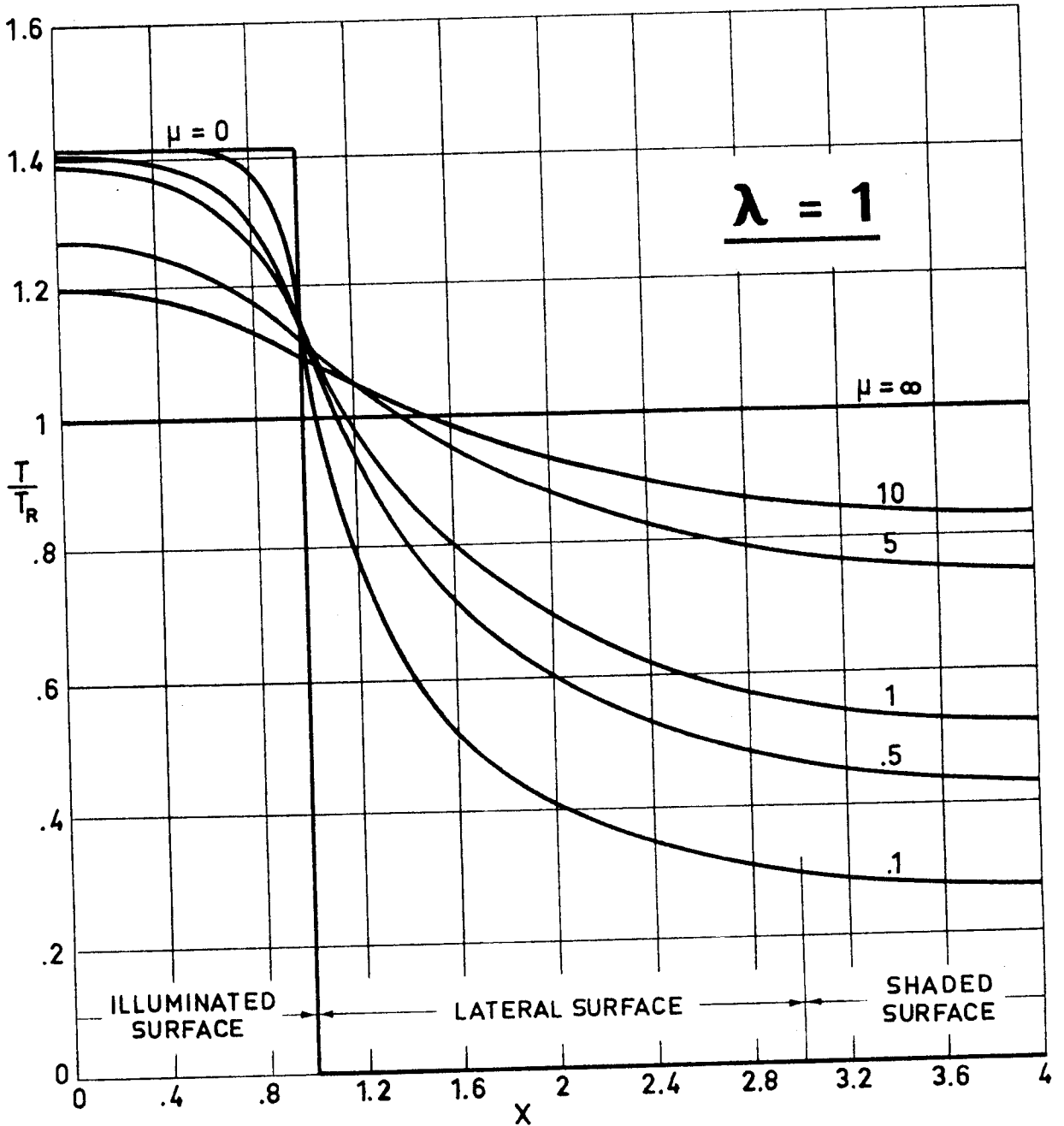


Fig 1-63. Temperature distribution on a cylindrical surface whose cross section is a rectangle of aspect-ratio $\lambda=1$. No internal radiation. Calculated by the compiler.

SOLAR RADIATION

Thin-Walled Cylindrical Bodies. Finite Conductivity

$\lambda = 2$

x	T/T _R					
	$\mu = 10$	$\mu = 5$	$\mu = 1$	$\mu = .5$	$\mu = .1$	$\mu = 0$
.0	1.1822	1.2682	1.3924	1.4088	1.4142	1.4142
.2	1.1781	1.2625	1.3874	1.4062	1.4141	1.4142
.4	1.1657	1.2451	1.3702	1.3959	1.4137	1.4142
.6	1.1446	1.2148	1.3333	1.3680	1.4098	1.4142
.8	1.1144	1.1698	1.2619	1.2980	1.3774	1.4142
1.0	1.0743	1.1079	1.1310	1.1312	1.1314	-
1.2	1.0316	1.0420	.9867	.9391	.7875	0
1.4	.9935	.9857	.8813	.8122	.6237	0
1.6	.9592	.9369	.8005	.7212	.5250	0
1.8	.9284	.8944	.7363	.6523	.4581	0
2.0	.9005	.8570	.6840	.5981	.4091	0
2.2	.8753	.8239	.6407	.5544	.3718	0
2.4	.8524	.7945	.6040	.5183	.3422	0
2.6	.8316	.7683	.5728	.4880	.3182	0
2.8	.8128	.7450	.5459	.4622	.2982	0
3.0	.7957	.7240	.5225	.4401	.2815	0
3.2	.7802	.7053	.5021	.4211	.2673	0
3.4	.7662	.6885	.4843	.4045	.2551	0
3.6	.7536	.6736	.4687	.3901	.2446	0
3.8	.7422	.6603	.4550	.3775	.2356	0
4.0	.7321	.6485	.4430	.3666	.2278	0
4.2	.7231	.6381	.4326	.3571	.2211	0
4.4	.7152	.6291	.4235	.3489	.2153	0
4.6	.7083	.6213	.4158	.3419	.2104	0
4.8	.7025	.6147	.4092	.3360	.2063	0
5.0	.6976	.6092	.4038	.3311	.2028	0
5.2	.6937	.6048	.3994	.3272	.2001	0
5.4	.6907	.6016	.3960	.3242	.1980	0
5.6	.6886	.5993	.3937	.3221	.1966	0
5.8	.6874	.5981	.3923	.3208	.1957	0
6.0	.6871	.5979	.3918	.3204	.1954	0

Table 1-7. Temperature distribution on a cylindrical surface whose cross section is a rectangle of aspect-ratio $\lambda = 2$. No internal radiation. Calculated by the compiler.

SOLAR RADIATION
Thin-Walled Cylindrical Bodies. Finite Conductivity

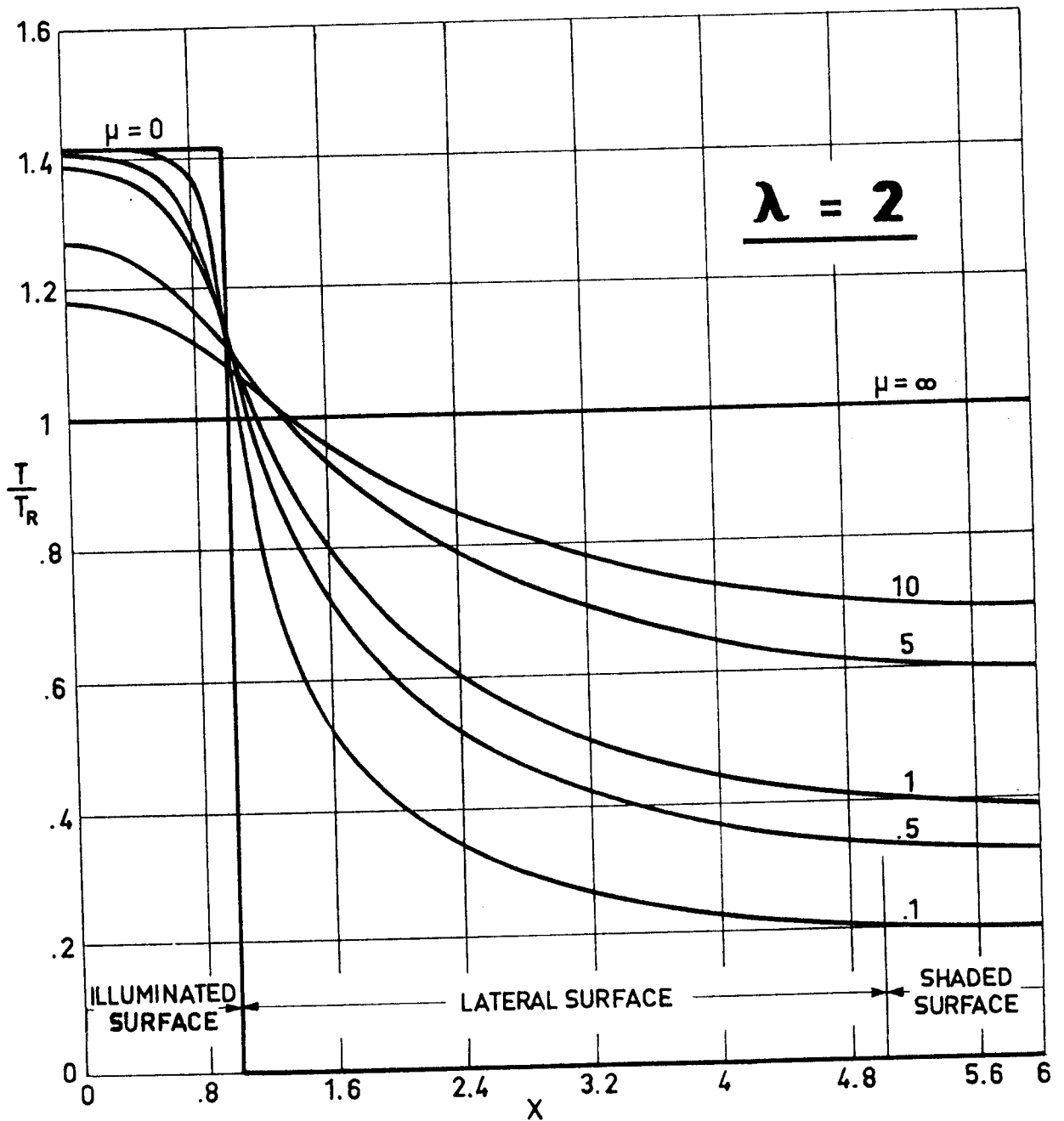


Fig 1-64. Temperature distribution on a cylindrical surface whose cross section is a rectangle of aspect-ratio $\lambda=2$. No internal radiation. Calculated by the compiler.

INTENTIONALLY BLANK PAGE

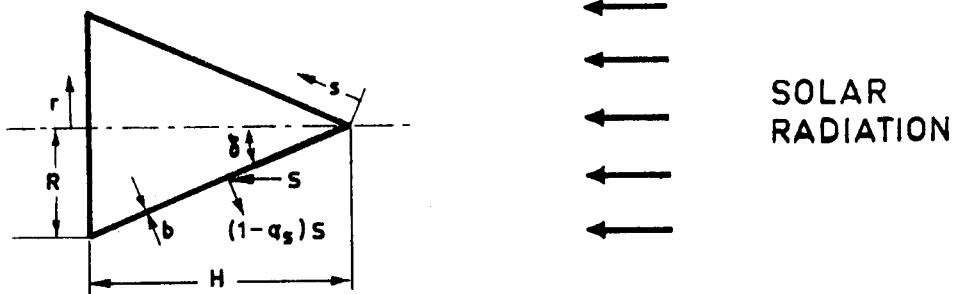
SOLAR RADIATION

Thin-Walled Conical Bodies. Finite Conductivity

1.12. THIN-WALLED CONICAL BODIES. FINITE CONDUCTIVITY

1.12.1. NON-SPINNING CONE

Sketch:



Dimensionless Parameters:

$$x = \frac{s}{\sqrt{R^2 + H^2}} \quad ,, \quad \text{when } 0 \leq x \leq 1$$

$$x = 2 - \frac{r}{R} \quad ,, \quad \text{when } 1 \leq x \leq 2$$

$$\tau(x) = \frac{T(x)}{T_R} \quad ,, \quad \mu = \frac{kb}{\epsilon \sigma T_R^3 R^2}$$

Differential Equations:

$$\frac{\mu \sin^2 \delta}{x} \frac{d}{dx} \left(x \frac{d\tau_1}{dx} \right) = \tau_1^4 - (1 + \sin \delta) \quad ,, \quad \text{when } 0 \leq x \leq 1$$

$$\frac{\mu}{2 - \mu} \frac{d}{dx} \left[(2 - x) \frac{d\tau_2}{dx} \right] = \tau_2^4 \quad ,, \quad \text{when } 1 \leq x \leq 2$$

Boundary Conditions:

$$\frac{d\tau_1}{dx} \Big|_{x=0} = \frac{d\tau_2}{dx} \Big|_{x=2} = 0 \quad ,, \quad \tau_1 \Big|_{x=1} = \tau_2 \Big|_{x=1}$$

$$\sin \delta \frac{d\tau_1}{dx} \Big|_{x=1} = \frac{d\tau_2}{dx} \Big|_{x=1}$$

Comments:

The results obtained by numerically solving this problem are given in the following six pages.

Reference: Nichols (1961).

SOLAR RADIATION

Thin-Walled Conical Bodies. Finite Conductivity

H/R = 1/2

X	T/T _R					
	$\mu = 12$	$\mu = 2$	$\mu = 1$	$\mu = 0.2$	$\mu = 0.1$	$\mu = 0.02$
0	1.02066	1.08620	1.12395	1.17067	1.17297	1.17319
.0625	1.02058	1.08590	1.12358	1.17057	1.17295	1.17319
.1250	1.02033	1.08497	1.12248	1.17026	1.17289	1.17319
.1875	1.01992	1.08342	1.12061	1.16970	1.17278	1.17319
.2500	1.01934	1.08124	1.11795	1.16882	1.17258	1.17319
.3125	1.01860	1.07839	1.11443	1.16752	1.17226	1.17319
.3750	1.01769	1.07485	1.10999	1.16565	1.17172	1.17319
.4375	1.01660	1.07060	1.10453	1.16295	1.17082	1.17318
.5000	1.01536	1.06559	1.09794	1.15911	1.16933	1.17317
.5625	1.01393	1.05977	1.09010	1.15364	1.16685	1.17314
.6250	1.01234	1.05311	1.08084	1.14586	1.16270	1.17303
.6875	1.01057	1.04553	1.07000	1.13482	1.15576	1.17267
.7500	1.00862	1.03697	1.05737	1.11916	1.14415	1.17144
.8125	1.00649	1.02737	1.04272	1.09704	1.12480	1.16730
.8750	1.00418	1.01664	1.02581	1.06598	1.09278	1.15342
.9375	1.00169	1.00471	1.00634	1.02273	1.04051	1.10753
1.0000	.99900	.99147	.98402	.96326	.95708	.96420
1.0625	.99660	.97951	.96369	.90662	.87478	.78436
1.1250	.99435	.96859	.94544	.85983	.81084	.67369
1.1875	.99227	.95864	.92910	.82073	.75990	.59819
1.2500	.99035	.94961	.91447	.78777	.71855	.54334
1.3125	.98859	.94146	.90142	.75983	.68456	.50182
1.3750	.98700	.93414	.88984	.73608	.65638	.46950
1.4375	.98555	.92762	.87962	.71588	.63291	.44388
1.5000	.98426	.92185	.87067	.69876	.61334	.42335
1.5625	.98313	.91683	.86293	.68433	.59709	.40681
1.6250	.98215	.91252	.85633	.67232	.58370	.39353
1.6875	.98132	.90891	.85083	.66248	.57284	.38298
1.7500	.98064	.90597	.84637	.65464	.56426	.37476
1.8125	.98012	.90370	.84294	.64867	.55776	.36862
1.8750	.97975	.90208	.84051	.64447	.55321	.36437
1.9375	.97952	.90111	.83905	.64198	.55051	.36189
2.0000	.97944	.90079	.83858	.64116	.54962	.36138

Table 1-8. Temperature distribution on cone for several μ values. No spin. No internal radiation. From Nichols (1961).

SOLAR RADIATION
Thin-Walled Conical Bodies. Finite Conductivity

$$\frac{H}{R} = \frac{1}{2}$$

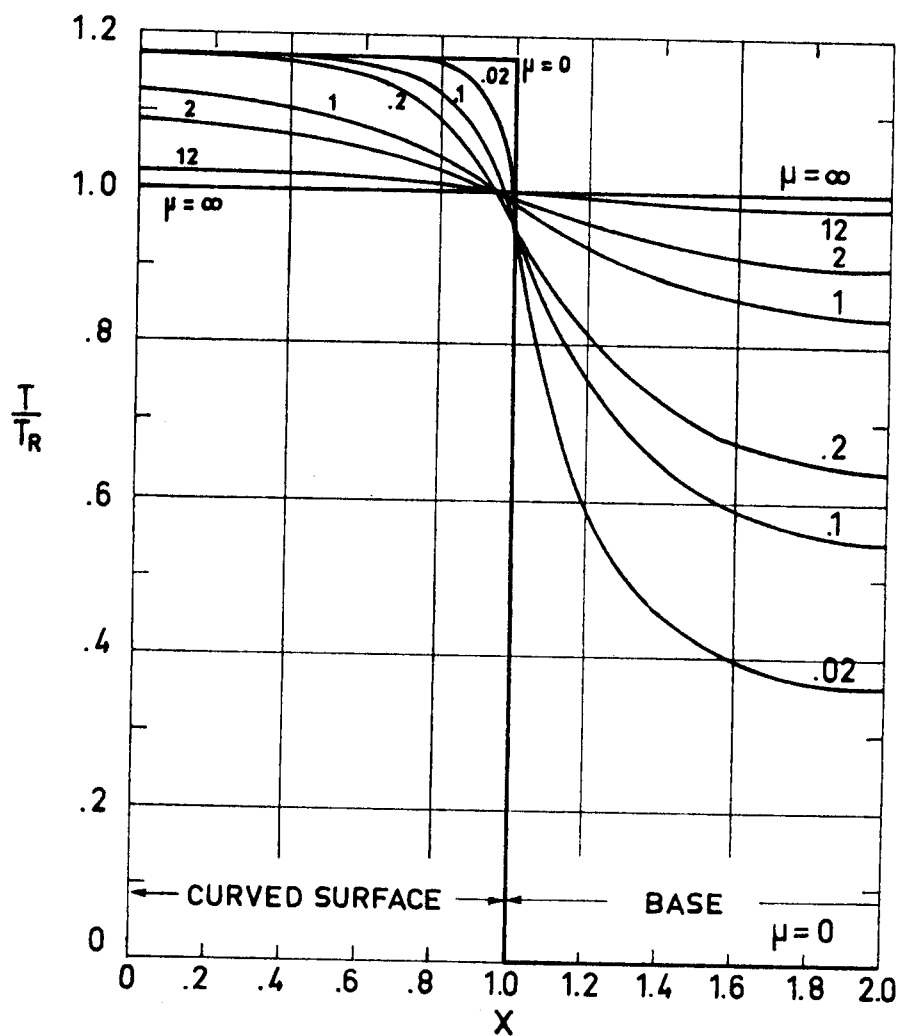


Fig 1-65. Temperature distribution on cone. No spin. No internal radiation. From Nichols (1961).

SOLAR RADIATION

Thin-Walled Conical Bodies. Finite Conductivity

H/R = 1

X	T/T _R					
	$\mu = 12$	$\mu = 2$	$\mu = 1$	$\mu = 0.2$	$\mu = 0.1$	$\mu = 0.02$
0	1.02286	1.08626	1.11580	1.14238	1.14302	1.14305
.0625	1.02276	1.08595	1.11549	1.14234	1.14301	1.14305
.1250	1.02246	1.08502	1.11456	1.14222	1.14300	1.14305
.1875	1.02196	1.08346	1.11297	1.14198	1.14297	1.14305
.2500	1.02126	1.08124	1.11068	1.14160	1.14292	1.14305
.3125	1.02036	1.07833	1.10760	1.14099	1.14282	1.14305
.3750	1.01925	1.07468	1.10364	1.14005	1.14264	1.14305
.4375	1.01793	1.07025	1.09867	1.13860	1.14230	1.14305
.5000	1.01641	1.06497	1.09254	1.13637	1.14166	1.14305
.5625	1.01467	1.05876	1.08504	1.13291	1.14047	1.14304
.6250	1.01272	1.05153	1.07595	1.12756	1.13822	1.14302
.6875	1.01054	1.04318	1.06498	1.11928	1.13397	1.14291
.7500	1.00814	1.03361	1.05182	1.10649	1.12593	1.14244
.8125	1.00551	1.02267	1.03608	1.08679	1.11076	1.14037
.8750	1.00265	1.01024	1.01731	1.05664	1.08234	1.13122
.9375	.99955	.99615	.99503	1.01098	1.02992	1.09138
1.0000	.99620	.98024	.96869	.94300	.93601	.92935
1.0625	.99381	.96875	.94939	.88962	.85836	.76390
1.1250	.99160	.95825	.93204	.84532	.79762	.66003
1.1875	.98954	.94868	.91647	.80814	.74897	.58833
1.2500	.98764	.93999	.90252	.77670	.70933	.53583
1.3125	.98590	.93214	.89007	.74998	.67663	.49857
1.3750	.98432	.92509	.87900	.72721	.64945	.46464
1.4375	.98289	.91880	.86923	.70782	.62677	.43980
1.5000	.98162	.91324	.86067	.69135	.60783	.41984
1.5625	.98050	.90840	.85326	.67746	.59207	.40375
1.6250	.97953	.90424	.84694	.66587	.57907	.39080
1.6875	.97871	.90075	.84166	.65638	.56853	.38049
1.7500	.97804	.89792	.83740	.64881	.56018	.37246
1.8125	.97752	.89573	.83411	.64305	.55386	.36644
1.8750	.97715	.89417	.83178	.63899	.54943	.36226
1.9375	.97693	.89323	.83038	.63658	.54681	.35980
2.0000	.97687	.89292	.82992	.63579	.54594	.35899

Table 1-9. Temperature distribution on cone for several μ values. No spin. No internal radiation. From Nichols (1961).

SOLAR RADIATION

Thin-Walled Conical Bodies. Finite Conductivity

$$\frac{H}{R} = 1$$

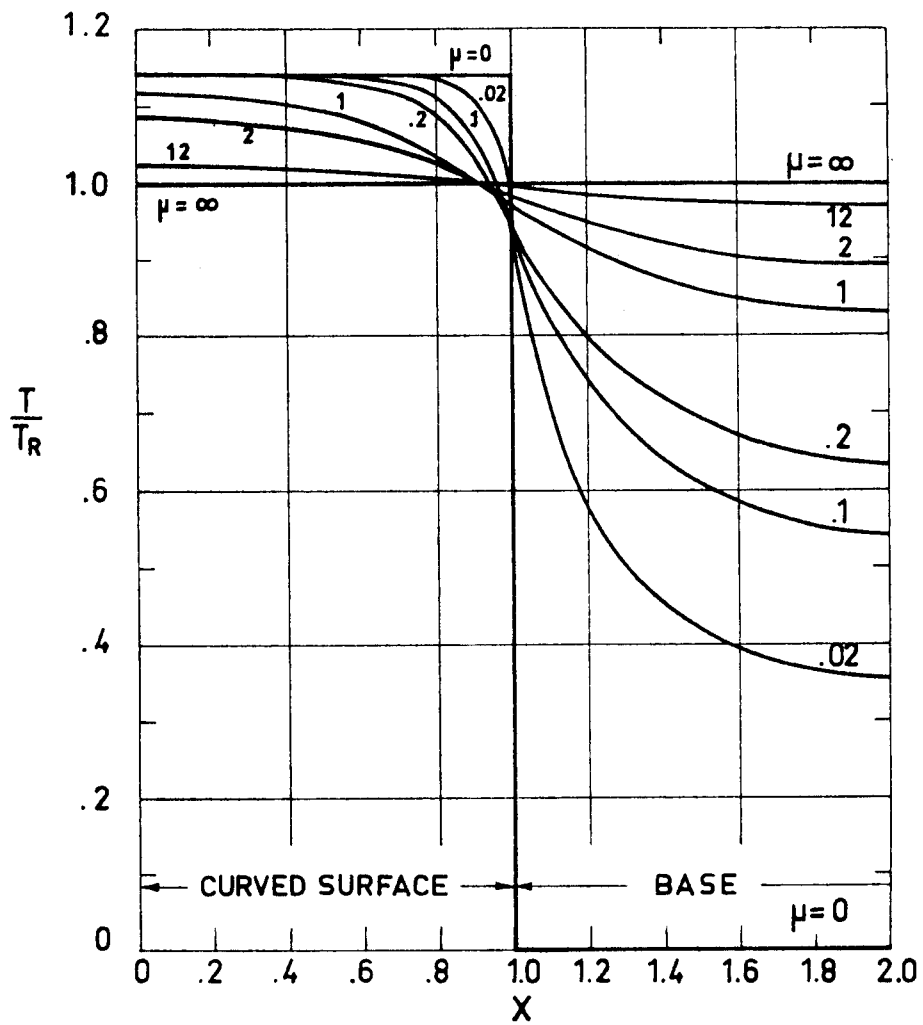


Fig 1-66. Temperature distribution on cone. No spin. No internal radiation. From Nichols (1961).

SOLAR RADIATION

Thin-Walled Conical Bodies. Finite Conductivity

$$H/R = 2$$

X	T/T _R					
	$\mu = 12$	$\mu = 2$	$\mu = 1$	$\mu = 0.2$	$\mu = 0.1$	$\mu = 0.02$
0	1.02765	1.07852	1.09132	1.09680	1.09682	1.09682
.0625	1.02751	1.07829	1.09118	1.09680	1.09682	1.09682
.1250	1.02711	1.07759	1.09074	1.09679	1.09682	1.09682
.1875	1.02643	1.07639	1.08998	1.09677	1.09682	1.09682
.2500	1.02547	1.07466	1.08884	1.09674	1.09682	1.09682
.3125	1.02424	1.07232	1.08722	1.09668	1.09681	1.09682
.3750	1.02271	1.06930	1.08499	1.09656	1.09680	1.09682
.4375	1.02089	1.06547	1.08200	1.09633	1.09678	1.09682
.5000	1.01877	1.06071	1.07800	1.09589	1.09673	1.09682
.5625	1.01633	1.05484	1.07267	1.09503	1.09659	1.09682
.6250	1.01356	1.04764	1.06561	1.09334	1.09621	1.09682
.6875	1.01044	1.03887	1.05627	1.09005	1.09522	1.09682
.7500	1.00697	1.02821	1.04393	1.08361	1.09261	1.09681
.8125	1.00312	1.01531	1.02769	1.07101	1.08571	1.09667
.8750	.99887	.99975	1.00638	1.04652	1.06758	1.09544
.9375	.99421	.98102	.97856	.99962	1.02072	1.08401
1.0000	.98911	.95858	.94248	.91241	.90495	.98257
1.0625	.98680	.94798	.92487	.86380	.83396	.79502
1.1250	.98464	.93827	.90901	.82315	.77786	.68078
1.1875	.98264	.92941	.89474	.78884	.73257	.60331
1.2500	.98079	.92137	.88193	.75968	.69544	.54724
1.3125	.97910	.91408	.87048	.73479	.66467	.50491
1.3750	.97757	.90754	.86028	.71352	.63899	.47202
1.4375	.97618	.90169	.85126	.69534	.61748	.44599
1.5000	.97494	.89653	.84335	.67987	.59948	.42513
1.5625	.97385	.89203	.83650	.66679	.58448	.40833
1.6250	.97291	.88816	.83064	.65586	.57208	.39483
1.6875	.97211	.88491	.82576	.64690	.56200	.38408
1.7500	.97146	.88227	.82180	.63974	.55402	.37568
1.8125	.97096	.88023	.81875	.63429	.54797	.36933
1.8750	.97060	.87877	.81658	.63045	.54372	.36482
1.9375	.97038	.87790	.81529	.62817	.54120	.36319
2.0000	.97031	.87762	.81486	.62741	.54037	.35769

Table 1-10. Temperature distribution on cone for several μ values. No spin. No internal radiation. From Nichols (1961).

SOLAR RADIATION

Thin-Walled Conical Bodies. Finite Conductivity

$$\frac{H}{R} = 2$$

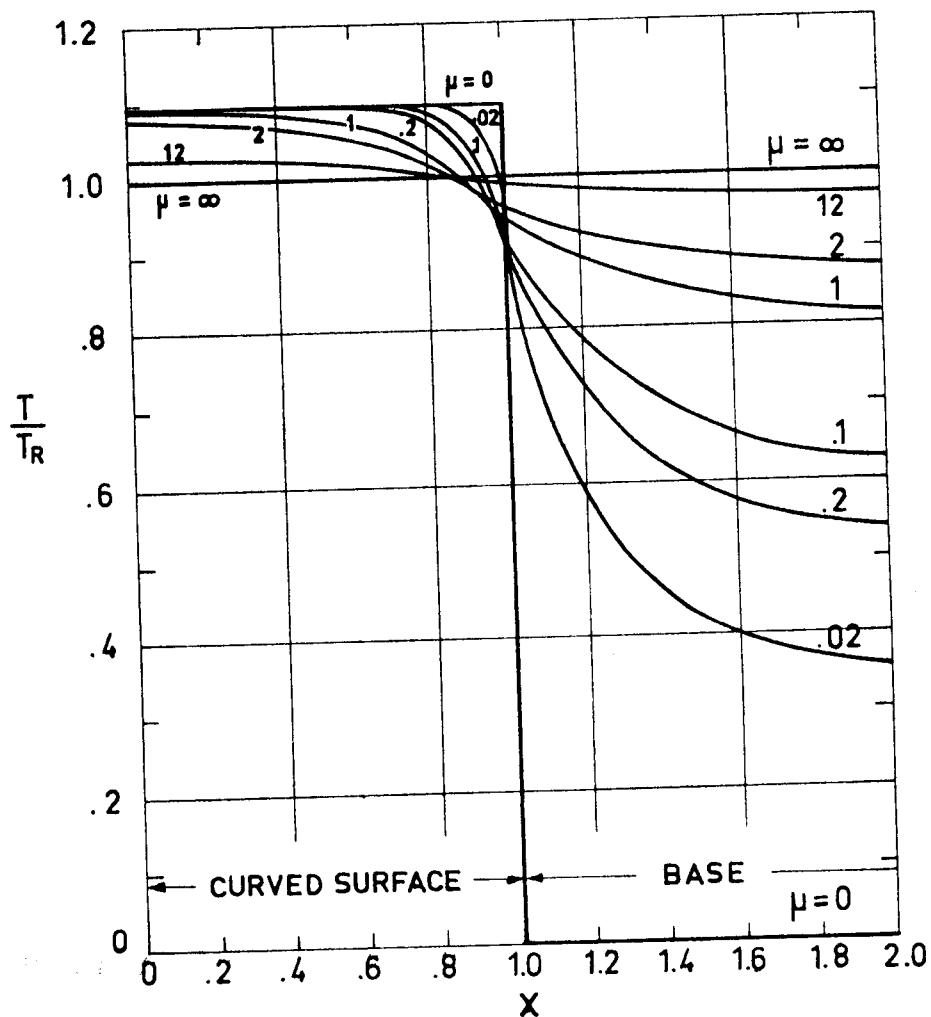


Fig 1-67. Temperature distribution on cone. No spin. No internal radiation. From Nichols (1961).

INTENTIONALLY BLANK PAGE

PLANETARY RADIATION

General

2. PLANETARY RADIATION2.1. GENERAL

Data on the equilibrium temperature of a satellite, heated by radiation from a planet, and cooled by radiation to the outer space, are presented in this Chapter. Only satellites of very simple geometrical configurations are considered.

The data presented have been calculated on the basis of the following assumptions:

- a) The satellite is constituted by a homogeneous solid body, exhibiting infinitely large thermal conductivity.
- b) The characteristic length of the satellite is small compared with the mean radius of the planet.
- c) The emission from the planet is assumed to follow Lambert's law.
- d) The Equivalent Surrounding Temperature, T_s , is assumed to be zero.
- e) Emittance and infrared absorptance of the satellite surface are independent of both temperature and wavelength.

The Spacecraft Planetary Radiation Equilibrium Temperature, T_{RP} , is given by

$$T_{RP} = \left[\frac{\alpha}{\epsilon} F_{SP} T_P^4 + T_s^4 \right]^{1/4} .$$

Once T_s has been assumed to be zero, the above expression gives the ratio T_{RP}/T_P as a function of the optical characteristics of the satellite surface (through α/ϵ) for arbitrary values of the view factor from spacecraft to planet, F_{SP} . The results are given in Fig 2-1.

PLANETARY RADIATION

General

These results can be also used to estimate the radiation from a satellite to a subsatellite or appendage provided that the above assumptions hold.

Values of T_{RP} as a function of T_{RP}/T_P for radiation from several planets are given in Fig 2-2. Radiation from the Earth is considered in Fig 2-3.

The remaining data are values of F_{SP} for simple geometries. For cylindrical and conical configurations F_{SP} is calculated by expansion in powers of $\sin\lambda$ and (or) $\cos\lambda$, λ being the angle defining the orientation of the spacecraft. The coefficients of these power expansions depend on the parameters B_i . The five first parameters B_i are given below, as calculated by Clark & Anderson (1965).

$$B_0 = \frac{2}{7\pi} \left[\frac{577}{105} - 7 \cos\alpha_L + \frac{4}{3} \cos^3\alpha_L - \frac{2}{5} \cos^5\alpha_L + \frac{4}{7} \cos^7\alpha_L \right]$$

$$B_1 = \frac{1}{2} \sin^2\alpha_L$$

$$B_2 = \frac{8}{7\pi} \left[\cos\alpha_L - 2 \cos^3\alpha_L + 4 \cos^5\alpha_L - 3 \cos^7\alpha_L \right]$$

$$B_3 = \frac{4}{7\pi} \left[-\cos\alpha_L + \frac{40}{3} \cos^3\alpha_L - \frac{91}{3} \cos^5\alpha_L + 18 \cos^7\alpha_L \right]$$

$$B_4 = \frac{8}{35\pi} \left[5 \cos\alpha_L - 35 \cos^3\alpha_L + 63 \cos^5\alpha_L - 33 \cos^7\alpha_L \right]$$

where:

$$\alpha_L = \sin^{-1} \frac{R_p}{h+R_p}$$

PLANETARY RADIATION
General

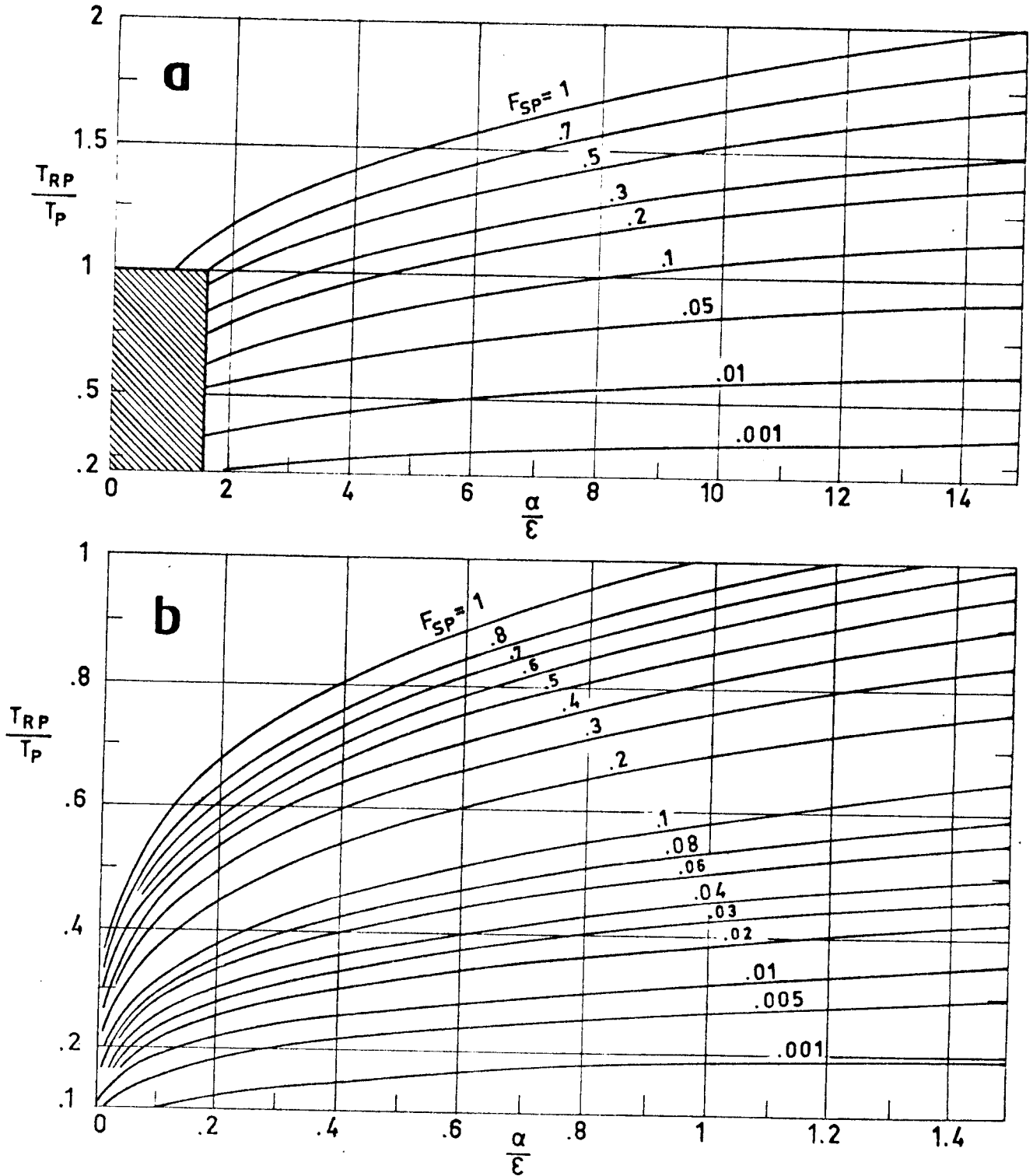


Fig 2-1. The ratio T_{RP}/T_P vs. the optical characteristics of the surface for different values of F_{SP} . Shaded zone of a is enlarged in b. Calculated by the compiler.

PLANETARY RADIATION
General

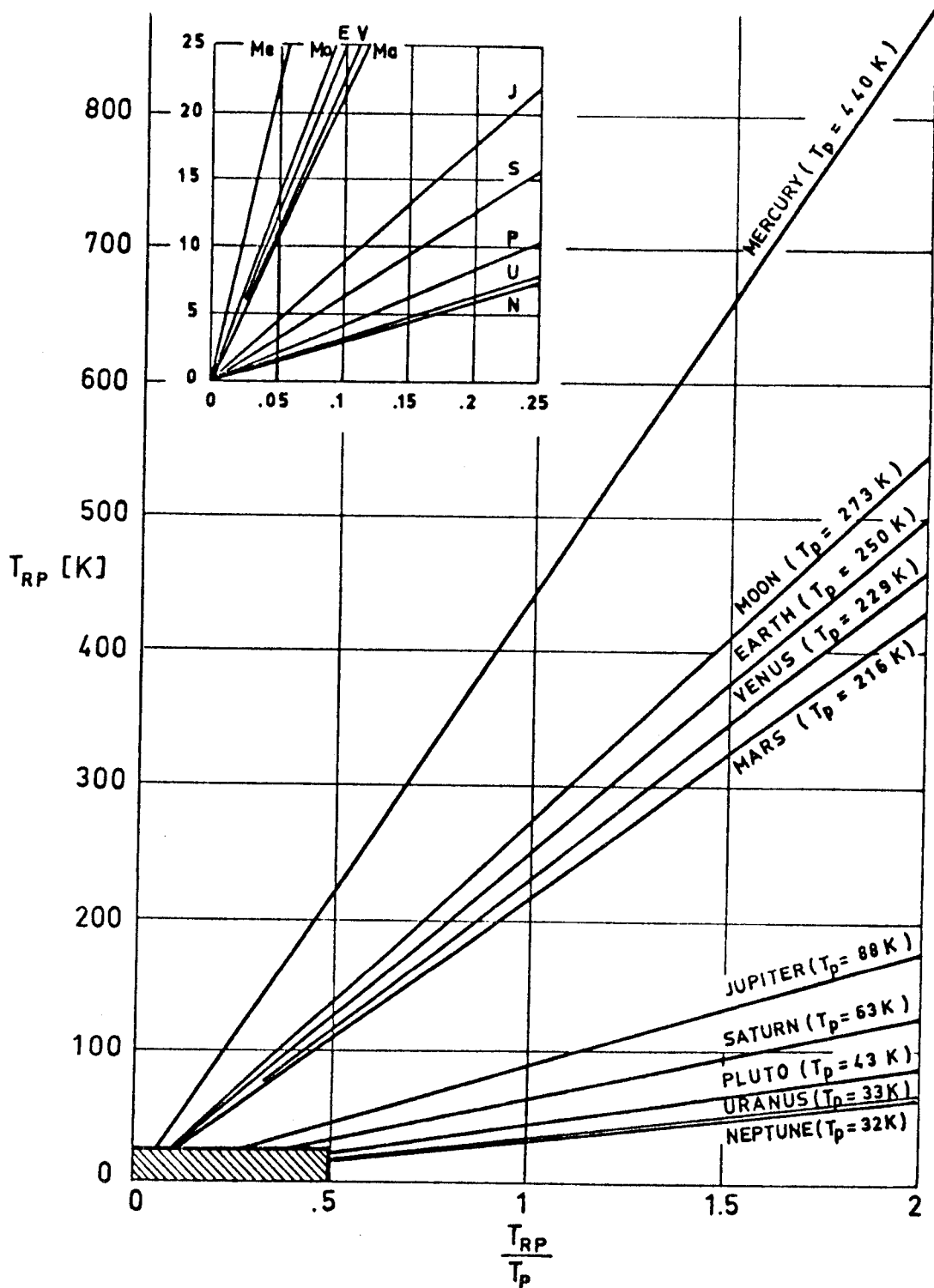


Fig 2-2. Radiation equilibrium temperature T_{RP} vs. ratio T_{RP}/T_p . Incoming radiation from different planets. After NASA-SP-3051 (1965).

PLANETARY RADIATION

General

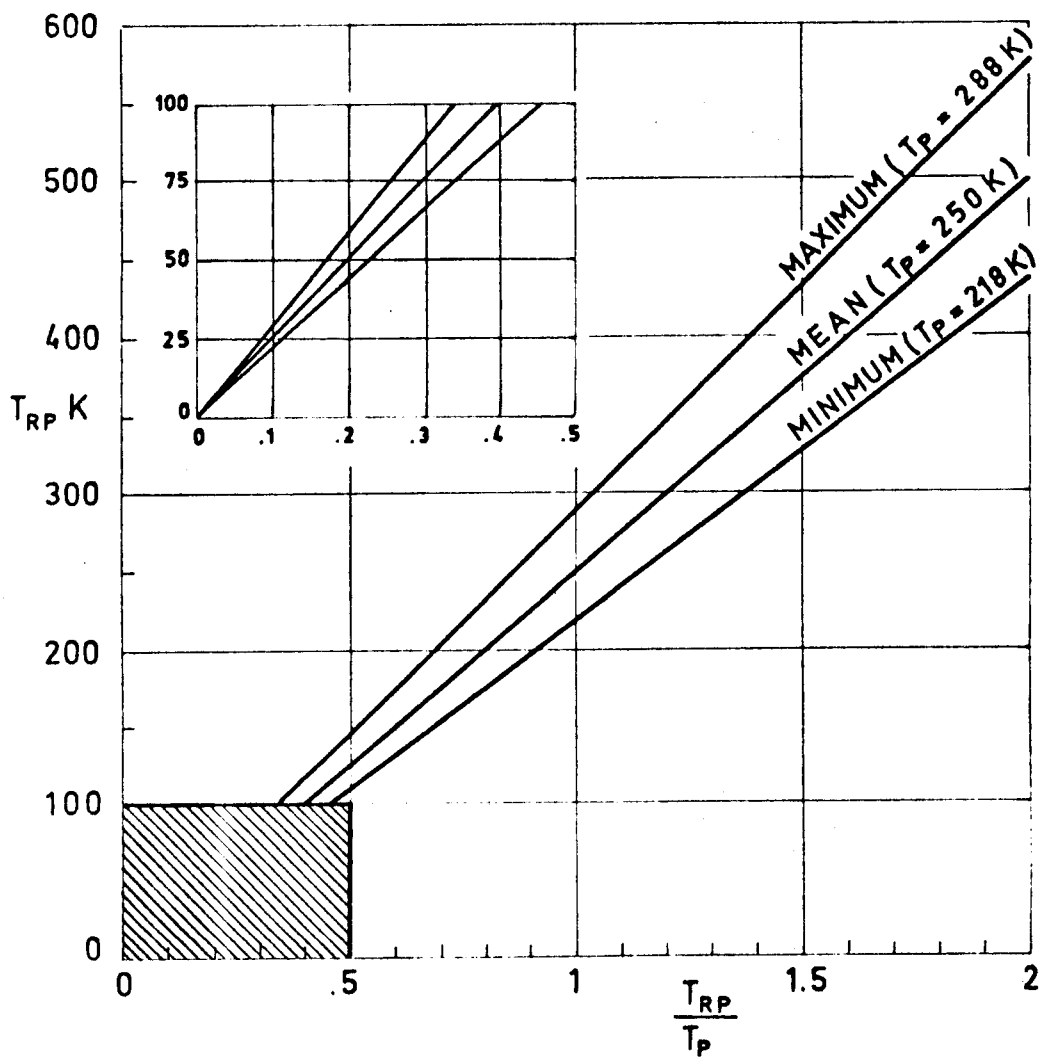


Fig 2-3. Different estimates of radiation equilibrium temperature T_{RP} vs. ratio $\frac{T_{RP}}{T_P}$, for radiation from the Earth. Plotted from data by Johnson (1965).

PLANETARY RADIATION
General

Table 2-1
Relevant data on the Planets and the Moon

	DISTANCE TO THE SUN $\times 10^{-9}$ [m]	DISTANCE TO THE SUN IN AU.	RADIUS OF THE PLANET $\times 10^{-3}$ [m]	PLANET TO EARTH RADIUS RATIO	SOLAR CONSTANT [W.m ⁻²]	EQUIVALENT TEMPERATURE OF THE PLANET [K]
MERCURY	57.9	.387	2330	.3659	9034	440
VENUS	108.1	.723	6100	.9580	2588	229
EARTH	149.5	1.	6367.5	1.	1353	250
MARS	227.4	1.521	3415	.5363	585	216
JUPITER	773.3	5.173	71375	11.2093	51	88
SATURN	1425.7	9.536	60500	9.5014	15	63
URANUS	2880.7	19.269	24850	3.9026	3.6	33
NEPTUNE	4490.1	30.034	25000	3.9262	1.5	32
PLUTO	5841.9	39.076	2930	.4600	.89	43
MOON	149.5	1.	1738	.2729	1353	273

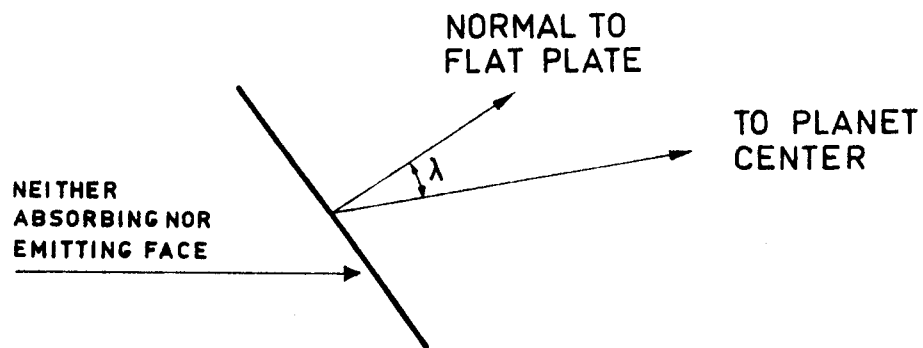
References: Kreith (1962), Wolverton (1963), Anderson (1969).

PLANETARY RADIATION
Infinitely Conductive Planar Surfaces

2.2. INFINITELY CONDUCTIVE PLANAR SURFACES

2.2.1. FLAT PLATE ABSORBING AND EMITTING ON ONE SIDE

Sketch:



Formula:

$$F_{SP} = B_0 + B_1 \cos \lambda + B_2 \cos^2 \lambda + B_3 \cos^4 \lambda + B_4 \cos^6 \lambda$$

where the parameters B_i ($i = 0, 1, \dots, 4$) are defined in § 2.1.

Reference: Clark & Anderson (1965).

PLANETARY RADIATION
Infinitely Conductive Planar Surfaces

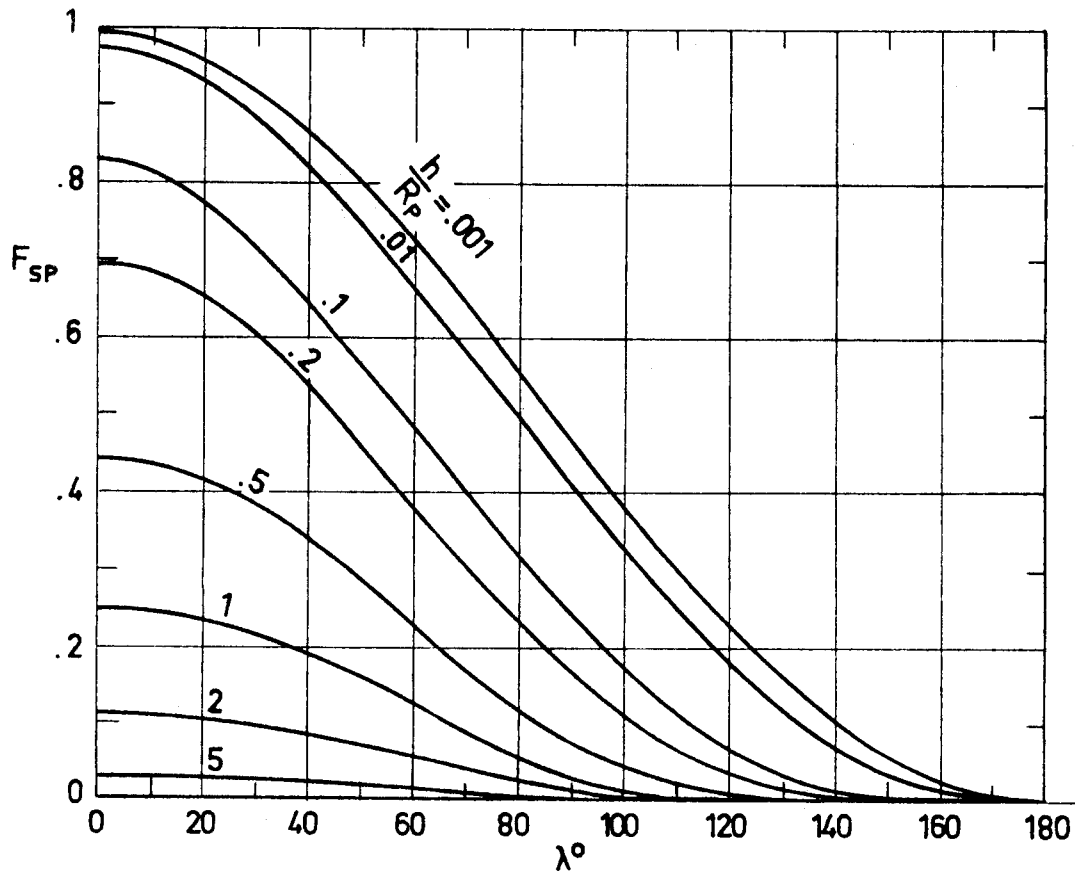


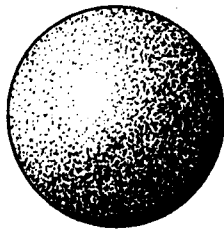
Fig 2-4. F_{SP} as a function of λ and $\frac{h}{R_P}$ in the case of a flat plate absorbing and emitting on one side. Calculated by the compiler.

PLANETARY RADIATION
Infinitely Conductive Spherical Surfaces

2.3. INFINITELY CONDUCTIVE SPHERICAL SURFACES

2.3.1. SPHERE

Sketch:



Formula:

$$F_{SP} = \frac{1}{2} \left[1 - \frac{\sqrt{\left(\frac{h}{R_P}\right)^2 + 2\left(\frac{h}{R_P}\right)}}{1 + \frac{h}{R_P}} \right]$$

References: Clark & Anderson (1965), Watts (1965).

PLANETARY RADIATION
Infinitely Conductive Spherical Surfaces

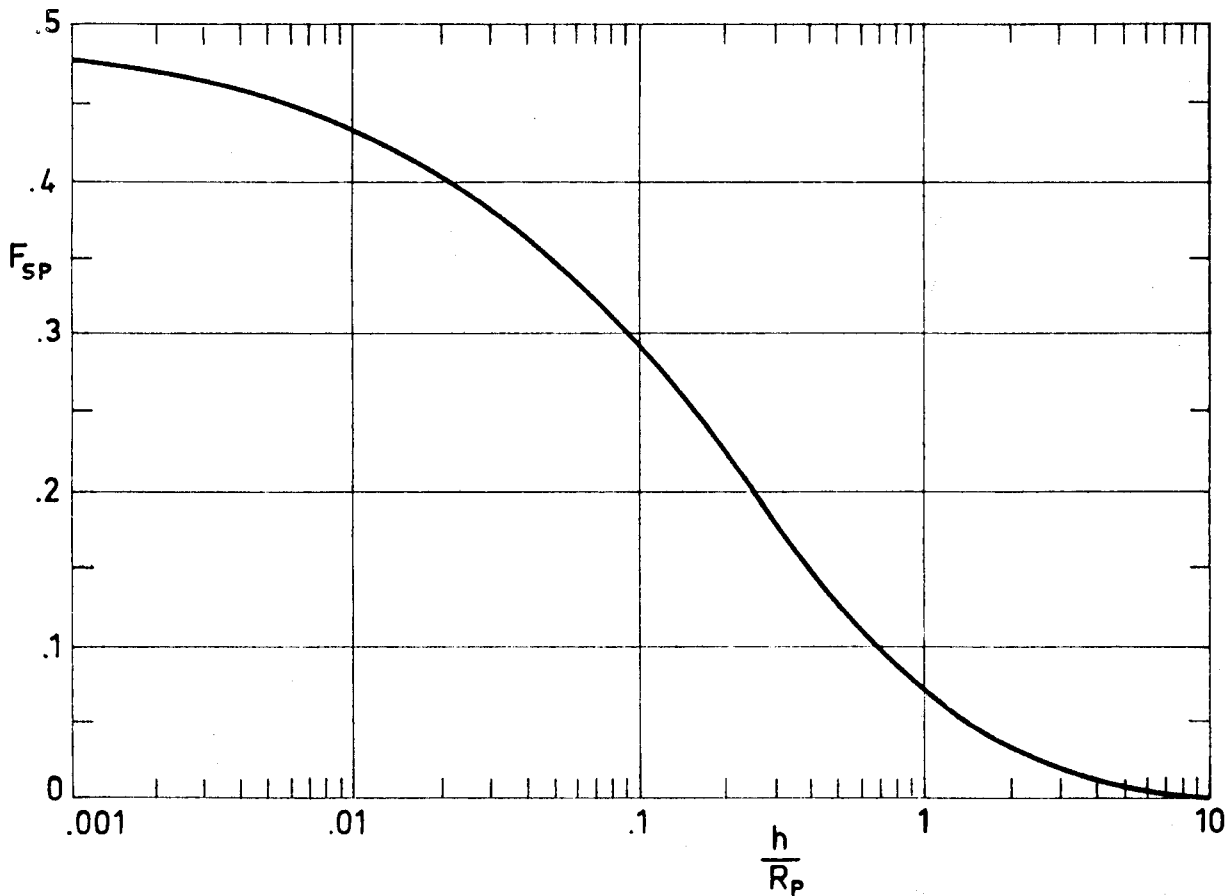
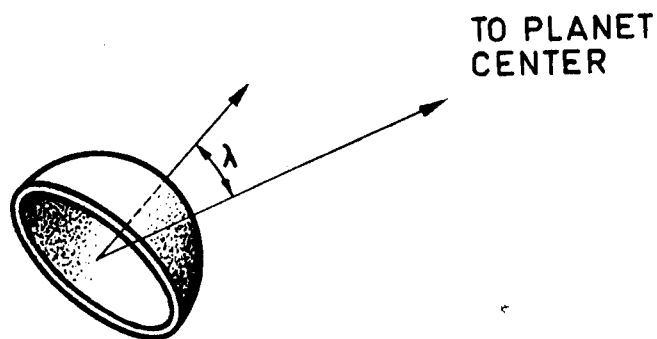


Fig 2-5. F_{SP} as a function of $\frac{h}{R_P}$ in the case of a sphere.
Calculated by the compiler.

PLANETARY RADIATION
 Infinitely Conductive Spherical Surfaces

2.3.2. HEMISPHERICAL SURFACE ABSORBING AND EMITTING ON OUTER FACE

Sketch:



Formula:

$$F_{SP} = \frac{1}{2} \left[1 - \frac{\sqrt{\left(\frac{h}{R_P}\right)^2 + 2 \left(\frac{h}{R_P}\right)}}{1 + \frac{h}{R_P}} + \frac{1}{1 + \frac{h}{R_P}} \cdot \frac{\cos \lambda}{2} \right]$$

Reference: Watts (1965).

PLANETARY RADIATION
Infinitely Conductive Spherical Surfaces

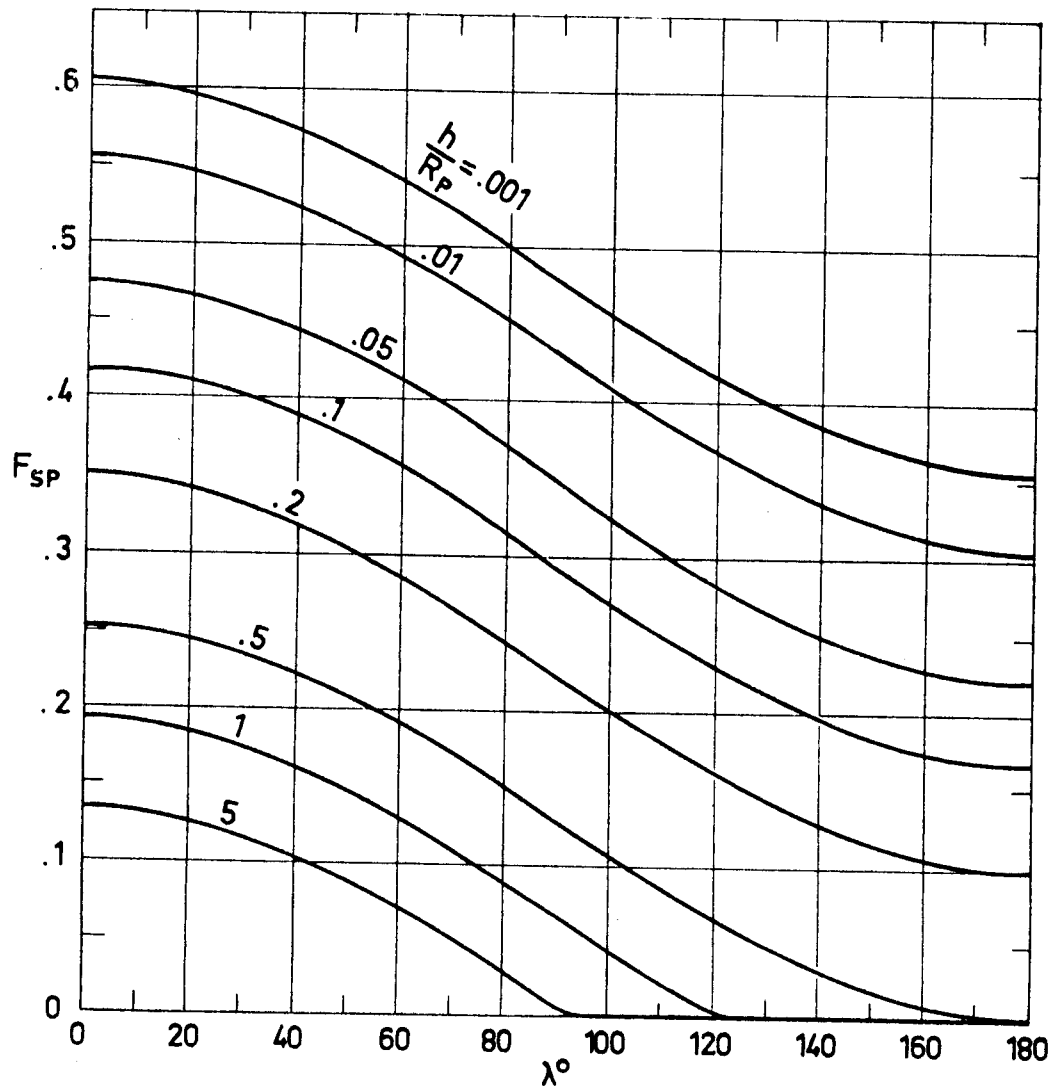


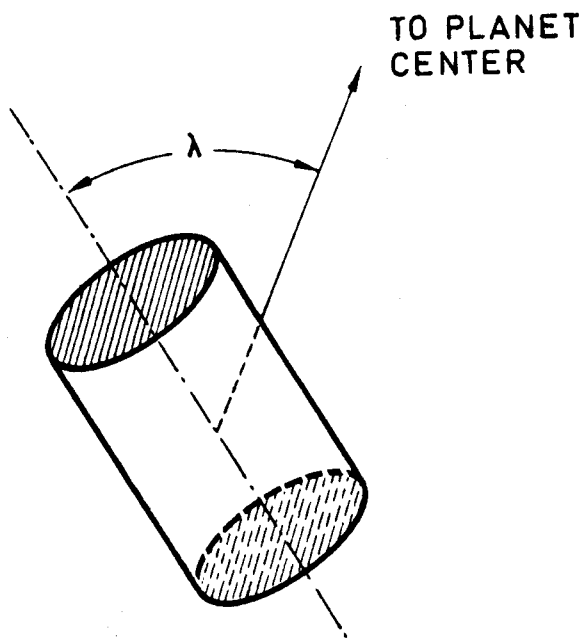
Fig 2-6. F_{SP} as a function of λ and $\frac{h}{R_P}$ in the case of a hemispherical surface absorbing and emitting on outer face. Calculated by the compiler.

PLANETARY RADIATION
Infinitely Conductive Cylindrical Surfaces

2.4. INFINITELY CONDUCTIVE CYLINDRICAL SURFACES

2.4.1. CIRCULAR CYLINDER WITH INSULATED BASES

Sketch:



Formula:

$$F_{SP} = B_0 + \frac{B_2}{2} \sin^2 \lambda + \frac{3B_3}{8} \sin^4 \lambda + \frac{5B_4}{16} \sin^6 \lambda$$

where the parameters B_i ($i = 0, 1, \dots, 4$) are defined in § 2.1.

References: Clark & Anderson (1965), Watts (1965).

PLANETARY RADIATION
 Infinitely Conductive Cylindrical Surfaces

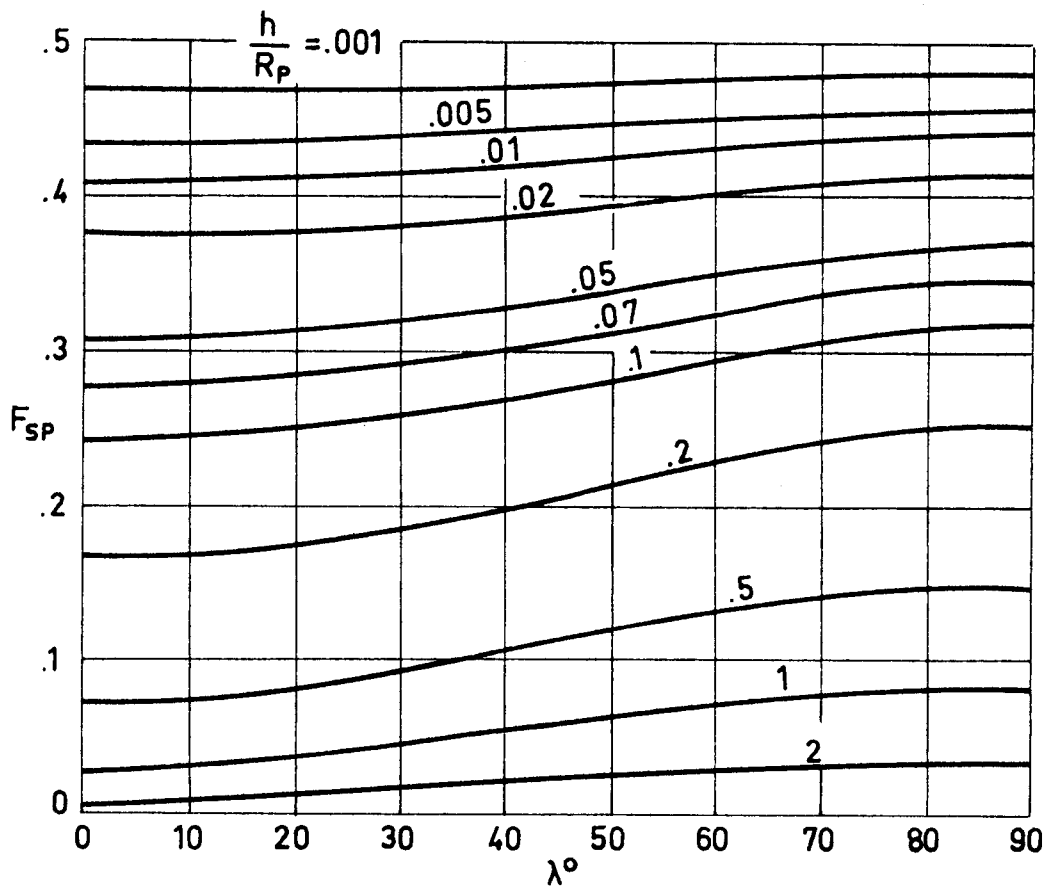
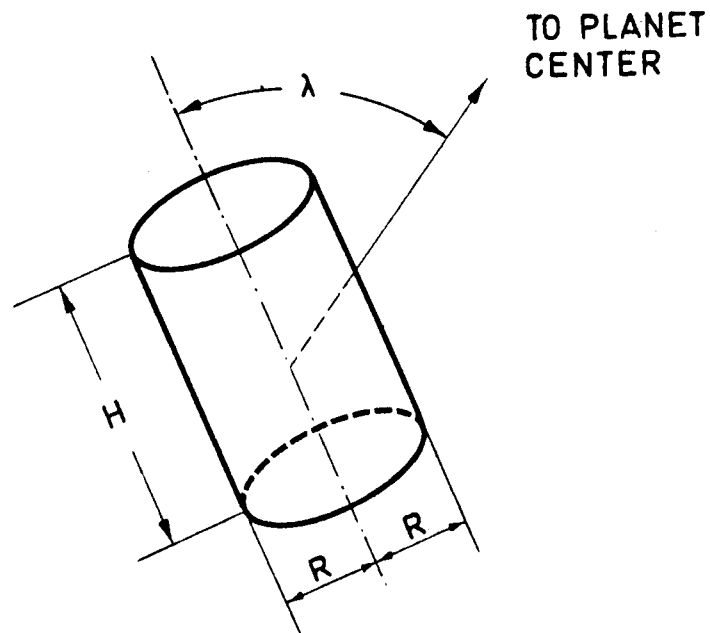


Fig 2-7. F_{SP} as a function of λ and $\frac{h}{R_p}$ in the case of a circular cylinder with insulated bases. Calculated by the compiler.

PLANETARY RADIATION
Infinitely Conductive Cylindrical Surfaces

2.4.2. FINITE HEIGHT CIRCULAR CYLINDER

Sketch:



Formula:

$$F_{SP} = \frac{1}{1 + \frac{H}{R}} \left[B_0 + B_2 \cos^2 \lambda + B_3 \cos^4 \lambda + B_4 \cos^6 \lambda + \right. \\ \left. + \frac{H}{R} \left(B_0 + \frac{B_2}{2} \sin^2 \lambda + \frac{3B_3}{8} \sin^4 \lambda + \frac{5B_4}{16} \sin^6 \lambda \right) \right]$$

where the parameters B_i ($i = 0, 1, \dots, 4$) are defined in § 2.1.

Reference: Clark & Anderson (1965).

PLANETARY RADIATION
Infinitely Conductive Cylindrical Surfaces

$$\frac{H}{R} = 0$$

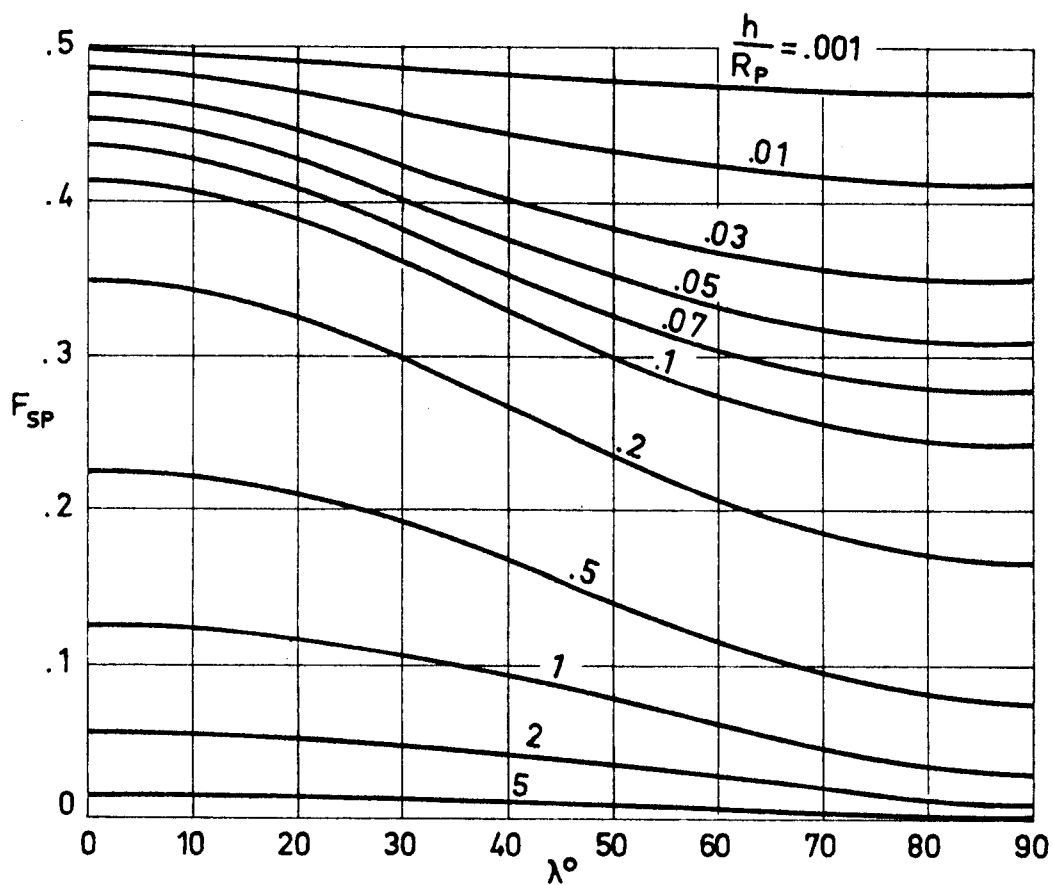


Fig 2-8. F_{SP} as a function of λ and $\frac{h}{R_P}$ in the case of a finite height circular cylinder. Calculated by the compiler.

PLANETARY RADIATION
 Infinitely Conductive Cylindrical Surfaces

$$\frac{H}{R} = 0.1$$

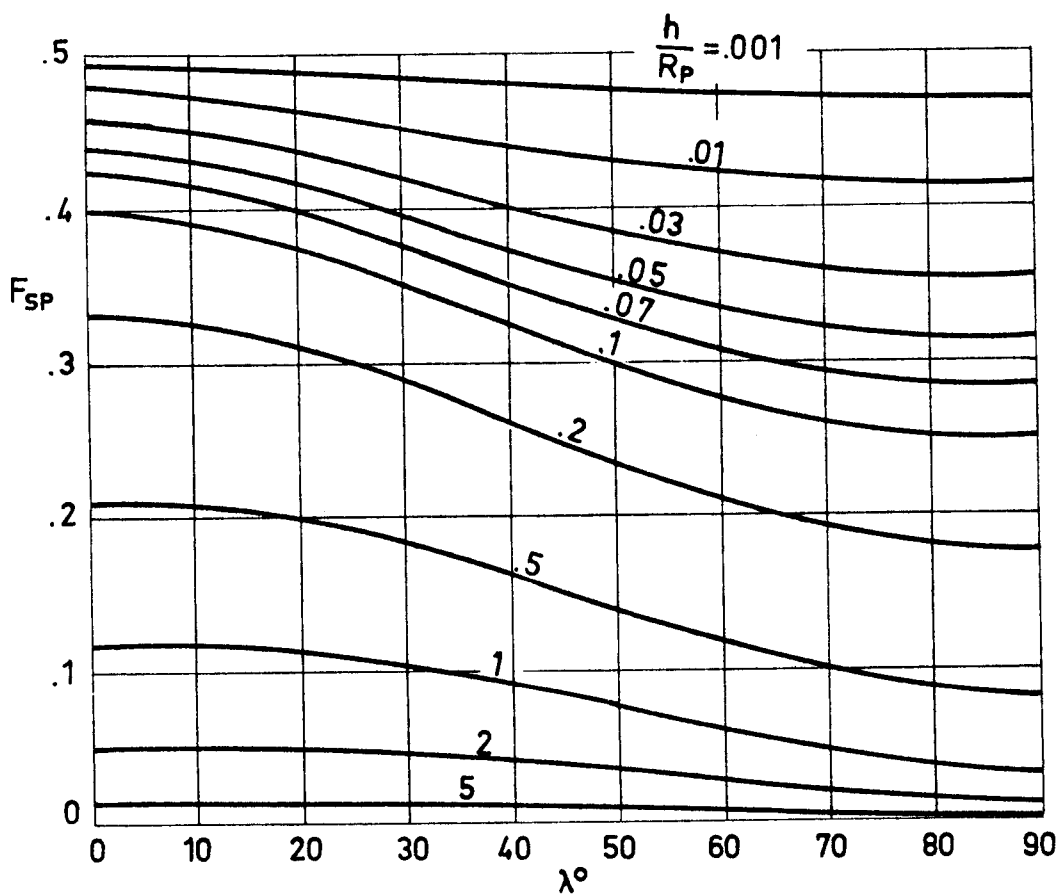


Fig 2-9. F_{SP} as a function of λ and $\frac{h}{R_p}$ in the case of a finite height circular cylinder. Calculated by the compiler.

PLANETARY RADIATION
 Infinitely Conductive Cylindrical Surfaces

$$\frac{H}{R} = 0.2$$

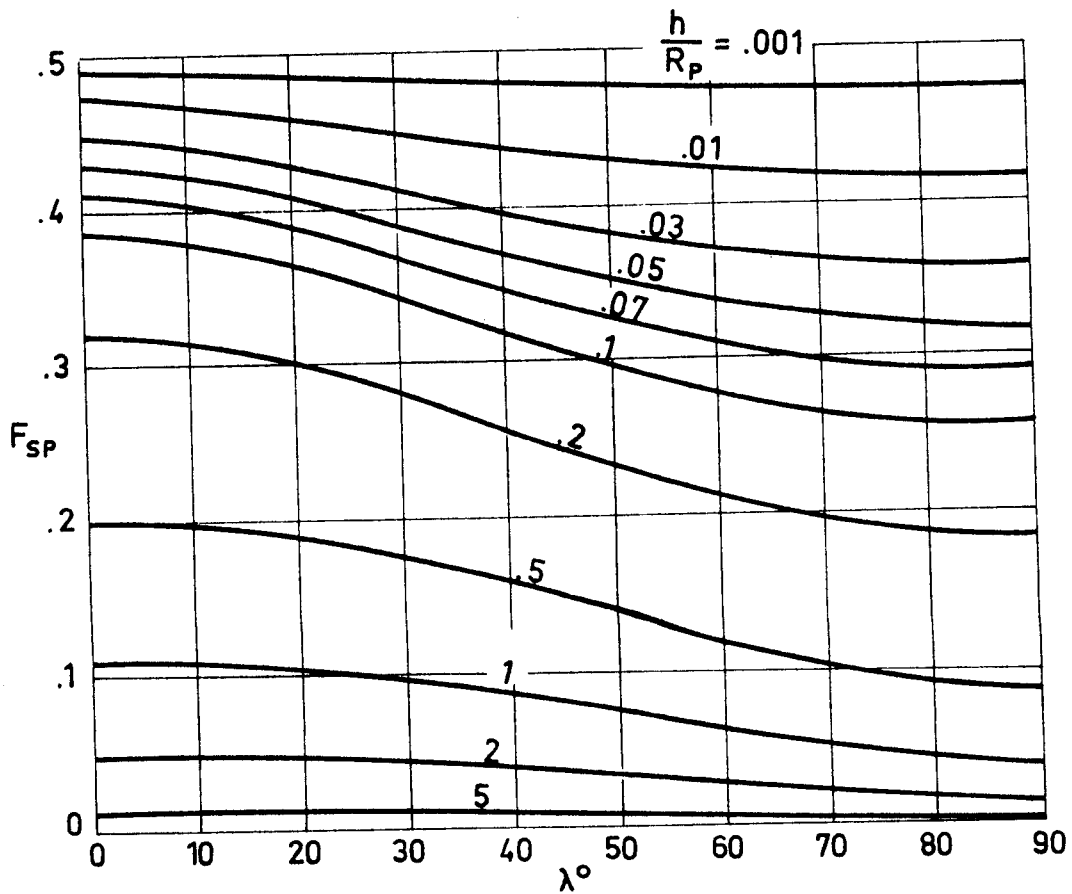


Fig 2-10. F_{SP} as a function of λ and $\frac{h}{R_P}$ in the case of a finite height circular cylinder. Calculated by the compiler.

PLANETARY RADIATION
 Infinitely Conductive Cylindrical Surfaces

$$\frac{H}{R} = 0.3$$

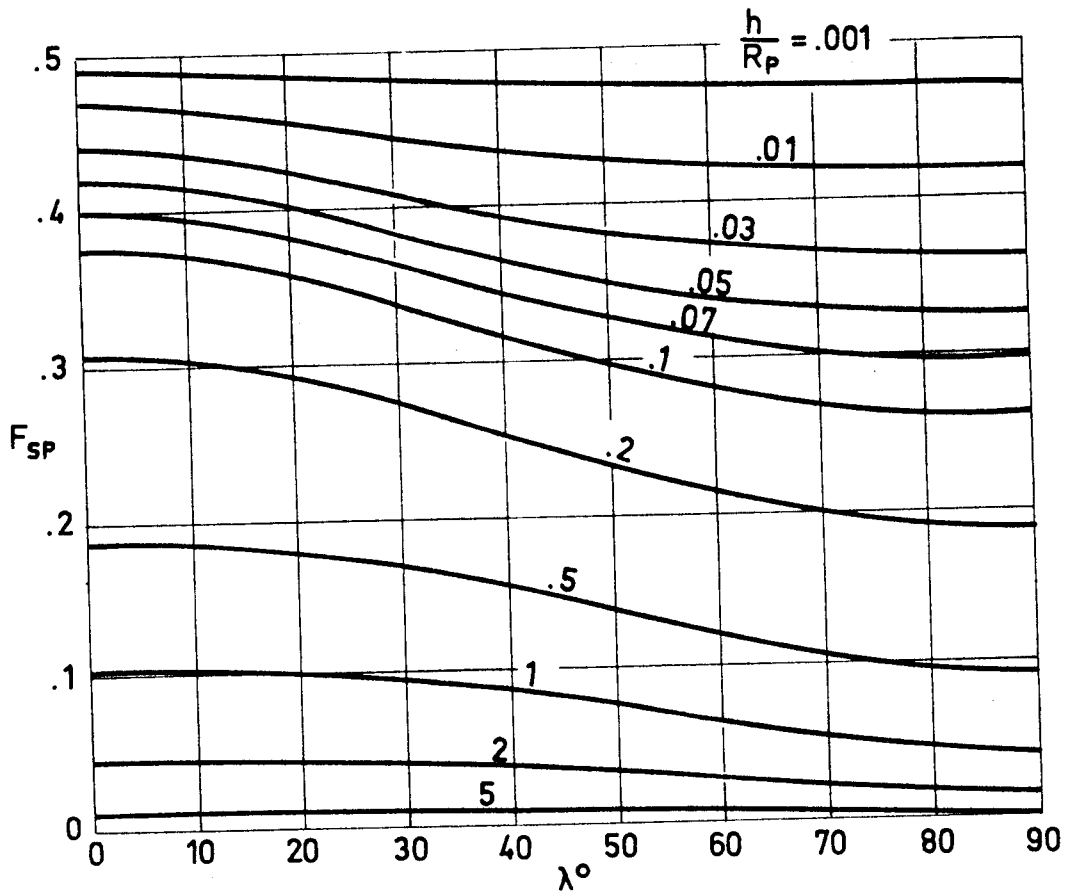


Fig 2-11. F_{SP} as a function of λ and $\frac{h}{R_p}$ in the case of a finite height circular cylinder. Calculated by the compiler.

PLANETARY RADIATION
 Infinitely Conductive Cylindrical Surfaces

$$\frac{H}{R} = 0.4$$

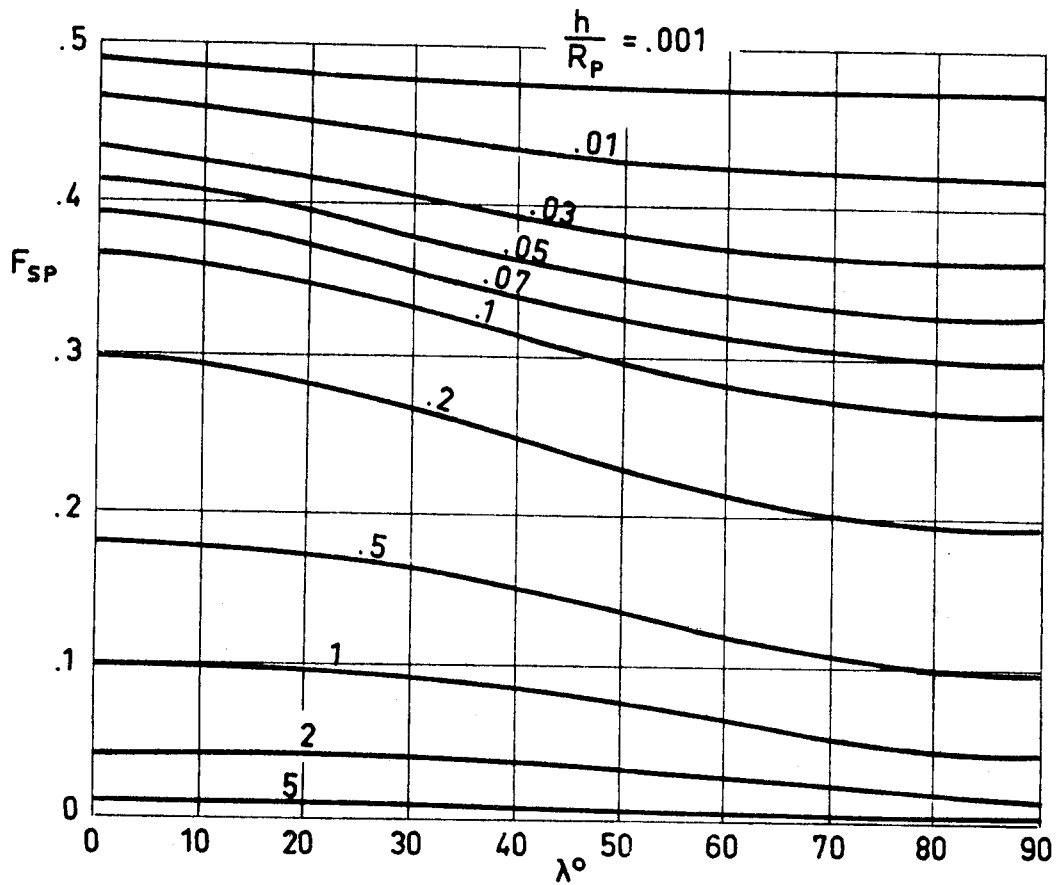


Fig 2-12. F_{SP} as a function of λ and $\frac{h}{R_p}$ in the case of a finite height circular cylinder. Calculated by the compiler.

PLANETARY RADIATION
 Infinitely Conductive Cylindrical Surfaces

$$\frac{H}{R} = 0.5$$

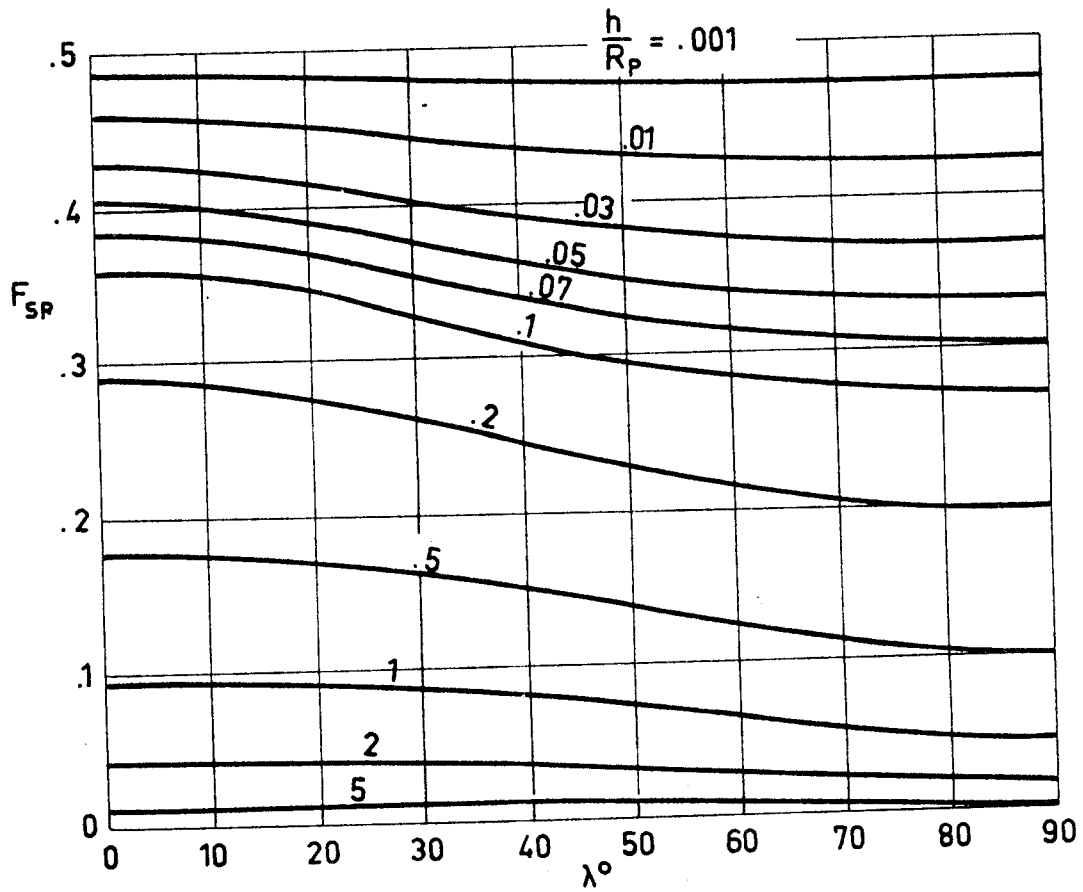


Fig 2-13. F_{SP} as a function of λ and $\frac{h}{R_p}$ in the case of a finite height circular cylinder. Calculated by the compiler.

PLANETARY RADIATION
 Infinitely Conductive Cylindrical Surfaces

$$\frac{H}{R} = 1$$

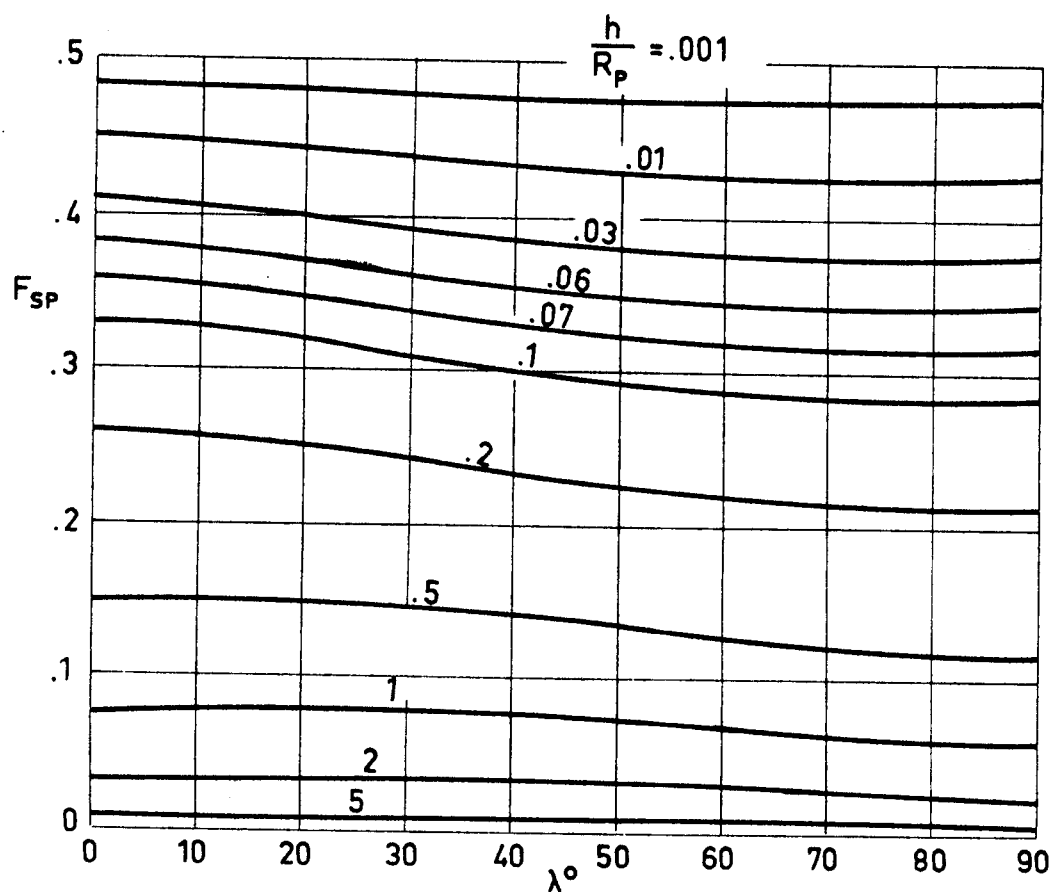


Fig 2-14. F_{SP} as a function of λ and $\frac{h}{R_p}$ in the case of a finite height circular cylinder. Calculated by the compiler.

PLANETARY RADIATION
 Infinitely Conductive Cylindrical Surfaces

$$\frac{H}{R} = 10$$

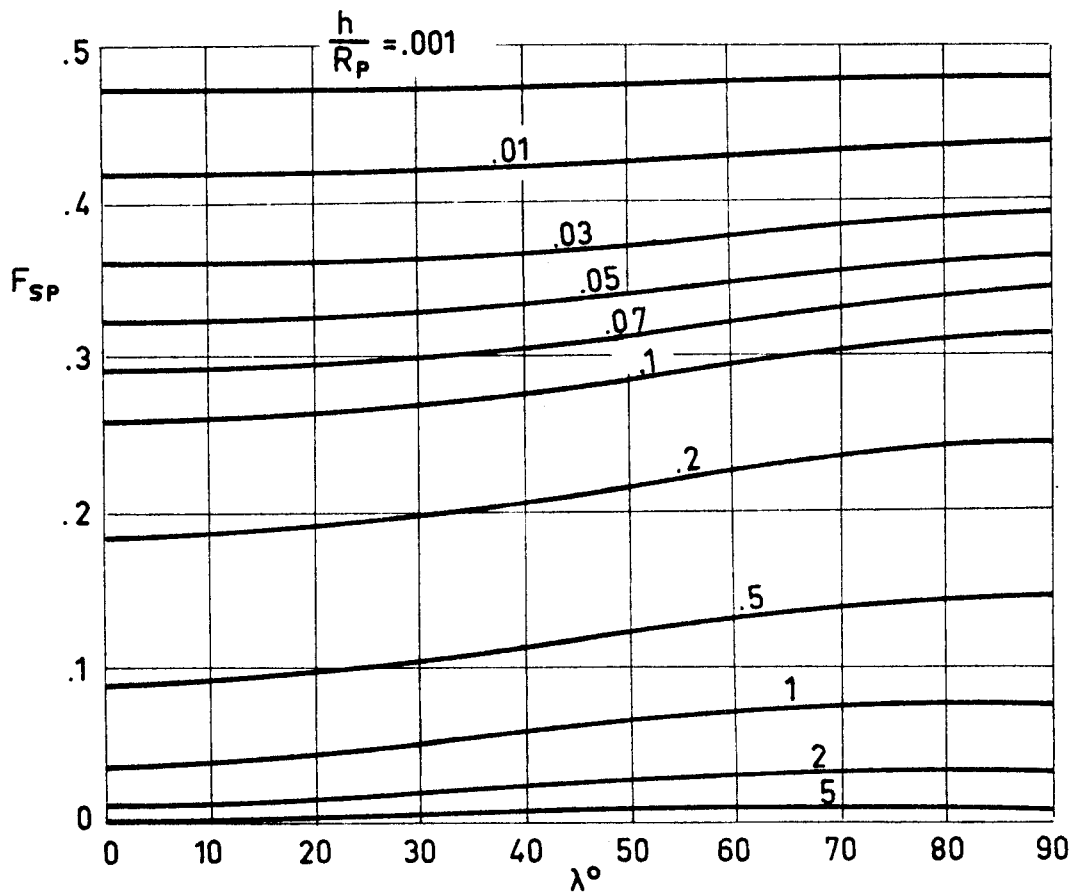


Fig 2-15. F_{SP} as a function of λ and $\frac{h}{R_p}$ in the case of a finite height circular cylinder. Calculated by the compiler.

PLANETARY RADIATION
 Infinitely Conductive Cylindrical Surfaces

$$\frac{H}{R} \geq 100$$

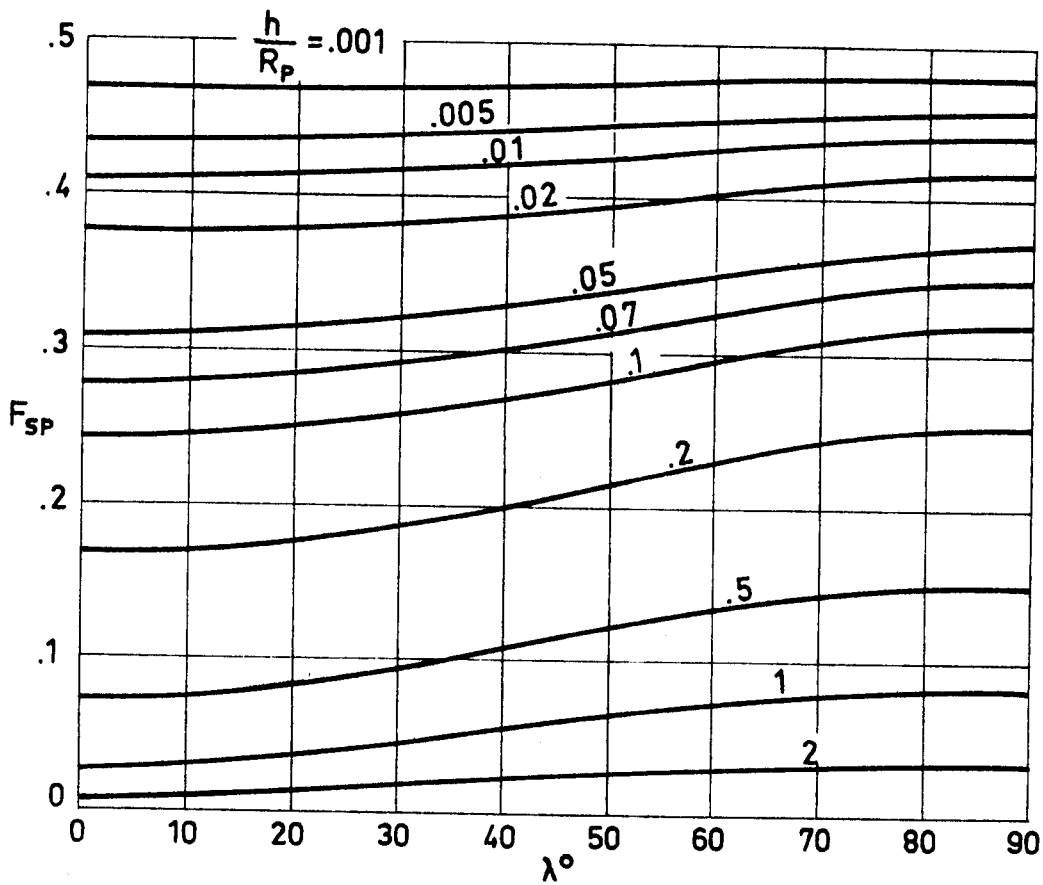


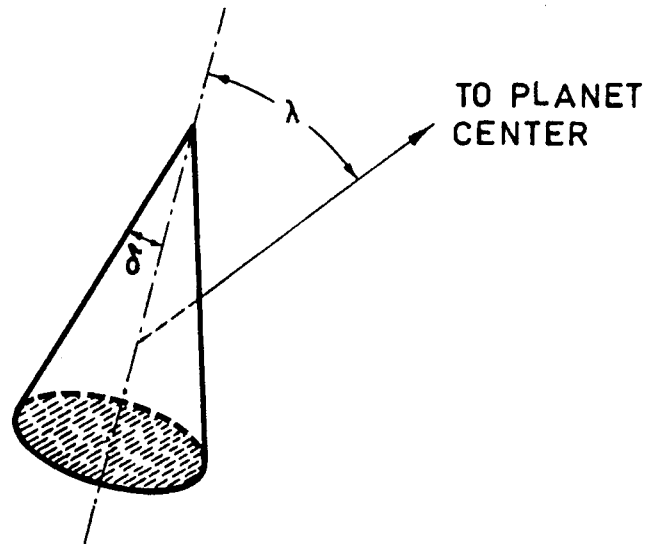
Fig 2-16. F_{SP} as a function of λ and $\frac{h}{R_P}$ in the case of a finite height circular cylinder. Calculated by the compiler.

PLANETARY RADIATION
Infinitely Conductive Conical Surfaces

2.5. INFINITELY CONDUCTIVE CONICAL SURFACES

2.5.1. CIRCULAR CONE WITH INSULATED BASE

Sketch:



Formula:

$$F_{SP} = B_0 + B_1 C + B_2 \left(C^2 + \frac{D^2}{2} \right) + B_3 \left(C^4 + 3C^2 D^2 + \frac{3}{8} D^4 \right) +$$

$$+ B_4 \left(C^6 + \frac{15}{2} C^4 D^2 + \frac{45}{8} C^2 D^4 + \frac{5}{16} D^6 \right)$$

where the parameters B_i ($i = 0, 1, \dots, 4$) are defined in § 2.1.

In addition:

$$C = \sin \delta \cos \lambda$$

$$D = \cos \delta \sin \lambda$$

Reference: Clark & Anderson (1965).

PLANETARY RADIATION
 Infinitely Conductive Conical Surfaces

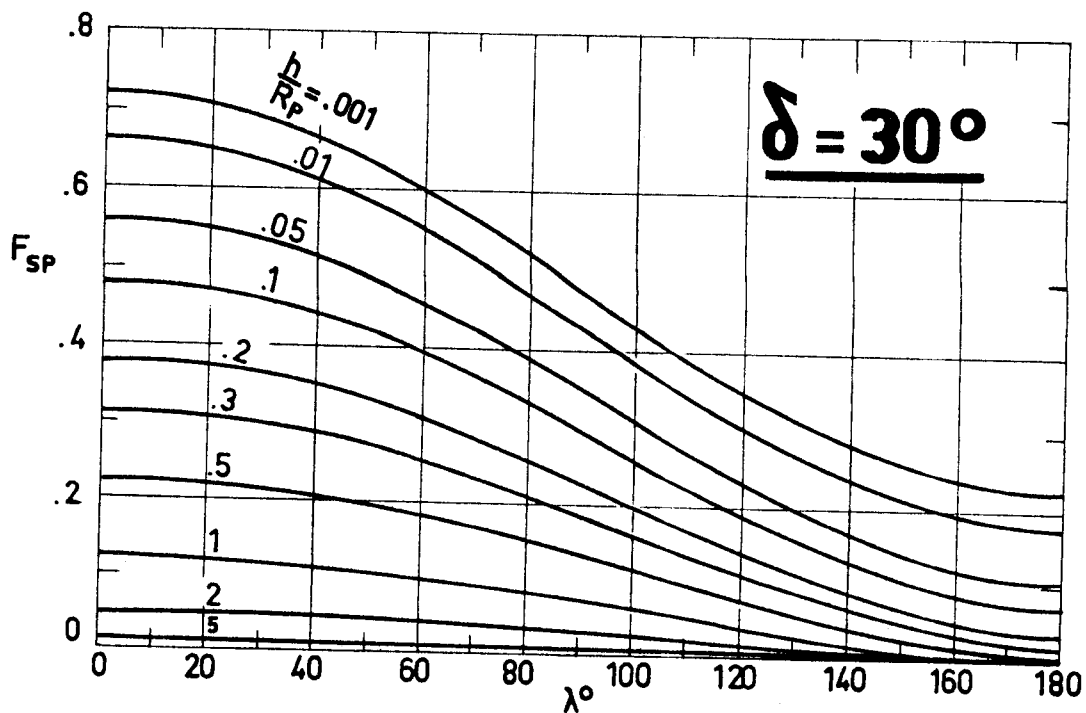
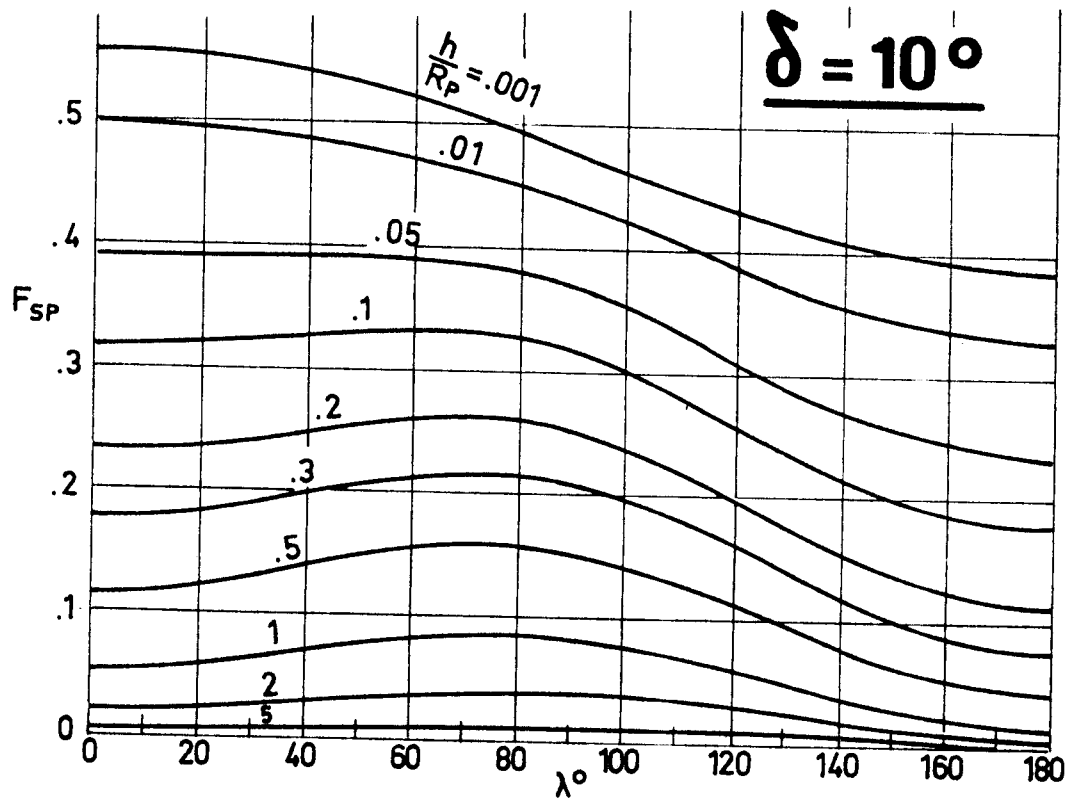


Fig 2-17. F_{SP} as a function of λ and $\frac{h}{R_P}$ in the case of a circular cone with insulated base. Calculated by the compiler.

PLANETARY RADIATION
 Infinitely Conductive Conical Surfaces

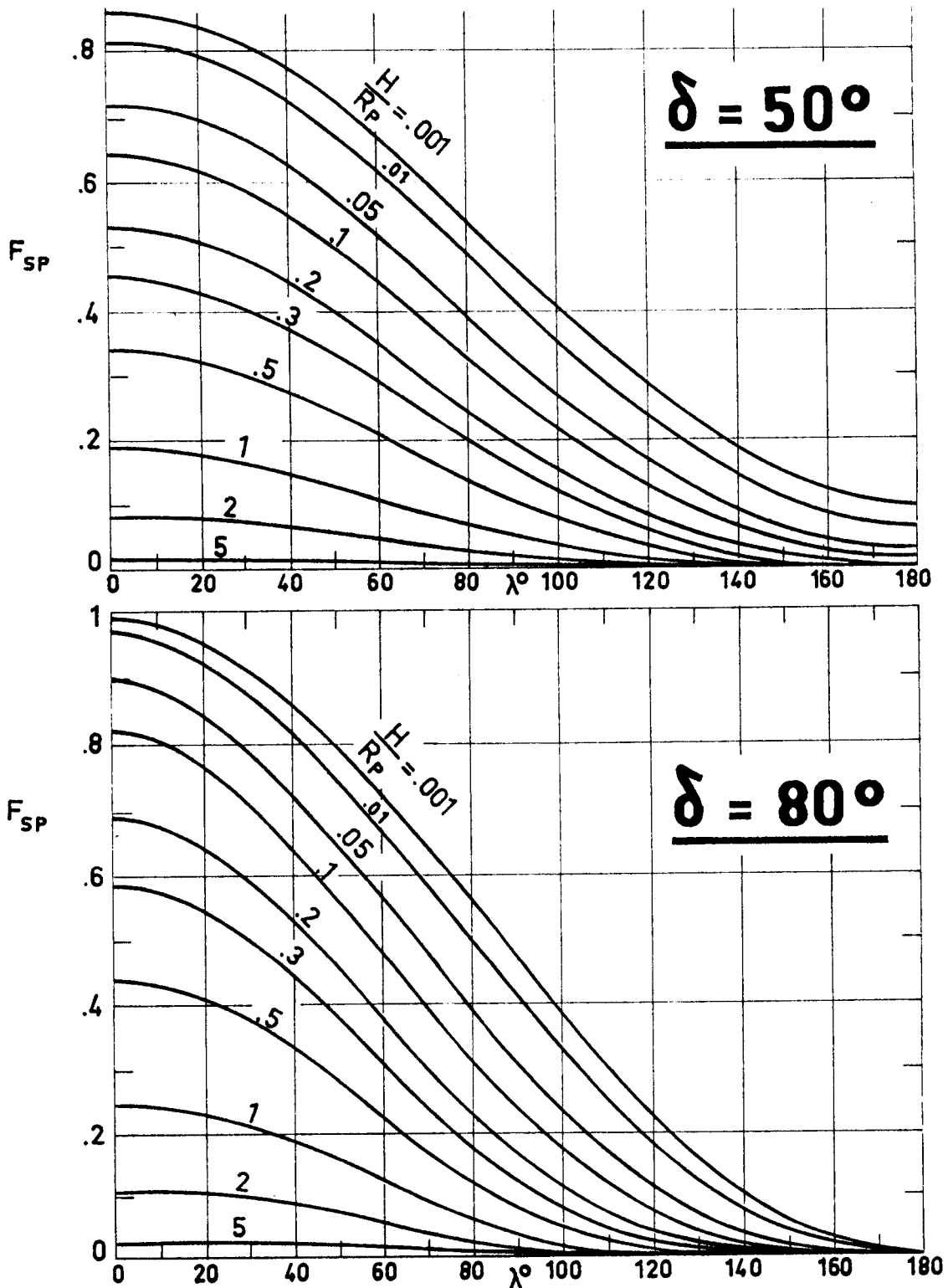


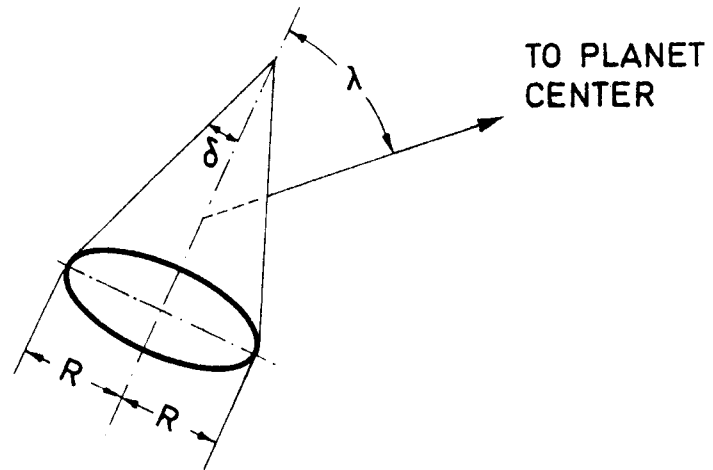
Fig 2-18. F_{SP} as a function of λ and $\frac{h}{R_P}$ in the case of a circular cone with insulated base. Calculated by the compiler.

INTENTIONALLY BLANK PAGE

PLANETARY RADIATION
Infinitely Conductive Conical Surfaces

2.5.2. FINITE HEIGHT CIRCULAR CONE

Sketch:



Formula:

$$F_{SP} = \frac{1}{1 + \sin \delta} \left[\sin \delta (B_0 - B_1 \cos \lambda + B_2 \cos^2 \lambda + B_3 \cos^4 \lambda + B_4 \cos^6 \lambda) + \right. \\ \left. + B_0 + B_1 C + B_2 \left(C^2 + \frac{D^2}{2} \right) + B_3 \left(C^4 + 3C^2 D^2 + \frac{3}{8} D^4 \right) + \right. \\ \left. + B_4 \left(C^6 + \frac{15}{2} C^4 D^2 + \frac{45}{8} C^2 D^4 + \frac{5}{16} D^6 \right) \right]$$

where the parameters B_i ($i = 0, 1, \dots, 4$) are defined in § 2.1. In addition:

$$C = \sin \delta \cos \lambda$$

$$D = \cos \delta \sin \lambda$$

Reference: Clark & Anderson (1965).

PLANETARY RADIATION
Infinitely Conductive Conical Surfaces

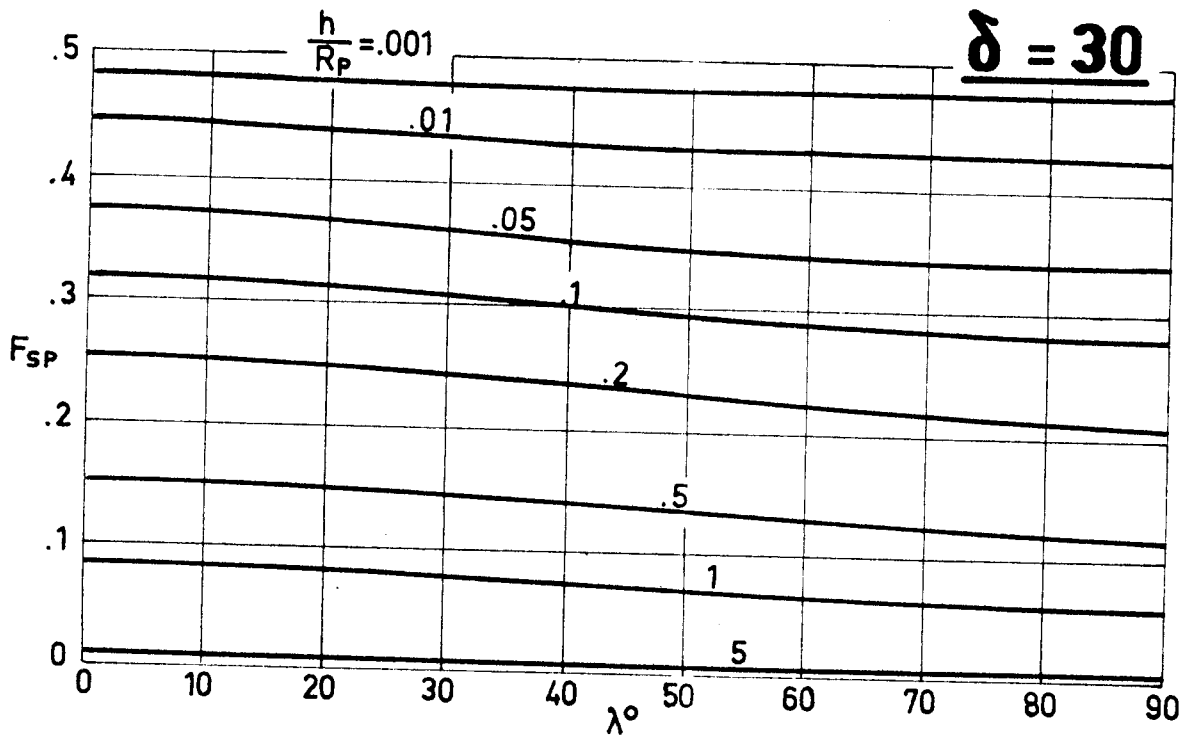
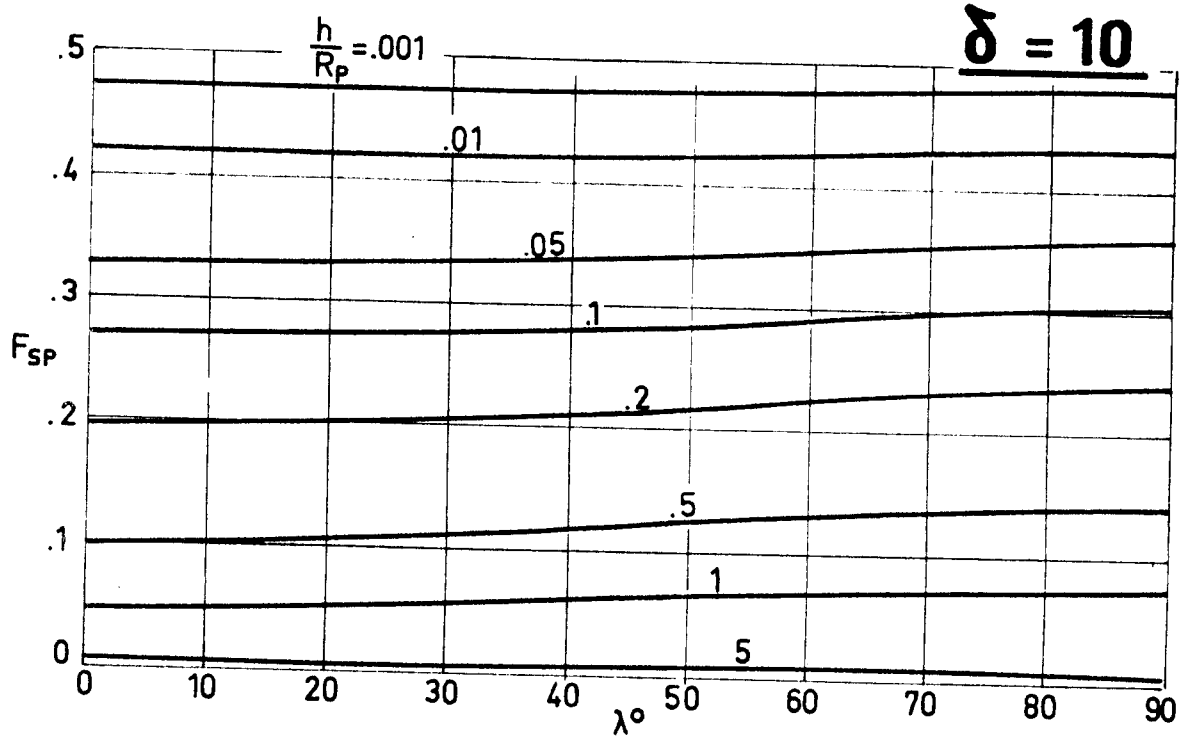


Fig 2-19. F_{SP} as a function of λ in the case of a finite height circular cone. Calculated by the compiler.

PLANETARY RADIATION
 Infinitely Conductive Conical Surfaces

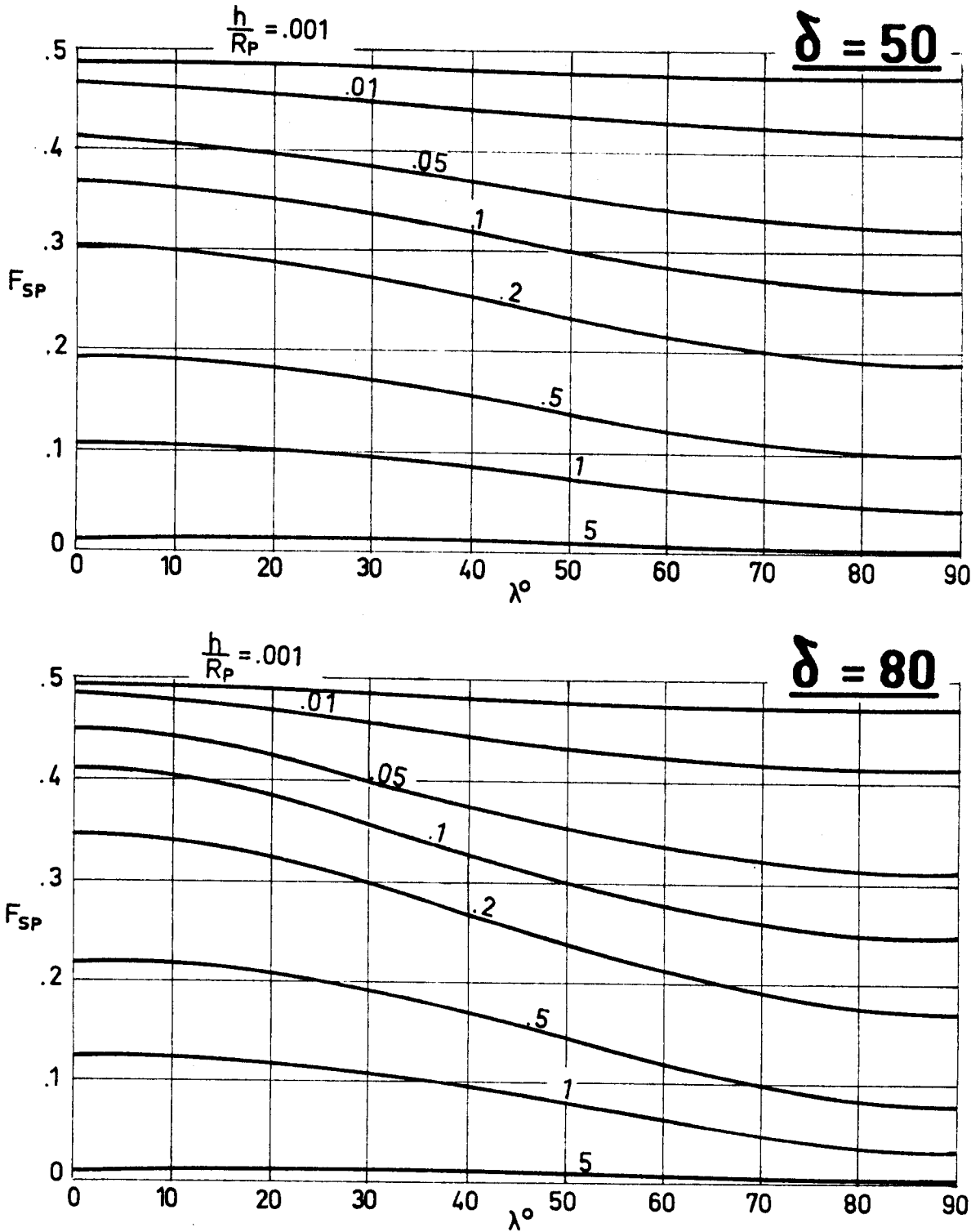


Fig 2-20. F_{SP} as a function of λ in the case of a finite height circular cone. Calculated by the compiler.

INTENTIONALLY BLANK PAGE

ALBEDO RADIATION

General

3. ALBEDO RADIATION3.1. GENERAL

Albedo radiation is that part of the solar radiation incident upon the planet which is reflected or scattered by the planet surface and atmosphere (if existent).

Data on the equilibrium temperature of a satellite, heated by the albedo radiation from a planet, and cooled by radiation to the outer space, are presented in this Chapter. These data are based on the assumptions a, b, d and e listed in § 2.1. In addition, the planet is supposed to be a diffusely reflecting sphere.

The Spacecraft Albedo Radiation Equilibrium Temperature, T_{RA} , as given by

$$T_{RA} = \left[\frac{\alpha}{\epsilon} F T_A^4 + T_s^4 \right]^{1/4},$$

where T_s is assumed to be zero as it has been indicated repeatedly. Values of T_{RA}/T_A vs. α/ϵ for arbitrary values of the albedo view factor, F , from spacecraft to planet are given in Fig 3-1. These values can be also used to estimate the effect on a subsatellite of the solar radiation reflected or scattered by a large satellite, provided that the above assumptions hold.

T_{RA} as function of T_{RA}/T_A for albedo radiation from several planets is given in Fig 3-2. Albedo radiation from the Earth is considered in Fig 3-3. Finally, values of F in three simple cases are presented.

ALBEDO RADIATION
General

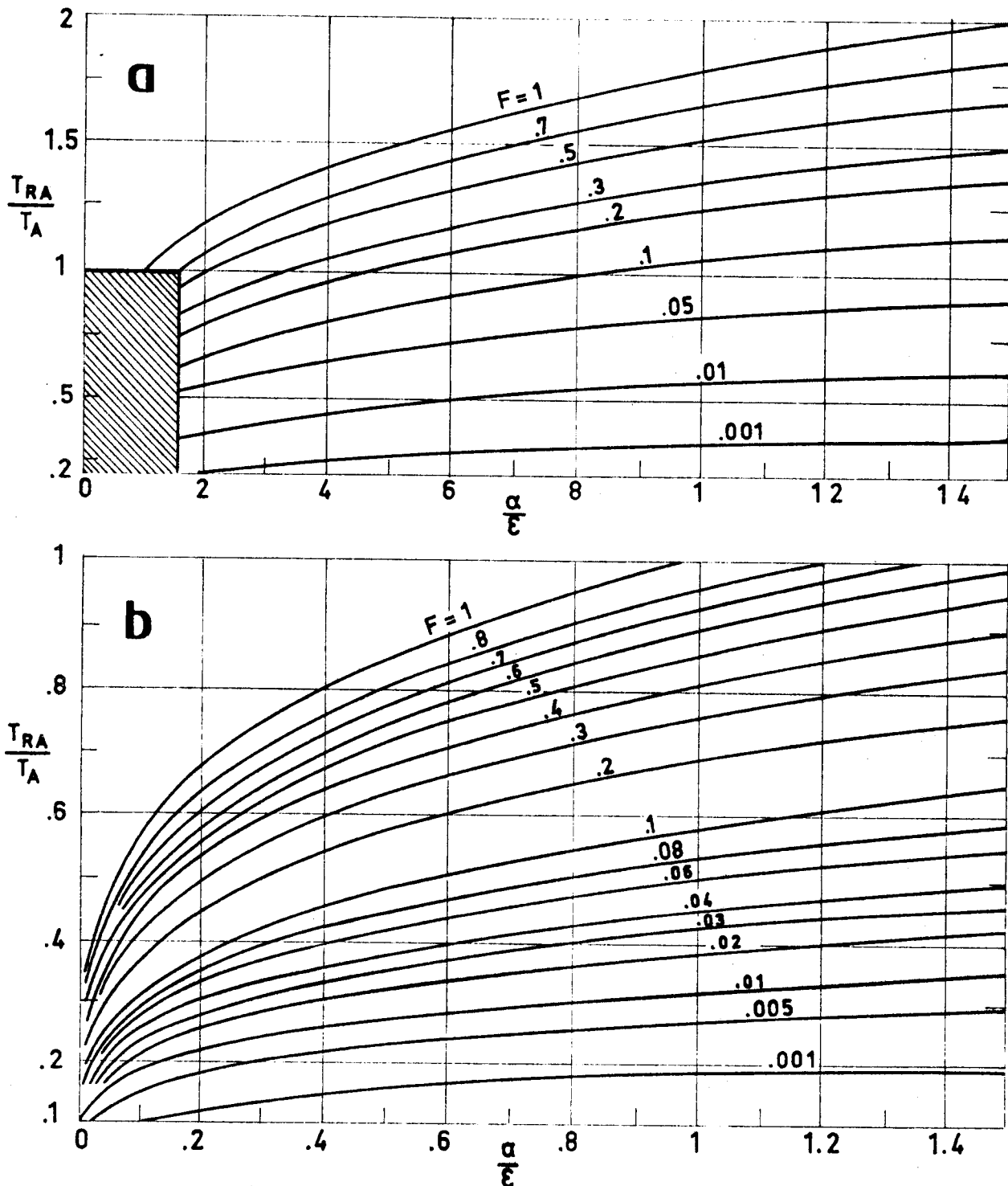


Fig 3-1. The ratio T_{RA}/T_A vs. the optical characteristics of the surface for different values of F . Shaded zone of a is enlarged in b. Calculated by the compiler.

ALBEDO RADIATION

General

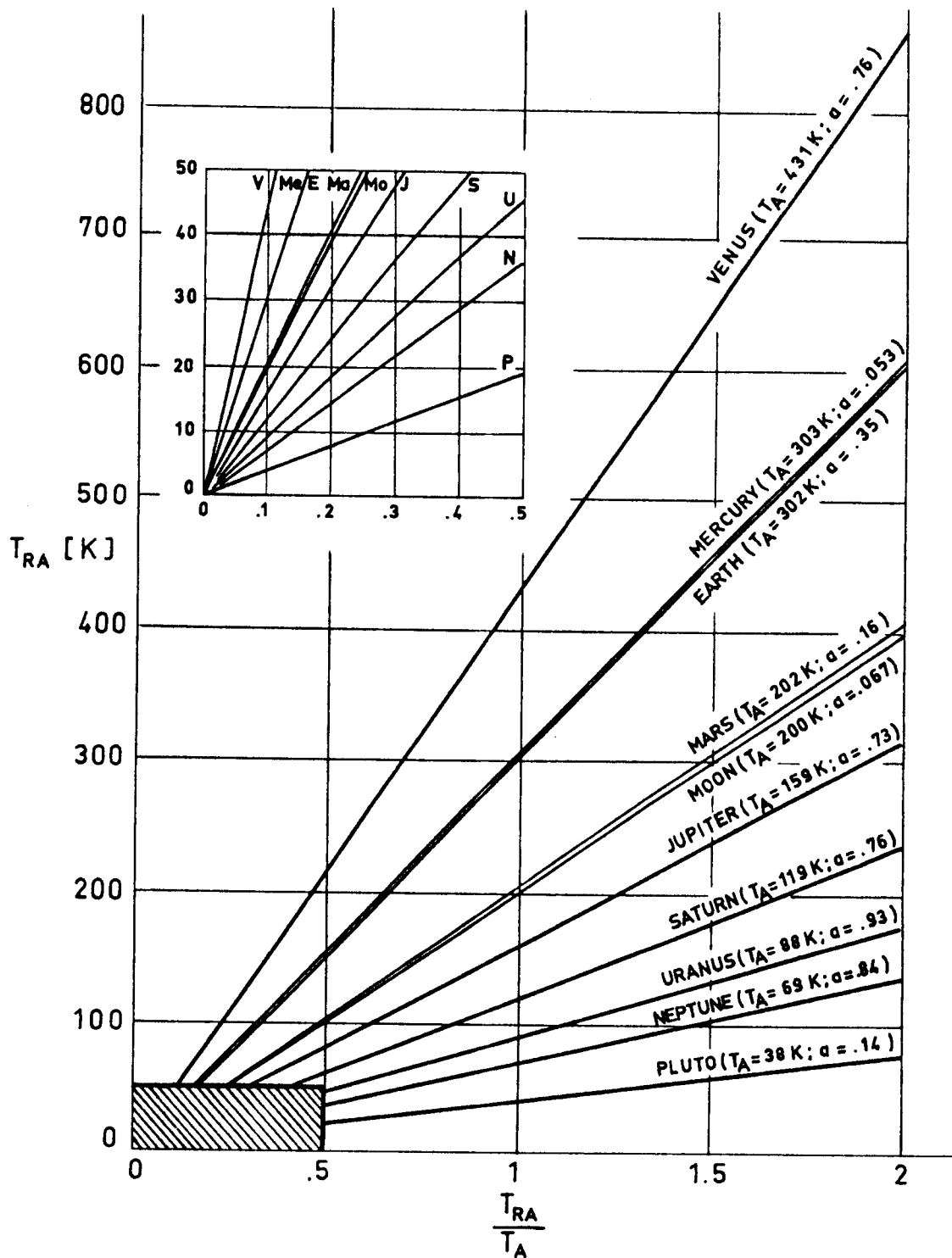


Fig 3-2. Albedo equilibrium temperature, T_{RA} , vs. dimensionless ratio T_{RA}/T_A . Incoming albedo from different planets. After Anderson (1969).

ALBEDO RADIATION
General

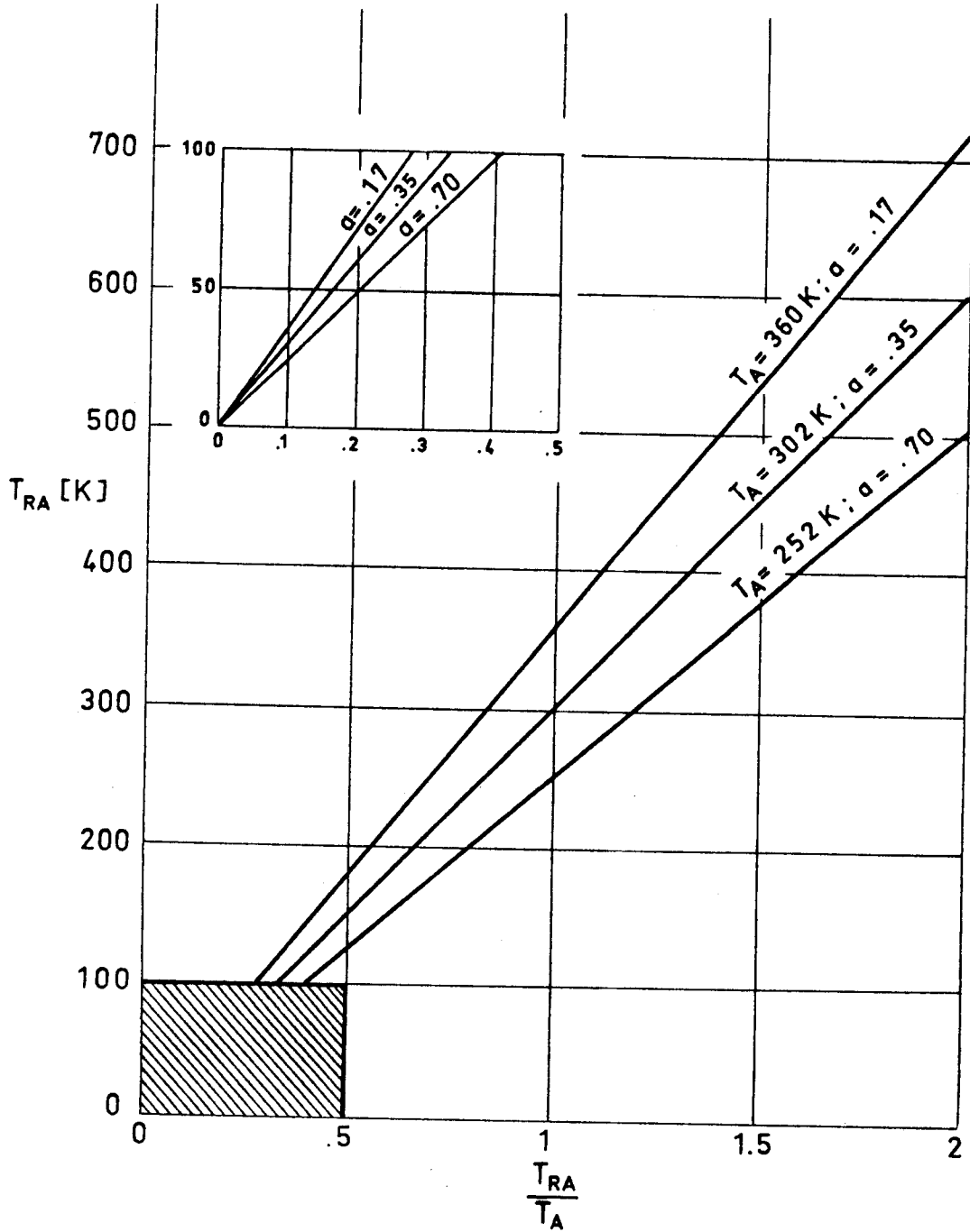


Fig 3-3. Different estimates of albedo equilibrium temperature T_{RA} , vs. T_{RA}/T_A in the case of the Earth. Calculated by the compiler.

ALBEDO RADIATION

General

Table 3-1
Relevant data on the Planets and the Moon

	DISTANCE TO THE SUN $\times 10^{-9}$ [m]	DISTANCE TO THE SUN IN AU.	RADIUS OF THE PLANET $\times 10^{-3}$ [m]	PLANET TO EARTH RADIUS RATIO	SOLAR CONSTANT [$\text{W}\cdot\text{m}^{-2}$]	MEAN ALBEDO
MERCURY	57.9	.387	2330	.3659	9034	.053
VENUS	108.1	.723	6100	.9580	2588	.76
EARTH	149.5	1.	6367.5	1.	1353	.35
MARS	227.4	1.521	3415	.5363	585	.16
JUPITER	773.3	5.173	71375	11.2093	51	.73
SATURN	1425.7	9.536	60500	9.5014	15	.76
URANUS	2880.7	19.269	24850	3.9026	3.6	.93
NEPTUNE	4490.1	30.034	25000	3.9262	1.5	.84
PLUTO	5841.9	39.076	2930	.4600	.89	.14
MOON	149.5	1.	1738	.2729	1353	.067

References: Kreith (1962), Wolverson (1963), Anderson (1969).

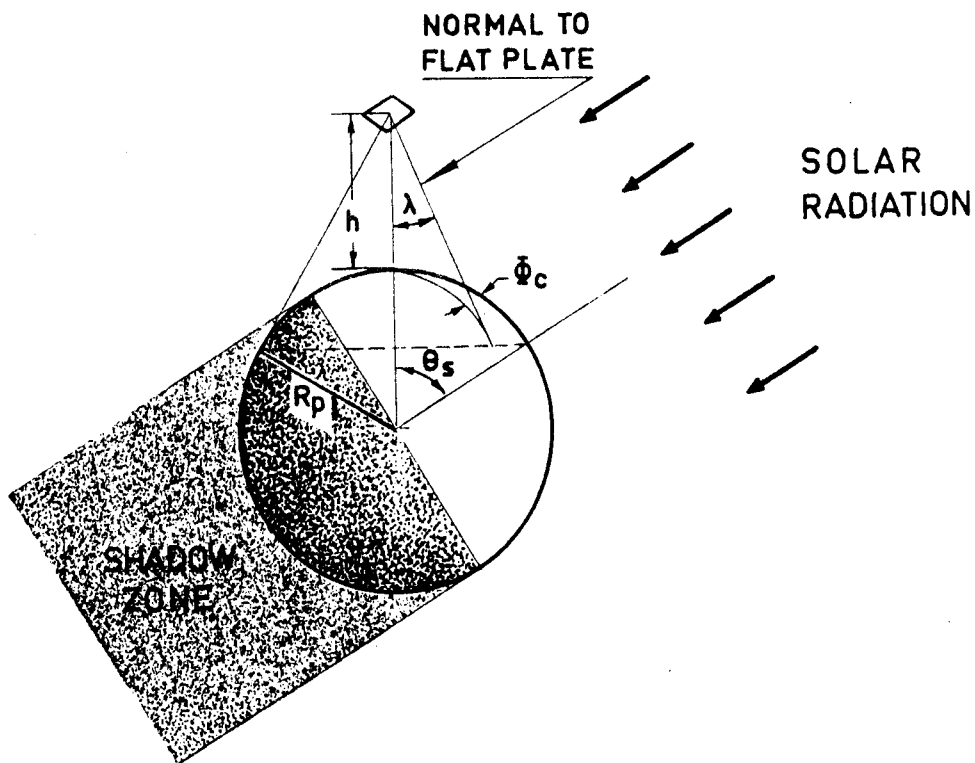
INTENTIONALLY BLANK PAGE

ALBEDO RADIATION
 Infinitely Conductive Planar Surfaces

3.2. INFINITELY CONDUCTIVE PLANAR SURFACES

3.2.1. FLAT PLATE ABSORBING AND EMITTING ON ONE SIDE

Sketch:



Formula: All results presented in the literature are obtained numerically.

Reference: Bannister (1965).

ALBEDO RADIATION
Infinitely Conductive Planar Surfaces

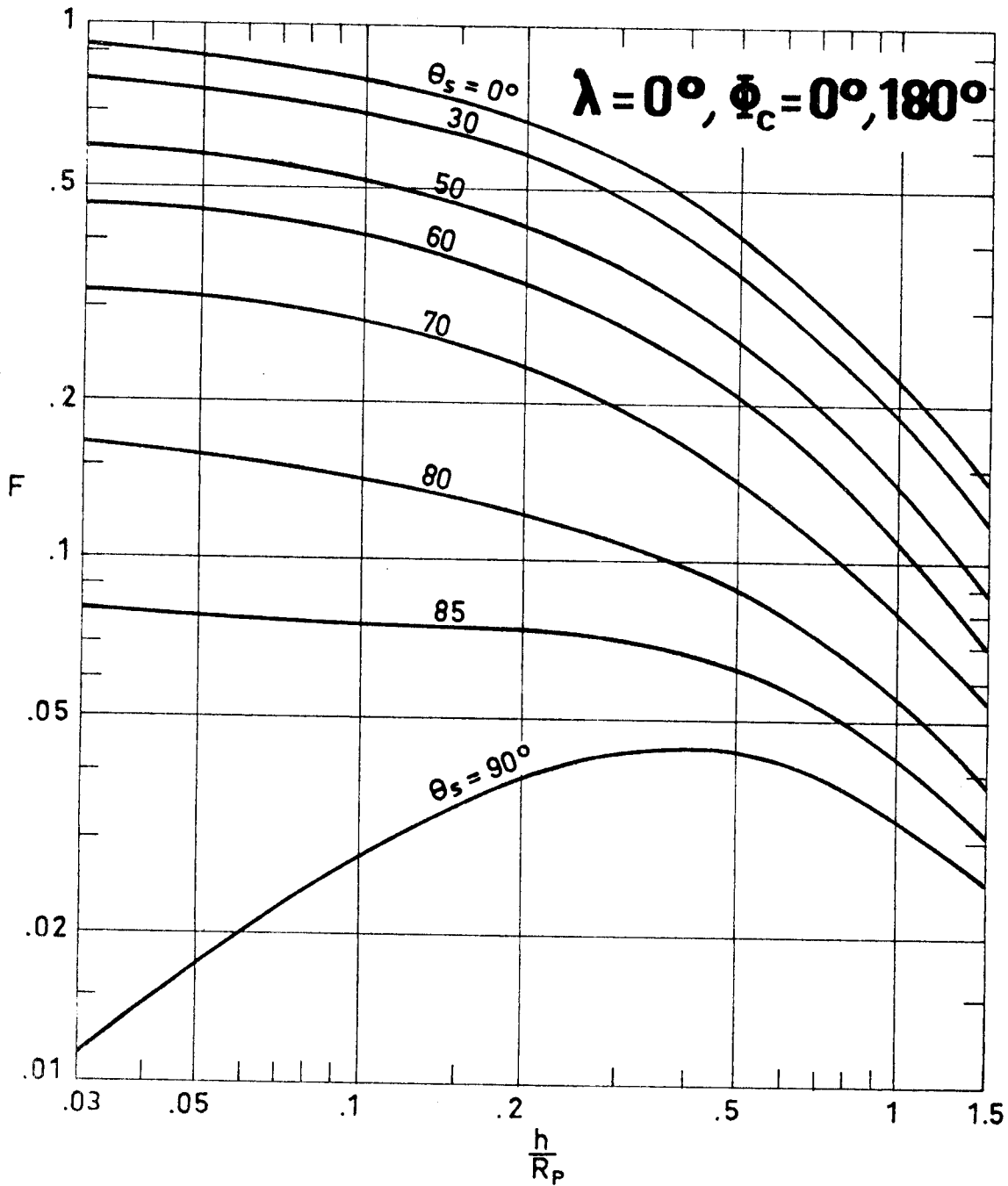


Fig 3-4. Albedo view factor F vs. h/R_p for different values of θ_s in the case of a flat plate ($\lambda=0^\circ, \phi_c=180^\circ$). From Bannister (1965).

ALBEDO RADIATION
 Infinitely Conductive Planar Surfaces

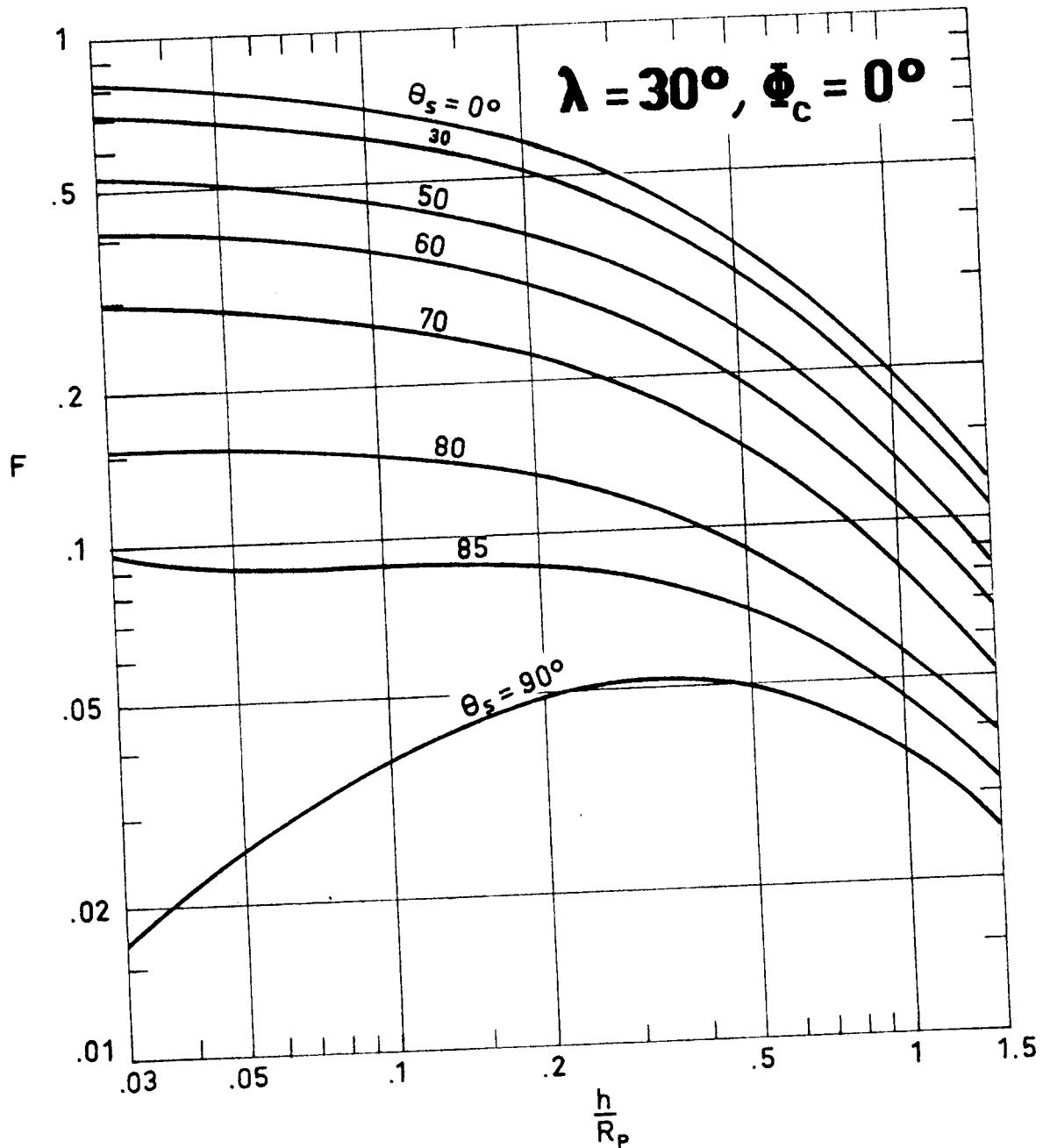


Fig 3-5. Albedo view factor F vs. h/R_p for different values of θ_s in the case of a flat plate ($\lambda=30^\circ, \phi_c=0^\circ$). From Bannister (1965).

ALBEDO RADIATION
 Infinitely Conductive Planar Surfaces

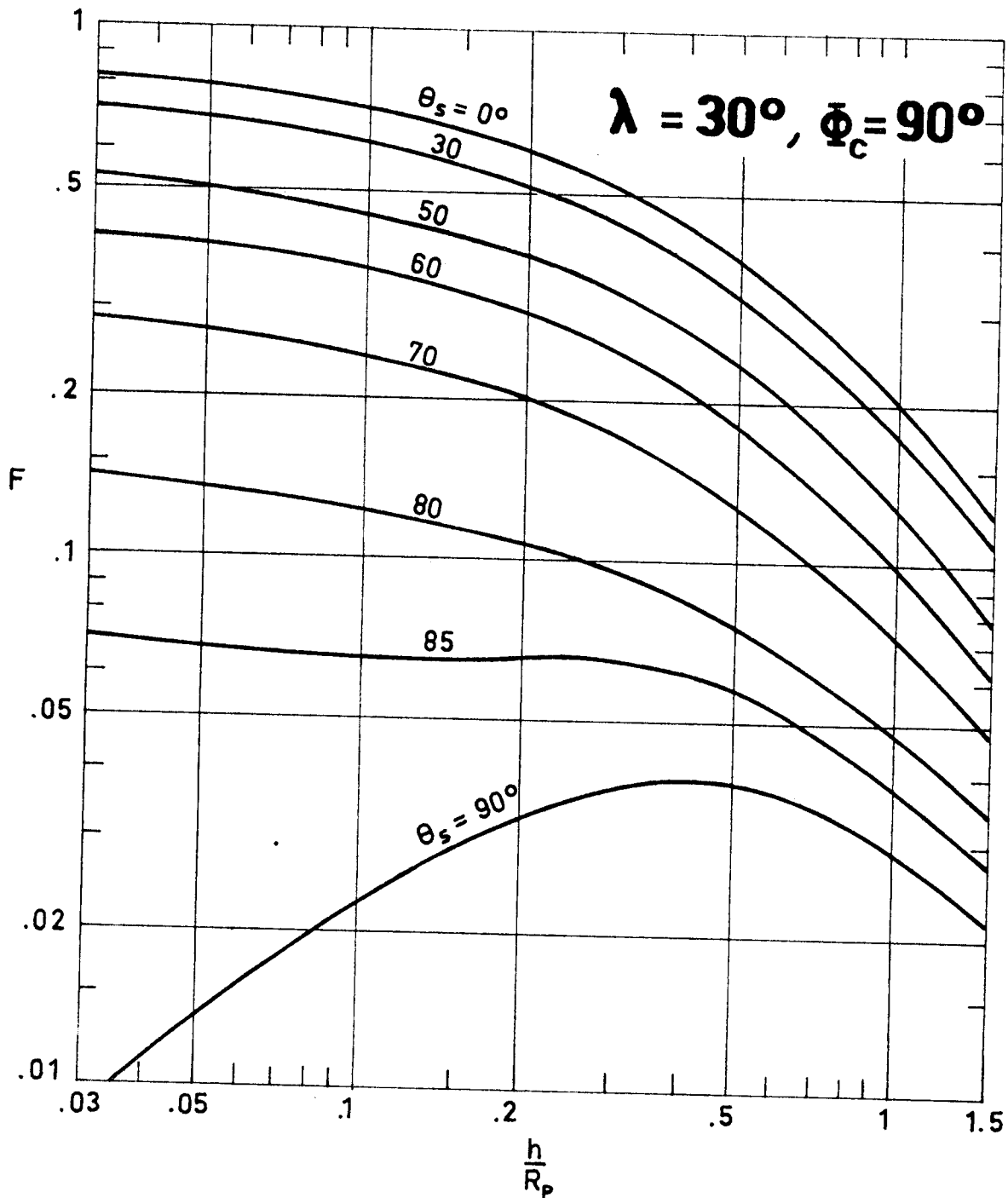


Fig 3-6. Albedo view factor F vs. h/R_p for different values of θ_s in the case of a flat plate ($\lambda=30^\circ$, $\phi_c=90^\circ$). From Bannister (1965).

ALBEDO RADIATION
 Infinitely Conductive Planar Surfaces

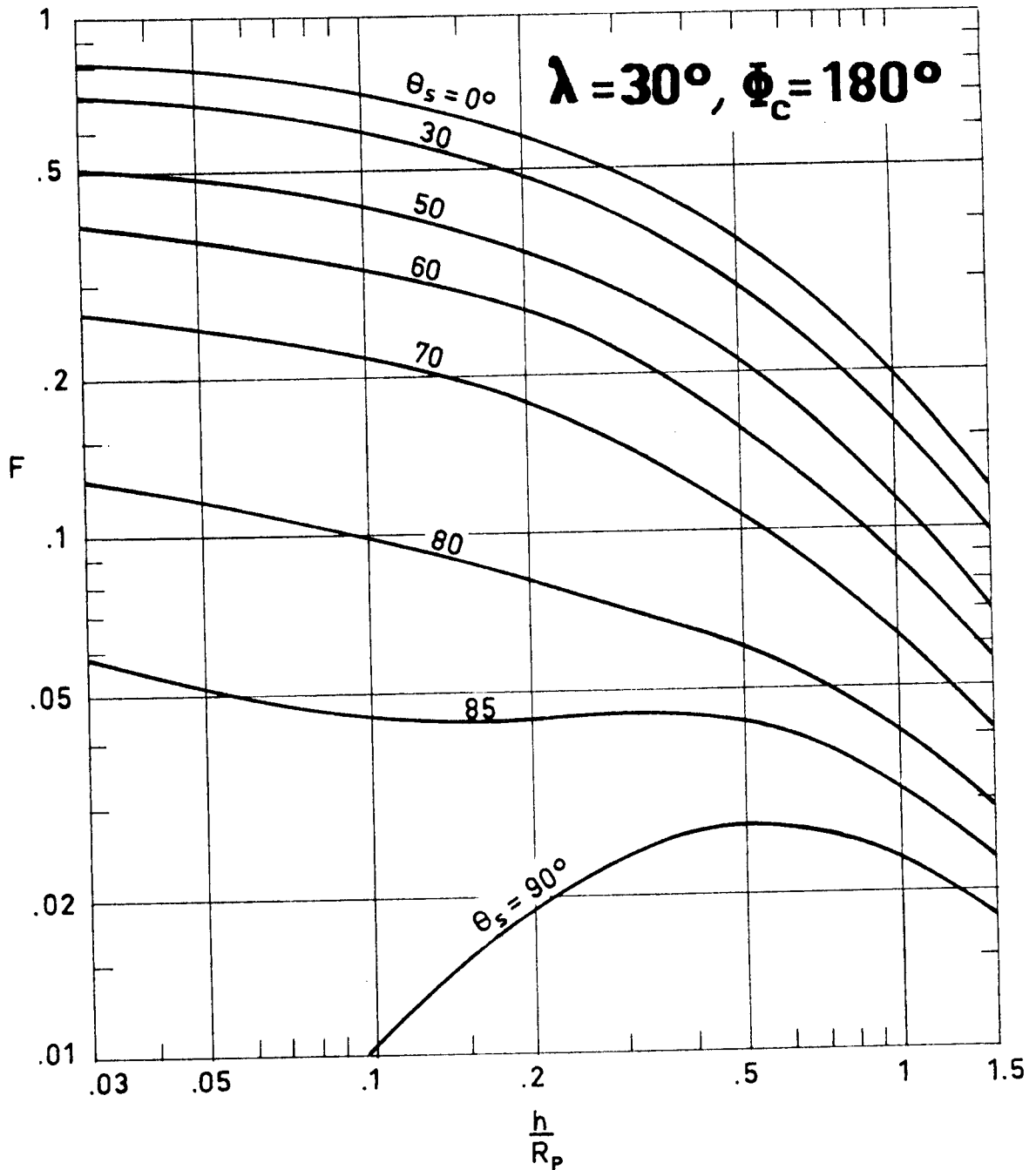


Fig 3-7. Albedo view factor F vs. h/R_p for different values of θ_s in the case of a flat plate ($\lambda=30^\circ$, $\phi_c=180^\circ$). From Bannister (1965).

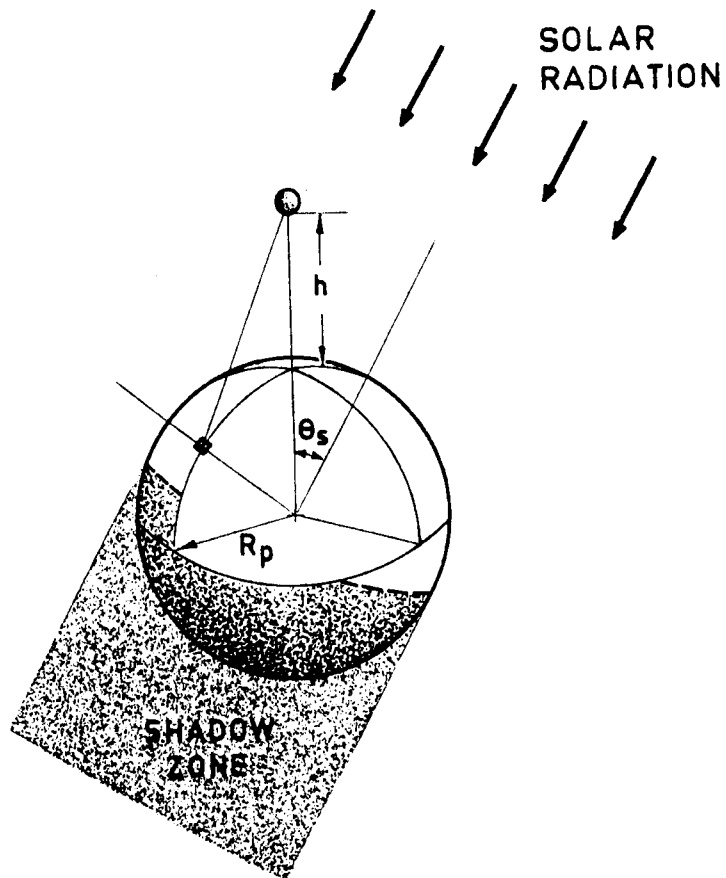
INTENTIONALLY BLANK PAGE

ALBEDO RADIATION
Infinitely Conductive Spherical Surfaces

3.3. INFINITELY CONDUCTIVE SPHERICAL SURFACES

3.3.1. SPHERE

Sketch:



Formula: All results presented in the literature are obtained numerically.

Reference: Cunningham (1961).

ALBEDO RADIATION
 Infinitely Conductive Spherical Surfaces

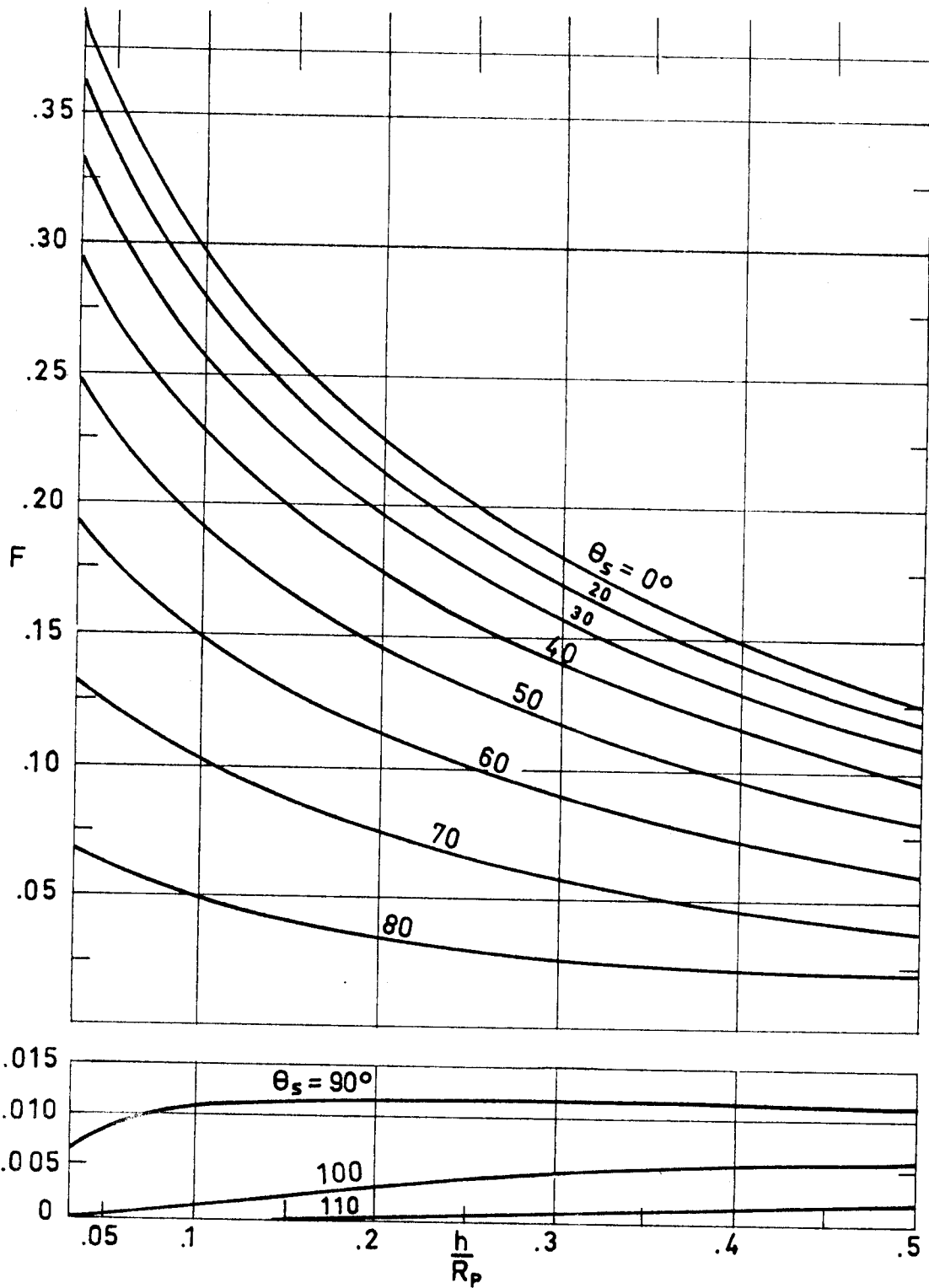


Fig 3-8. Albedo view factor F vs. h/R_p for different values of θ_s in the case of a sphere. From Cunningham (1961).

ALBEDO RADIATION
 Infinitely Conductive Spherical Surfaces

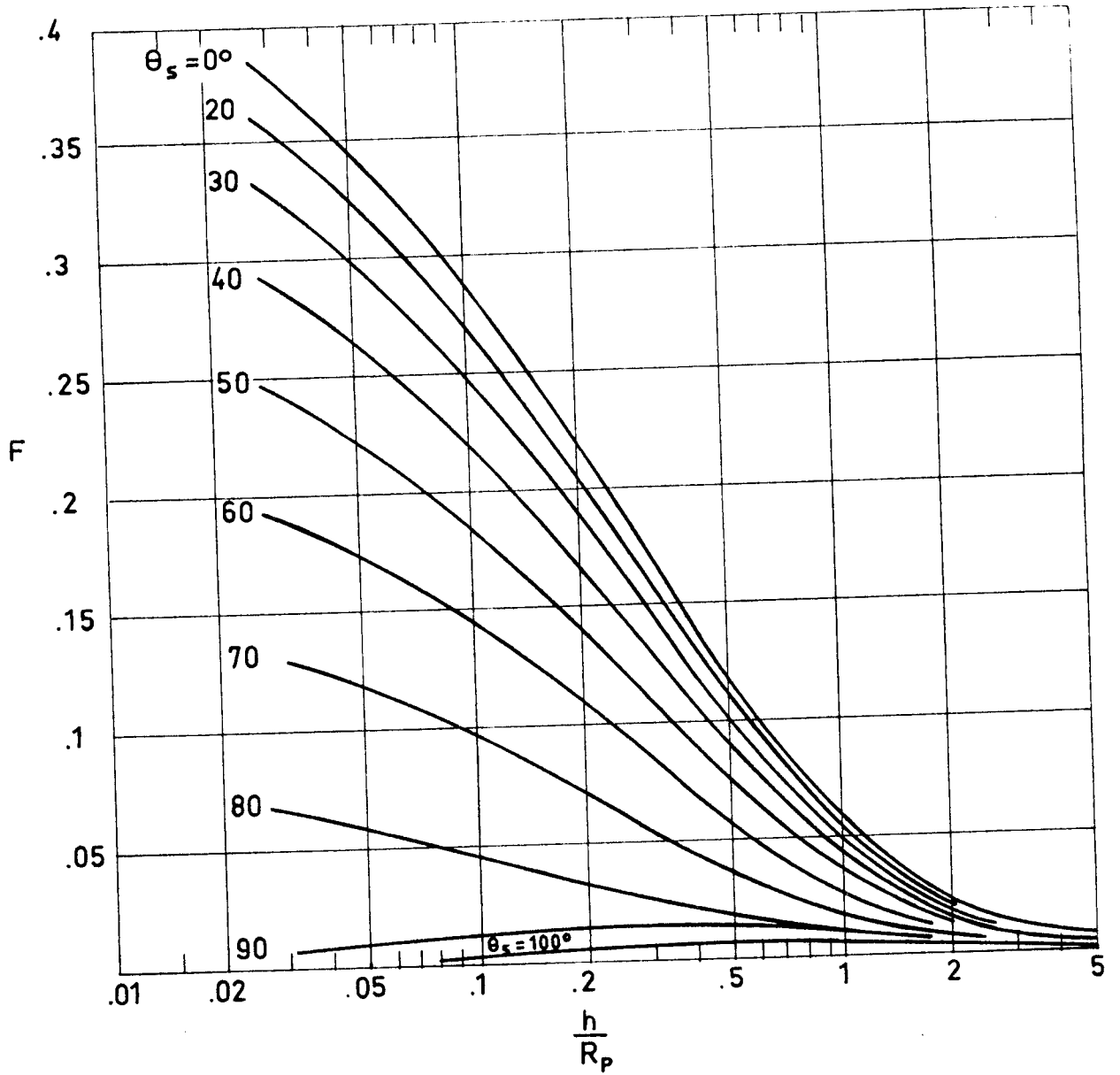


Fig 3-9. Albedo view factor F vs. h/R_p for different values of θ_s in the case of a sphere. From Cunningham (1961).

ALBEDO RADIATION
Infinitely Conductive Spherical Surfaces

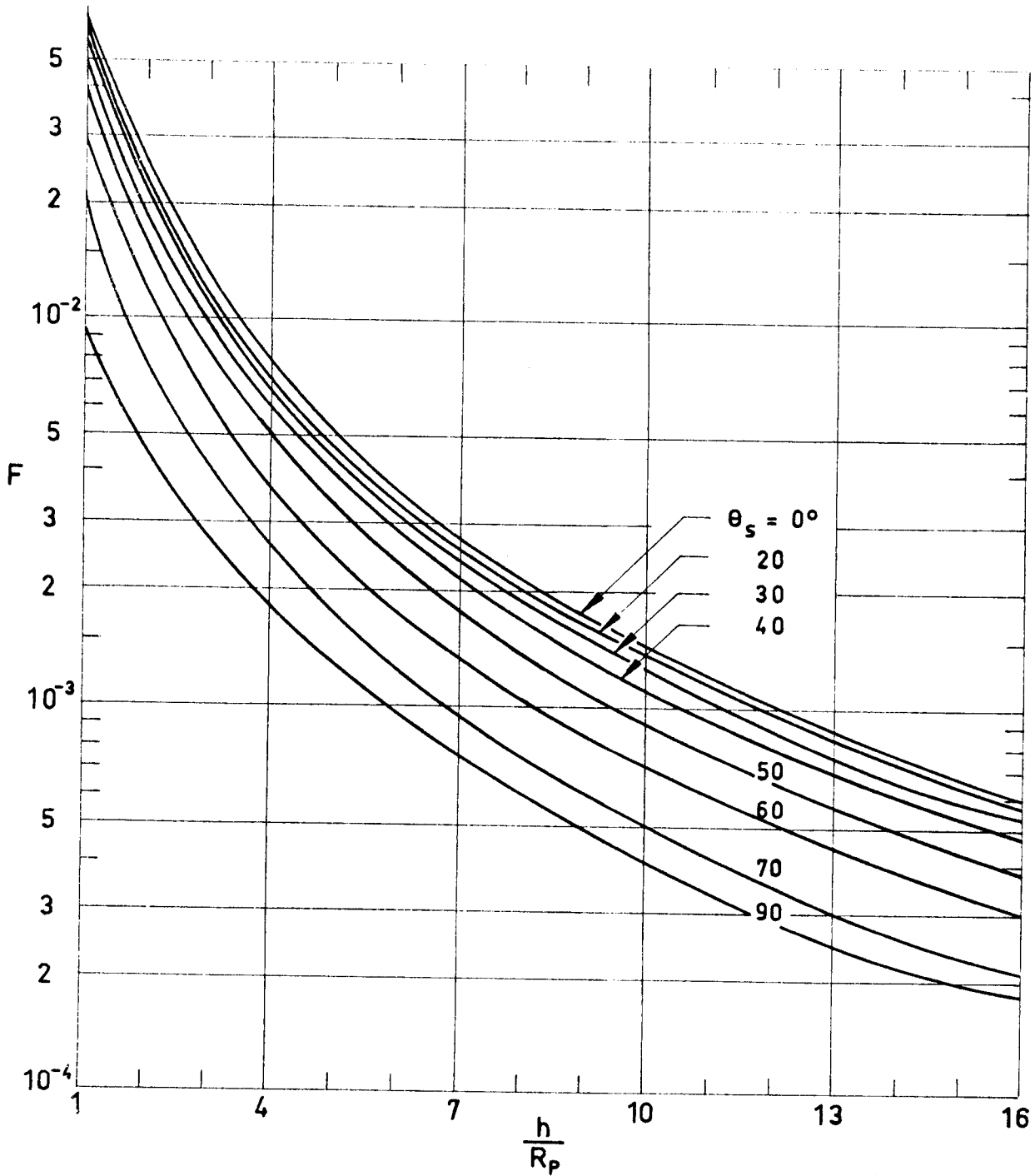


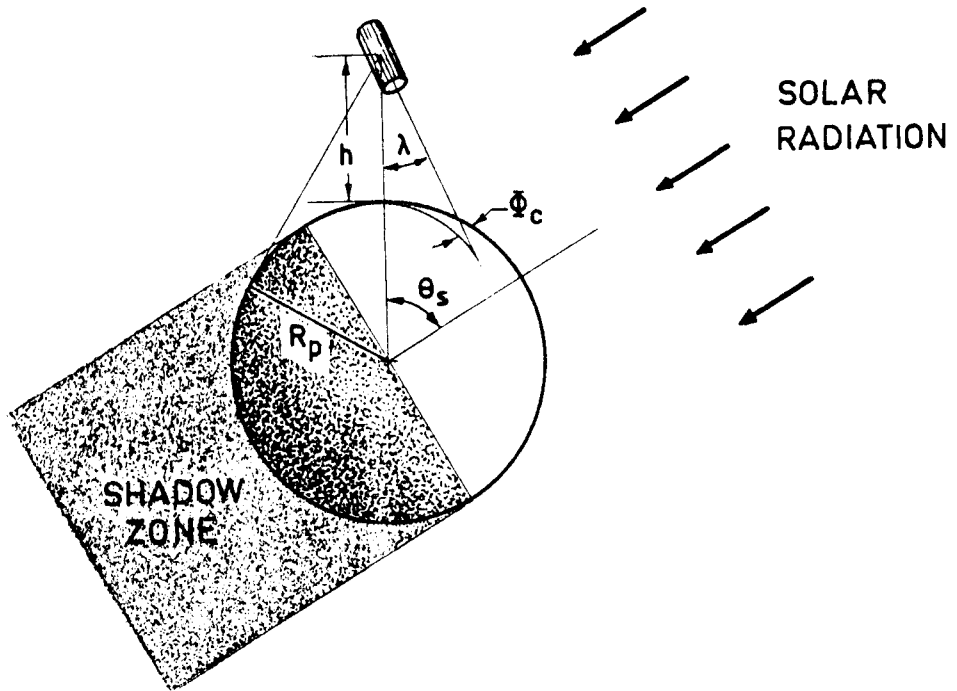
Fig 3-10. Albedo view factor F vs. h/R_p for different values of θ_s in the case of a sphere. Calculated by the compiler.

ALBEDO RADIATION
Infinitely Conductive Cylindrical Surfaces

3.4. INFINITELY CONDUCTIVE CYLINDRICAL SURFACES

3.4.1. CIRCULAR CYLINDER WITH INSULATED BASES

Sketch:



Formula: All results presented in the literature are obtained numerically.

Reference: Bannister (1965).

ALBEDO RADIATION
Infinitely Conductive Cylindrical Surfaces

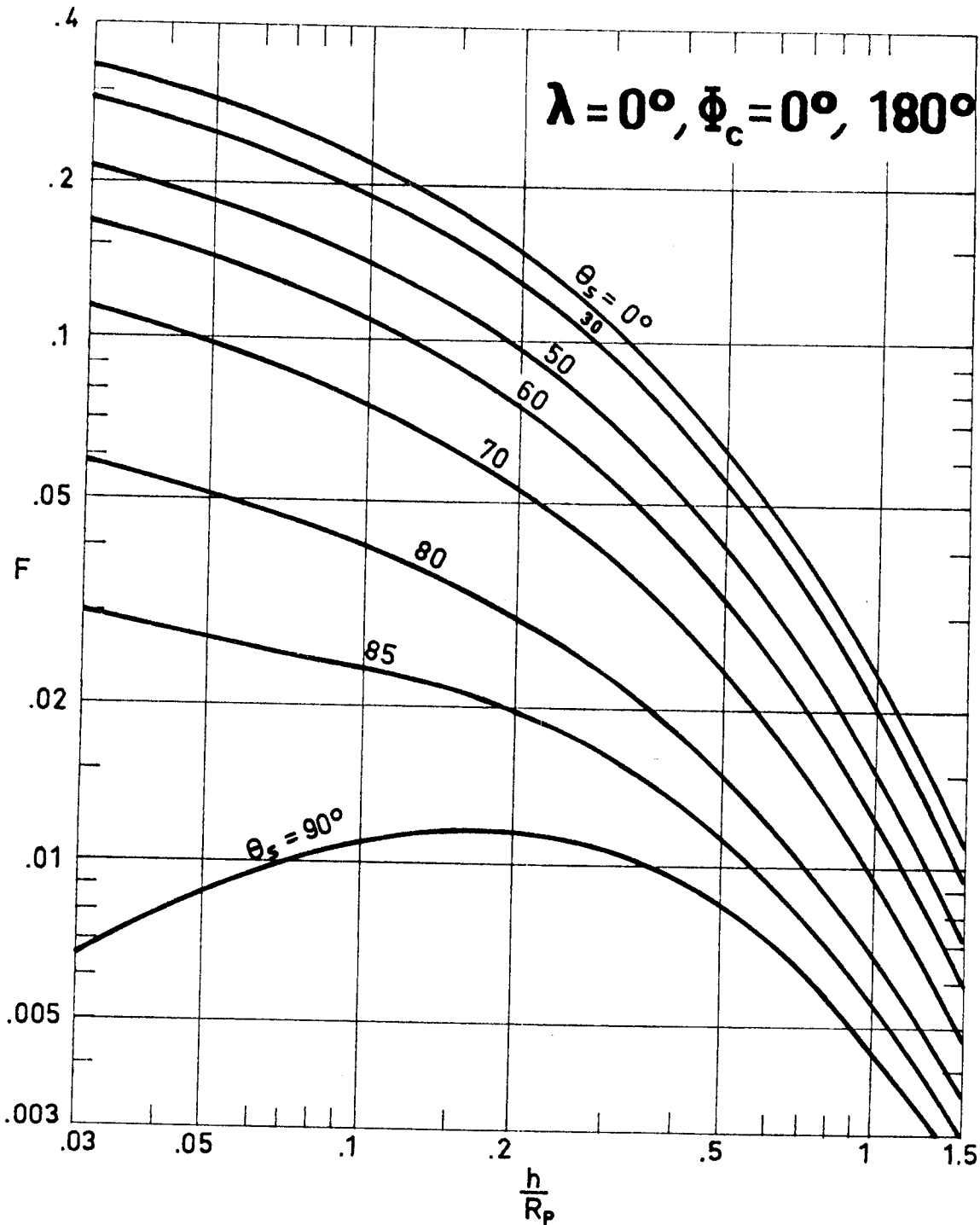


Fig 3-11. Albedo view factor F vs. h/R_p for different values of θ_s in the case of a cylinder ($\lambda=0^\circ, \phi_c=0^\circ, 180^\circ$). From Bannister (1965).

ALBEDO RADIATION
 Infinitely Conductive Cylindrical Surfaces

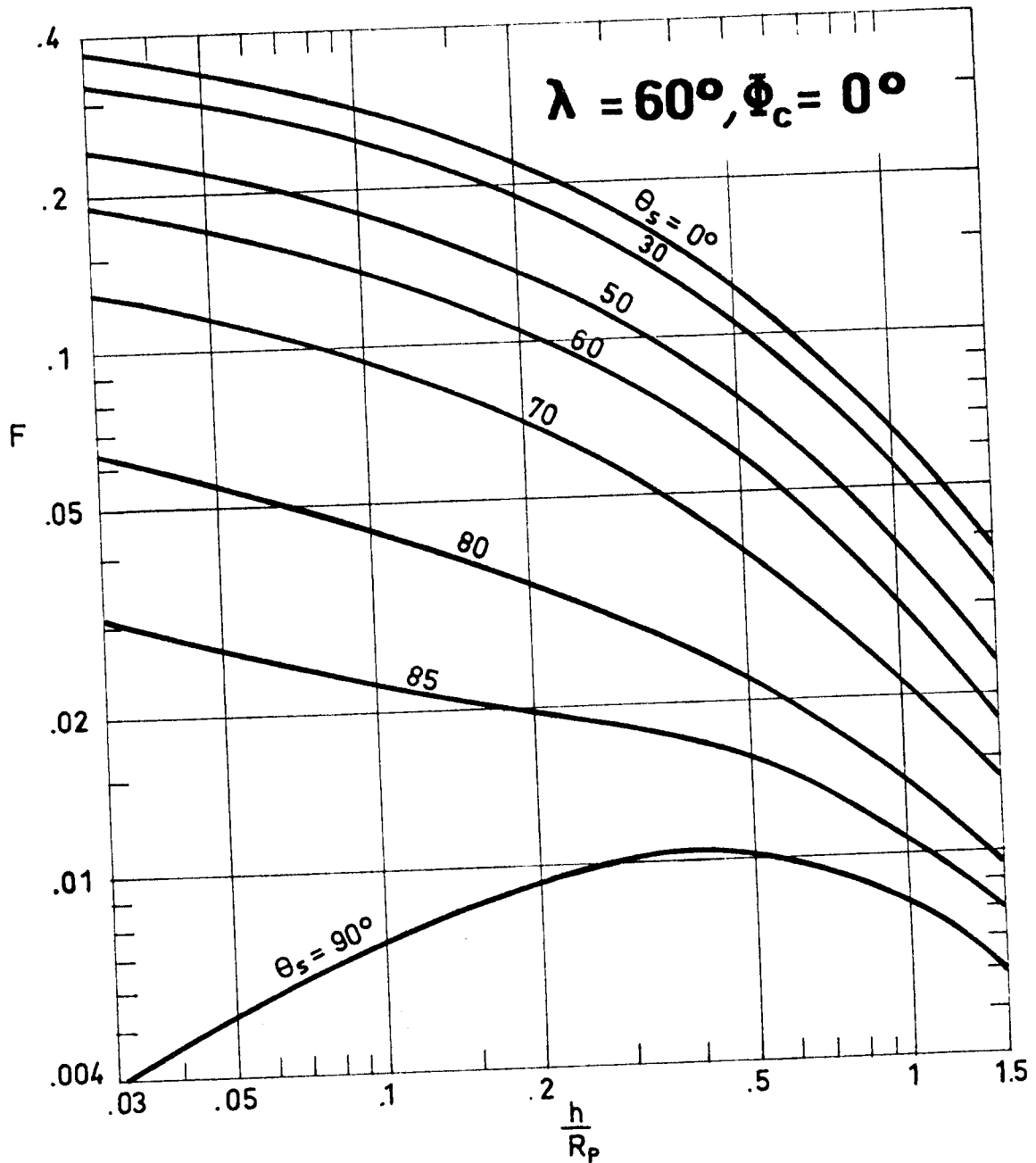


Fig 3-12. Albedo view factor F vs. h/R_p for different values of θ_s in the case of a cylinder ($\lambda=60^\circ, \phi_c=0^\circ$). From Bannister (1965).

ALBEDO RADIATION
 Infinitely Conductive Cylindrical Surfaces

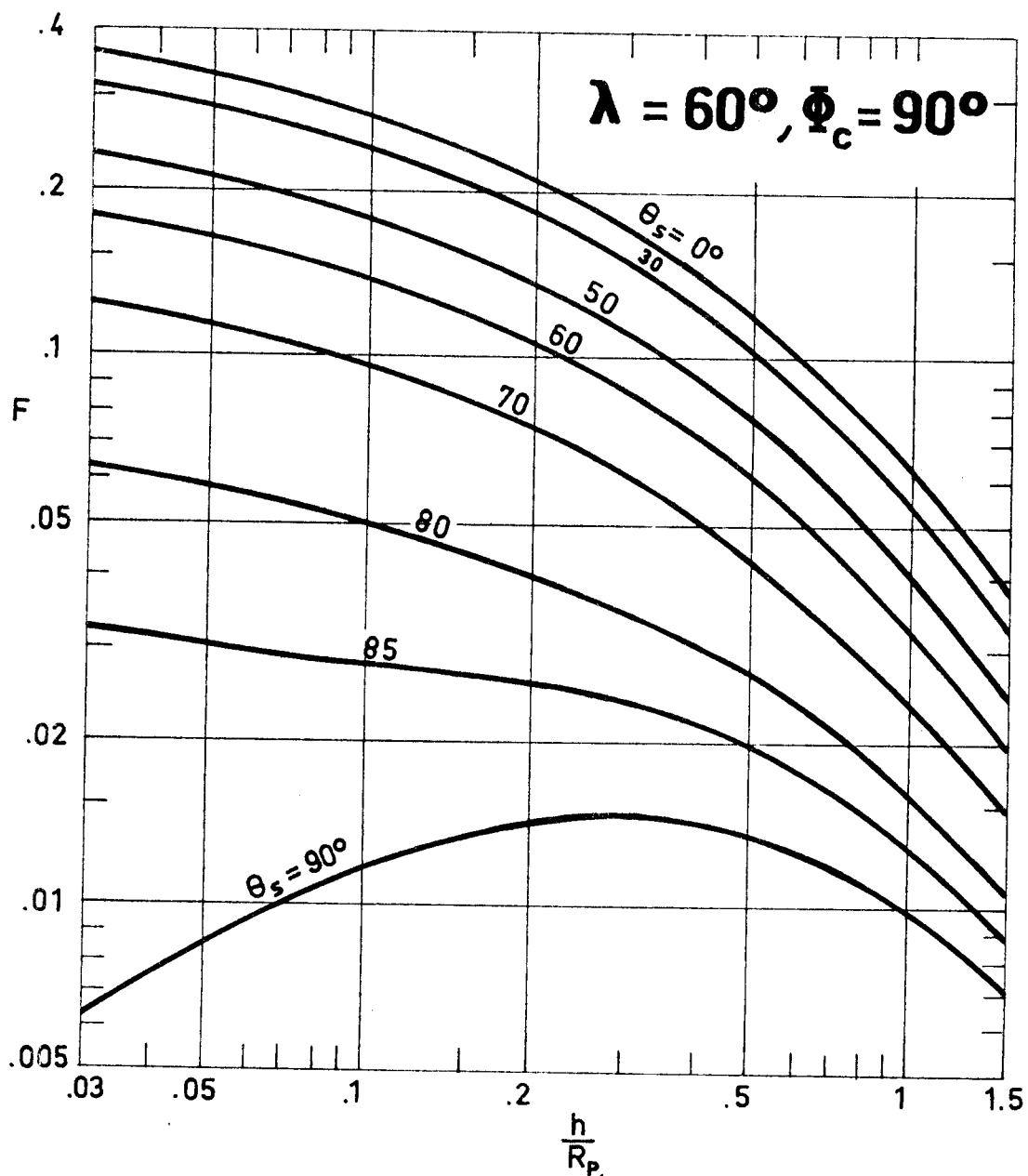


Fig 3-13. Albedo view factor F vs. h/R_p for different values of θ_s in the case of a cylinder ($\lambda=60^\circ$, $\phi_c=90^\circ$). From Bannister (1965).

ALBEDO RADIATION
 Infinitely Conductive Cylindrical Surfaces

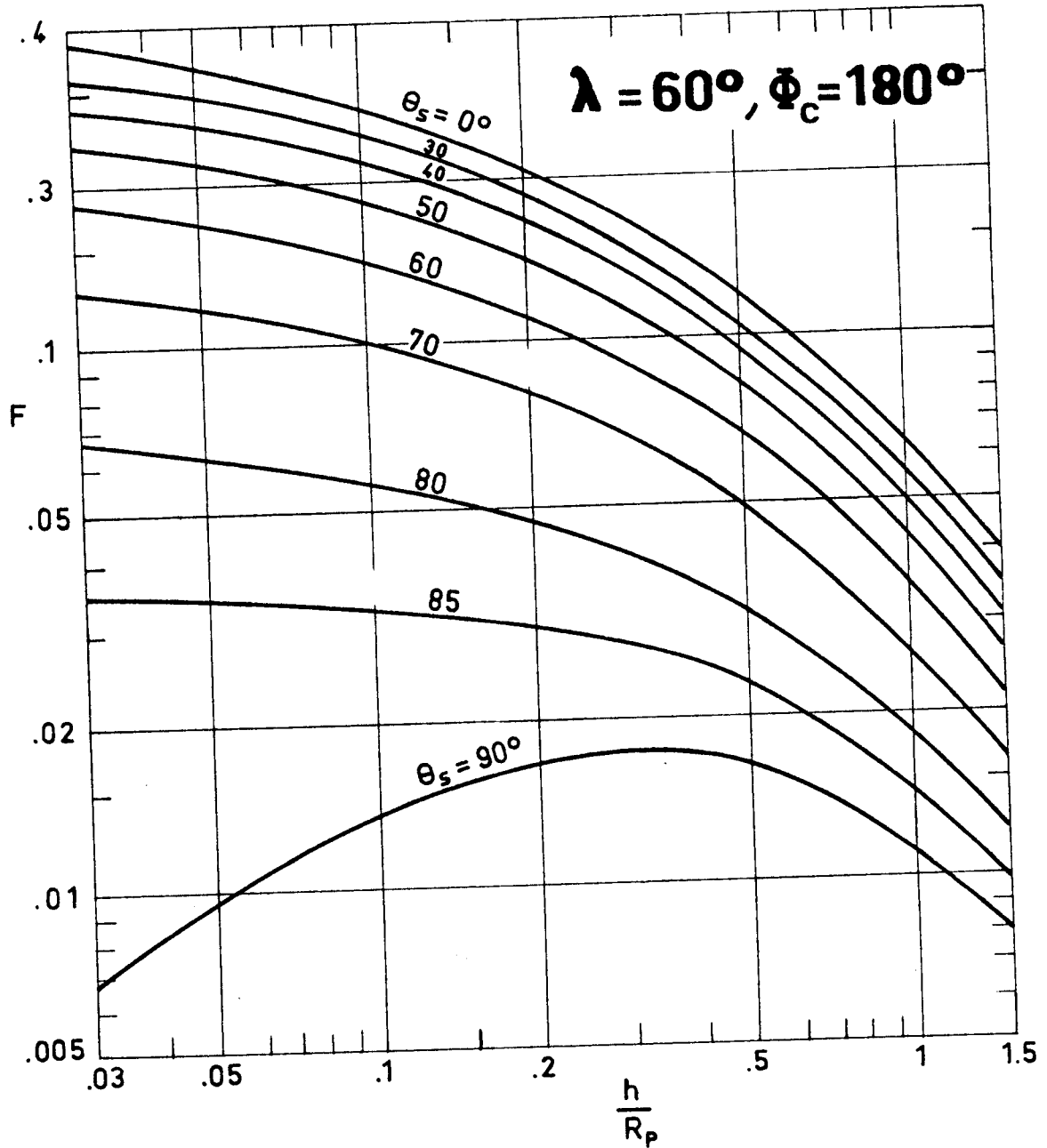


Fig 3-14. Albedo view factor F vs. h/R_p for different values of θ_s in the case of a cylinder ($\lambda=60^\circ, \phi_c=180^\circ$). From Bannister (1965).

INTENTIONALLY BLANK PAGE

SPACECRAFT SURFACE TEMPERATURE

References

- Gast, P.R. 1965 "Insolation of the Upper Atmosphere and of a Satellite",
in "Scientific Uses of Earth Satellites",
J.A. Van Allen, Ed., 2nd Edition, The
University of Michigan Press, Ann Arbor,
1965.
- Charnes, A., 1960 "Solar Heating of a Rotating Cylindrical
Raynor, S. Space Vehicle",
ARS Journal, Vol. 30, No. 5, May 1960,
pp. 479-484.
- Cunningham, F.G. 1961 "Earth Reflected Solar Radiation Input to
Spherical Satellites",
NASA TN D-1099, October 1961.
- Nichols, L.D. 1961 "Surface-Temperature Distribution on Thin-
Walled Bodies Subjected to Solar Radiation
in Interplanetary Space",
NASA TN D-584, 1961.
- Kreith, F. 1962 "Radiation Heat Transfer for Spacecraft and
Solar Power Plant Design",
International Textbook Co., Scranton, Penn-
sylvania, 1962, pp. 57-79.
- Wolverton, R. 1963 "Flight Performance Handbook for Orbital
Operations",
John Wiley & Sons, Inc., New York, 1963,
pp. B-14/B-15.
- Bannister, T.C. 1965 "Radiation Geometry Factor between the Earth
and a Satellite",
NASA TN D-2750, July 1965.

SPACECRAFT SURFACE TEMPERATURE

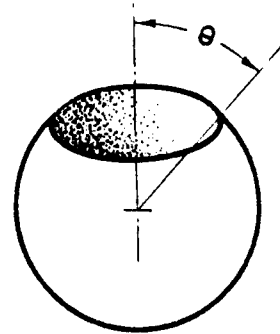
References

- Camack, W.G. 1965 "Albedo and Earth Radiation",
in "Space Materials Handbook",
C.G. Goetzl, J.B. Rittenhouse & J.B.
Singletary, Eds., Addison-Wesley Publish-
ing Co. Inc., Mass., 1965, pp. 31-49
- Clark, L.G.,
Anderson, E.C. 1965 "Geometric Shape Factors for Planetary-
-Thermal and Planetary-Reflected Radiation
Incident upon Spinning and Non-Spinning
Spacecraft",
NASA TN D-2835, May 1965.
- Johnson, F.S. 1965 "Solar Radiation",
in "Satellite Environment Handbook",
F.S. Johnson, Ed., 2nd Edition, Stanford
University Press, Stanford, California,
1966, pp. 95-105.
- Watts, R.G. 1965 "Radiant Heat Transfer to Earth Satellites",
Journal of Heat Transfer, Vol. 87c, No. 3,
August 1965, pp. 369-373.
- Fontana, A. 1967 "The Effect of Planetary Albedo on Solar
Orientation of Spacecraft",
NASA TN D-4133, September 1967.
- Anderson, A.D. 1969 "Nonpenetrating Radiations",
in "Space Materials Handbook",
J.B. Rittenhouse & J.B. Singletary, Eds.,
3rd Edition, NASA SP-3051, 1969, pp.25-35.

GRAY DIFFUSE SURFACES
Diffuse Incident Radiation

1.2.6. SPHERICAL CAVITY

Inner surface of a sphere emitting and absorbing radiation through the circle forming the cavity opening.



Formulae:

$$\alpha_a = \frac{2\alpha}{2 - (1-\alpha)(1+\cos\theta)} \quad (1)$$

$$\epsilon_a = \frac{2\epsilon}{2 - (1-\alpha)(1+\cos\theta)} \quad (2)$$

Comments:

Formula (1) is valid for any spatial and directional distribution of the incoming radiation.

When $\epsilon \approx \alpha$ (gray body), Fig 1-7 overleaf may be used in order to estimate ϵ_a . If $\epsilon \neq \alpha$, then Fig 1-7 can still be used although the ordinate values must be multiplied by ϵ/α .

References: Sparrow & Jonsson (1962a, 1962b), Sparrow (1965).

GRAY DIFFUSE SURFACES
Diffuse Incident Radiation

θ°	10	20	30	40	50	60
α A_h/A_c	.00760	.03015	.06699	.11698	.17861	.25000
.1	.93601	.78655	.62388	.48714	.38352	.30769
.2	.97051	.89237	.78868	.68124	.58329	.50000
.3	.98258	.93427	.86483	.78558	.70584	.63158
.4	.98873	.95673	.90869	.85073	.78870	.72727
.5	.99246	.97073	.93722	.89527	.84846	.80000
.6	.99496	.98029	.95725	.92766	.89360	.85714
.7	.99676	.98724	.97209	.95226	.92890	.90323
.8	.99810	.99252	.98353	.97159	.95726	.94118
.9	.99916	.99666	.99261	.98717	.98054	.97297
θ°	70	90	110	130	150	170
α A_h/A_c	.32899	.50000	.67101	.82139	.93301	.99240
.1	.25247	.18182	.14206	.11915	.10642	.10069
.2	.43179	.33333	.27144	.23334	.21132	.20122
.3	.56573	.46154	.38976	.34287	.31476	.30160
.4	.66957	.57143	.49838	.44801	.41675	.40183
.5	.75245	.66667	.59844	.54903	.51733	.50191
.6	.82012	.75000	.69092	.64616	.61652	.60183
.7	.87643	.82353	.77665	.73963	.71436	.70160
.8	.92400	.88889	.85635	.82964	.81086	.80122
.9	.96473	.94737	.93062	.91637	.90607	.90068

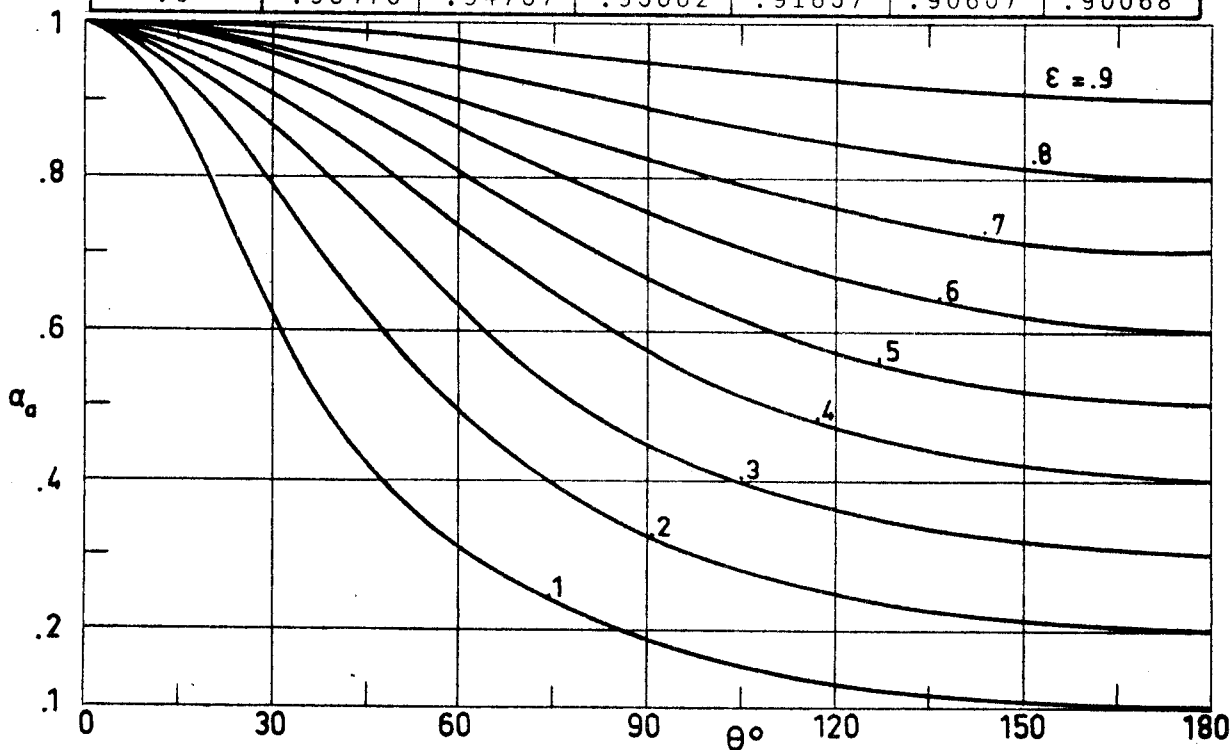


Fig 1-7. Apparent absorptance, α_a , of a spherical cavity vs. opening semiangle, θ , for different values of the surface absorptance, α . Calculated by the compiler.

HOLES, GROOVES, AND CAVITIES

References

- Hottel, H.C., 1933 "Effect of Reradiation on Heat Transmission
Keller, J.D. in Furnaces and through Openings",
Transactions of the American Society of Mechanical Engineers, Vol. IS-55-6, 1933, pp. 39-49.
- Vollmer, J. 1957 "Study of the Effective Thermal Emittance of
Cylindrical Cavities",
Journal of the Optical Society of America, Vol. 47, No. 10, Oct. 1957, pp. 926-932.
- Parkes, E.W. 1960 "Influence Coefficients for Radiation in a
Circular Cylinder",
International Journal of Heat and Mass Transfer, Vol. 2, Sep. 1960, pp. 155-162.
- Sparrow, E.M., 1960 "Apparent Emissivity and Heat Transfer in a
Albers, L.U. Long Cylindrical Hole",
Journal of Heat Transfer, Vol. C82, Aug. 1960, pp. 253-255.
- Usiskin, C.M., 1960 "Thermal Radiation from a Cylindrical Enclo-
Siegel, R. sure with Specified Wall Heat Flux",
Journal of Heat Transfer, Vol. C82, No. 4, Nov. 1960, pp. 369-374.
- Eckert, E.R.G., 1961 "Radiative Heat Exchange between Surfaces
Sparrow, E.M. with Specular Reflection",
International Journal of Heat and Mass Transfer, Vol. 3, 1961, pp. 42-54.
- Stephens, C.W., 1961 "Internal Design Consideration for Cavity-
Haire, A.M. Type Solar Absorbers",
ARS Journal, July 1961, pp. 896-901.

HOLES, GROOVES, AND CAVITIES

References

- Heaslet, M.A., 1962 "Radiative Heat-Transfer Calculations for
Lomax, H. Infinite Shells with Circular-Arc Sections,
Including Effects of an External Source
Field",
International Journal of Heat and Mass
Transfer, Vol. 5, 1962, pp. 457-468.
- Sparrow, E.M. 1962 "Radiant Absorption Characteristics of Concave
Cylindrical Surfaces",
Journal of Heat Transfer, Vol. C84, No. 4,
Nov. 1962, pp. 283-293.
- Sparrow, E.M., 1962 "Thermal Radiation Characteristics of Cylin-
Albers, L.U., drical Enclosures",
Eckert, E.R.G. Journal of Heat Transfer, Vol. C84, No. 1,
Feb. 1962, pp. 73-81.
- Sparrow, E.M., 1962 "An Enclosure Theory for Radiative Exchange
Eckert, E.R.G., between Specularly and Diffusely Reflecting
Jonsson, V.K. Surfaces",
Journal of Heat Transfer, Vol. C84, No. 4,
Nov. 1962, pp. 294-300.
- Sparrow, E.M., 1962 "Radiant Emission from a Parallel-Walled
Gregg, J.L. Groove",
Journal of Heat Transfer, Vol. C84, No. 3,
Aug. 1962, pp. 270-271.
- Sparrow, E.M., 1962a "Absorption and Emission Characteristics of
Jonsson, V.K. Diffuse Spherical Enclosures",
Journal of Heat Transfer, Vol. C84, No. 2,
May 1962, pp. 188-189.

HOLES, GROOVES, AND CAVITIES

References

- Sparrow, E.M.,
Jonsson, V.K. 1962b "Absorption and Emission Characteristics of Diffuse Spherical Enclosures", NASA TN D-1289, 1962.
- Sparrow, E.M.,
Lin, S.H. 1962 "Absorption of Thermal Radiation in a V-Groove Cavity", International Journal of Heat and Mass Transfer, Vol. 5, 1962, pp. 1111-1115.
- Howell, J.R.,
Perlmutter, M. 1963 "Directional Behavior of Emitted and Reflected Radiant Energy from a Specular, Gray, Asymmetric Groove", NASA TN D-1874, Aug. 1963.
- Jones, W.P. 1963 "Radiative Heat Transfer between Planar Surfaces with Filleted Junctions", NASA TR R-157, 1963.
- Perlmutter, M.,
Howell, J.R. 1963 "A Strongly Directional Emitting and Absorbing Surface", Journal of Heat Transfer, Vol. C85, Aug. 1963, pp. 282-283.
- Perlmutter, M.,
Siegel, R. 1963 "Effect of a Specularly Reflecting Gray Surface on Thermal Radiation through a Tube and from Its Heated Wall", Journal of Heat Transfer, Vol. C85, No. 1, Feb. 1963, pp. 55-62.
- Sparrow, E.M.,
Jonsson, V.K. 1963a "Thermal Radiation Absorption in Rectangular-Groove Cavities", Journal of Applied Mechanics, Vol. E30, No. 2, June 1963, pp. 237-244.

HOLES, GROOVES, AND CAVITIES

References

- Sparrow, E.M.,
Jonsson, V.K. 1963b "Radiant Emission Characteristics of Diffuse
Conical Cavities",
Journal of the Optical Society of America,
Vol. 53, No. 7, July 1963, pp. 816-821.
- Lin, S.H.,
Sparrow, E.M. 1965 "Radiant Interchange among Curved Specularly
Reflecting Surfaces - Application to Cylindrical and Conical Cavities",
Journal of Heat Transfer, Vol. C87, No. 2,
May 1965, pp. 295-307.
- Sparrow, E.M. 1965 "Radiation Heat Transfer between Surfaces",
in "Advances in Heat Transfer", Vol. 2, J.P.
Hartnett and T.F. Irvine, Jr., Eds., Academic
Press, New York, 1965, pp. 399-452.
- Sparrow, E.M.,
Lin, S.H. 1965 "Radiation Heat Transfer at a Surface Having
both Specular and Diffuse Reflectance Components",
International Journal of Heat and Mass
Transfer, Vol. 8, No. 5, May 1965, pp. 769-
779.
- Parmer, J.F.,
Wiebelt, J.A. 1966 "Thermal Radiation Characteristics of a
Specular Walled Groove",
Journal of Spacecraft and Rockets, Vol. 3,
No. 11, Nov. 1966, pp. 1678-1680.
- Sarofim, A.F.,
Hottel, H.C. 1966 "Radiative Exchange among Non-Lambert Sur-
faces",
Journal of Heat Transfer, Vol. C88, No. 1,
Feb. 1966, pp. 37-44.

HOLES, GROOVES, AND CAVITIES

References

- Black, W.Z., 1968 "A Study of Directional Radiation Properties
Schoenhals, R.J. of Specially Prepared V-Groove Cavities",
Journal of Heat Transfer, Vol. C90, No. 4,
Nov. 1968, pp. 420-428.
- Sparrow, E.M., 1971 "Efficiencies of Honeycomb Absorbers of Solar
Bifano, W.J., Radiation",
Healy, J.A. NASA TN D-6337, May 1971.
- Siegel, R., 1972 "Thermal Radiation Heat Transfer",
Howell, J.R. McGraw-Hill Book Co., New York, 1972, pp.
235-373.
- Black, W.Z. 1973 "Optimization of the Directional Emission
from V-Groove Rectangular Cavities",
Journal of Heat Transfer, Vol. C95, Feb.
1973, pp. 31-36.
- Siegel, R. 1973 "Net Radiation Method for Enclosure Systems
Involving Partially Transparent Walls",
NASA TN D-7384, Aug. 1973.

INTENTIONALLY BLANK PAGE

CONDUCTIVE HEAT TRANSFER

- 1 CONDUCTIVE SHAPE FACTORS
- 2 THERMAL JOINT CONDUCTANCE

CONDUCTIVE HEAT TRANSFER

Table of Contents

	Page
TABLE OF CONTENTS	0-1
LIST OF SYMBOLS	0-3
1. CONDUCTIVE SHAPE FACTORS	1-1
1.1. General	1-1
1.2. Planar-Planar Surfaces	1-3
1.2.1. Two-Dimensional Configurations	1-3
1.2.1.1. Strips of Equal Width	1-3
1.2.1.2. Strips of Unequal Width	1-5
1.3. Planar Surface - Cylindrical Surface	1-7
1.3.1. Two-Dimensional Configurations	1-7
1.3.1.1. Plane and Cylinder of Rectangular Cross Section	1-7
1.3.1.2. Plane and Circular Cylinder	1-9
1.3.2. Axisymmetrical Configurations	1-11
1.3.2.1. Plane and Circular Cylinder	1-11
1.4. Planar Surface - Spherical Surface	1-13
1.4.1. Plane and Sphere	1-13
1.5. Cylindrical-Cylindrical Surfaces	1-15
1.5.1. Two-Dimensional Configurations	1-15
1.5.1.1. Circular Cylinders	1-15
1.5.1.2. Circular Rods with Holes	1-17
1.5.1.3. Rectangular Bars with Holes	1-23
1.5.1.4. Polygonal Bars with Holes	1-29
1.6. Spherical-Spherical Surfaces	1-31
1.6.1. Two Concentric Spheres	1-31
2. THERMAL JOINT CONDUCTANCE	2-1
2.1. General	2-1
2.2. Empirical Correlations	2-3
2.2.1. Fletcher & Gyroog Correlation	2-3
2.2.2. Thomas & Probert Correlation	2-5
2.3. Bare Metallic Joints	2-7
2.4. Metallic Foils between Similar Metals	2-19
2.5. Metallic Oxide Powders between Similar Metals	2-21
2.6. Porous Metallic Materials between Similar Metals ...	2-23
2.7. Insulating Spacers between Similar Metals	2-29
2.8. Thermal Greases between Similar Metals	2-45
2.9. Elastomeric Materials between Similar Metals	2-47

CONDUCTIVE HEAT TRANSFER

Table of Contents

	Page
2.10. Outgassing Data	2-49
REFERENCES	3-1

CONDUCTIVE HEAT TRANSFER

List of Symbols

LIST OF SYMBOLS

- A , Cross-Sectional Area Normal to Temperature Gradient. $[m^2]$.
- E , Modulus of Elasticity. $[Pa]$.
- L , Length Normal to the Plane of the Figure in Two-Dimensional Configurations. $[m]$.
- M , Surface Hardness. $[Pa]$.
- P , Applied Compressive Load. Also called Contact Pressure. $[Pa]$.
- Q , Heat Transfer Rate. $[W]$.
- S , Langmuir Conductive Shape Factor. $[m]$.
- T , Temperature. $[K]$.
- T_m , Arithmetic Mean Temperature. $[K]$.
- b , Chap. 2: Radius of the Specimen. $[m]$.
- d , Surface Parameter in Fletcher & Gyrog Correlation. $[m]$.
- h_c , Thermal Joint Conductance. $[W.m^{-2}.K^{-1}]$.
- h_f , Interstitial Contribution to Thermal Joint Conductance. $[W.m^{-2}.K^{-1}]$.
- h_r , Radiative Contribution to Thermal Joint Conductance. $[W.m^{-2}.K^{-1}]$.
- h_s , Solid Contribution to Thermal Joint Conductance. $[W.m^{-2}.K^{-1}]$.
- k , Thermal Conductivity. $[W.m^{-1}.K^{-1}]$.
- km , Mean Thermal Conductivity. $[W.m^{-1}.K^{-1}]$. $km = 2k_1k_2/(k_1+k_2)$.
- l , Heat Path Length. $[m]$.
- p , Ambient Pressure. $[Pa]$.
- r , Filter Rating. $[m]$.

CONDUCTIVE HEAT TRANSFER

List of Symbols

- t , Thickness. [m].
- ΔT , Interfacial Temperature Drop. [K].
- ϕ , Porosity.
- β , Coefficient of Linear Thermal Expansion. [K^{-1}].
- δ_o , Gap Thickness Parameter in Fletcher & Gyroog Correlation.
[m].
- ρ , Density. [$kg \cdot m^{-3}$].
- σ , rms Surface Roughness. [m].

Acronyms

- FD , Flatness Deviation. [m].
- RD , Roughness Deviation. [m].
- TWL , Total Weight Loss, Percent.
- VCM , Volatile Condensable Materials, Percent by Weight.

Other symbols, mainly used to define the geometry of the configuration, are introduced when required.

CONDUCTIVE SHAPE FACTORS

General

1. CONDUCTIVE SHAPE FACTORS1.1. GENERAL

The conductive heat transfer rate through fairly complicated two-or three-dimensional configurations can be estimated on the basis of the so-called conductive shape factor, S.

In order to introduce the concept of conductive shape factor it is customary to start with the expression giving the one-dimensional conductive heat transfer rate, Q, between two parallel planar surfaces, 1 and 2, of cross-sectional area A. Assuming that the thermal conductance, k, of the space between the planes is constant, Fourier's law yields the following equation:

$$Q = k \frac{A}{l} (T_2 - T_1) = kS (T_2 - T_1) ,$$

l being the distance between the planes.

The factor S, known as Langmuir conductive shape factor, is, in this case, the ratio of the cross-sectional area, A, to the heat path length, l.

When two-or three-dimensional configurations are involved, the temperature field can be calculated by use of one of the methods available to solve Laplace differential equations. In many instances, however, only the overall heat transfer rate between arbitrary surfaces, 1 and 2, is required, and the above expression giving Q can be used, provided that S represents the ratio of the average cross-sectional area to the average heat path length. Although the mathematical problem must be solved in full, in order to calculate S, the

CONDUCTIVE SHAPE FACTORS

General

resulting values of S can be displayed in a very compact and useful way, as it is shown in this Chapter.

It should be mentioned that for two-dimensional configurations, that is to say, configurations which do not depend on the coordinate normal to the plane of the figure, the heat transfer rate is to be understood as that corresponding to the unit length normal to the mentioned plane. In order to keep unchanged the physical dimensions of S , the conductive shape factor for two-dimensional configurations is defined as S/L , which is a dimensionless magnitude.

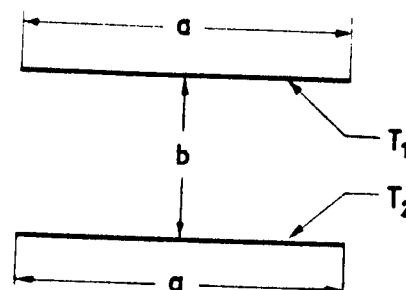
CONDUCTIVE SHAPE FACTORS
Planar-Planar Surfaces

1.2. PLANAR-PLANAR SURFACES

1.2.1. TWO-DIMENSIONAL CONFIGURATIONS

1.2.1.1. STRIPS OF EQUAL WIDTH

Two parallel strips of equal width.



Formula:

$$\frac{S}{L} = \frac{a}{b}$$

Comments:

The configuration is two-dimensional.

S/L is the conductive shape factor per unit length normal to the plane of the figure.

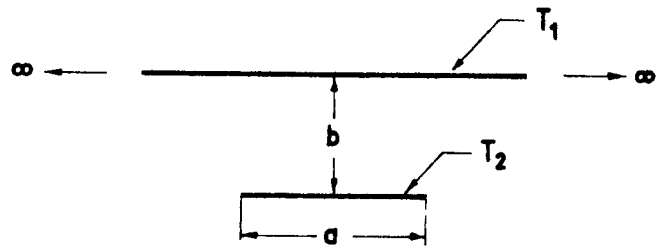
References: Andrews (1955), Sunderland & Johnson (1964).

INTENTIONALLY BLANK PAGE

CONDUCTIVE SHAPE FACTORS
Planar-Planar Surfaces

1.2.1.2. STRIPS OF UNEQUAL WIDTH

Finite width strip and
infinite parallel plane.



$$\chi = \frac{a}{b}$$

Formula:

$$\frac{S}{L} = 1.45 \left[\ln \left(1 + \frac{1}{\chi} \right) \right]^{-.59}$$

Comments:

The configuration is two-dimensional.

S/L is the conductive shape factor per unit length normal to the plane of the figure.

The results are given in Fig 1-1 overleaf.

Reference: Andrews (1955).

CONDUCTIVE SHAPE FACTORS
Planar-Planar Surfaces

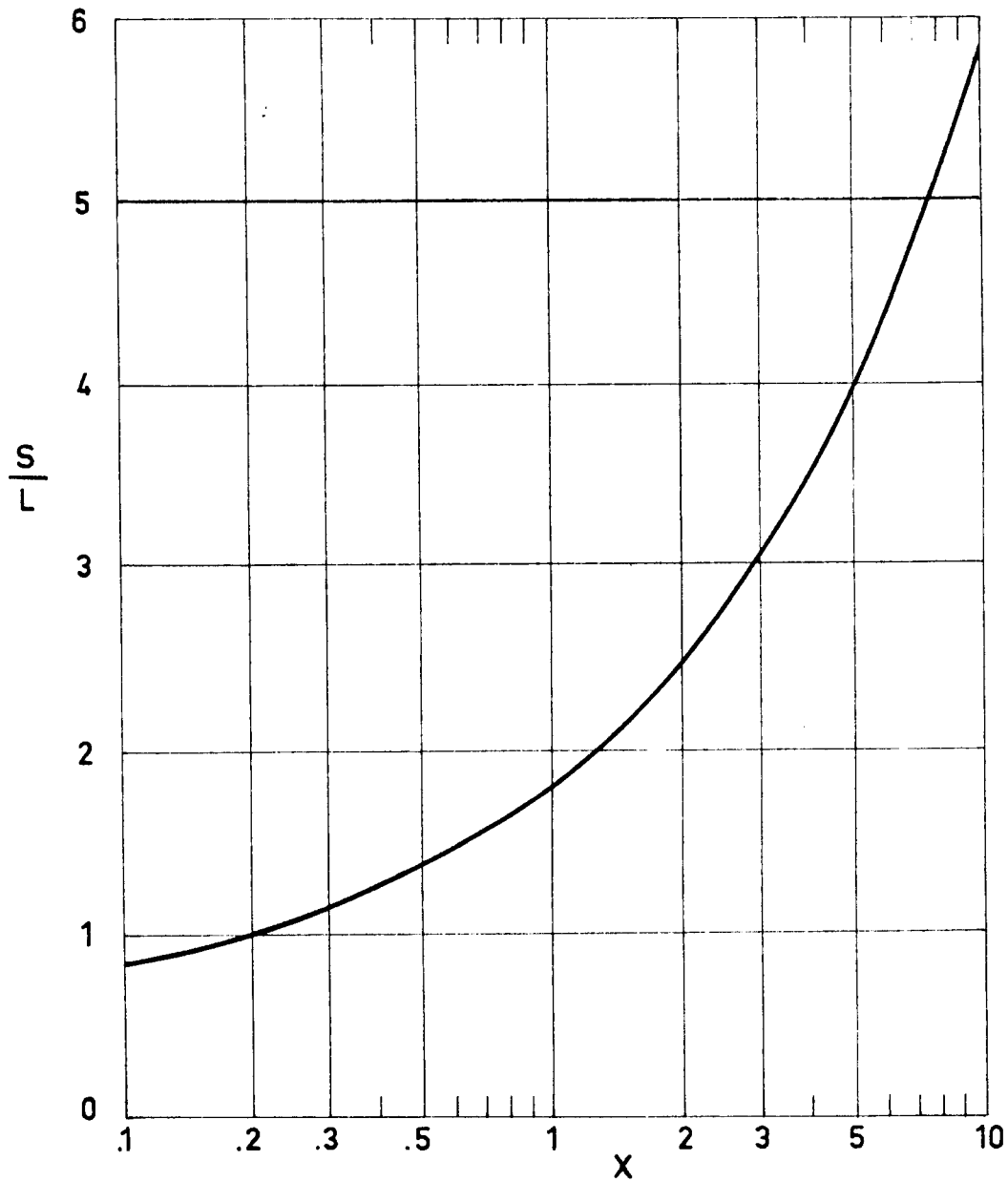


Fig 1-1. Values of the conductive shape factor per unit length, S/L , vs. the dimensionless width of the strip, X . Calculated by the compiler.

CONDUCTIVE SHAPE FACTORS
Planar Surface-Cylindrical Surface

1.3. PLANAR SURFACE-CYLINDRICAL SURFACE

1.3.1. TWO-DIMENSIONAL CONFIGURATIONS

1.3.1.1. PLANE AND CYLINDER OF
RECTANGULAR CROSS SECTION

Plane and cylinder of rectangular cross section. The plane is parallel to the base of the rectangle.

The cylinder is assumed to be infinitely conductive.

Formula:

$$\frac{S}{L} = 1.685 \left[\ln \left(1 + \frac{1}{X} \right) \right]^{-.59} \left[\frac{1}{Y} \right]^{-.078}$$

Comments:

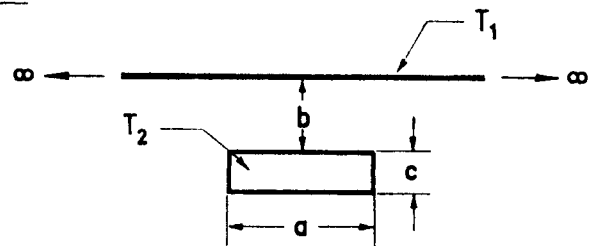
The configuration is two-dimensional.

S/L is the conductive shape factor per unit length normal to the plane of the figure.

The above expression has been obtained by means of the electric analogy, using a conducting paper of finite dimensions (Andrews (1955)). Since it is not stated in the reference how the point at infinity has been taken into account, results for small values of Y, which presumably correspond to large values of b, are doubtful. In the figure overleaf the finite strip case (see § 1.2.1.2) has been taken to bound below the recommended values.

The results are given in Fig 1-2 overleaf.

References: Andrews (1955), Sunderland & Johnson (1964).



$$X = \frac{d}{b}$$

$$Y = \frac{c}{b}$$

CONDUCTIVE SHAPE FACTORS
Planar Surface-Cylindrical Surface

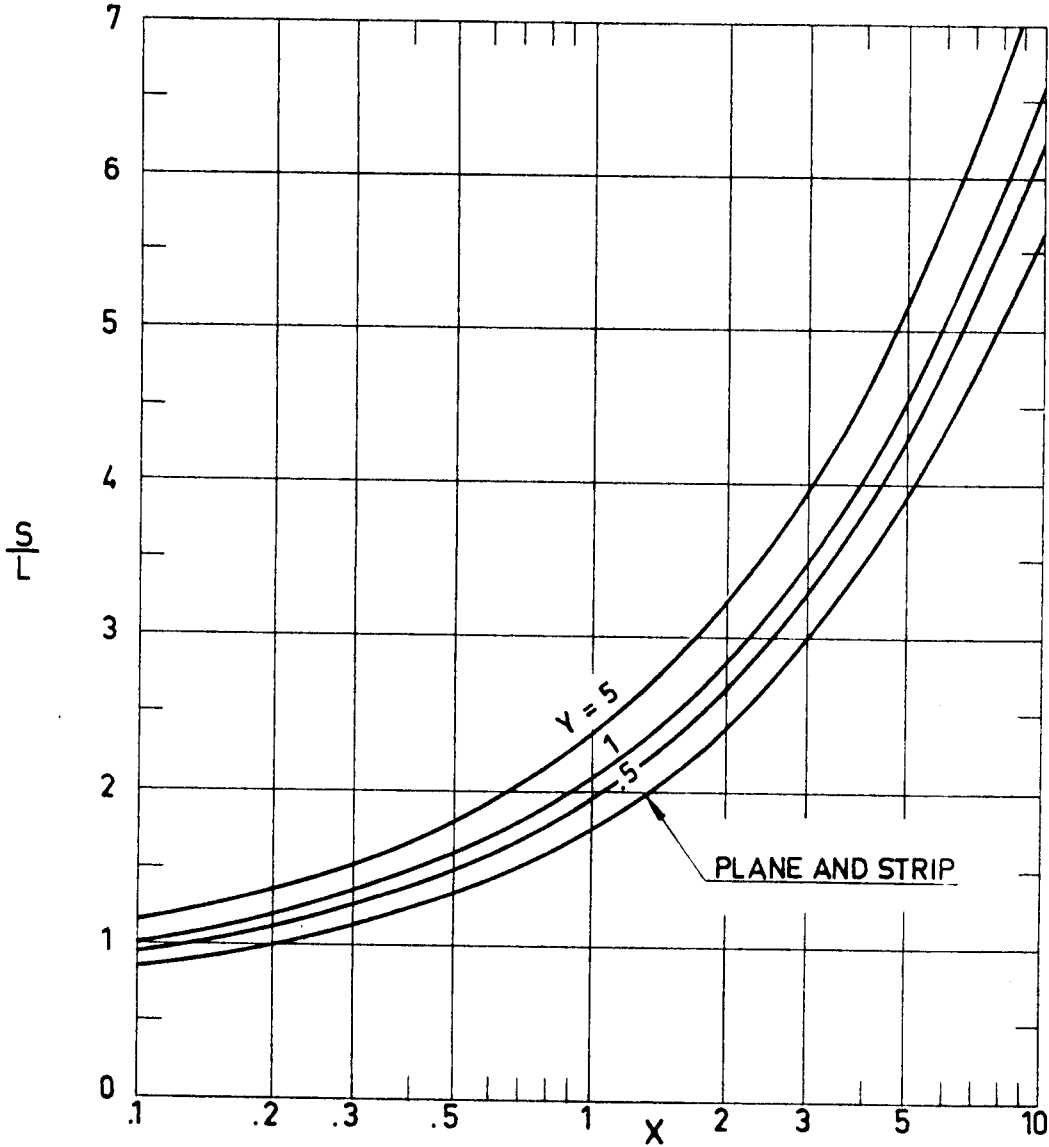


Fig 1-2. Values of the conductive shape factor per unit length, S/L , vs. X for different values of Y . Calculated by the compiler.

CONDUCTIVE SHAPE FACTORS
Planar Surface-Cylindrical Surface

1.3.1.2. PLANE AND CIRCULAR CYLINDER

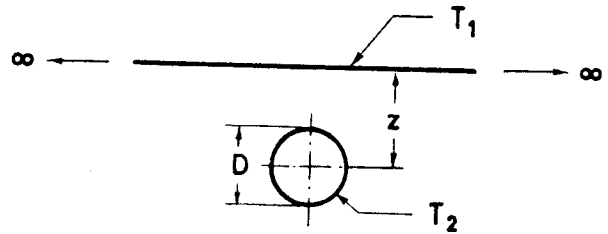
Plane and circular cylinder whose axis is parallel to the plane.

The cylinder is assumed to be infinitely conductive.

$$Z = \frac{D}{z}$$

Formula:

$$\frac{S}{L} = \frac{2\pi}{\cosh^{-1}\left(\frac{2}{Z}\right)}$$



Comments:

The configuration is two-dimensional.

S/L is the conductive shape factor per unit length normal to the plane of the figure.

The results are given in Fig 1-3 overleaf.

References: Sunderland & Johnson (1964), Kutateladze & Borishanskii (1966).

CONDUCTIVE SHAPE FACTORS
Planar Surface-Cylindrical Surface

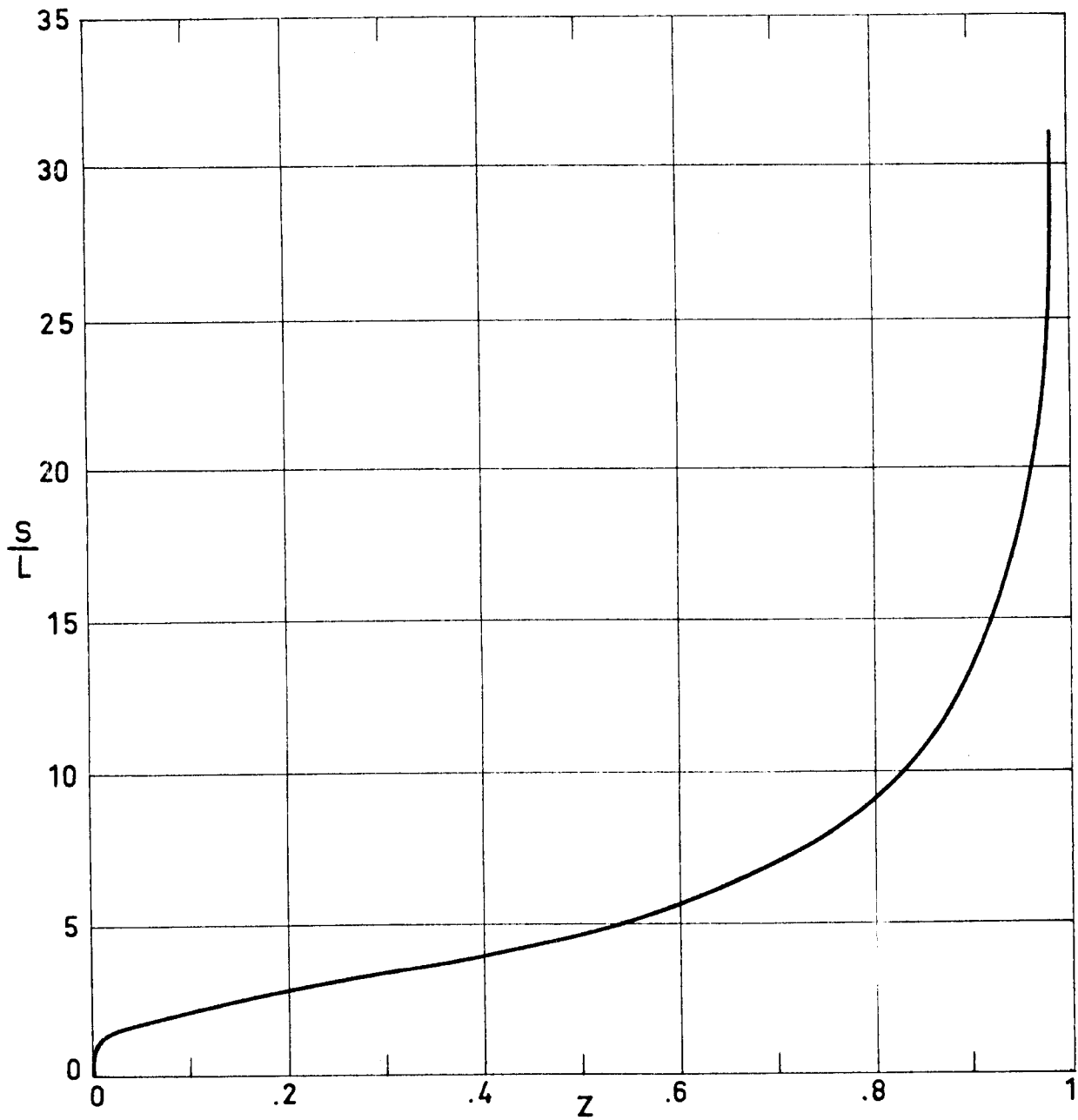


Fig 1-3. Values of the conductive shape factor per unit length S/L , vs. dimensionless diameter of the cylinder cross section. Calculated by the compiler.

CONDUCTIVE SHAPE FACTORS
Planar Surface-Cylindrical Surface

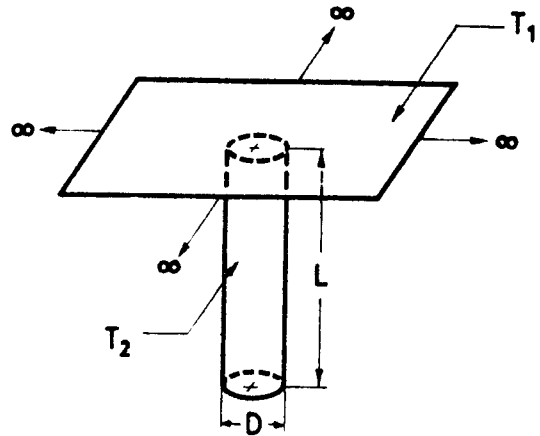
1.3.2. AXISYMMETRICAL CONFIGURATION

1.3.2.1. PLANE AND CIRCULAR CYLINDER

Plane and circular cylinder of finite length with its base on the plane.

The cylinder is assumed to be infinitely conductive.

$$D \ll L$$



Formulae:

$$\frac{S}{L} = \frac{2\pi}{\ln \frac{4L}{D}} \tag{a}$$

$$\frac{S}{L} = \frac{2\pi}{\ln \frac{4L}{D}} - \frac{2\pi(2\ln\sqrt{2}-1)}{\left(\ln \frac{4L}{D}\right)^2} \tag{b}$$

Comments:

To obtain expression (a) the end effects corresponding to the free end of the cylinder have been neglected, so that this expression is only valid when the cylinder is slender enough.

Expression (b), which includes the second asymptotic term of the three-dimensional solution, has been obtained by the compiler.

The results are given in Fig 1-4 overleaf.

References: Sunderland & Johnson (1964), Kutateladze & Borishanskii (1966); Parker, Boggs & Blick (1969).

CONDUCTIVE SHAPE FACTORS
Planar Surface-Cylindrical Surface

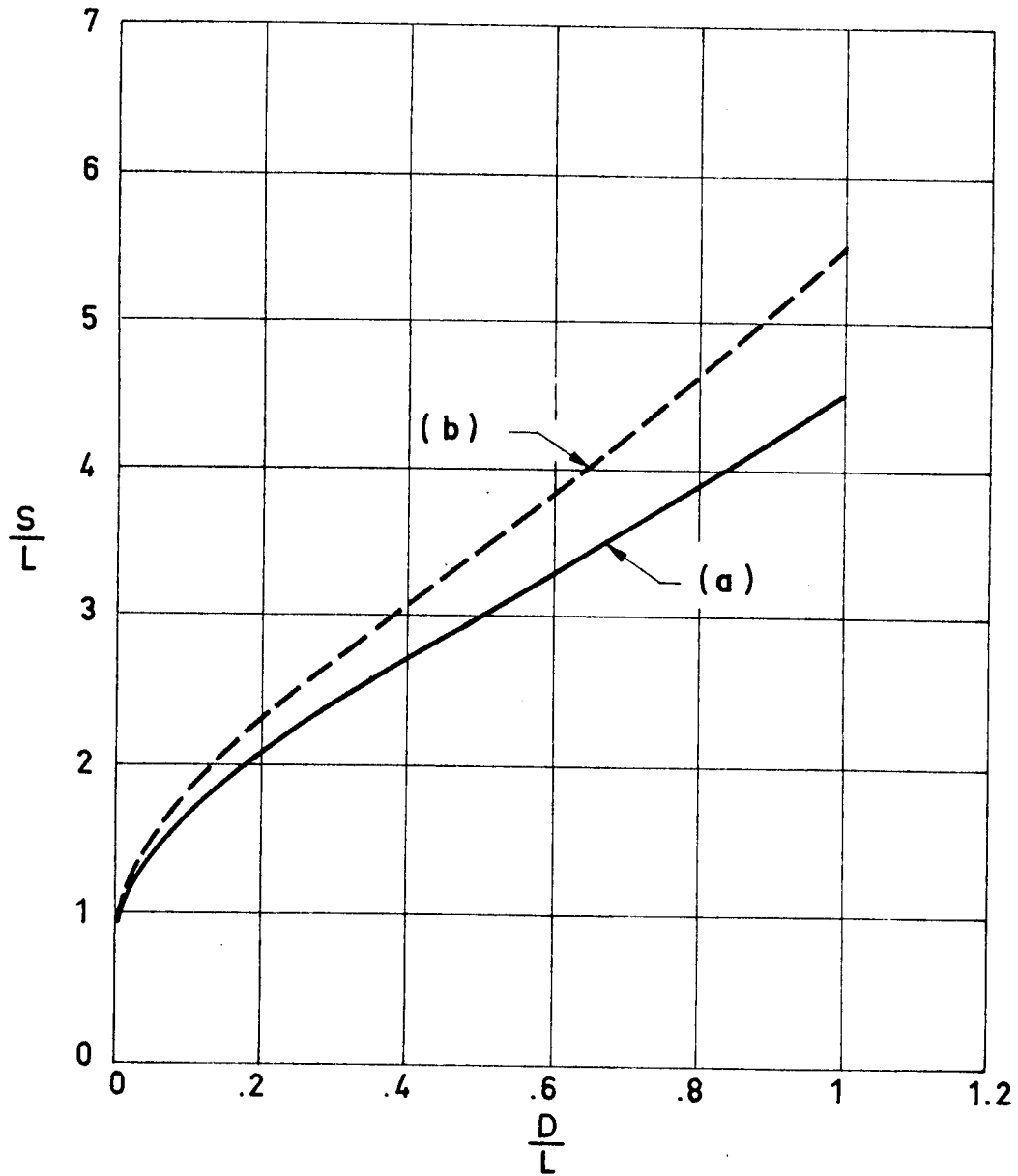


Fig 1-4. Values of the dimensionless conductive shape factor, S/L, vs. cylinder diameter to length ratio, D/L. Calculated by the compiler.

CONDUCTIVE SHAPE FACTORS
Planar Surface-Spherical Surface

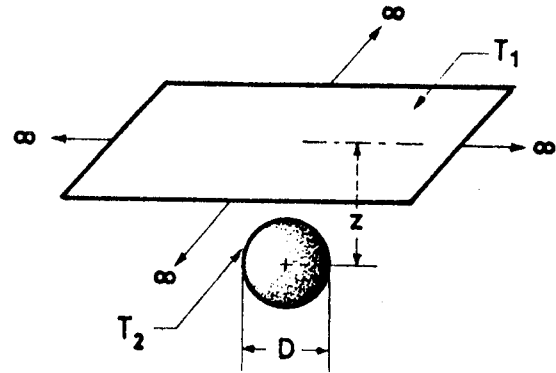
1.4. PLANAR SURFACE-SPHERICAL SURFACE

1.4.1. PLANE AND SPHERE

Plane and sphere.

The sphere is assumed to be infinitely conductive.

$$Z = \frac{D}{z}$$



Formula:

$$\frac{S}{D} = \frac{2\pi}{1 + \frac{z}{4}}$$

The results are given in Fig 1-5 overleaf.

References: Andrews (1955), Sunderland & Johnson (1964), Kutateladze & Borishanskii (1966); Parker, Boggs & Blick (1969).

CONDUCTIVE SHAPE FACTORS.
Planar Surface-Spherical Surface

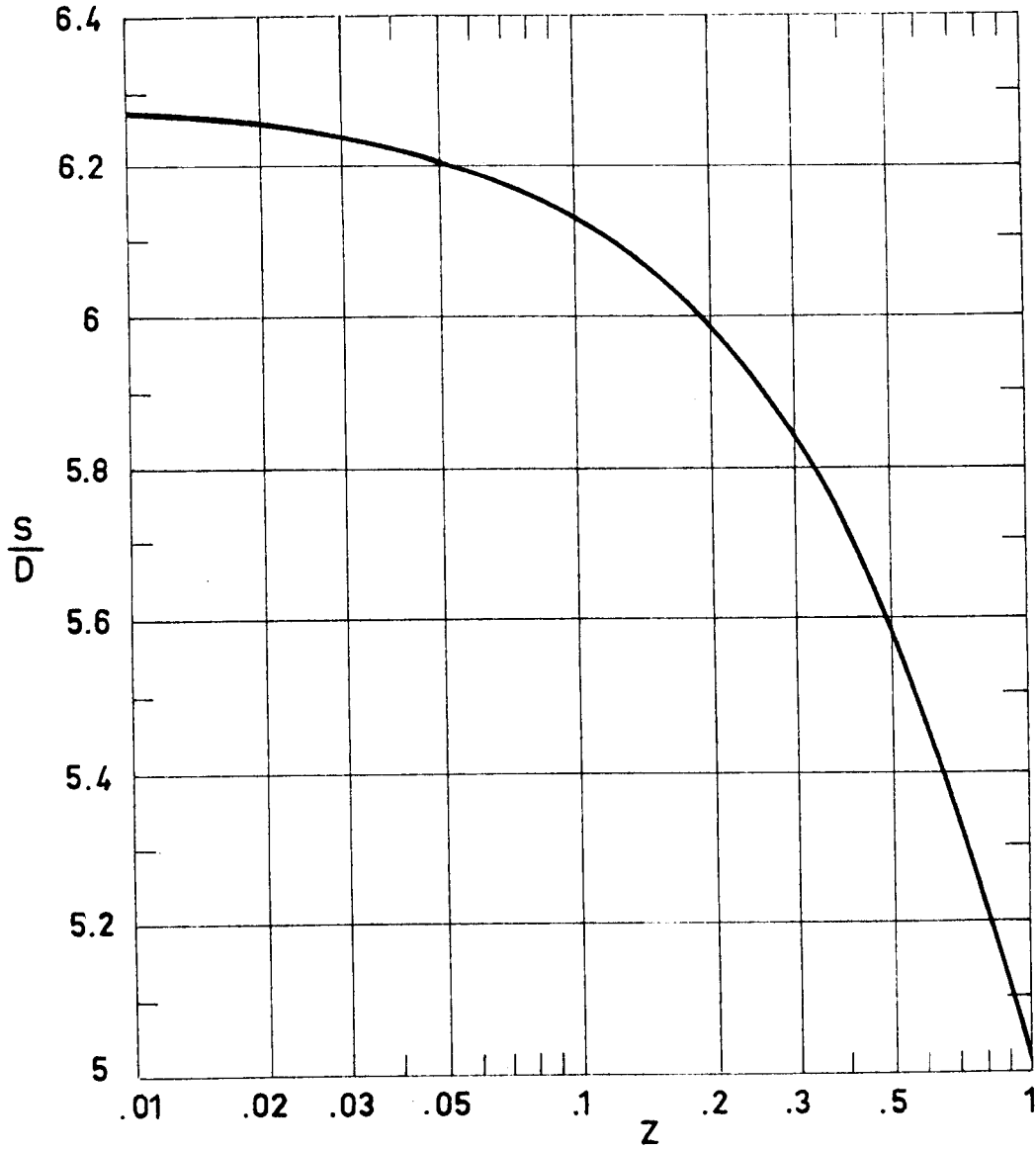


Fig 1-5. Values of the dimensionless conductive shape factor, S/D, vs. the dimensionless diameter of the sphere, Z. Calculated by the compiler.

CONDUCTIVE SHAPE FACTORS
Cylindrical-Cylindrical Surfaces

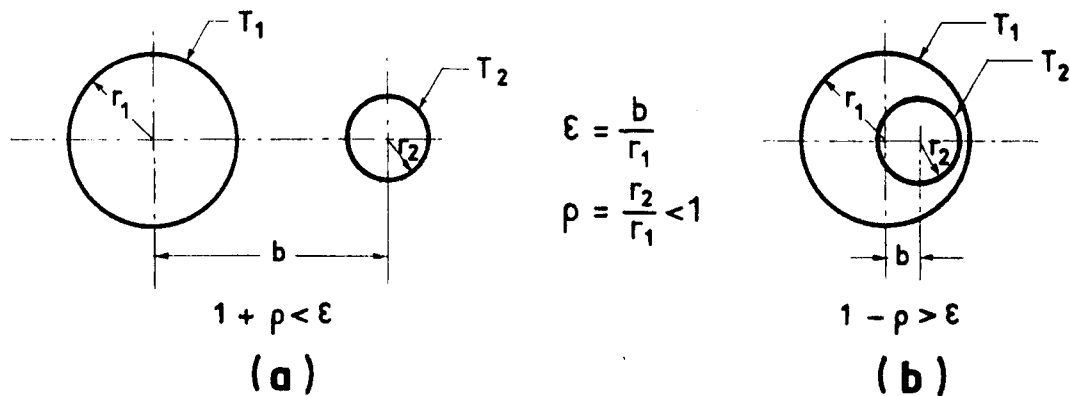
1.5. CYLINDRICAL-CYLINDRICAL SURFACES

1.5.1. TWO-DIMENSIONAL CONFIGURATIONS

1.5.1.1. CIRCULAR CYLINDERS

Parallel circular cylinders.

Both cylinders are assumed to be infinitely conductive.



Formula:

$$\frac{S}{L} = \frac{2\pi}{\cosh^{-1} \left[\frac{1 + \rho^2 - \epsilon^2}{2\rho} \right]}$$

Comments:

Both configurations are two-dimensional.

S/L is the conductive shape factor per unit length normal to the plane of the figure.

The results are given in Fig 1-6 overleaf.

References: Andrews (1955), Sunderland & Johnson (1964); Parker, Boggs & Blick (1969).

CONDUCTIVE SHAPE FACTORS
Cylindrical-Cylindrical Surfaces

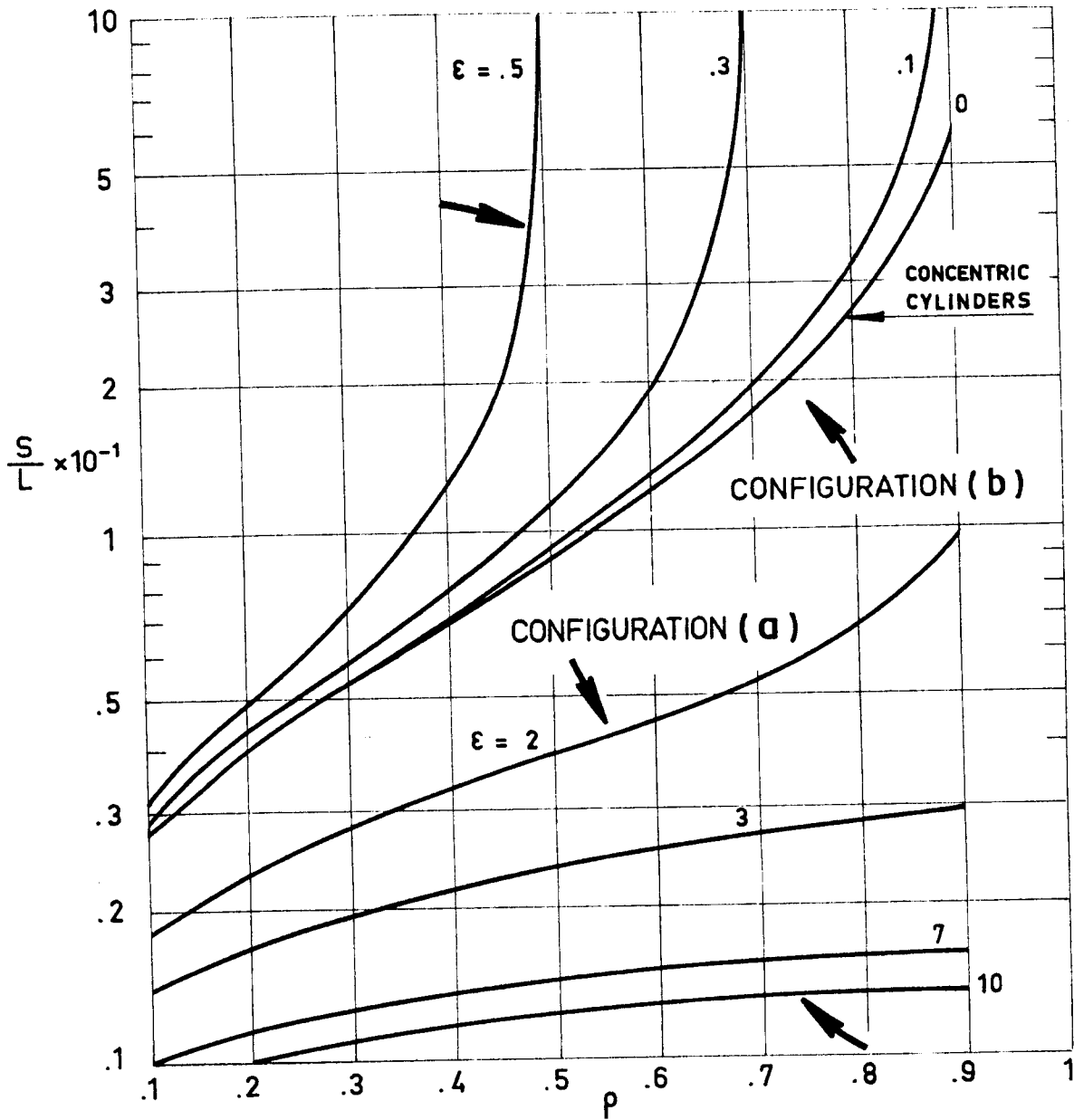


Fig 1-6. Values of the conductive shape factor per unit length, S/L , vs. radius ratio, ρ ; for different values of the dimensionless distance between cylinder axes, ϵ . Calculated by the compiler.

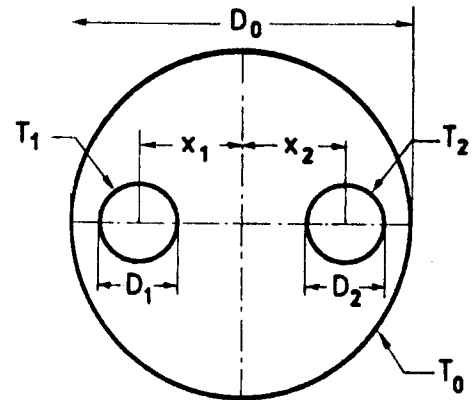
CONDUCTIVE SHAPE FACTORS
Cylindrical-Cylindrical Surfaces

1.5.1.2. CIRCULAR RODS WITH HOLES

Circular rod with two circular holes.

$$X_i = \frac{x_i}{D_0}$$

$$d_i = \frac{D_i}{D_0}$$



The results presented have been obtained by using an electrical analogue method.

Comments:

The configuration is two-dimensional.

S/L is the conductive shape factor per unit length normal to the plane of the figure.

The results are given in Fig 1-7 overleaf.

Reference: Faulkner & Andrews (1955).

CONDUCTIVE SHAPE FACTORS
Cylindrical-Cylindrical Surfaces

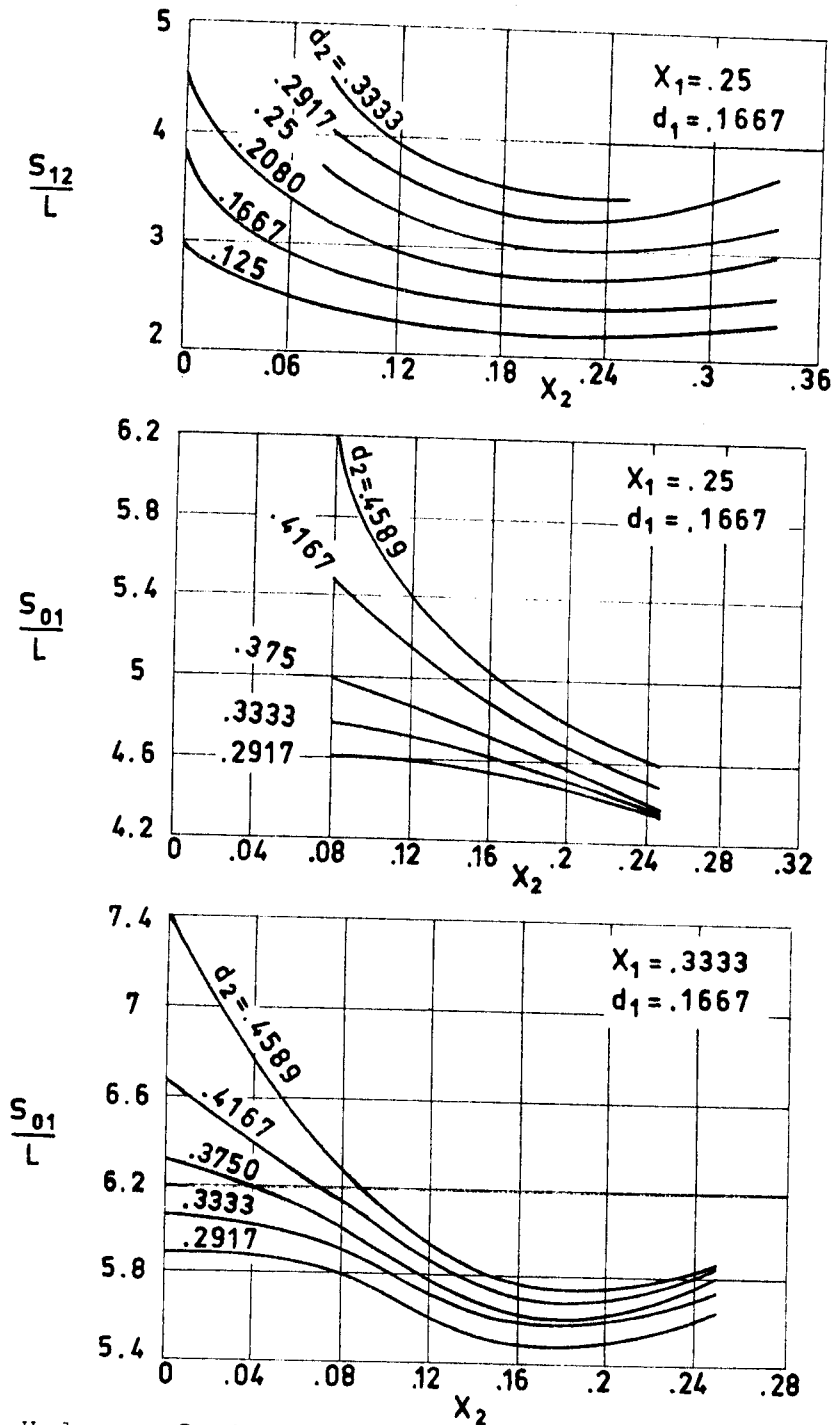


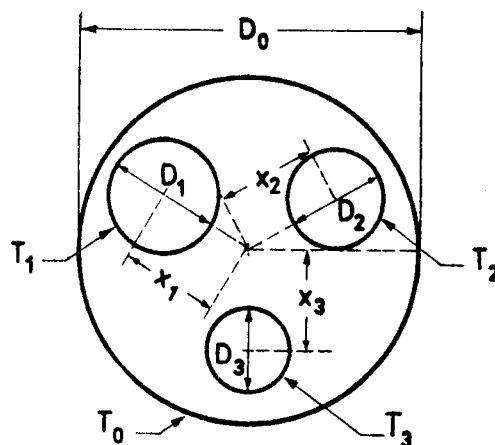
Fig 1-7. Values of the dimensionless conductive shape factors per unit length, S_{ij}/L , vs. the eccentricity of one of the holes X_2 , for different values of the relevant geometrical parameters. From Faulkner & Andrews (1955).

CONDUCTIVE SHAPE FACTORS
Cylindrical-Cylindrical Surfaces

Circular rod with three circular holes.

$$X_i = \frac{x_i}{D_0}$$

$$d_i = \frac{D_i}{D_0}$$



The results presented have been obtained by using an electrical analogue method.

Comments:

The configuration is two-dimensional.

S/L is the conductive shape factor per unit length normal to the plane of the figure.

The results are given in Fig 1-8 overleaf.

Reference: Faulkner & Andrews (1955).

CONDUCTIVE SHAPE FACTORS
Cylindrical-Cylindrical Surfaces

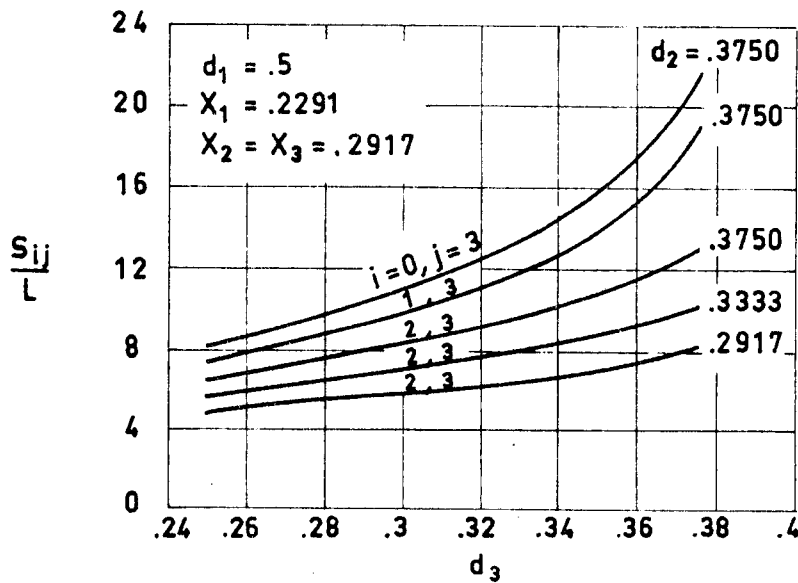
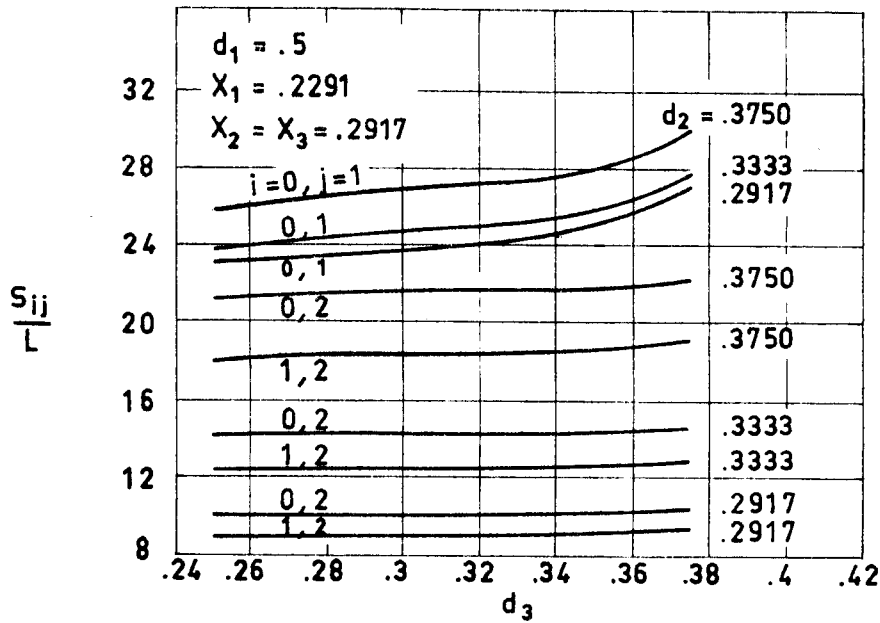
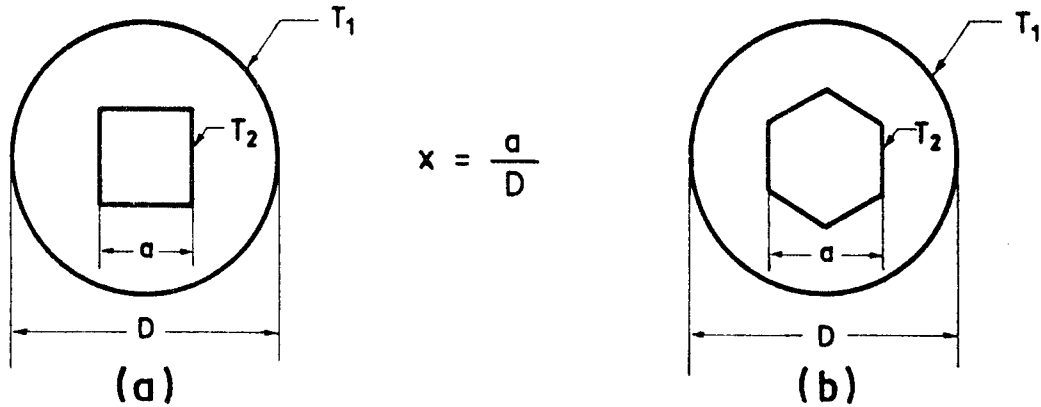


Fig 1-8. Values of the conductive shape factors per unit length, S_{ij}/L , vs. the diameter ratio d_3 , for different values of the relevant geometric parameters. From Faulkner & Andrews (1955).

CONDUCTIVE SHAPE FACTORS
Cylindrical-Cylindrical Surfaces

Circular rod with square or hexagonal concentric holes.



Formulae:

$$(a) \quad \frac{S}{L} = \frac{6.533}{\ln \frac{1}{x} - .15921}$$

$$(b) \quad \frac{S}{L} = \frac{6.46}{\ln \frac{1}{x} - .03147}$$

Comments:

The configuration is two-dimensional.

S/L is the conductive shape factor per unit length normal to the plane of the figure.

The results are given in Fig 1-9 overleaf.

Reference: Ramachandra Murthy & Ramachandran (1967).

CONDUCTIVE SHAPE FACTORS
Cylindrical-Cylindrical Surfaces

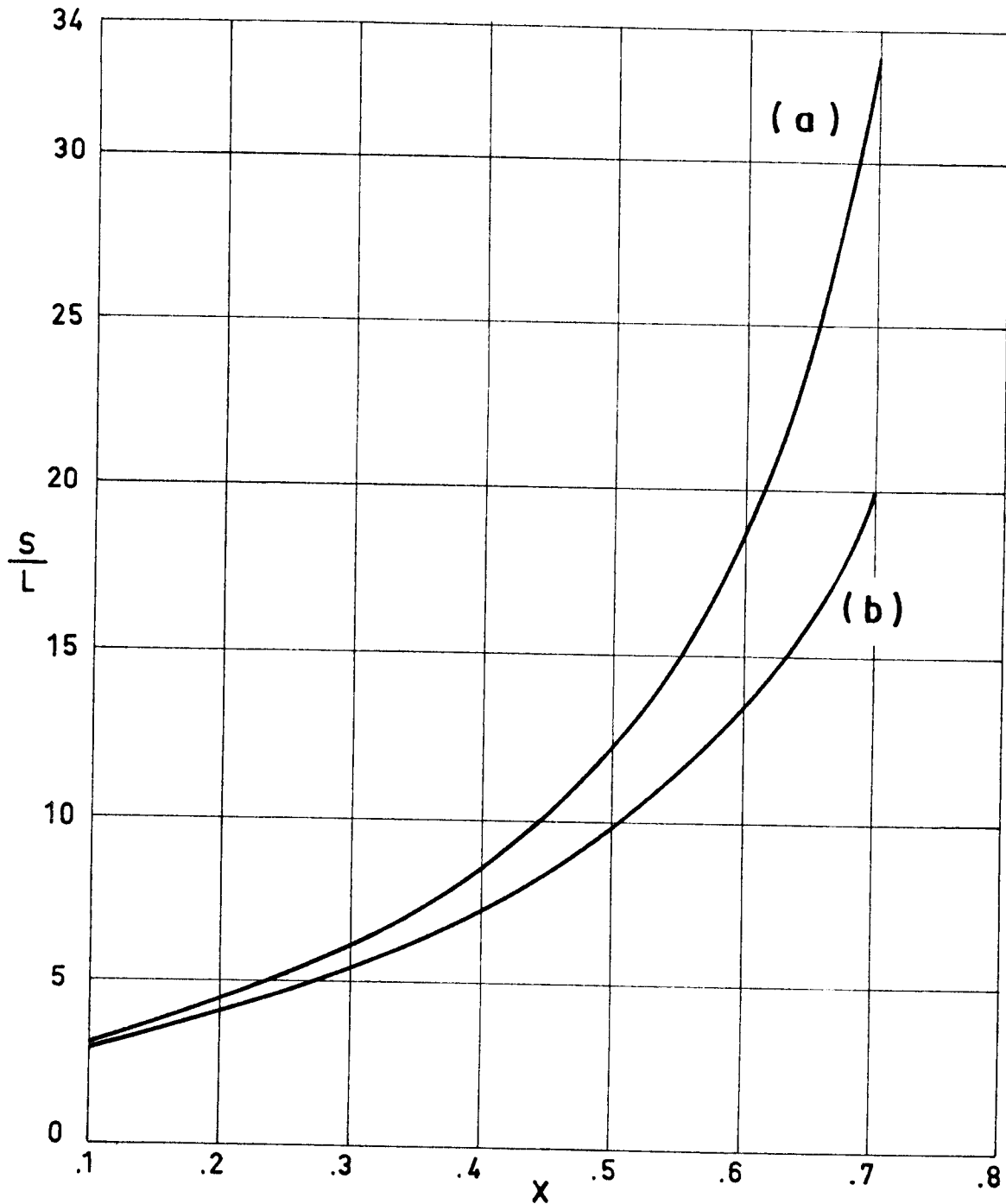


Fig 1-9. Values of the conductive shape factor per unit length, S/L , vs. the dimensionless characteristic length of the holes, X . Calculated by the compiler.

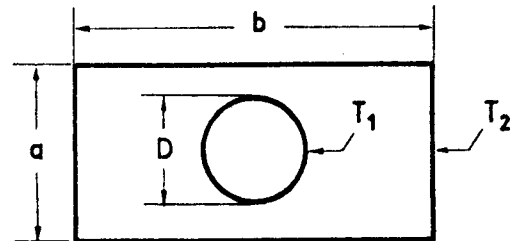
CONDUCTIVE SHAPE FACTORS
Cylindrical-Cylindrical Surfaces

1.5.1.3. RECTANGULAR BARS WITH HOLES

Rectangular bar with a concentric circular hole.

$$X = \frac{D}{a}$$

$$Y = \frac{b}{a}$$



Formula:

$$\frac{S}{L} = \frac{2\pi}{\ln \frac{4}{\pi X} - 2k}$$

where k is a coefficient which depends upon Y as indicated below

Y	k
1.00	.08290
1.25	.03963
1.50	.01781
1.75	.00816
2.00	.00373
2.25	.00170
2.50	.00078
3.00	.00016
4.00	6.9748×10^{-6}
5.00	3.0140×10^{-7}
10.00	4.5422×10^{-14}
∞	0

Comments:

The configuration is two-dimensional.

S/L is the conductive shape factor per unit length normal to the plane of the figure.

The results are given in Fig 1-10 overleaf.

Reference: Sunderland & Johnson (1964).

CONDUCTIVE SHAPE FACTORS
Cylindrical-Cylindrical Surfaces

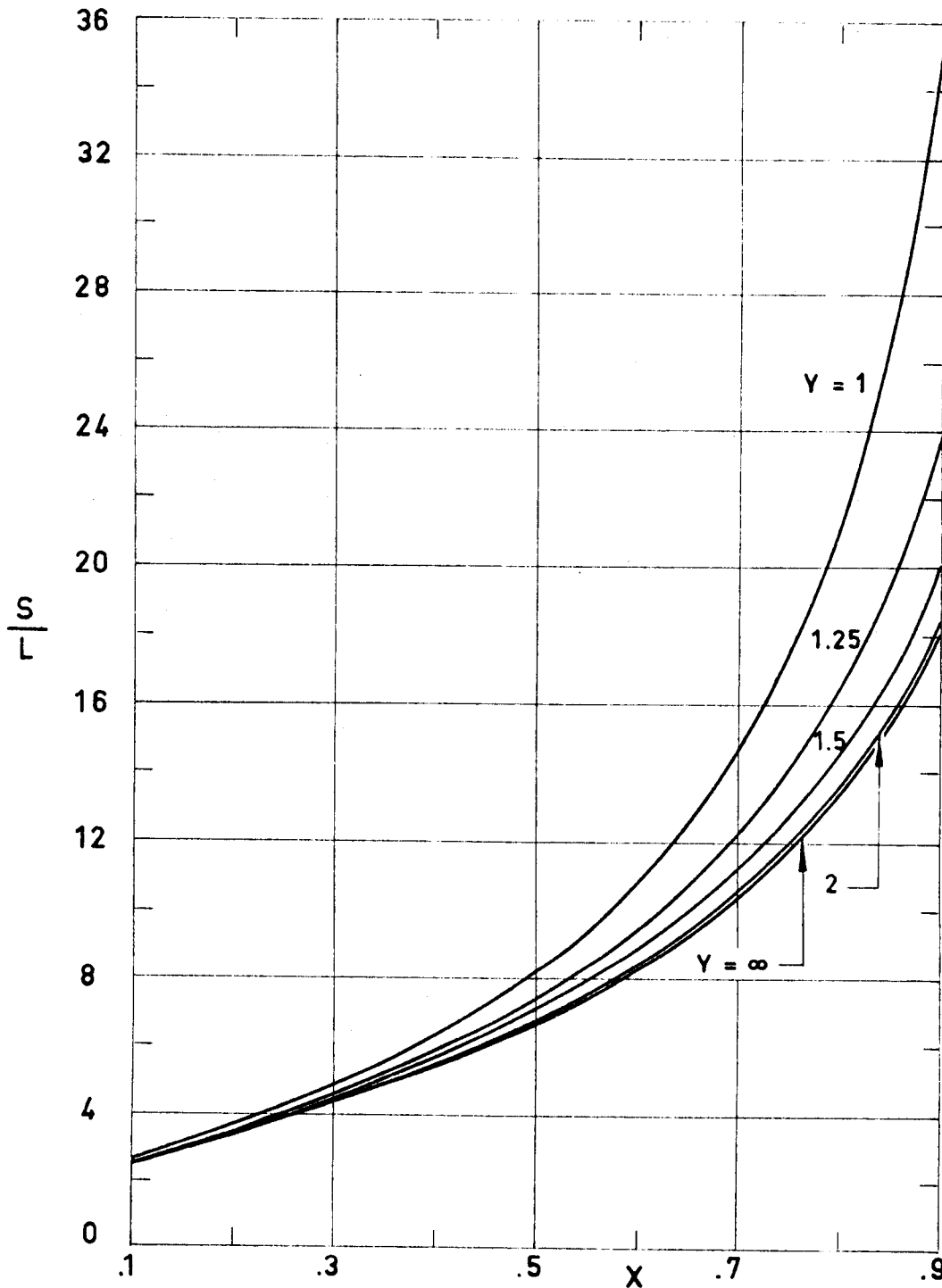


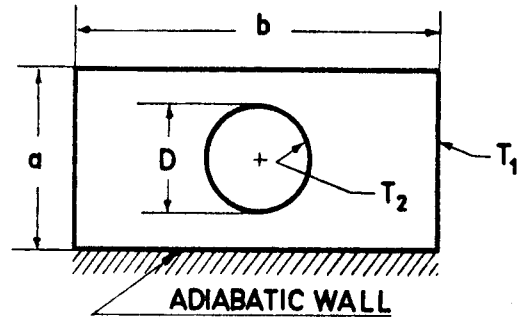
Fig 1-10. Values of the conductive shape factor per unit length, S/L , vs. the dimensionless diameter of the hole, X , for several values of the aspect ratio, Y , of the rectangular bar cross-section. Calculated by the compiler.

CONDUCTIVE SHAPE FACTORS
Cylindrical-Cylindrical Surfaces

Rectangular bar having one adiabatic face and a concentric circular hole.

$$X = \frac{D}{a}$$

$$Y = \frac{b}{a}$$



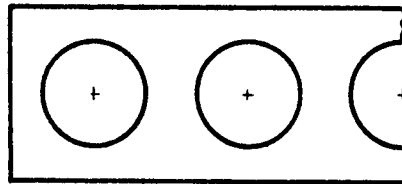
The results presented were obtained numerically.

Comments:

The configuration is two-dimensional.

S/L is the conductive shape factor per unit length normal to the plane of the figure.

These results can be used to study configurations similar to the one sketched below.



The results are given in Fig 1-11 overleaf.

Reference: Griggs, Pitts & Goyal (1973).

CONDUCTIVE SHAPE FACTORS
Cylindrical-Cylindrical Surfaces

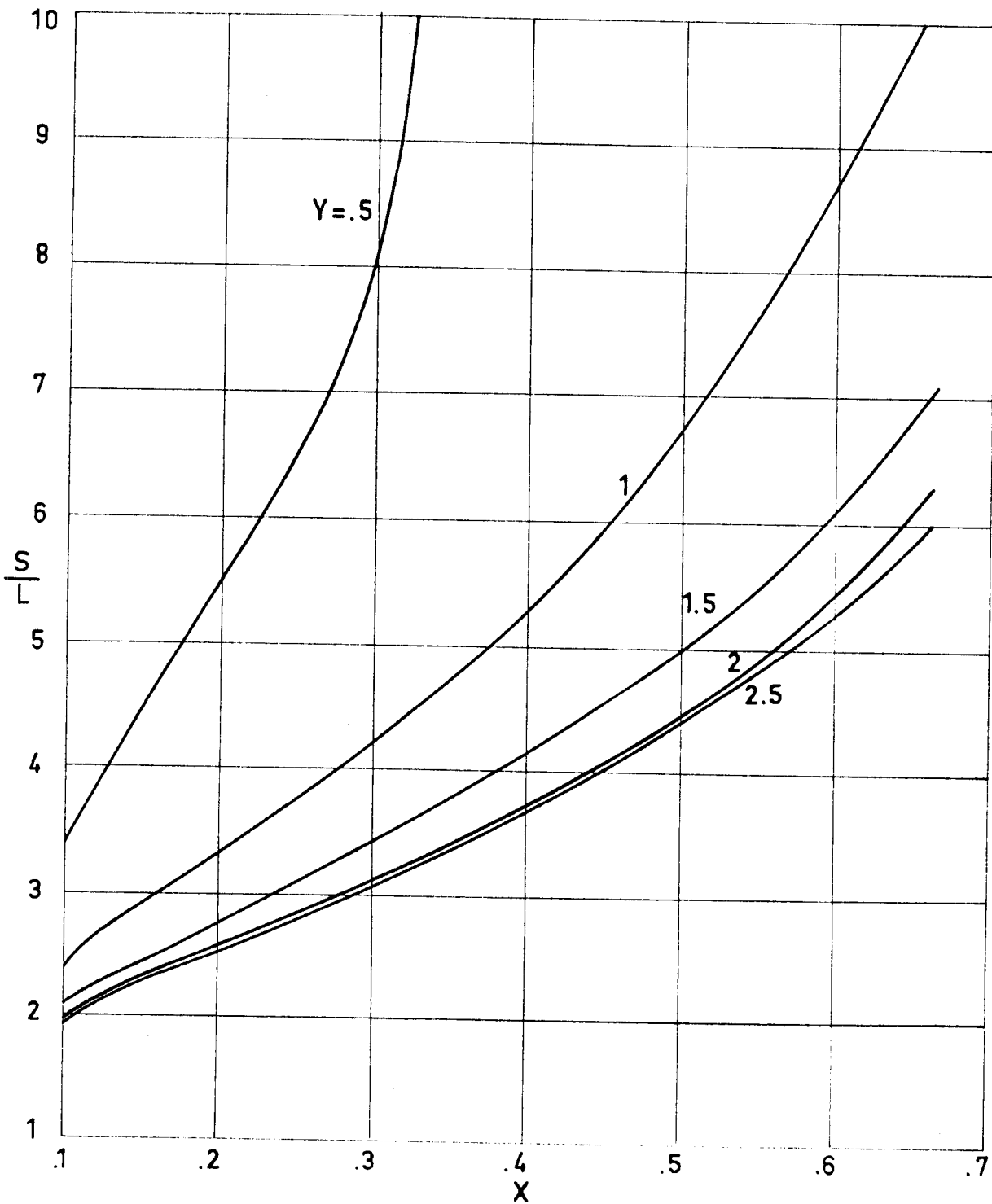


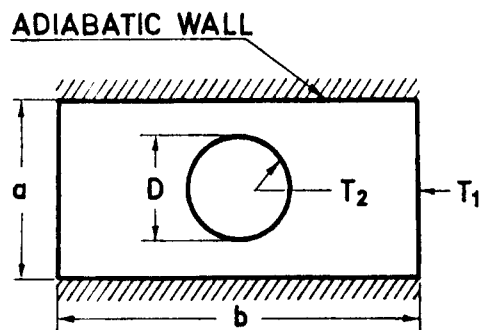
Fig 1-11. Values of the conductive shape factor per unit length, S/L , vs. the dimensionless diameter of the hole, X , for different values of the aspect ratio, Y , of the rectangular bar cross section. After Griggs, Pitts & Goyal (1973).

CONDUCTIVE SHAPE FACTORS
Cylindrical-Cylindrical Surfaces

Rectangular bar having two opposite adiabatic faces and a concentric circular hole.

$$X = \frac{D}{a}$$

$$Y = \frac{b}{a}$$



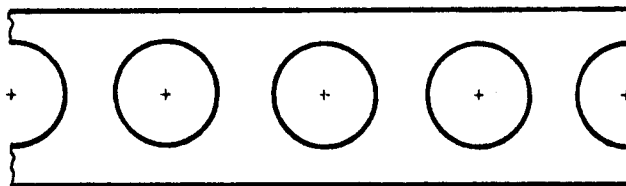
The results presented were obtained numerically.

Comments:

The configuration is two-dimensional.

S/L is the conductive shape factor per unit length normal to the plane of the figure.

These results can be used to study configurations similar to the one sketched below.



The results are given in Fig 1-12 overleaf.

Reference: Griggs, Pitts & Goyal (1973).

CONDUCTIVE SHAPE FACTORS
Cylindrical-Cylindrical Surfaces

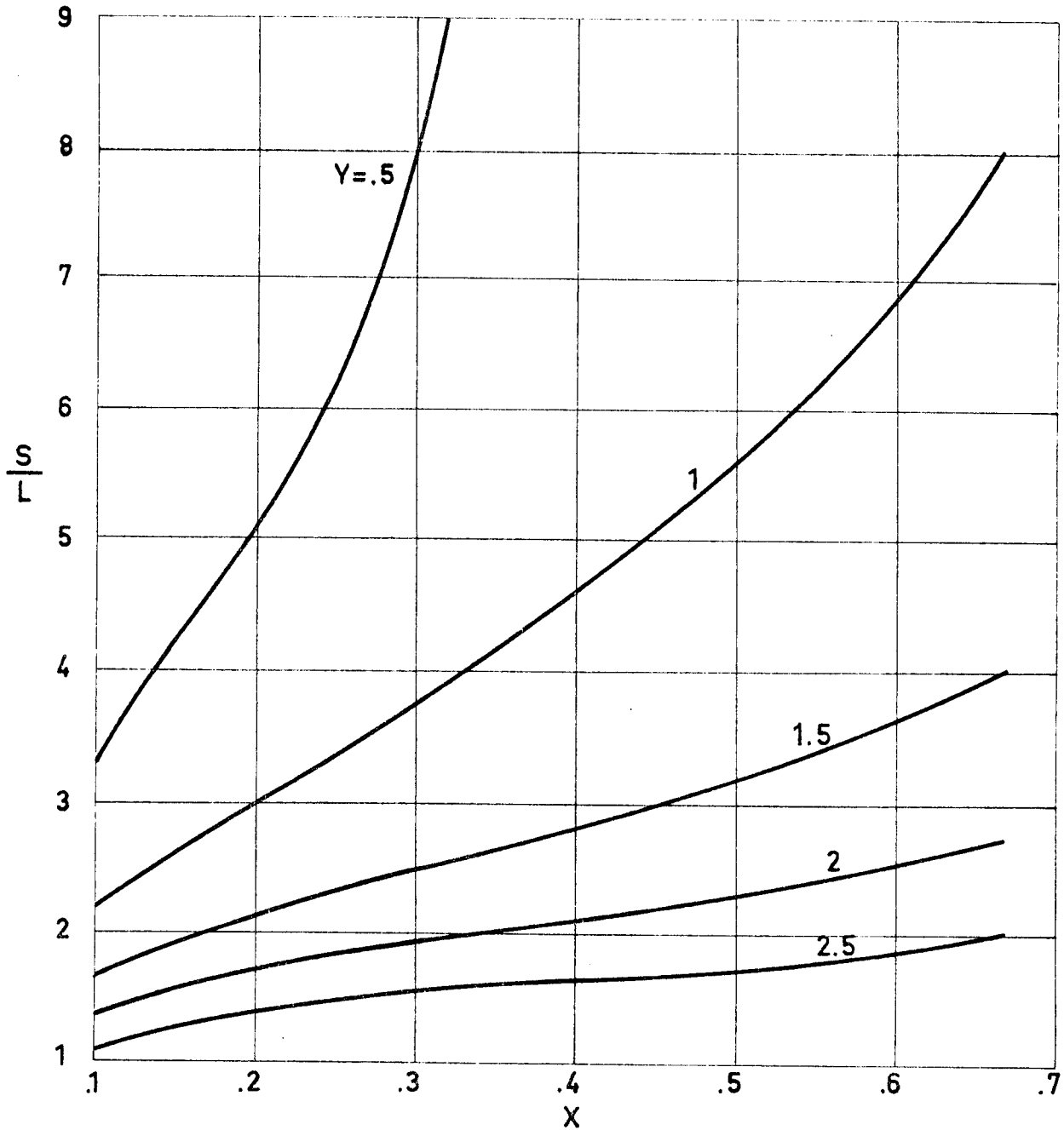
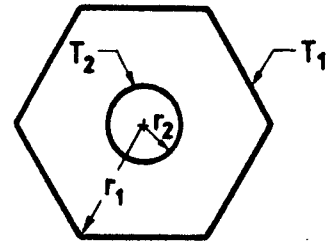


Fig 1-12. Values of the conductive shape factor per unit length, S/L , vs. the dimensionless diameter of the hole, X , for several values of the aspect ratio, Y , of the rectangular bar cross section. After Griggs, Pitts & Goyal (1973).

CONDUCTIVE SHAPE FACTORS
Cylindrical-Cylindrical Surfaces

1.5.1.4. POLYGONAL BARS WITH HOLES

Cylinder with an n-sided regular cross section and a concentric circular hole.



$$\rho = \frac{r_2}{r_1}$$

Formula:

$$\frac{S}{L} = \frac{2\pi}{\ln\left(\frac{1}{\rho} - \frac{B}{2}\right)}$$

where B is a coefficient which depends upon n as indicated in the table below.

n	B
3	1.13916
4	.54159
5	.32131
6	.21339
∞	0

Comments:

The configuration is two-dimensional.

S/L is the conductive shape factor per unit length normal to the plane of the figure.

The results are given in Fig 1-13 overleaf.

Reference: Sunderland & Johnson (1964).

CONDUCTIVE SHAPE FACTORS
Cylindrical-Cylindrical Surfaces

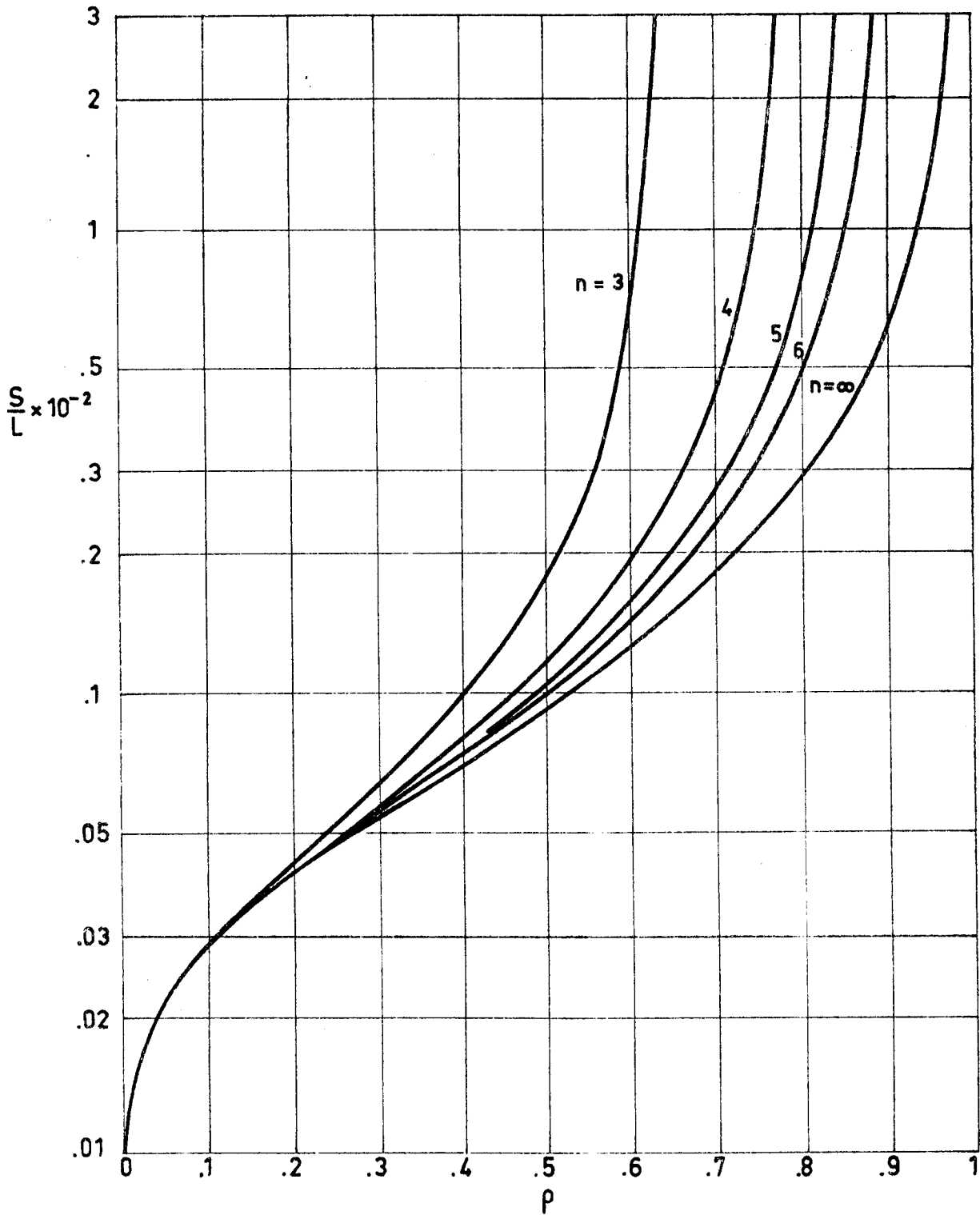


Fig 1-13. Values of the conductive shape factor per unit length, S/L , vs. the dimensionless hole radius, ρ , for several values of n . Calculated by the compiler.

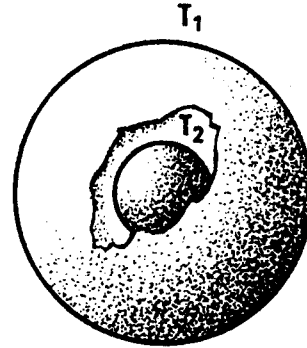
CONDUCTIVE SHAPE FACTORS
Spherical-Spherical Surfaces

1.6. SPHERICAL-SPHERICAL SURFACES

1.6.1. TWO CONCENTRIC SPHERES

Two concentric spheres.

$$\rho = \frac{r_2}{r_1}$$



where r_1 and r_2 are the radii of the outer and inner sphere, respectively.

Formula:

$$\frac{S}{r_1} = \frac{4\pi}{\frac{1}{\rho} - 1}$$

The results are given in Fig 1-14 overleaf.

Reference: Parker, Boggs & Blick (1969).

CONDUCTIVE SHAPE FACTORS
Spherical-Spherical Surfaces

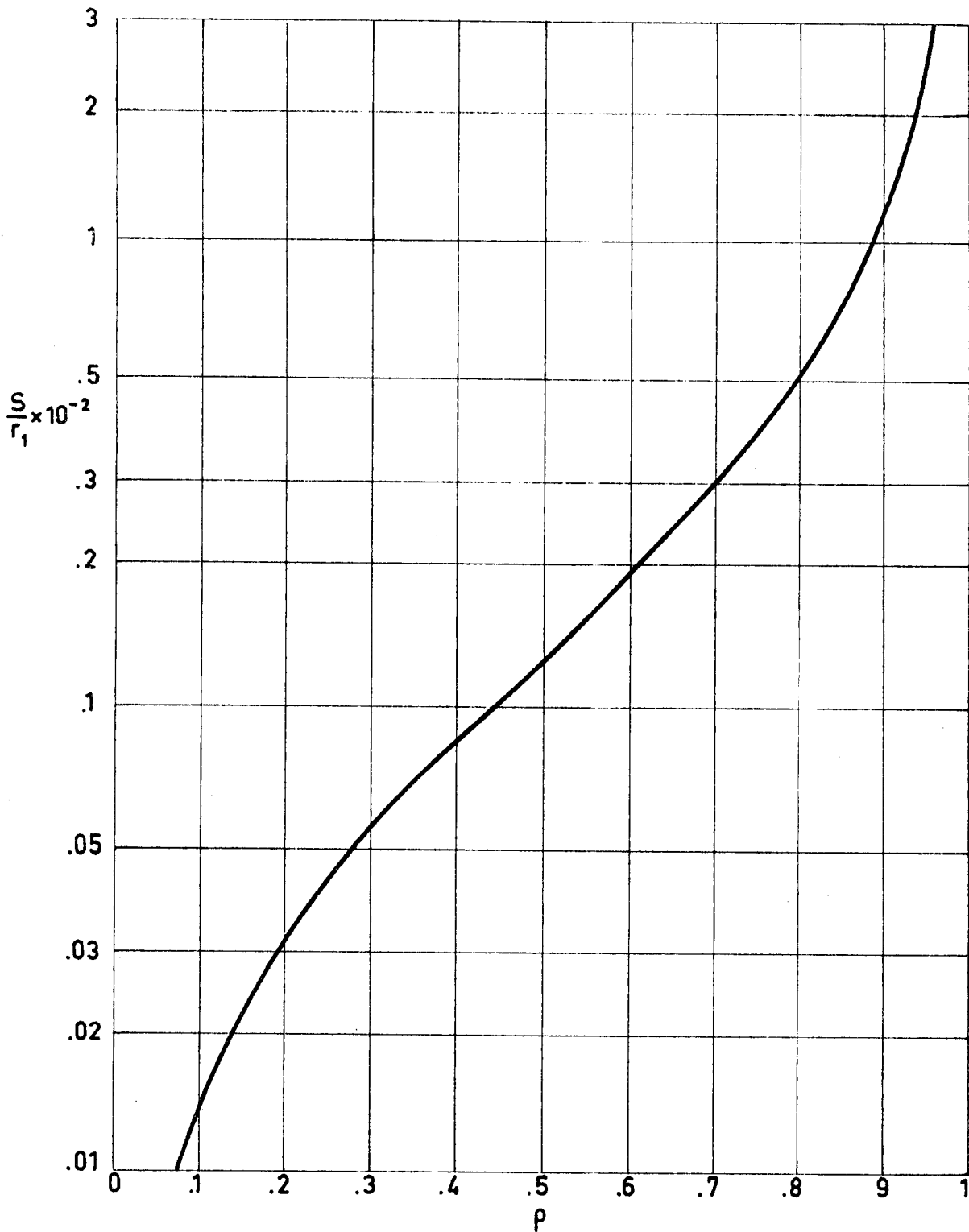


Fig 1-14. Values of the dimensionless conductive shape factor, S/r_1 , vs. radius ratio, ρ . Calculated by the compiler.

THERMAL JOINT CONDUCTANCE

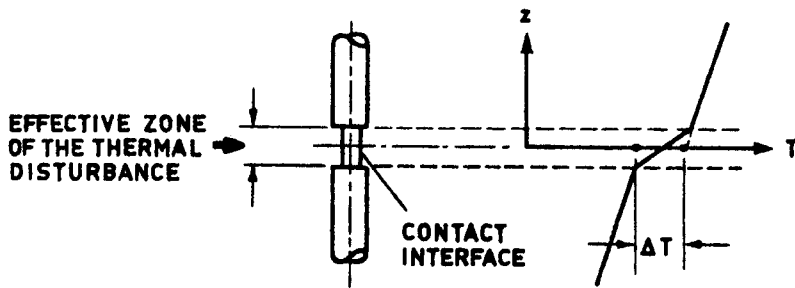
General

2. THERMAL JOINT CONDUCTANCE

2.1. GENERAL

The interface existing between two surfaces in contact introduces a resistance to heat transfer between the materials making up the contact. The thermal conductance, h_c , between these surfaces is given by:

$$h_c = \frac{Q/A}{\Delta T} ,$$



where:

Q/A , Heat flux across the interface. [$W.m^{-2}$].

ΔT , Interfacial temperature drop, estimated as in Fig 2-1. [K].

Fig 2-1. Estimation of the temperature drop at the interface.

The thermal conductance, h_c , which depends on the actual contact area and on the physical properties of the mating materials, can be split into three contributions, namely: the radiative, h_r , interstitial, h_f , and solid, h_s , contributions

$$h_c = h_r + h_f + h_s .$$

The radiative contribution, h_r , can be neglected for temperatures below 900K, as shown by Fenech & Rohsenow (1959) and by Clausing & Chao (1965).

Concerning h_f , no generally valid method has been developed up to the moment to predict its contribution. The problem has been considered, among others, by Cetinkale & Fishended (1951), La-

THERMAL JOINT CONDUCTANCE

General

ming (1961), Fenech & Rohsenow (1963), and Henry & Fenech (1964).

The contribution, h_s , of the solid contacting materials has been calculated, in the case of very simple geometrical configurations, by Roess (1949), Laming (1961), Clausing & Chao (1965), Fenech & Rohsenow (1963), and Henry & Fenech (1964). However, the direct application of these data is impeded by the impossibility of correctly defining the geometrical characteristics of the contact area under practical conditions.

Because of the difficulties which have been mentioned, the use of empirical correlations based on directly measurable parameters should be recommended. These correlations, which are based on dimensional considerations for the selection of the relevant dimensionless groups of parameters, include together the contributions of h_r , h_f , and h_s .

Unfortunately, only correlations for bare contacting metals have reached widespread use, thence, when information on the contact conductance between similar metals separated by a suitable spacer material is required, one must resort to the use of experimental data on systems which resemble as much as possible the configuration which is expected to be used in the real case.

Recently Al-Astrabadi et al. (1977) correlated data on thermal contact conductances for stacks of thin layers in high vacuum. Data from different sources, for both bare metals and plastic layers, correlate fairly in terms of appropriate dimensionless parameters.

THERMAL JOINT CONDUCTANCE

Empirical Correlations

2.2. EMPIRICAL CORRELATIONS2.2.1. FLETCHER & GYOROG CORRELATION

The following expression to predict the thermal conductance of contacting metal surfaces in a vacuum has been suggested by Fletcher & Gyrog (1970).

$$h_c = \frac{km}{\delta_o} \left[5.22 \times 10^{-6} \frac{\delta_o}{b} + .036 \frac{P}{E} \beta T_m \right]^{.56} \exp \left[170 \left(\frac{P}{E} \frac{\beta T_m}{\delta_o / b} \right) \right], \quad (1)$$

where: E, Modulus of Elasticity. [Pa].

P, Applied Compressive Load. [Pa].

T_m, Mean Temperature. [K].

b, Specimen Radius. [m].

h_c, Thermal Contact Conductance. [W.m⁻².K⁻¹].

km, Mean Thermal Conductivity. [W.m⁻¹.K⁻¹].

km = 2k₁k₂/(k₁+k₂). k₁ and k₂ are the thermal conductivities of the mating materials.

β, Coefficient of Linear Thermal Expansion. [K⁻¹].

δ_o, Gap Thickness Parameter. [m].

$$\delta_o = .519 \times 10^{-6} + .806 \times 10^{-1} d - .622 \times 10^3 d^2 + .211 \times 10^7 d^3 \quad (2)$$

$$d = (FD + 2RD)_{\text{rough surface}} - \frac{1}{2} (FD + 2RD)_{\text{smooth surface}} \quad [\text{m}].$$

FD, Flatness Deviation. [m].

RD, Roughness Deviation. [m].

The gap thickness parameter δ_o is represented as a function of d in Fig 2-2. Experimental data from different sources are included in this figure.

The thermal conductance, h_c, is plotted vs. the load pressure, P, in Fig 2-3. Again the empirical correlation is compared with data from several sources. A mean error of 24% is reported by the authors.

THERMAL JOINT CONDUCTANCE
Empirical Correlations

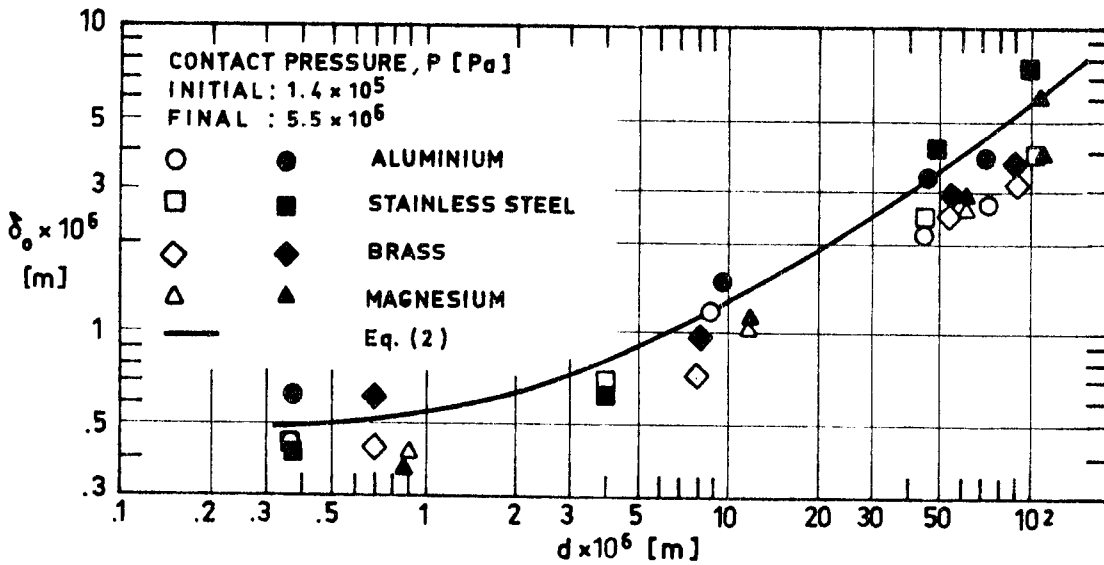


Fig 2-2. Variation of gap thickness parameter, δ_o , with contact surface parameter, d. After Fletcher & Gyrog (1970).

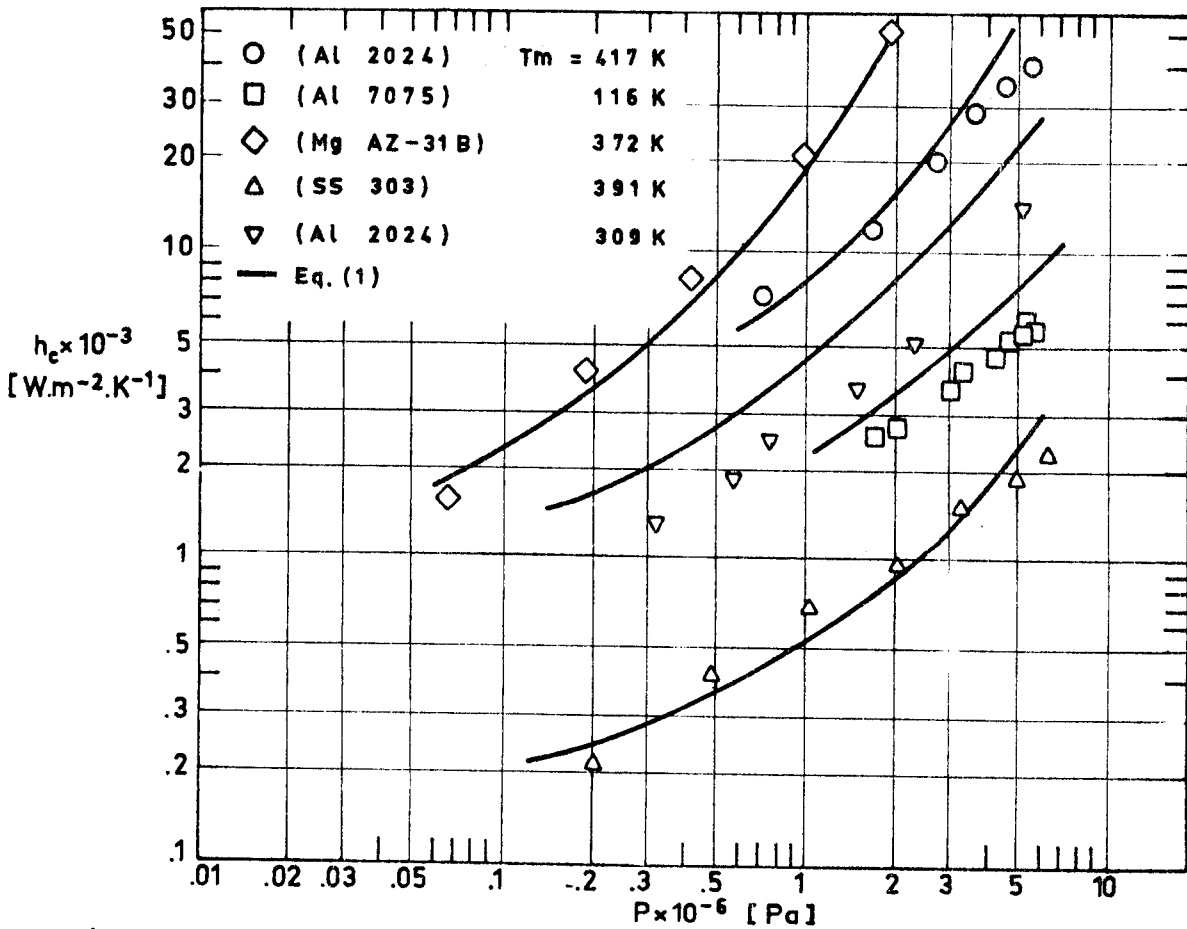


Fig 2-3. Variation of contact conductance with apparent interface pressure. After Fletcher & Gyrog (1970).

Rev. 2. 1984

THERMAL JOINT CONDUCTANCE
Empirical Correlations

2.2.2. THOMAS & PROBERT CORRELATION

This correlation has been set forth by Thomas & Probert (1972) and extensively verified, under vacuum conditions, both by the mentioned authors and by O'Callaghan & Probert (1973).

$$\log \frac{h_c A}{\sigma k m} = C \log \frac{P A}{\sigma^2 M} + D \quad (3)$$

where:

- A , Nominal Contact Area. [m²].
- C = .743 ± .067 for stainless steel.
= .720 ± .044 for aluminium.
- D = 2.26 ± .88 for stainless steel.
= .66 ± .62 for aluminium.
- M , Surface Hardness. [Pa].
- σ , rms Surface Roughness. [m].
σ = ((RD)₁² + (RD)₂²)^{1/2}. (RD)₁ and (RD)₂ are the roughness desviations of the mating materials.

Fig 2-4 gives the dimensionless conductance vs. the dimensionless load for stainless steel contacts in a vacuum, while Fig 2-5 shows similar data when one or both surfaces are aluminium.

Rev. 2. 1984

THERMAL JOINT CONDUCTANCE
Empirical Correlations

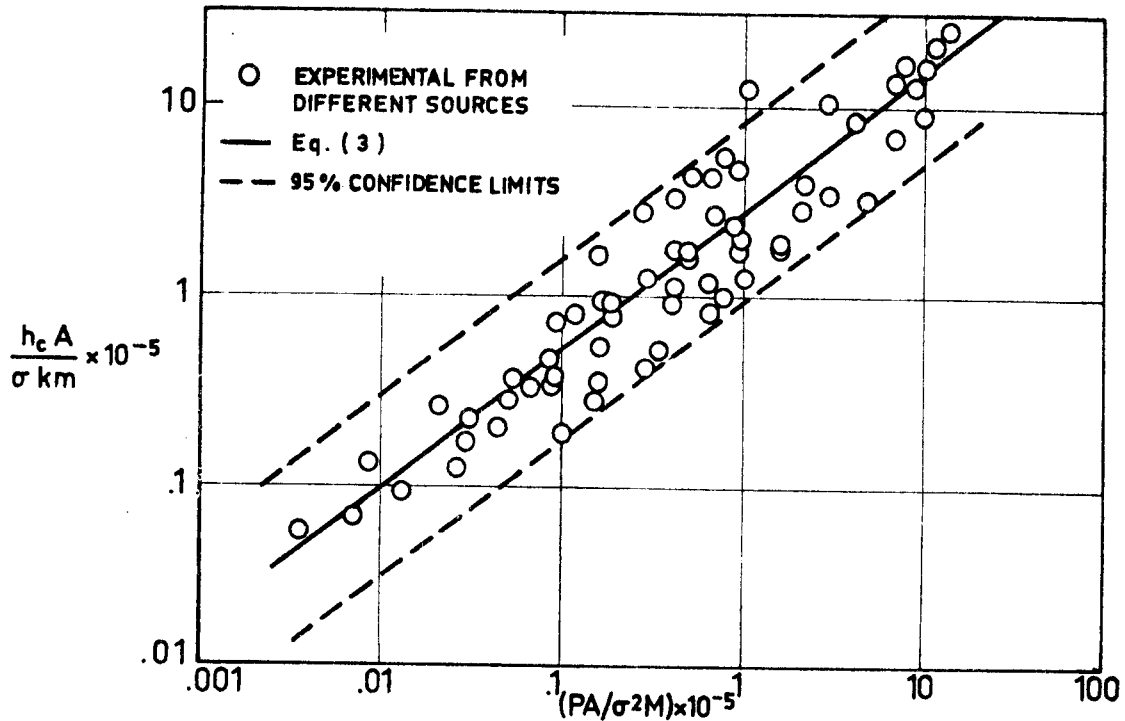


Fig 2-4. Dimensionless conductance vs. dimensionless load. Stainless steel under vacuum conditions. From Thomas & Probert (1972).

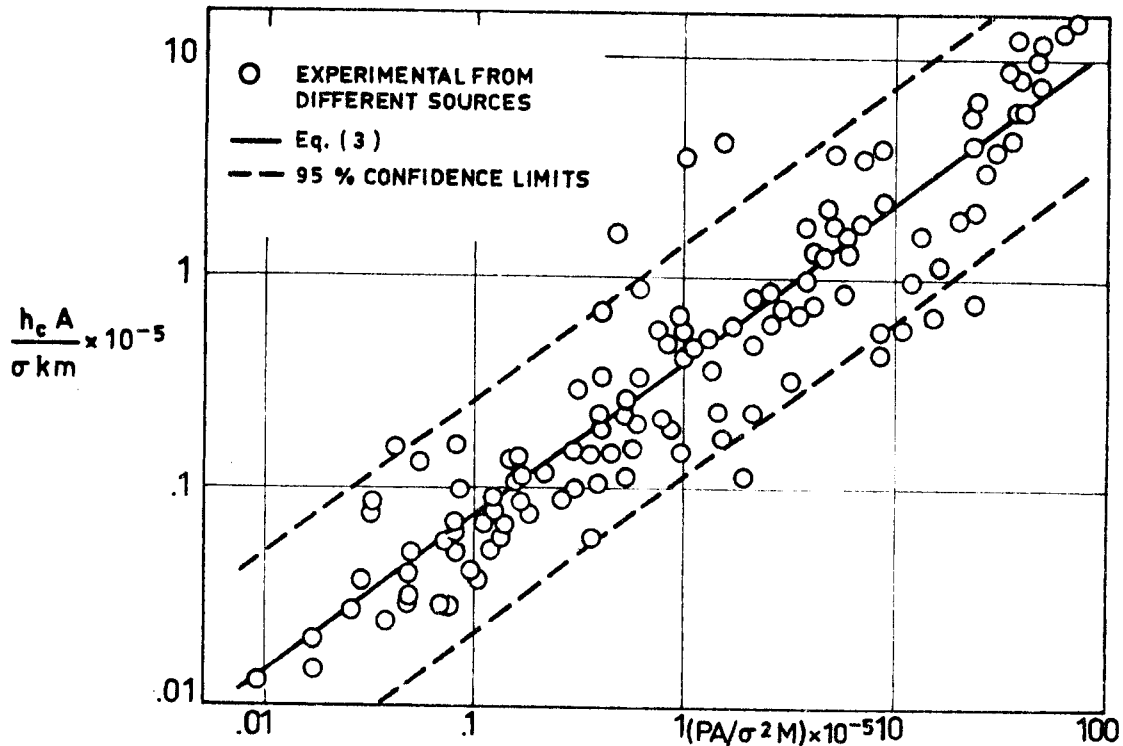


Fig 2-5. Dimensionless conductance vs. dimensionless load. One or both surfaces are aluminium. Vacuum conditions. From Thomas & Probert (1972).

THERMAL JOINT CONDUCTANCE
Bare Metallic Joints

2.3. BARE METALLIC JOINTS

SPECIMENS: Two cylinders, Al - 4.3 Cu - 1.5 Mg - 0.6 Mn. (Al 2024-T4).

Radius, $b = 2.54 \times 10^{-2}$ m.

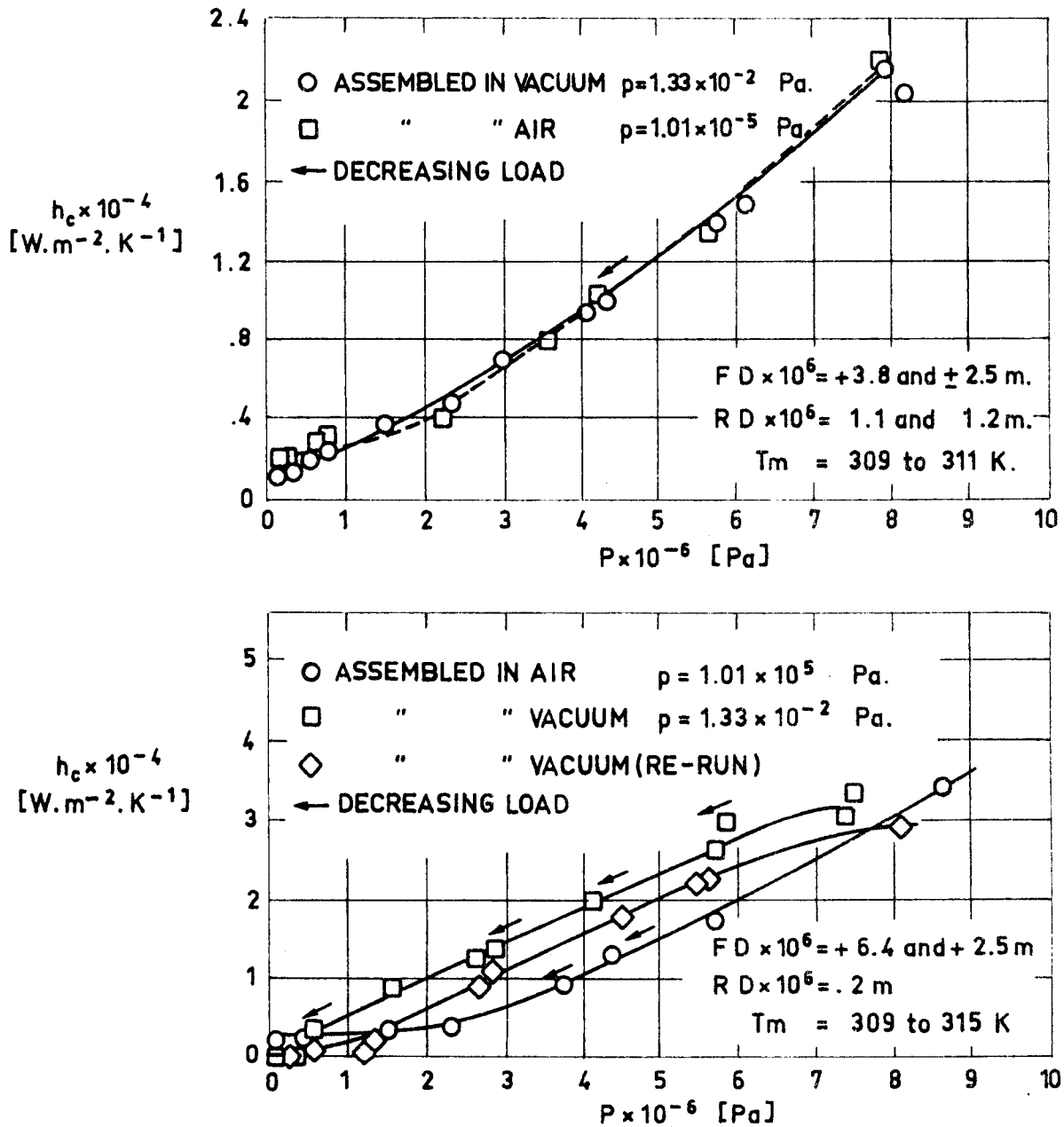


Fig 2-6. Plots of contact conductance vs. contact pressure for two different surface finishes. From Fried & Kelley (1966).

THERMAL JOINT CONDUCTANCE
Bare Metallic Joints

SPECIMENS: Two cylinders, Al - 1 Mg - 0.6 Si. (Al 6061-T6).

Radius, $b = 2.54 \times 10^{-2}$ m.

Ambient Pressure, $p = 1.33 \times 10^{-2}$ Pa.

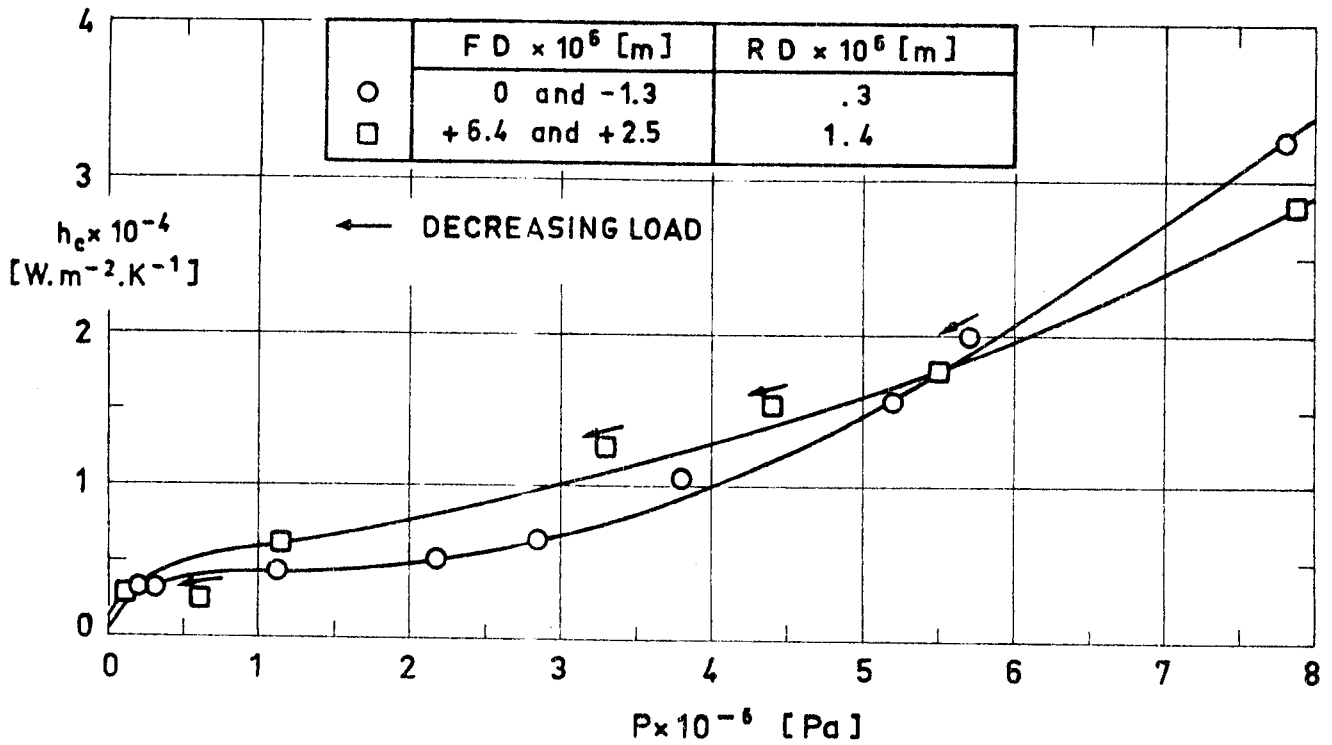


Fig 2-7. Plot of contact conductance vs. contact pressure for two different surface finishes. From Fried & Atkins (1965).

THERMAL JOINT CONDUCTANCE
Bare Metallic Joints

SPECIMENS: Two cylinders, Al - 5.5 Zn - 2.5 Mg - 1.5 Cu. (Al 7075-T6).

Radius, $b = 1.27 \times 10^{-2}$ m.

Ambient Pressure, $p = 1.33 \times 10^{-3}$ Pa.

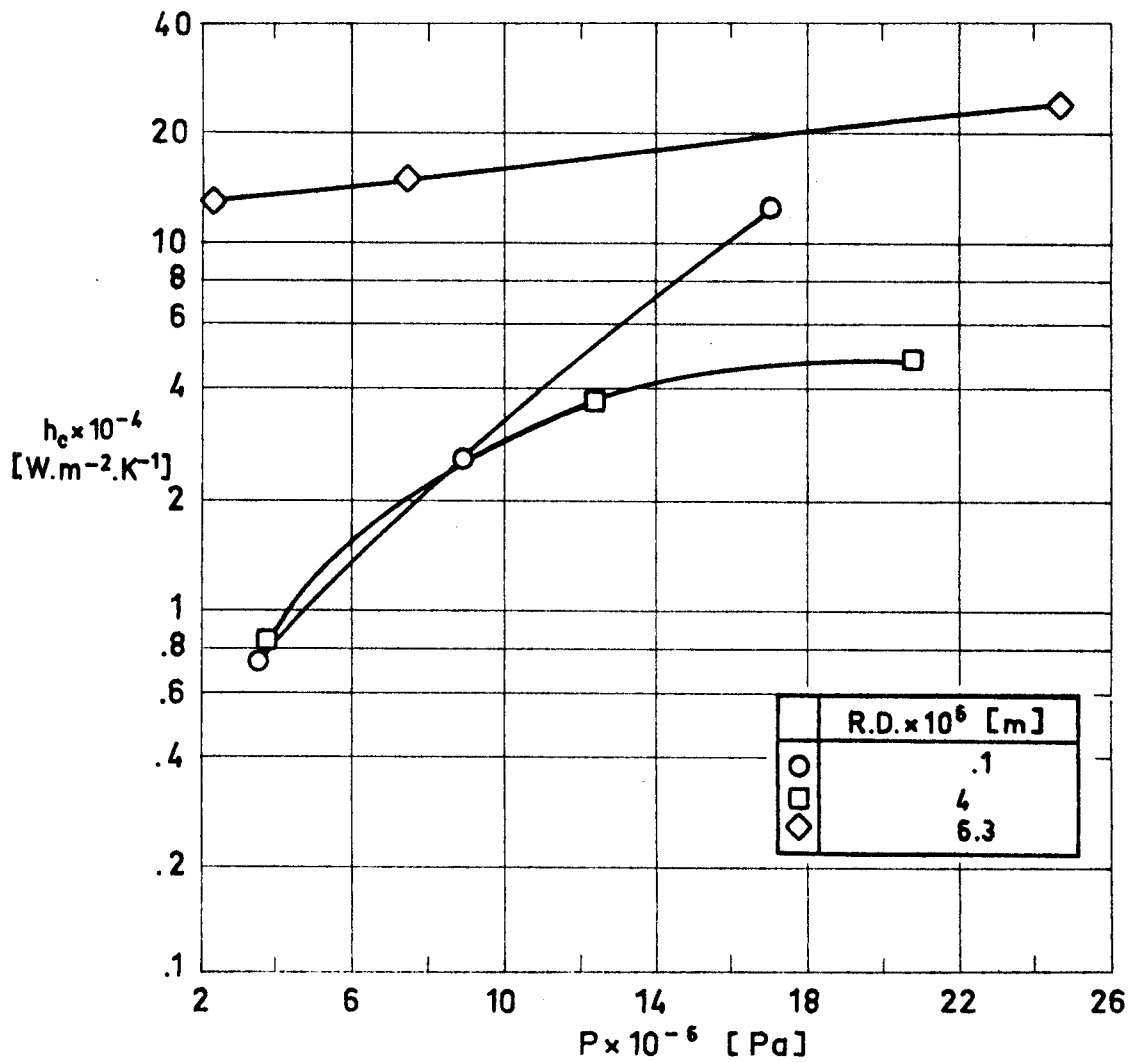


Fig 2-8. Plot of contact conductance vs. contact pressure for different surface finishes. From Fried (1966) quoted by Scollon & Carpitella (1970).

THERMAL JOINT CONDUCTANCE
Bare Metallic Joints

SPECIMENS: Two cylinders, Be

Radius, $b = 2.54 \times 10^{-2}$ m.

Flatness Deviation, $FD = +3.8 \times 10^{-6}$ and $+3 \times 10^{-6}$ m.

Roughness Deviation, $RD = .1 \times 10^{-6}$ m.

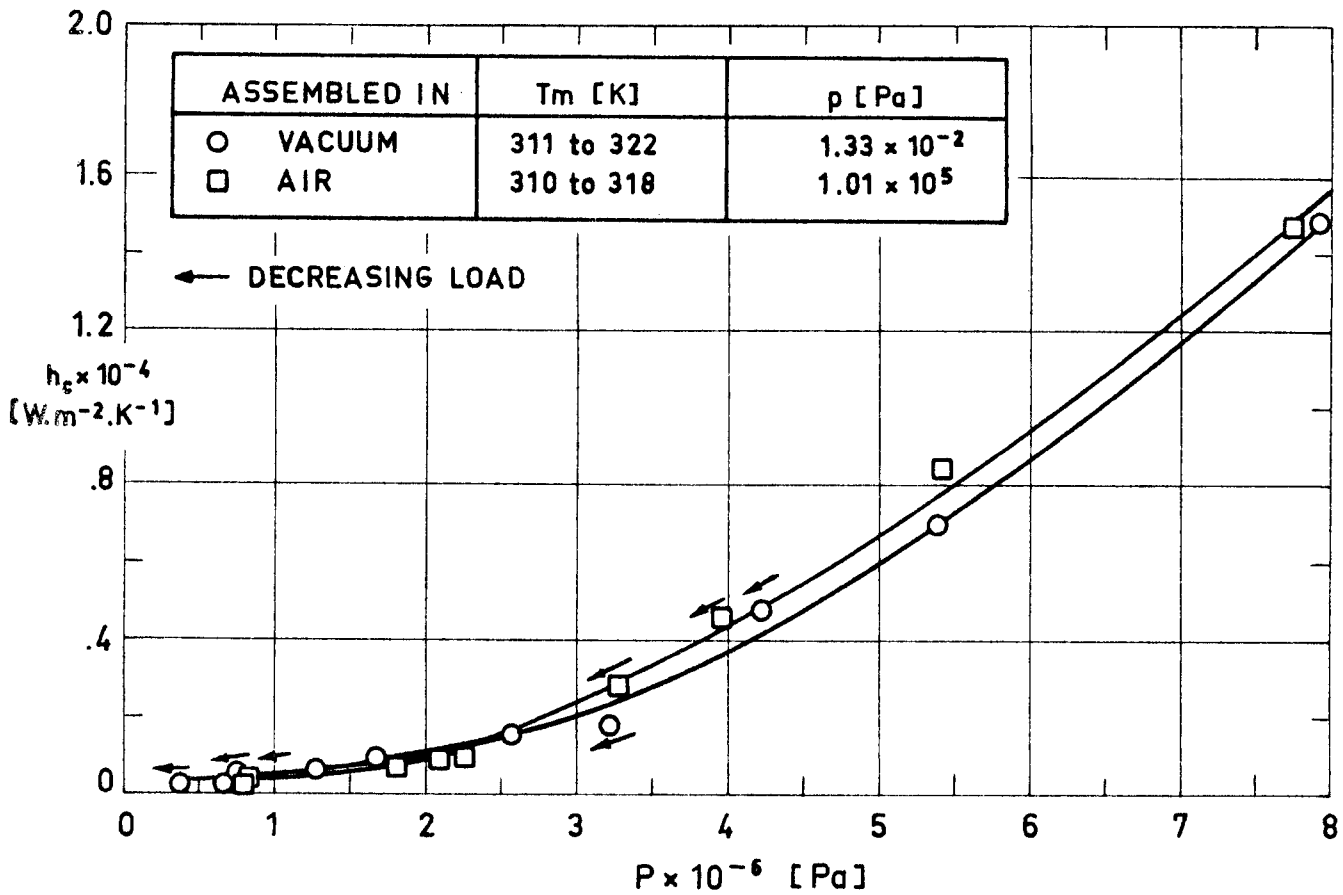


Fig 2-9. Plot of contact conductance vs. contact pressure for different ambient pressures. From Fried & Kelley (1966).

THERMAL JOINT CONDUCTANCE
Bare Metallic Joints

SPECIMENS: Two cylinders, Cu OFHC
(OFHC: Oxygen Free High Conductivity).

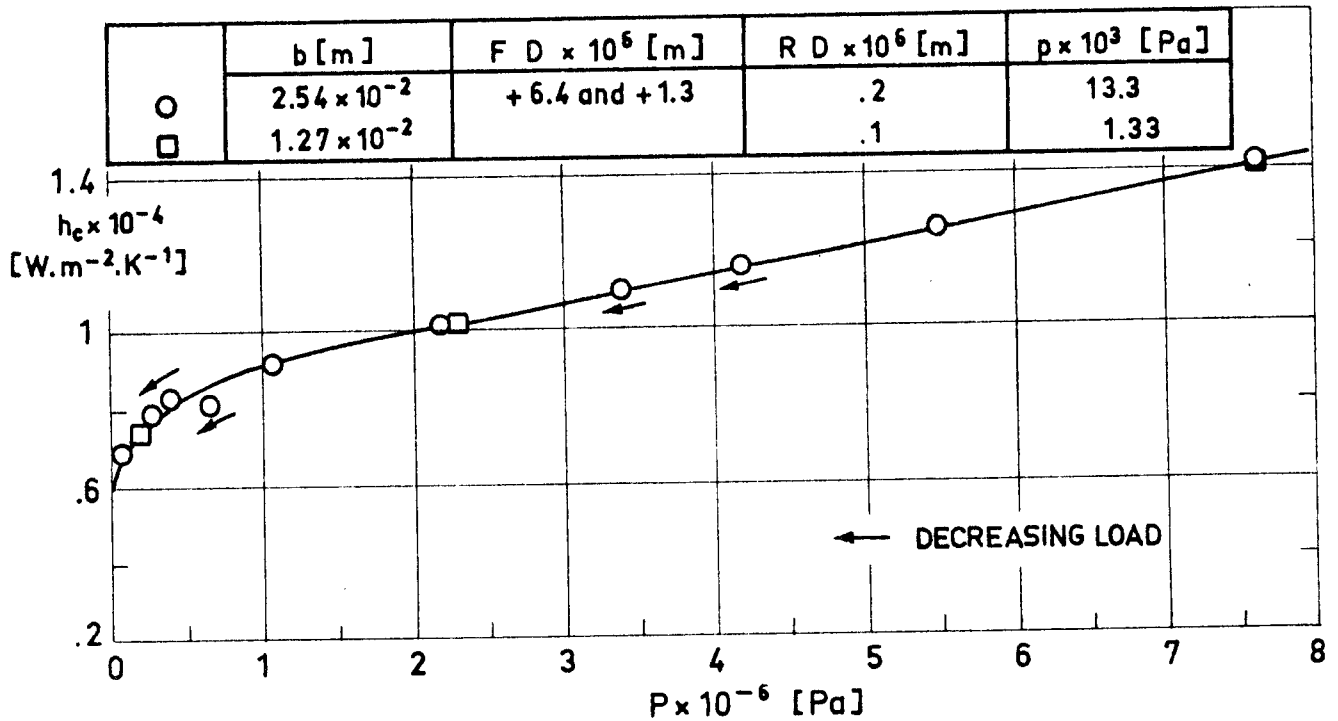
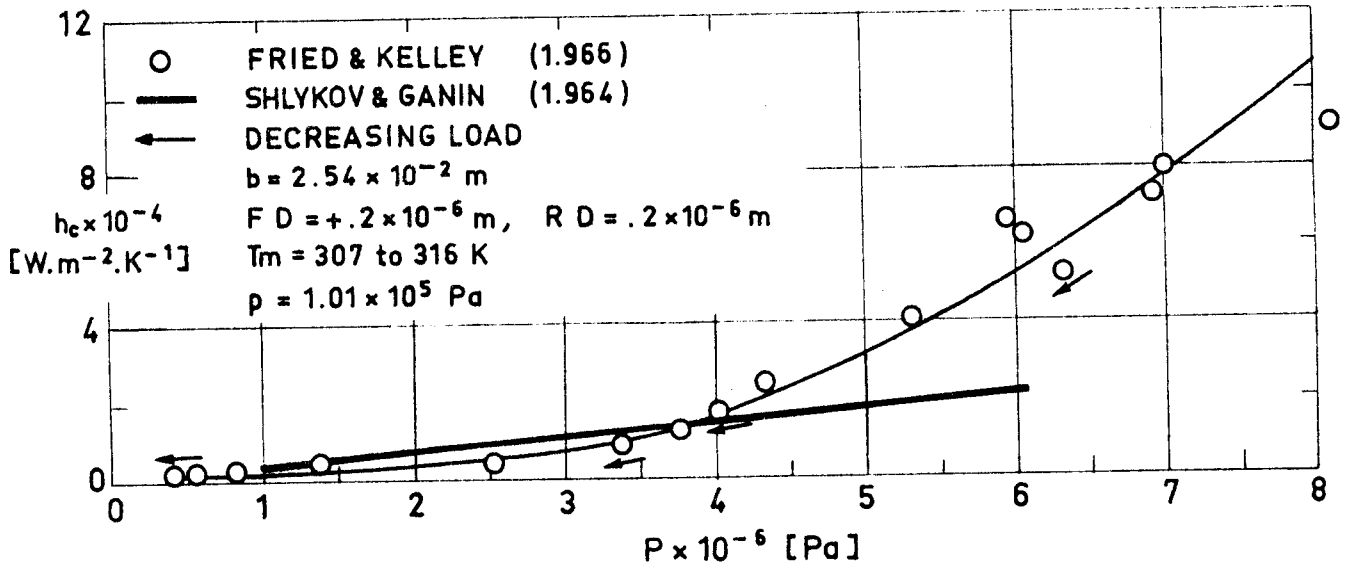


Fig 2-10. Plots of contact conductance vs. contact pressure for different surface finishes and ambient pressures. ○ From Fried & Atkins (1965). □ From Fried (1966) quoted by Scollon & Carpitella (1970).

THERMAL JOINT CONDUCTANCE
Bare Metallic Joints

SPECIMENS: Two cylinders, Cu - 35 Zn - 3 Pb (Brass, Anaconda alloy 271)

Radius, $b = 1.27 \times 10^{-2}$ m.

Roughness Deviation, $RD = .1 \times 10^{-6}$ m.

Ambient Pressure, $p = .66 \times 10^{-3}$ Pa.

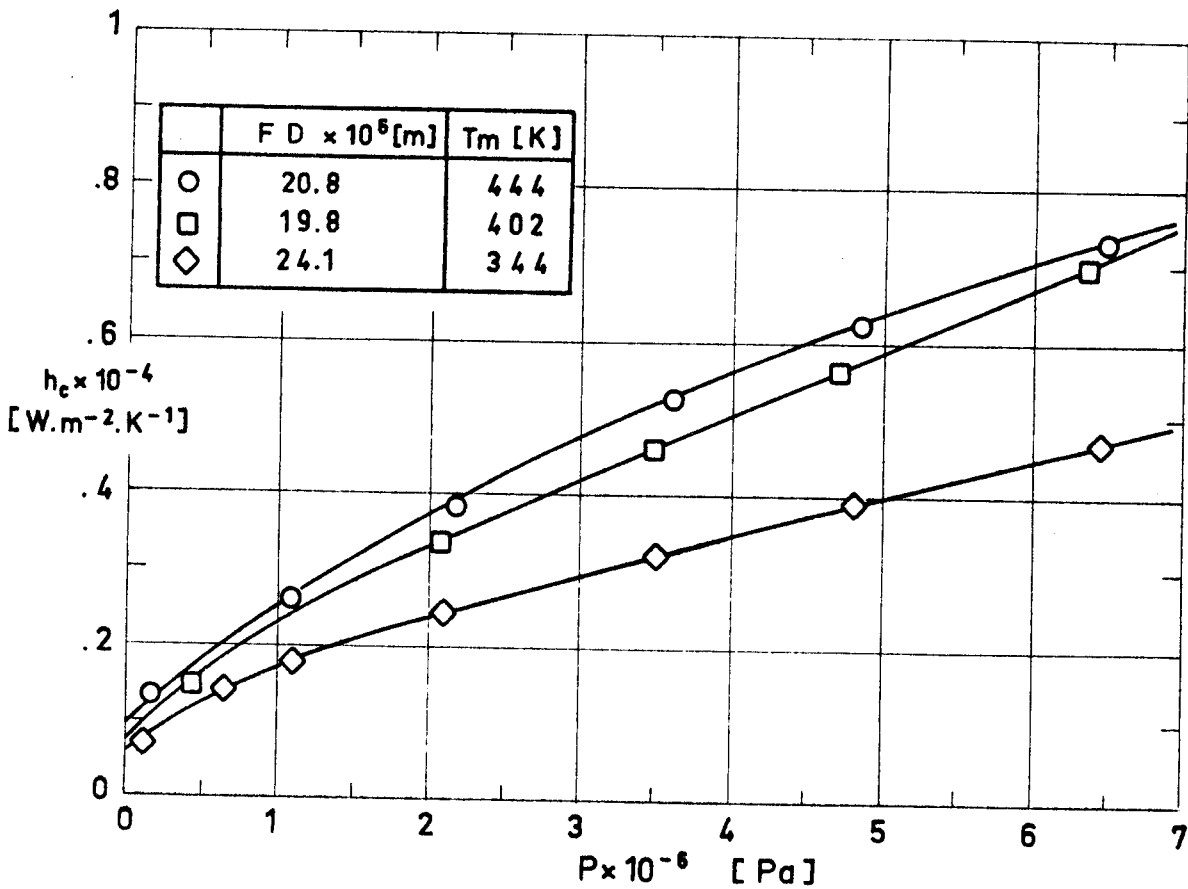


Fig 2-11. Plot of contact conductance vs. contact pressure for different surface finishes. From Clausing & Chao (1965).

THERMAL JOINT CONDUCTANCE
Bare Metallic Joints

SPECIMENS: Two cylinders, Mg - 3 Al - 1 Zn - .2 Mn. (Mg AZ-31B).

Radius, $b = 2.54 \times 10^{-2}$ m.

Ambient Pressure, $p = 1.33 \times 10^{-2}$ Pa.

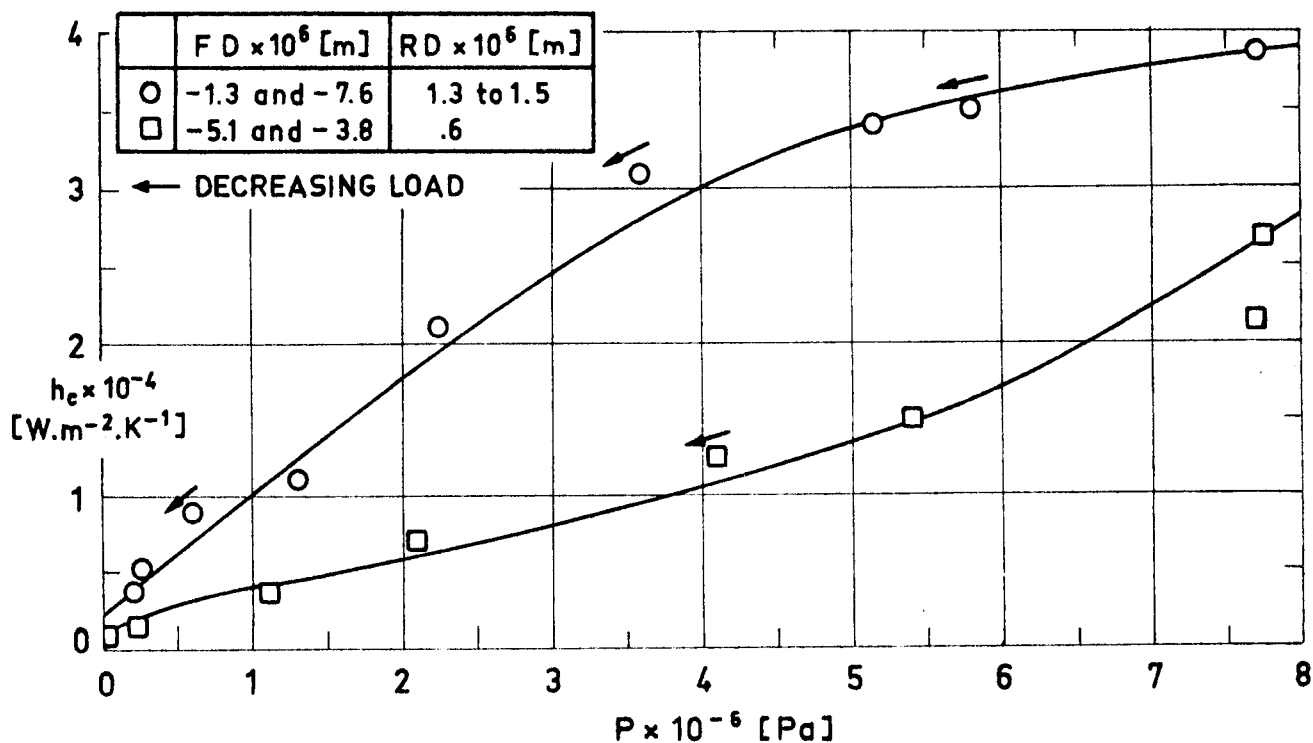


Fig 2-12. Plot of contact conductance vs. contact pressure for different surface finishes. From Fried & Atkins (1965).

Comments: Oxide films were detected on both test surfaces. This could be the explanation of the higher conductance exhibited by the coarse finish.

THERMAL JOINT CONDUCTANCE
Bare Metallic Joints

SPECIMENS: Two cylinders, Mg - 3 Al - 1 Zn - 0.2 Mn. (Mg AZ-31B).

Radius, $b = 1.27 \times 10^{-2}$ m.

Roughness Deviation, $RD = .1 \times 10^{-6}$ m.

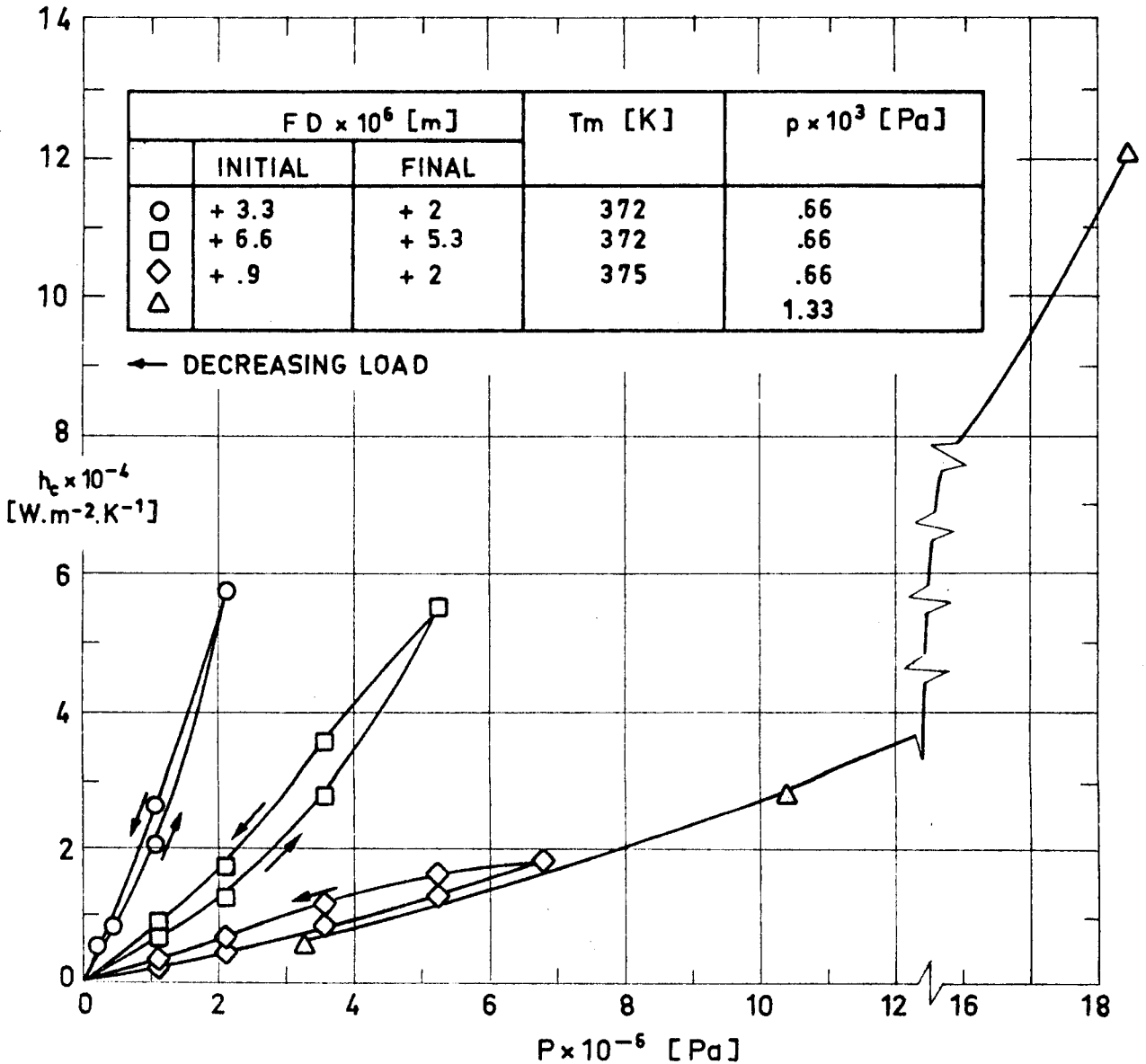


Fig 2-13. Plot of contact conductance vs. contact pressure for various surface finishes, mean temperatures and ambient pressures. —○—, —◻—, —◊— from Clausing & Chao (1965). —△— from Fried (1966) quoted by Scollon & Carpitella (1970).

Comments: Notice the effect of loading and unloading. In the case of the curve —◊—, a film was detected on both test surfaces.

THERMAL JOINT CONDUCTANCE
Bare Metallic Joints

SPECIMENS: Two cylinders, Fe - 19 Cr - 10 Ni (SS 304) and Al - 4.3 Cu - 1.5 Mg - 0.6 Mn (Al 2024-T4).

Radius, $b = 2.54 \times 10^{-2}$ m.

Flatness Deviation, $FD = -1.3 \times 10^{-6}$ and $+6.4 \times 10^{-6}$ m.

Roughness Deviation, $RD = .3 \times 10^{-6}$ and $.2 \times 10^{-6}$ m.

Mean Temperature, $T_m = 302$ to 321 K.

Ambient Pressure, $p = 1.33 \times 10^{-2}$ Pa.

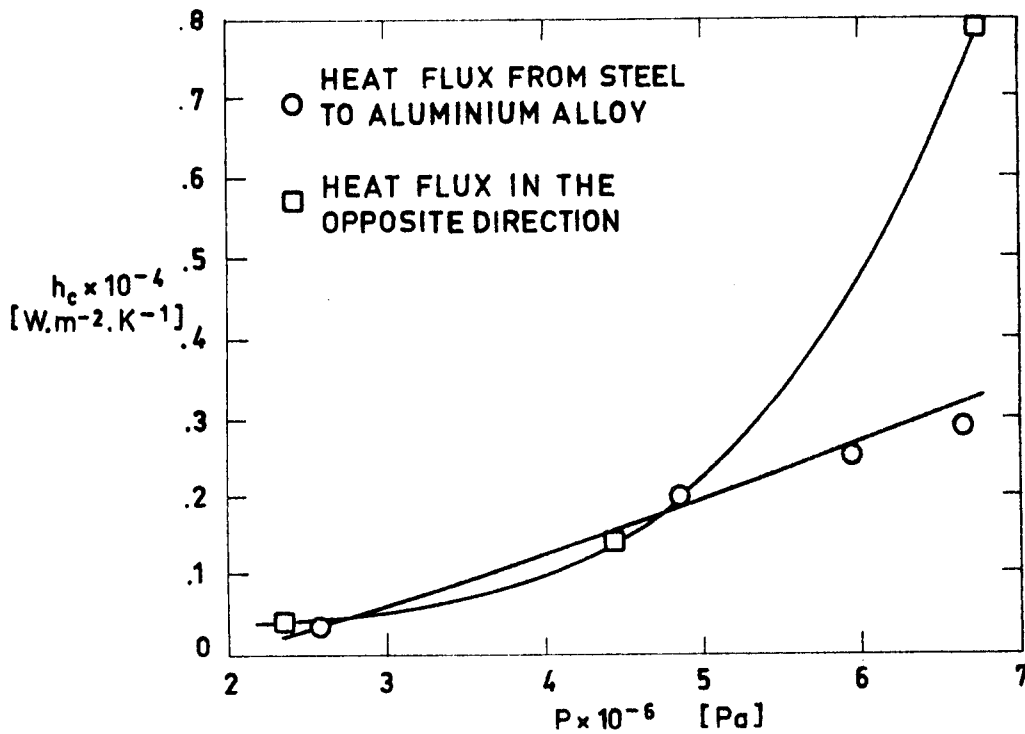


Fig 2-14. Plot of contact conductance vs. contact pressure. Notice the directional effect on contact conductance. From Fried & Kelley (1966).

THERMAL JOINT CONDUCTANCE
Bare Metallic Joints

SPECIMENS: Two cylinders, Fe - 19 Cr - 10 Ni (SS 304).

Radius, $b = 2.54 \times 10^{-2}$ m.

Ambient Pressure, $p = 1.33 \times 10^{-2}$ Pa.

$h_c \times 10^{-4}$
[W.m⁻².K⁻¹]

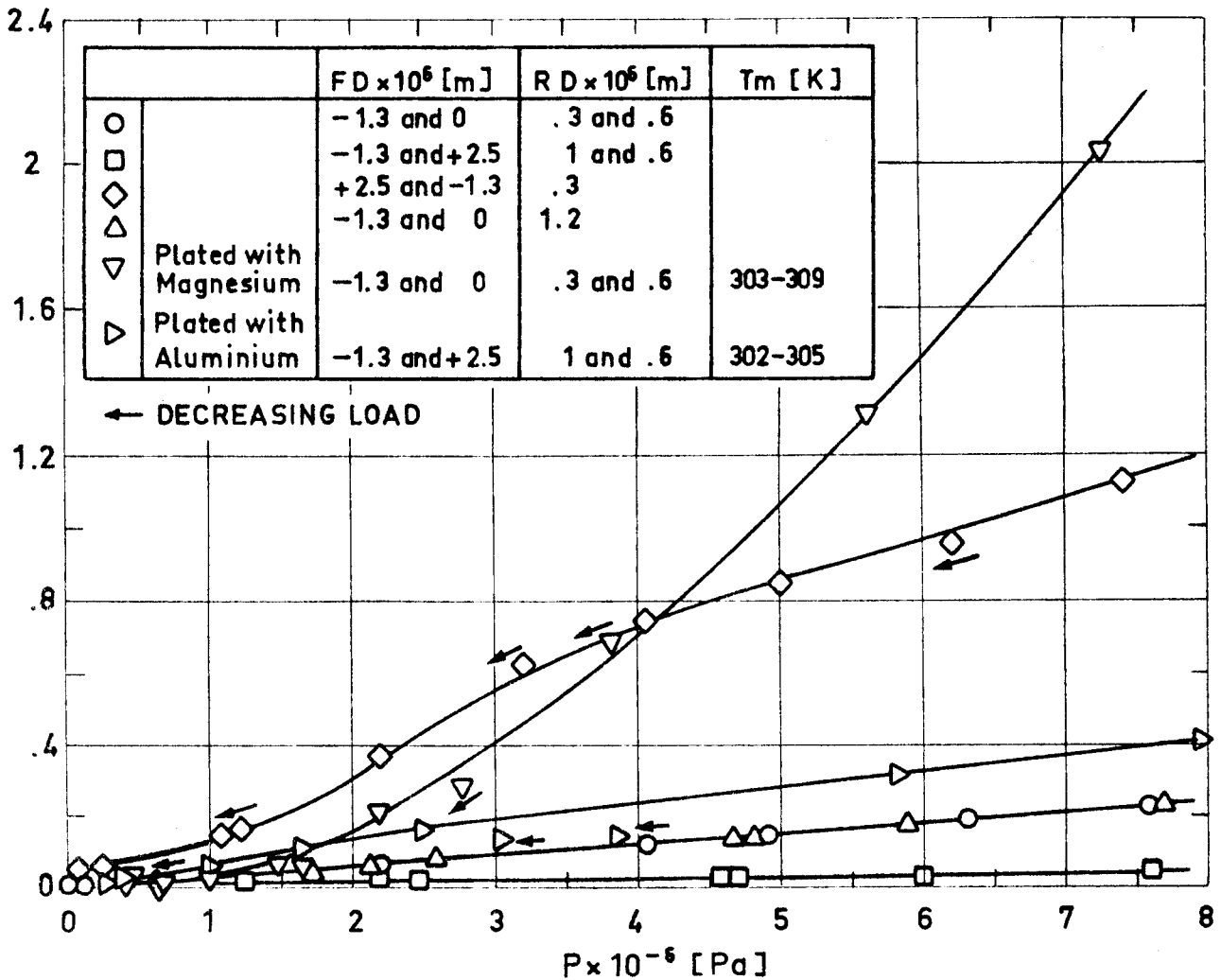


Fig 2-15. Plot of contact conductance vs. contact pressure for different surface finishes. —○—, —□— from Fried (1965). —◇—, —△— from Fried & Atkins (1965). —▽—, —▷— from Fried & Kelley (1966).

THERMAL JOINT CONDUCTANCE
Bare Metallic Joints

SPECIMENS: Two cylinders, Fe - 19 Cr - 10 Ni. (SS-304).

Radius, $b = 1.27 \times 10^{-2}$ m.

Ambient Pressure, $p = 1.33 \times 10^{-3}$ Pa.

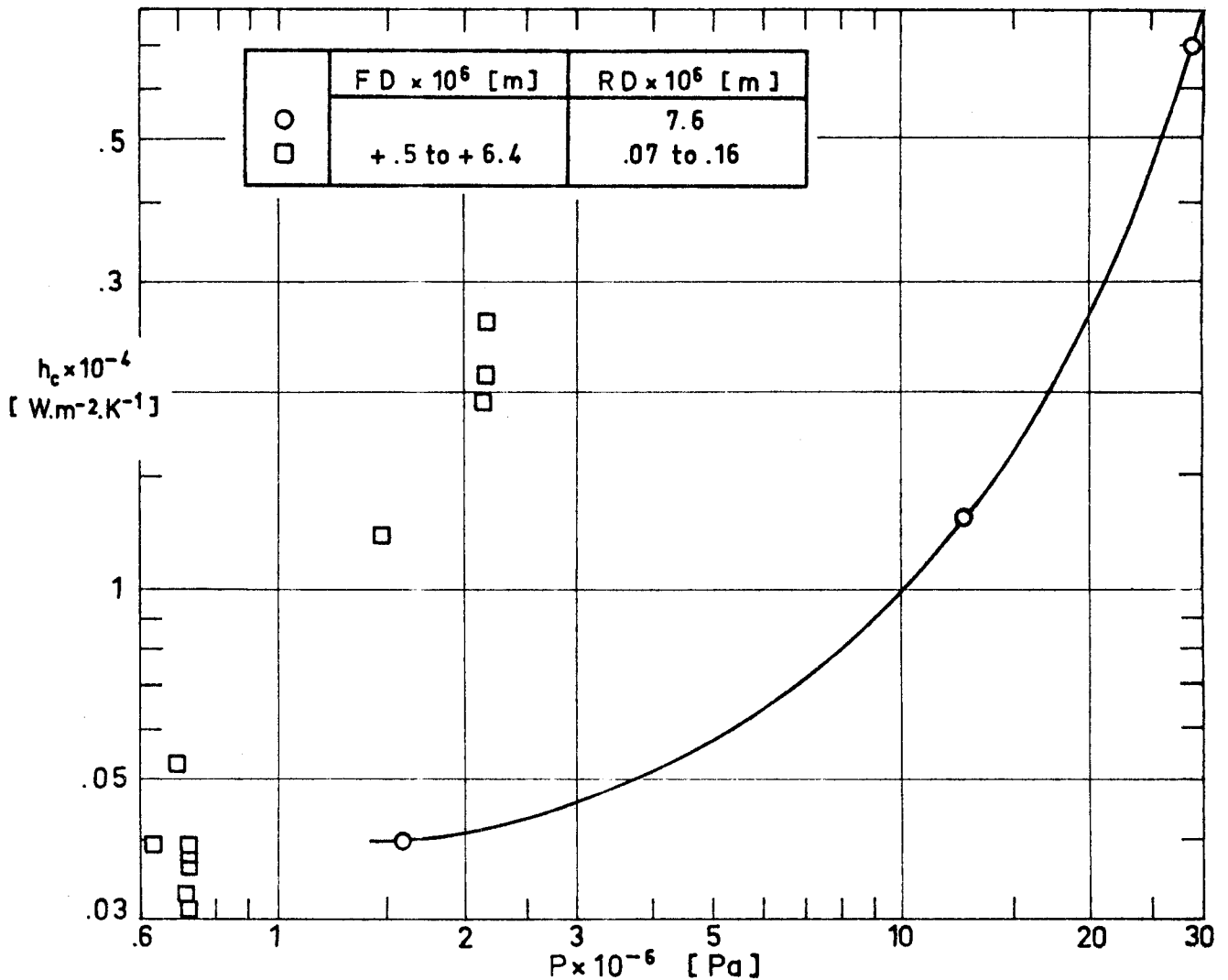


Fig 2-16. Plot of contact conductance vs. contact pressure for different surface finishes. —○— From Fried (1966) quoted by Scollon & Carpitella (1970). —□— From Gyrog (1970).

THERMAL JOINT CONDUCTANCE
Bare Metallic Joints

SPECIMENS: Two cylinders, Ti - 6 Al - 4 V . (Ti 6 Al 4 V) .

Radius, $b = 1.27 \times 10^{-2}$ m.

Ambient Pressure, $p = 1.33 \times 10^{-3}$ Pa.

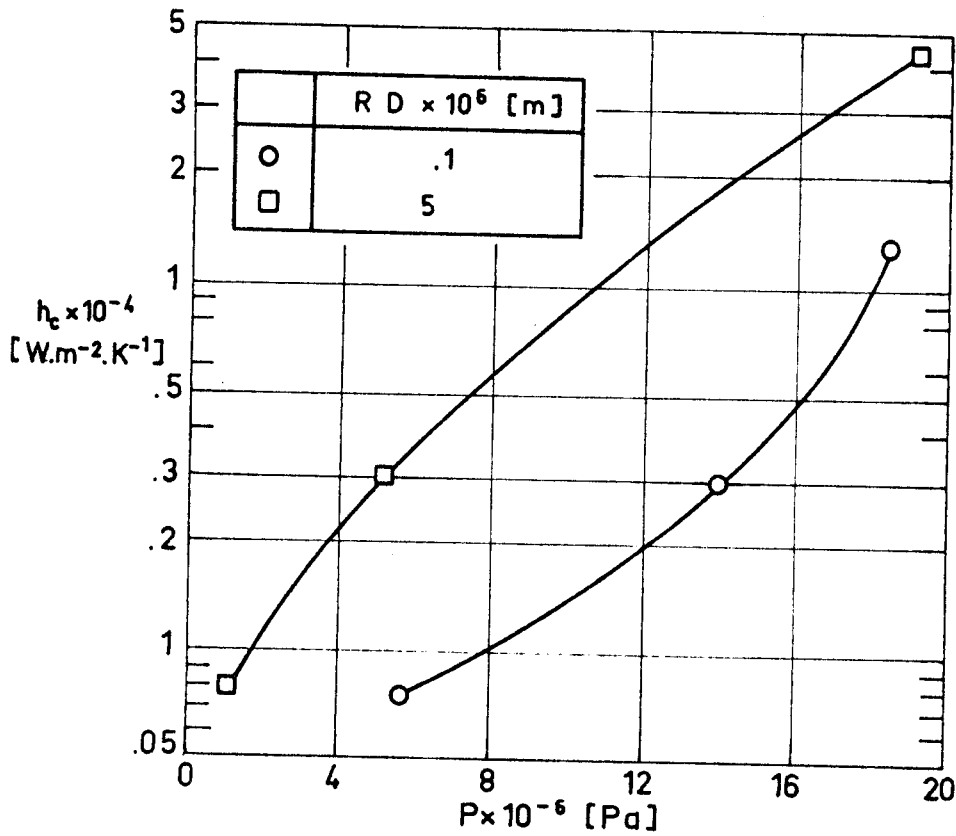


Fig 2-17. Plot of contact conductance vs. contact pressure for different surface finishes. From Fried (1966) quoted by Scollon & Carpitella (1970).

THERMAL JOINT CONDUCTANCE
Metallic Foils between Similar Metals

2.4. METALLIC FOILS BETWEEN SIMILAR METALS

FILLER: Indium Foil, 99.99 percent pure.

Density, $\rho = 7\,310 \text{ kg.m}^{-3}$

Initial Thickness, $t = 2.5 \times 10^{-5} \text{ m}$.

SPECIMENS: Two cylinders as indicated below.

Radius, $b = 1.27 \times 10^{-2} \text{ m}$.

Ambient Pressure, $p = 1.33 \times 10^{-3} \text{ Pa}$.

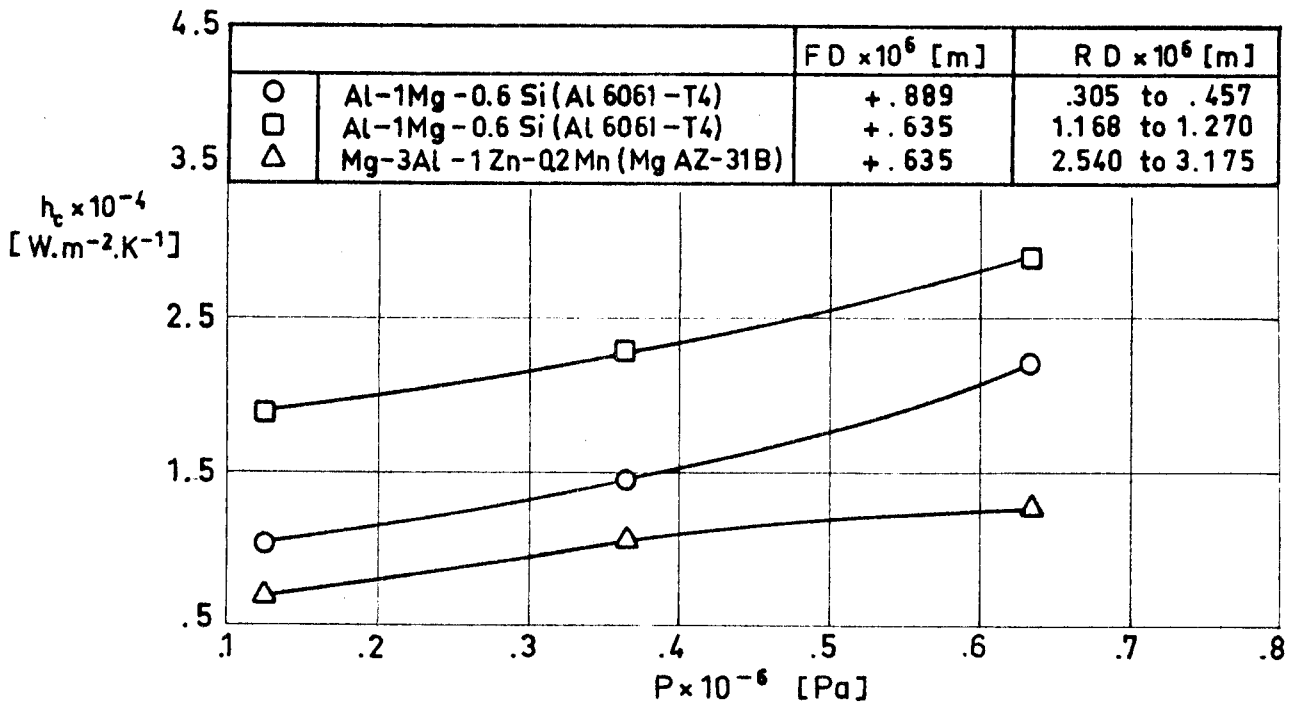


Fig 2-18. Plot of contact conductance vs. contact pressure.
From Cunnington (1964).

Cost of the filler: $1\,300 \text{ SF.kg}^{-1}$ (Fluka).

INTENTIONALLY BLANK PAGE

THERMAL JOINT CONDUCTANCE
Metallic Oxide Powders between Similar Metals

2.5. METALLIC OXIDE POWDERS BETWEEN SIMILAR METALS

FILLER: Rutile powder.

SPECIMENS: Two cylinders, Fe - 19 Cr - 10 Ni. (SS 304).

Radius, $b = 1.27 \times 10^{-2}$ m.
 Flatness Deviation, $FD = +.508 \times 10^{-6}$ to $+.635 \times 10^{-6}$ m.
 Roughness Deviation, $RD = .076 \times 10^{-6}$ to $.152 \times 10^{-6}$ m.
 Mean Temperature, $T_m = 387$ K.
 Ambient Pressure, $p = 1.33 \times 10^{-3}$ Pa.

Table 2-1

Values of contact conductance vs. contact pressure.

$P \times 10^{-3}$ [Pa]	h_c [$W \cdot m^{-2} \cdot K^{-1}$]
627	128
2 137	271

From Gyrog (1970).

Cost of the filler: 0.5 US \$.kg⁻¹

INTENTIONALLY BLANK PAGE

THERMAL JOINT CONDUCTANCE

Porous Metallic Materials between Similar Metals

2.6. POROUS METALLIC MATERIALS BETWEEN SIMILAR METALS

Understanding of the data in this Section requires some familiarity with the following concepts concerning porous materials.

The porosity, ϕ , of a porous material is the fraction of the bulk volume of the material occupied by voids.

Filters may be rated according to its degree of filtration. A filter rated, for example, $r = 25 \times 10^{-6}$ m., will, when new and clean, stop 98 per cent of the particles measuring 25×10^{-6} m or more while operating under its designed flow conditions.

Filter Rating, in m, should not be mixed up with Filtration Rate, which is the volume of liquid passing through a unit area of the filter medium in a unit time, for a given pressure loss. This rate is measured in $m.s^{-1}$.

THERMAL JOINT CONDUCTANCE
 Porous Metallic Materials between Similar Metals

FILLER: Porous Copper.

Porosity, $\phi = .8$
 Fiber Diameter, $d = .4 \times 10^{-4}$ m.
 Filter Rating, $r = .145 \times 10^{-3}$ m.
 Initial Thickness, $t = .66 \times 10^{-3}$ m.

SPECIMENS: Two cylinders, Al - 4.3 Cu - 1.5 Mg - 0.6 Mn. (Al 2024-T4).

Radius, $b = 1.27 \times 10^{-2}$ m.
 Ambient Pressure, $p = 1.33 \times 10^{-3}$ Pa.

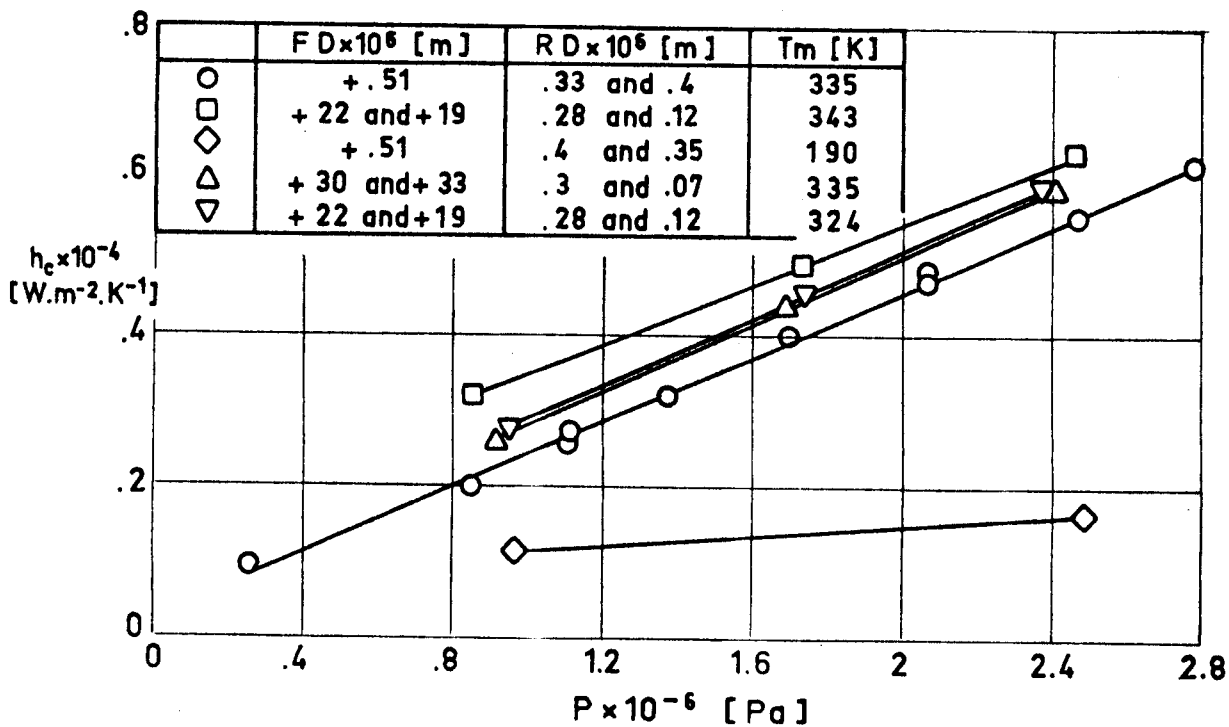


Fig 2-19. Plot of contact conductance vs. contact pressure for different surface finishes and mean temperatures. From Miller & Fletcher (1973).

The filler is an structure of sintered metallic fibers. In this particular case it has been manufactured by Huyck Metals Co., USA.

Cost of the filler:

THERMAL JOINT CONDUCTANCE

Porous Metallic Materials between Similar Metals

FILLER: Porous Nickel.

Porosity, $\phi = .8$
 Fiber Diameter, $d = .12 \times 10^{-4}$ m.
 Filter Rating, $r = .6 \times 10^{-4}$ m.
 Initial Thickness, $t = 2.05 \times 10^{-3}$ m.

SPECIMENS: Two cylinders, Al - 4.3 Cu - 1.5 Mg - 0.6 Mn. (Al 2024-T4).

Radius, $b = 1.27 \times 10^{-2}$ m.
 Ambient Pressure, $p = 1.33 \times 10^{-3}$ Pa.

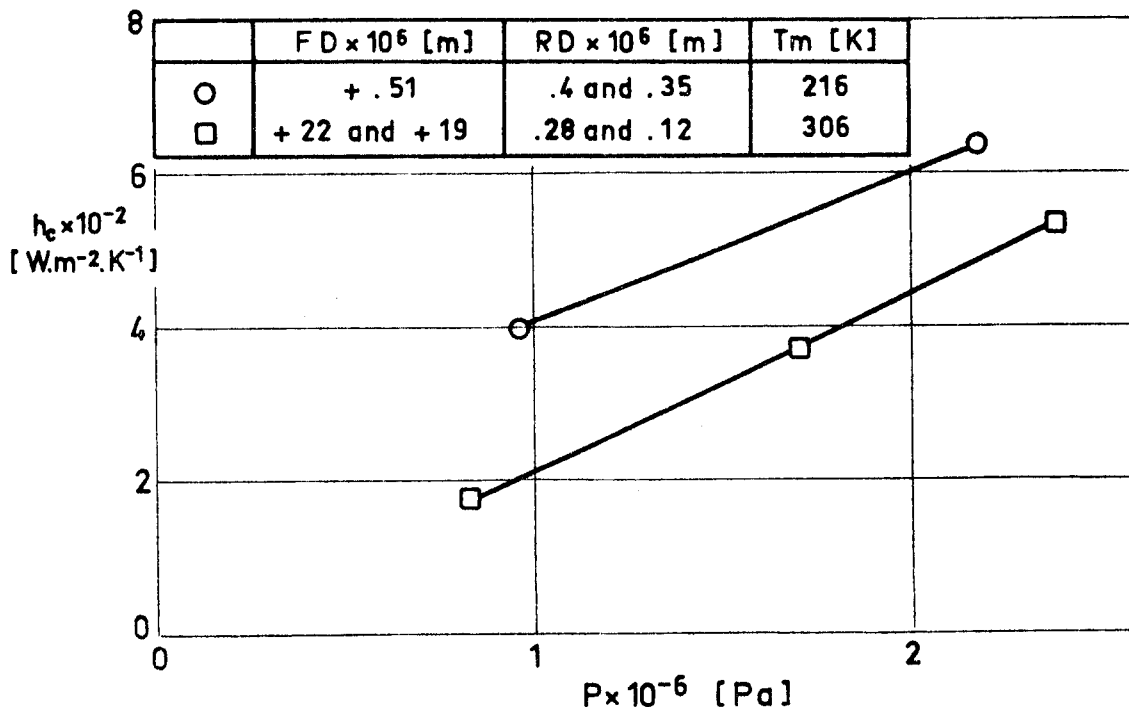


Fig 2-20. Plot of contact conductance vs. contact pressure for different surface finishes and mean temperatures. From Miller & Fletcher (1973).

The filler is an structure of sintered metallic fibers. In this particular case it has been manufactured by Huyck Metals Co., USA.

Cost of the filler:

THERMAL JOINT CONDUCTANCE
 Porous Metallic Materials between Similar Metals

FILLER: Porous Fe - 16 Cr (SS 430).

Porosity, $\phi = .68$ and $.80$
 Fiber Diameter, $d = .43 \times 10^{-4}$ and $.45 \times 10^{-4}$ m.
 Filter Rating, $r = 1 \times 10^{-4}$ and 1.5×10^{-4} m.
 Initial Thickness, $t = 1.67 \times 10^{-3}$ and 1.62×10^{-3} m.

SPECIMENS: Two cylinders, Al - 4.3 Cu - 1.5 Mg - 0.6 Mn. (Al 2024-T4).

Radius, $b = 1.27 \times 10^{-2}$ m.
 Flatness Deviation, $FD = +.30 \times 10^{-4}$ and $+.33 \times 10^{-4}$ m.
 Roughness Deviation, $RD = .30 \times 10^{-6}$ and $.07 \times 10^{-6}$ m.
 Mean Temperature, $T_m = 341$ K.
 Ambient Pressure, $p = 1.33 \times 10^{-3}$ Pa.

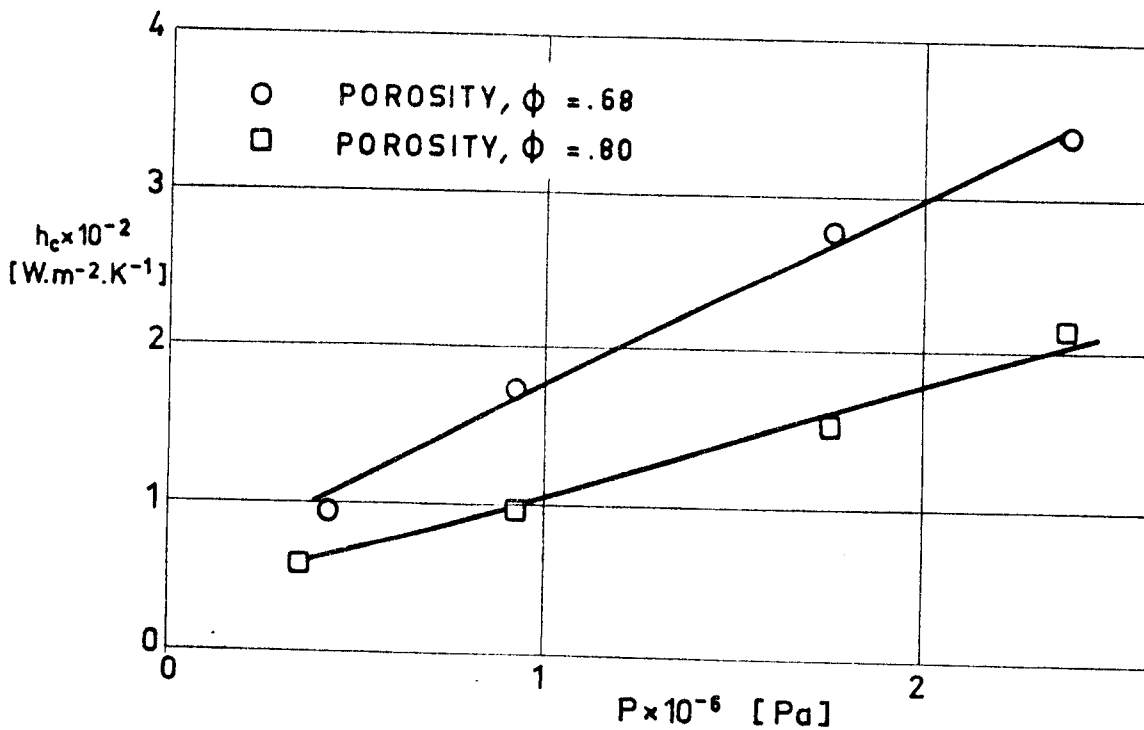


Fig 2-21. Plot of contact conductance vs. contact pressure for different porosities. From Miller & Fletcher (1973). The filler is an structure of sintered metallic fibers. In this particular case it has been manufactured by Huyck Metals Co., USA. Cost of the filler:

THERMAL JOINT CONDUCTANCE

Porous Metallic Materials between Similar Metals

FILLER: Stainless Steel 149×10^{-6} m. Mesh Screen.Density, $\rho = 8\,009 \text{ kg.m}^{-3}$ Initial Thickness, $t = 2.29 \times 10^{-3}$ m.

SPECIMENS: Two cylinders, Fe - 19 Cr - 10 Ni. (SS 304).

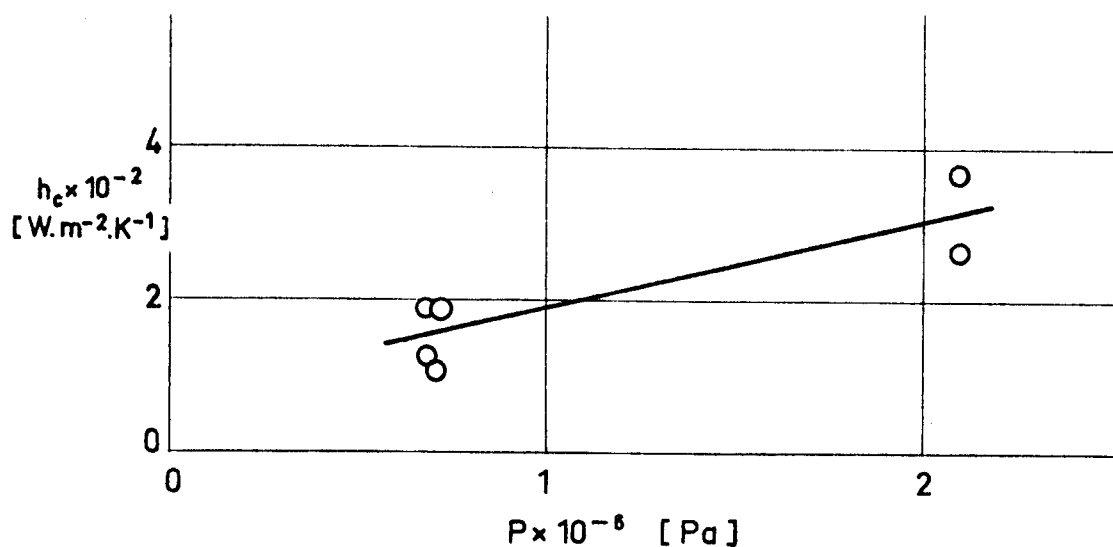
Radius, $b = 1.27 \times 10^{-6}$ m.Flatness Deviation, $FD = +.508 \times 10^{-6}$ to $+.635 \times 10^{-6}$ m.Roughness Deviation, $RD = .076 \times 10^{-6}$ to $.152 \times 10^{-6}$ m.Mean Temperature, $T_m = 236$ to 418 K.Ambient Pressure, $p = 1.33 \times 10^{-3}$ Pa.

Fig 2-22. Plot of contact conductance vs. contact pressure.
From Gyrog (1970).

Cost of the filler: 20 US \$.m⁻²

THERMAL JOINT CONDUCTANCE
Porous Metallic Materials between Similar Metals

FILLER: Stainless Steel 2×10^{-3} m. Mesh Screen.

Density, $\rho = 8\ 009\ \text{kg.m}^{-3}$

Initial Thickness, $t = 1.27 \times 10^{-3}$ m.

SPECIMENS: Two cylinders, Fe - 19 Cr - 10 Ni. (SS 304).

Radius, $b = 1.27 \times 10^{-2}$ m.

Flatness Deviation, $FD = +.508 \times 10^{-6}$ to $+.635 \times 10^{-6}$ m.

Roughness Deviation, $RD = .076 \times 10^{-6}$ to $.152 \times 10^{-6}$ m.

Mean Temperature, $T_m = 219$ to 385 K.

Ambient Pressure, $p = 1.33 \times 10^{-3}$ Pa.

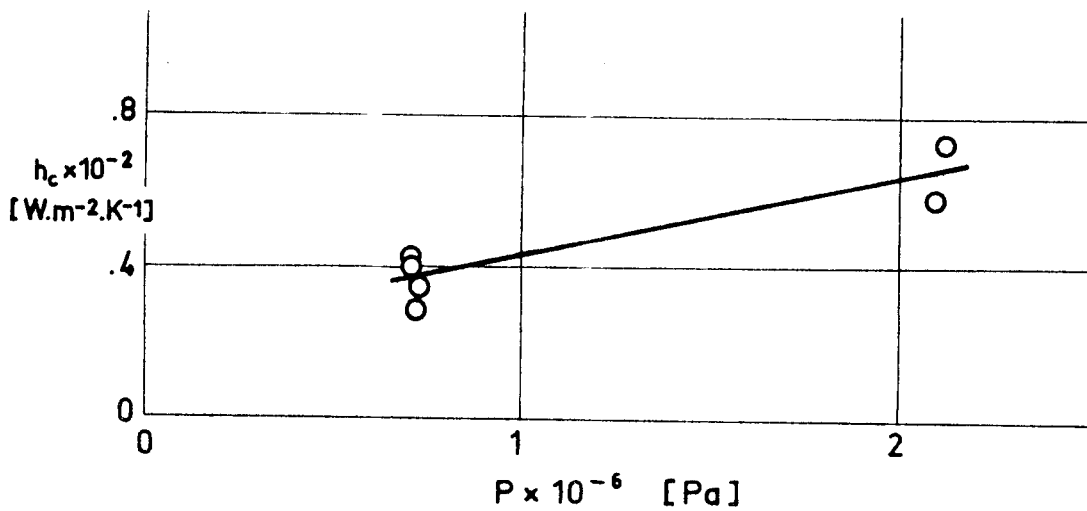


Fig 2-23. Plot of contact conductance vs. contact pressure.
From Gyrog (1970).

Cost of the filler: 11 US \$.m⁻²

THERMAL JOINT CONDUCTANCE
Insulating Spacers between Similar Metals

2.7. INSULATING SPACERS BETWEEN SIMILAR METALS

FILLER: Asbestos Board

Density, $\rho = 2\ 178\ \text{kg.m}^{-3}$

Initial Thickness, $t = 3.38 \times 10^{-3}\ \text{m}$.

Appearance after thermal test: No apparent effect

SPECIMENS: Two cylinders, Al - 4.3 Cu - 1.5 Mg - 0.6 Mn. (Al 2024).

Radius, $b = 1.27 \times 10^{-2}\ \text{m}$.

Flatness Deviation, $FD = +.635 \times 10^{-6}\ \text{m}$.

Roughness Deviation, $RD = .127 \times 10^{-6}\ \text{m}$.

Mean Temperature, $T_m = 366\ \text{K}$.

Ambient Pressure, $p = 1.33 \times 10^{-3}\ \text{to}\ 1.33 \times 10^{-4}\ \text{Pa}$.

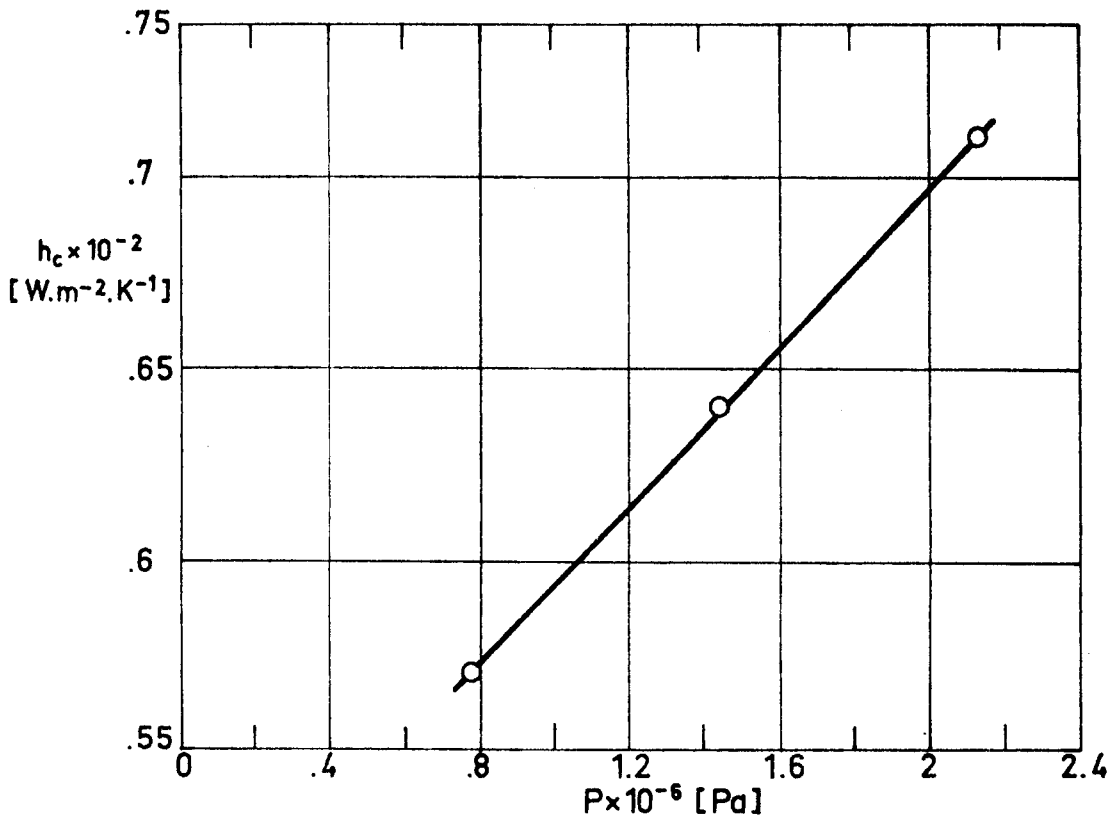


Fig 2-24. Plot of contact conductance vs. contact pressure.

From Fletcher, Smuda & Gyrog (1969).

Cost of the filler: 1 US \$.kg⁻¹, 7 US \$.m⁻² (on basis of density).

THERMAL JOINT CONDUCTANCE
Insulating Spacers between Similar Metals

FILLER: Asbestos Tape (No. 2074)

Density, $\rho = 880 \text{ kg.m}^{-3}$

Initial Thickness, $t = 1.67 \times 10^{-3} \text{ m.}$

Appearance after thermal test: No apparent effect

SPECIMENS: Two cylinders, Al - 4.3 Cu - 1.5 Mg - 0.6 Mn. (Al 2024).

Radius, $b = 1.27 \times 10^{-2} \text{ m.}$

Flatness Deviation, $FD = +.635 \times 10^{-6} \text{ m.}$

Roughness Deviation, $RD = .127 \times 10^{-6} \text{ m.}$

Mean Temperature, $T_m = 369 \text{ K.}$

Ambient Pressure, $p = 1.33 \times 10^{-3} \text{ to } 1.33 \times 10^{-4} \text{ Pa.}$

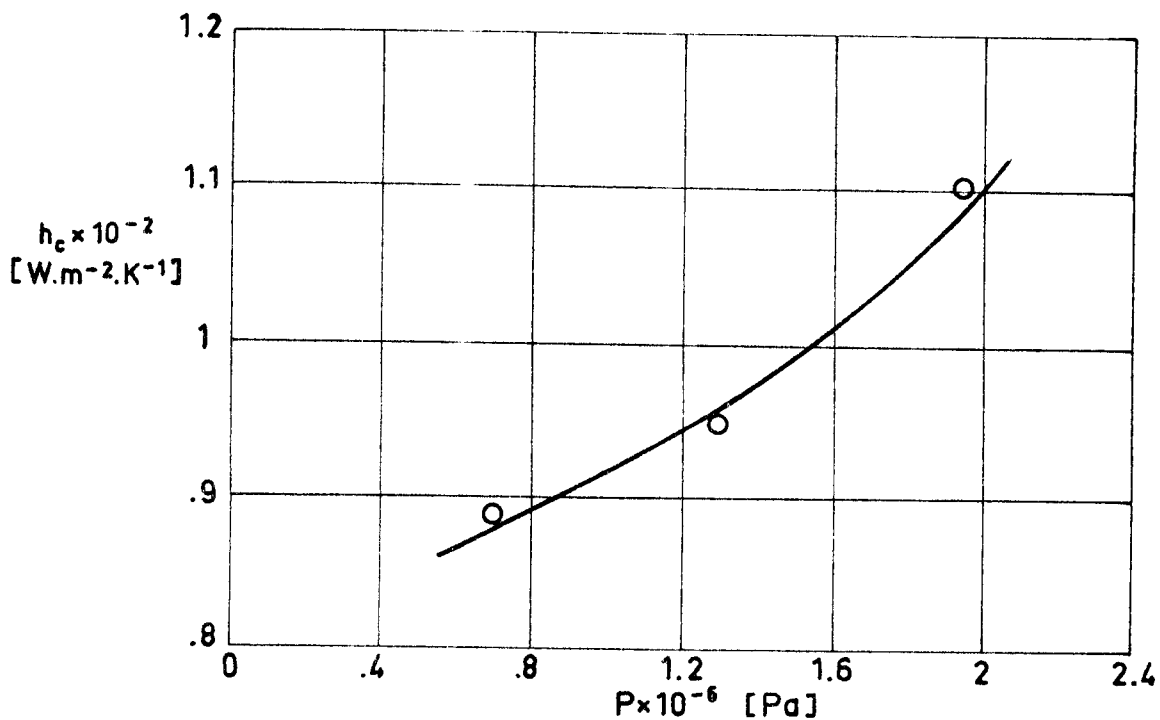


Fig 2-25. Plot of contact conductance vs. contact pressure.
From Fletcher, Smuda & Gyrog (1969).

Asbestos Tape (No. 2074) is produced by Atlas Asbestos Co. USA.
Cost of the filler: 1 US \$.kg⁻¹, 2 US \$.m⁻² (on basis of density).

THERMAL JOINT CONDUCTANCE
Insulating Spacers between Similar Metals

FILLER: Carbon Paper (F-907)

Density, $\rho = 144 \text{ kg.m}^{-3}$

Thickness, t , as given by the following compression test data:

$P \times 10^{-3}$ [Pa]	0	690	1380	2070
$t \times 10^{-3}$ [m]	1.19	.43	.33	.25

Appearance after thermal test: Slightly compressed

SPECIMENS: Two cylinders, Al - 4.3 Cu - 1.5 Mg - 0.6 Mn. (Al 2024).

Radius, $b = 1.27 \times 10^{-2} \text{ m}$.

Flatness Deviation, $FD = +.635 \times 10^{-6} \text{ m}$.

Roughness Deviation, $RD = .127 \times 10^{-6} \text{ m}$.

Mean Temperature, $T_m = 365 \text{ K}$.

Ambient Pressure, $p = 1.33 \times 10^{-3}$ to $1.33 \times 10^{-4} \text{ Pa}$.

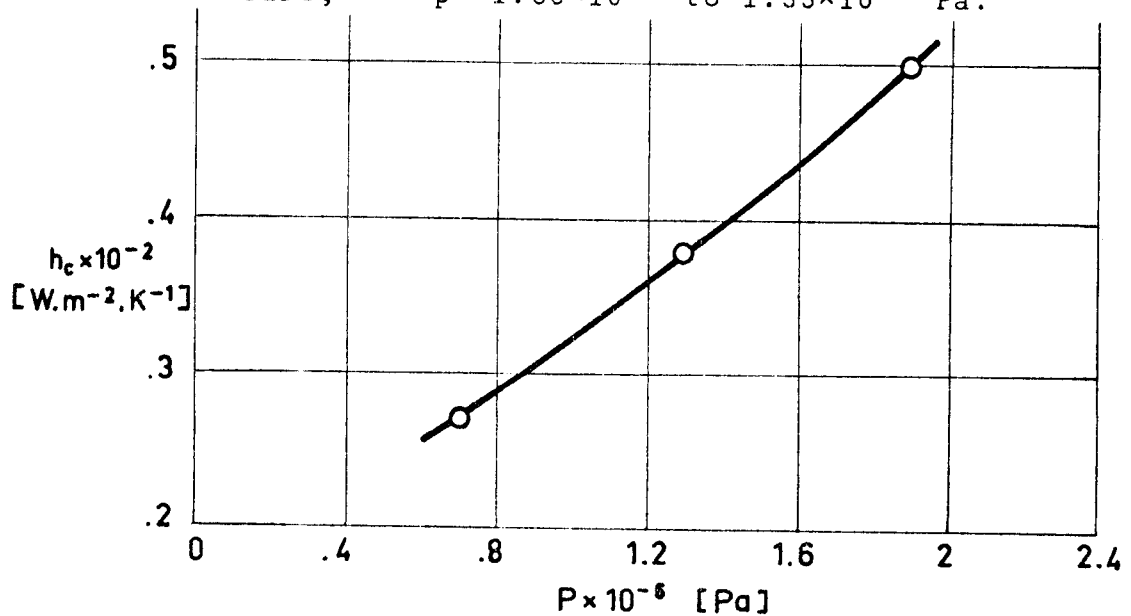


Fig 2-26. Plot of contact conductance vs. contact pressure.
From Fletcher, Smuda & Gyrog (1969).

Paper F-907 is a product of Fiberite Corp. USA.

Cost of the filler:

THERMAL JOINT CONDUCTANCE
 Insulating Spacers between Similar Metals

FILLER: Ceramic Paper (970-J)

Density, $\rho = 192 \text{ kg.m}^{-3}$

Thickness, t , as given by the following compression test data:

$P \times 10^{-3} \text{ [Pa]}$	0	690	1380	2070
$t \times 10^3 \text{ [m]}$	2	.86	.71	.64

Appearance after thermal test: Slightly deformed.

SPECIMENS: Two cylinders, Al - 4.3 Cu - 1.5 Mg - 0.6 Mn. (Al 2024).

Radius, $b = 1.27 \times 10^{-2} \text{ m}$.

Flatness Deviation, $FD = +.635 \times 10^{-6} \text{ m}$.

Roughness Deviation, $RD = .127 \times 10^{-6} \text{ m}$.

Mean Temperature, $T_m = 366 \text{ K}$.

Ambient Pressure, $p = 1.33 \times 10^{-3} \text{ to } 1.33 \times 10^{-4} \text{ Pa}$.

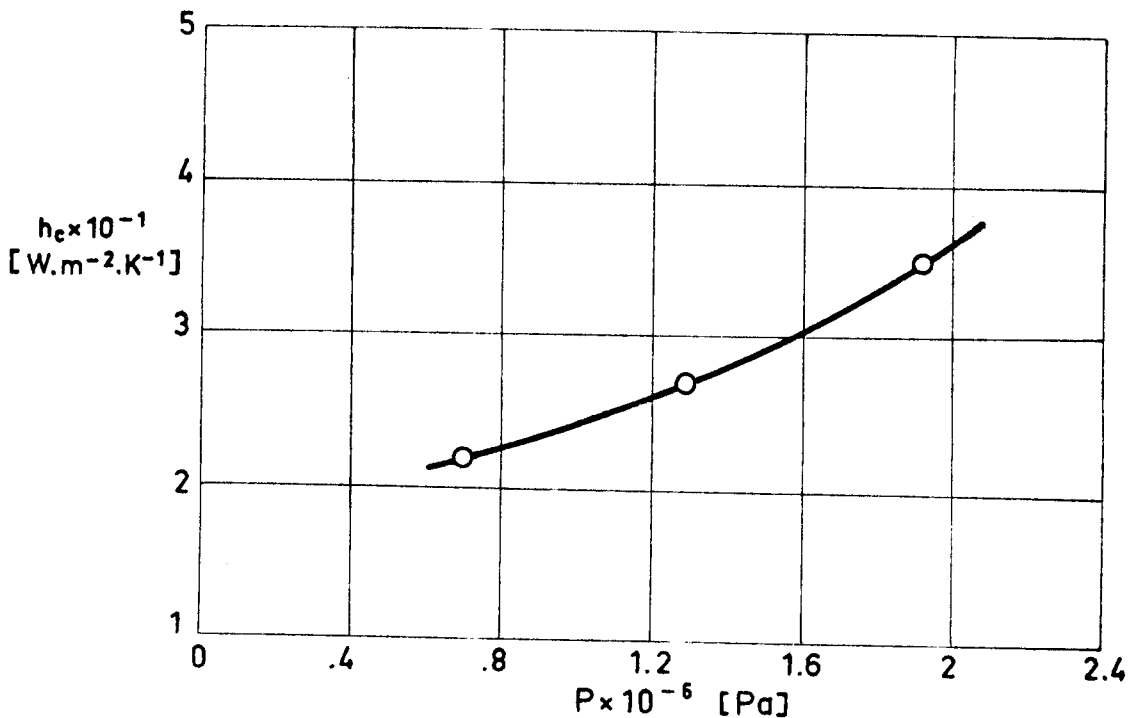


Fig 2-27. Plot of contact conductance vs. contact pressure.
 From Fletcher, Smuda & Gyrog (1969).

Paper 970 is made of Fiberfrax, which is a fiber composed mainly of Alumina and Silica. Fiberfrax is a Trade Name of Carborundum Co. USA

Cost of the filler: 14 US \$.m⁻²

THERMAL JOINT CONDUCTANCE
 Insulating Spacers between Similar Metals

FILLER: Laminate T-30-LR

Density, $\rho = 801 \text{ kg.m}^{-3}$

Initial Thickness, $t = 3.33 \times 10^{-3} \text{ m.}$

Appearance after thermal test: No apparent effect.

SPECIMENS: Two cylinders, Al - 4.3 Cu - 1.5 Mg - 0.6 Mn. (Al 2024).

Radius, $b = 1.27 \times 10^{-2} \text{ m.}$

Flatness Deviation, $FD = +.635 \times 10^{-6} \text{ m.}$

Roughness Deviation, $RD = .127 \times 10^{-6} \text{ m.}$

Mean Temperature, $T_m = 365 \text{ K.}$

Ambient Pressure, $p = 1.33 \times 10^{-3} \text{ to } 1.33 \times 10^{-4} \text{ Pa.}$

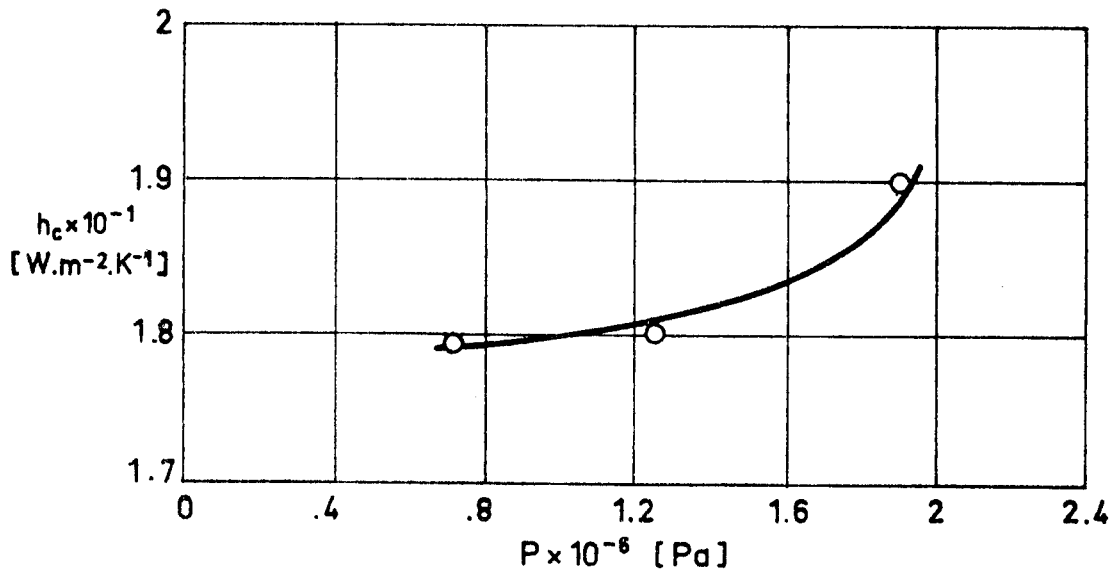


Fig 2-28. Plot of contact conductance vs. contact pressure.
 From Fletcher, Smuda & Gyrog (1969).

T-30-LR is a laminate of impregnated Fiberfrax; which is a fiber composed mainly of Alumina and Silica. Fiberfrax is a Trade Name of Carborundum Co., USA.

Cost of the filler:

THERMAL JOINT CONDUCTANCE
 Insulating Spacers between Similar Metals

FILLER: Laminate T-30-LR

Density, $\rho = 801 \text{ kg.m}^{-3}$

Initial Thickness, $t = 3.15 \times 10^{-3} \text{ m}$.

SPECIMENS: Two cylinders, Fe - 19 Cr - 10 Ni. (SS 304).

Radius, $b = 1.27 \times 10^{-2} \text{ m}$.

Flatness Deviation, $FD = +.508 \times 10^{-6} \text{ to } +.635 \times 10^{-6} \text{ m}$.

Roughness Deviation, $RD = .076 \times 10^{-6} \text{ to } .152 \times 10^{-6} \text{ m}$.

Ambient Pressure, $p = 1.33 \times 10^{-3} \text{ Pa}$.

Table 2-2

Values of contact conductance as a function
 of contact pressure and mean temperature.

$P \times 10^{-3} \text{ [Pa]}$	$T_m \text{ [K]}$	$h_c \text{ [W.m}^{-2}.\text{K}^{-1}]$
738	377	29
745	374	16
717	369	13
731	365	8
703	370	8
717	369	10

From Gyrog (1970).

T-30-LR is a laminate of impregnated Fiberfrax; which is a fiber composed mainly of Alumina and Silica. Fiberfrax is a Trade Name of Carborundum Co. USA.

Cost of the filler:

THERMAL JOINT CONDUCTANCE
Insulating Spacers between Similar Metals

FILLER: Mica (bonded)

Density, $\rho = 208 \text{ kg.m}^{-3}$

Initial Thickness, $t = .5 \times 10^{-4} \text{ m.}$

Appearance after thermal test: Slightly deformed.

SPECIMENS: Two cylinders, Al - 4.3 Cu - 1.5 Mg - 0.6 Mn. (Al 2024).

Radius, $b = 1.27 \times 10^{-2} \text{ m.}$

Flatness Deviation, $FD = +.635 \times 10^{-6} \text{ m.}$

Roughness Deviation, $RD = .127 \times 10^{-6} \text{ m.}$

Mean Temperature, $T_m = 376 \text{ to } 385 \text{ K.}$

Ambient Pressure, $p = 1.33 \times 10^{-3} \text{ to } 1.33 \times 10^{-4} \text{ Pa.}$

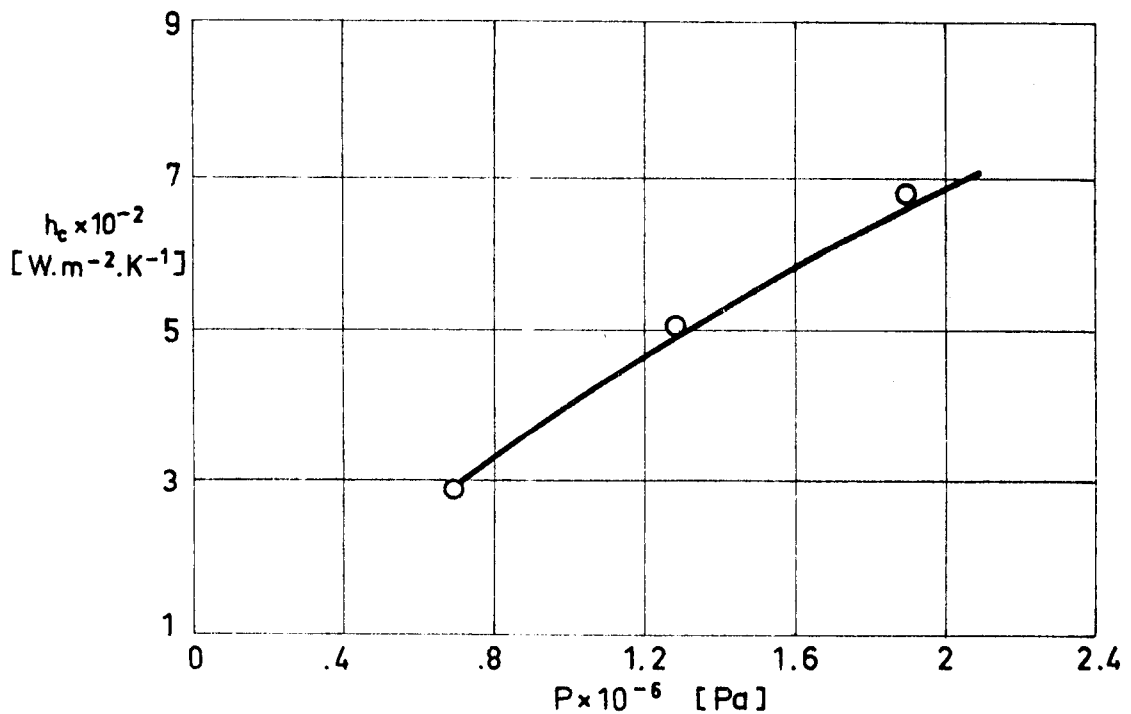


Fig 2-29. Plot of contact conductance vs. contact pressure.

From Fletcher, Smuda & Gyrog (1969).

Cost of the filler: 2.5 US \$.kg⁻¹, .05 US \$.m⁻² (on basis of density).

THERMAL JOINT CONDUCTANCE
Insulating Spacers between Similar Metals

FILLER: Mica

Density, $\rho = 208 \text{ kg.m}^{-3}$

Initial Thickness, $t = .7 \times 10^{-4} \text{ m.}$

SPECIMENS: Two cylinders, Fe - 19 Cr - 10 Ni. (SS 304).

Radius, $b = 1.27 \times 10^{-2} \text{ m.}$

Flatness Deviation, $FD = +.508 \times 10^{-6} \text{ to } +.635 \times 10^{-6} \text{ m.}$

Roughness Deviation, $RD = .076 \times 10^{-6} \text{ to } .152 \times 10^{-6} \text{ m.}$

Mean Temperature, $T_m = 351 \text{ to } 401 \text{ K.}$

Ambient Pressure, $p = 1.33 \times 10^{-3} \text{ Pa.}$

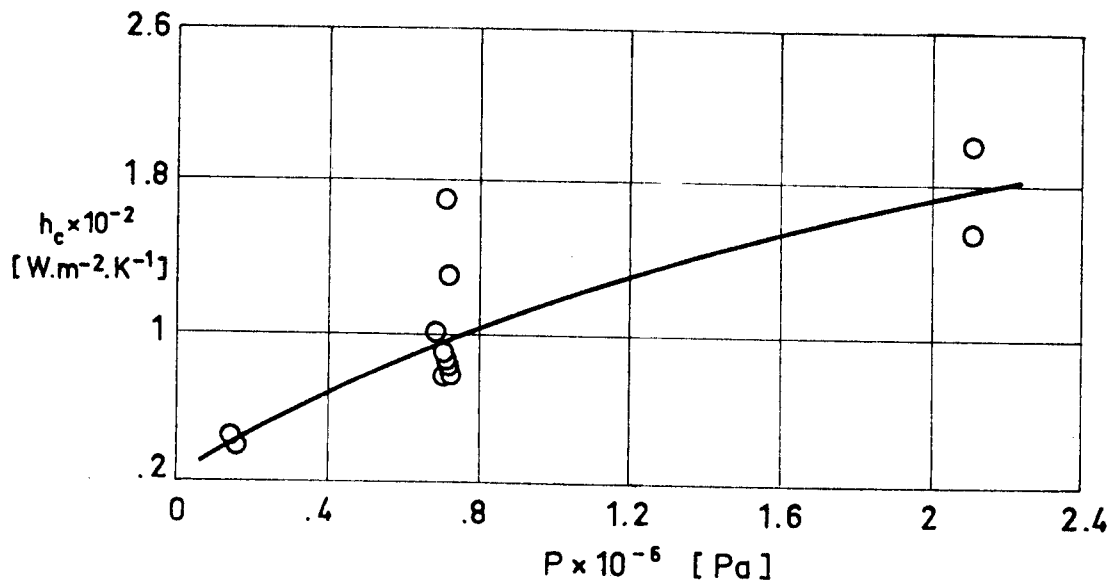


Fig 2-30. Plot of contact conductance vs. contact pressure.

From Gyrog (1970).

Cost of the filler: $2.5 \text{ US } \$.\text{kg}^{-1}$, $.05 \text{ US } \$.\text{m}^{-2}$ (on basis of density).

THERMAL JOINT CONDUCTANCE
Insulating Spacers between Similar Metals

FILLER: Pluton B-1 Cloth

Density, $\rho = 1\,394 \text{ kg.m}^{-3}$

Initial Thickness, $t = 3.16 \times 10^{-3} \text{ m.}$

Appearance after thermal test: Slightly compressed.

SPECIMENS: Two cylinders, Al - 4.3 Cu - 1.5 Mg - 0.6 Mn. (Al 2024).

Radius, $b = 1.27 \times 10^{-2} \text{ m.}$

Flatness Deviation, $FD = +.635 \times 10^{-6} \text{ m.}$

Roughness Deviation, $RD = .127 \times 10^{-6} \text{ m.}$

Mean Temperature, $T_m = 362 \text{ to } 364 \text{ K.}$

Ambient Pressure, $p = 1.33 \times 10^{-3} \text{ to } 1.33 \times 10^{-4} \text{ Pa.}$

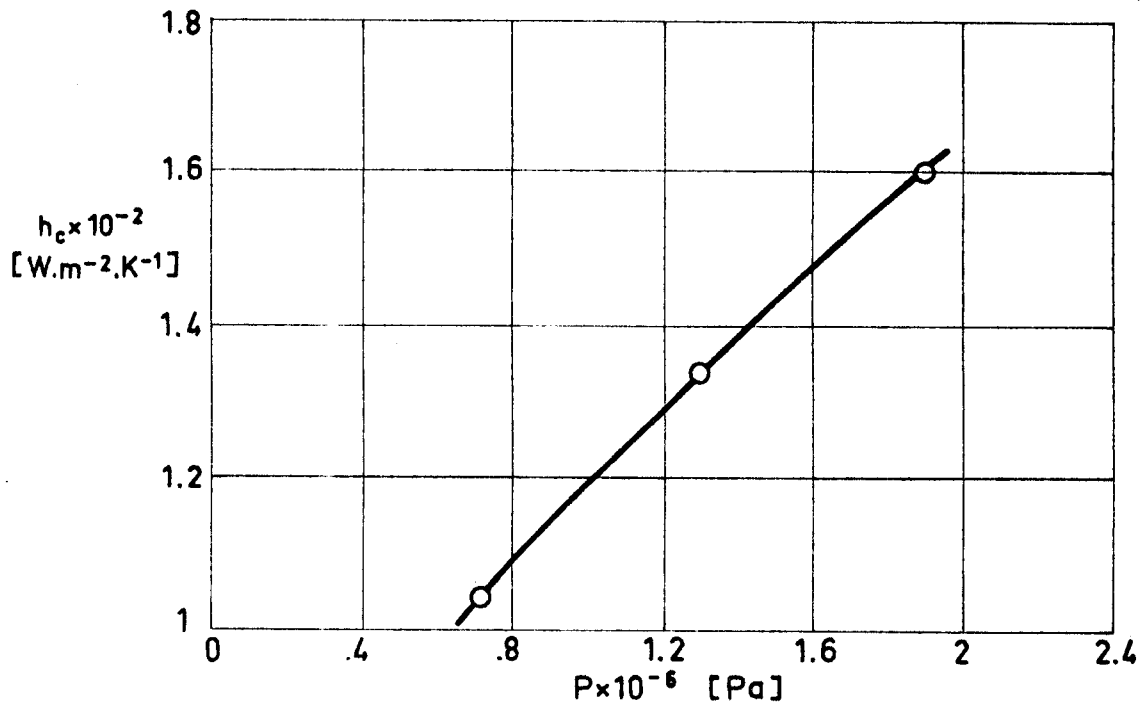


Fig 2-31. Plot of contact conductance vs. contact pressure.

From Fletcher, Smuda & Gyrog (1969).

Cost of the filler:

THERMAL JOINT CONDUCTANCE
Insulating Spacers between Similar Metals

FILLER: Pyroid

Density, $\rho = 2\,595 \text{ kg}\cdot\text{m}^{-3}$

Initial Thickness, $t = 2.95 \times 10^{-3} \text{ m}$.

Appearance after thermal test: No apparent effect.

SPECIMENS: Two cylinders, Al - 4.3 Cu - 1.5 Mg - 0.6 Mn. (Al 2024).

Radius, $b = 1.27 \times 10^{-2} \text{ m}$.

Flatness Deviation, $FD = +.635 \times 10^{-6} \text{ m}$.

Roughness Deviation, $RD = .127 \times 10^{-6} \text{ m}$.

Mean Temperature, $T_m = 376 \text{ to } 378 \text{ K}$.

Ambient Pressure, $p = 1.33 \times 10^{-3} \text{ to } 1.33 \times 10^{-4} \text{ Pa}$.

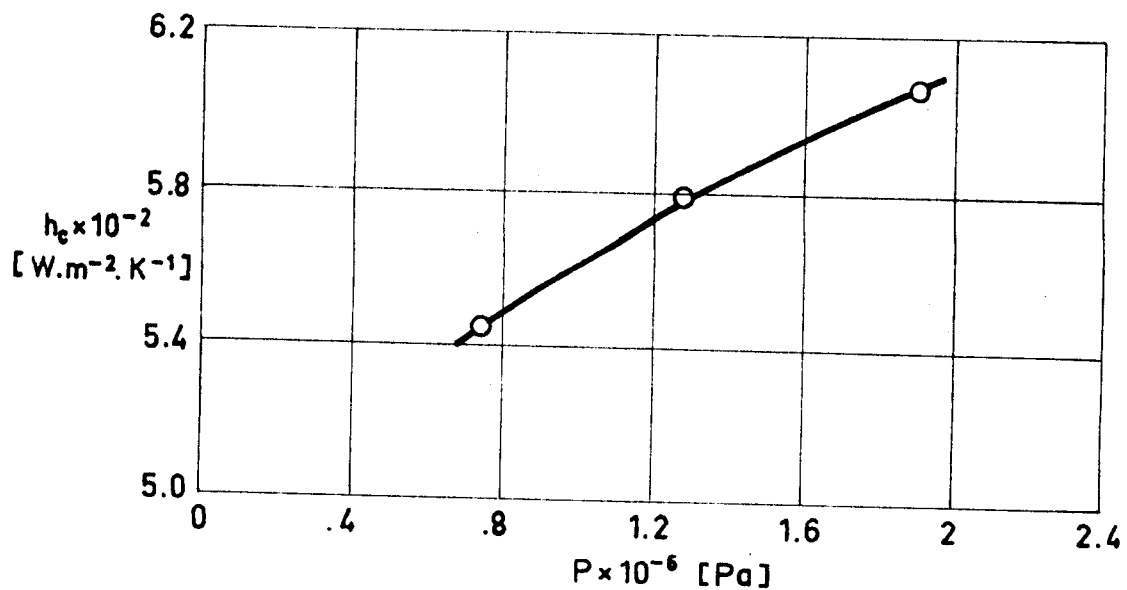


Fig 2-32. Plot of contact conductance vs. contact pressure.
From Fletcher, Smuda & Gyrog (1969).

Cost of the filler:

THERMAL JOINT CONDUCTANCE
Insulating Spacers between Similar Metals

FILLER: Pyrotex 23RPD

Density, $\rho = 1\,396 \text{ kg.m}^{-3}$

Initial Thickness, $t = 2.84 \times 10^{-3} \text{ m}$.

SPECIMENS: Two cylinders, Fe - 19 Cr - 10 Ni. (SS 304).

Radius, $b = 1.27 \times 10^{-2} \text{ m}$.

Flatness Deviation, $FD = +.508 \times 10^{-6} \text{ to } +.635 \times 10^{-6} \text{ m}$.

Roughness Deviation, $RD = .076 \times 10^{-6} \text{ to } .152 \times 10^{-6} \text{ m}$.

Ambient Pressure, $p = 1.33 \times 10^{-3} \text{ Pa}$.

Table 2-3

Values of contact conductance as a function
of contact pressure and mean temperature.

$P \times 10^{-3} \text{ [Pa]}$	$T_m \text{ [K]}$	$h_c \text{ [W.m}^{-2}.\text{K}^{-1}]$
648	393	69
2 137	394	78

From Gyorog (1970).

Pyrotex 23RPD is the Trade Name of an asbestos reinforced plastic from International Raybestos Manhattan Co. USA.

Cost of the filler:

THERMAL JOINT CONDUCTANCE
 Insulating Spacers between Similar Metals

FILLER: Silica paper

Density, $\rho = 160 \text{ kg.m}^{-3}$

Thickness, t , as given by the following compression test data

$P \times 10^{-3} \text{ [Pa]}$	0	690	1380	2070
$t \times 10^3 \text{ [m]}$	1.24	.43	.30	.27

Appearance after thermal test: Discoloring, considerably compressed.

SPECIMENS: Two cylinders, Al - 4.3 Cu - 1.5 Mg - 0.6 Mn. (Al 2024).

Radius, $b = 1.27 \times 10^{-2} \text{ m}$.

Flatness Deviation, $FD = +.635 \times 10^{-6} \text{ m}$.

Roughness Deviation, $RD = .127 \times 10^{-6} \text{ m}$.

Mean Temperature, $T_m = 366 \text{ K}$.

Ambient Pressure, $p = 1.33 \times 10^{-3} \text{ to } 1.33 \times 10^{-4} \text{ Pa}$.

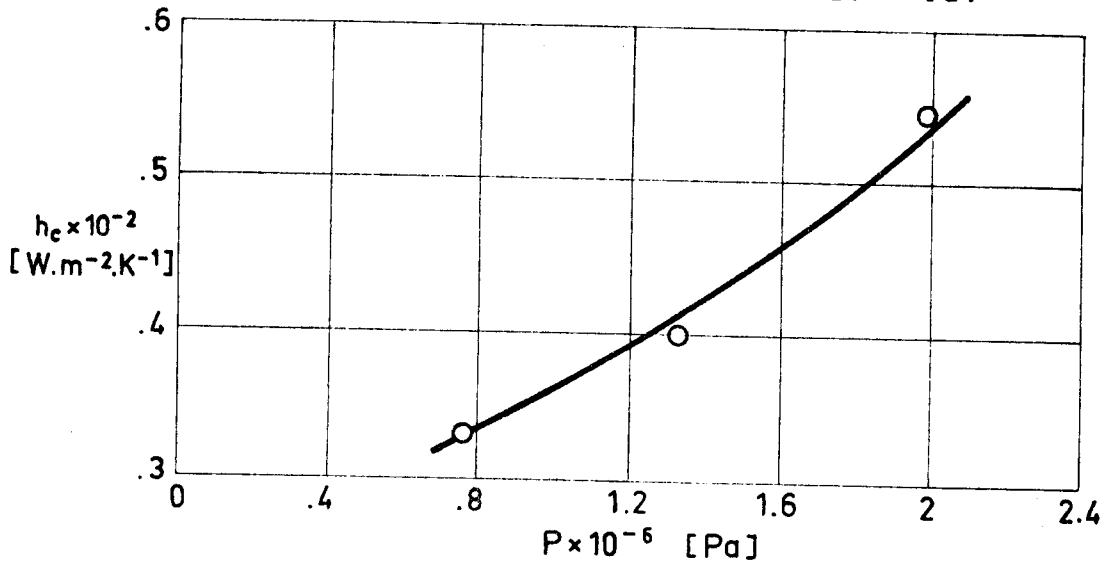


Fig 2-33. Plot of contact conductance vs. contact pressure.

From Fletcher, Smuda & Gyrog (1969).

Silica paper is a product of Fiberite Corp., USA.

Cost of the filler:

THERMAL JOINT CONDUCTANCE
Insulating Spacers between Similar Metals

FILLER: Teflon (TFE) Sheet

Density, $\rho = 160 \text{ kg.m}^{-3}$

Initial Thickness, $t = .5 \times 10^{-4} \text{ m.}$

Appearance after thermal test: No apparent effect.

SPECIMENS: Two cylinders, Al - 4.3 Cu - 1.5 Mg - 0.6 Mn. (Al 2024).

Radius, $b = 1.27 \times 10^{-2} \text{ m.}$

Flatness Deviation, $FD = +.635 \times 10^{-6} \text{ m.}$

Roughness Deviation, $RD = .127 \times 10^{-6} \text{ m.}$

Mean Temperature, $T_m = 398 \text{ to } 401 \text{ K.}$

Ambient Pressure, $p = 1.33 \times 10^{-3} \text{ to } 1.33 \times 10^{-4} \text{ Pa.}$

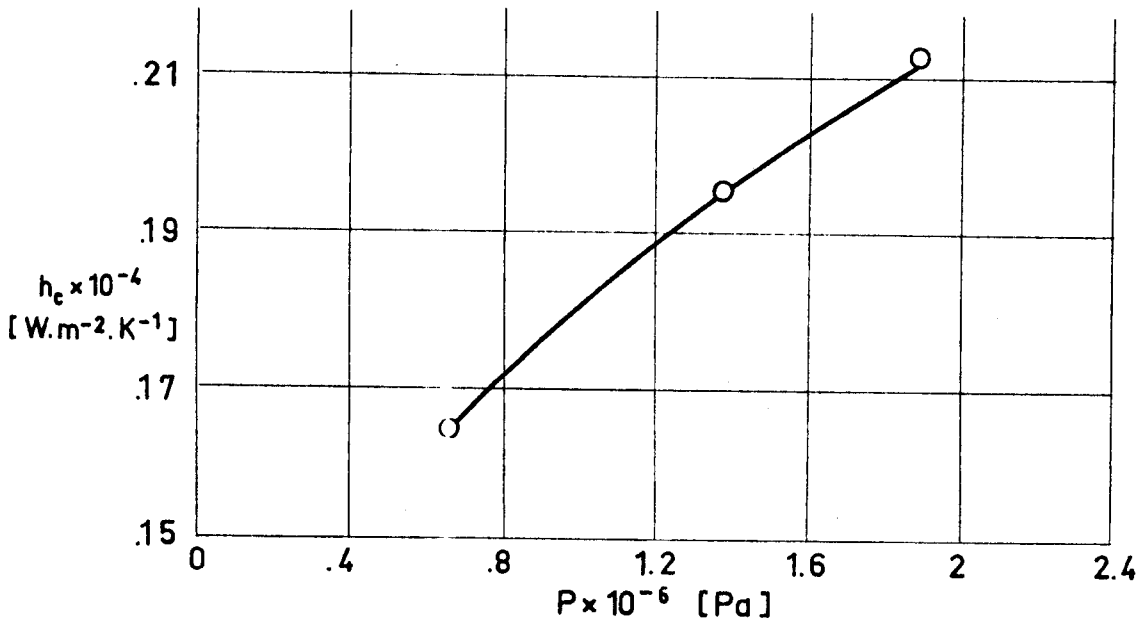


Fig 2-34. Plot of contact conductance vs. contact pressure.

From Fletcher, Smuda & Gyrog (1969).

Teflon polytetrafluoroethylene (TFE) is a Trade Name of E.I. DuPont de Nemours Co., Inc. USA.

Cost of the filler: 20 US \$.kg⁻¹, .16 US \$.m⁻² (on basis of density).

THERMAL JOINT CONDUCTANCE
Insulating Spacers between Similar Metals

FILLER: Teflon (TFE) Sheet

Density, $\rho = 160 \text{ kg.m}^{-3}$
Initial Thickness, $t = 3.07 \times 10^{-3} \text{ m}$.

SPECIMENS: Two cylinders, Fe - 19 Cr - 10 Ni. (SS 304).

Radius, $b = 1.27 \times 10^{-2} \text{ m}$.
Flatness Deviation, $FD = +.508 \times 10^{-6}$ to $+.635 \times 10^{-6} \text{ m}$.
Roughness Deviation, $RD = .076 \times 10^{-6}$ to $.152 \times 10^{-6} \text{ m}$.
Ambient Pressure, $p = 1.33 \times 10^{-3} \text{ Pa}$.

Table 2-4

Values of contact conductance as a function
of contact pressure and mean temperature.

$P \times 10^{-3} \text{ [Pa]}$	$T_m \text{ [K]}$	$h_c \text{ [W.m}^{-2}.\text{K}^{-1}]$
731	414	162
717	390	163
2 110	392	170

From Gyrog (1970).

Teflon polytetrafluoroethylene (TFE) is a Trade Name of E.I. DuPont de Nemours Co., Inc. USA.

Cost of the filler: 20 US \$.kg⁻¹, 9.6 US \$.m⁻² (on basis of density).

THERMAL JOINT CONDUCTANCE
 Insulating Spacers between Similar Metals

FILLER: Textolite

Initial Thickness, $t = 1.57 \times 10^{-3}$ m.

SPECIMENS: Two cylinders, Fe - 19 Cr - 10 Ni. (SS 304).

Radius, $b = 1.27 \times 10^{-2}$ m.

Flatness Deviation, $FD = +.508 \times 10^{-6}$ to $+.635 \times 10^{-6}$ m.

Roughness Deviation, $RD = .076 \times 10^{-6}$ to $.152 \times 10^{-6}$ m.

Mean Temperature, $T_m = 386$ to 393 K.

Ambient Pressure, $p = 1.33 \times 10^{-3}$ Pa.

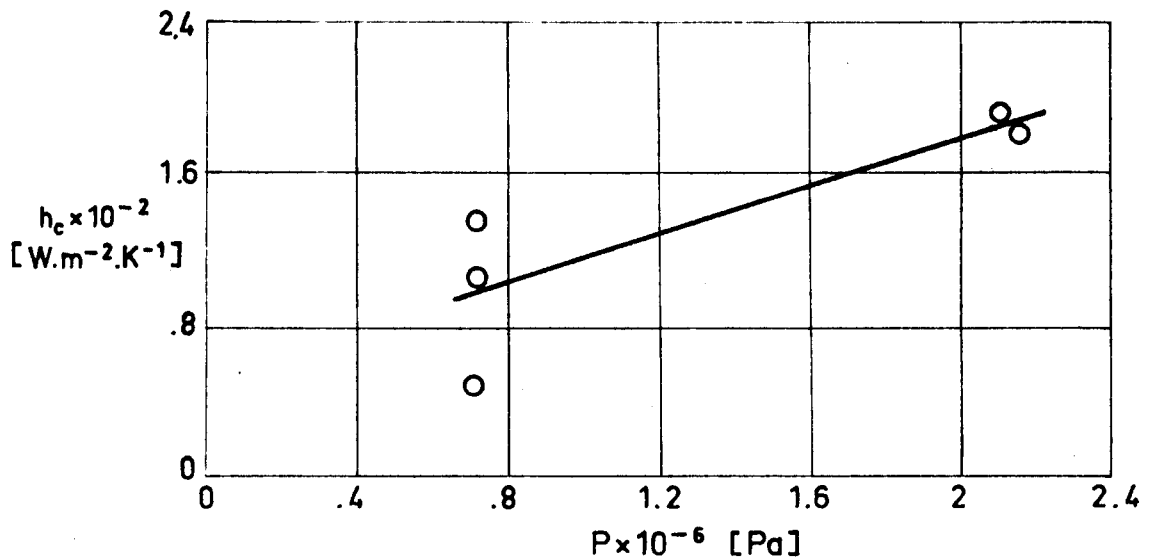


Fig 2-35. Plot of contact conductance vs. contact pressure.
 From Gyorog (1970).

Textolite, Trade Name of General Electric Co. USA, is a phenol formaldehyde laminated compound.

Cost of the filler:

THERMAL JOINT CONDUCTANCE
 Insulating Spacers between Similar Metals

FILLER: WRP-X-AQ Felt

Density, $\rho = 288 \text{ kg.m}^{-3}$

Thickness, t , as given by the following compression test data

$P \times 10^{-3} \text{ [Pa]}$	0	690	1380	2070
$t \times 10^3 \text{ [m]}$	4.47	2.33	1.93	1.72

Appearance after thermal test: Slightly compressed

SPECIMENS: Two cylinders, Al - 4.3 Cu - 1.5 Mg - 0.6 Mn. (Al 2024).

Radius, $b = 1.27 \times 10^{-2} \text{ m}$.

Flatness Deviation, $FD = +.635 \times 10^{-6} \text{ m}$.

Roughness Deviation, $RD = .127 \times 10^{-6} \text{ m}$.

Mean Temperature, $T_m = 357 \text{ K}$.

Ambient Pressure, $p = 1.33 \times 10^{-3} \text{ to } 1.33 \times 10^{-4} \text{ Pa}$.

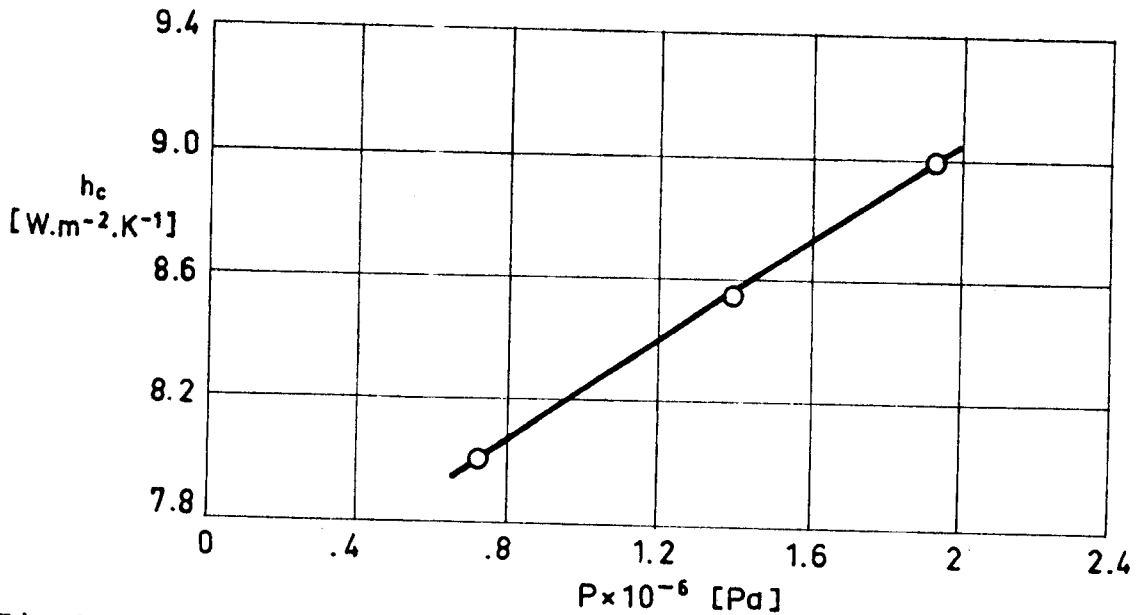


Fig 2-36. Plot of contact conductance vs. contact pressure.
 From Fletcher, Smuda & Gyorog (1969).

Cost of the filler:

THERMAL JOINT CONDUCTANCE

Thermal Greases between Similar Metals

2.8. THERMAL GREASES BETWEEN SIMILAR METALS

FILLER: DC-340 Grease

Density, $\rho = 2\ 300\ \text{kg}\cdot\text{m}^{-3}$

SPECIMENS: Two cylinders as indicated below.

Radius, $b = 1.27 \times 10^{-2}\ \text{m}$.

Ambient Pressure, $p = 1.33 \times 10^{-3}\ \text{Pa}$.

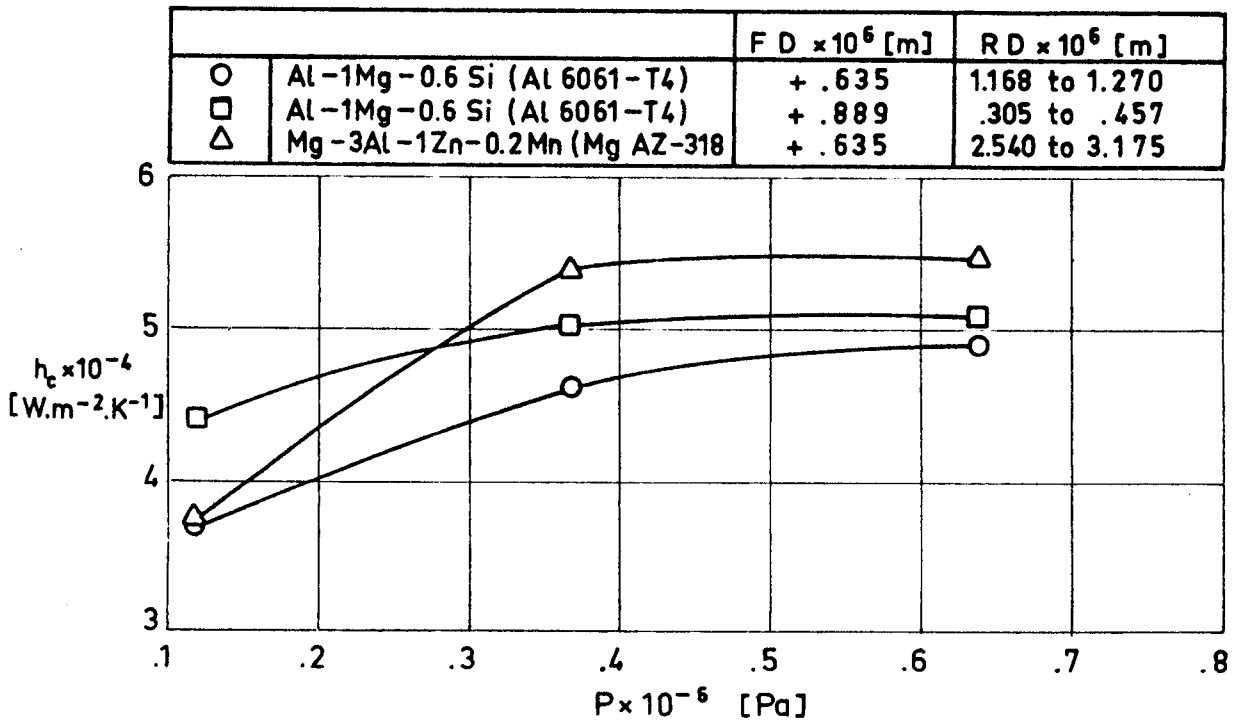


Fig 2-37. Plot of contact conductance vs contact pressure. From Cunnington (1964).

DC-340 is a silicone heat transfer compound, heavily filled with metal oxides. It is produced by Dow-Corning. USA.

Cost of the filler: 10 US \$.kg⁻¹

THERMAL JOINT CONDUCTANCE
Thermal Greases between Similar Metals

FILLER: Silicone High Vacuum Grease

Density, $\rho = 1\ 000\ \text{kg.m}^{-3}$

SPECIMENS: Two cylinders, Mg - 3 Al - 1 Zn - 0.2 Mn. (Mg AZ-31B).

Radius, $b = 1.27 \times 10^{-2}\ \text{m}$.

Flatness Deviation, $FD = +.635 \times 10^{-6}\ \text{m}$.

Roughness Deviation, $RD = 2.54\ \text{to}\ 3.175 \times 10^{-6}\ \text{m}$.

Ambient Pressure, $p = 1.33 \times 10^{-3}\ \text{Pa}$.

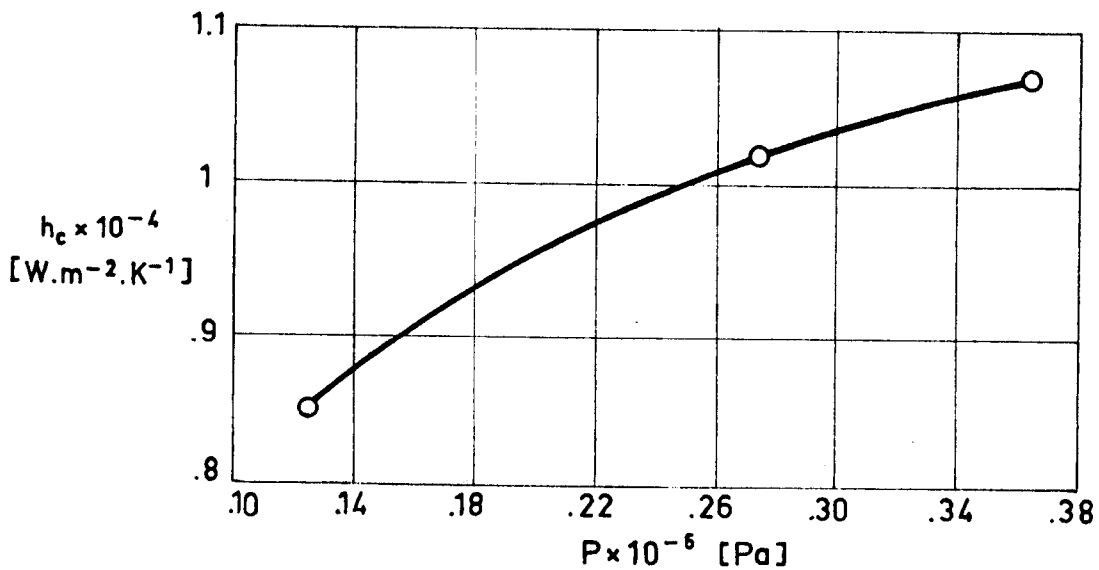


Fig 2-38. Plot of contact conductance vs. contact pressure.
From Cunnington (1964).

The filler is a stiff, nonmelting, silicone material that maintains its consistence over a temperature range 233 to 533 K. It is produced by Dow-Corning. USA.

Cost of the filler: 25 US \$. kg^{-1}

Rev. 3. 1986

THERMAL JOINT CONDUCTANCE

Elastomeric Materials between Similar Metals

2.9. ELASTOMERIC MATERIALS BETWEEN SIMILAR METALS

Elastomeric materials are used as gaskets because of their superior environmental resistance, excellent sealing capability and durability through repeated loadings. These materials may contain fillers to improve their mechanical or thermophysical properties.

The enclosed table, reproduced from Fletcher & Miller (1973), shows the relevant characteristics of the elastomers used to obtain the joint conductance data presented in the following page.

Code	Name	Material	Filler	Density [kg.m ⁻³]	Temperature Range [K]	Thick. tx10 ³ [m]
N1		Neoprene Rubber		1 350	244-366	2.92
IP1	D84-1 ^a	Fluoro- carbon	Carbon black	1 875	233-533	2.08
IP2	EXN-117-3 ^a	Nitrile	Graphite, Talc	1 450	233-422	1.98
IP3	SIL-181-3 ^a	Silicone	Diatomaceous earth	1 340	219-533	2.05
IP4	R36-1 ^a	Nitrile	Carbon black, Organic per- oxide	1 215	244-394	2.36
IP5	4658-2 ^a	Poly- acrilate	Silica, Alu- mina Complex	1 360	255-450	1.90
C1	1224 ^b	Silicone	Silver flakes	3 250	218-473	.76
C2	1215 ^b	Silicone	Silver coated copper powder	3 650	218-398	.71
C3	X-4044-3 ^b	Silicone	Inorganic-die- lectric, therm- ally conduc- tive material	1 750	218-473	.43
TW1	CONCIL R350 ^c	Silicone	Silver flakes	1 700	222-450	.74
TW2	CONCIL R600 ^c	Silicone	Silver flakes	1 800	222-450	.71
TW3	CONCIL G450 ^c	Silicone	Silver coated inert parti- cles	1 700	200-478	.74
TW4	CONCIL G750 ^c	Silicone	Silver coated inert parti- cles	1 800	200-478	.76

^a International Packings Corporation, Bristol, New Hampshire 03222.

^b Chomerics, 77 Dragon Court, Woburn, Massachusetts 01801.

^c Technical Wire Products, Inc., 129 Dermody Street, Cranford, New Jersey 07016.

Rev. 3. 1986

THERMAL JOINT CONDUCTANCE

Elastomeric Materials between Similar Metals

SPECIMENS: Three cylinders, Al - 4.3 Cu - 1.5 Mg - 0.6 Mn. (Al 2024-T4).

Two identical contacting junctions placed as sketched.

Radius, $b = 1.27 \times 10^{-2}$ m.

Surface	$FD \times 10^{-6}$ [m]	$RD \times 10^6$ [m]
S1	+ .51	.40
S2	+ .51	.35
S3	+ .51	.33
S4	+ .51	.40

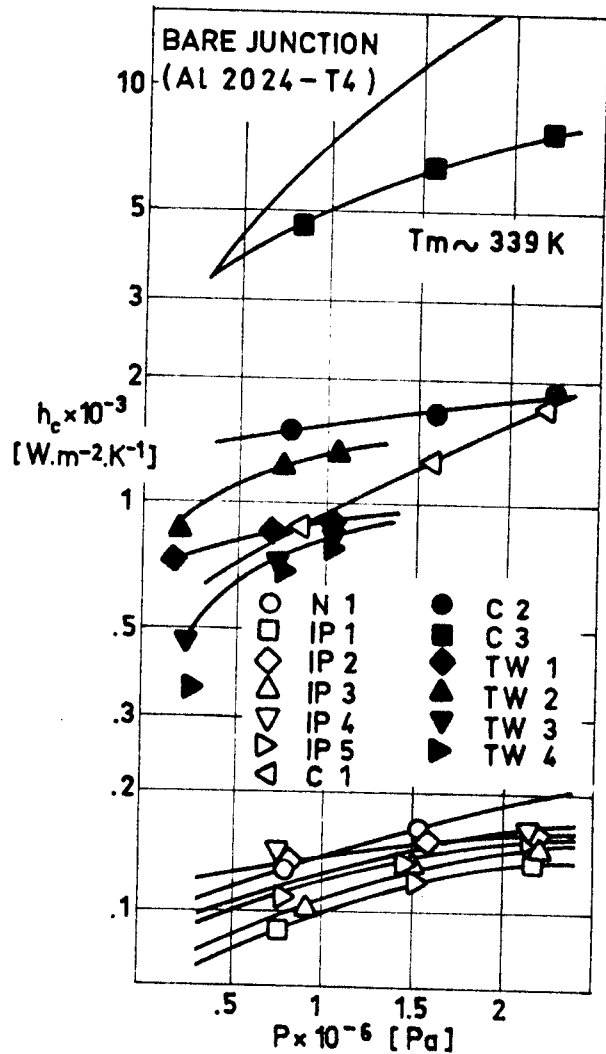
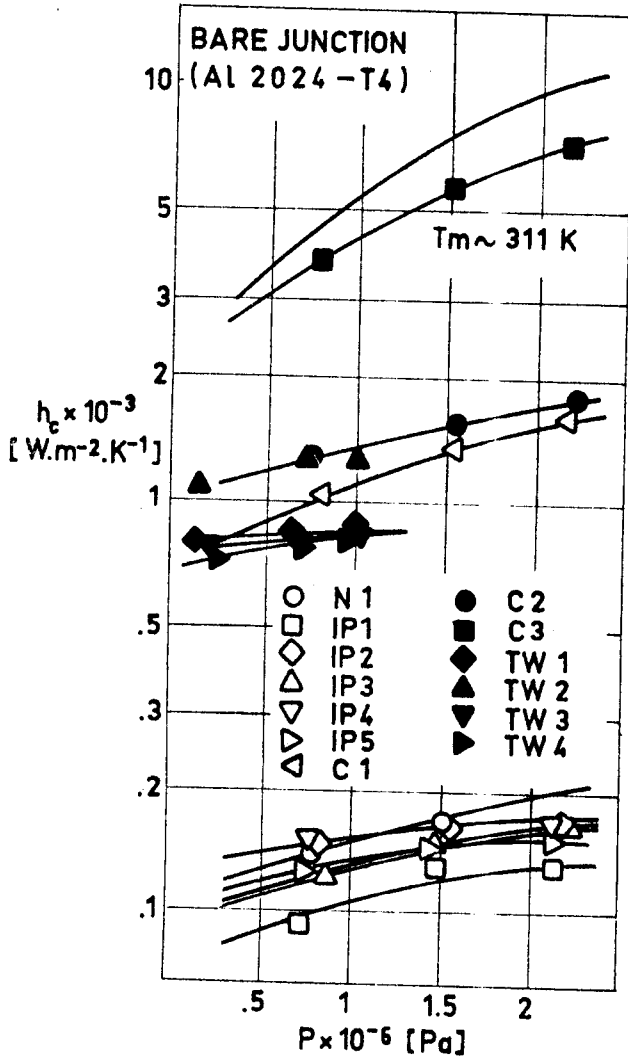
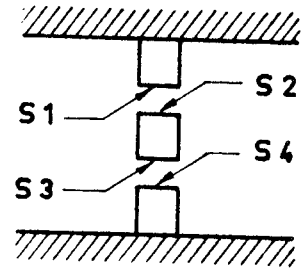


Fig 2-39. Plot of contact conductance vs. contact pressure for various elastomeric materials at two mean temperatures. From Fletcher & Miller (1973).

THERMAL JOINT CONDUCTANCE

Outgassing Data

2.10. OUTGASSING DATA

Outgassing data, consisting of total weight loss (TWL) and volatile condensable materials (VCM), of several non-metallic materials included in this part, are presented in the following table.

Table 2-5

Outgassing Data of Several Non-Metallic Materials

MATERIAL	% TWL	% VCM	CURE TIME [h]	CURE TEMPERATURE [K]	ATMOSPHERE
DC-340 Grease	.350	.110		273	
DC-340 Grease	.840	.310	24	298	AIR
Neoprene	3.010	1.720		273	
Silicone High Vacuum Grease	1.520	.340		273	
Silver Filled Silicone	.261	.055		273	
Silver Filled Silicone	.048	.023	24	450	AIR

From Campbell, Marrott & Park (1973).

INTENTIONALLY BLANK PAGE

CONDUCTIVE HEAT TRANSFER

References

- Roess, L.C. 1949 "Theory of Spreading Conductance"
Appendix to "Thermal Resistance Measurements of Joints Formed between Stationary Metal Surfaces", by N.D. Weills & E.A. Ryder.
Transactions of the ASME, Vol. 71, No. 3, 1949.
- Cetinkale, T.N.,
Fishenden, M. 1951 "Thermal Conductance of Metal Surfaces in Contact",
Proceedings International Conference of Heat Transfer, Inst. Mech. Eng., London 1951, pp. 271-275.
- Andrews, R.V. 1955 "Solving Conductive Heat Transfer Problems with Electrical-Analogue Shape Factors",
Chemical Engineering Progress, Vol. 51, No. 2, Feb. 1955, pp. 67-71.
- Faulkner, R.C.,
Andrews, R.V. 1955 "Shape Factors in Multiple-Pipe Systems",
Amer. Inst. Chem. Engrs. (AIChE) Journal, Vol. 1, No. 4, Dec. 1955.
- Fenech, H.,
Rohsenow, W.M. 1959 "Thermal Conductance of Metallic Surfaces in Contact",
U.S. Atomic Energy Commission, Report NYO-2316, May 1959.
- Laming, L.C. 1961 "Thermal Conductance of Machined Metal Contacts",
Proceedings International Conference on Developments in Heat Transfer, ASME, Part I, 1961, pp. 65-76.

CONDUCTIVE HEAT TRANSFER

References

- Fenech, H,
Rohsenow, W.M. 1963 "Prediction of Thermal Conductance of Metallic Surfaces in Contact",
Journal of Heat Transfer, Vol. 85-C,
No. 1, Feb. 1963, pp. 15-24.
- Cunnington, Jr., G.R. 1964 "Thermal Conductance of Filled Aluminium and Magnesium Joints in a Vacuum Environment",
ASME paper No. 64-WA/TH-40, 1964.
- Henry, J.J.,
Fenech, H. 1964 "The Use of Analog Computer for Determining Surface Parameters Required for Prediction of Thermal Contact Conductance",
Journal of Heat Transfer, Vol. 86-C,
No. 4, Nov. 1964, pp. 543-551.
- Shlykov, Yu.P.,
Ganin, Ye.A. 1964 "Thermal Resistance of Metallic Contacts",
International Journal of Heat and Mass Transfer, Vol. 7, No. 8, Aug. 1964, pp. 921-929.
- Sunderland, J.E.,
Johnson, K.R. 1964 "Shape Factors for Heat Conduction through Bodies with Isothermal or Convective Boundary Conditions",
Trans. of the Amer. Soc. of Heating, Refrigeration and Air-Conditioning Engrs. (ASHRAE), Vol. 10, 1964, pp. 237-241.
- Clausing, A.M.,
Chao, B.T. 1965 "Thermal Contact Resistance in a Vacuum Environment",
Journal of Heat Transfer, Vol. 87-C,
No. 2, May 1965, pp. 243-251.

CONDUCTIVE HEAT TRANSFER

References

- Fried, E. 1965 "Study of Interface Thermal Control Conductance",
Summary Report, General Electric Doc. 65SD4395, 1965.
- Fried, E.,
Atkins, H.L. 1965 "Interface Thermal Conductance in a Vacuum",
Journal of Spacecraft and Rockets, Vol. 2, No. 4, July-Aug. 1965, pp. 591-593.
- Fried, E. 1966 "Study of Interface Thermal Contact Conductance - Summary Report",
General Electric Report 66SD4471, July 1966.
- Fried, E.,
Kelley, M.J. 1966 "Thermal Conductance of Metallic Contacts in a Vacuum",
in "Progress in Astronautics and Aeronautics", Vol. 18, G.B. Heller, Ed., Academic Press. New York, 1966, pp. 697-718.
- Kutateladze, S.S.,
Borishanskii, V.M. 1966 "A Concise Encyclopedia of Heat Transfer",
Translated from the Russian by J.B. Arthur, Pergamon Press, Oxford, 1956, Chap. 3, pp. 36-44.
- Ramachandra Murthy, M.L.,
Ramachandran, A. 1967 "Shape Factors in Conduction Heat Transfer",
British Chemical Engineering, Vol. 12, No. 5, 1967, pp. 730-731.
- Fletcher, L.S.,
Smuda, P.A.,
Gyorog, D.A. 1969 "Thermal Contact Resistance of Selected Low-Conductance Interstitial Materials",
AIAA Journal, Vol. 7, No. 7, July 1969, pp. 1302-1309.

CONDUCTIVE HEAT TRANSFER

References

- Parker, J.D.,
Boggs, J.H.,
Blick, E.F. 1969 "Introduction to Fluid Mechanics and Heat Transfer", Addison-Wesley Publishing Company, Inc., Reading Mass. 1969, Chap. 14. pp. 427-431.
- Fletcher, L.S.,
Gyorog, D.A. 1970 "Prediction of Thermal Contact Conductance between Similar Metal Surfaces", in "Progress in Astronautics and Aeronautics", Vol. 24, J.W. Lucas, Ed., MIT Press, Cambridge, Mass., 1970, pp. 273-288.
- Gyorog, D.A. 1970 "Investigation of Thermal Isolation Materials for Contacting Surfaces", in "Progress in Astronautics and Aeronautics", Vol. 24, J.W. Lucas, Ed., MIT Press, Cambridge, Mass., 1970, pp. 310-336.
- Scollon, T.R.,
Carpitella, M.J. 1970 "Long Life Reliability Thermal Control Systems Study Data Handbook", Prepared under Contract NAS 8-26252 by Space Systems Organization, General Electric Co., 1970.
- Thomas, T.R.,
Probert, S.D. 1972 "Correlations for Thermal Contact Conductance in Vacuo", Journal of Heat Transfer, Vol. 94-C, No. 2, May 1972, pp. 276-281.
- Campbell, Jr., W.A.,
Marriott, R.S.,
Park, J.J. 1973 "A Compilation of Outgassing Data for Spacecraft Materials", NASA TN D-7362, Sep. 1973.
- Fletcher, L.S.,
Miller, R.G. 1973 "Thermal Conductance of Gasket Materials for Spacecraft Joints", AIAA Paper No. 73-119, Jan. 1973.

CONDUCTIVE HEAT TRANSFER

References

- Griggs, E.I.,
Pitts, D.R.,
Goyal, A.B. 1973 "Conductive Shape Factors for a Circular Cylinder Centered in a Rectangular Slab Having One and Two Adiabatic Surfaces", Journal of Heat Transfer, Vol. 95-C, No. 1, Feb. 1973, pp. 129-130.
- Miller, R.G.,
Fletcher, L.S. 1973 "Thermal Contact Conductance of Porous Materials in a Vacuum Environment", AIAA Paper No. 73-747, July 1973.
- O'Callaghan, P.W.,
Probert, S.D. 1973 "Correlations for Thermal Conductance in Vacuo", Journal of Heat Transfer, Vol. 95-C, No. 1, Feb. 1973, pp. 141-142.
- Al-Astrabadi, F.R.,
O'Callaghan, P.W.,
Probert, S.D.,
Jones, A.M. 1977 "Thermal Contact Conductance Correlation for Stacks of Thin Layers in High Vacuums", Journal of Heat Transfer, Vol. 99-C, No. 1, Feb. 1977, pp. 139-142.

INTENTIONALLY BLANK PAGE

SPACECRAFT SURFACE TEMPERATURE

- 1 SOLAR RADIATION
- 2 PLANETARY RADIATION
- 3 ALBEDO RADIATION

E

S/C SURFACE
TEMPERATURE

SPACECRAFT SURFACE TEMPERATURE

Table of Contents

	Page
TABLE OF CONTENTS	0-1
LIST OF SYMBOLS	0-3
1. SOLAR RADIATION	1-1
1.1. General	1-1
1.2. Infinitely Conductive Planar Surfaces	1-7
1.2.1. Flat Plate Emitting on One or Both Sides	1-7
1.3. Infinitely Conductive Spherical Surfaces	1-9
1.3.1. Sphere	1-9
1.4. Infinitely Conductive Cylindrical Surfaces	1-11
1.4.1. Two-Dimensional Circular Cylinder	1-11
1.4.2. Three Dimensional Circular Cylinder	1-13
1.5. Infinitely Conductive Conical Surfaces	1-15
1.5.1. Semi-Infinite Circular Cone	1-15
1.5.2. Finite Circular Cone with Insulated Base (Axial Configuration)	1-17
1.5.3. Finite Height Circular Cone	1-19
1.6. Infinitely Conductive Cylindrical-Conical Surfaces .	1-21
1.6.1. Cone-Cylinder-Cone	1-21
1.7. Infinitely Conductive Prismatic Surfaces	1-39
1.7.1. Prism with an n-Sided Regular Polygonal Section	1-39
1.8. Infinitely Conductive Pyramidal Surfaces	1-51
1.8.1. Pyramid with an n-Sided Regular Polygonal Section	1-51
1.9. Infinitely Conductive Prismatic-Pyramidal Surfaces .	1-63
1.9.1. Pyramid-Prism-Pyramid with an n-Sided Regular Polygonal Section	1-63
1.10. Thin-Walled Spherical Bodies. Finite Conductivity ..	1-75
1.10.1. Non-Spinning Sphere	1-75
1.10.2. Non-Spinning Sphere. Including Internal Radiation	1-79
1.11. Thin-Walled Cylindrical Bodies. Finite Conductivity.	1-83
1.11.1. Non-Spinning Two-Dimensional Circular Cylinder	1-83
1.11.2. Spinning Two-Dimensional Circular Cylinder ..	1-87
1.11.3. Circular Cylinder. Solar Radiation Parallel to Axis of Symmetry	1-91
1.11.4. Cylindrical Surface of Rectangular Cross Sec- tion. Solar Radiation Normal to a Face	1-95
1.12. Thin-Walled Conical Bodies. Finite Conductivity	1-103
1.12.1. Non-Spinning Cone	1-103

SPACECRAFT SURFACE TEMPERATURE

Table of Contents

	Page
2. PLANETARY RADIATION	2-1
2.1. General	2-1
2.2. Infinitely Conductive Planar Surfaces	2-7
2.2.1. Flat Plate Absorbing and Emitting on One Side	2-7
2.3. Infinitely Conductive Spherical Surfaces	2-9
2.3.1. Sphere	2-9
2.3.2. Hemispherical Surface Absorbing and Emitting on Outer Face	2-11
2.4. Infinitely Conductive Cylindrical Surfaces	2-13
2.4.1. Circular Cylinder with Insulated Bases	2-13
2.4.2. Finite Height Circular Cylinder	2-15
2.5. Infinitely Conductive Conical Surfaces	2-25
2.5.1. Circular Cone with Insulated Base	2-25
2.5.2. Finite Height Circular Cone	2-29
3. ALBEDO RADIATION	3-1
3.1. General	3-1
3.2. Infinitely Conductive Planar Surfaces	3-7
3.2.1. Flat Plate Absorbing and Emitting on One Side	3-7
3.3. Infinitely Conductive Spherical Surfaces	3-13
3.3.1. Sphere	3-13
3.4. Infinitely Conductive Cylindrical Surfaces	3-17
3.4.1. Circular Cylinder with Insulated Bases	3-17
REFERENCES	4-1

SPACECRAFT SURFACE TEMPERATURE

List of Symbols

LIST OF SYMBOLS

- A_E , Emitting Area of the Spacecraft. [m^2].
- A_I , Area of the Spacecraft Projected from the Sun. [m^2].
- B_i , Parameters of the Truncated Power Series Development of F_{SP} .
See p. 2-2.
- F , Albedo View Factor from Spacecraft to Planet.
- F_{SP} , View Factor from Spacecraft to Planet.
- R_P , Mean Radius of the Planet. [m].
- S , Solar Flux. [$W.m^{-2}$]. $S = S_0 . d^{-2}$.
- S_0 , Solar Constant. $S_0 = 1\ 353\ W.m^{-2}$.
- T , Temperature. [K].
- T_A , Albedo Temperature. [K]. $T_A = \left[\frac{aS_0}{\sigma d^2} \right]^{1/4}$.
- T_R , Radiation Equilibrium Temperature of the Infinitely Conductive Spacecraft. [K].
- T_{RA} , Radiation Equilibrium Temperature of the Infinitely Conductive Spacecraft under Albedo Radiation. [K].
- T_{RP} , Radiation Equilibrium Temperature of the Infinitely Conductive Spacecraft under Planetary Radiation. [K].
- T_P , Equivalent Planet Temperature. [K]. $T_P = \left(\frac{e}{\sigma} \right)^{1/4}$.
- T_S , Equivalent Surrounding Temperature. [K].
- a , Mean Albedo of the Planet.
- b , Wall Thickness. [m].
- c , Specific Heat. [$J.kg^{-1}.K^{-1}$].
- d , Chap. 1: Distance from the Sun Center to the Spacecraft.
[AU].

SPACECRAFT SURFACE TEMPERATURE

List of Symbols

- d , Chap. 3: Distance between Sun Center and Planet Center. [AU].
- e , Mean Emissive Power of the Planet per Unit Area. [W.m^{-2}].
- h , Distance from the Spacecraft to the Planet Surface. [m].
- k , Thermal Conductivity. [$\text{W.m}^{-1}.\text{K}^{-1}$].
- γ , Dimensionless Specific Heat in the Spinning Thin-Walled Spacecraft. $\gamma = \frac{\rho b c \omega}{\epsilon \sigma T_R^3}$.
- α , Hemispherical Absorptance.
- α_s , Solar Absorptance.
- ϵ , Hemispherical Total Emittance.
- μ , Dimensionless Thermal Conductance in the Thin-Walled Spacecraft. $\mu = \frac{k b}{\epsilon \sigma T_R^3 R^2}$, where R is a characteristic length of the spacecraft surface.
- ρ , Density, [kg.m^{-3}].
- σ , Stefan-Boltzmann Constant. $\sigma = 5.6697 \times 10^{-8} \text{ W.m}^{-2}.\text{K}^{-4}$.
- τ , Dimensionless Temperature. $\tau = T/T_R$.
- ω , Angular Velocity of the Spinning Spacecraft.

Other symbols, mainly used to define the geometry of the configuration, are introduced when required.

SOLAR RADIATION

General

1. SOLAR RADIATION1.1. GENERAL

Data on the equilibrium temperature of a satellite, heated by the Sun, and cooled by radiation to the outer space, are presented in this Chapter. Fairly simple geometrical configurations are considered. The temperature field within the satellite corresponds to either of the following two simplifying assumptions.

1) Infinitely conductive satellite. The satellite is constituted by a homogeneous solid body, exhibiting infinitely large thermal conductivity. The temperature of the satellite is uniform. This temperature is usually named Spacecraft Radiation Equilibrium Temperature, and is represented by T_R . The following additional assumptions have been used for the calculations:

- a) The heat addition is by parallel radiation from the Sun.
- b) The Equivalent Surrounding Temperature, T_s , is assumed to be zero.
- c) Emittance and solar absorptance of the satellite surface are independent of both temperature and wavelength.
- d) Absorptance is independent of the angle between the surface normal and the direction of the incoming radiation.

The Spacecraft Radiation Equilibrium Temperatures, T_R , is given by

$$T_R = \left[\frac{\alpha_s}{\epsilon} \frac{A_I}{A_E} \frac{S_o}{\sigma d^2} + T_s^4 \right]^{1/4},$$

where T_s is assumed to be zero as it has been indicated above.

SOLAR RADIATION

General

2) Satellites of finite thermal conductivity. A limited amount of the data presented in this Chapter concerns bodies of finite thermal conductivity. Some knowledge of the internal structure of the satellite is required to evaluate the temperature field. Here it is assumed that the satellite is a thin-walled body with no internal conductive structure, furthermore, in most cases the gas contained within the body is assumed to be opaque and non conducting.

The data presented are based on the following assumptions:

- a) The heat addition is by parallel radiation from the Sun.
- b) The Equivalent Surrounding Temperature, T_s , is assumed to be zero.
- c) The configuration has an axis of symmetry, solar radiation being parallel to this axis.
- d) Emittance and solar absorptance of the satellite surface are independent of both temperature and wavelength.
- e) Thermal conductivity is temperature independent.
- f) Lambert's law is assumed to govern reflection and emission.
- g) The body is filled with an opaque non-conducting gas.

The results are presented in terms of the local temperature, T , made dimensionless with the Spacecraft Radiation Equilibrium Temperature, T_R .

SOLAR RADIATION
General

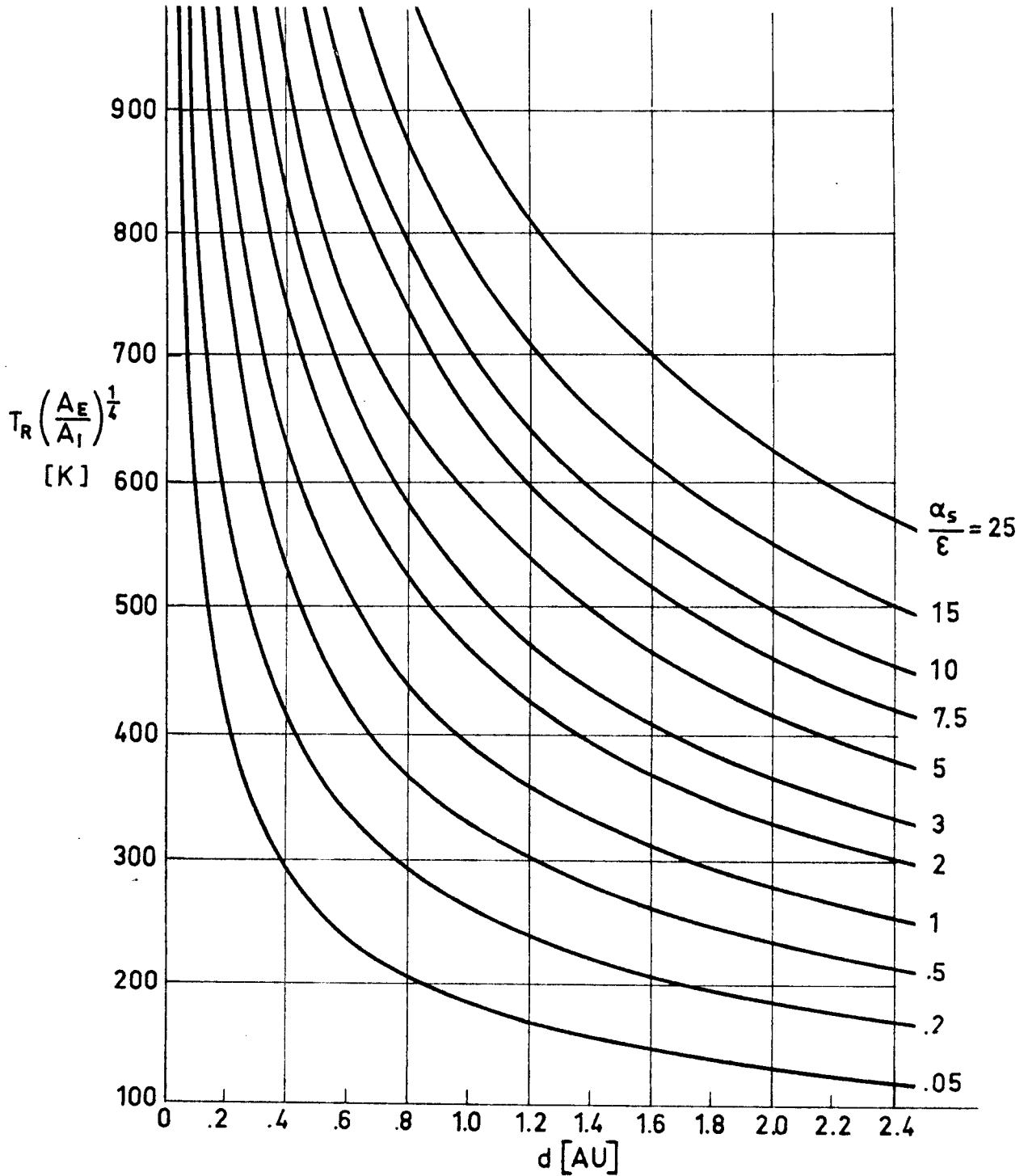


Fig 1-1. The function $T_R \left(\frac{A_E}{A_I}\right)^{1/4}$ vs. the distance to the Sun.
Calculated by the compiler.

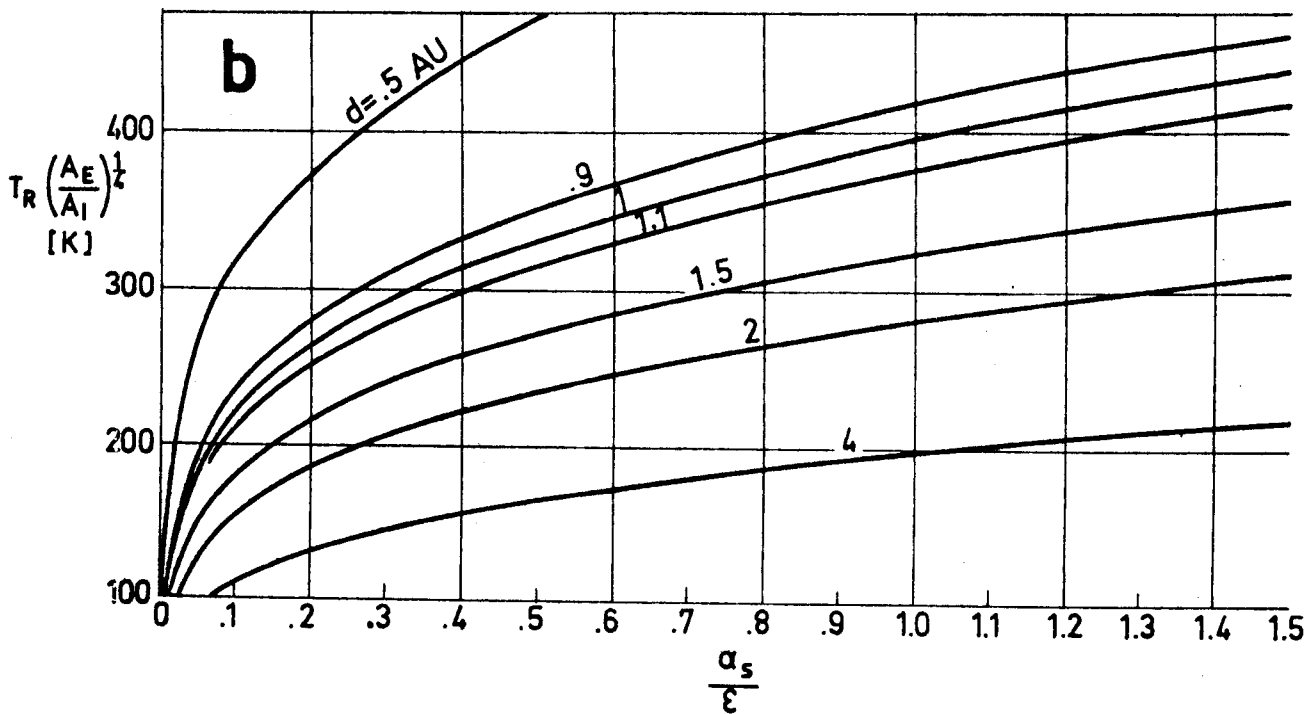
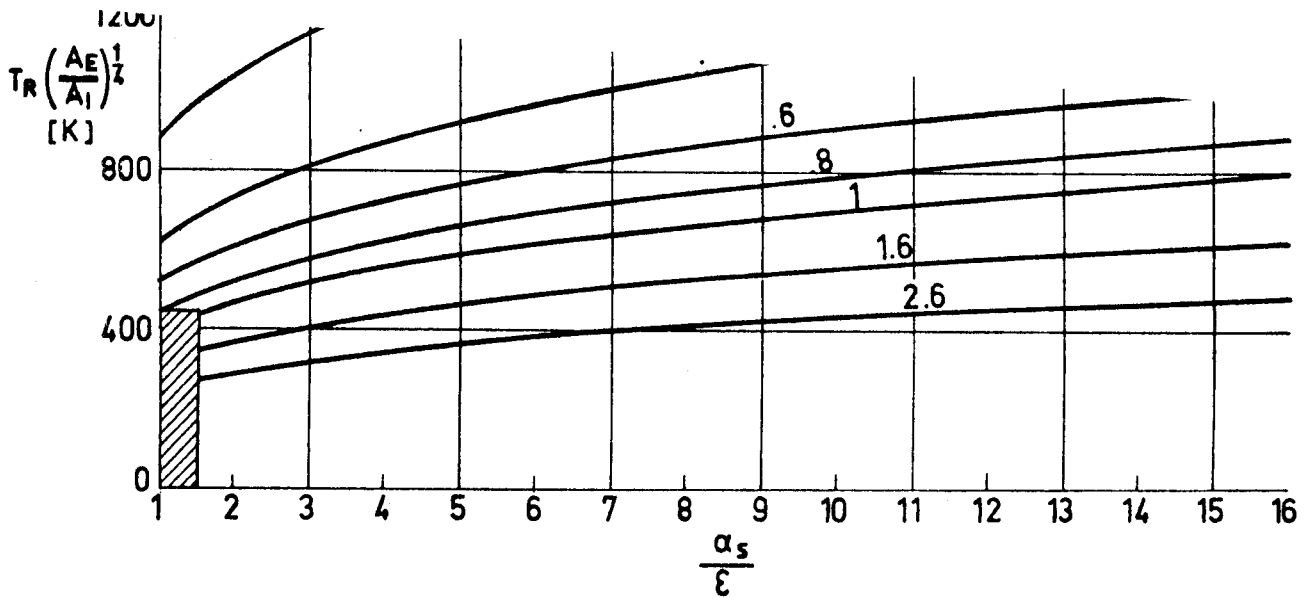


Fig 1-2. The function $T_R \left(\frac{AE}{AI} \right)^{1/4}$ vs. the optical characteristics of the surface. Shaded zone of a is enlarged in b. Calculated by the compiler.

SOLAR RADIATION
General

d = 1 AU

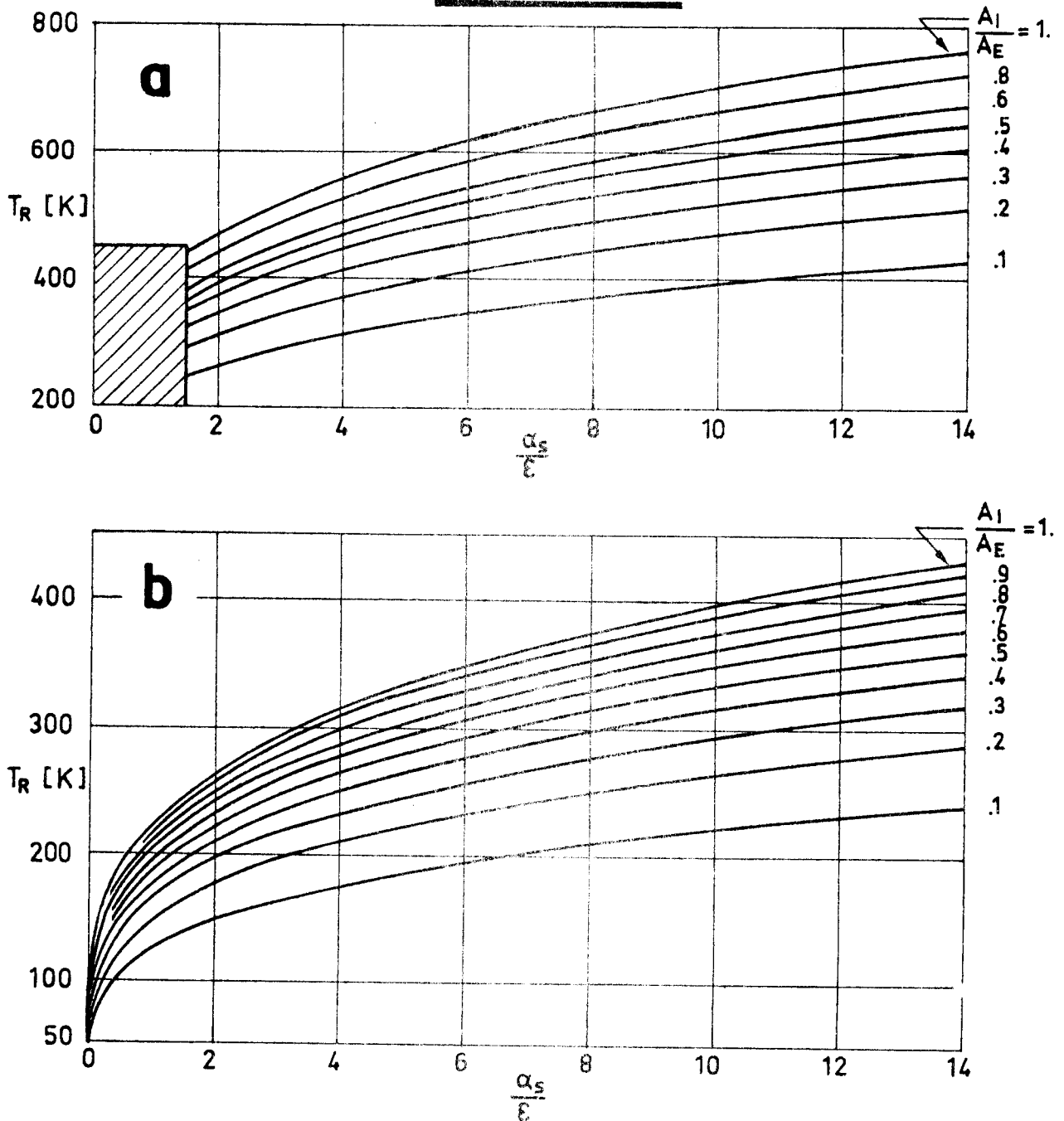


Fig 1-3. Temperature T_R as a function of α_s/ϵ and A_I/A_E for $d=1$ AU. Shaded zone of a is enlarged in b. Calculated by the compiler.

INTENTIONALLY BLANK PAGE

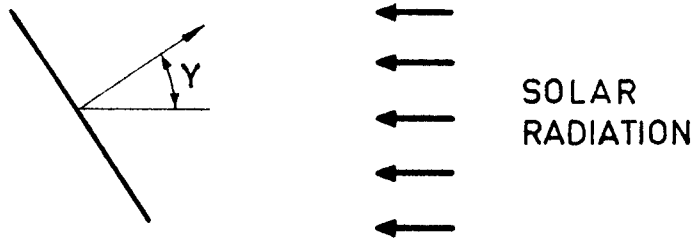
SOLAR RADIATION
Infinitely Conductive Planar Surfaces

1.2. INFINITELY CONDUCTIVE PLANAR SURFACES

1.2.1. FLAT PLATE EMITTING ON ONE OR BOTH SIDES

I.- FLAT PLATE EMITTING ON ONE SIDE.

Sketch:

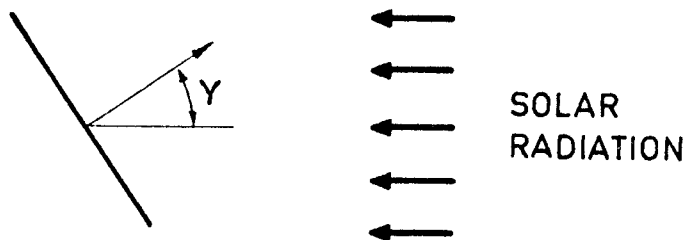


Formula:

$$\frac{A_I}{A_E} = \cos \gamma$$

II.- FLAT PLATE EMITTING ON BOTH SIDES.

Sketch:



Formula:

$$\frac{A_I}{A_E} = \frac{\cos \gamma}{2}$$

SOLAR RADIATION
 Infinitely Conductive Planar Surfaces

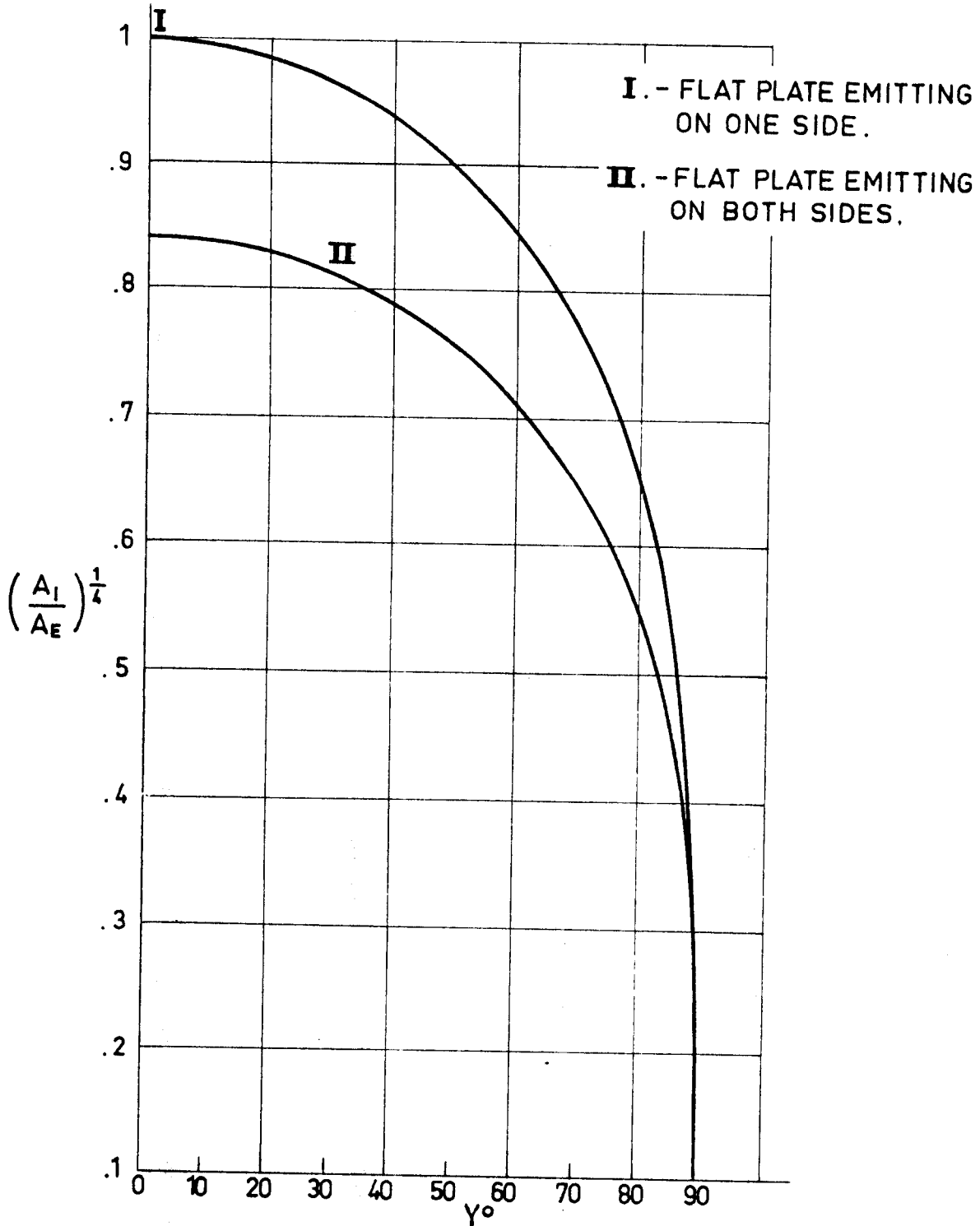


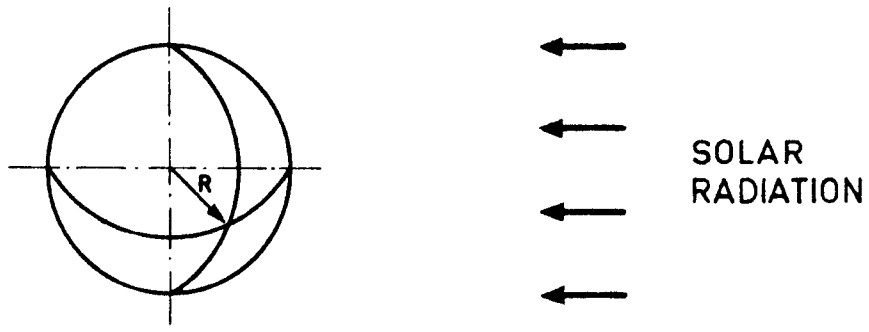
Fig 1-4. Ratio $\left(\frac{A_I}{A_E}\right)^{1/4}$ as a function of γ , in the case of a flat plate. Calculated by the compiler.

SOLAR RADIATION
 Infinitely Conductive Spherical Surfaces

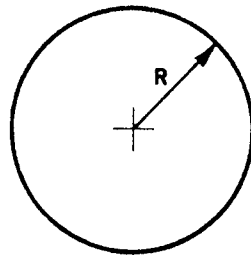
1.3. INFINITELY CONDUCTIVE SPHERICAL SURFACES

1.3.1. SPHERE

Sketch:



Area Projected from the Sun, A_I :



Formula:

$$\frac{A_I}{A_E} = \frac{1}{4}$$

$$\left(\frac{A_I}{A_E}\right)^{1/4} = 0.707$$

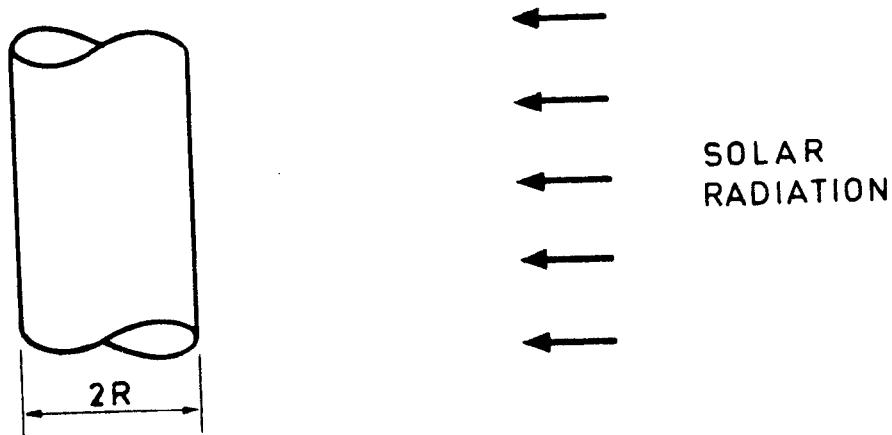
INTENTIONALLY BLANK PAGE

SOLAR RADIATION
 Infinitely Conductive Cylindrical Surfaces

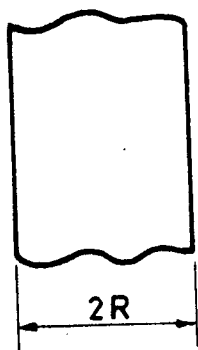
1.4. INFINITELY CONDUCTIVE CYLINDRICAL SURFACES

1.4.1. TWO-DIMENSIONAL CIRCULAR CYLINDER

Sketch:



Area Projected from the Sun, A_I :



Formula:

$$\frac{A_I}{A_E} = \frac{1}{\pi}$$

$$\left(\frac{A_I}{A_E}\right)^{1/4} = 0.751$$

Comments:

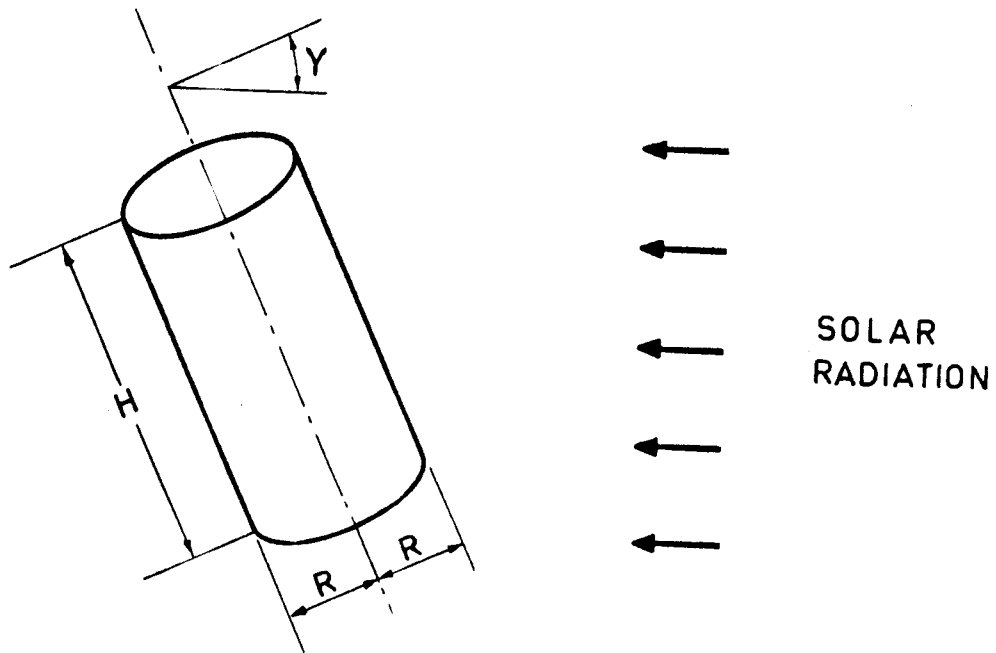
This expression can be also applied to the finite circular cylinder with isolated bases.

INTENTIONALLY BLANK PAGE

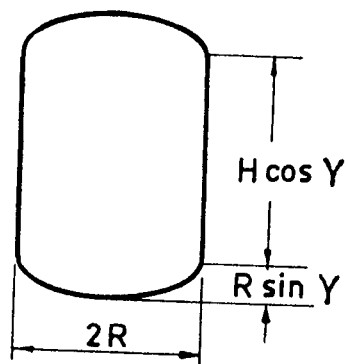
SOLAR RADIATION
 Infinitely Conductive Cylindrical Surfaces

1.4.2. THREE DIMENSIONAL CIRCULAR CYLINDER

Sketch:



Area Projected from the Sun, A_I :



Formula :

$$\frac{A_I}{A_E} = \frac{\pi \sin \gamma + 2 \left(\frac{H}{R}\right) \cos \gamma}{2 \pi \left[1 + \left(\frac{H}{R}\right) \right]}$$

SOLAR RADIATION
 Infinitely Conductive Cylindrical Surfaces

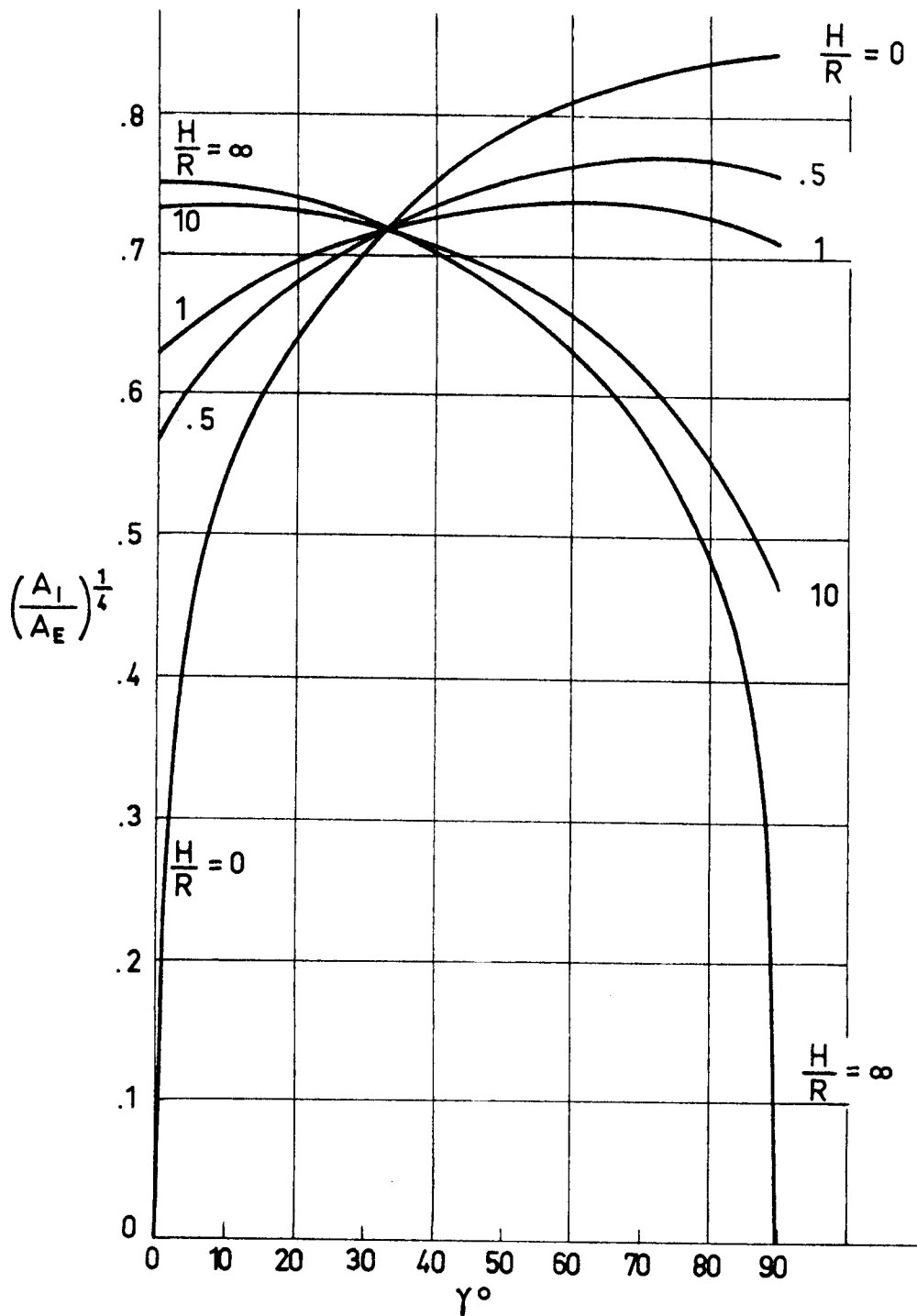


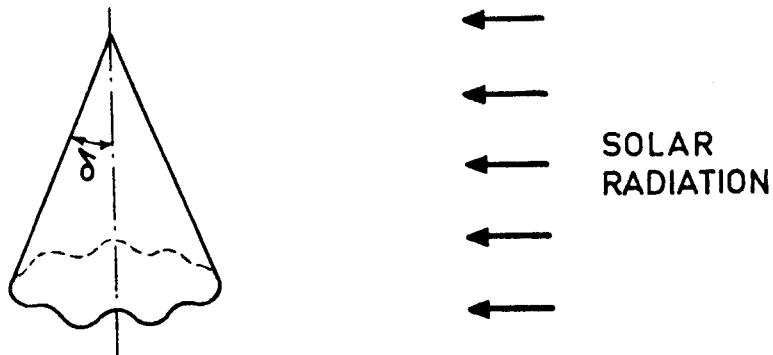
Fig 1-5. Ratio $\left(\frac{A_I}{A_E}\right)^{1/4}$ as a function of γ and $\frac{H}{R}$, in the case of a finite height circular cylinder. Calculated by the compiler.

SOLAR RADIATION
 Infinitely Conductive Conical Surfaces

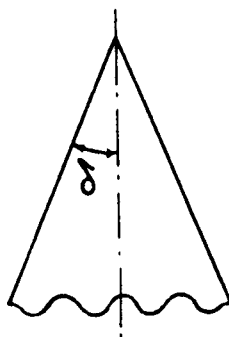
1.5. INFINITELY CONDUCTIVE CONICAL SURFACES

1.5.1. SEMI-INFINITE CIRCULAR CONE

Sketch:



Area Projected from the Sun, A_I :



Formula:

$$\frac{A_I}{A_E} = \frac{\cos \delta}{\pi}$$

Comments:

This expression can be also applied to the finite circular cone with isolated base provided that the incoming radiation is normal to the cone axis.

SOLAR RADIATION
Infinitely Conductive Conical Surfaces

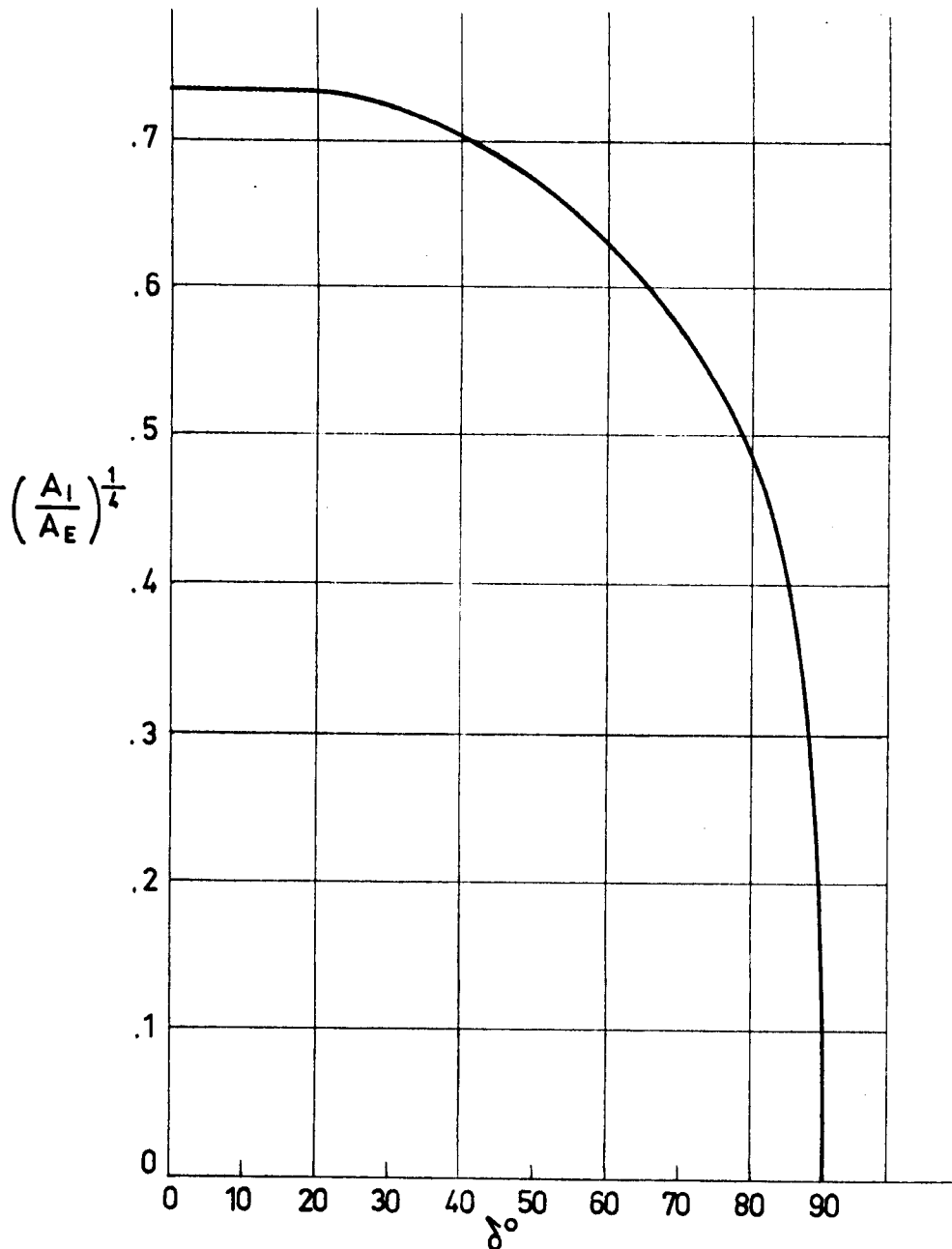
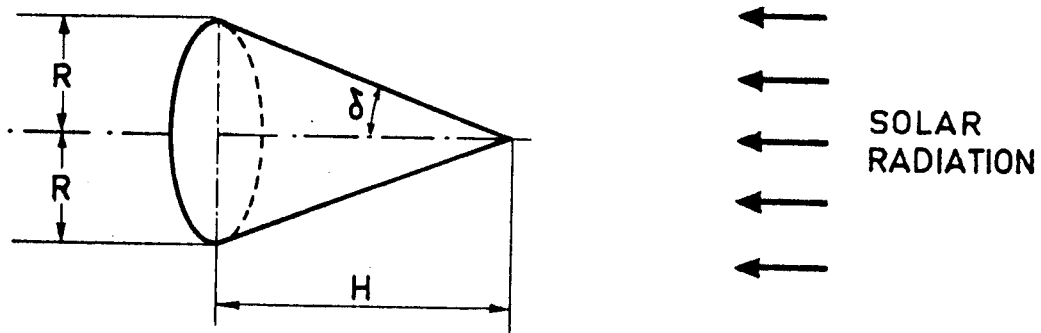


Fig 1-6. Ratio $\left(\frac{A_I}{A_E}\right)^{1/4}$ as a function of δ , in the case of a semi-infinite circular cone. Calculated by the compiler.

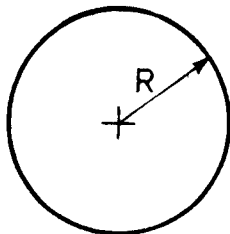
SOLAR RADIATION
 Infinitely Conductive Conical Surfaces

1.5.2. FINITE CIRCULAR CONE WITH INSULATED BASE. (AXIAL CONFIGURATION)

Sketch:



Area Projected from the Sun, A_I :



Formula:

$$\frac{A_I}{A_E} = \sin \delta$$

SOLAR RADIATION
Infinitely Conductive Conical Surfaces

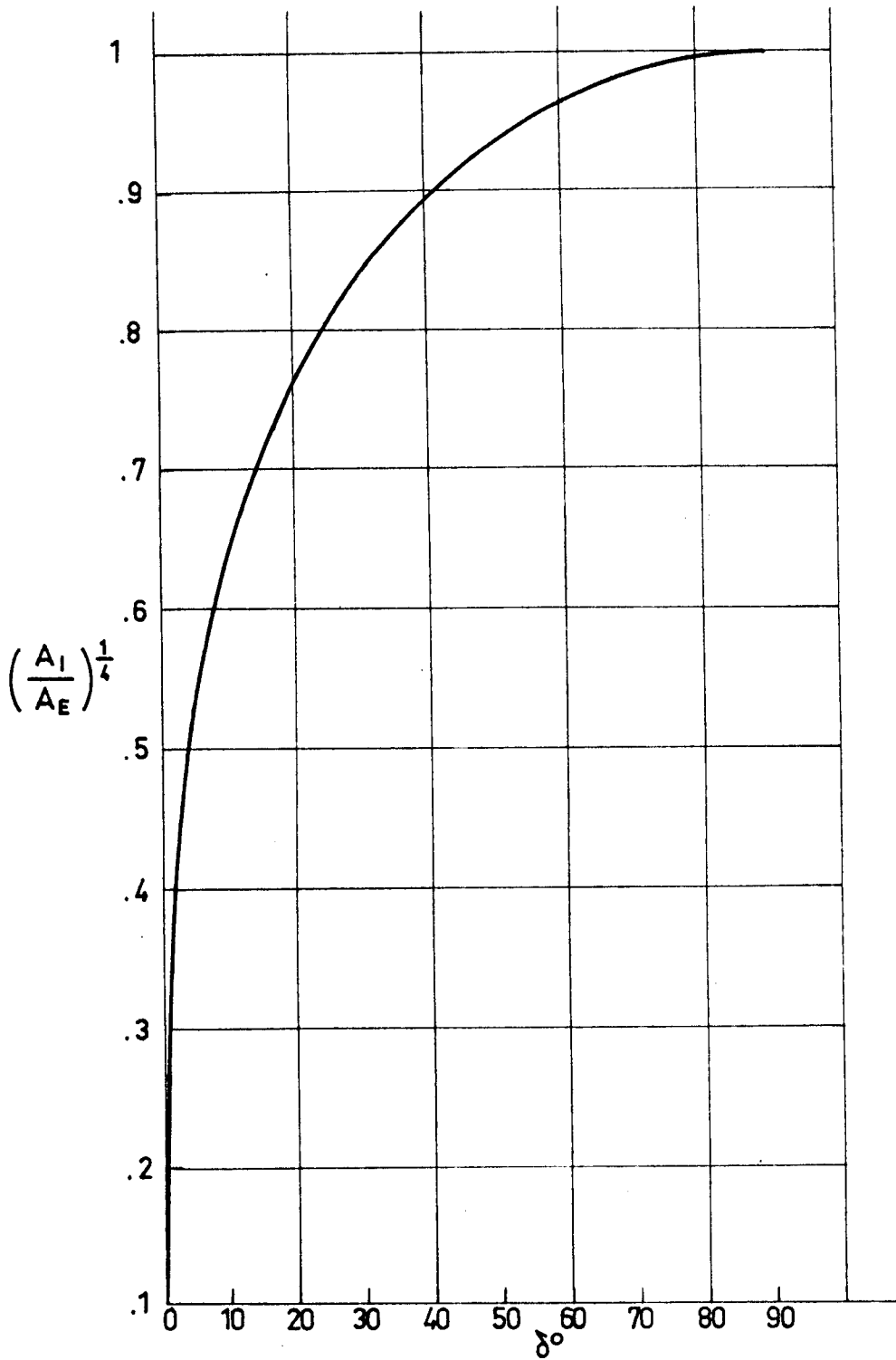
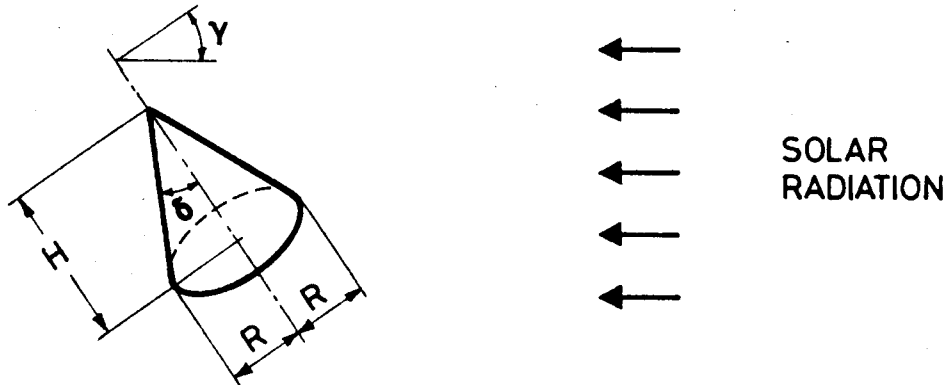


Fig 1-7. Ratio $\left(\frac{A_I}{A_E}\right)^{1/4}$ as a function of δ , in the case of a finite circular cone with insulated base (axial configuration). Calculated by the compiler.

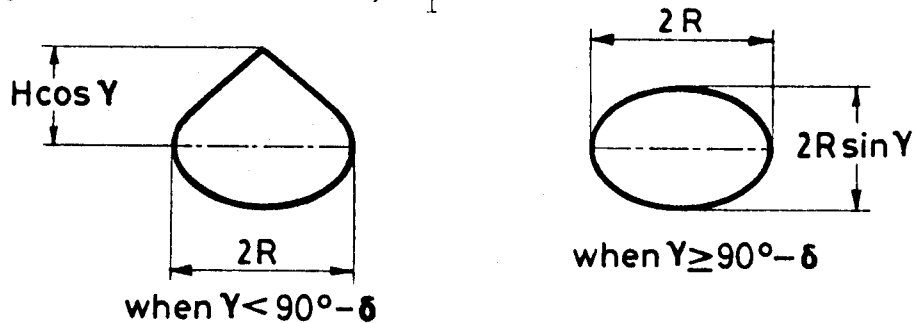
SOLAR RADIATION
 Infinitely Conductive Conical Surfaces

1.5.3. FINITE HEIGHT CIRCULAR CONE

Sketch:



Area Projected from the Sun, A_I :



Formula:

a) when $0 \leq \gamma \leq 90^\circ - \delta$,

$$\frac{A_I}{A_E} = \frac{\sin \gamma \sin \delta}{\pi(1 + \sin \delta)} \left[\pi + \frac{\sqrt{1 - \tan^2 \gamma \tan^2 \delta}}{\tan \gamma \tan \delta} - \sin^{-1} \sqrt{1 - \tan^2 \gamma \tan^2 \delta} \right]$$

when $\gamma = 0$ the above expression becomes

$$\frac{A_I}{A_E} = \frac{\cos \delta}{\pi(1 + \sin \delta)}$$

b) when $\gamma \geq 90^\circ - \delta$,

$$\frac{A_I}{A_E} = \frac{\sin \delta \sin \gamma}{1 + \sin \delta}$$

Rev. 3. 1986

SOLAR RADIATION
 Infinitely Conductive Conical Surfaces

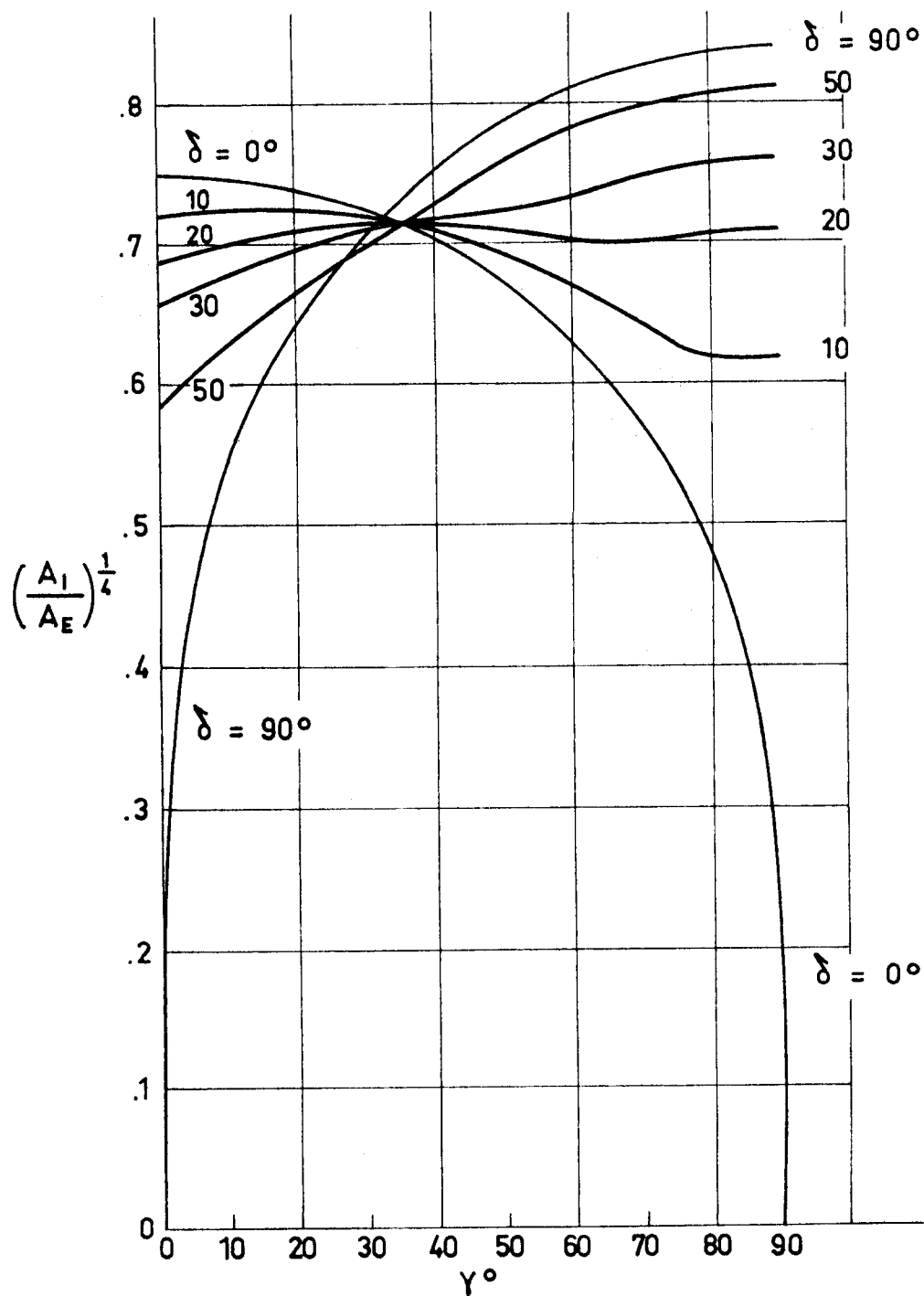


Fig 1-8. Ratio $\left(\frac{A_I}{A_E}\right)^{1/4}$ as a function of γ and δ , in the case of a finite height cone. Calculated by the compiler.

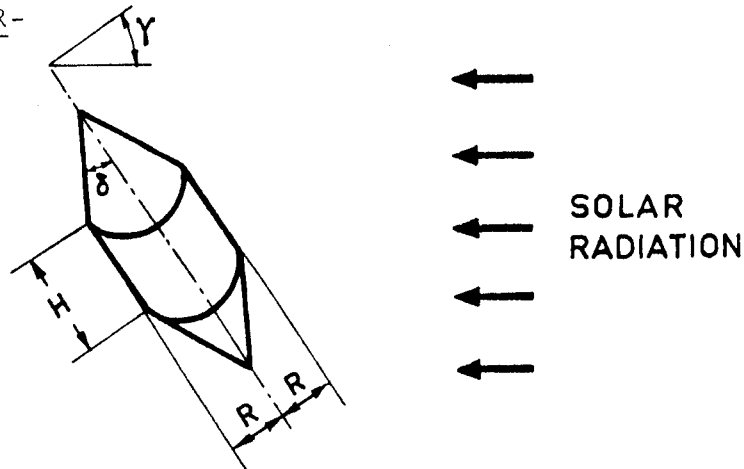
SOLAR RADIATION

Infinitely Conductive Cylindrical-Conical Surfaces

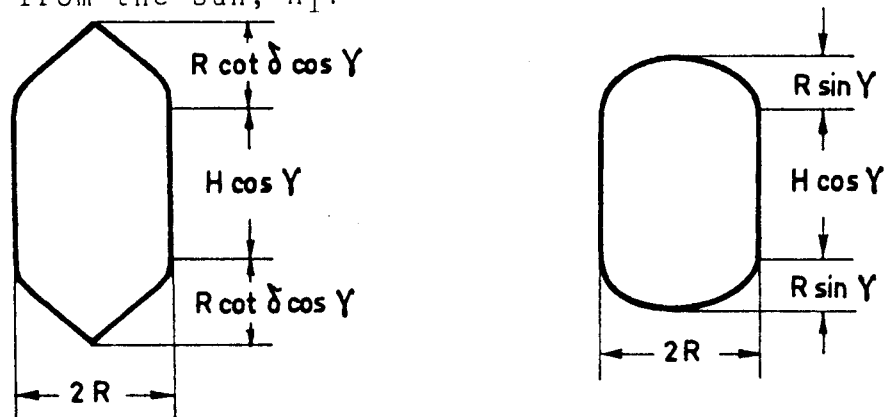
1.6. INFINITELY CONDUCTIVE CYLINDRICAL-CONICAL SURFACES

1.6.1. CONE-CYLINDER-
CONE

Sketch:



Area Projected from the Sun, A_I :



Formula:

a) When $\gamma \leq 90^\circ - \delta$

$$\frac{A_I}{A_E} = \frac{\sin \gamma \sin \delta \left[\frac{\pi}{2} - \sin^{-1} \sqrt{1 - \tan^2 \gamma \tan^2 \delta} \right]}{\pi \left[1 + \frac{H}{R} \sin \delta \right]} + \frac{\cos \gamma \left[\frac{H}{R} \sin \delta + \cos \delta \sqrt{1 - \tan^2 \gamma \tan^2 \delta} \right]}{\pi \left[1 + \frac{H}{R} \sin \delta \right]}$$

b) When $\gamma \geq 90^\circ - \delta$

$$\frac{A_I}{A_E} = \frac{\sin \delta \left[\sin \gamma + \frac{2H}{\pi R} \cos \gamma \right]}{\pi \left[1 + \frac{H}{R} \sin \delta \right]}$$

SOLAR RADIATION

Infinitely Conductive Cylindrical-Conical Surfaces

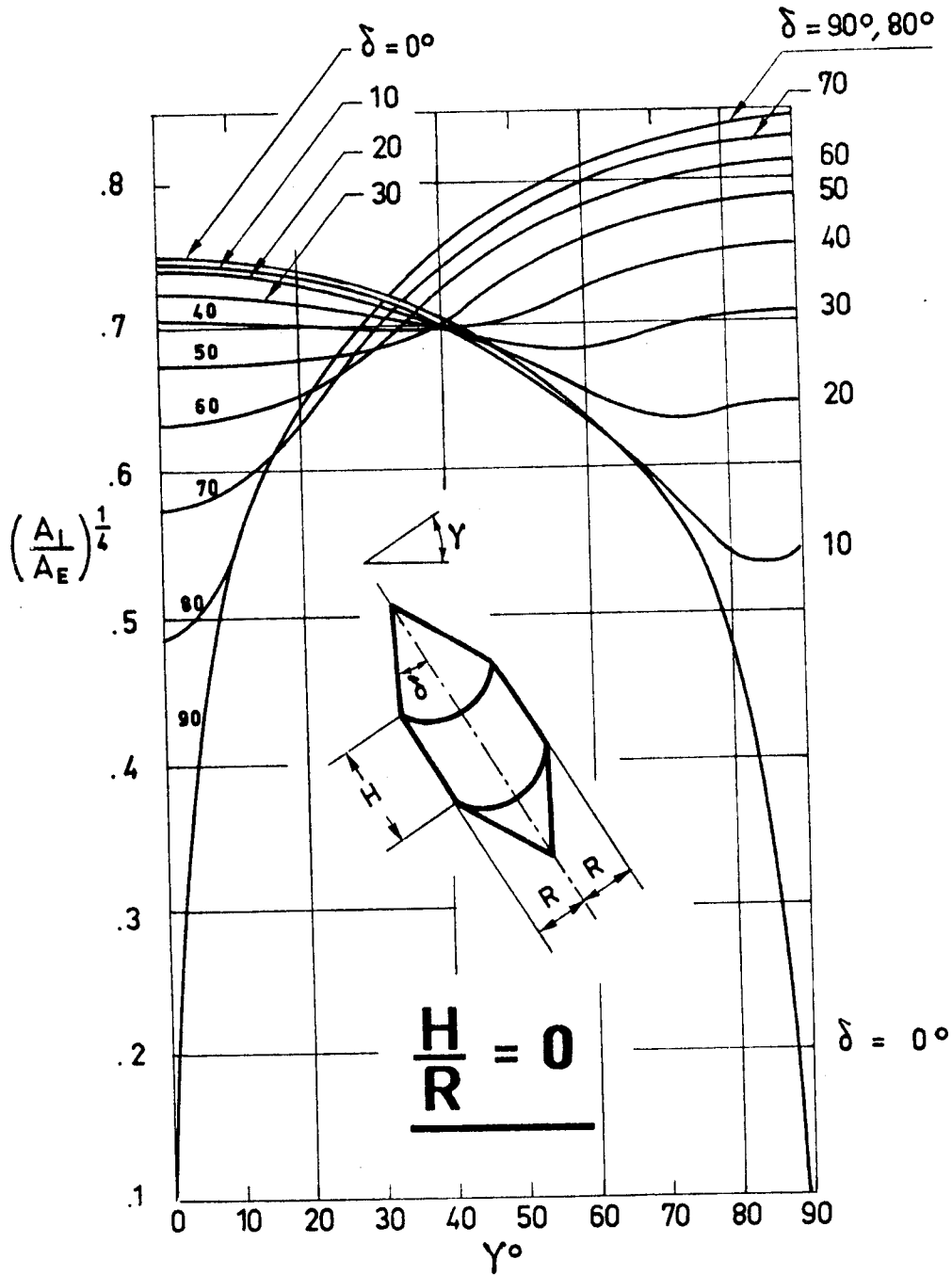


Fig 1-9. Ratio $(\frac{A_I}{A_E})^{1/4}$ as a function of γ and δ , in the case of a cone-cylinder-cone. Calculated by the compiler.

SOLAR RADIATION

Infinitely Conductive Cylindrical-Conical Surfaces

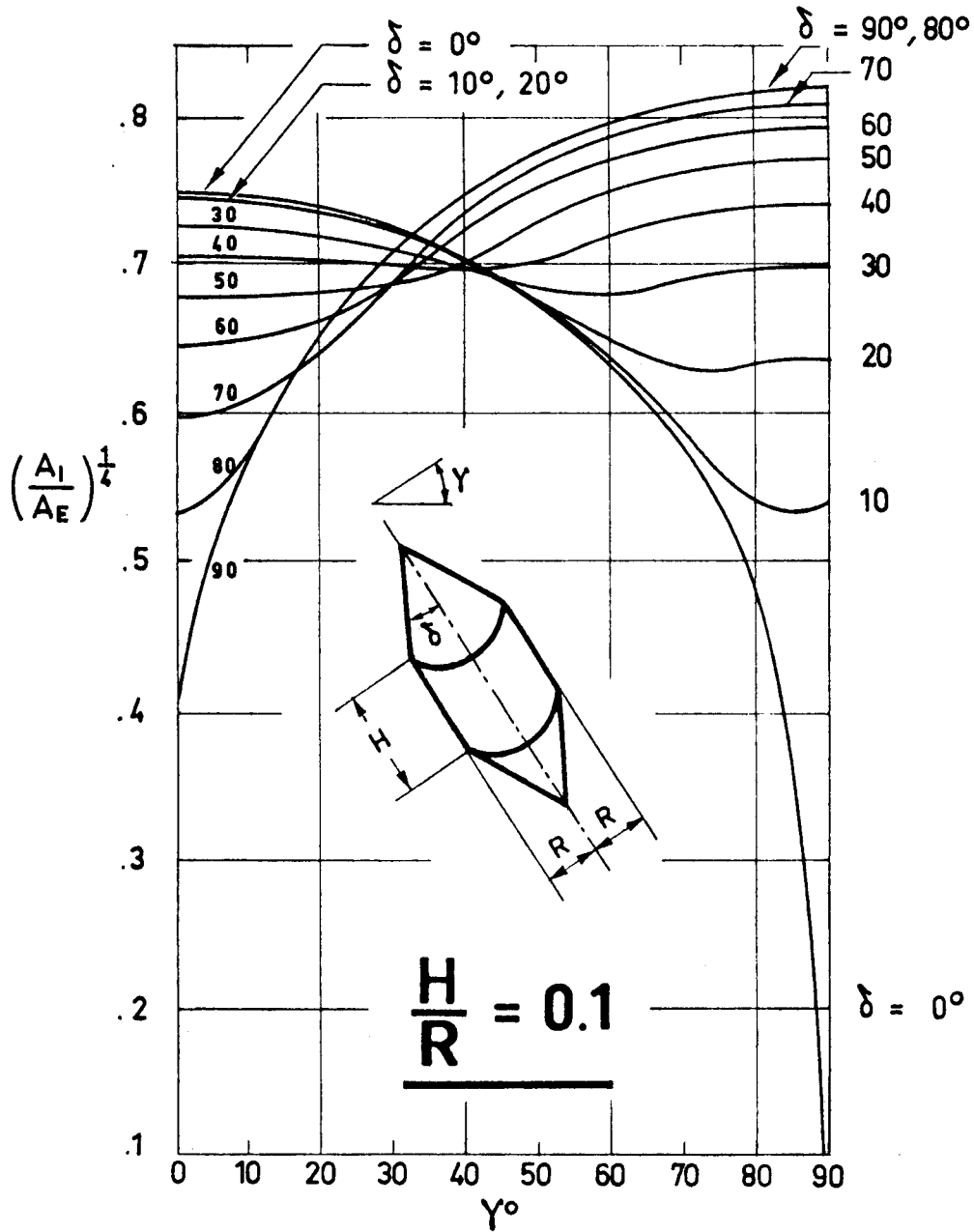


Fig 1-10. Ratio $(\frac{A_I}{A_E})^{1/4}$ as a function of γ and δ , in the case of a cone-cylinder-cone. Calculated by the compiler.

SOLAR RADIATION
Infinitely Conductive Cylindrical-Conical Surfaces

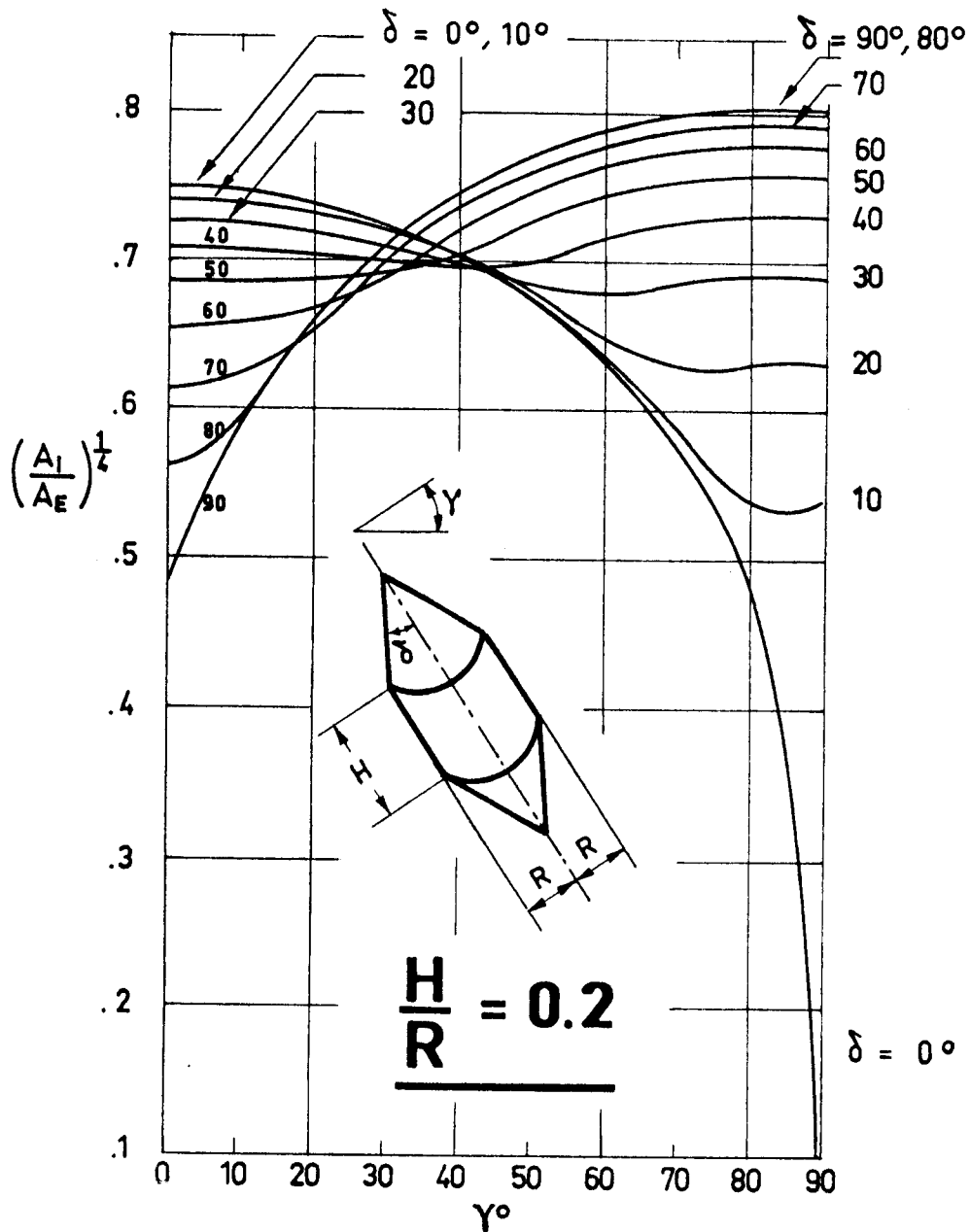


Fig 1-11. Ratio $(\frac{A_I}{A_E})^{1/4}$ as a function of γ and δ , in the case of a cone-cylinder-cone. Calculated by the compiler.

SOLAR RADIATION
 Infinitely Conductive Cylindrical-Conical Surfaces

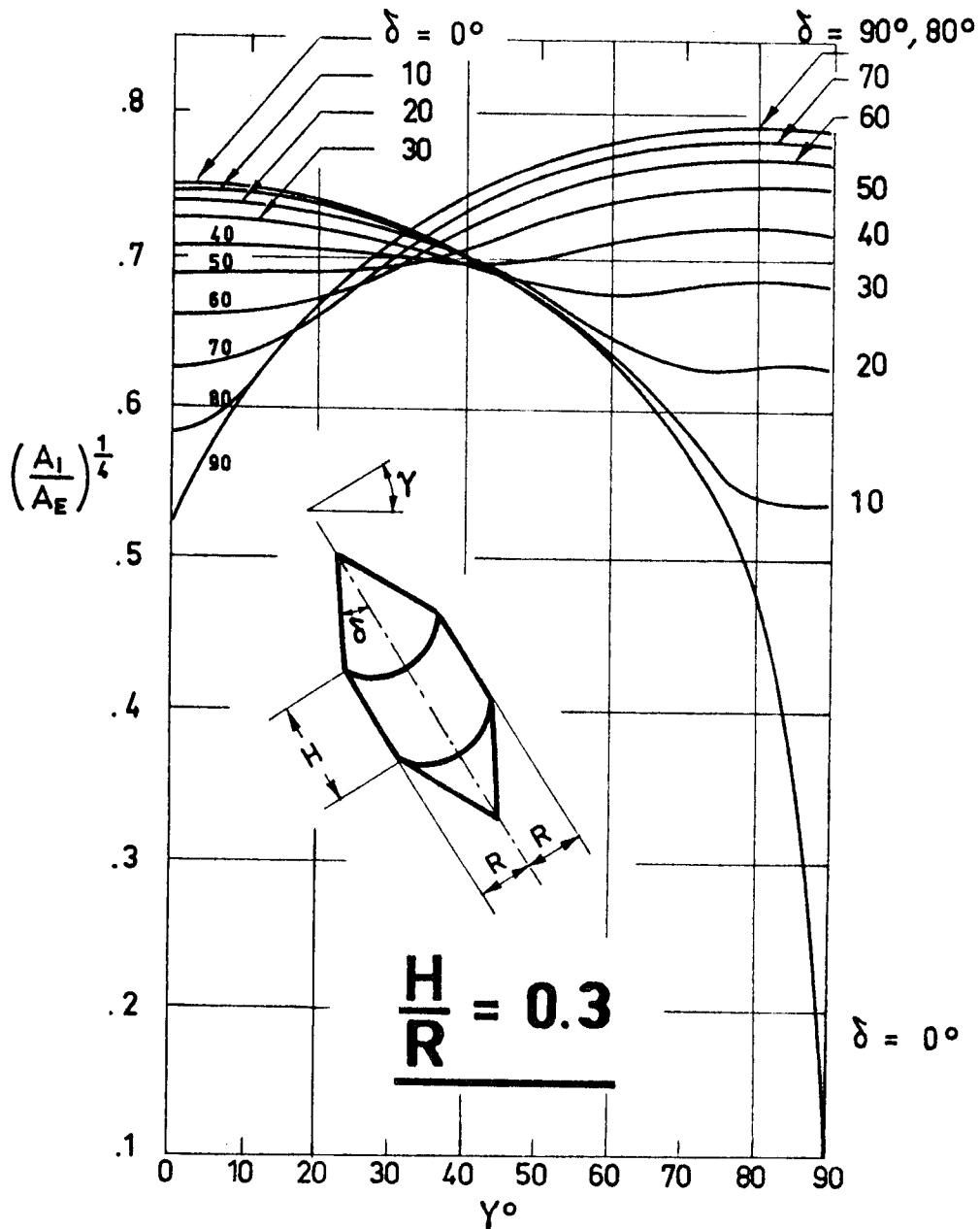


Fig 1-12. Ratio $(\frac{A_I}{A_E})^{1/4}$ as a function of γ and δ , in the case of a cone-cylinder-cone. Calculated by the compiler.

SOLAR RADIATION

Infinitely Conductive Cylindrical-Conical Surfaces

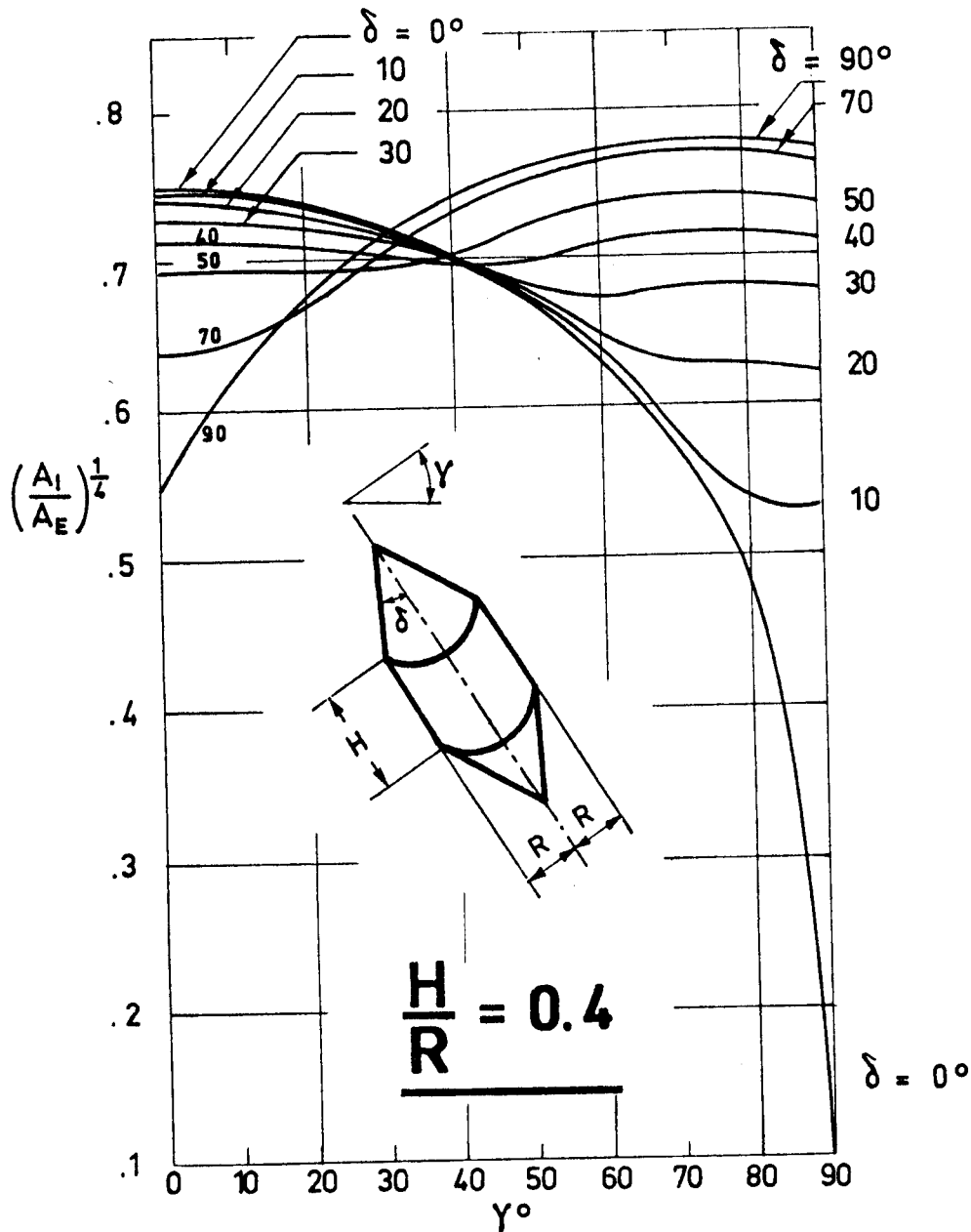


Fig 1-13. Ratio $(\frac{A_I}{A_E})^{1/4}$ as a function of γ and δ , in the case of a cone-cylinder-cone. Calculated by the compiler.

SOLAR RADIATION
 Infinitely Conductive Cylindrical-Conical Surfaces

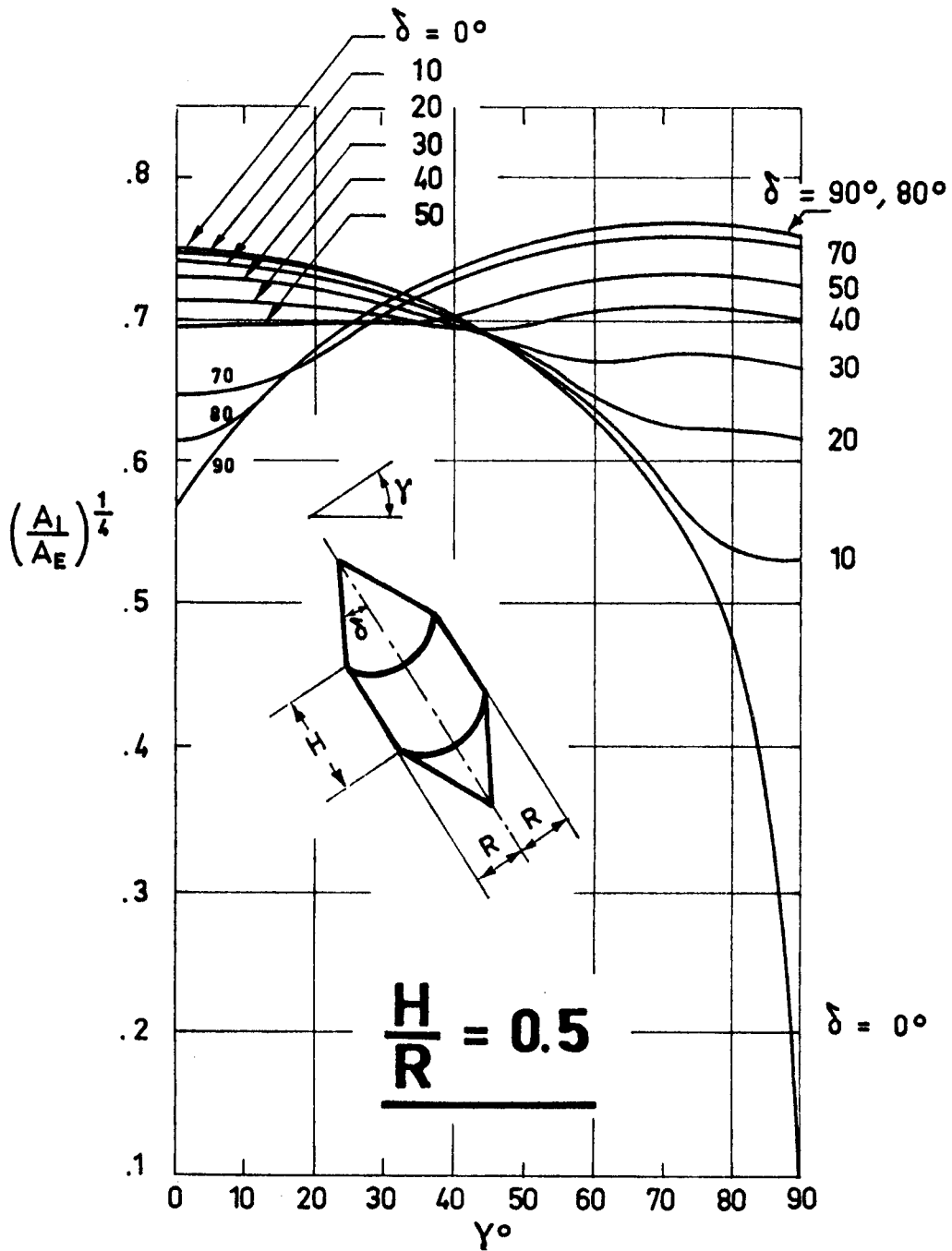


Fig 1-14. Ratio $(\frac{A_I}{A_E})^{1/4}$ as a function of γ and δ , in the case of a cone-cylinder-cone. Calculated by the compiler.

SOLAR RADIATION

Infinitely Conductive Cylindrical-Conical Surfaces

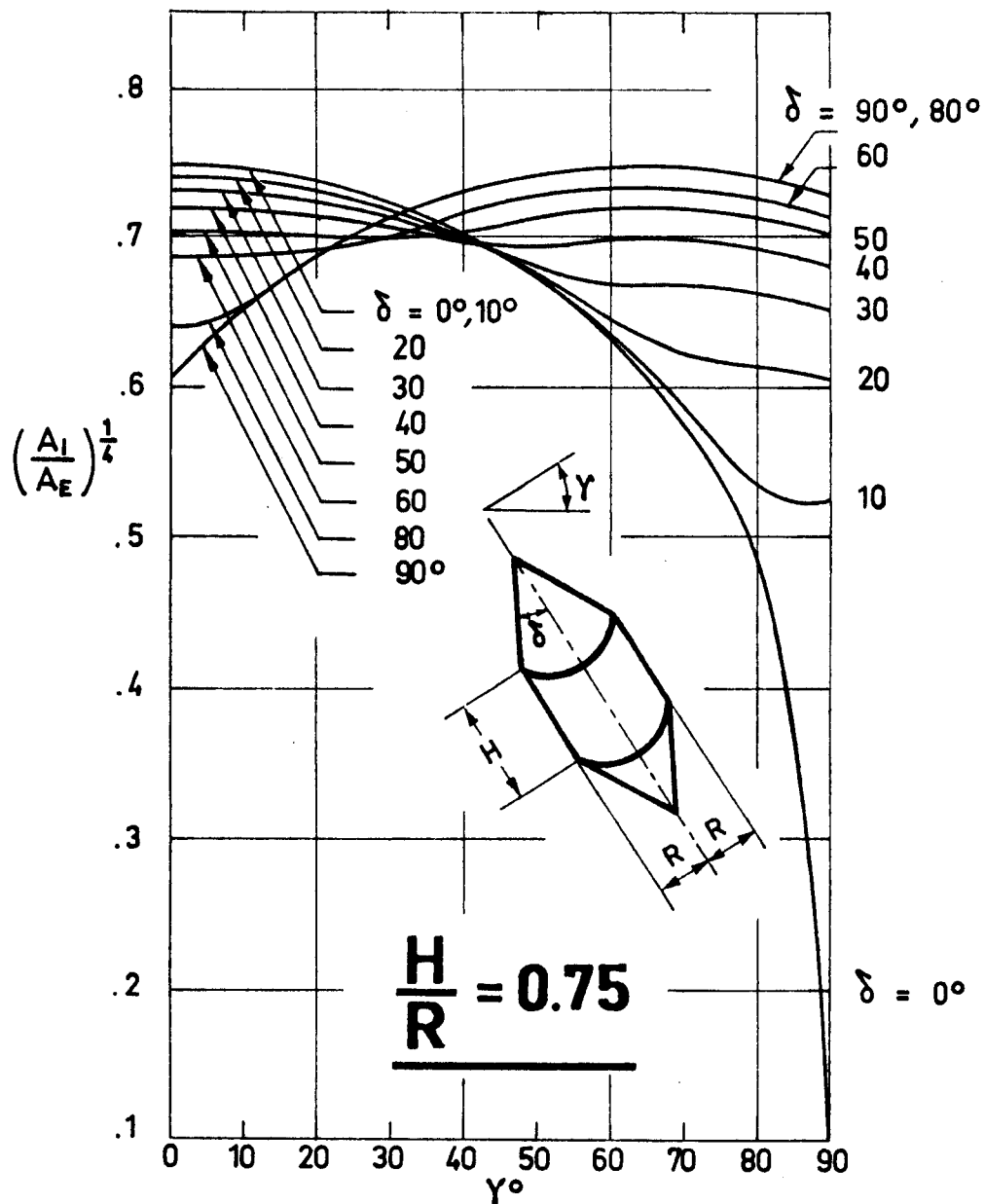


Fig 1-15. Ratio $(\frac{A_I}{A_E})^{1/4}$ as a function of γ and δ , in the case of a cone-cylinder-cone. Calculated by the compiler.

SOLAR RADIATION
 Infinitely Conductive Cylindrical-Conical Surfaces

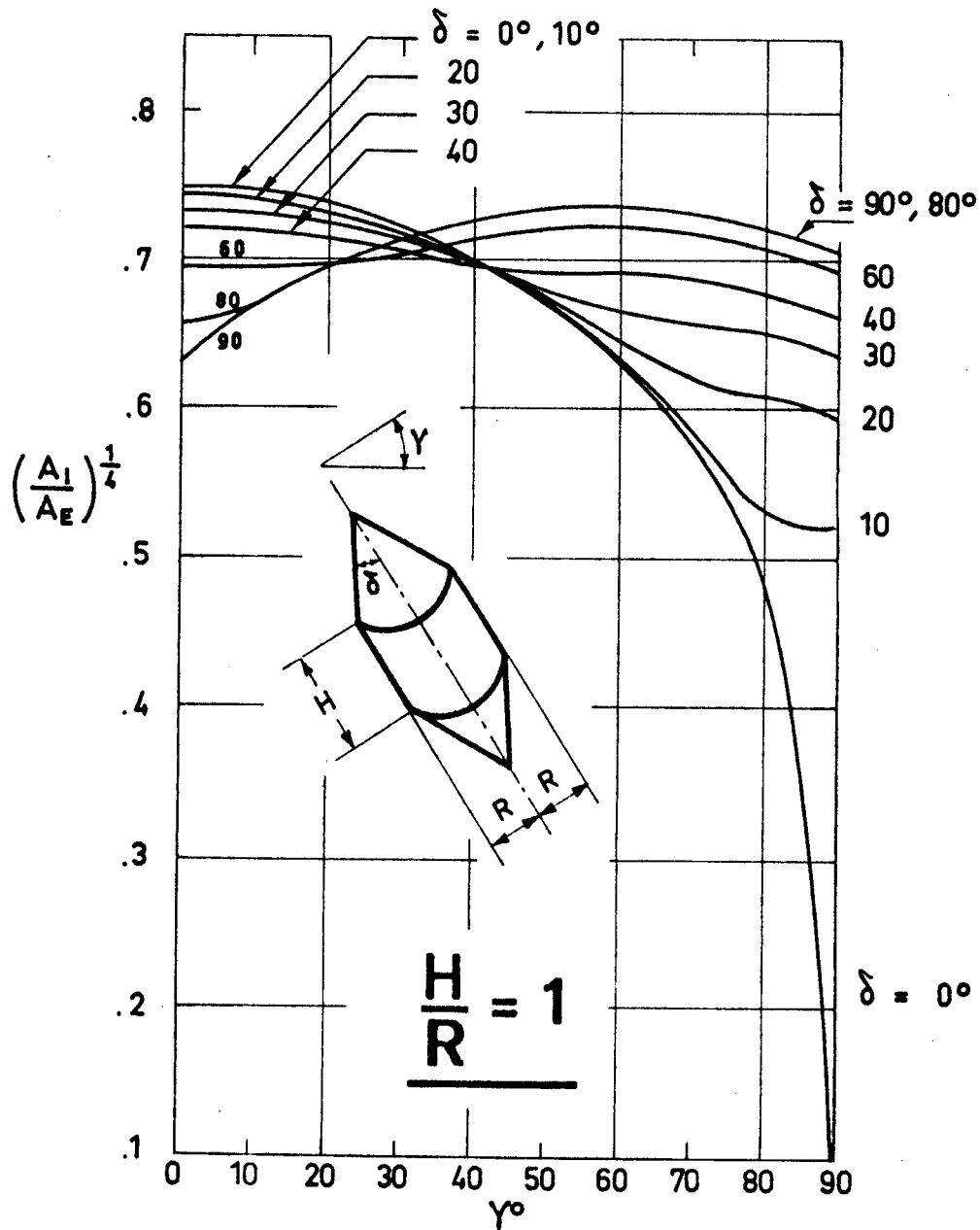


Fig 1-16. Ratio $(\frac{A_I}{A_E})^{1/4}$ as a function of γ and δ , in the case of a cone-cylinder-cone. Calculated by the compiler.

SOLAR RADIATION

Infinitely Conductive Cylindrical-Conical Surfaces

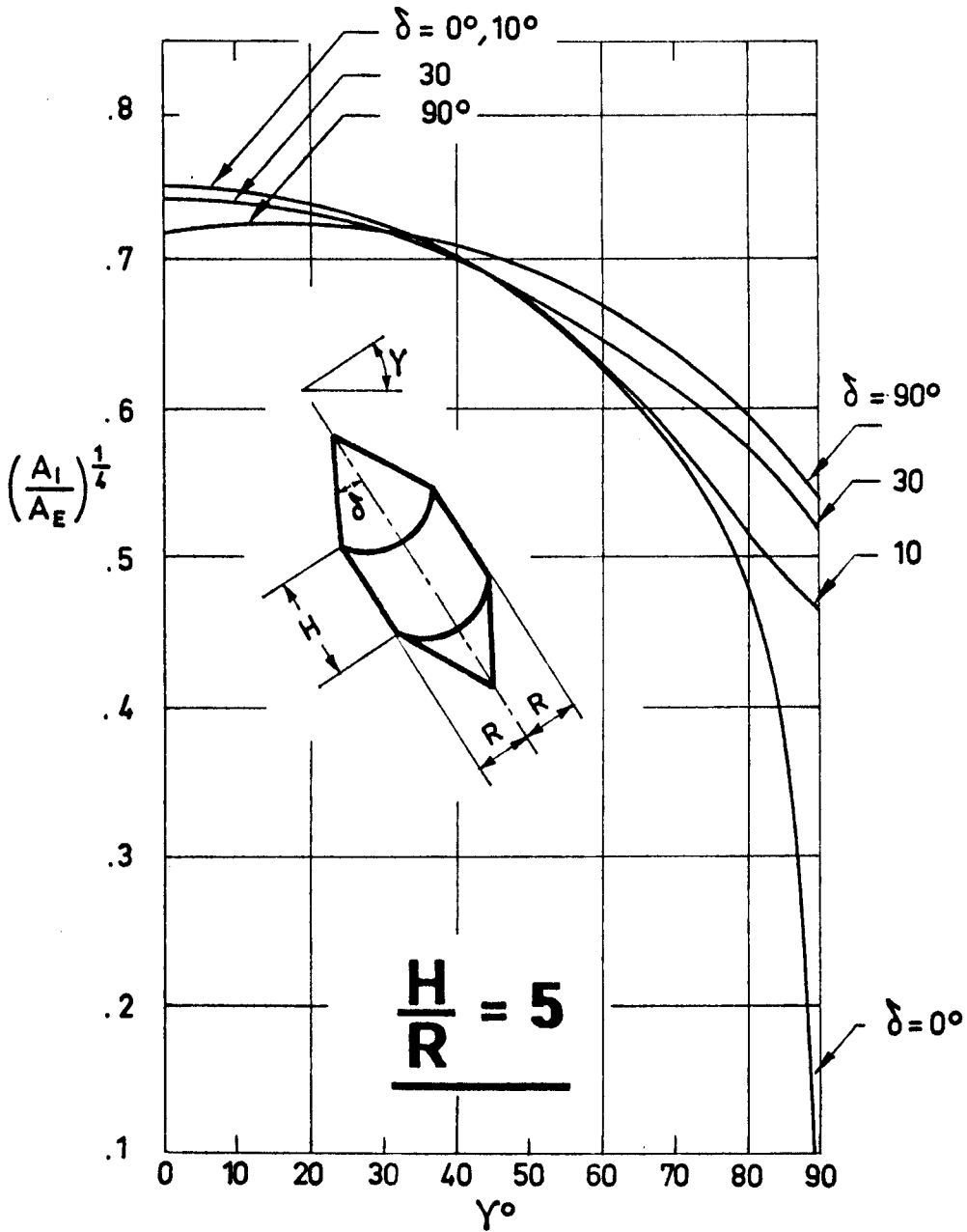


Fig 1-17. Ratio $(\frac{A_I}{A_E})^{1/4}$ as a function of γ and δ , in the case of a cone-cylinder-cone. Calculated by the compiler.

SOLAR RADIATION
 Infinitely Conductive Cylindrical-Conical Surfaces

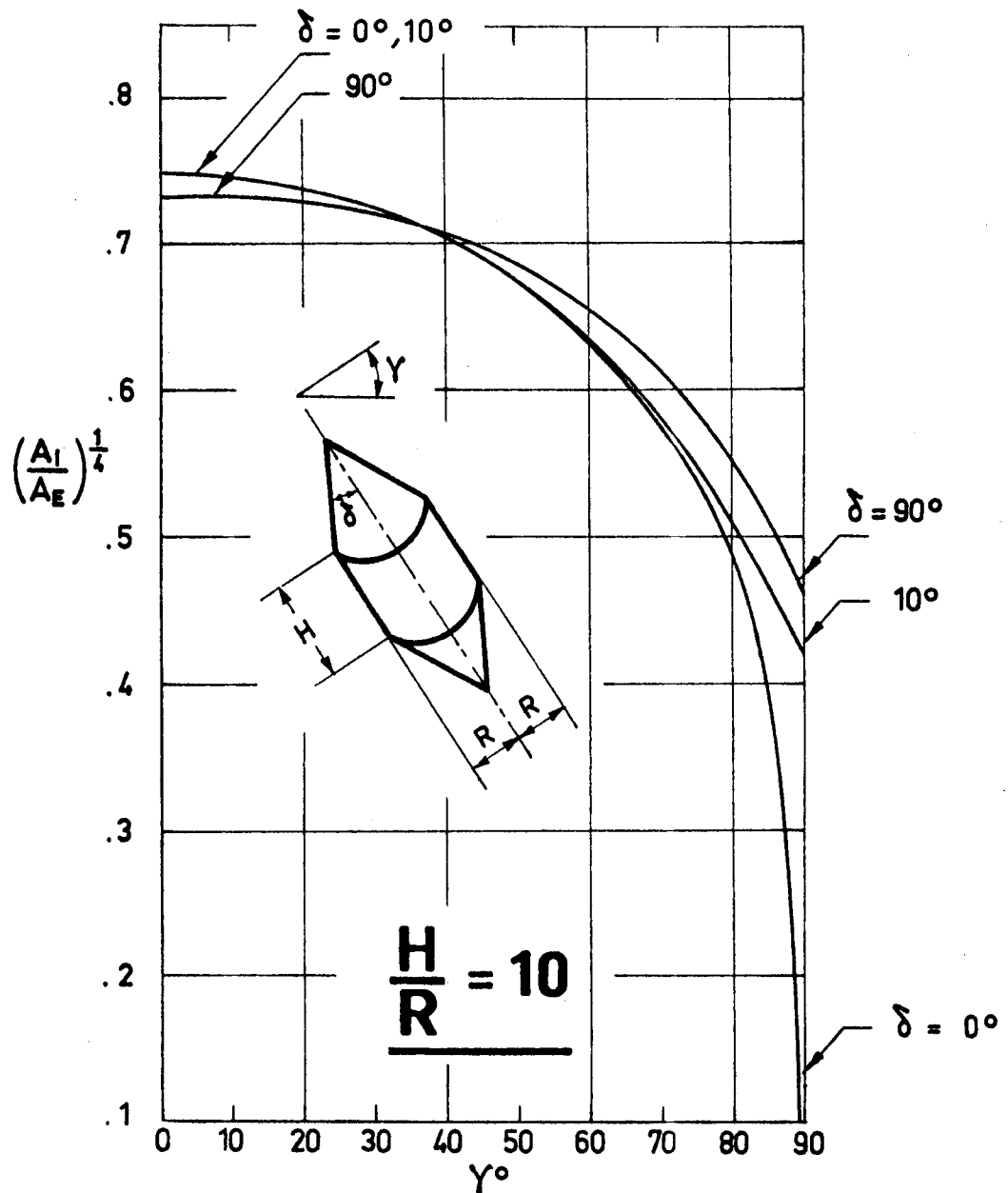


Fig 1-18. Ratio $(\frac{A_I}{A_E})^{1/4}$ as a function of γ and δ , in the case of a cone-cylinder-cone. Calculated by the compiler.

SOLAR RADIATION

Infinitely Conductive Cylindrical-Conical Surfaces

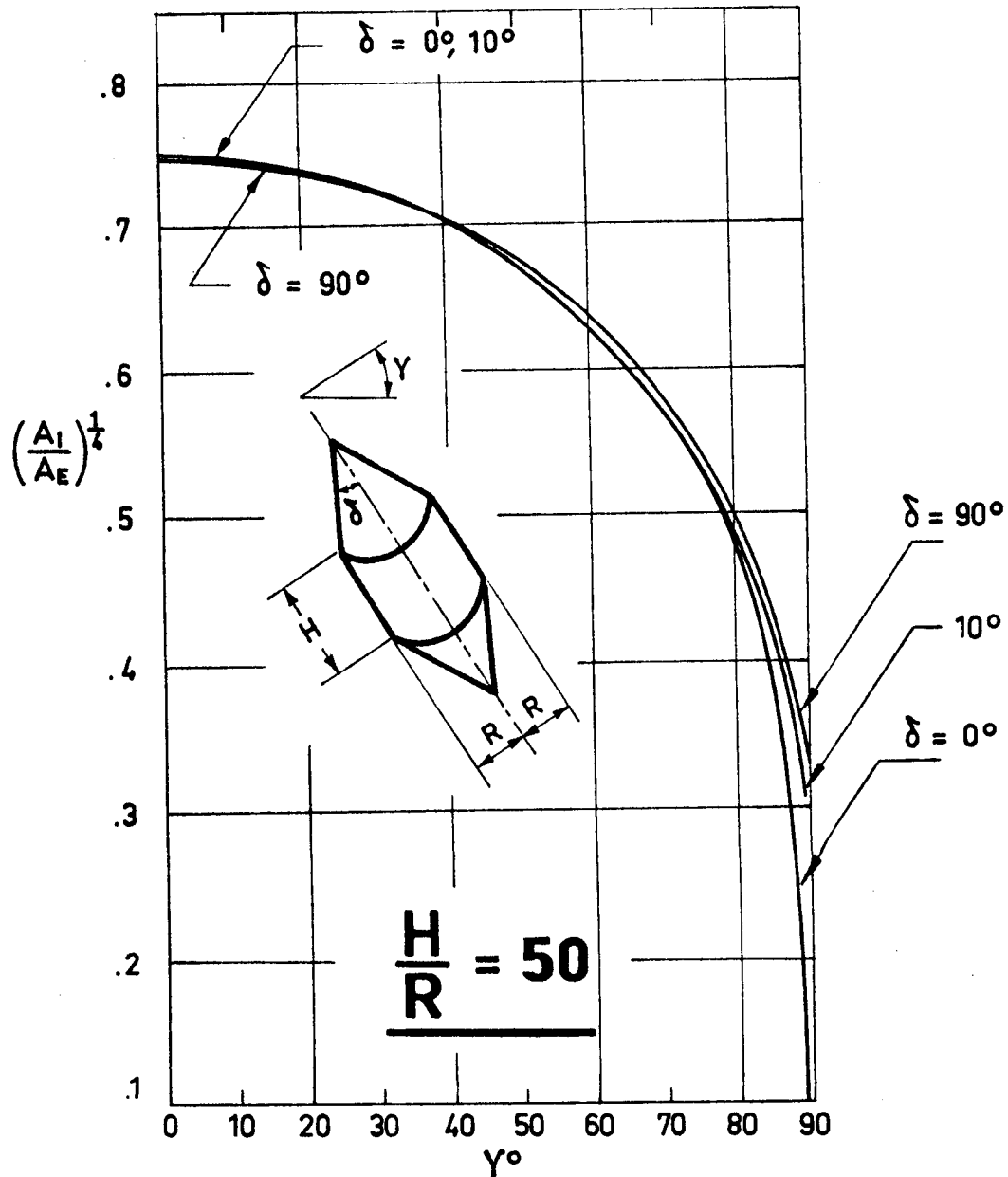


Fig 1-19. Ratio $(\frac{A_I}{A_E})^{1/4}$ as a function of γ and δ , in the case of a cone-cylinder-cone. Calculated by the compiler.

SOLAR RADIATION
 Infinitely Conductive Cylindrical-Conical Surfaces

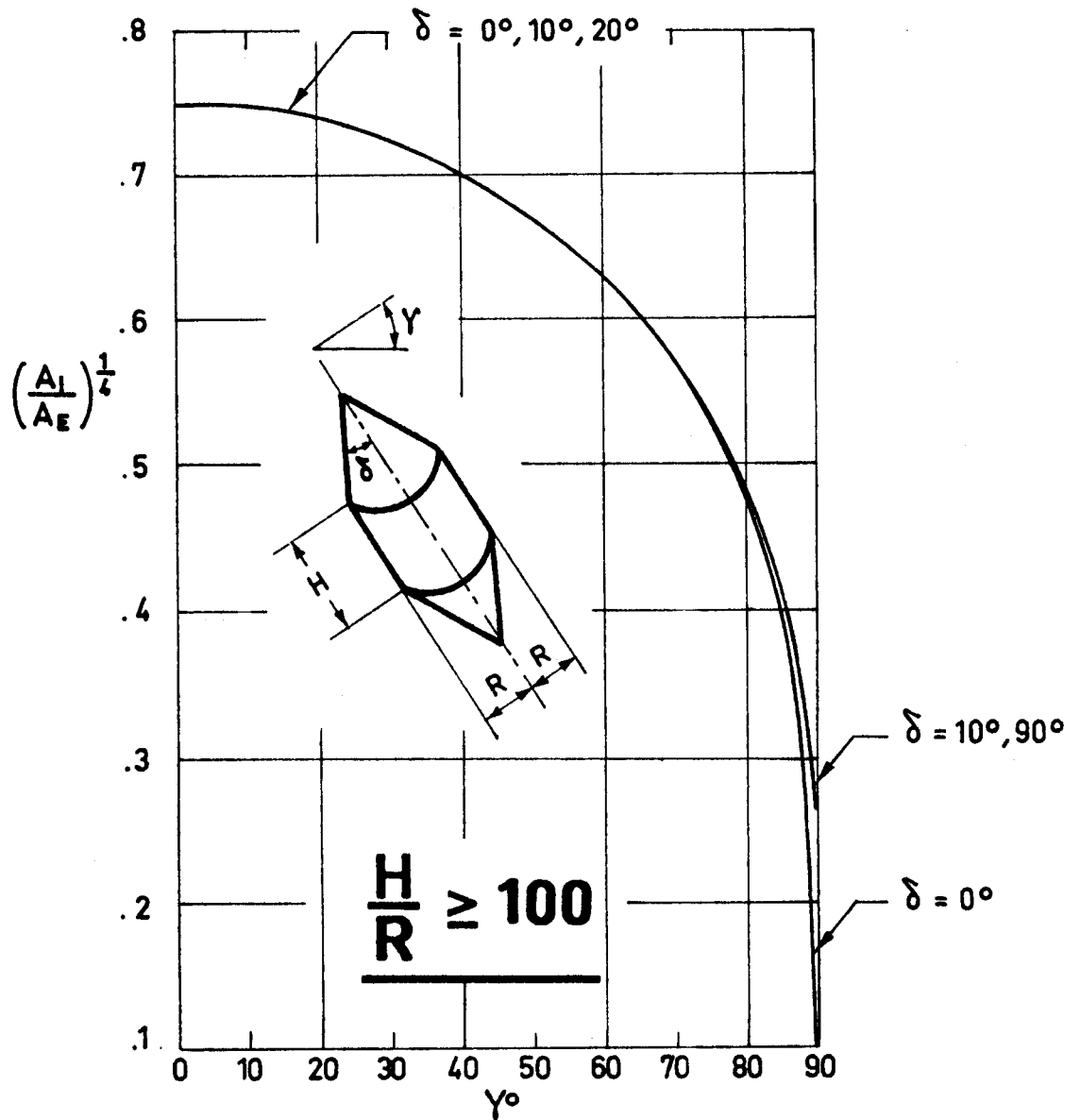


Fig 1-20. Ratio $(\frac{A_I}{A_E})^{1/4}$ as a function of γ and δ , in the case of a cone-cylinder-cone. Calculated by the compiler.

SOLAR RADIATION

Infinitely Conductive Cylindrical-Conical Surfaces

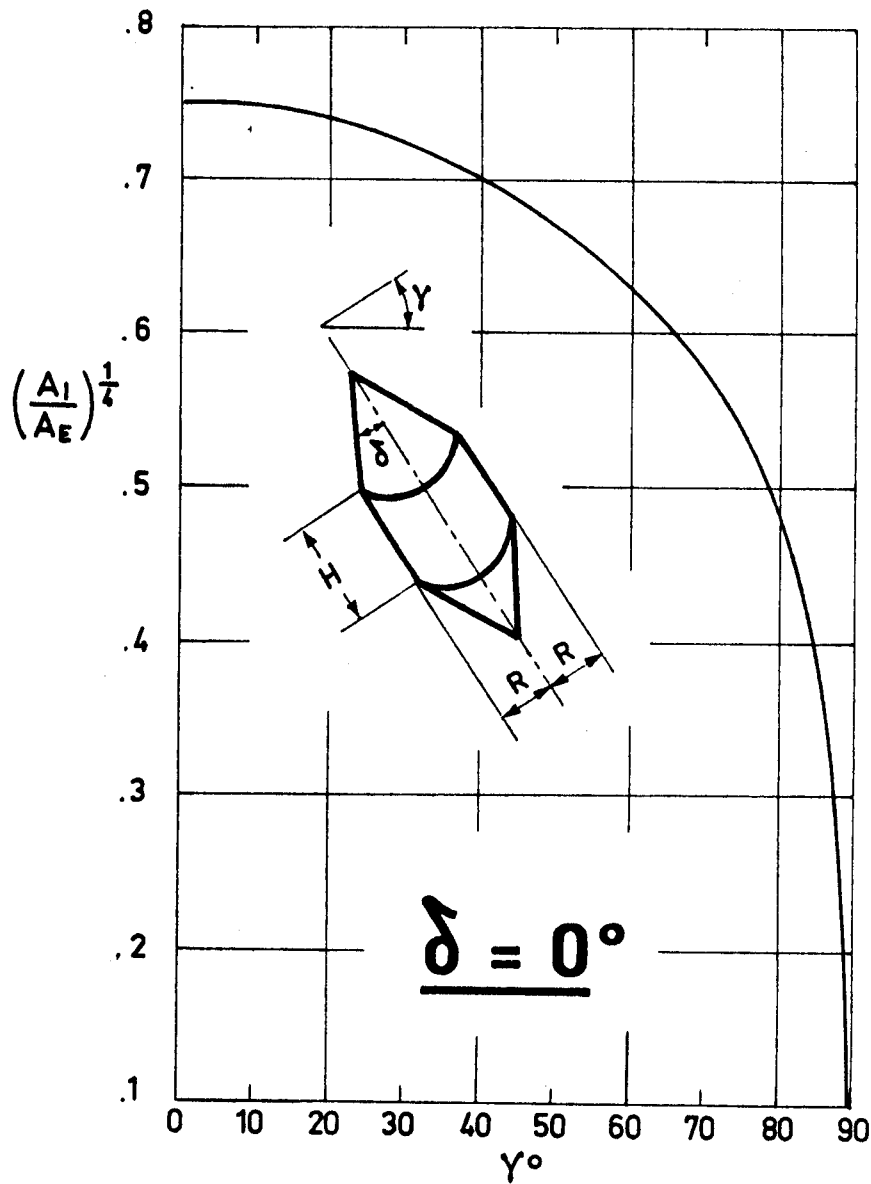


Fig 1-21. Ratio $\left(\frac{A_I}{A_E}\right)^{1/4}$ as a function of γ for any value of $\frac{H}{R}$, in the case of a cone-cylinder-cone. Calculated by the compiler.

SOLAR RADIATION
 Infinitely Conductive Cylindrical-Conical Surfaces

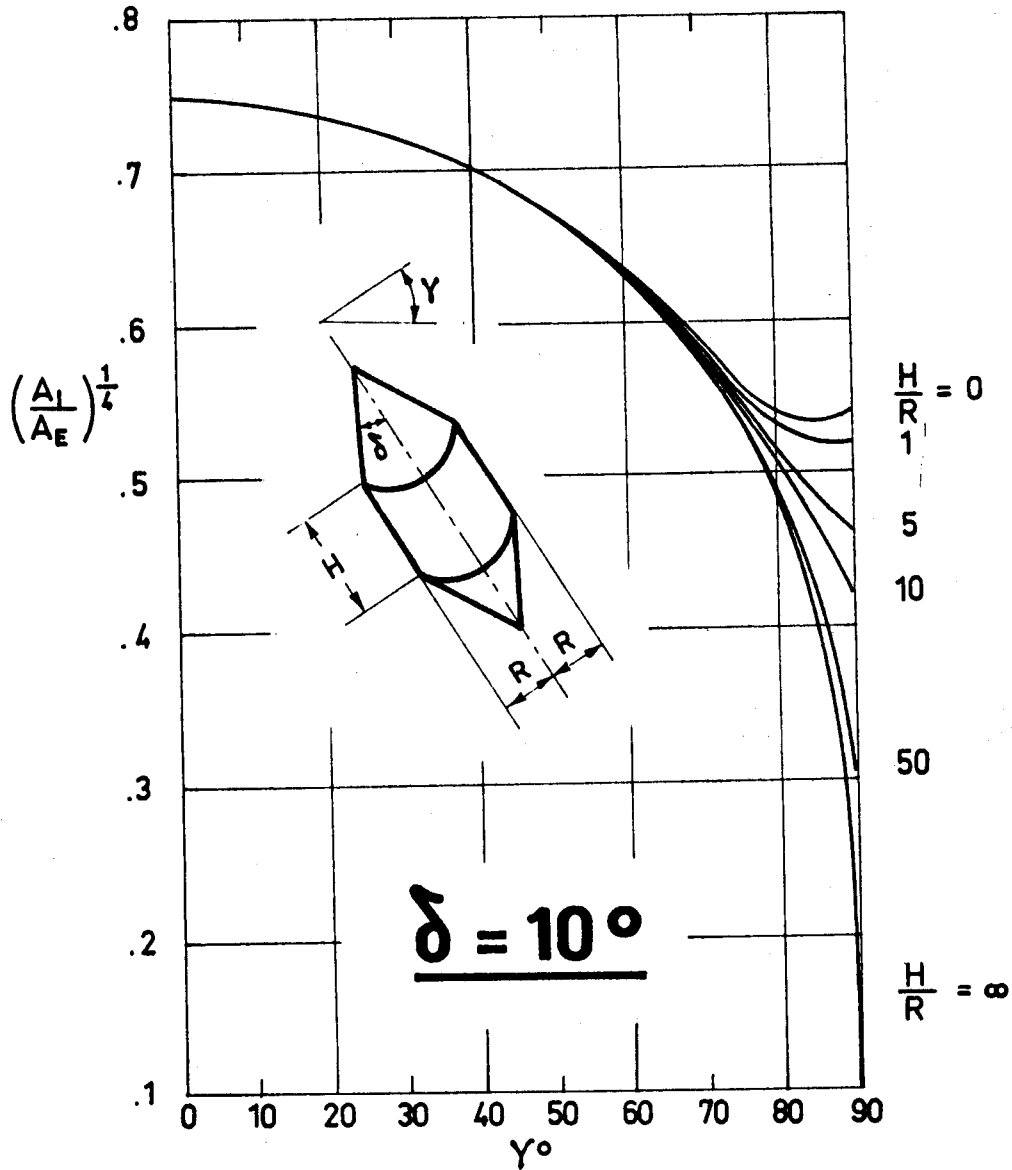


Fig 1-22. Ratio $(\frac{A_I}{A_E})^{1/4}$ as a function of γ and $\frac{H}{R}$, in the case of a cone-cylinder-cone. Calculated by the compiler.

SOLAR RADIATION

Infinitely Conductive Cylindrical-Conical Surfaces

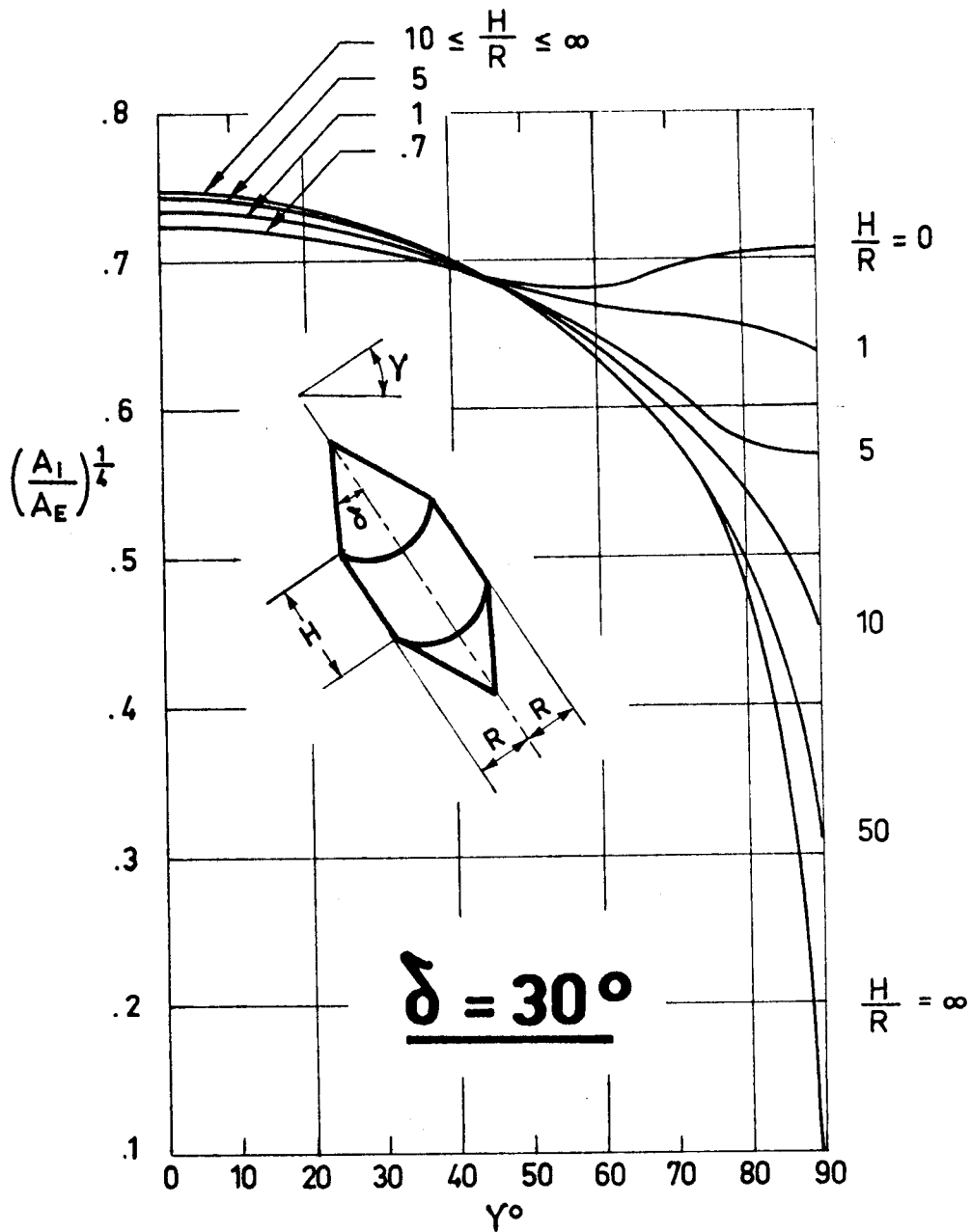


Fig 1-23. Ratio $(\frac{A_I}{A_E})^{1/4}$ as a function of γ and $\frac{H}{R}$, in the case of a cone-cylinder-cone. Calculated by the compiler.

SOLAR RADIATION
 Infinitely Conductive Cylindrical-Conical Surfaces

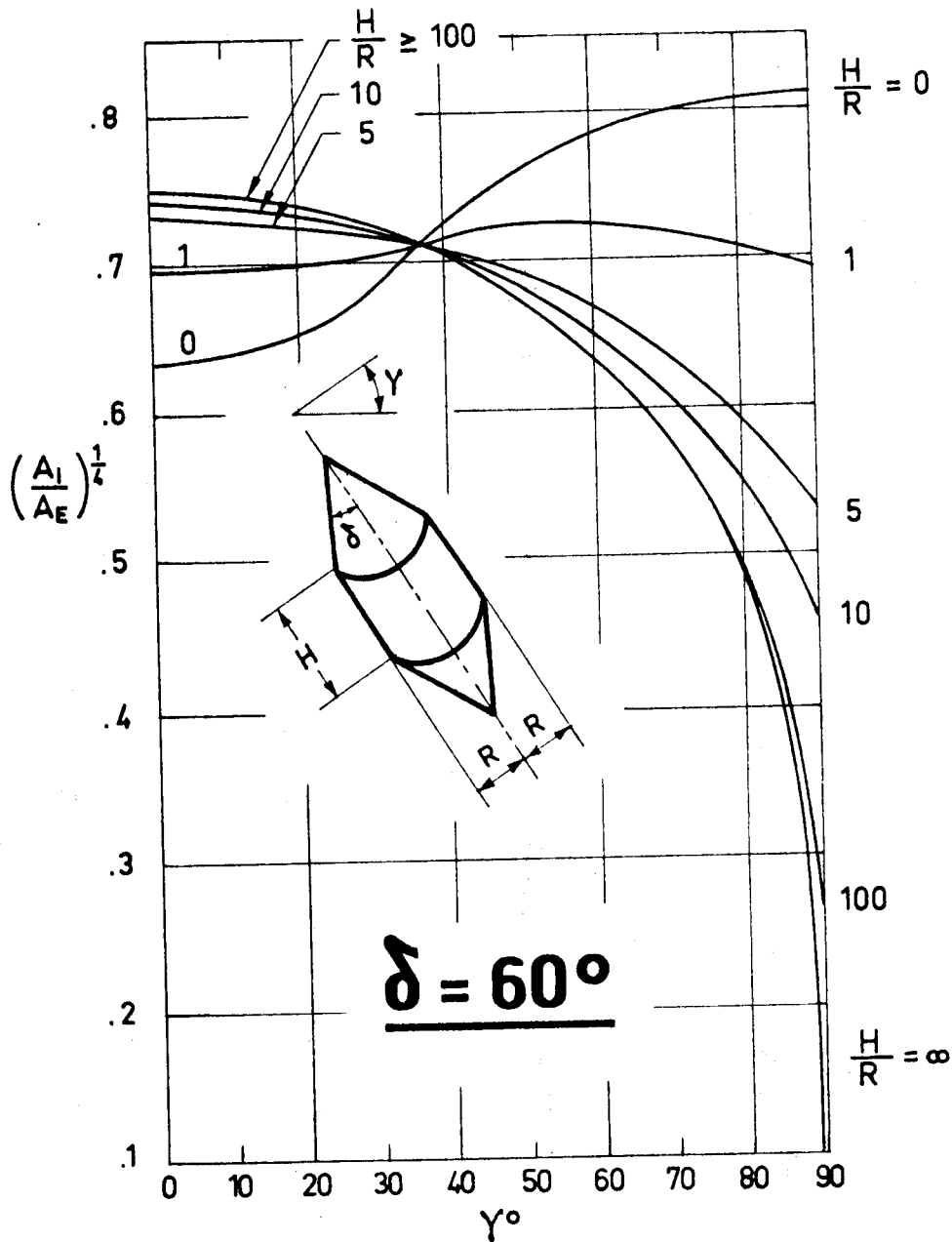


Fig 1-24. Ratio $(\frac{A_I}{A_E})^{1/4}$ as a function of γ and $\frac{H}{R}$, in the case of a cone-cylinder-cone. Calculated by the compiler.

SOLAR RADIATION
 Infinitely Conductive Cylindrical-Conical Surfaces

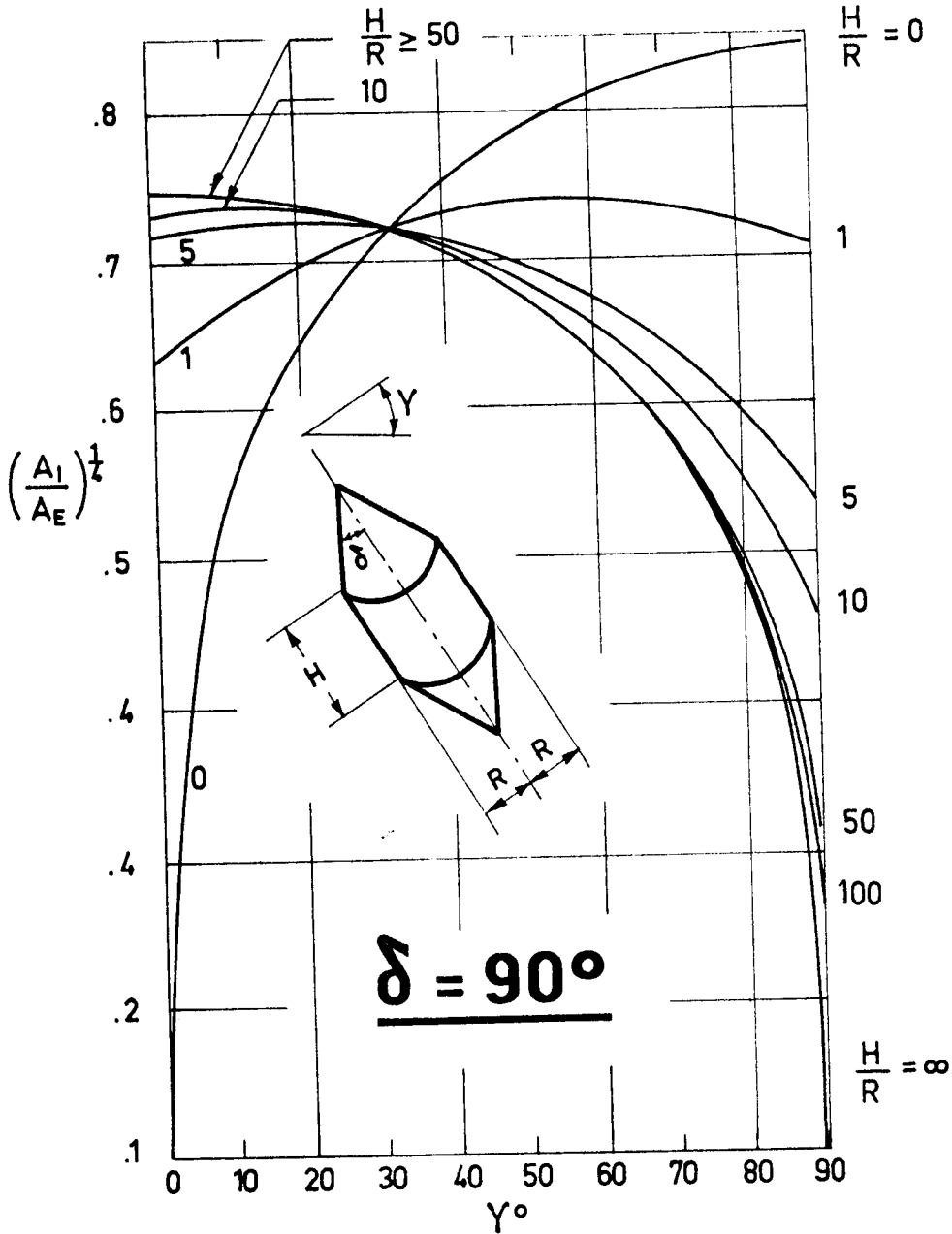


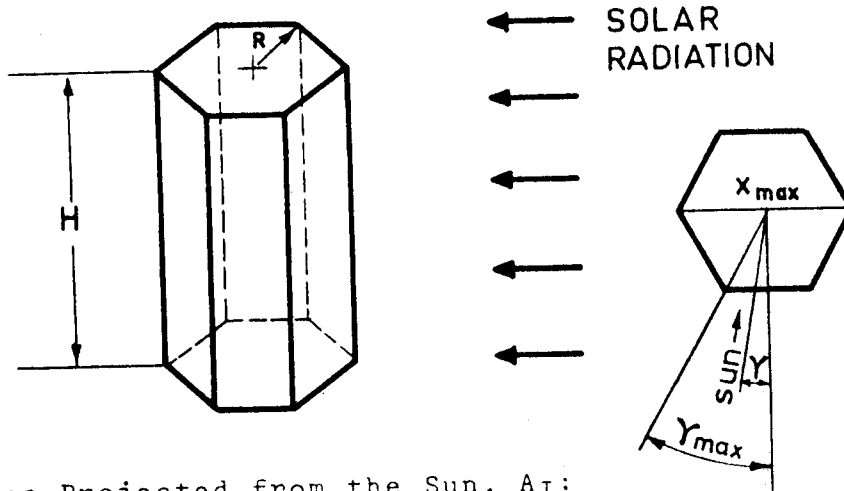
Fig 1-25. Ratio $(\frac{A_I}{A_E})^{1/4}$ as a function of γ and $\frac{H}{R}$, in the case of a cone-cylinder-cone. Calculated by the compiler.

SOLAR RADIATION
Infinitely Conductive Prismatic Surfaces

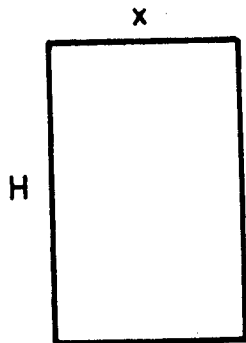
1.7. INFINITELY CONDUCTIVE PRISMATIC SURFACES

1.7.1. PRISM WITH AN n-SIDED REGULAR POLYGONAL SECTION

Sketch:



Area Projected from the Sun, A_I :



$$\frac{X}{R} = 2 \cos \gamma, \text{ for } n \text{ even.}$$

$$\frac{X}{R} = 2 \cos\left(\frac{\pi}{2n}\right) \cos \gamma, \text{ for } n \text{ odd.}$$

Formula:

$$\frac{A_I}{A_E} = \frac{\frac{H}{R} \frac{X}{R}}{n \left[\sin\left(\frac{2\pi}{n}\right) + 2 \left(\frac{H}{R}\right) \sin\left(\frac{\pi}{n}\right) \right]}$$

SOLAR RADIATION
 Infinitely Conductive Prismatic Surfaces

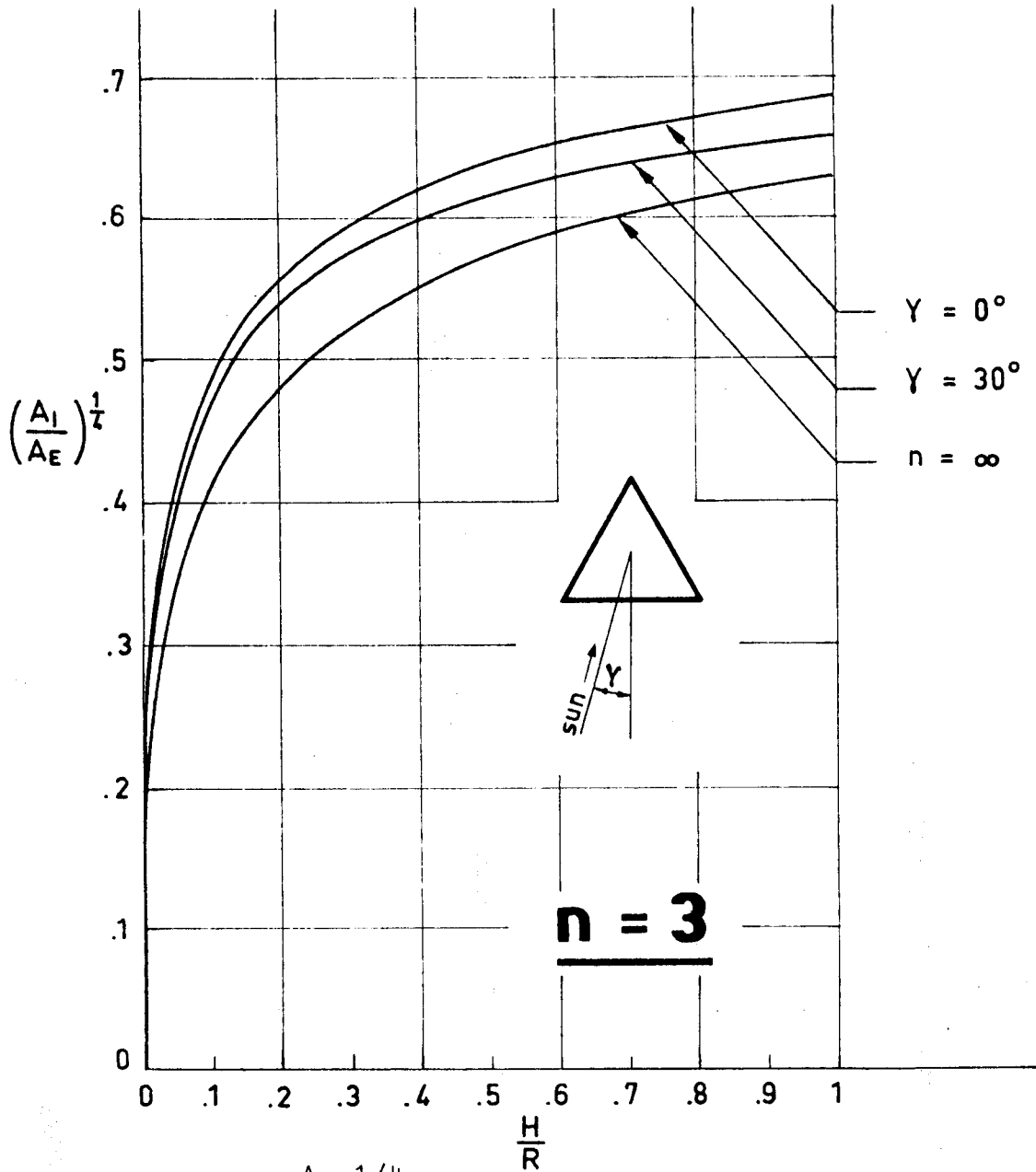


Fig 1-26. Ratio $(\frac{A_I}{A_E})^{1/4}$ as a function of $\frac{H}{R}$, in the case of a prism. The curves plotted are those corresponding to the largest and smallest areas projected from the Sun. Circular cylinder, $n=\infty$. Calculated by the compiler.

SOLAR RADIATION
 Infinitely Conductive Prismatic Surfaces

n = 3

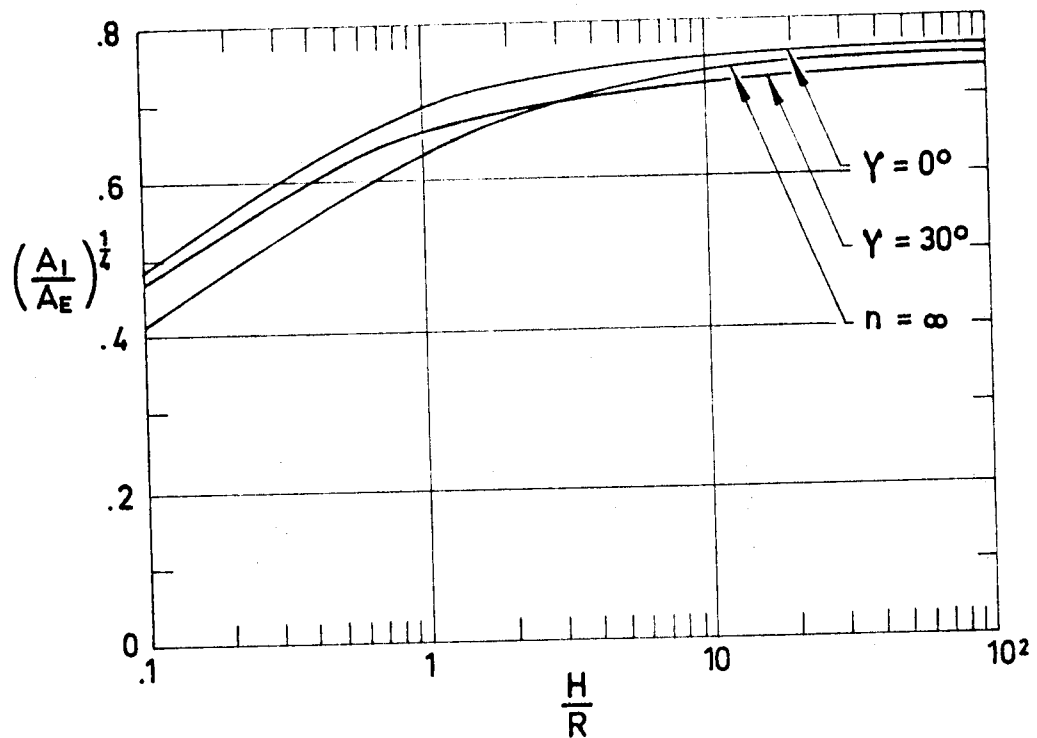


Fig 1-27. Ratio $\left(\frac{A_I}{A_E}\right)^{1/4}$ as a function of $\frac{H}{R}$, in the case of a prism. The curves plotted are those corresponding to the largest and smallest areas projected from the Sun. The values corresponding to $\frac{H}{R} \leq 1$ are also plotted in the previous figure. Circular cylinder, $n = \infty$. Calculated by the compiler.

SOLAR RADIATION
Infinitely Conductive Prismatic Surfaces

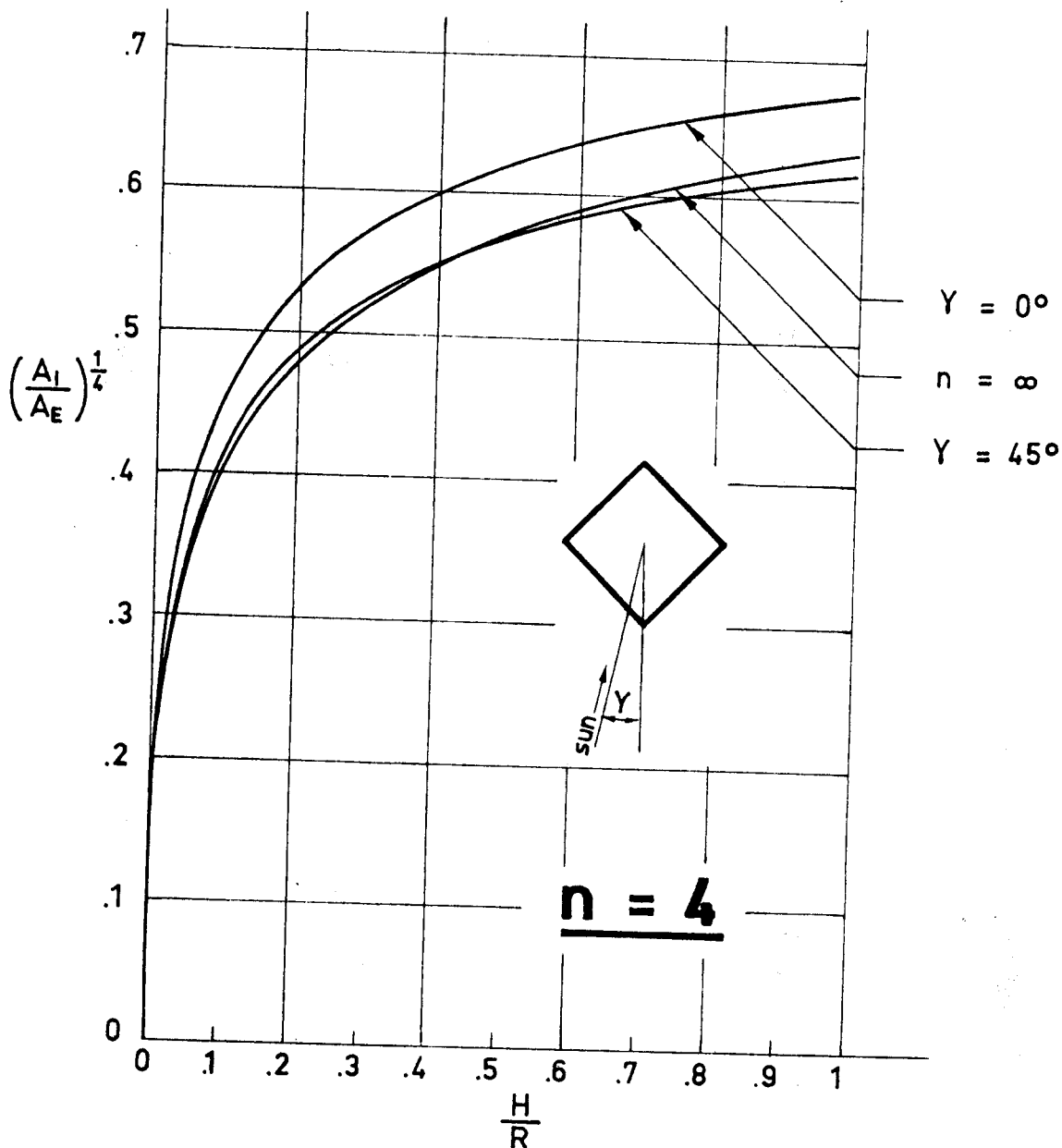


Fig 1-28. Ratio $\left(\frac{A_I}{A_E}\right)^{1/4}$ as a function of $\frac{H}{R}$, in the case of a prism. The curves plotted are those corresponding to the largest and smallest areas projected from the Sun. Circular cylinder, $n = \infty$. Calculated by the compiler.

SOLAR RADIATION
 Infinitely Conductive Prismatic Surfaces

n = 4

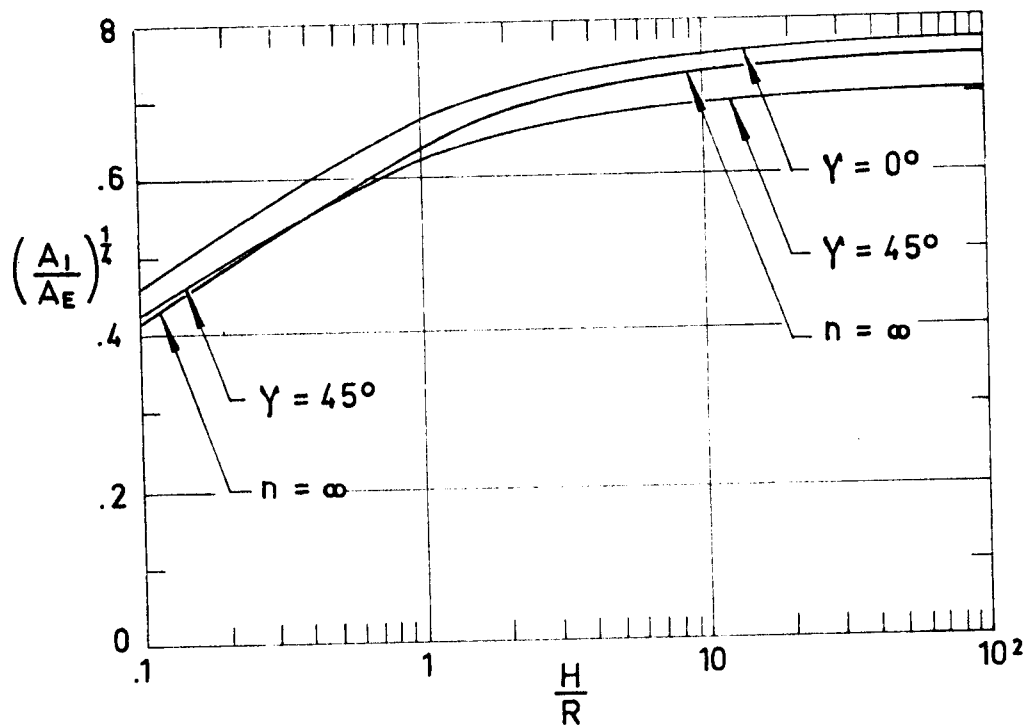


Fig 1-29. Ratio $\left(\frac{A_I}{A_E}\right)^{1/4}$ as a function of $\frac{H}{R}$, in the case of a prism. The curves plotted are those corresponding to the largest and smallest areas projected from the Sun. The values corresponding to $\frac{H}{R} \leq 1$ are also plotted in the previous figure. Circular cylinder, $n = \infty$. Calculated by the compiler.

SOLAR RADIATION
 Infinitely Conductive Prismatic Surfaces

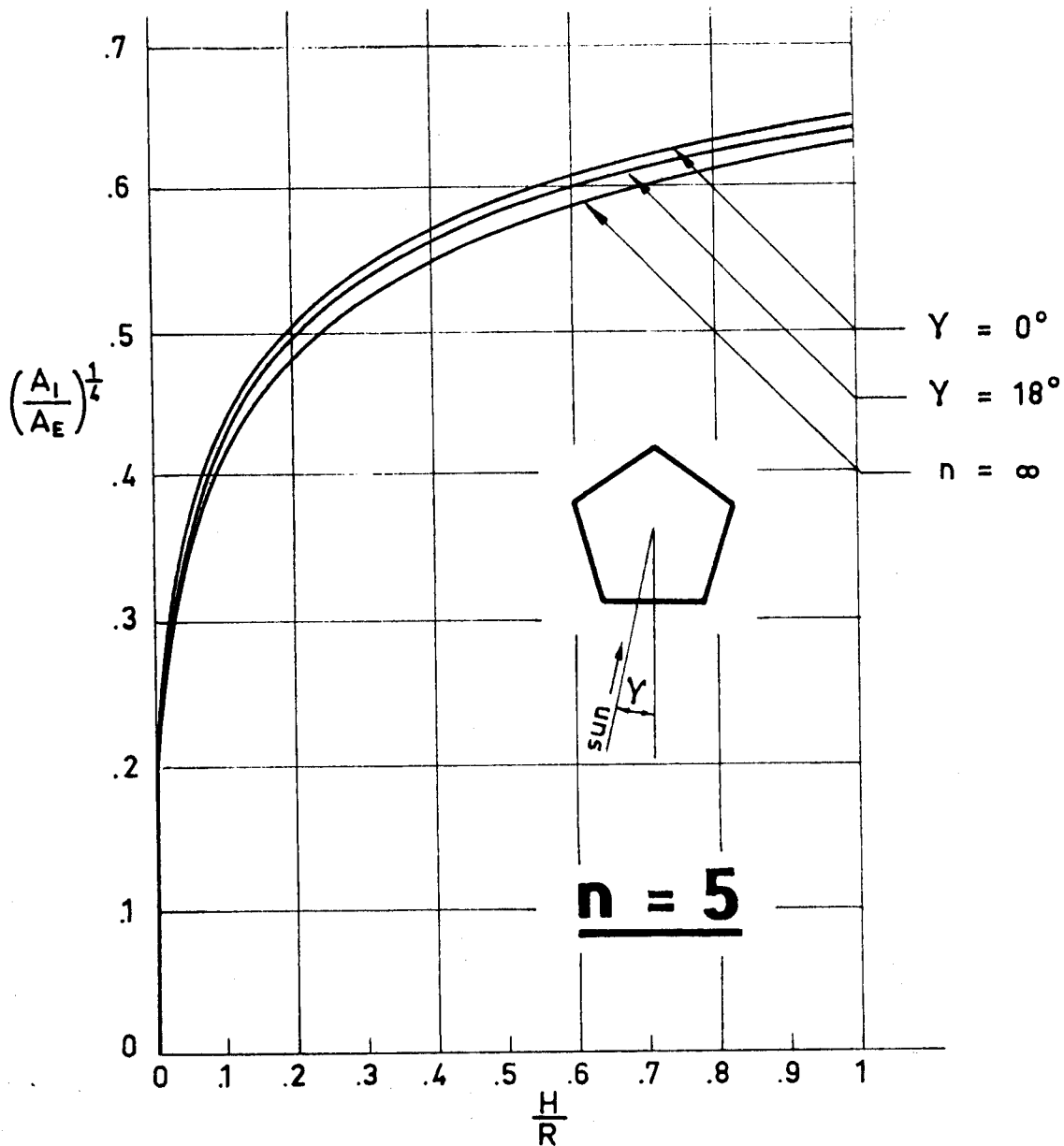


Fig 1-30. Ratio $(\frac{A_I}{A_E})^{1/4}$ as a function of $\frac{H}{R}$, in the case of a prism. The curves plotted are those corresponding to the largest and smallest areas projected from the Sun. Circular cylinder, $n=\infty$. Calculated by the compiler.

SOLAR RADIATION
 Infinitely Conductive Prismatic Surfaces

n = 5

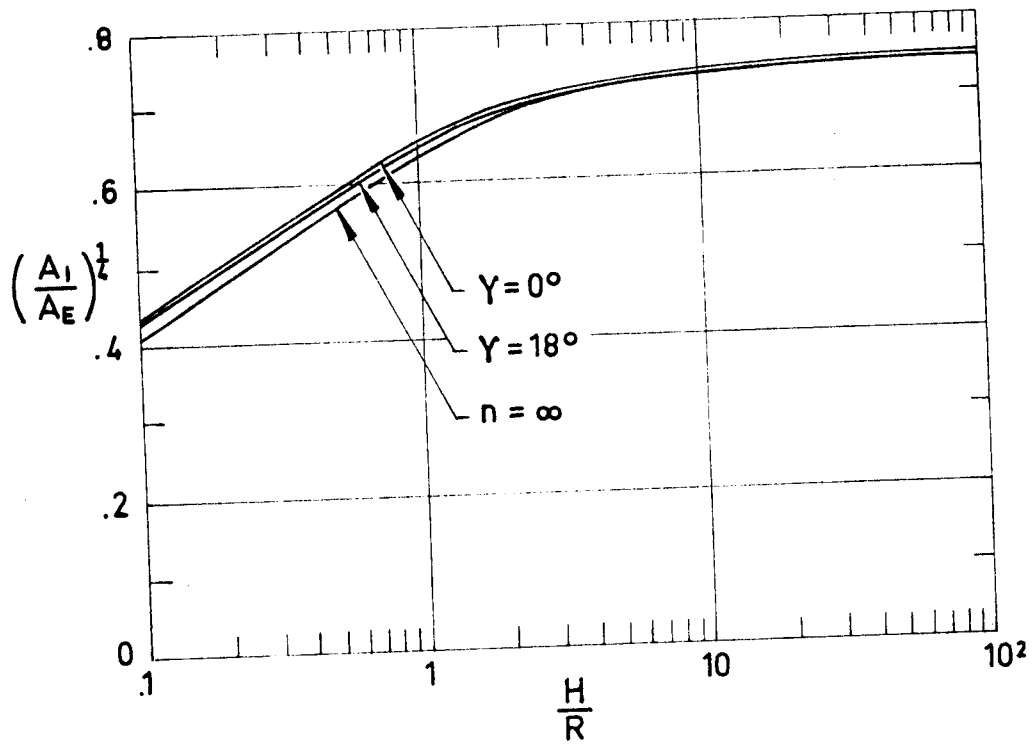


Fig 1-31. Ratio $\left(\frac{A_I}{A_E}\right)^{1/4}$ as a function of $\frac{H}{R}$, in the case of a prism. The curves plotted are those corresponding to the largest and smallest areas projected from the Sun. The values corresponding to $\frac{H}{R} \leq 1$ are also plotted in the previous figure. Circular cylinder, $n=\infty$. Calculated by the compiler.

SOLAR RADIATION
 Infinitely Conductive Prismatic Surfaces

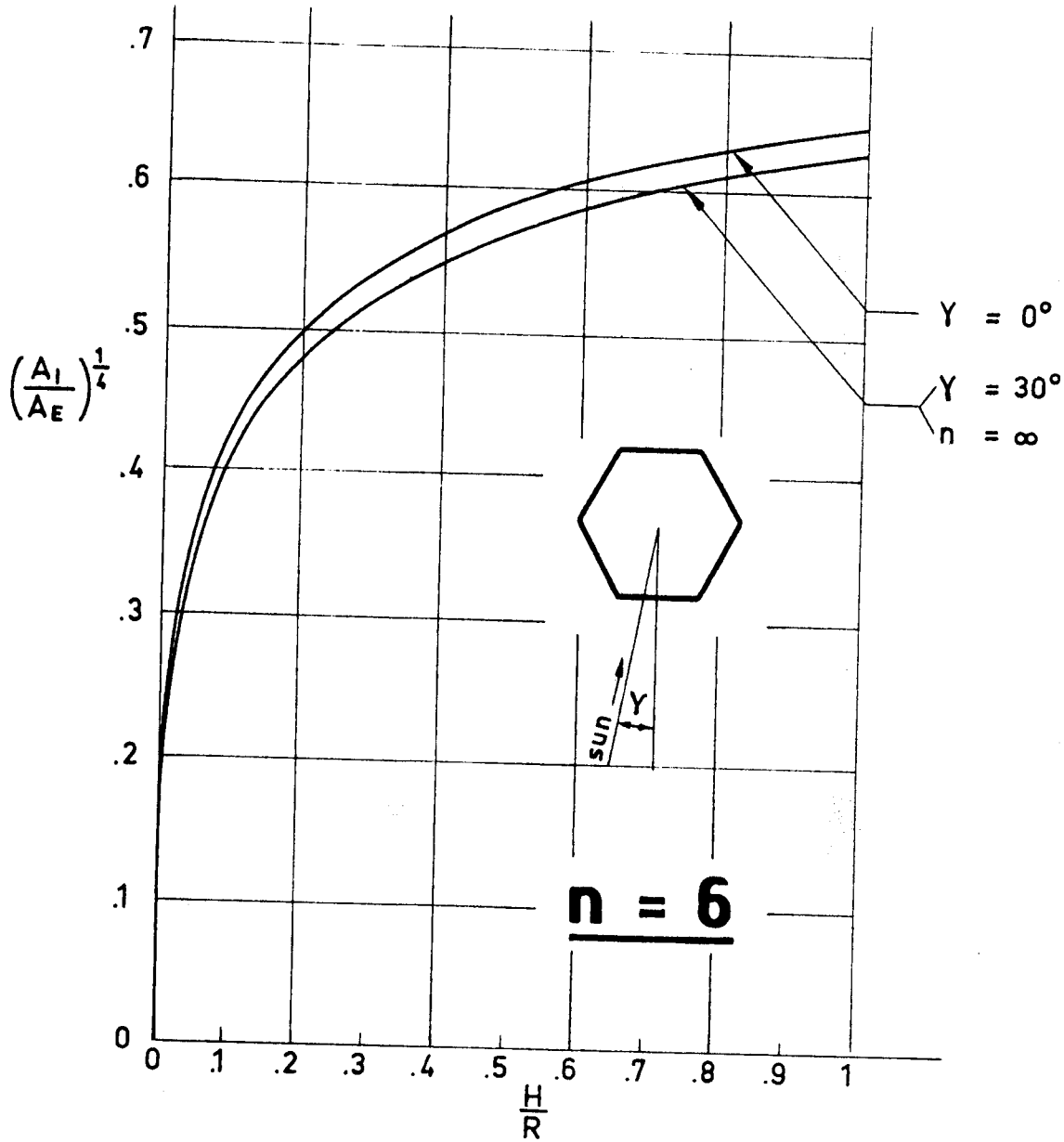


Fig 1-32. Ratio $(\frac{A_I}{A_E})^{1/4}$ as a function of $\frac{H}{R}$, in the case of a prism. The curves plotted are those corresponding to the largest and smallest areas projected from the Sun. Circular cylinder, $n = \infty$. Calculated by the compiler.

SOLAR RADIATION
 Infinitely Conductive Prismatic Surfaces

n = 6

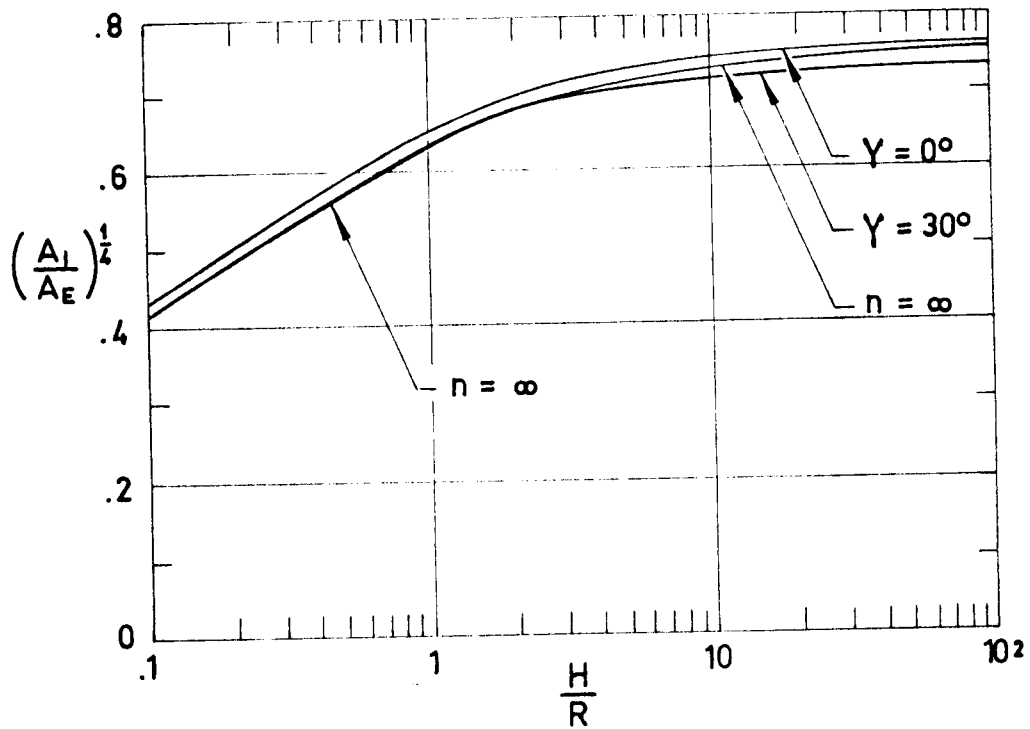


Fig 1-33. Ratio $\left(\frac{A_I}{A_E}\right)^{1/4}$ as a function of $\frac{H}{R}$, in the case of a prism. The curves plotted are those corresponding to the largest and smallest areas projected from the Sun. The values corresponding to $\frac{H}{R} \leq 1$ are also plotted in the previous figure. Circular cylinder, $n = \infty$. Calculated by the compiler.

SOLAR RADIATION
 Infinitely Conductive Prismatic Surfaces

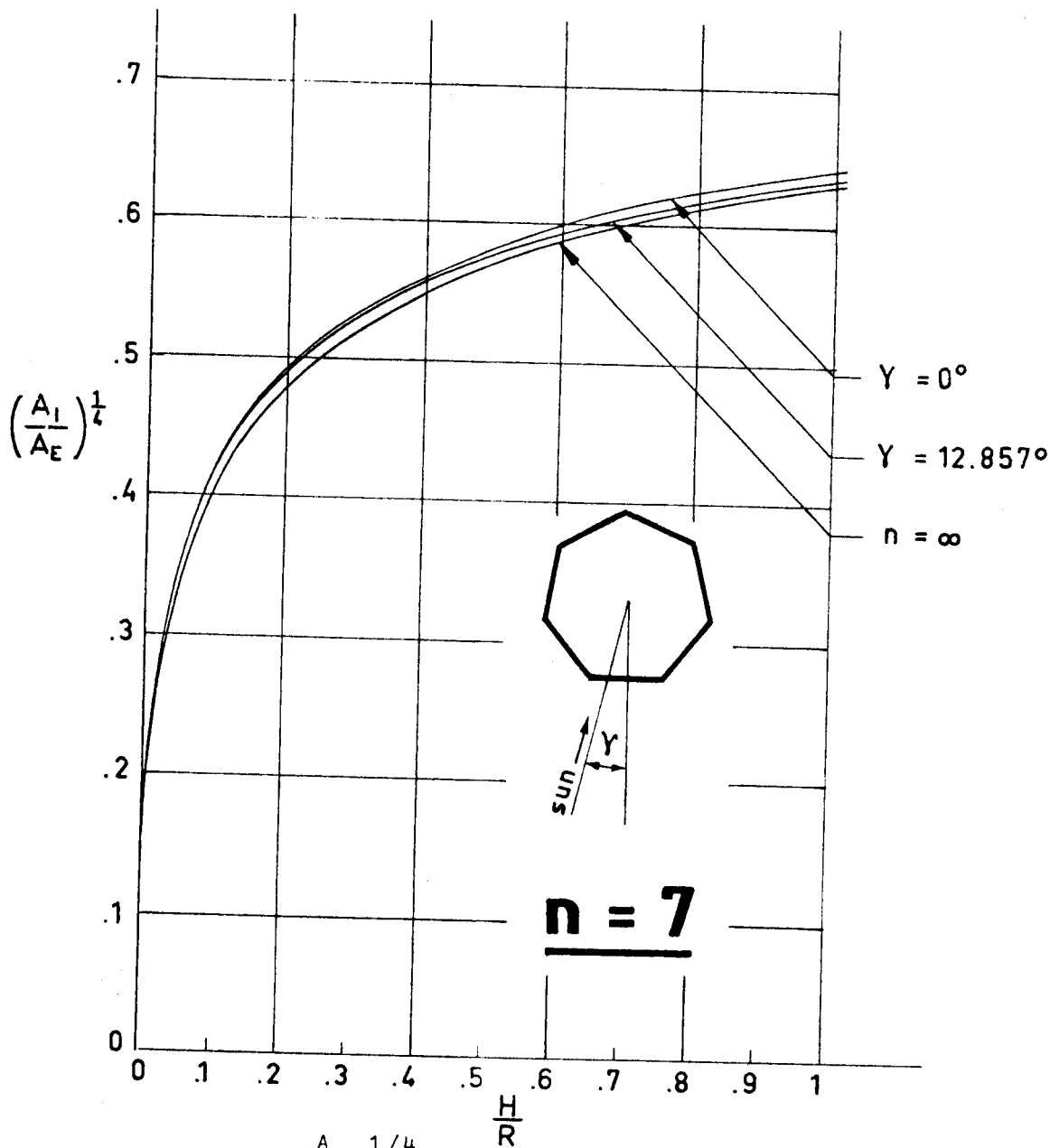


Fig 1-34. Ratio $(\frac{A_I}{A_E})^{1/4}$ as a function of $\frac{H}{R}$, in the case of a prism. The curves plotted are those corresponding to the largest and smallest areas projected from the Sun. Circular cylinder, $n=\infty$. Calculated by the compiler.

SOLAR RADIATION
 Infinitely Conductive Prismatic Surfaces

n = 7

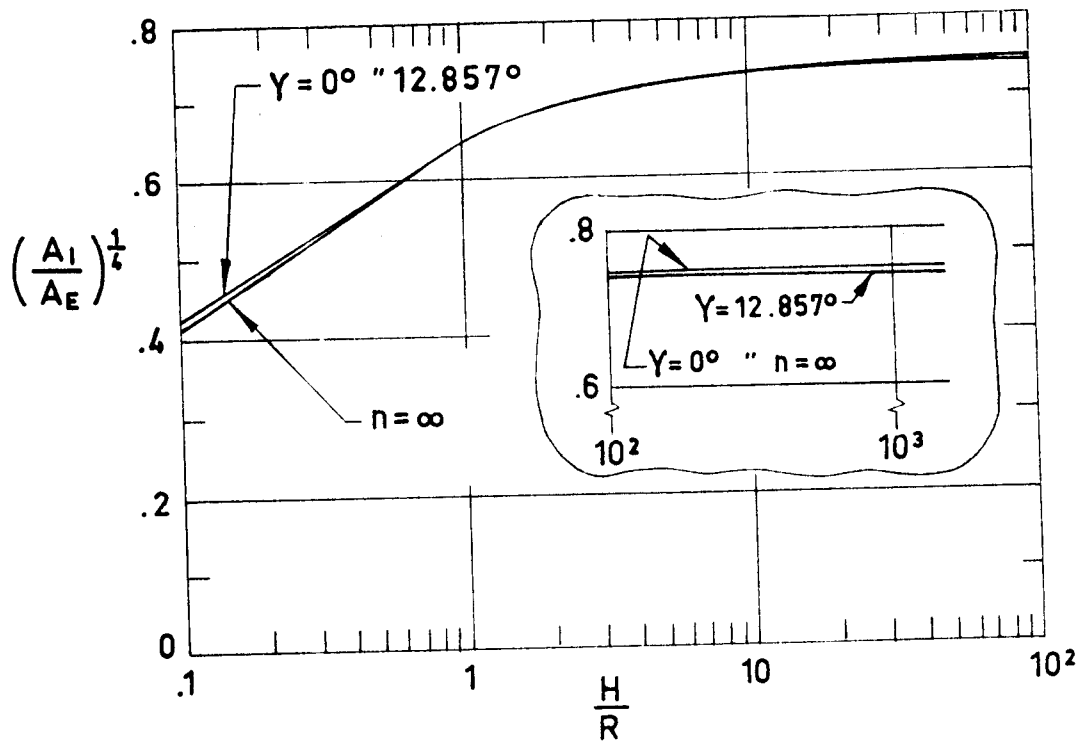


Fig 1-35. Ratio $(\frac{A_I}{A_E})^{1/4}$ as a function of $\frac{H}{R}$, in the case of a prism. The curves plotted are those corresponding to the largest and smallest areas projected from the Sun. The values corresponding to $\frac{H}{R} \leq 1$ are also plotted in the previous figure. Circular cylinder, $n = \infty$. Calculated by the compiler.

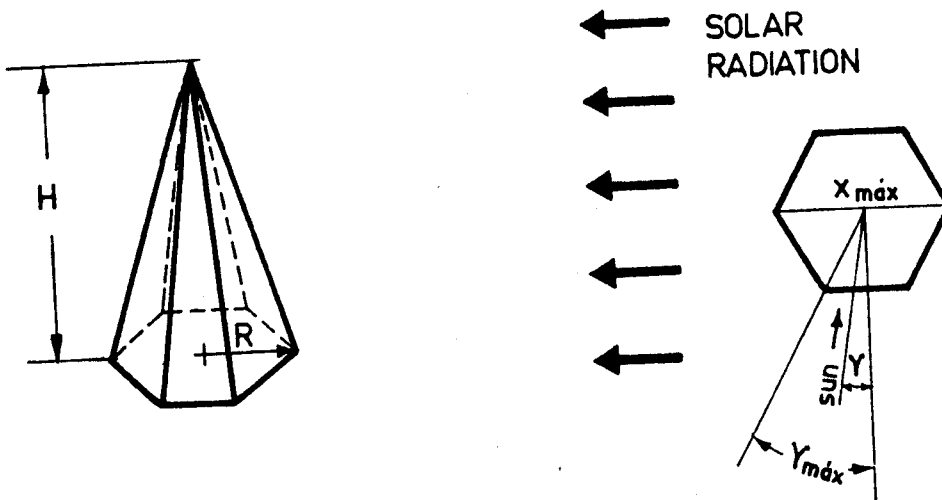
INTENTIONALLY BLANK PAGE

SOLAR RADIATION
 Infinitely Conductive Pyramidal Surfaces

1.8. INFINITELY CONDUCTIVE PYRAMIDAL SURFACES

1.8.1. PYRAMID WITH AN n-SIDED REGULAR POLYGONAL SECTION

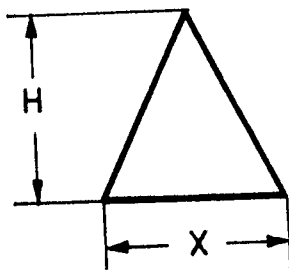
Sketch:



Area Projected from the Sun, A_I :

$$\frac{X}{R} = 2 \cos \gamma, \quad \text{for } n \text{ even.}$$

$$\frac{X}{R} = 2 \cos \left(\frac{\pi}{2n} \right) \cos \gamma, \quad \text{for } n \text{ odd.}$$



Formula:

$$\frac{A_I}{A_E} = \frac{\frac{H}{R} \frac{X}{R}}{n \sin \left(\frac{2\pi}{n} \right) \left[1 + \sqrt{1 + \left(\frac{H/R}{\cos \frac{\pi}{n}} \right)^2} \right]}$$

SOLAR RADIATION
Infinitely Conductive Pyramidal Surfaces

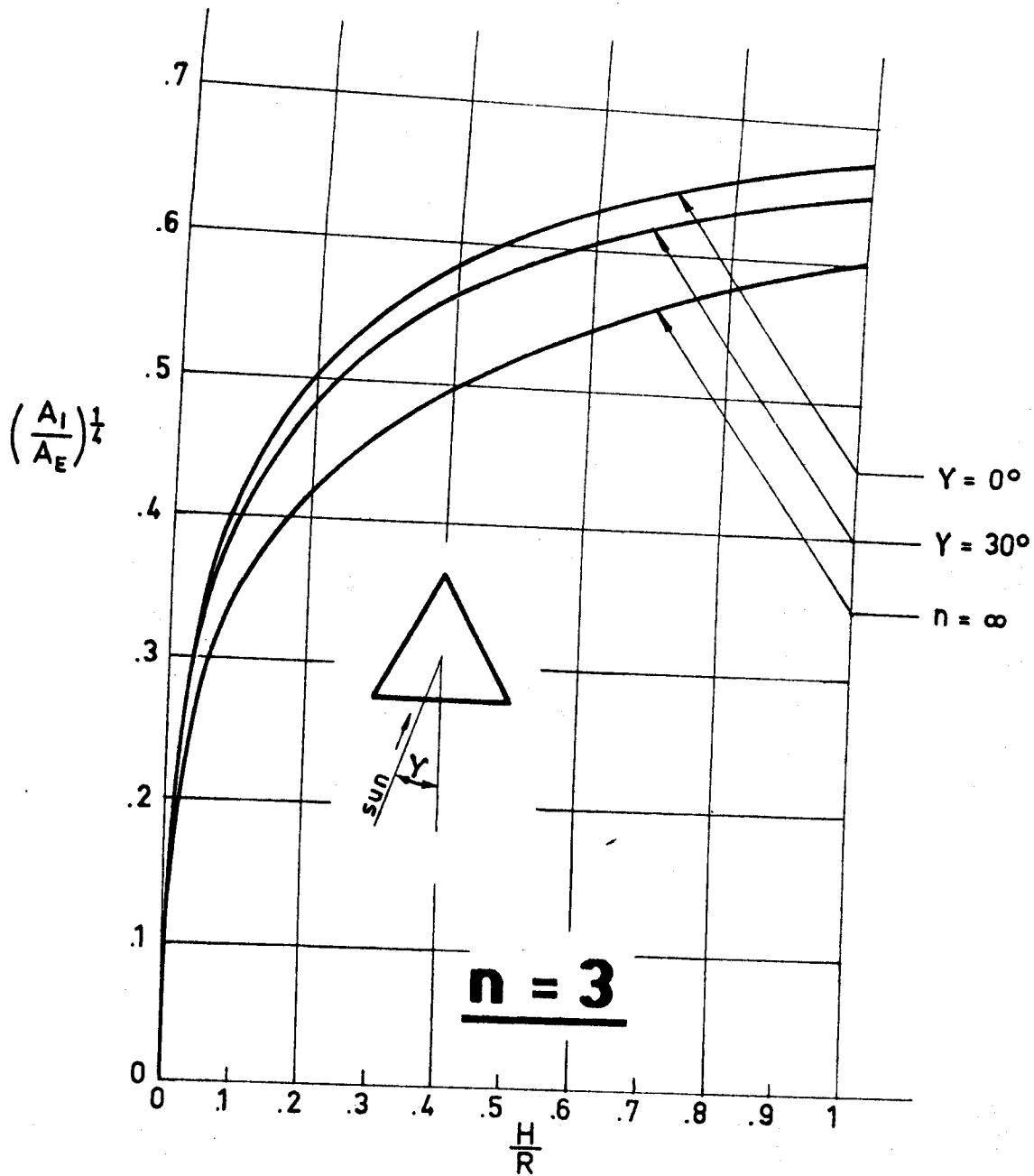


Fig 1-36. Ratio $\left(\frac{A_I}{A_E}\right)^{1/4}$ as a function of $\frac{H}{R}$, in the case of a pyramid. The curves plotted are those corresponding to the largest and smallest areas projected from the Sun. Circular cone, $n = \infty$. Calculated by the compiler.

SOLAR RADIATION
 Infinitely Conductive Pyramidal Surfaces

n = 3

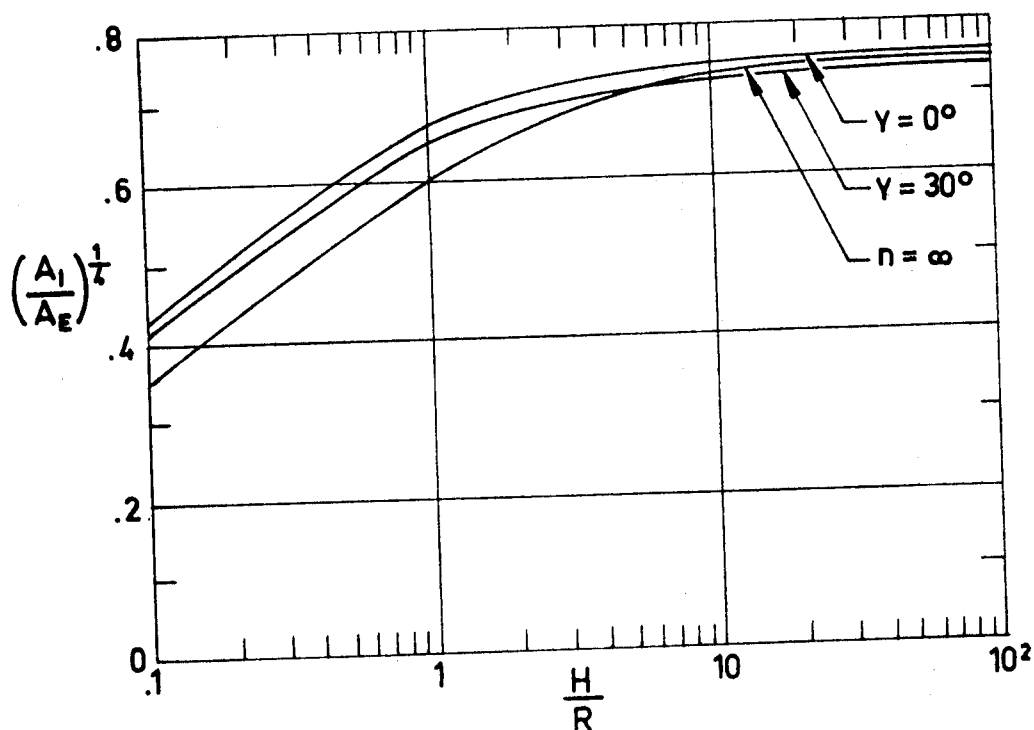


Fig 1-37. Ratio $(\frac{A_I}{A_E})^{1/4}$ as a function of $\frac{H}{R}$, in the case of a pyramid. The curves plotted are those corresponding to the largest and smallest areas projected from the Sun. The values corresponding to $\frac{H}{R} \leq 1$ are also plotted in the previous figure. Circular cone, $n = \infty$. Calculated by the compiler.

SOLAR RADIATION
 Infinitely Conductive Pyramidal Surfaces

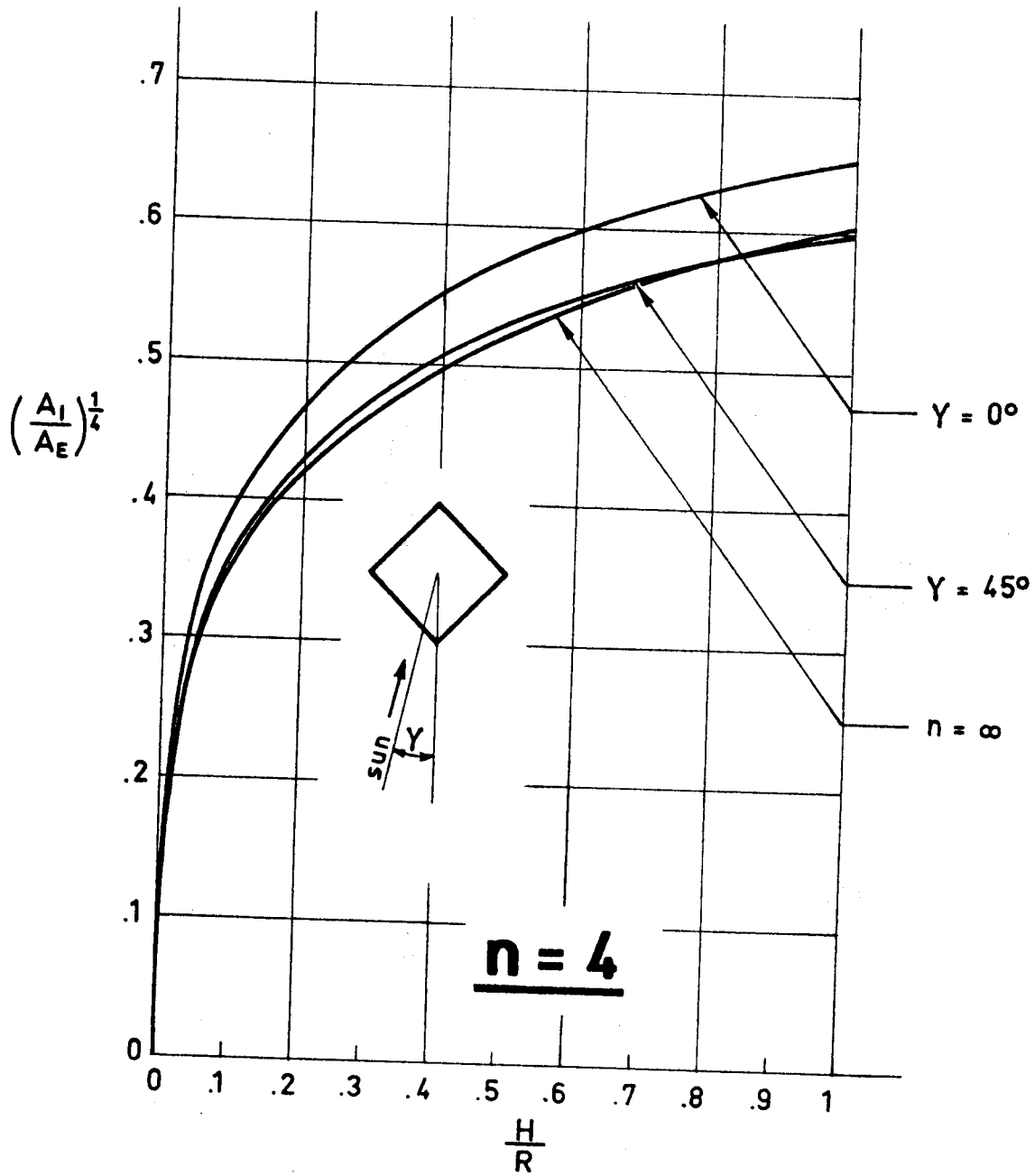


Fig 1-38. Ratio $(\frac{A_I}{A_E})^{1/4}$ as a function of $\frac{H}{R}$, in the case of a pyramid. The curves plotted are those corresponding to the largest and smallest areas projected from the Sun. Circular cone, $n = \infty$. Calculated by the compiler.

SOLAR RADIATION
 Infinitely Conductive Pyramidal Surfaces

$n = 4$

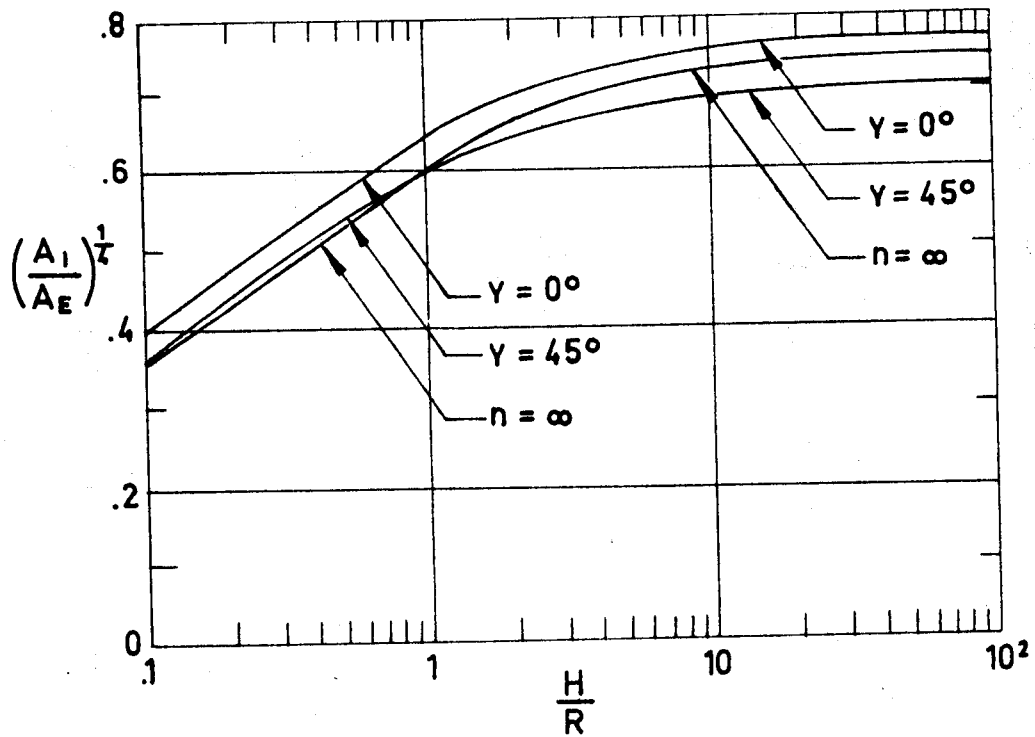


Fig 1-39. Ratio $\left(\frac{A_I}{A_E}\right)^{1/4}$ as a function of $\frac{H}{R}$, in the case of a pyramid. The curves plotted are those corresponding to the largest and smallest areas projected from the Sun. The values corresponding to $\frac{H}{R} \leq 1$ are also plotted in the previous figure. Circular cone, $n = \infty$. Calculated by the compiler.

SOLAR RADIATION
Infinitely Conductive Pyramidal Surfaces

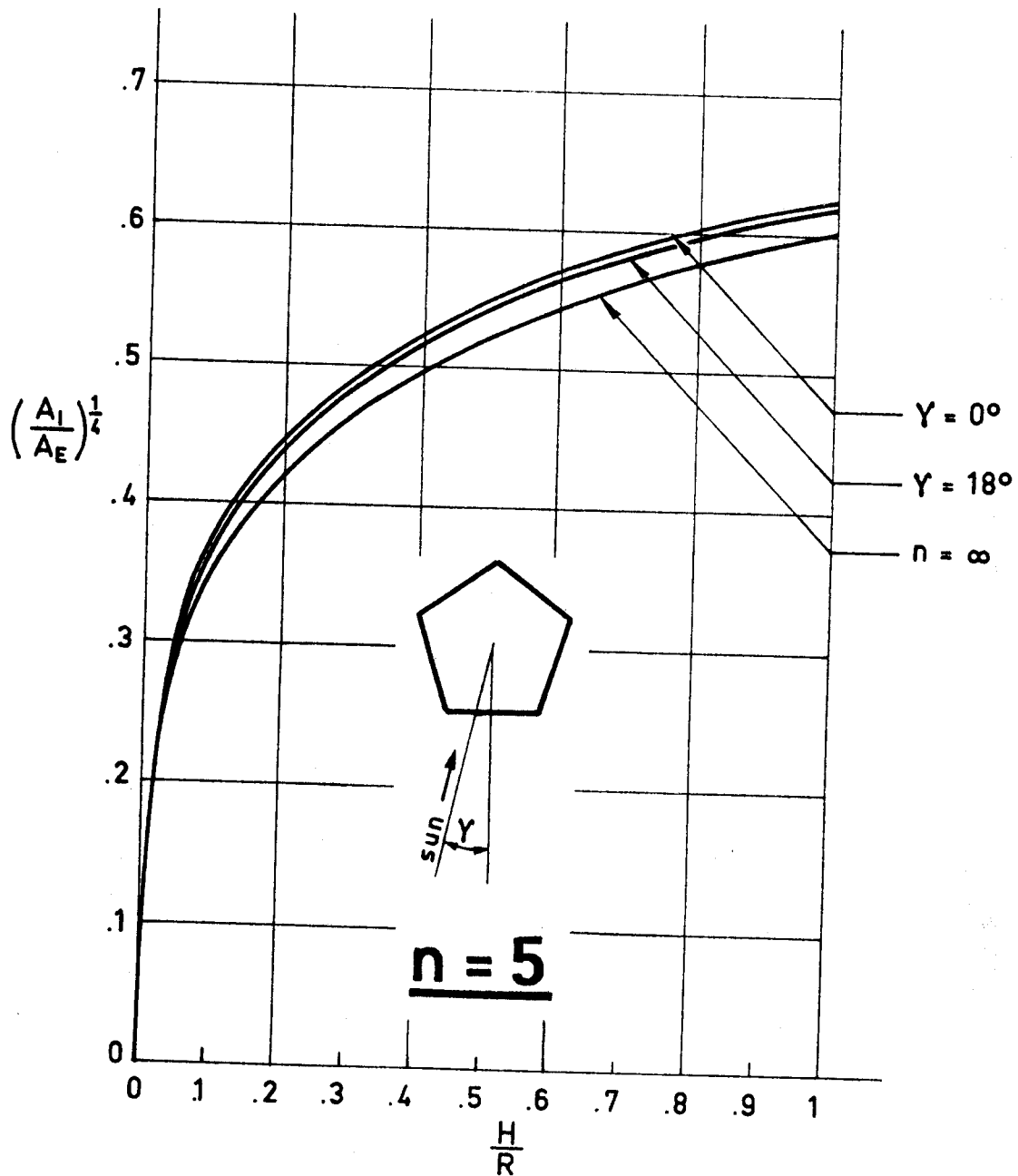


Fig 1-40. Ratio $\left(\frac{A_I}{A_E}\right)^{1/4}$ as a function of $\frac{H}{R}$, in the case of a pyramid. The curves plotted are those corresponding to the largest and smallest areas projected from the Sun. Circular cone, $n = \infty$. Calculated by the compiler.

SOLAR RADIATION
 Infinitely Conductive Pyramidal Surfaces

n = 5

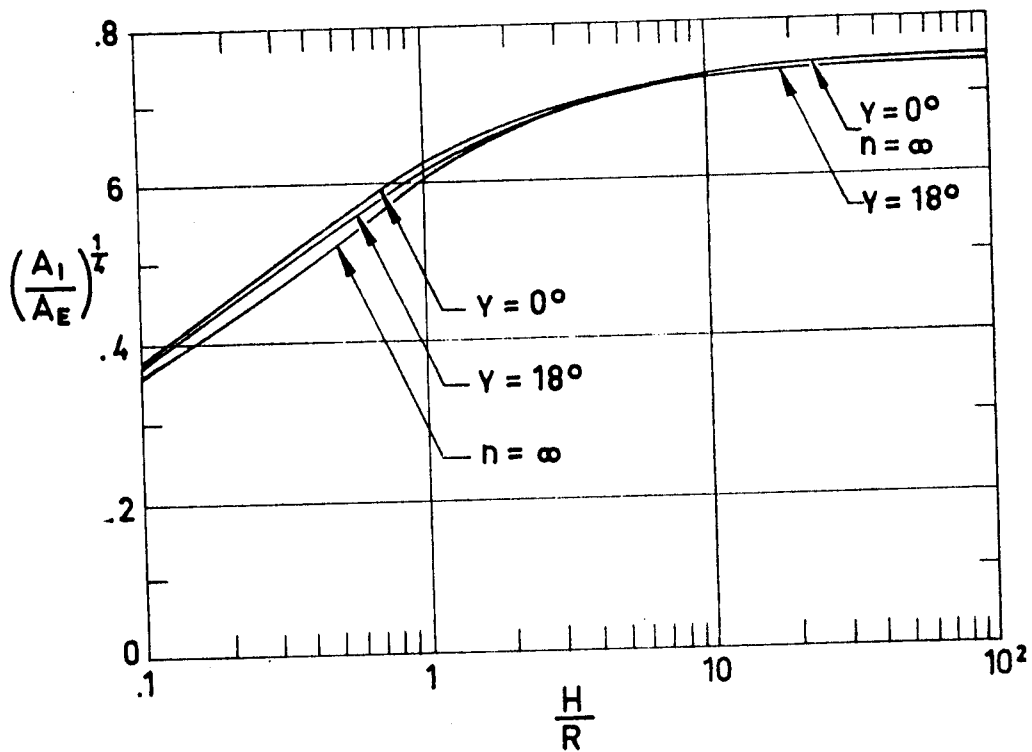


Fig 1-41. Ratio $\left(\frac{A_I}{A_E}\right)^{1/4}$ as a function of $\frac{H}{R}$, in the case of a pyramid. The curves plotted are those corresponding to the largest and smallest areas projected from the Sun. The values corresponding to $\frac{H}{R} \leq 1$ are also plotted in the previous figure. Circular cone, $n = \infty$. Calculated by the compiler.

SOLAR RADIATION
 Infinitely Conductive Pyramidal Surfaces

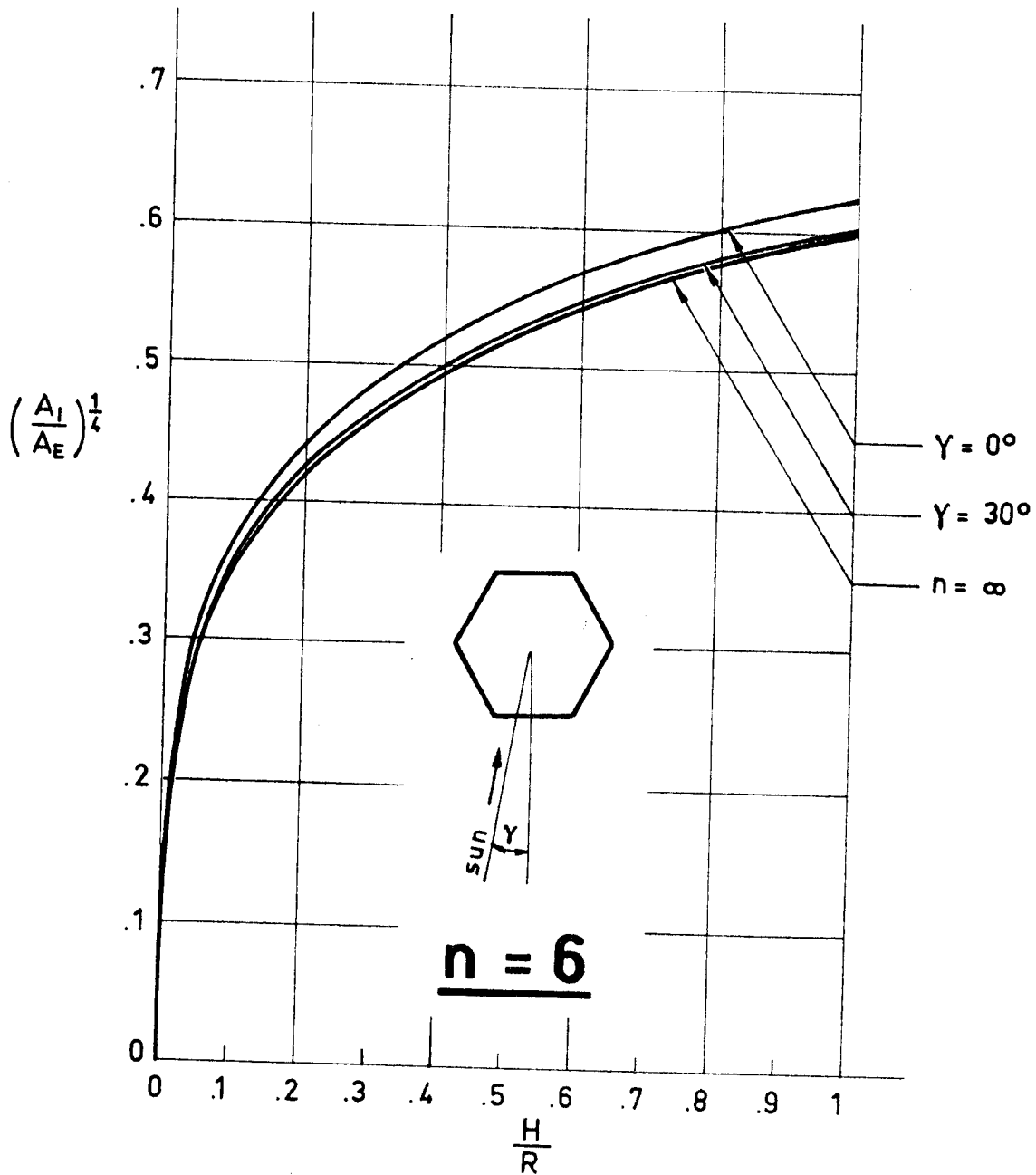


Fig 1-42. Ratio $(\frac{A_I}{A_E})^{1/4}$ as a function of $\frac{H}{R}$, in the case of a pyramid. The curves plotted are those corresponding to the largest and smallest areas projected from the Sun. Circular cone, $n = \infty$. Calculated by the compiler.

SOLAR RADIATION
 Infinitely Conductive Pyramidal Surfaces

n = 6

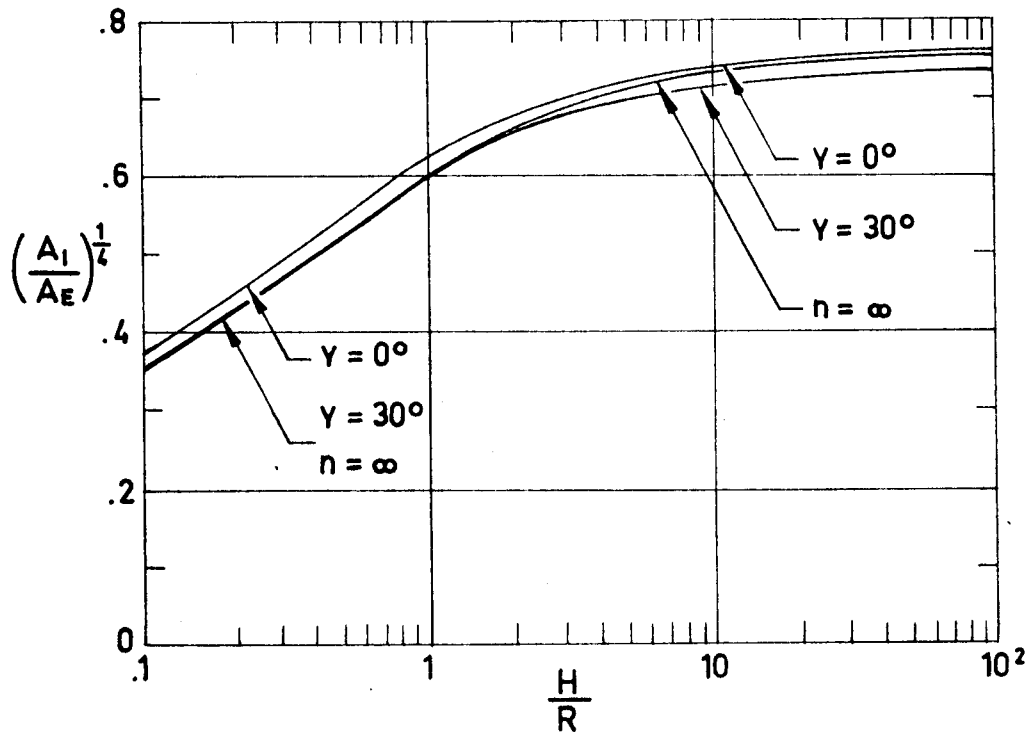


Fig 1-43. Ratio $\left(\frac{A_I}{A_E}\right)^{1/4}$ as a function of $\frac{H}{R}$, in the case of pyramid. The curves plotted are those corresponding to the largest and smallest areas projected from the Sun. The values corresponding to $\frac{H}{R} \leq 1$ are also plotted in the previous figure. Circular cone, $n=\infty$. Calculated by the compiler.

SOLAR RADIATION
 Infinitely Conductive Pyramidal Surfaces

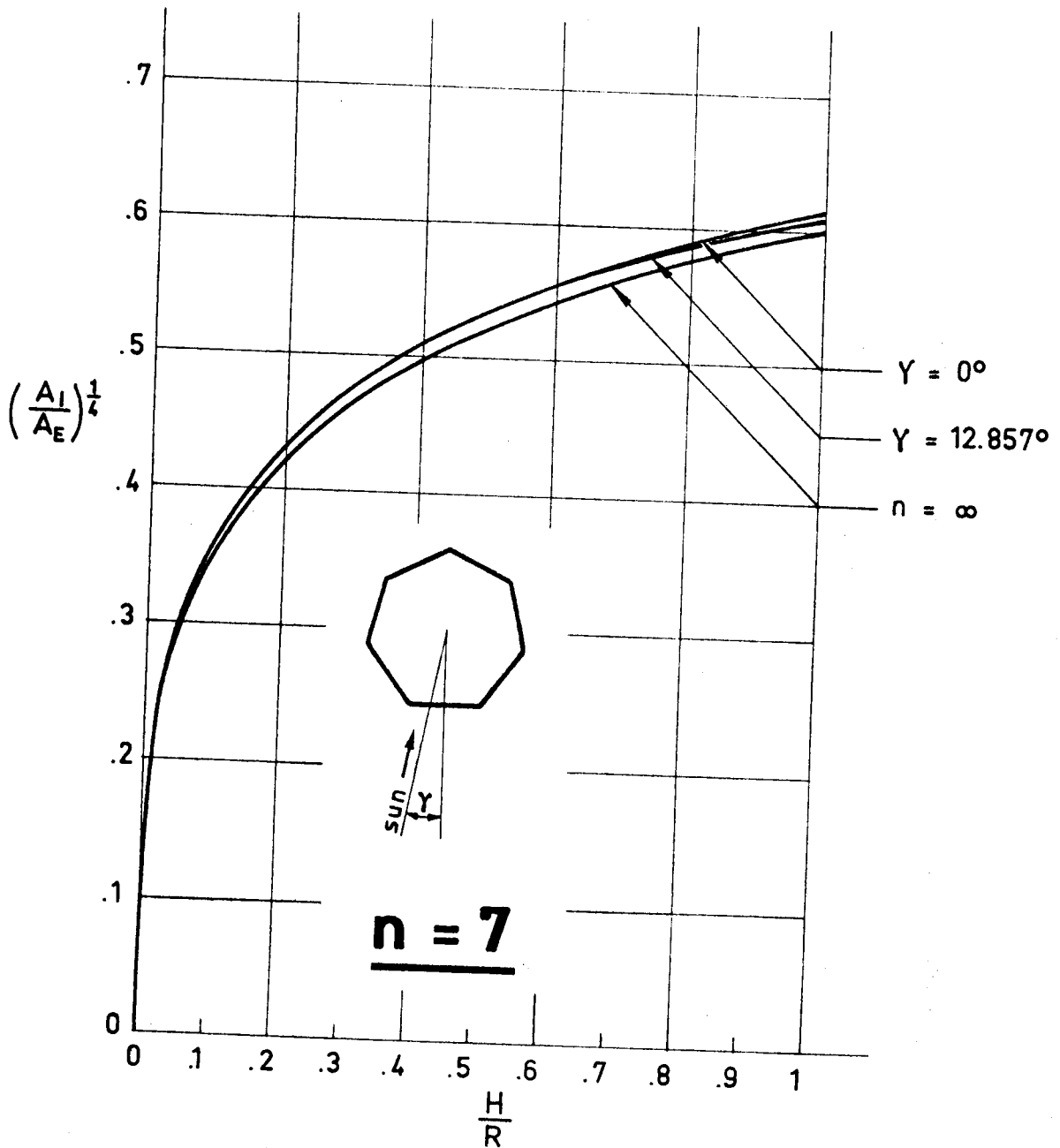


Fig 1-44. Ratio $(\frac{A_I}{A_E})^{1/4}$ as a function of $\frac{H}{R}$, in the case of a pyramid. The curves plotted are those corresponding to the largest and smallest areas projected from the Sun. Circular cone, $n = \infty$. Calculated by the compiler.

SOLAR RADIATION
 Infinitely Conductive Pyramidal Surfaces

n = 7

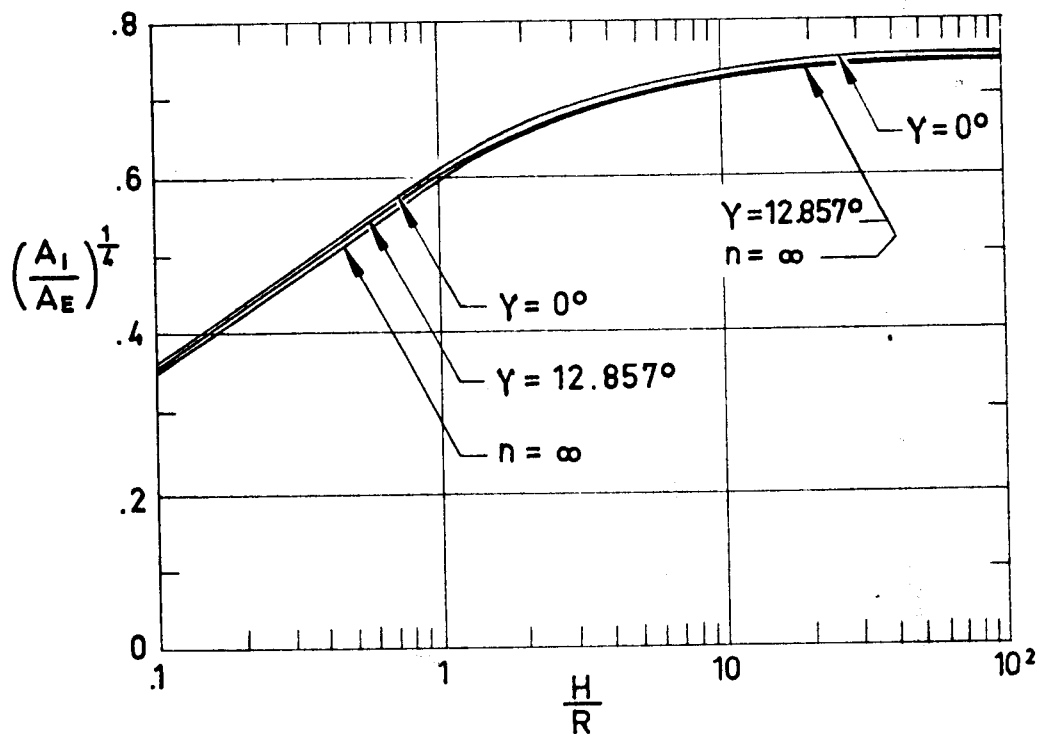


Fig 1-45. Ratio $\left(\frac{A_I}{A_E}\right)^{\frac{1}{4}}$ as a function of $\frac{H}{R}$, in the case of a pyramid. The curves plotted are those corresponding to the largest and smallest areas projected from the Sun. The values corresponding to $\frac{H}{R} \leq 1$ are also plotted in the previous figure. Circular cone, $n = \infty$. Calculated by the compiler.

INTENTIONALLY BLANK PAGE

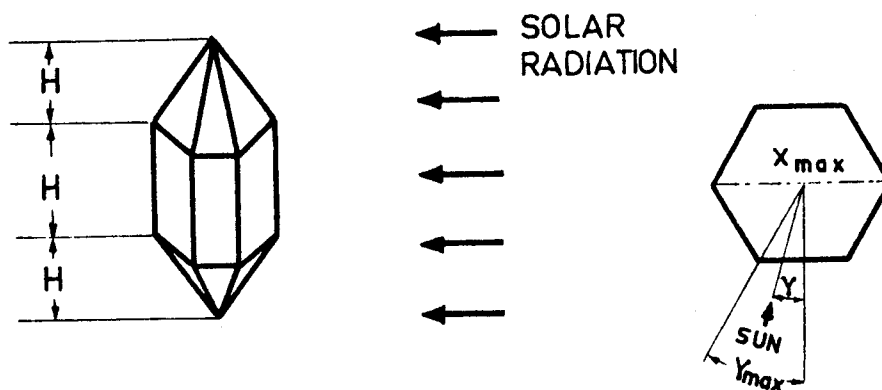
SOLAR RADIATION

Infinitely Conductive Prismatic-Pyramidal Surfaces

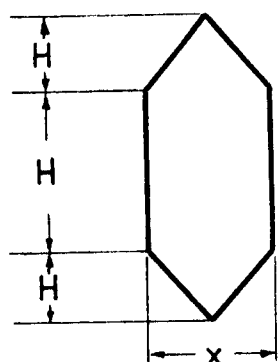
1.9. INFINITELY CONDUCTIVE PRISMATIC-PYRAMIDAL SURFACES

1.9.1. PYRAMID-PRISM-PYRAMID WITH AN n-SIDED REGULAR POLYGONAL SECTION

Sketch:



Area Projected from the Sun, A_I :



$$\frac{X}{R} = 2 \cos \gamma, \text{ for } n \text{ even.}$$

$$\frac{X}{R} = 2 \cos\left(\frac{\pi}{2n}\right) \cos \gamma, \text{ for } n \text{ odd.}$$

Formula:

$$\frac{A_I}{A_E} = \frac{\frac{X}{R}}{n \sin\left(\frac{\pi}{n}\right) \left[1 + \sqrt{1 + \frac{\cos^2\left(\frac{\pi}{n}\right)}{(H/R)^2}}\right]}$$

SOLAR RADIATION
Infinitely Conductive Prismatic-Pyramidal Surfaces

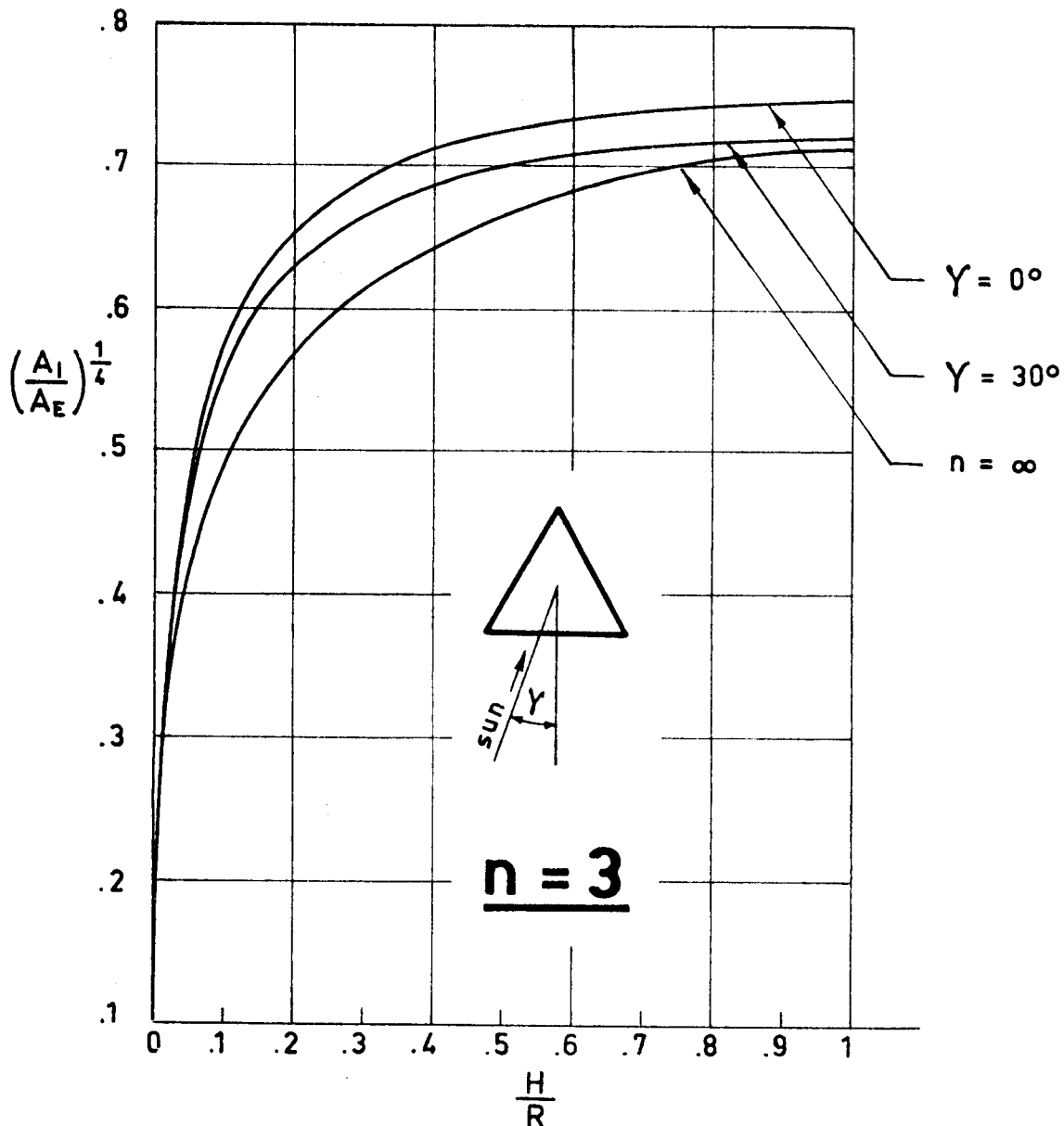


Fig 1-46. Ratio $\left(\frac{A_I}{A_E}\right)^{1/4}$ as a function of $\frac{H}{R}$, in the case of a pyramid-prism-pyramid. The curves plotted are those corresponding to the largest and smallest areas projected from the Sun. Cone-cylinder-cone, $n=\infty$. Calculated by the compiler.

SOLAR RADIATION
 Infinitely Conductive Prismatic-Pyramidal Surfaces

n = 3

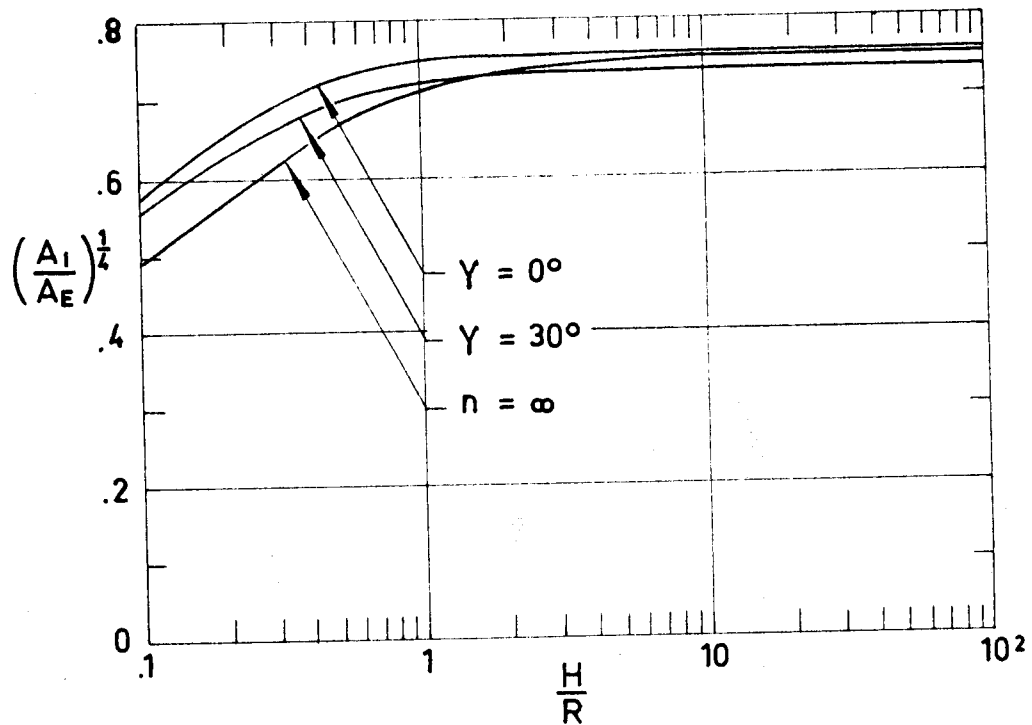


Fig 1-47. Ratio $\left(\frac{A_I}{A_E}\right)^{1/4}$ as a function of $\frac{H}{R}$, in the case of a pyramid-prism-pyramid. The curves plotted are those corresponding to the largest and smallest areas projected from the Sun. The values corresponding to $\frac{H}{R} \leq 1$ are also plotted in the previous figure. Cone-cylinder-cone, $n=\infty$. Calculated by the compiler.

SOLAR RADIATION

Infinitely Conductive Prismatic-Pyramidal Surfaces

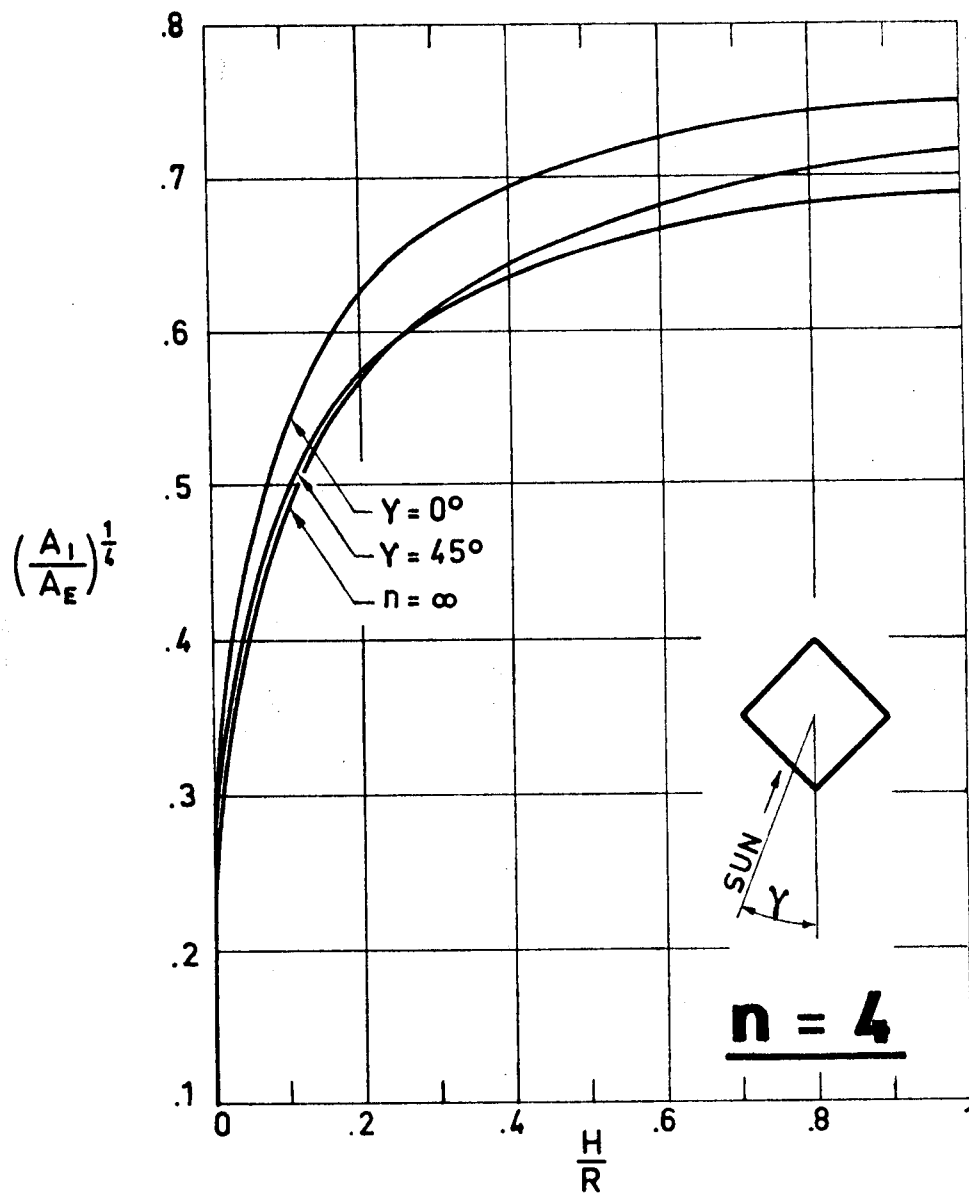


Fig 1-48. Ratio $\left(\frac{A_I}{A_E}\right)^{1/4}$ as a function of $\frac{H}{R}$, in the case of a pyramid-prism-pyramid. The curves plotted are those corresponding to the largest and smallest areas projected from the Sun. Cone-cylinder-cone, $n=\infty$. Calculated by the compiler.

SOLAR RADIATION
 Infinitely Conductive Prismatic-Pyramidal Surfaces

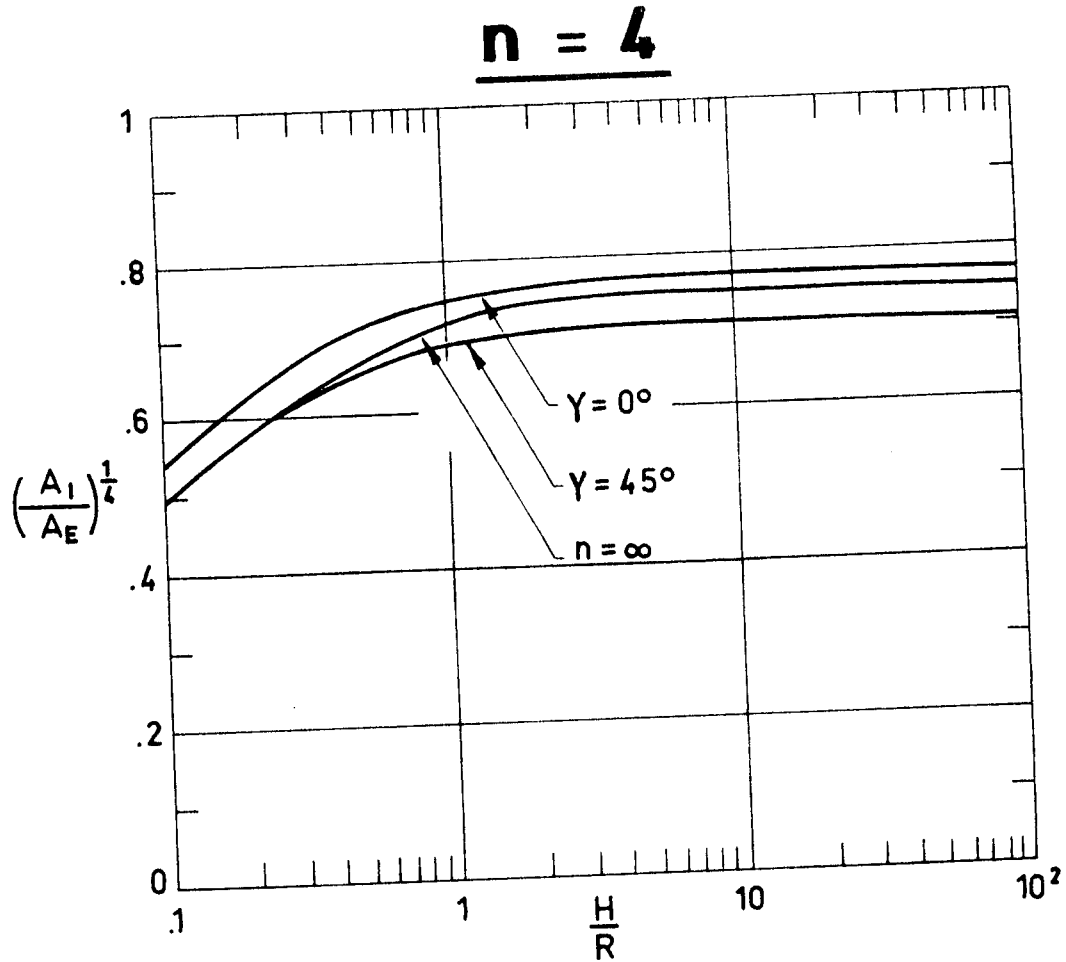


Fig 1-49. Ratio $(\frac{A_I}{A_E})^{1/4}$ as a function of $\frac{H}{R}$, in the case of a pyramid-prism-pyramid. The curves plotted are those corresponding to the largest and smallest areas projected from the Sun. The values corresponding to $\frac{H}{R} \leq 1$ are also plotted in the previous figure. Cone-cylinder-cone, $n = \infty$. Calculated by the compiler.

SOLAR RADIATION

Infinitely Conductive Prismatic-Pyramidal Surfaces

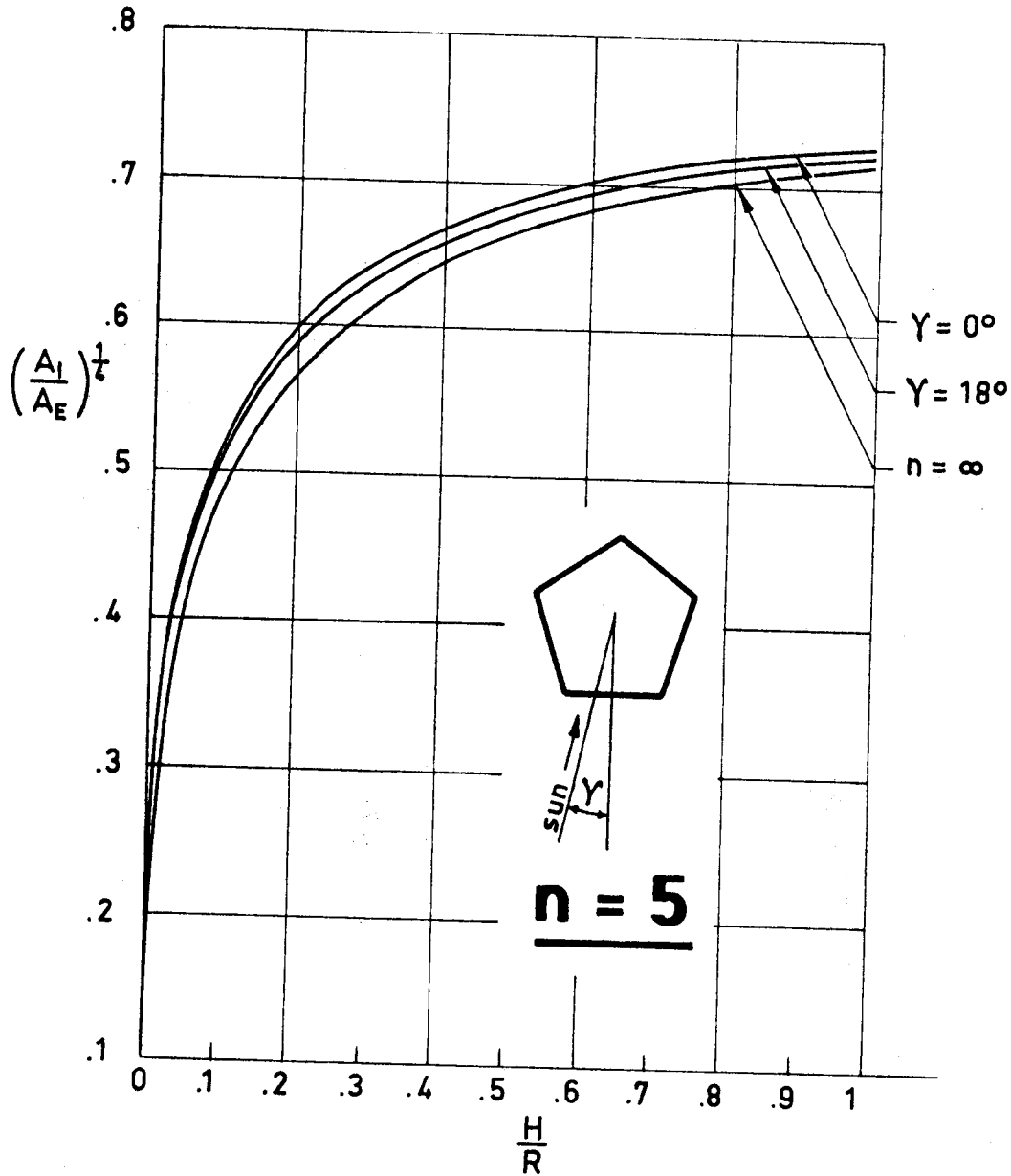


Fig 1-50. Ratio $(\frac{A_I}{A_E})^{1/4}$ as a function of $\frac{H}{R}$, in the case of a pyramid-prism-pyramid. The curves plotted are those corresponding to the largest and smallest areas projected from the Sun. Cone-cylinder-cone, $n=\infty$. Calculated by the compiler.

SOLAR RADIATION
 Infinitely Conductive Prismatic-Pyramidal Surfaces

n = 5

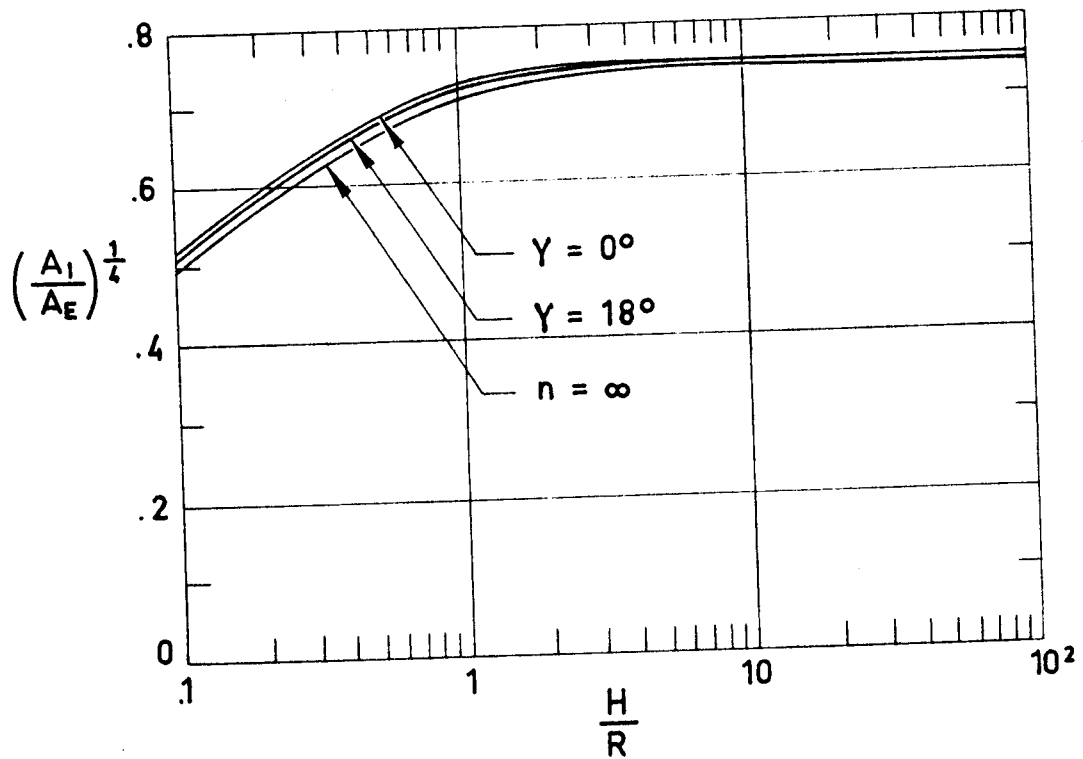


Fig 1-51. Ratio $\left(\frac{A_I}{A_E}\right)^{1/4}$ as a function of $\frac{H}{R}$, in the case of a pyramid-prism-pyramid. The curves plotted are those corresponding to the largest and smallest areas projected from the Sun. The values corresponding to $\frac{H}{R} \leq 1$ are also plotted in the previous figure. Cone-cylinder-cone, $n = \infty$. Calculated by the compiler.

SOLAR RADIATION

Infinitely Conductive Prismatic-Pyramidal Surfaces

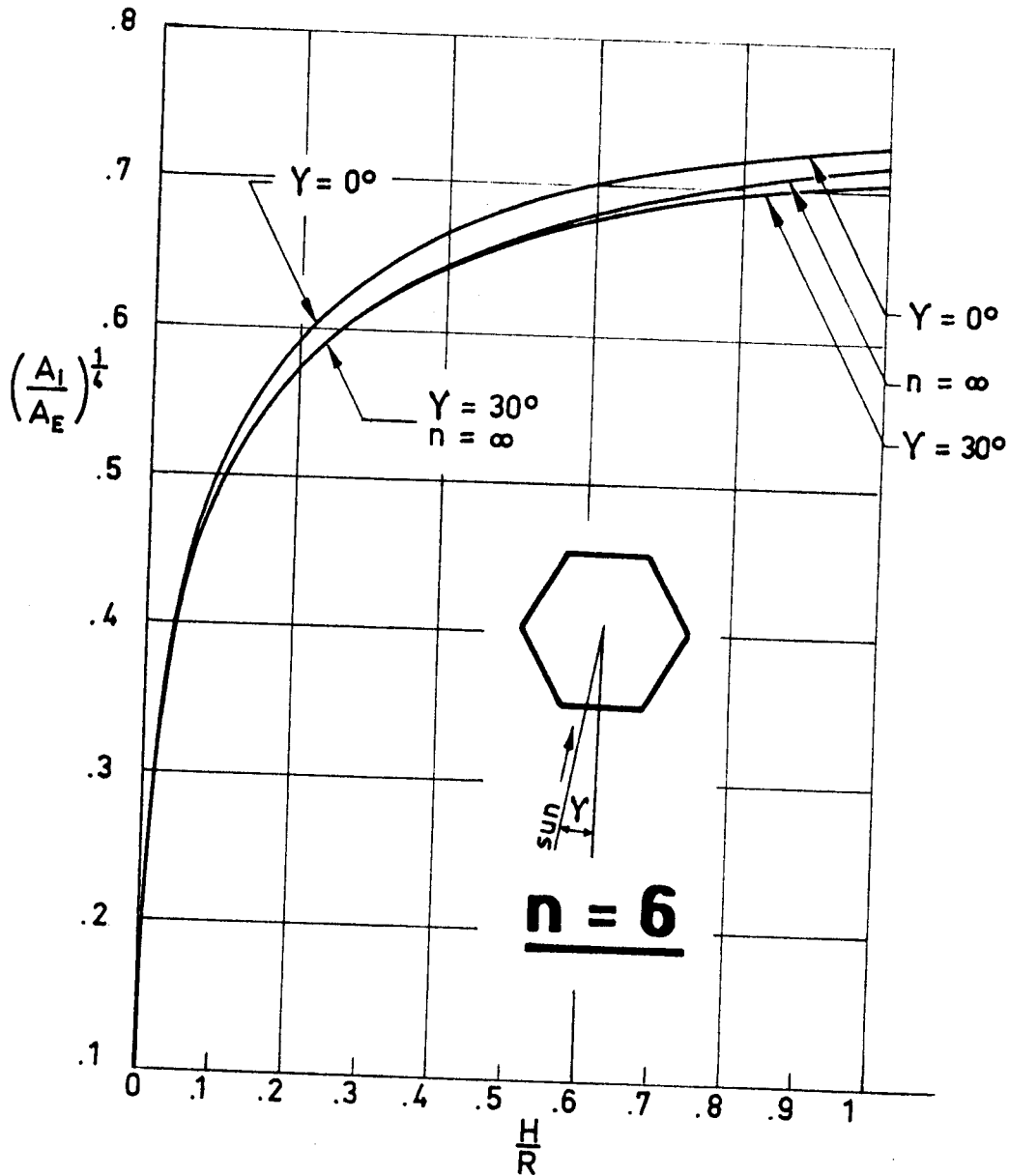


Fig 1-52. Ratio $(\frac{A_I}{A_E})^{1/4}$ as a function of $\frac{H}{R}$, in the case of a pyramid-prism-pyramid. The curves plotted are those corresponding to the largest and smallest areas projected from the Sun. Cone-cylinder-cone, $n=\infty$. Calculated by the compiler.

SOLAR RADIATION

Infinitely Conductive Prismatic-Pyramidal Surfaces

n = 6

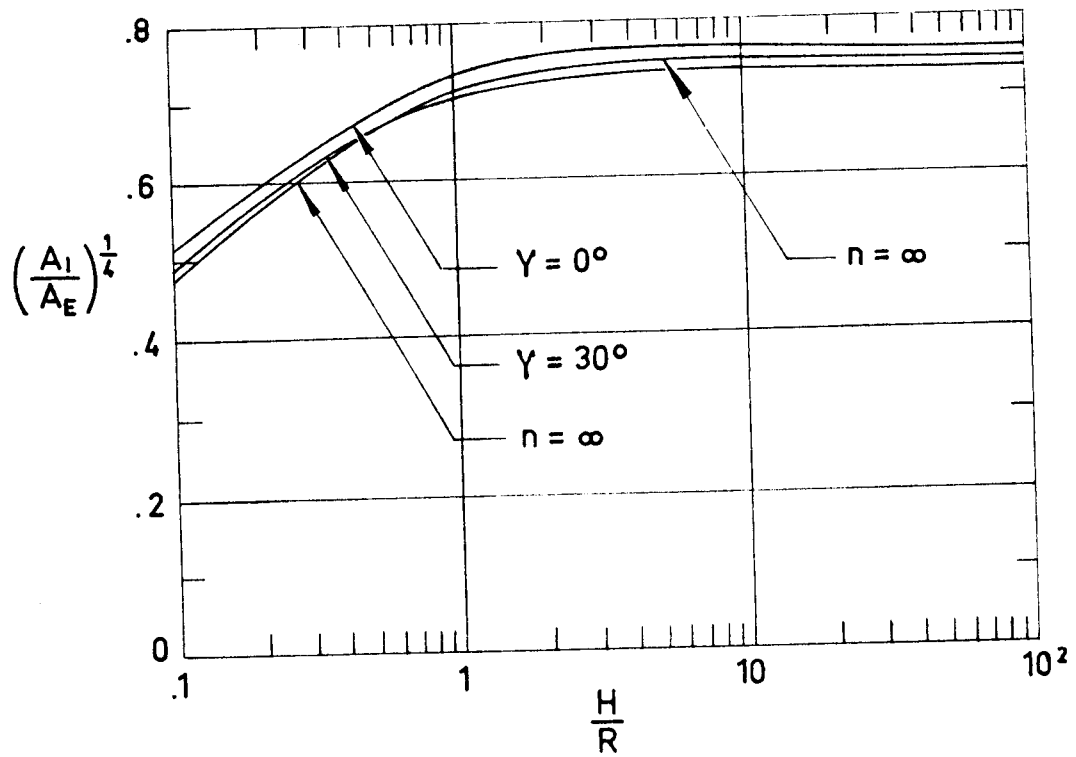


Fig 1-53. Ratio $\left(\frac{A_I}{A_E}\right)^{1/4}$ as a function of $\frac{H}{R}$, in the case of a pyramid-prism-pyramid. The curves plotted are those corresponding to the largest and smallest areas projected from the Sun. The values corresponding to $\frac{H}{R} \leq 1$ are also plotted in the previous figure. Cone-cylinder-cone, $n = \infty$. Calculated by the compiler.

SOLAR RADIATION
 Infinitely Conductive Prismatic-Pyramidal Surfaces

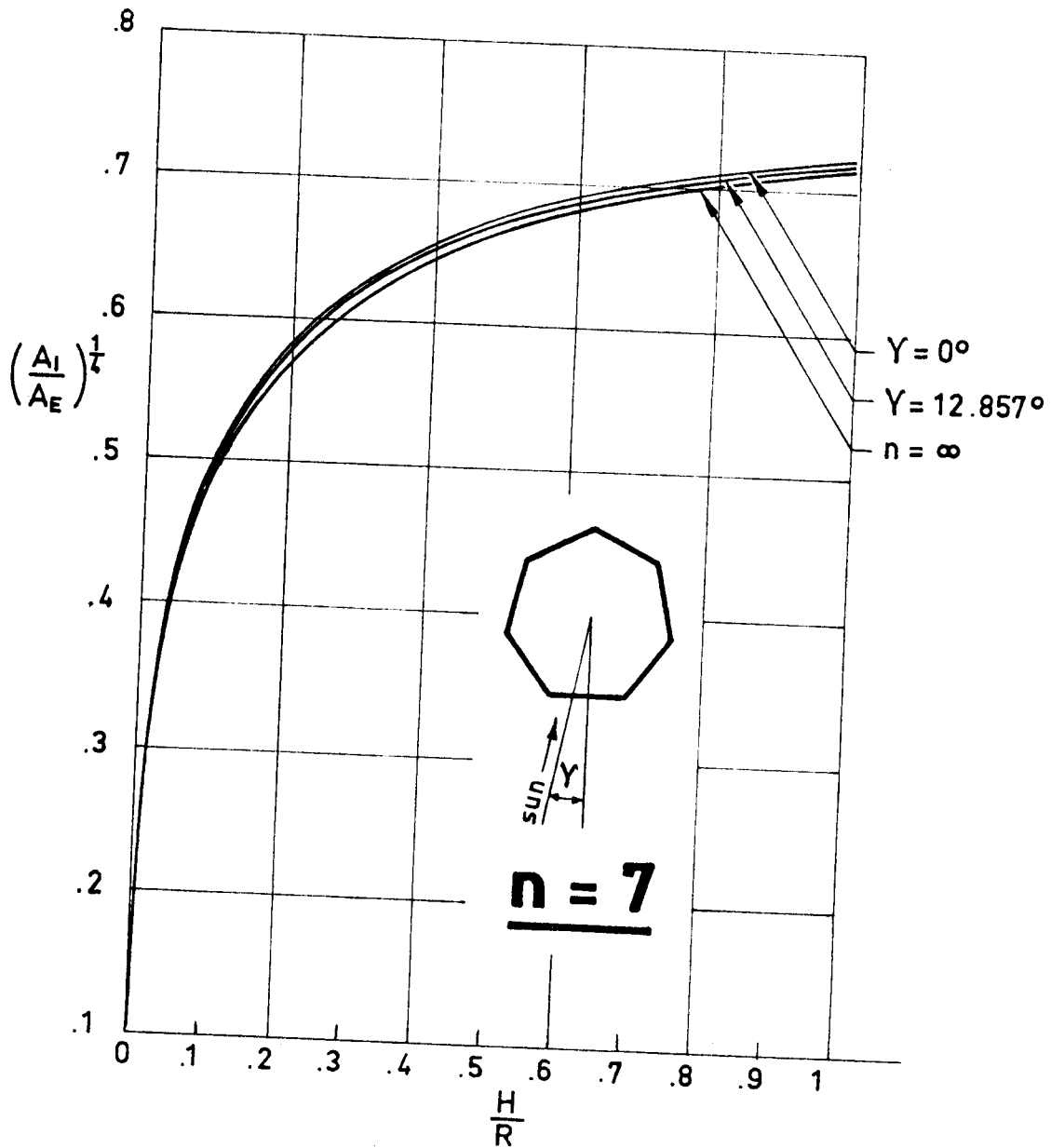


Fig 1-54. Ratio $(\frac{A_I}{A_E})^{1/4}$ as a function of $\frac{H}{R}$, in the case of a pyramid-prism-pyramid. The curves plotted are those corresponding to the largest and smallest areas projected from the Sun. Cone-cylinder-cone, $n = \infty$. Calculated by the compiler.

SOLAR RADIATION
 Infinitely Conductive Prismatic-Pyramidal Surfaces

n = 7

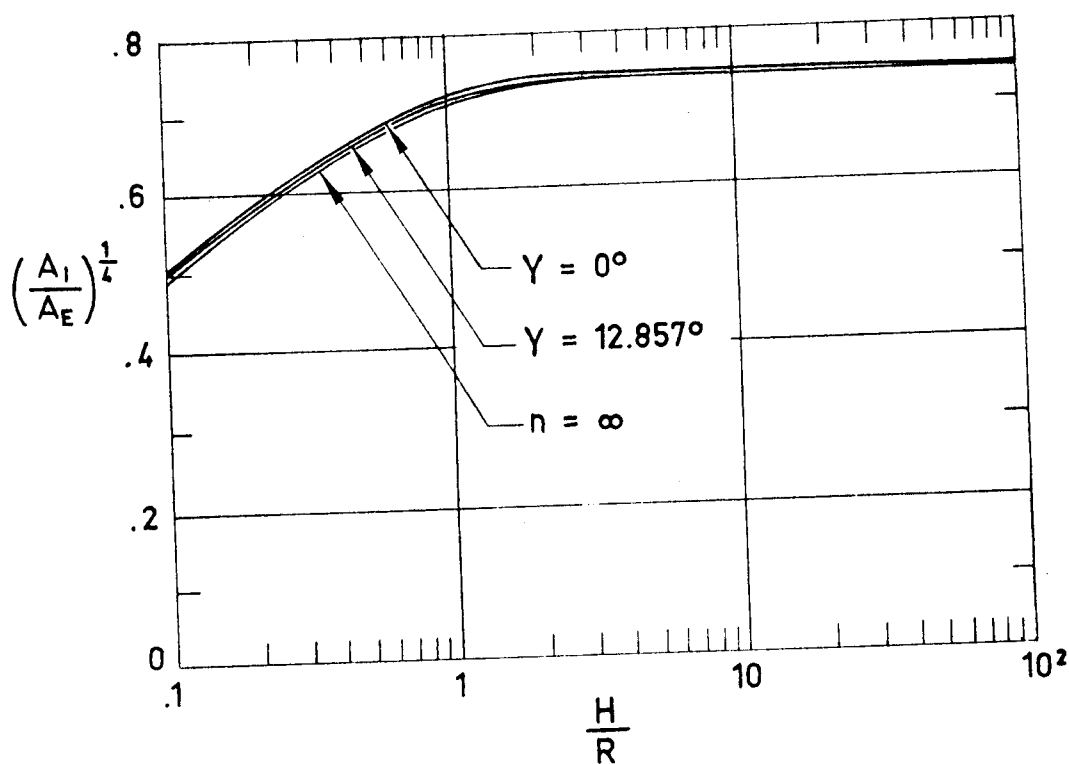


Fig 1-55. Ratio $\left(\frac{A_I}{A_E}\right)^{1/4}$ as a function of $\frac{H}{R}$, in the case of a pyramid-prism-pyramid. The curves plotted are those corresponding to the largest and smallest areas projected from the Sun. The values corresponding to $\frac{H}{R} \leq 1$ are also plotted in the previous figure. Cone-cylinder-cone, $n = \infty$. Calculated by the compiler.

INTENTIONALLY BLANK PAGE

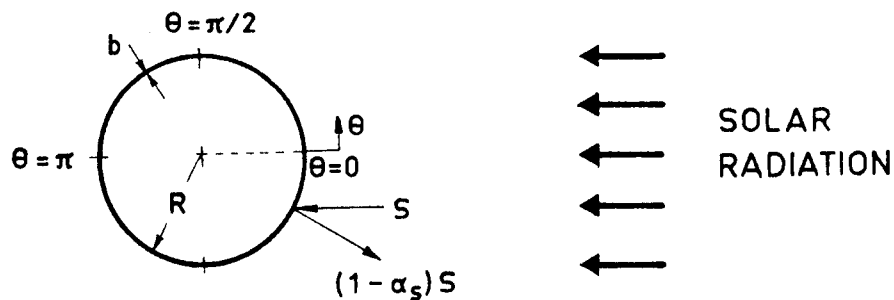
SOLAR RADIATION

Thin-Walled Spherical Bodies. Finite Conductivity

1.10. THIN-WALLED SPHERICAL BODIES. FINITE CONDUCTIVITY

1.10.1. NON-SPINNING SPHERE

Sketch:



Dimensionless Parameters:

$$\tau(\theta) = \frac{T(\theta)}{T_R} \quad , , \quad \mu = \frac{kb}{\epsilon\sigma T_R^3 R^2}$$

Differential Equations:

$$\frac{\mu}{\sin\theta} \frac{d}{d\theta} \left[\sin\theta \frac{d\tau}{d\theta} \right] = \begin{cases} \tau^4 - 4 \cos\theta & , , \quad \text{when } 0 \leq \theta \leq \pi/2 \\ \tau^4 & , , \quad \text{when } \pi/2 \leq \theta \leq \pi \end{cases}$$

Boundary Conditions:

$$\frac{d\tau}{d\theta} \Big|_{\theta=0} = \frac{d\tau}{d\theta} \Big|_{\theta=\pi} = 0 \quad , , \quad \tau \Big|_{\theta=\pi/2} \text{ and } \frac{d\tau}{d\theta} \Big|_{\theta=\pi/2} \text{ continuous.}$$

Comments:

The results obtained by numerically solving this problem are given in the following two pages.

Reference: Nichols (1961).

SOLAR RADIATION

Thin-Walled Spherical Bodies. Finite Conductivity

θ°	T/T _R						
	$\mu=10$	$\mu=5$	$\mu=1$	$\mu=.5$	$\mu=.1$	$\mu=.01$	$\mu=0$
0	1.09700	1.16215	1.33458	1.37639	1.40777	1.41340	1.41421
5	1.09652	1.16134	1.33300	1.37497	1.40638	1.41138	1.41287
10	1.09507	1.15887	1.32827	1.37027	1.40221	1.40620	1.40881
15	1.09267	1.15477	1.32037	1.36237	1.39522	1.39975	1.40201
20	1.08935	1.14909	1.30928	1.35120	1.38532	1.39001	1.39239
25	1.08514	1.14190	1.29499	1.33662	1.37237	1.37528	1.37986
30	1.08010	1.13325	1.27748	1.31850	1.35619	1.36300	1.36426
35	1.07428	1.12325	1.25676	1.29666	1.33651	1.34241	1.34541
40	1.06774	1.11202	1.23288	1.27093	1.31296	1.31999	1.32306
45	1.06058	1.09968	1.20591	1.24116	1.28503	1.29412	1.29684
50	1.05288	1.08638	1.17599	1.20724	1.25198	1.26213	1.26629
55	1.04474	1.07229	1.14336	1.16916	1.21283	1.22708	1.23073
60	1.03627	1.05760	1.10835	1.12706	1.16691	1.18724	1.18921
65	1.02759	1.04253	1.07144	1.08133	1.13321	1.13937	1.14026
70	1.01883	1.02730	1.03323	1.03263	1.07412	1.08069	1.08150
75	1.01012	1.01217	.99453	.98203	.96475	.98960	1.00870
80	1.00162	.99741	.95631	.93106	.90253	.91131	.91292
85	.99349	.98333	.91977	.88179	.77965	.76880	.76840
90	.98590	.97024	.88632	.83684	.72340	.58532	0
95	.97898	.95843	.85714	.79850	.65631	.46727	0
100	.97271	.94781	.83187	.76613	.60415	.40045	0
105	.96703	.93827	.80991	.73857	.57227	.36310	0
110	.96190	.92969	.79075	.71497	.53393	.32352	0
115	.95726	.92200	.77400	.69466	.51476	.30373	0
120	.95308	.91512	.75937	.67716	.49304	.28349	0
125	.94933	.90898	.74656	.66201	.47515	.26772	0
130	.94599	.90352	.73540	.64895	.46025	.25831	0
135	.94302	.89870	.72571	.63771	.45000	.24752	0
140	.94041	.89449	.71735	.62808	.43732	.23341	0
145	.93815	.89084	.71020	.61991	.42828	.23019	0
150	.93621	.88773	.70417	.61305	.42049	.22362	0
155	.93459	.88513	.69918	.60740	.41436	.21873	0
160	.93328	.88303	.69518	.60288	.40957	.21506	0
165	.93227	.88141	.69210	.59941	.40596	.21235	0
170	.93155	.88026	.68993	.59696	.40343	.21048	0
175	.93112	.87958	.68861	.59545	.40194	.20937	0
180	.93097	.87935	.68828	.59519	.40144	.20901	0

Table 1-1. Temperature distribution on sphere for several μ values. No spin. No internal radiation. Calculated by the compiler.

SOLAR RADIATION

Thin-Walled Spherical Bodies. Finite Conductivity

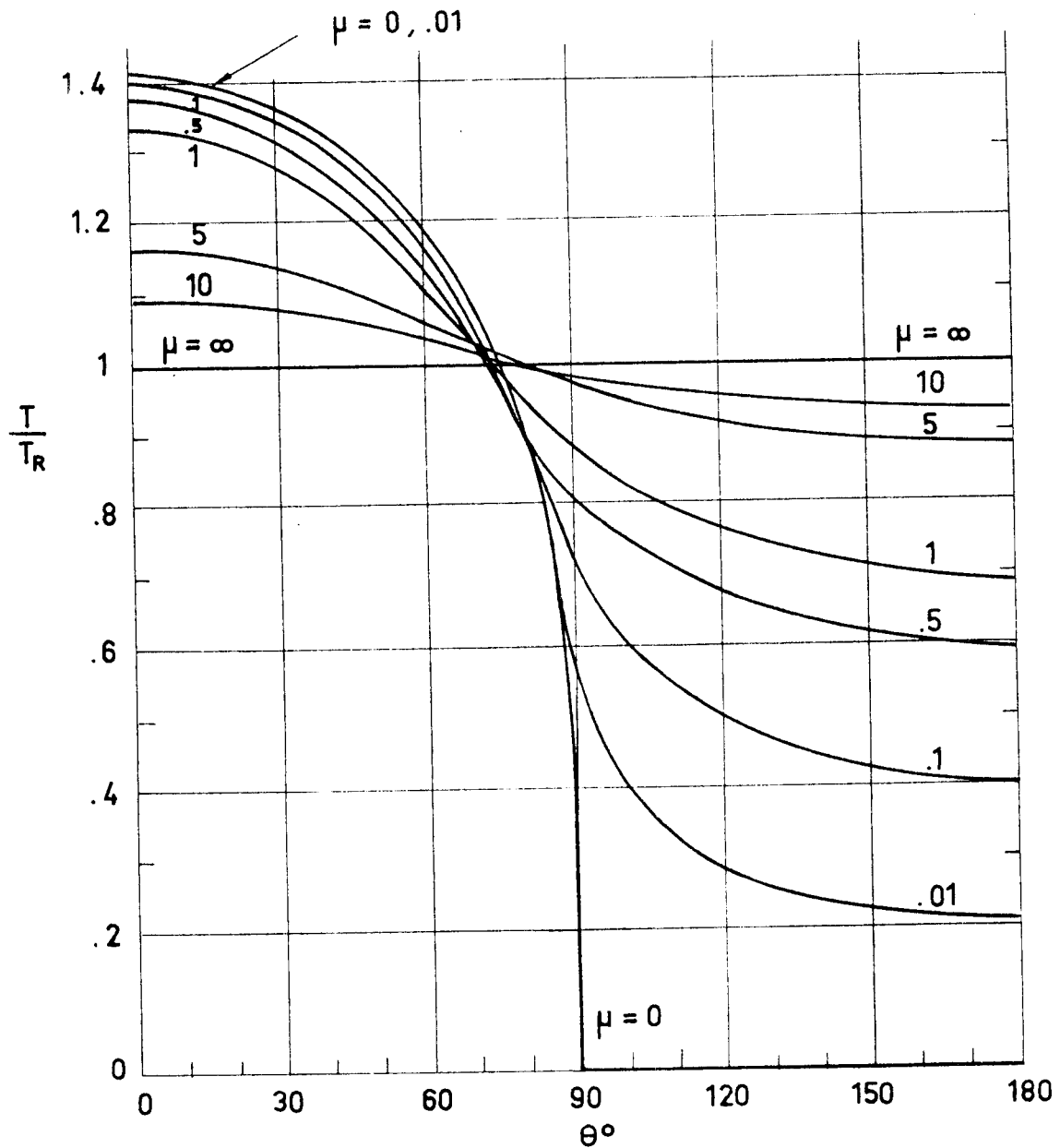
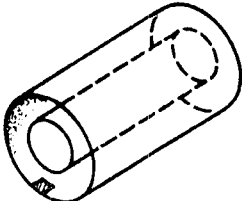
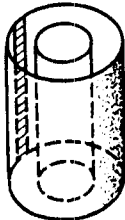
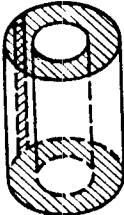
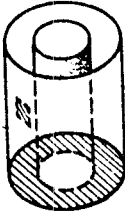
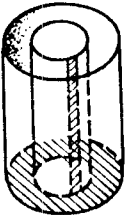


Fig 1-56. Temperature distribution on sphere. No spin. No internal radiation. Calculated by the compiler.

INTENTIONALLY BLANK PAGE

DIFFUSE SURFACES
Additional Sources of Data

Definition	Sketch	Sources
Element is at end of wall on inside of finite length cylinder enclosing concentric cylinder of same length; factor is from element to inside surface of outer cylinder		Hamilton & Morgan (1952), Leuenberger & Person (1956), Kreith (1962).
Elemental strip on inner surface of outer concentric cylinder to interior surface of outer concentric cylinder		Hamilton & Morgan (1952), Leuenberger & Person (1956), Kreith (1962).
Elemental strip on inner surface of outer concentric cylinder to either annular end		Hamilton & Morgan (1952), Leuenberger & Person (1956), Kreith (1962).
Element on inside of outer finite concentric cylinder to inside cylinder or annular end		Leuenberger & Person (1956).
Strip element on exterior of inner finite length concentric cylinder to inside of outer cylinder or to annular end		Leuenberger & Person (1956).
Reference: Siegel & Howell (1972).		

DIFFUSE SURFACES

Additional Sources of Data

Definition	Sketch	Sources
Strip on plane inside cylinder of finite length to inside of cylinder		Leuenberger & Person (1956).
Exterior element on tube surface to finite area on adjacent parallel tube of same diameter		Sparrow & Jonsson (1963 a). Journal of Heat Transfer, vol. 85, No. 4, 1963, pp. 382-384.
Exterior element on tube surface of partitioned tube to finite area on adjacent parallel tube of same diameter		Sparrow & Jonsson (1963 a).
Element on wall of right circular cone to base of cone		Joerg & McFarland (1962). Report S62-245, Aerojet-General Corporation, 1962.
Spherical point source to rectangle. Point source is on one corner of rectangle that intersects with receiving rectangle at angle ϕ		Hamilton & Morgan (1952), Jakob (1957), Kreith (1962).
Reference: Siegel & Howell (1972).		

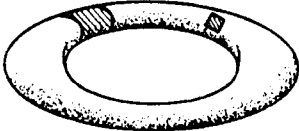
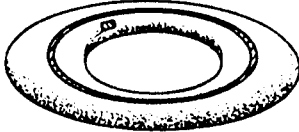
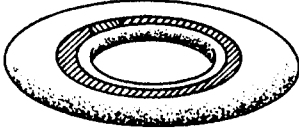
DIFFUSE SURFACES

Additional Sources of Data

Definition	Sketch	Sources
Sphere to ring element oriented normal to sphere axis		Feingold & Gupta (1970).
Elemental area on sphere to finite area on second sphere		Grier (1969). NASA SP-3050, 1969.
Area element to axisymmetric surface -paraboloid, cone, cylinder (formulation given-factors are not evaluated)		Morizumi (1964). AIAA Journal, vol. 2, No. 11, 1964, pp. 2028-2030.
Element on interior (or exterior) of any axisymmetric body of revolution to band of finite length on interior (or exterior)		Robbins (1961). NASA TN D-586, 1961. Robbins & Todd (1962). NASA TN D-878, 1962.
Slender torus to element on perpendicular axis		Moon (1961).
Reference: Siegel & Howell (1972).		

DIFFUSE SURFACES

Additional Sources of Data

Definition	Sketch	Sources
Element on exterior of toroid to toroidal segment of finite width		Grier & Sommers (1969). NASA TN D-5006, 1969.
Element on exterior of toroid to toroidal band of finite width		Grier & Sommers (1969).
Element and ring element on exterior of toroid to entire exterior of toroid		Grier & Sommers (1969). Sommers & Grier (1969). Journal of Heat Transfer, vol. 91, No. 3, 1969, pp. 459-461.
Reference: Siegel & Howell (1972).		

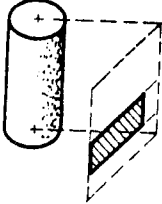
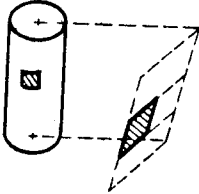
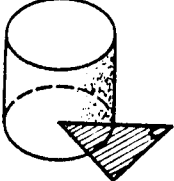

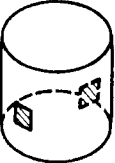
DIFFUSE SURFACES

Additional Sources of Data

Definition	Sketch	Sources
Circular disc to arbitrarily placed rectangle in parallel plane		<p>Tripp, Hwang & Crank (1962). Special Report 16, Kansas State University Bulletin, vol. 46, No. 4, 1962.</p>
Circle to arbitrarily placed rectangle in plane parallel to normal to circle		<p>Tripp, Hwang & Crank (1962).</p>
Circular disc to parallel right triangle; normal from center of circle passes through one acute vertex		<p>Tripp, Hwang & Crank (1962).</p>
Cylinder to any rectangle in plane perpendicular to cylinder axis		<p>Tripp, Hwang & Crank (1962).</p>
Finite area on exterior of cylinder to finite area on plane parallel to cylinder axis		<p>Stevenson & Grafton (1961). Report SID-61-91, North American Aviation (AFASD TR 61-119, pt. 1), 1961.</p>
<p>Reference: Siegel & Howell (1972).</p>		

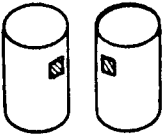
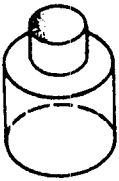
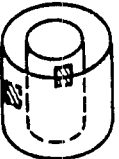
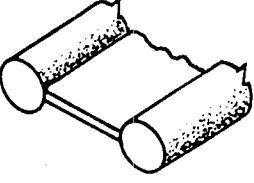
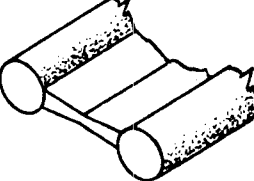
DIFFUSE SURFACES

Additional Sources of Data

Definition	Sketch	Sources
Cylinder to any rectangle in plane parallel to cylinder axis		Tripp, Hwang & Crank (1962). Special Report 16, Kansas State University Bulletin, vol. 46, No. 4, 1962.
Finite area on exterior of cylinder to finite area on skewed plane		Stevenson & Grafton (1961). Report SID-61-91, North American Aviation (AFASD TR 61-119, pt. 1), 1961.
Outside surface of cylinder to perpendicular right triangle; triangle is in plane of cylinder base with one vertex of triangle at center of base		Tripp, Hwang & Crank (1962).
Cylinder and plane of equal length parallel to cylinder axis; plane inside cylinder; all factors between plane and inner surface of cylinder		Leuenberger & Person (1956).
Finite areas on interior of right circular cylinder		Stevenson & Grafton (1961).
Reference: Siegel & Howell (1972).		

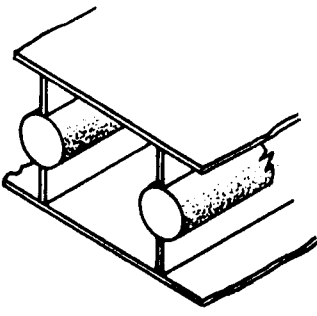
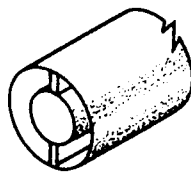
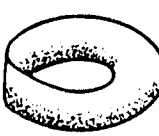
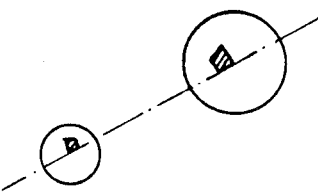
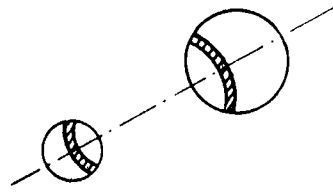
DIFFUSE SURFACES

Additional Sources of Data

Definition	Sketch	Sources
Finite area on exterior of cylinder to finite area on exterior of parallel cylinder		Stevenson & Grafton (1961). Report SID-61-91, North American Aviation (AFASD TR 61-119, pt. 1, 1961).
Concentric cylinders of different radii, one atop other; factors between inside of upper cylinder and inside or base of lower cylinder		Leuenberger & Person (1956).
Finite area on exterior of inner cylinder to finite area on interior of concentric outer cylinder		Stevenson & Grafton (1961).
Two tubes connected with fin of finite thickness; length can be finite or infinite; all factors between finite surfaces formulated in terms of integrations between differential strips		Sotos & Stockman (1964). NASA TN D-2556, 1964.
Two tubes connected with tapered fins of finite thickness; tube length can be finite or infinite; all factors between finite surfaces formulated in terms of integrations between differential strips		Sotos & Stockman (1964).
Reference: Siegel & Howell (1972).		

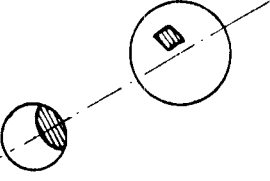
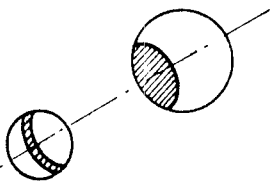
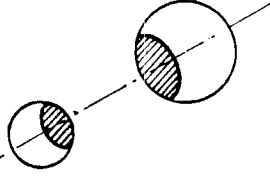


DIFFUSE SURFACES

Additional Sources of Data

Definition	Sketch	Sources
Sandwich tube and fin structure of infinite or finite length; all factors between finite surfaces formulated in terms of integrations between differential strips		Sotos & Stockman (1964). NASA TN D-2556, 1964.
Concentric cylinders connected by fin of finite thickness; length finite or infinite; all factors between finite surfaces formulated in terms of integrations between differential strips		Sotos & Stockman (1964).
From Moebius strip to itself		Stasenko (1967). Akad. Nauk SSSR, Izv. Energetika Transport, pp. 104-107, 1967.
Area on sphere to area on another sphere		Grier (1969). NASA SP-3050, 1969.
Band on one sphere to band on another sphere		Grier (1969).
Reference: Siegel & Howell (1972).		

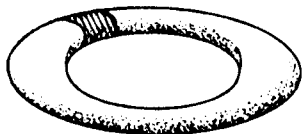
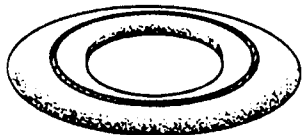
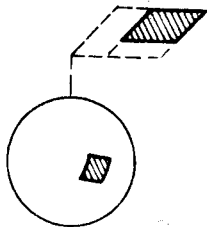
DIFFUSE SURFACES

Additional Sources of Data

Definition	Sketch	Sources
Area on sphere to cap on another sphere		Grier (1969). NASA SP-3050, 1969.
Cap on sphere to band on another sphere		Grier (1969).
Cap on sphere to cap on another sphere		Grier (1969):
Hemisphere to coaxial hemisphere in contact		Wakao, Kato & Furuya (1969). Int. J. Heat Mass Transfer, vol. 12, No. 1, 1969, pp. 118-120.
Exterior of toroid to itself		Sommers & Grier (1969). Journal of Heat Transfer, vol. 91, No. 3, 1969, pp. 459-461.
Reference: Siegel & Howell (1972).		

DIFFUSE SURFACES

Additional Sources of Data

Definition	Sketch	Sources
Segment of finite width on toroid to exterior of toroid		Grier & Sommers (1969). NASA TN D-5006, 1969.
Toroidal band of finite width to exterior of toroid		Grier & Sommers (1969).
Area on surface of sphere to rectangle in plane perpendicular to axis of sphere		Stevenson & Grafton (1961). Report SID-61-91, North American Aviation (AFASD TR 61-119, pt. 1, 1961.
Reference: Siegel & Howell (1972).		

SPECULAR SURFACES

General

2. SPECULAR SURFACES2.1. GENERAL

The specular view factor, F_{12}^s , between two specularly reflecting gray surfaces A_1 and A_2 is defined, (Perlmutter & Siegel (1963)) as the fraction of the energy leaving diffusely the isothermal surface A_1 that impinges A_2 , either directly or through any number of specular reflections from these or other gray surfaces of the whole system. Notice that a given amount of energy leaving A_1 , if specularly reflected, may be counted several times on its arrival to A_2 , so that F_{12}^s may be larger than one. On the other hand, the ratio of the energy absorbed by A_2 to that emitted by A_1 is smaller than one, depending its value, for a given geometrical system, on the specular reflectances of the surfaces forming the system.

The above definition of specular view factor shows some peculiarities that were not present in the definition of diffuse view factors. Such peculiarities are:

1) When calculating the radiant interchange between gray diffuse surfaces, the effect of the diffuse reflectance of the surfaces is not included in the view factor, since it is accounted for by means of the radiosity, B , which takes into account both the emitted and the diffusely reflected radiations.

$$B = \epsilon \sigma T^4 + \rho^d H ,$$

H represents the radiant flux incident on the emitting surfaces per unit time and unit area, and ρ^d is the diffuse reflectance. Thus $B_1 A_1 F_{12}$ is the heat arriving directly to A_2 from A_1 without being

SPECULAR SURFACES

General

reflected in any surface after the last time it leaves A_1 .

On the other hand, when specular surfaces are involved, it is usual to leave unchanged the factor corresponding to diffuse radiosity, and to include specular reflections in the view factor F_{12}^S . In any case $B_1 A_1 F_{12}^S$ measures the heat arriving to A_2 from A_1 both directly and through all possible specular inter-reflections, but it should be emphasized that B_1 indicates the diffusely-tributed radiant flux leaving A_1 per unit time and unit area.

A ray, that leaving A_1 reaches A_2 after a reflection from A_j , is accounted for as coming from A_j if this surface is diffuse reflecting and as coming from A_1 if A_j is specularly reflecting.

2) The concept of diffuse view factor involves only the emitting surface, A_1 , and the receiving surface, A_2 , while the parallel concept of specular view factor involves, in addition to A_1 and A_2 , all partially or totally specular surfaces of the system where rays coming from A_1 can be reflected before reaching A_2 .

3) It is obvious that, for a given geometrical system, the radiative transfer equation may be written in a unified fashion in terms of the temperature, optical characteristics of the surfaces, and view factors, no matter whether some of these surfaces are specular or not, provided that the diffuse radiosity and the appropriate view factors are used for the computation.

For a system of N specular surfaces, having specular reflectances ρ_j^S , the specular view factor, F_{12}^S , between two of them is:

SPECULAR SURFACES

General

$$F_{12}^s = \sum_{i=0}^{\infty} \sum_{j=0}^{\infty} \sum_{k=0}^{\infty} \dots \sum_{p=0}^{\infty} \sum_{q=0}^{\infty} (\rho_1^s)^i (\rho_2^s)^j (\rho_3^s)^k \dots (\rho_{N-1}^s)^p (\rho_N^s)^q K_{12}(i, j, k, p, q)$$

with $\lim_{\rho_j^s \rightarrow 0} (\rho_j^s)^0 = 1$ for every ρ_j^s .

The factor K_{12} may be interpreted as the fraction of the radiative energy leaving A_1 which reaches A_2 after i specular reflections from A_1 , j from A_2 , k from A_3, \dots, p from A_{N-1} , and q from A_N , under the assumption that there is no absorption, so that the mirrors do nothing except to change the direction of the impinging rays. Due to some geometrical constraints, several K factors may vanish.

A reasoning based on the fact that the reversal of the rays arriving to A_2 from A_1 , after reflection from several surfaces of the system, is exactly equivalent to the system of the rays arriving to A_1 from A_2 , after reflection from the same surfaces, indicates that, independently of what surfaces A_1 and A_2 are considered, their specular view factors satisfy the reciprocity relation:

$$A_1 F_{12}^s = A_2 F_{21}^s$$

When an enclosure of N surfaces A_1, A_2, \dots, A_N is considered, the specular view factors satisfy the relation:

$$\sum_{j=1}^N (1 - \rho_j^s) F_{ij} = 1$$

for any surface A_i . This relationship results from the fact that the overall heat transfer in the enclosure must be zero.

INTENTIONALLY BLANK PAGE

SPECULAR SURFACES
Two Planar Specular Surfaces

2.2. TWO PLANAR SPECULAR SURFACES

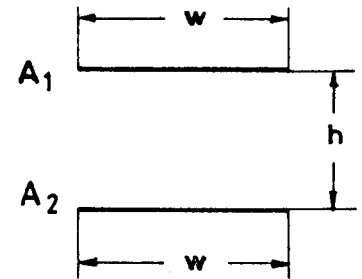
2.2.1. TWO-DIMENSIONAL CONFIGURATIONS

2.2.1.1. PARALLEL STRIPS OF EQUAL WIDTH

Two infinitely long directly opposed parallel strips of same finite width.

$$H = \frac{w}{h}$$

$$R = \rho_1^s \rho_2^s$$



Formulae:

$$F_{12}^s = F_{21}^s = K(1) + \sum_{n=1}^{\infty} R^n K(2n+1)$$

$$\frac{F_{11}^s}{\rho_2^s} = \frac{F_{22}^s}{\rho_1^s} = K(2) + \sum_{n=1}^{\infty} R^n K(2n+2)$$

where:

$$K(m) = \frac{1}{H} (\sqrt{H^2 + m^2} - m)$$

n is the number of specular reflections which a ray suffers before reaching the receiving surface.

Reference: These expressions have been obtained by the compiler.

SPECULAR SURFACES
Two Planar Specular Surfaces

R \ H	.1	.2	.4	.6	1	2
.05	.05073	.10074	.19601	.28209	.42258	.63367
.20	.05368	.10662	.20773	.29959	.45131	.68762
.30	.05603	.11131	.21710	.31358	.47432	.73117
.40	.05881	.11688	.22820	.33017	.50164	.78314
.50	.06220	.12364	.24171	.35036	.53494	.84688
.60	.06647	.13219	.25877	.37588	.57709	.92810
.70	.07218	.14361	.28157	.41000	.63354	1.03765
.80	.08058	.16039	.31510	.46021	.71677	1.20039
.90	.09576	.19069	.37561	.55087	.86737	1.49732
.95	.11191	.22260	.43925	.64624	1.02596	1.81208

R \ H	4	6	10	20	50	100
.05	.80669	.87925	.94380	.99635	1.02967	1.04107
.20	.89734	.99301	1.08354	1.16166	1.21337	1.23147
.30	.97181	1.08779	1.20276	1.30625	1.37719	1.40246
.40	1.06208	1.20471	1.35234	1.49219	1.59217	1.62860
.50	1.17464	1.35253	1.54615	1.74038	1.88674	1.94170
.60	1.32058	1.54750	1.80863	2.08901	2.31524	2.40386
.70	1.52124	1.82072	2.18801	2.61669	2.99633	3.15489
.80	1.82569	2.24439	2.79856	3.51889	4.24958	4.58937
.90	2.39482	3.05724	4.02632	5.49479	7.35852	8.43256
.95	3.00983	3.95438	5.43867	7.96304	11.84370	14.62470

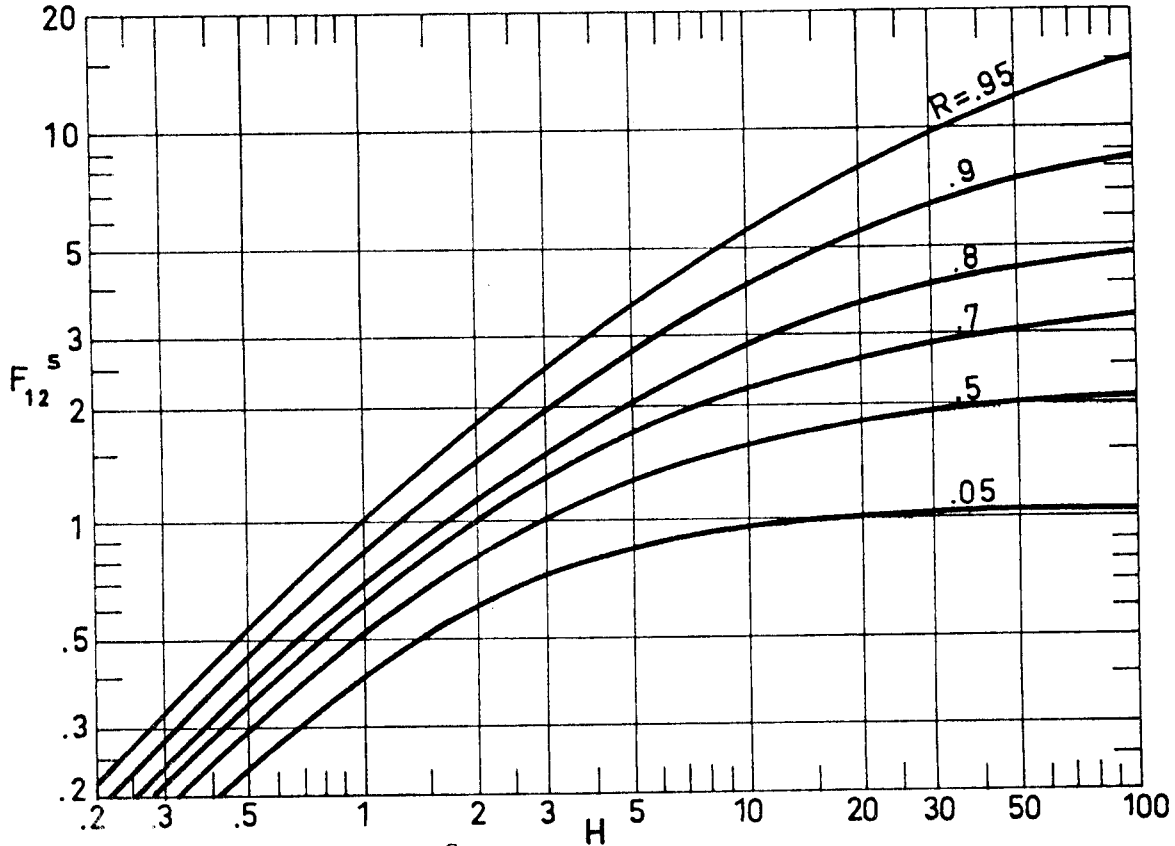


Fig 2-1. Values of F_{12}^s as a function of R and H. Calculated by the compiler.

SPECULAR SURFACES
Two Planar Specular Surfaces

R \ H	.1	.2	.4	.6	1	2
.00	.02499	.04988	.09902	.14677	.23607	.41421
.10	.02633	.05255	.10437	.15477	.24927	.43958
.20	.02788	.05566	.11057	.16404	.26459	.46909
.30	.02971	.05932	.11787	.17497	.28267	.50404
.40	.03191	.06372	.12667	.18814	.30447	.54632
.50	.03464	.06918	.13757	.20447	.33151	.59897
.60	.03817	.07622	.15164	.22553	.36644	.66724
.70	.04298	.08586	.17090	.25438	.41432	.76123
.85	.05583	.11146	.22206	.33105	.54174	1.01288
.95	.07925	.15768	.31424	.46921	.77165	1.46999

R \ H	4	6	10	20	50	100
.00	.61803	.72076	.81980	.90499	.96080	.98020
.10	.66274	.77878	.89370	.99515	1.06293	1.08672
.20	.71525	.84757	.98251	1.10534	1.18937	1.21922
.30	.77802	.93062	1.09140	1.24308	1.34996	1.38851
.40	.85475	1.03325	1.22833	1.42029	1.56071	1.61241
.50	.95139	1.16405	1.40626	1.65700	1.84951	1.92239
.60	1.07818	1.33792	1.64815	1.98985	2.26966	2.37998
.70	1.25502	1.58403	1.99968	2.49446	2.93762	3.12359
.85	1.73786	2.27142	3.02477	4.08585	5.27772	5.88321
.95	2.63412	3.58166	5.08668	7.66349	11.63700	14.48770

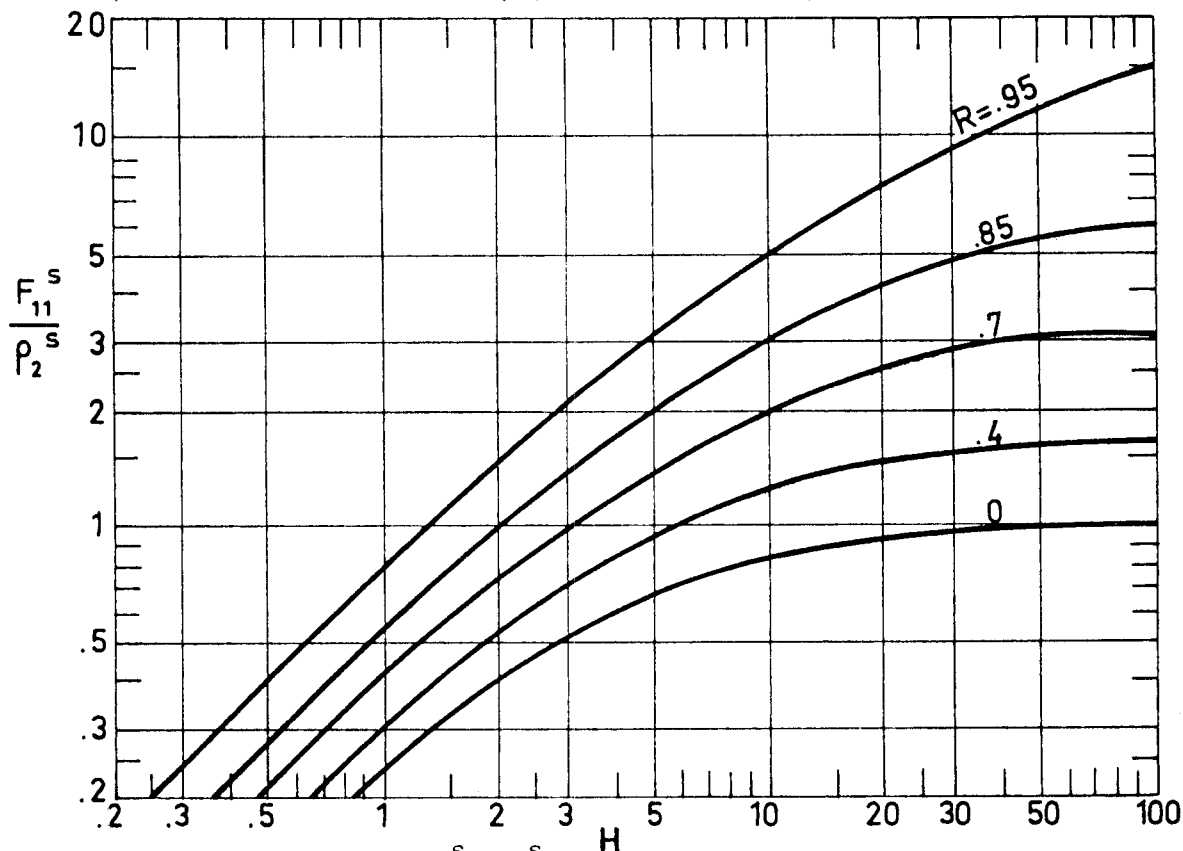


Fig 2-2. Values of F_{11}^s / ρ_2^s as a function of R and H. Calculated by the compiler.

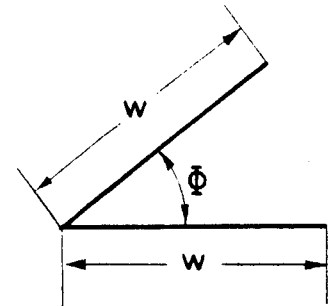
INTENTIONALLY BLANK PAGE

SPECULAR SURFACES

Two Planar Specular Surfaces

2.2.1.2. STRIPS OF EQUAL WIDTH AT ANY ANGLE

Two infinitely long plates of equal finite width w , having one common edge, and at an included angle ϕ to each other.



$$R = \rho_1^s \rho_2^s$$

Formulae:

$$F_{12}^s = F_{21}^s = K(1) + \sum_{n=1}^{n < \frac{1}{2} \left(\frac{180}{\phi} - 1 \right)} R^n K(2n+1)$$

$$\frac{F_{11}^s}{\rho_2^s} = \frac{F_{22}^s}{\rho_1^s} = K(2) + \sum_{n=1}^{n < \left(\frac{180}{\phi} - 1 \right)} R^n K(2n+2)$$

where:

$$K(m) = 1 - \sin \frac{m\phi}{2} .$$

n is the number of specular reflections which a ray suffers before reaching the receiving surface.

Comments:

When $\phi \geq 60^\circ$, the rays reaching the second surface did not suffer any specular reflection by the first.

$$F_{12}^s = F_{21}^s = K(1) .$$

When $\phi \geq 45^\circ$, the rays reaching the first surface did not suffer more than one specular reflection by the second.

$$\frac{F_{11}^s}{\rho_2^s} = \frac{F_{22}^s}{\rho_2^s} = K(2) .$$

Reference: These expressions have been obtained by the compiler.

SPECULAR SURFACES
Two Planar Specular Surfaces

R \ ϕ°	5	10	20	30	40	50
.10	1.05193	.99319	.87875	.77081	.67138	.58079
.20	1.16841	1.08812	.93619	.80112	.68477	.58420
.30	1.31338	1.20156	.99904	.83212	.69817	.58760
.40	1.49846	1.33878	1.06764	.86379	.71157	.59101
.50	1.74221	1.50679	1.14238	.89615	.72497	.59442
.60	2.07590	1.71493	1.22360	.92918	.73836	.57783
.70	2.55515	1.97562	1.31168	.96290	.75176	.60123
.80	3.28446	2.30522	1.40696	.99730	.76516	.60464
.90	4.47036	2.72513	1.50982	1.03238	.77856	.60805
1.00	6.53721	3.26314	1.62061	1.06815	.79195	.61146

ϕ°	60	65	70	75	80	85	90
any R	.50000	.46270	.42642	.39124	.35721	.32841	.29289

Notice that, when $\phi \geq 60^\circ$, F_{12}^S is independent of R.

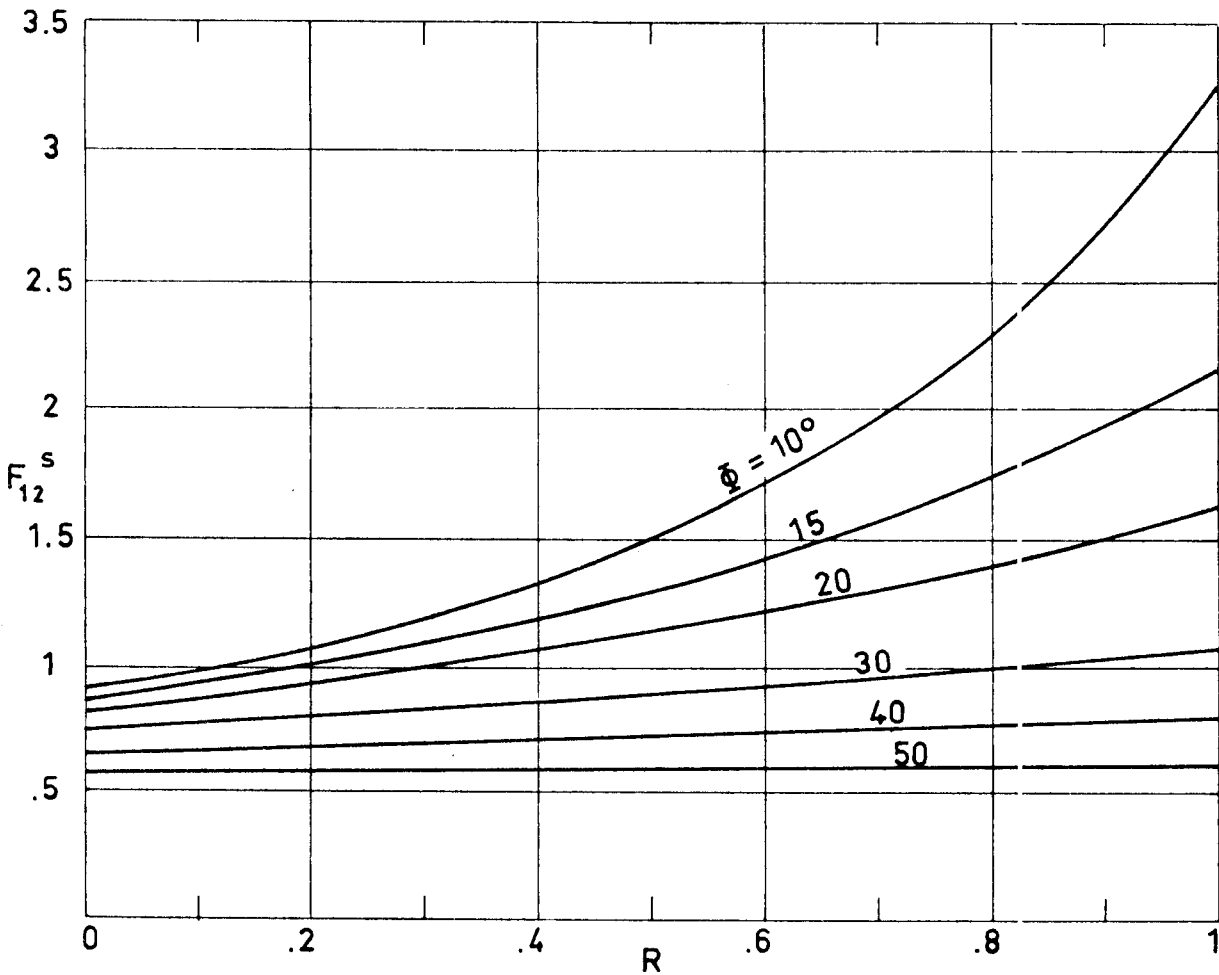


Fig 2-3. Values of F_{12}^S as a function of R for different values of ϕ . Calculated by the compiler.

SPECULAR SURFACES
Two Planar Specular Surfaces

R \ ϕ°	5	10	15	20	30	40	
.00	.91284	.82635	.74118	.65798	.5	.35721	
.10	1.00361	.89753	.79425	.69506	.51340	.35873	
.20	1.11414	.98123	.85402	.73490	.52679	.36025	
.30	1.25153	1.08066	.92143	.77761	.54019	.36177	
.45	1.53329	1.26887	1.03910	.84724	.56029	.36405	
.55	1.80054	1.42897	1.13019	.89750	.57369	.36557	
.70	2.41869	1.74150	1.28883	.97889	.59378	.36785	
.80	3.09556	2.01435	1.41118	1.03727	.60718	.36937	
.90	4.18336	2.35587	1.54845	1.09907	.62058	.37089	
1.00	6.04812	2.78497	1.70212	1.16436	.63397	.37240	
ϕ°	50	60	70	75	80	85	90
any R	.23396	.13397	.06031	.03407	.01519	.00381	0

Notice that, when $\phi \geq 45^\circ$, F_{11}^s/ρ_2^s is independent of R.

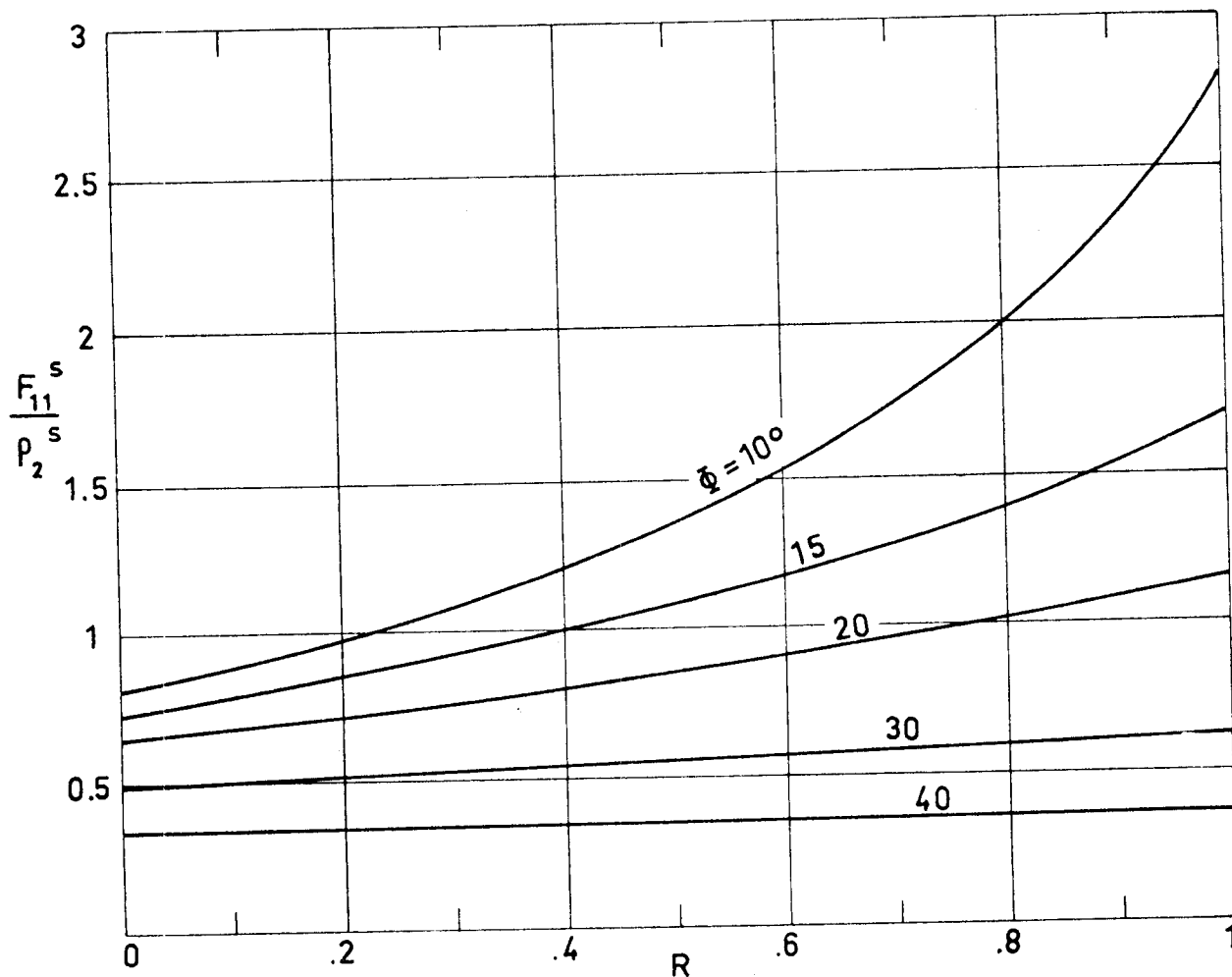


Fig 2-4. Values of F_{11}^s/ρ_2^s as a function of R for different values of ϕ . Calculated by the compiler.

INTENTIONALLY BLANK PAGE

SPECULAR SURFACES

Two Planar Specular Surfaces

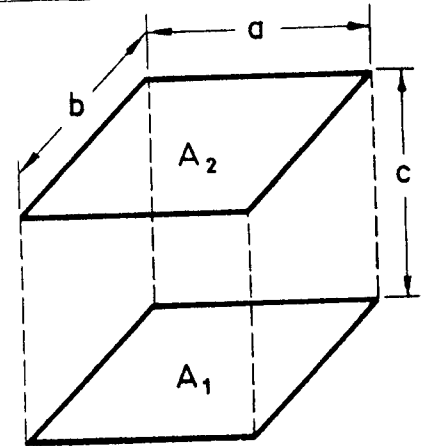
2.2.3. PARALLEL RECTANGLES OF SAME WIDTH AND LENGTH

Parallel, directly opposed rectangles of same width and length.

$$X = \frac{a}{c}$$

$$Z = \frac{b}{a}$$

$$R = \rho_1^s \rho_2^s$$



Formulae:

$$F_{12}^s = F_{21}^s = K(1) + \sum_{n=1}^{\infty} R^n K(2n+1)$$

$$\frac{F_{11}^s}{\rho_2^s} = \frac{F_{22}^s}{\rho_1^s} = K(2) + \sum_{n=1}^{\infty} R^n K(2n+2)$$

where:

$$K(m) = \frac{2}{\pi m^2 X^2 Z} \left\{ \ln \left[\frac{\{1+(mX)^2\} \{1+(mXZ)^2\}}{1+(mX)^2(1+Z^2)} \right]^{1/2} + \right.$$

$$+ mX \sqrt{1+(mXZ)^2} \tan^{-1} \left(\frac{mX}{\sqrt{1+(mXZ)^2}} \right) + mXZ \sqrt{1+(mX)^2} \tan^{-1} \left(\frac{mXZ}{\sqrt{1+(mX)^2}} \right) -$$

$$\left. - mX \tan^{-1}(mX) - mXZ \tan^{-1}(mXZ) \right\} .$$

n is the number of specular reflections which a ray suffers before reaching the receiving surface.

Reference: These expressions have been obtained by the compiler.

SPECULAR SURFACES
Two Planar Specular Surfaces

R \ X	.1	.2	.4	.6	1	2
.05	.00317	.01247	.04642	.09399	.20151	.42091
.20	.00323	.01271	.04735	.09605	.20697	.43947
.30	.00328	.01288	.04803	.09757	.21105	.45344
.40	.00332	.01307	.04879	.09925	.21555	.46904
.50	.00338	.01328	.04963	.10112	.22059	.48669
.60	.00344	.01352	.05059	.10325	.22633	.50703
.70	.00351	.01380	.05170	.10573	.23304	.53113
.80	.00359	.01414	.05305	.10874	.24121	.56088
.90	.00370	.01458	.05482	.11268	.25195	.60072
.95	.00378	.01488	.05601	.11536	.25929	.62840

R \ X	4	6	10	20	50	100
.05	.64655	.75400	.85705	.94725	1.00820	1.02996
.20	.69523	.82717	.96238	1.08924	1.18030	1.21402
.30	.73293	.88525	1.04886	1.21048	1.33198	1.37827
.40	.77605	.95317	1.15322	1.36251	1.52856	1.59398
.50	.82618	1.03408	1.28203	1.55900	1.79350	1.88988
.60	.88570	1.13280	1.44585	1.82337	2.17022	2.32100
.70	.95855	1.25747	1.66306	2.19973	2.74905	3.00780
.80	1.05205	1.42353	1.97027	2.78428	3.75561	4.27523
.90	1.18341	1.66806	2.45981	3.84963	5.97218	7.41699
.95	1.27892	1.85405	2.86239	4.85810	8.60281	11.83080

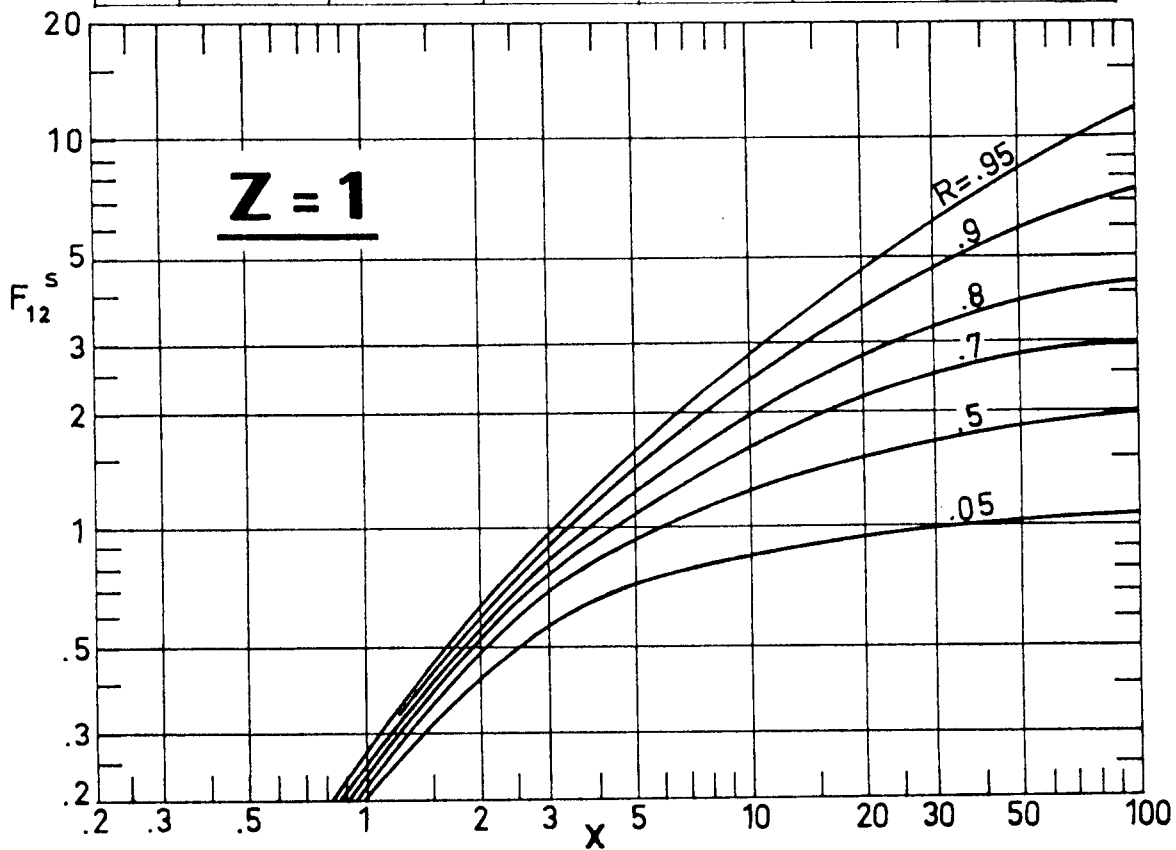


Fig 2-5. Values of F_{12}^s as a function of R and X for $Z=1$.
Calculated by the compiler.

SPECULAR SURFACES
Two Planar Specular Surfaces

R \ X	.1	.2	.4	.6	1	2
.00	.00079	.00316	.01240	.02705	.06859	.19983
.10	.00082	.00324	.01273	.02779	.07059	.20704
.20	.00084	.00333	.01310	.02860	.07280	.21504
.30	.00086	.00343	.01350	.02951	.07527	.22401
.40	.00089	.00355	.01396	.03053	.07805	.23420
.50	.00093	.00368	.01448	.03170	.08124	.24596
.60	.00096	.00383	.01509	.03306	.08496	.25983
.70	.00101	.00402	.01583	.03470	.08946	.27668
.85	.00110	.00439	.01733	.03807	.09869	.31175
.95	.00121	.00480	.01895	.04170	.10870	.35037

R \ X	4	6	10	20	50	100
.00	.41525	.54738	.69025	.82700	.92525	.96149
.10	.43642	.58153	.74300	.90235	1.01986	1.06387
.20	.46028	.62063	.80475	.99294	1.13607	1.19068
.30	.48749	.66595	.87813	1.10396	1.28224	1.35184
.40	.51895	.71929	.96694	1.24330	1.47171	1.56352
.50	.55597	.78332	1.07696	1.42359	1.72715	1.85392
.60	.60056	.86219	1.21752	1.66652	2.09049	2.27707
.70	.65610	.96299	1.40510	2.01313	2.64904	2.95130
.85	.77610	1.18978	1.85861	2.96052	4.44239	5.32104
.95	.91477	1.46616	2.46829	4.49068	8.31719	11.62380

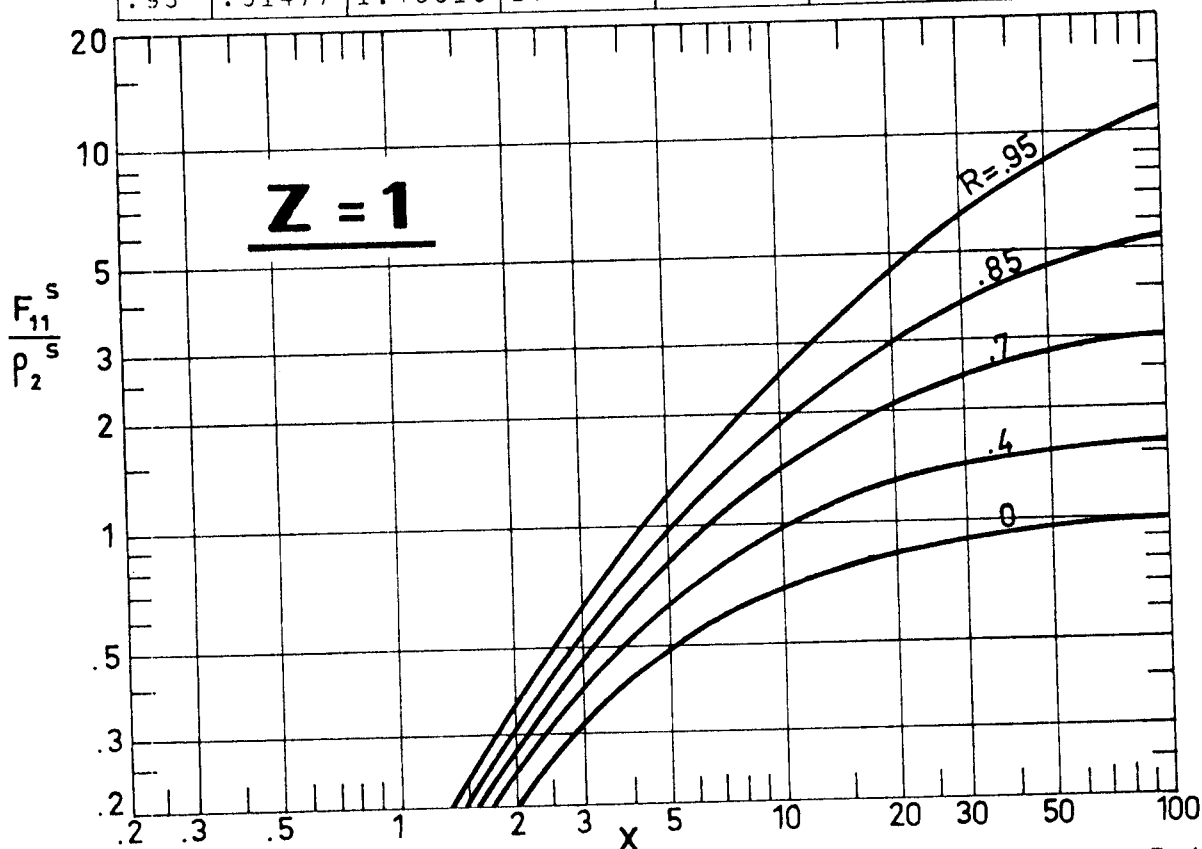


Fig 2-6. Values of F_{11}^s / ρ_2^s as a function of R and X for Z=1. Calculated by the compiler.

SPECULAR SURFACES
Two Planar Specular Surfaces

R \ X	.1	.2	.4	.6	1	2
.05	.01480	.04975	.13640	.22141	.36460	.58597
.20	.01509	.05088	.14053	.22969	.38261	.62856
.30	.01531	.05172	.14362	.23592	.39637	.66194
.40	.01555	.05264	.14704	.24288	.41192	.70056
.50	.01582	.05367	.15089	.25076	.42978	.74610
.60	.01613	.05485	.15528	.25984	.45069	.80113
.70	.01649	.05622	.16044	.27059	.47593	.87000
.80	.01692	.05789	.16673	.28388	.50779	.96101
.90	.01749	.06011	.17498	.30172	.55169	1.09429
.95	.01788	.06164	.18055	.31418	.58298	1.19552

R \ X	4	6	10	20	50	100
.05	.77309	.85346	.92617	.98642	1.02536	1.03885
.20	.85331	.95798	1.05856	1.14698	1.20673	1.22797
.30	.91813	1.04419	1.17061	1.28672	1.36809	1.39761
.40	.99535	1.14888	1.31003	1.46553	1.57932	1.62165
.50	1.08944	1.27927	1.48872	1.70268	1.86784	1.93127
.60	1.20765	1.44739	1.72711	2.03287	2.28568	2.38714
.70	1.36775	1.67511	2.06980	2.52608	2.94541	3.12508
.80	1.58063	2.00846	2.58553	3.35060	4.14566	4.52511
.90	1.92836	2.57367	3.54719	5.06595	7.04731	8.21814
.95	2.21803	3.07711	4.48968	7.00567	11.03080	13.99550

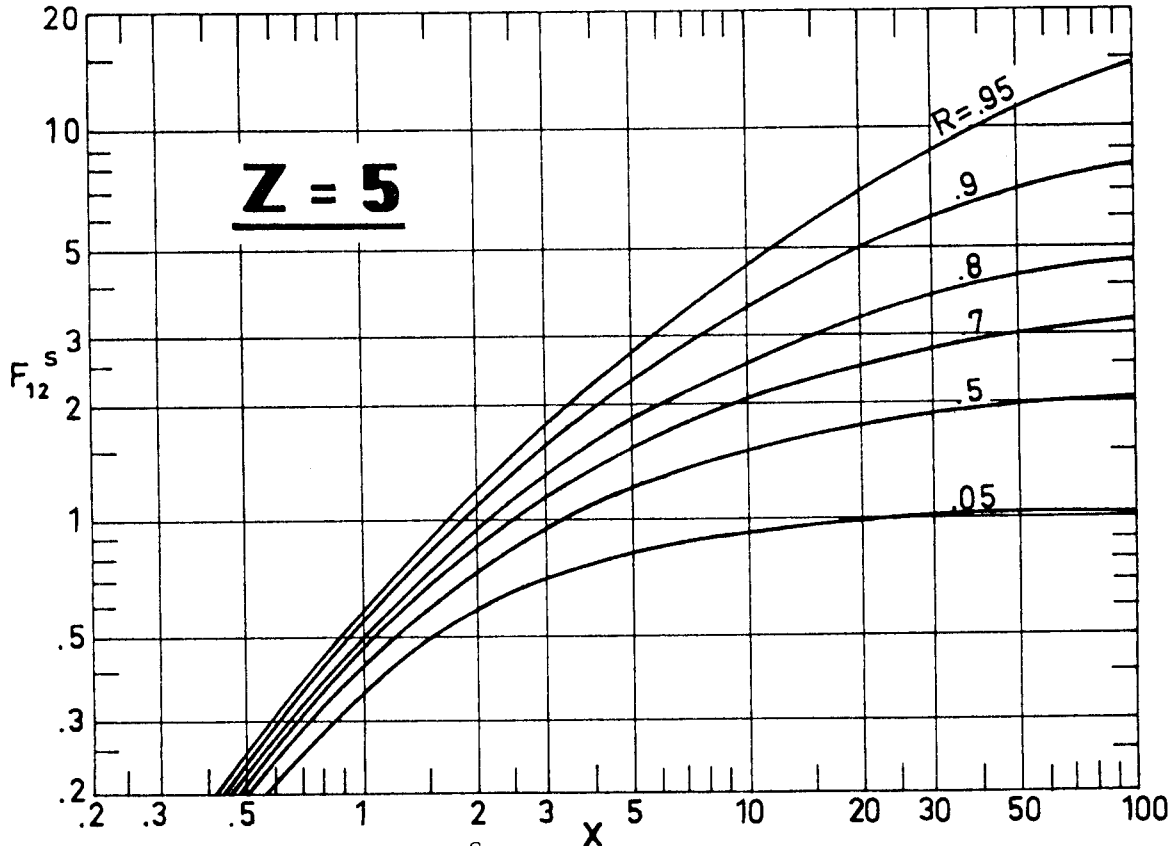


Fig 2-7. Values of F_{12}^s as a function of R and X for Z=5. Calculated by the compiler.

SPECULAR SURFACES
Two Planar Specular Surfaces

R \ X	.1	.2	.4	.6	1	2
.00	.00389	.01471	.04941	.09152	.17792	.35917
.10	.00400	.01512	.05095	.09473	.18531	.37809
.20	.00412	.01557	.05266	.09829	.19359	.39964
.30	.00425	.01607	.05457	.10228	.20296	.42449
.40	.00440	.01664	.05672	.10682	.21372	.45359
.50	.00458	.01729	.05920	.11206	.22628	.48835
.60	.00479	.01805	.06210	.11824	.24128	.53099
.70	.00503	.01898	.06562	.12576	.25979	.58532
.85	.00554	.02091	.07290	.14139	.29924	.70733
.95	.00608	.02301	.08096	.15845	.34401	.85652

R \ X	4	6	10	20	50	100
.00	.57338	.68413	.79316	.88920	.95366	.97645
.10	.61194	.73657	.86248	.97631	1.05427	1.08214
.20	.65669	.79822	.94535	1.08243	1.17864	1.21349
.30	.70941	.87190	1.04629	1.21458	1.33630	1.38115
.40	.77269	.96180	1.17215	1.38376	1.54272	1.60258
.50	.85048	1.07441	1.33391	1.60831	1.82469	1.90861
.60	.94921	1.22064	1.55049	1.92130	2.23311	2.35921
.70	1.08036	1.42043	1.85801	2.38957	2.87815	3.08867
.85	1.39793	1.93009	2.70147	3.81485	5.09800	5.76702
.95	1.83305	2.68923	4.11800	6.68380	10.80410	13.84260

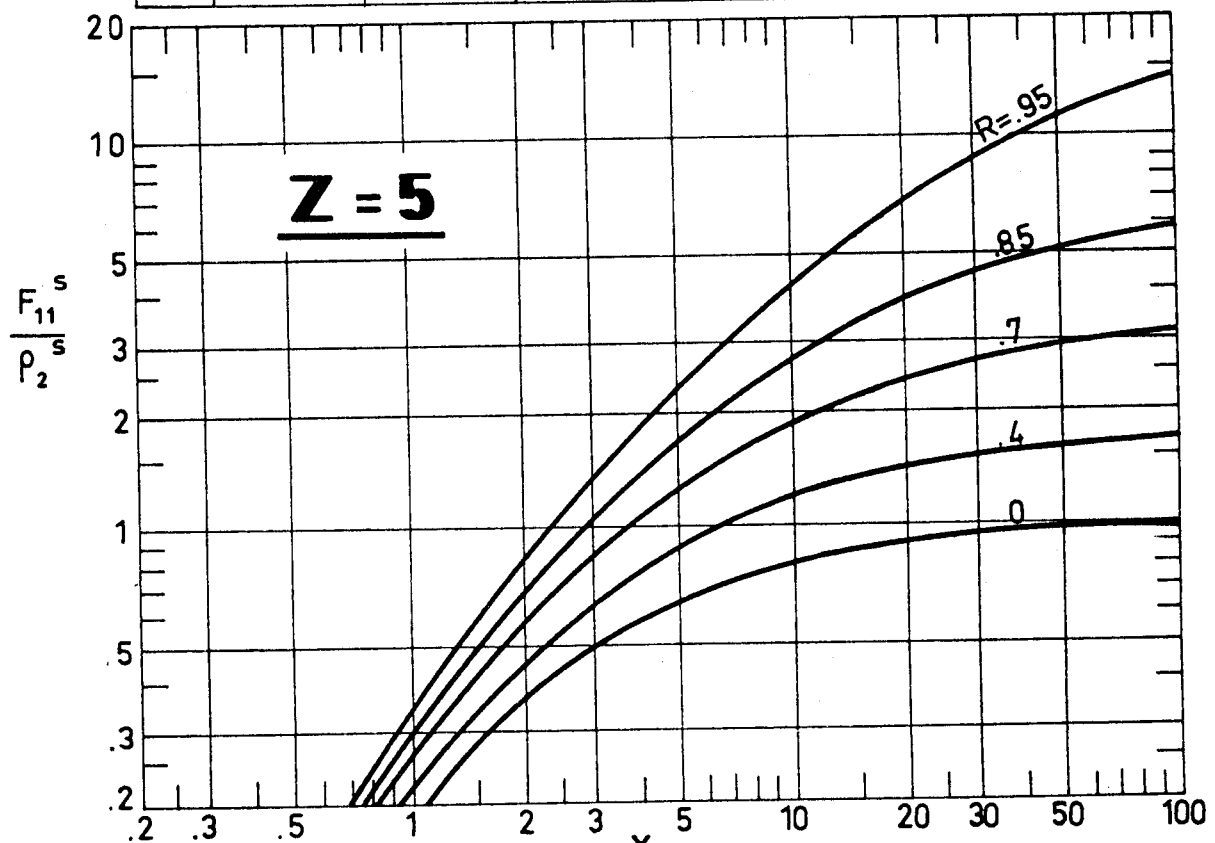


Fig 2-8. Values of F_{11}^s / ρ_2^s as a function of R and X for Z=5. Calculated by the compiler.

SPECULAR SURFACES
Two Planar Specular Surfaces

R \ X	.1	.2	.4	.6	1	2
.05	.02510	.06971	.16419	.25069	.39316	.60971
.20	.02567	.07233	.17074	.26256	.41596	.65778
.30	.02608	.07384	.17568	.27163	.43370	.69599
.40	.02654	.07551	.18121	.28189	.45412	.74086
.50	.02706	.07739	.18748	.29369	.47803	.79470
.60	.02765	.07955	.19476	.30752	.50667	.86124
.70	.02833	.08210	.20345	.32426	.54217	.94693
.80	.02916	.08522	.21429	.34552	.58857	1.06466
.90	.03025	.08936	.22905	.37514	.65577	1.24742
.95	.03099	.09221	.23948	.39658	.70648	1.39617

R \ X	4	6	10	20	50	100
.05	.78986	.86634	.93498	.99141	1.02751	1.03996
.20	.87524	.97546	1.07104	1.15432	1.21005	1.22972
.30	.94481	1.06601	1.18666	1.29648	1.37264	1.40003
.40	1.02842	1.17665	1.33113	1.47885	1.58574	1.62512
.50	1.13145	1.31562	1.51733	1.72150	1.87728	1.93648
.60	1.26295	1.49684	1.76764	2.06088	2.30045	2.39550
.70	1.43918	1.74643	2.12539	2.57123	2.97085	3.13998
.80	1.69521	2.12181	2.68997	3.43415	4.19752	4.55722
.90	2.12810	2.79207	3.77391	5.27581	7.20205	8.32512
.95	2.51631	3.43379	4.90714	7.45775	11.43070	14.30830

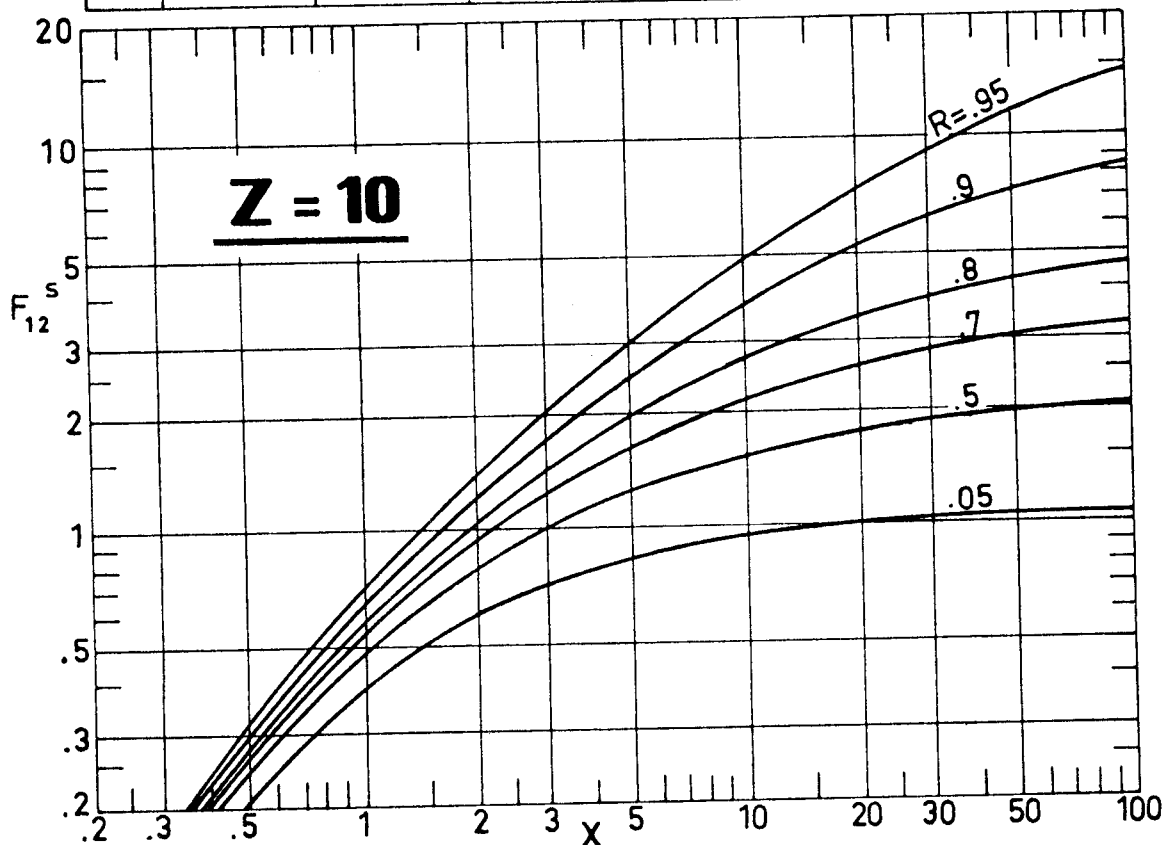


Fig 2-9. Values of F_{12}^s as a function of R and X for $Z=10$.
Calculated by the compiler.

SPECULAR SURFACES
Two Planar Specular Surfaces

R \ X	.1	.2	.4	.6	1	2
.00	.00729	.02493	.06971	.11650	.20586	.38638
.10	.00749	.02569	.07233	.12143	.21576	.40839
.20	.00772	.02654	.07524	.12696	.22699	.43371
.30	.00797	.02748	.07852	.13323	.23990	.46327
.40	.00825	.02856	.08224	.14043	.25496	.49840
.50	.00857	.02979	.08656	.14886	.27287	.54114
.60	.00895	.03123	.09168	.15895	.29471	.59477
.70	.00941	.03298	.09795	.17144	.32235	.66510
.85	.01034	.03660	.11116	.19829	.38383	.83168
.95	.01135	.04055	.12596	.22924	.45841	1.05385

R \ X	4	6	10	20	50	100
.00	.59563	.70241	.80647	.89709	.95723	.97833
.10	.63722	.75762	.87807	.98573	1.05860	1.08443
.20	.68579	.82281	.96390	1.09388	1.18400	1.21636
.30	.74343	.90113	1.06880	1.22882	1.34313	1.38483
.40	.81325	.99731	1.20016	1.40200	1.55171	1.60749
.50	.90011	1.11884	1.36994	1.63262	1.83709	1.91550
.60	1.01213	1.27850	1.59903	1.95549	2.25137	2.36959
.70	1.16433	1.50045	1.92812	2.44182	2.90786	3.10612
.85	1.55153	2.09049	2.85813	3.94880	5.18758	5.82505
.95	2.13409	3.05160	4.54397	7.14637	11.21380	14.16330

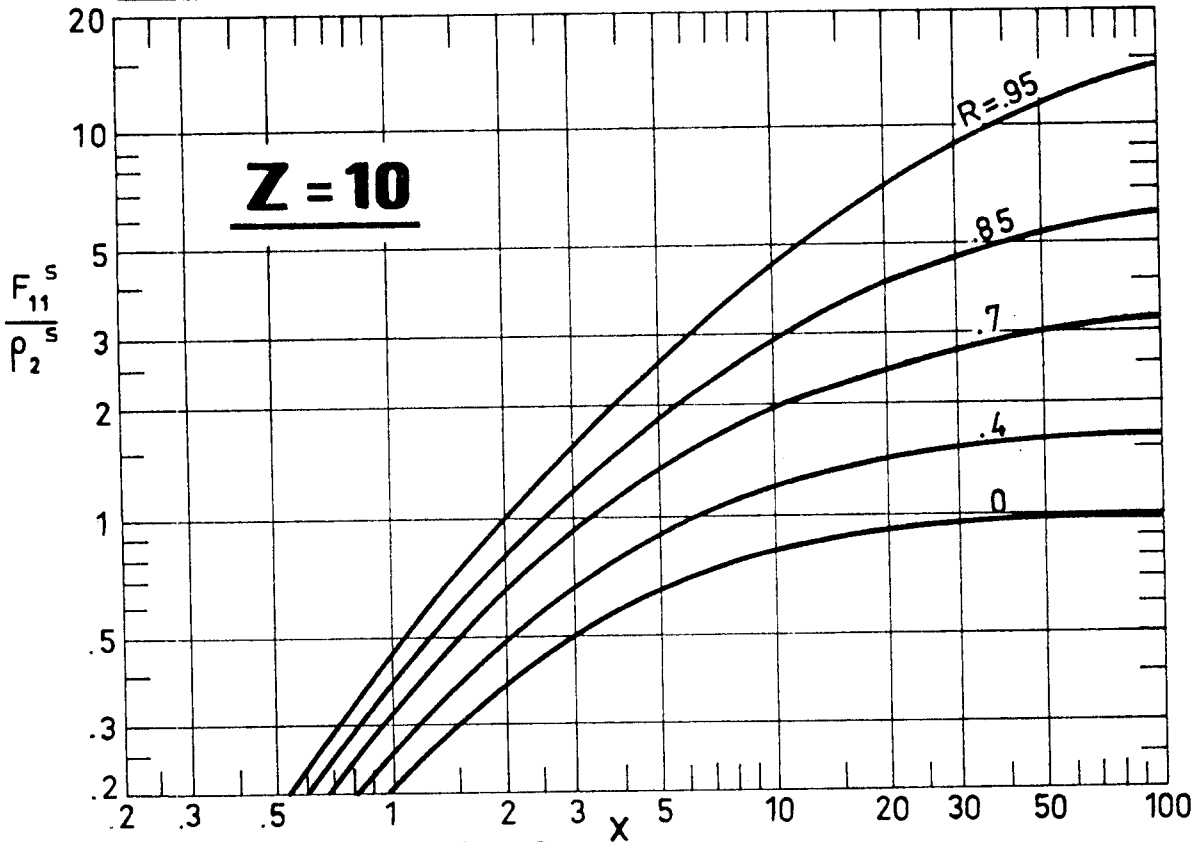


Fig 2-10. Values of F_{11}^S / ρ_2^S as a function of R and X for Z=10. Calculated by the compiler.

SPECULAR SURFACES
Two Planar Specular Surfaces

R \ X	.1	.2	.4	.6	1	2
.05	.03144	.07940	.17447	.26101	.40291	.61768
.20	.03225	.08180	.18218	.27448	.42758	.66769
.30	.03285	.08364	.18794	.28479	.44695	.70764
.40	.03352	.08571	.19436	.29644	.46937	.75480
.50	.03426	.08809	.20168	.30983	.49573	.81179
.60	.03512	.09086	.21023	.32558	.52746	.88281
.70	.03611	.09420	.22059	.34479	.56696	.97515
.80	.03733	.09837	.23384	.36963	.61909	1.10327
.90	.03893	.10405	.25254	.40547	.69660	1.30519
.95	.04002	.10805	.26626	.43258	.75772	1.47473

R \ X	4	6	10	20	50	100
.05	.79546	.87064	.93792	.99306	1.02823	1.04033
.20	.88260	.98130	1.07520	1.15676	1.21116	1.23030
.30	.95379	1.07332	1.19203	1.29974	1.37415	1.40084
.40	1.03960	1.18599	1.33819	1.48329	1.58788	1.62628
.50	1.14577	1.32789	1.52692	1.72779	1.88043	1.93822
.60	1.28195	1.51365	1.78127	2.07025	2.30538	2.39828
.70	1.46607	1.77098	2.14618	2.58636	2.97934	3.14495
.80	1.73679	2.16187	2.72587	3.46232	4.21486	4.56793
.90	2.20264	2.87279	3.85539	5.34815	7.25410	8.36090
.95	2.62890	3.56738	5.06246	7.62055	11.56740	14.41350

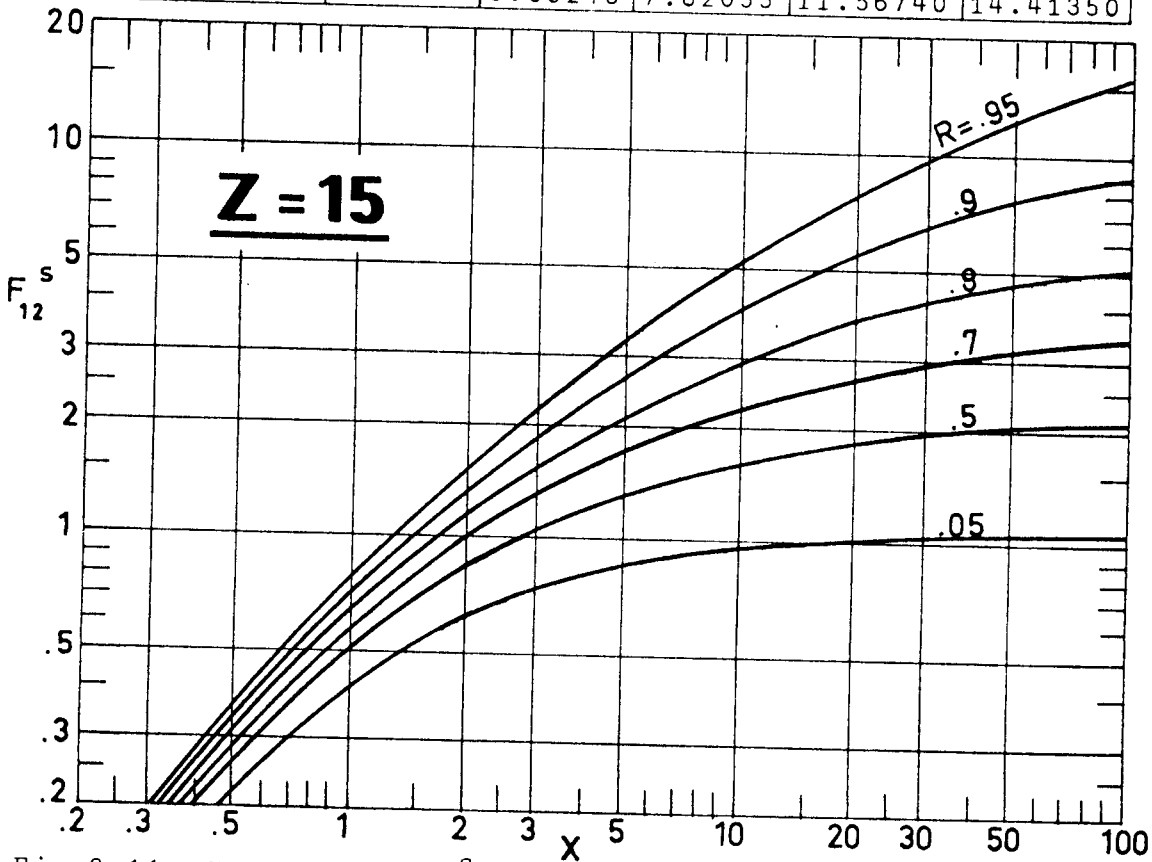


Fig 2-11. Values of F_{12}^s as a function of R and X for $Z=15$. Calculated by the compiler.

SPECULAR SURFACES
Two Planar Specular Surfaces

R \ X	.1	.2	.4	.6	1	2
.00	.00969	.03119	.07868	.12620	.21578	.39562
.10	.00999	.03221	.08195	.13199	.22671	.41873
.20	.01032	.03335	.08557	.13853	.23920	.44542
.30	.01068	.03463	.08964	.14596	.25366	.47672
.40	.01110	.03610	.09428	.15452	.27063	.51414
.50	.01157	.03779	.09968	.16456	.29095	.56000
.60	.01213	.03980	.10614	.17465	.31587	.61807
.70	.01280	.04225	.11416	.19177	.34763	.69499
.85	.01418	.04739	.13150	.22514	.41960	.88001
.95	.01568	.05310	.15170	.26551	.51132	1.13554
R \ X	4	6	10	20	50	100
.00	.60309	.70852	.81091	.89972	.95842	.97895
.10	.64571	.76467	.88328	.98887	1.06005	1.08519
.20	.69559	.83105	.97010	1.09769	1.18579	1.21731
.30	.75492	.91094	1.07633	1.23357	1.34541	1.38606
.40	.82702	1.00926	1.20954	1.40810	1.55471	1.60913
.50	.91709	1.13386	1.38203	1.64074	1.84123	1.91780
.60	1.03392	1.29820	1.61537	1.96693	2.25746	2.37305
.70	1.19401	1.52806	1.95188	2.45934	2.91777	3.11194
.85	1.60872	2.14859	2.91290	3.99428	5.21759	5.84443
.95	2.25046	3.18902	4.70312	7.31301	11.35400	14.27120

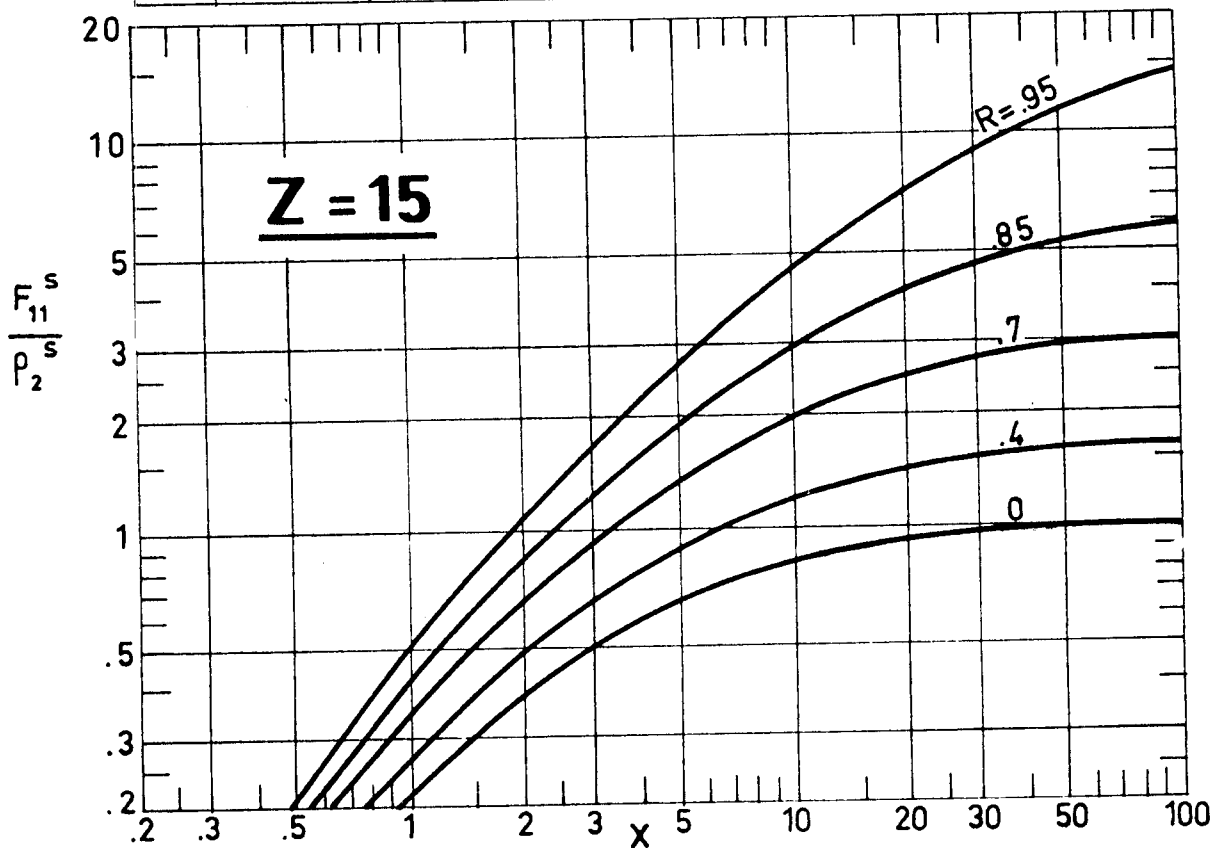


Fig 2-12. Values of F_{11}^s / ρ_2^s as a function of R and X for Z=15. Calculated by the compiler.

SPECULAR SURFACES
Two Planar Specular Surfaces

R \ X	.1	.2	.4	.6	1	2
.05	.03545	.08412	.17973	.26623	.40781	.62167
.20	.03646	.08619	.18774	.28047	.43346	.67266
.30	.03721	.08785	.19345	.29118	.45364	.71350
.40	.03805	.08980	.19966	.30304	.47694	.76184
.50	.03899	.09213	.20661	.31633	.50415	.82044
.60	.04007	.09496	.21472	.33163	.53639	.89362
.70	.04135	.09850	.22468	.35004	.57562	.98856
.80	.04291	.10312	.23784	.37397	.62623	1.11839
.90	.04498	.10970	.25745	.40989	.70155	1.31683
.95	.04641	.11451	.27272	.43876	.76355	1.48236

R \ X	4	6	10	20	50	100
.05	.79827	.87279	.93939	.99388	1.02859	1.04052
.20	.88628	.98423	1.07729	1.15799	1.21171	1.23059
.30	.95829	1.07698	1.19471	1.30137	1.37491	1.40125
.40	1.04521	1.19066	1.34173	1.48552	1.58895	1.62686
.50	1.15297	1.33404	1.53172	1.73094	1.88201	1.93909
.60	1.29156	1.52209	1.78810	2.07494	2.30784	2.39968
.70	1.47967	1.78336	2.15661	2.59394	2.98359	3.14743
.80	1.75734	2.18214	2.74397	3.47644	4.22353	4.57329
.90	2.23051	2.90966	3.89628	5.38463	7.28017	8.37881
.95	2.65013	3.60608	5.12739	7.70208	11.63620	14.46620

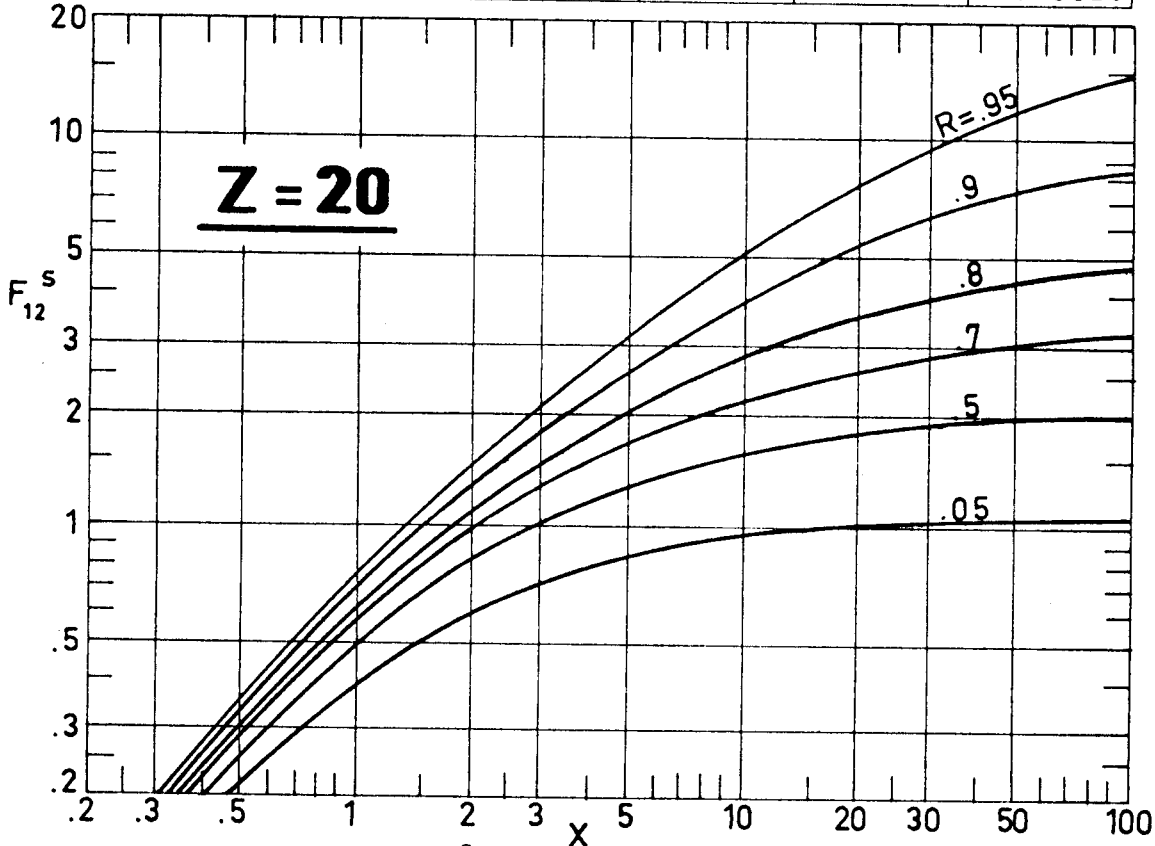


Fig 2-13. Values of F_{12}^s as a function of R and X for $Z=20$. Calculated by the compiler.

SPECULAR SURFACES
Two Planar Specular Surfaces

R \ X	.1	.2	.4	.6	1	2
.00	.01060	.03515	.08353	.13123	.22081	.40026
.10	.01098	.03627	.08717	.13752	.23229	.42392
.20	.01140	.03754	.09112	.14459	.24545	.45131
.30	.01188	.03899	.09548	.15255	.26072	.48351
.40	.01241	.04067	.10040	.16160	.27864	.52212
.50	.01303	.04264	.10611	.17208	.29997	.56959
.60	.01375	.04502	.11296	.18455	.32583	.62987
.70	.01463	.04797	.12158	.20012	.35827	.70958
.85	.01644	.05429	.14086	.23513	.43084	.89758
.95	.01841	.06151	.16457	.28006	.52672	1.15204

R \ X	4	6	10	20	50	100
.00	.60682	.71158	.81314	.90104	.95901	.97926
.10	.64997	.76820	.88588	.99044	1.06077	1.08558
.20	.70050	.83518	.97320	1.09961	1.18669	1.21779
.30	.76069	.91586	1.08010	1.23595	1.34655	1.38667
.40	.83394	1.01525	1.21424	1.41114	1.55621	1.60995
.50	.92563	1.41139	1.38808	1.64480	1.84330	1.91895
.60	1.04492	1.30810	1.62356	1.97266	2.26051	2.37478
.70	1.20905	1.54198	1.96380	2.46812	2.92273	3.11485
.85	1.63564	2.17769	2.94060	4.01711	5.23261	5.85412
.95	2.27784	3.23205	4.77077	7.39656	11.42450	14.32530

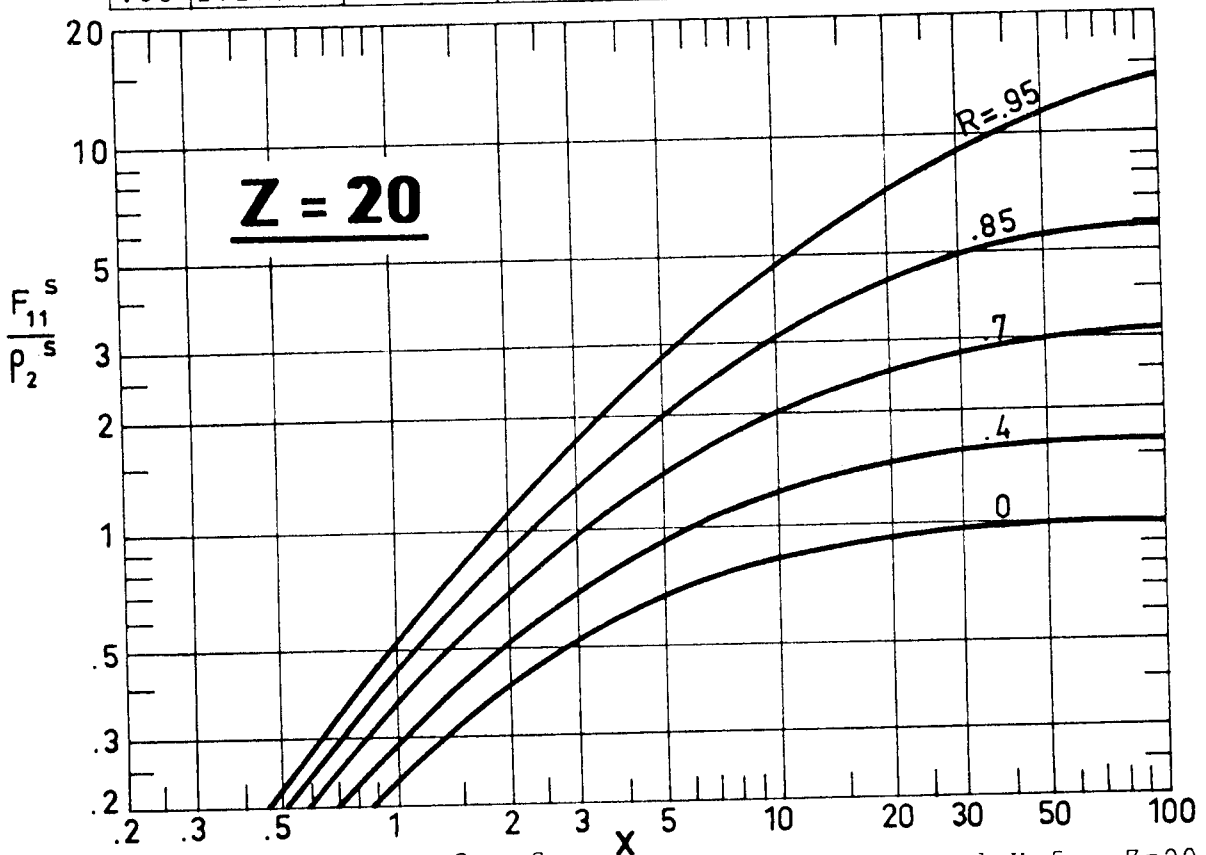


Fig 2-14. Values of F_{11}^s / ρ_2^s as a function of R and X for Z=20. Calculated by the compiler.

INTENTIONALLY BLANK PAGE

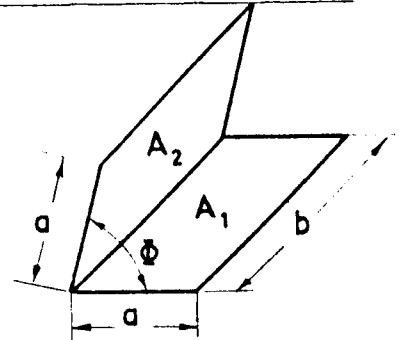
SPECULAR SURFACES
Two Planar Specular Surfaces

2.2.4. RECTANGLES OF SAME WIDTH AND LENGTH WITH ONE COMMON EDGE

Two specular finite rectangles of the same dimensions having a common edge and at an included angle ϕ .

$$L = \frac{a}{b}$$

$$R = \rho_1^s \rho_2^s$$



Formulae:

$$F_{12}^s = F_{21}^s = K(1) + \sum_{n=1}^{n < \frac{1}{2} \left(\frac{180}{\phi} - 1 \right)} R^n K(2n+1)$$

$$\frac{F_{11}^s}{\rho_2^s} = \frac{F_{22}^s}{\rho_1^s} = K(2) + \sum_{n=1}^{n < \left(\frac{180}{\phi} - 1 \right)} R^n K(2n+2)$$

In these expressions $K(m)$ is the diffuse view factor between two rectangles having the same width and length of that considered and at an included angle $m\phi$. The value of this diffuse view factor has been obtained by using the results by Feingold (1966) See § 1.3.2.3.

n is the number of specular reflections which a ray suffers before reaching the receiving surface.

Comments:

When $\phi \geq 60^\circ$, the rays reaching the second surface did not suffer any specular reflection by the first.

$$F_{12}^s = F_{21}^s = K(1) \quad .$$

When $\phi \geq 45^\circ$, the rays reaching the first surface did not suffer more than one specular reflection by the second.

$$\frac{F_{11}^s}{\rho_2^s} = \frac{F_{22}^s}{\rho_1^s} = K(2) \quad .$$

Reference: These expressions have been obtained by the compiler.

SPECULAR SURFACES
Two Planar Specular Surfaces

R \ L	.1	.2	.4	.6	1
.1	.75690	.74304	.71570	.68913	.63925
.2	.78606	.77107	.74157	.71304	.65989
.3	.81587	.79972	.76800	.73746	.68096
.4	.84633	.82898	.79498	.76238	.70246
.5	.87744	.85886	.82253	.78781	.72439
.6	.90920	.88936	.85063	.81374	.74674
.7	.94161	.92048	.87929	.84019	.76952
.8	.97466	.95221	.90851	.86714	.79272
.9	1.00837	.98456	.93829	.89459	.81636
1.0	1.04272	1.01753	.96862	.92256	.84042
R \ L	2	4	6	10	20
.1	.53639	.40478	.32767	.24152	.15165
.2	.55178	.41522	.33573	.24718	.15505
.3	.56749	.42587	.34394	.25296	.15851
.4	.58349	.43672	.35231	.25884	.16204
.5	.59981	.44777	.36083	.26483	.16563
.6	.61644	.45903	.36951	.27093	.16929
.7	.63337	.47050	.37835	.27714	.17301
.8	.65061	.48217	.38734	.28346	.17680
.9	.66816	.49404	.39649	.28989	.18065
1.0	.68602	.50612	.40580	.29642	.18457

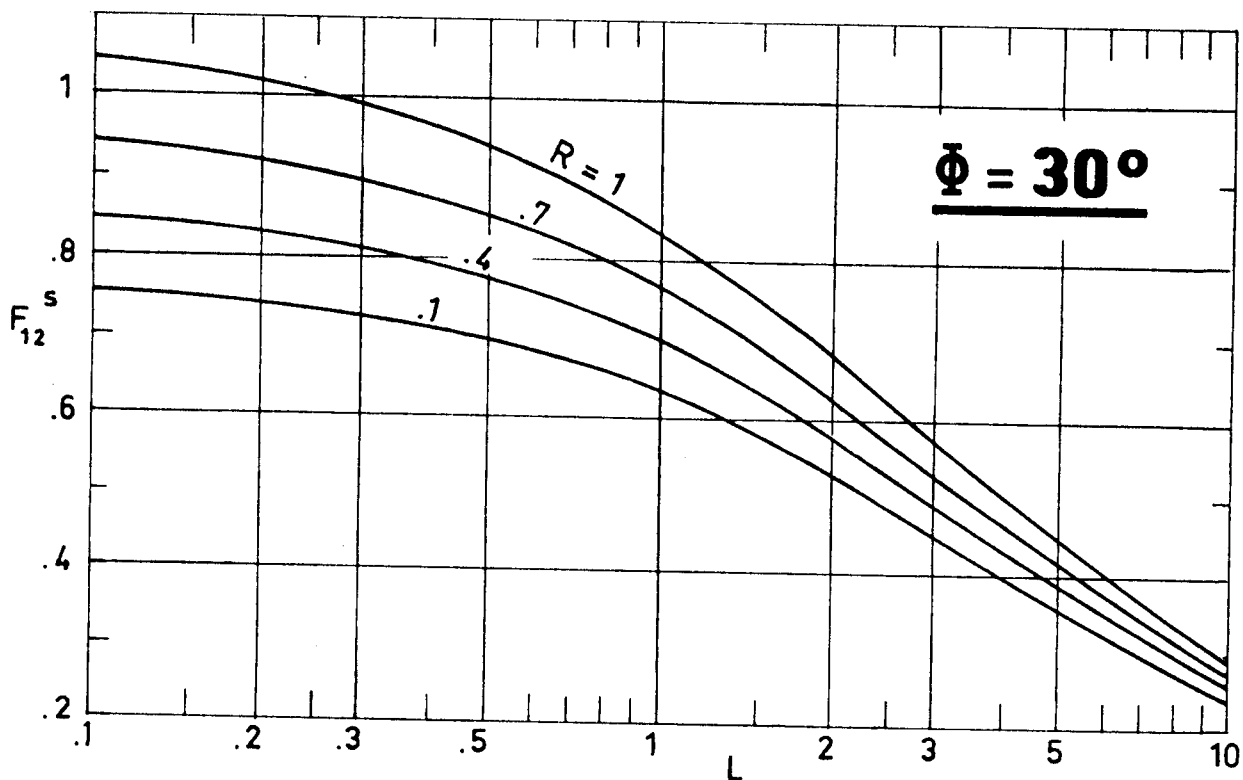


Fig 2-15. Values of F_{12}^s vs. aspect ratio, L , for different values of R . $\phi=30^\circ$. Calculated by the compiler.

SPECULAR SURFACES
Two Planar Specular Surfaces

R \ L	.1	.2	.4	.6	1
.00	.48559	.47129	.44348	.41725	.37091
.10	.49840	.48352	.45463	.42744	.37957
.20	.51121	.49576	.46578	.43764	.38823
.30	.52402	.50799	.47693	.44783	.39689
.45	.54323	.52634	.49366	.46312	.40988
.55	.55604	.53857	.50481	.47332	.41854
.70	.57525	.55692	.52153	.48861	.43154
.80	.58806	.56916	.53268	.49880	.44020
.90	.60087	.58139	.54384	.50900	.44806
1.00	.61368	.59363	.55499	.51919	.45752

R \ L	2	4	6	10	20
.00	.28827	.20204	.15805	.11266	.06849
.10	.29460	.20626	.16129	.11493	.06984
.20	.30092	.21049	.16453	.11719	.07119
.30	.30725	.21471	.16777	.11945	.07254
.45	.31674	.22105	.17262	.12285	.07456
.55	.32306	.22528	.17586	.12511	.07591
.70	.33255	.23162	.18072	.12851	.07794
.80	.33887	.23584	.18396	.13077	.07929
.90	.34520	.24007	.18720	.13304	.08064
1.00	.35152	.24430	.19044	.13530	.08199

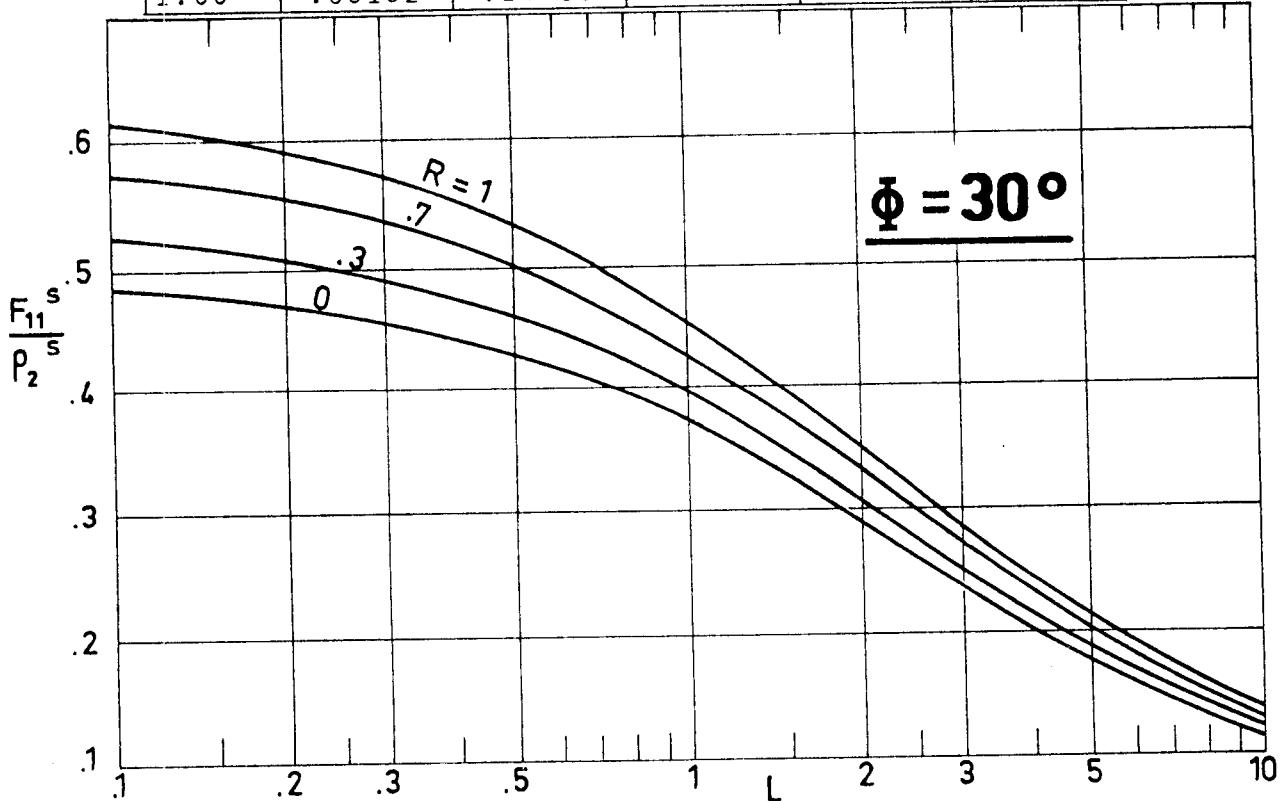


Fig 2-16. Values of F_{11}^s / ρ_2^s vs. aspect ratio, L, for different values of R. $\phi = 30^\circ$. Calculated by the compiler.

SPECULAR SURFACES
Two Planar Specular Surfaces

R \ L	.1	.2	.4	.6	1
.1	.61010	.59535	.56644	.53872	.48810
.2	.61736	.60227	.57271	.54444	.49301
.3	.62462	.60919	.57899	.55016	.49784
.4	.63188	.61610	.58527	.55588	.50267
.5	.63914	.62302	.59155	.56159	.50750
.6	.64640	.62994	.59782	.56713	.51233
.7	.65366	.63686	.60410	.57303	.51716
.8	.66093	.64378	.61038	.57874	.52200
.9	.66819	.65069	.61666	.58446	.52683
1.0	.67545	.65761	.62293	.59018	.53166
R \ L	2	4	6	10	20
.1	.39173	.28235	.23365	.16136	.09925
.2	.39523	.28468	.22543	.16260	.09999
.3	.39874	.28701	.22721	.16385	.10073
.4	.40224	.28935	.22900	.16509	.10147
.5	.40575	.29168	.23078	.16633	.10221
.6	.40925	.29401	.23256	.16758	.10295
.7	.41275	.29634	.23434	.16882	.10369
.8	.41626	.29867	.23613	.17006	.10443
.9	.41976	.30100	.23791	.17131	.10517
1.0	.42327	.30333	.23969	.17255	.10591

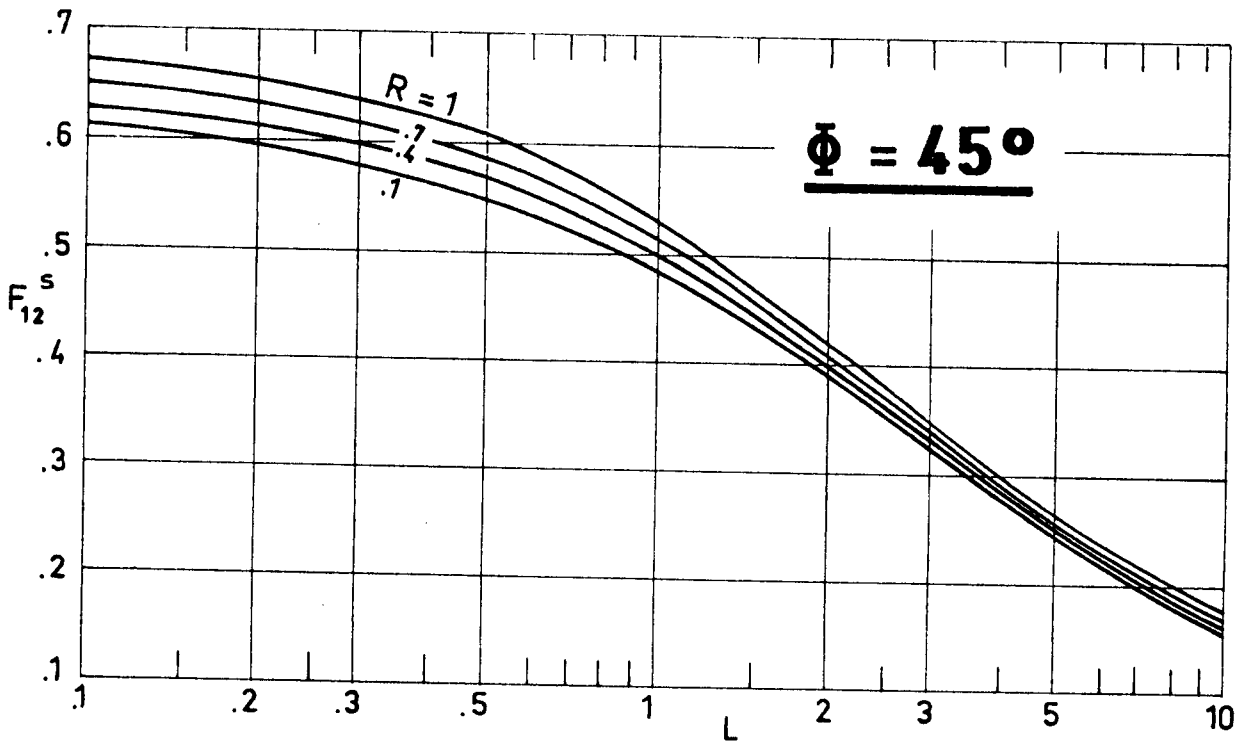


Fig 2-17. Values of F_{12}^s vs. aspect ratio, L, for different values of R. $\phi=45^\circ$. Calculated by the compiler.

SPECULAR SURFACES
Two Planar Specular Surfaces

L	F_{11}^s / ρ_2^s for $\phi = 45^\circ$	F_{12}^s for $\phi = 60^\circ$	F_{11}^s / ρ_2^s for $\phi = 60^\circ$
.1	.28189	.48559	.12810
.2	.27104	.47129	.12234
.4	.25032	.44348	.11151
.6	.23147	.41725	.10194
1.0	.20004	.37091	.08662
2.0	.14930	.28827	.06325
4.0	.10136	.20204	.04226
6.0	.07822	.15805	.03239
10.0	.05502	.11266	.02264
20.0	.03302	.06849	.01350

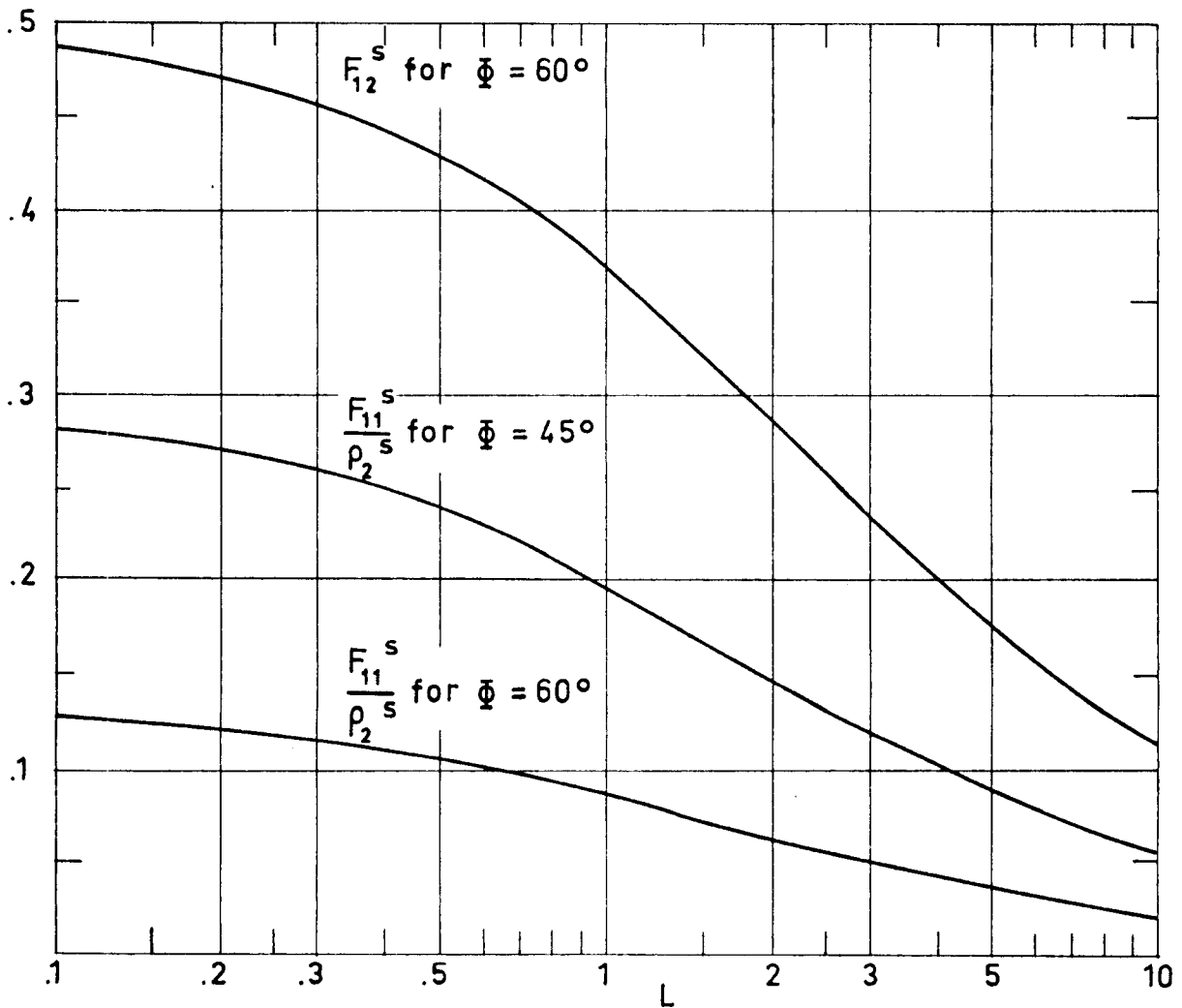


Fig 2-18. Values of F_{12}^s and F_{11}^s / ρ_2^s vs. aspect ratio, L, for the limiting values of ϕ . Calculated by the compiler.

INTENTIONALLY BLANK PAGE

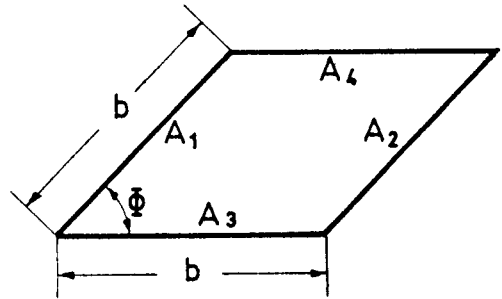
SPECULAR SURFACES

Planar Specular and Planar Diffuse Surfaces

2.3. PLANAR SPECULAR AND PLANAR DIFFUSE SURFACES

2.3.1. TWO DIMENSIONAL CAVITIES. CYLINDERS OF QUADRANGULAR CROSS SECTION

Specular view factors between the different inner surfaces of a cylinder of quadrangular cross section formed by two specular and two diffuse parallel strips.



The surfaces A_1 and A_2 are specular-reflecting while A_3 and A_4 are diffuse reflecting.

$$\rho_1^s = \rho_2^s = \rho^s$$

Formulae:

$$F_{11}^s = F_{22}^s = \sum_{n=0}^{n=K-1} (\rho^s)^{2n+1} \left[\sqrt{(2n+2)^2 \sin^2 \Phi + 1} - (2n+1) \sin \Phi - 1 \right] + \sum_{n=K}^{\infty} (\rho^s)^{2n+1} \left[\sqrt{(1 - \cos \Phi)^2 + (2n+1)^2 \sin^2 \Phi} - (2n+1) \sin \Phi \right]$$

$$F_{12}^s = F_{21}^s = \sum_{n=0}^{n=K} (\rho^s)^{2n} \left[\frac{\sqrt{(1 + \cos \Phi)^2 + (2n+1)^2 \sin^2 \Phi} + \sqrt{(1 - \cos \Phi)^2 + (2n+1)^2 \sin^2 \Phi}}{2} - 1 - 2n \sin \Phi \right] + \sum_{n=K+1}^{\infty} (\rho^s)^{2n} \left[\frac{\sqrt{(2n+1) \sin^2 \Phi + (1 - \cos \Phi)^2} + \sqrt{(2n-1)^2 \sin^2 \Phi + (1 - \cos \Phi)^2}}{2} - 2n \sin \Phi \right]$$

SPECULAR SURFACES

Planar Specular and Planar Diffuse Surfaces

$$\begin{aligned}
 F_{31}^S = F_{13}^S = F_{42}^S = F_{24}^S = & \left[1 - \frac{\sqrt{\sin^2 \Phi + (1 - \cos \Phi)^2}}{2} \right] + \\
 & + \sum_{n=1}^K \left\{ (\rho^S)^{2n-1} \left[\frac{\sqrt{(2n-1)^2 \sin^2 \Phi + (1 - \cos \Phi)^2} + 1 - \sqrt{(2n \sin \Phi)^2 + 1}}{2} \right] + \right. \\
 & + \left. (\rho^S)^{2n} \left[\frac{\sqrt{(2n \sin \Phi)^2 + 1} - 1 - \sqrt{(2n+1)^2 \sin^2 \Phi + (1 - \cos \Phi)^2}}{2} + \sin \Phi \right] \right\} + \\
 & + \sum_{n=K+1}^{\infty} (\rho^S)^{2n} \left[\frac{\sqrt{(2n-1)^2 \sin^2 \Phi + (1 - \cos \Phi)^2} - \sqrt{(2n+1)^2 \sin^2 \Phi + (1 - \cos \Phi)^2} + \sin \Phi}{2} \right]
 \end{aligned}$$

$$\begin{aligned}
 F_{32}^S = F_{23}^S = F_{41}^S = F_{14}^S = & \sum_{n=0}^{n=K} (\rho^S)^{2n} \left[\frac{\sqrt{1 + (2n \sin \Phi)^2} + 1 - \sqrt{(2n+1)^2 \sin^2 \Phi + (1 + \cos \Phi)^2}}{2} \right] + \\
 & + \sum_{n=0}^{n=K-1} (\rho^S)^{2n+1} \left[\frac{\sqrt{(1 + \cos \Phi)^2 + (2n+1)^2 \sin^2 \Phi} - 1 - \sqrt{(2n+2)^2 \sin^2 \Phi + 1}}{2} + \sin \Phi \right] + \\
 & + \sum_{n=K+1}^{\infty} \left\{ (\rho^S)^{2n+1} \left[\frac{\sqrt{(2n-1)^2 \sin^2 \Phi + (1 - \cos \Phi)^2} - \sqrt{(2n+1)^2 \sin^2 \Phi + (1 - \cos \Phi)^2}}{2} + \sin \Phi \right] + \right. \\
 & + \left. (\rho^S)^{2n+1} \left[\frac{\sqrt{(2n+1)^2 \sin^2 \Phi + (1 + \cos \Phi)^2} - \sqrt{(2n+1)^2 \sin^2 \Phi + (1 - \cos \Phi)^2}}{2} + \sin \Phi - 1 \right] \right\}
 \end{aligned}$$

In all these expressions K is the largest integer which is smaller than $1/(2 \cos \Phi)$

$$F_{33}^S = F_{44}^S = \rho^S (1 - \sin \Phi)$$

$$F_{34}^S = F_{43}^S = 1 - (1 - \rho^S) (F_{31}^S + F_{32}^S) - F_{33}^S$$

Reference: These expressions have been obtained by the compiler.

SPECULAR SURFACES

Planar Specular and Planar Diffuse Surfaces

$\rho^s \backslash \phi^\circ$	5	10	20	30	40
.05	.00000	.00003	.00026	.00088	.00206
.20	.00002	.00013	.00107	.00358	.00837
.30	.00003	.00021	.00163	.00546	.01278
.40	.00004	.00028	.00224	.00748	.01750
.50	.00005	.00036	.00290	.00970	.02272
.60	.00006	.00046	.00366	.01225	.02871
.70	.00007	.00058	.00458	.01534	.03598
.80	.00009	.00073	.00581	.01946	.04568
.90	.00012	.00098	.00779	.02613	.06144
.95	.00015	.00122	.00970	.03257	.07668

$\rho^s \backslash \phi^\circ$	50	60	70	80	90
.05	.00396	.00670	.00947	.01122	.01182
.20	.01606	.02719	.03846	.04573	.04823
.30	.02455	.04155	.05892	.07038	.07436
.40	.03364	.05697	.08105	.09747	.10327
.50	.04368	.07405	.10581	.12841	.13662
.60	.05523	.09373	.13472	.16547	.17713
.70	.06930	.11776	.17057	.21280	.22996
.80	.08812	.15002	.21951	.27964	.30689
.90	.11878	.20277	.30114	.39543	.44685
.95	.14849	.25406	.38170	.51304	.59695

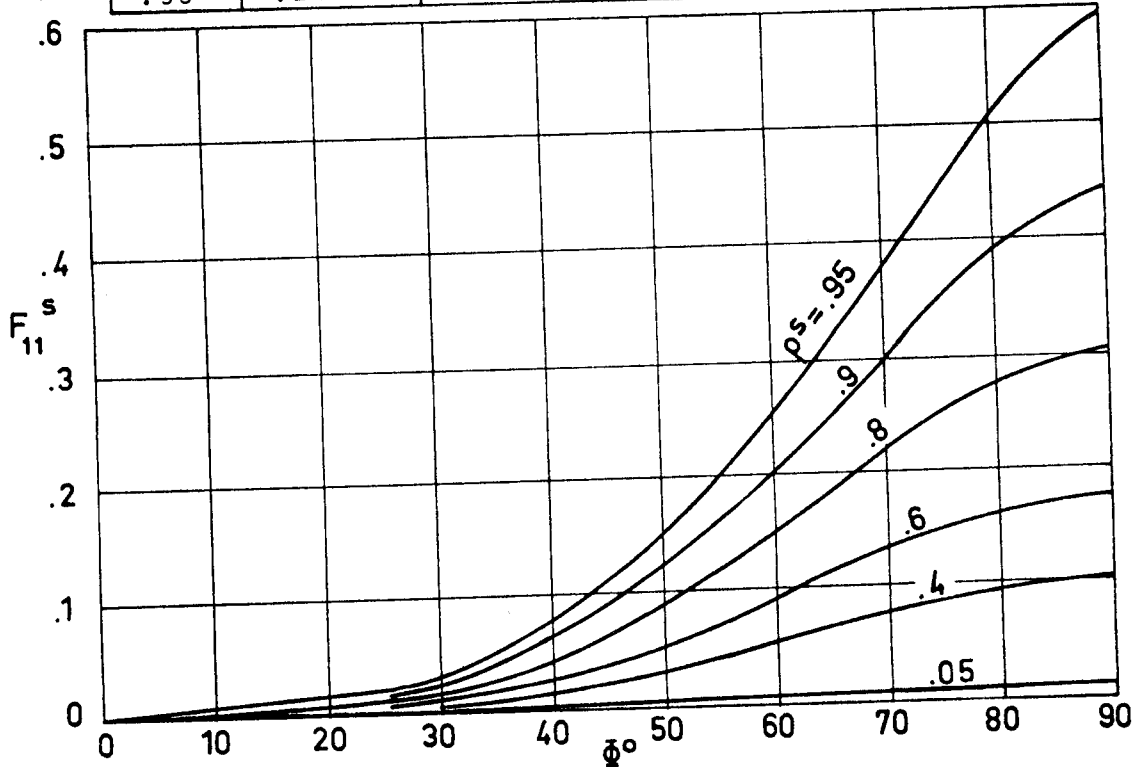


Fig 2-19. Values of F_{11}^s vs. ϕ for different values of the specular reflectance, ρ^s . Calculated by the compiler.

SPECULAR SURFACES

Planar Specular and Planar Diffuse Surfaces

$\rho^s \backslash \phi^\circ$	5	10	20	30	40
.00	.00095	.00381	.01519	.03407	.06031
.10	.00521	.01207	.03051	.05479	.08437
.20	.00947	.02034	.04584	.07554	.10851
.30	.01373	.02862	.06119	.09637	.13282
.40	.01799	.03689	.07658	.11730	.15739
.50	.02225	.04518	.09201	.13840	.18233
.60	.02651	.05347	.10751	.15971	.20777
.70	.03077	.06177	.12310	.18131	.23389
.85	.03717	.07426	.14672	.21452	.27497
.95	.04144	.08261	.16275	.23762	.30460

$\rho^s \backslash \phi^\circ$	50	60	70	80	90
.00	.09369	.13397	.18085	.23396	.29289
.10	.11869	.15722	.20038	.24879	.30219
.20	.14385	.18073	.22029	.26418	.31236
.30	.16932	.20478	.24095	.28042	.32359
.40	.19530	.22966	.26273	.29785	.33610
.50	.22198	.25573	.28608	.31693	.35026
.60	.24962	.28341	.31161	.33829	.36655
.70	.27855	.31327	.34014	.36289	.38582
.85	.32561	.36427	.39167	.40991	.42403
.95	.36132	.40568	.43694	.45519	.46325

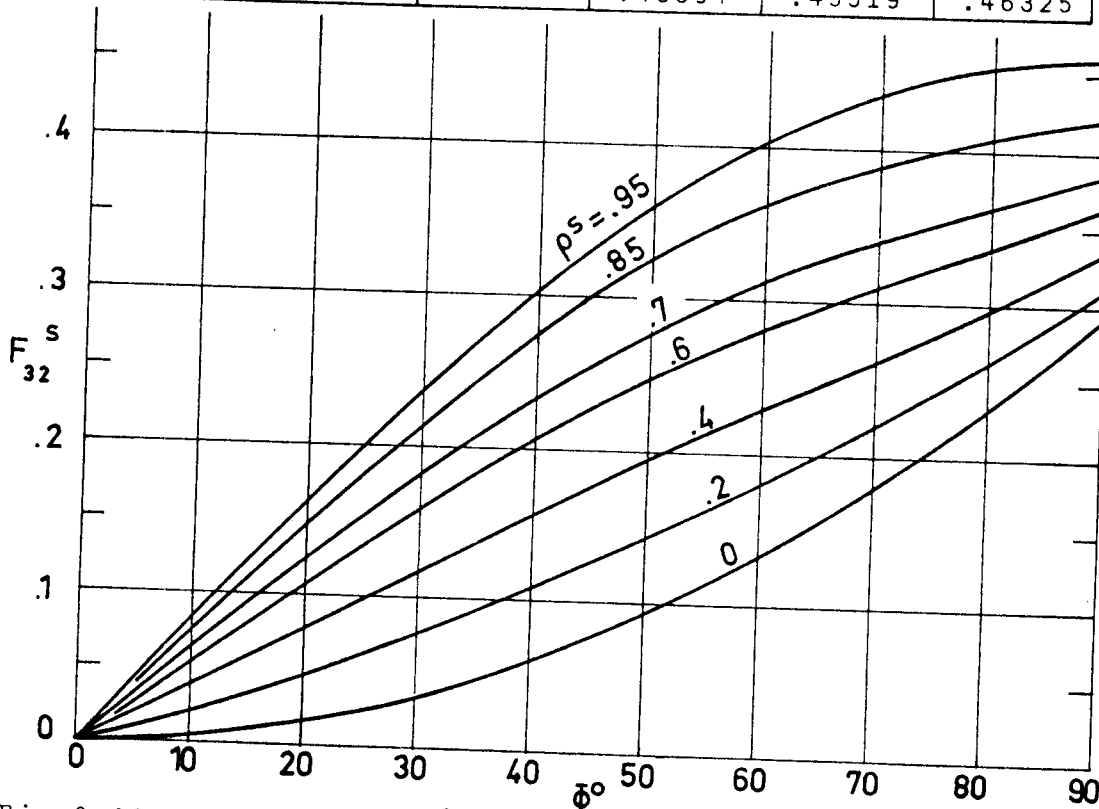


Fig 2-22. Values of F_{32}^s vs. ϕ for different values of the specular reflectance, ρ^s . Calculated by the compiler.

SPECULAR SURFACES

Planar Specular and Planar Diffuse Surfaces

$\rho^s \backslash \phi^\circ$	5	10	20	30	40
.00	.95638	.91284	.82635	.74118	.65798
.10	.95638	.91285	.82637	.74124	.65812
.20	.95638	.91285	.82642	.74142	.65853
.30	.95638	.91286	.82651	.74172	.65922
.40	.95639	.91288	.82664	.74215	.66023
.50	.95639	.91290	.82681	.74272	.66157
.60	.95639	.91293	.82704	.74347	.66330
.70	.95640	.91297	.82732	.74441	.66550
.85	.95641	.91304	.82791	.74636	.67007
.95	.95641	.91311	.82849	.74833	.67467

$\rho^s \backslash \phi^\circ$	50	60	70	80	90
.00	.57738	.50000	.42642	.35721	.29289
.10	.57764	.50043	.42791	.36160	.30219
.20	.57842	.50174	.43054	.36714	.31236
.30	.57975	.50396	.43440	.37391	.32359
.40	.58166	.50716	.43956	.38208	.33610
.50	.58422	.51145	.44622	.39190	.35026
.60	.58752	.51700	.45464	.40375	.36655
.70	.59173	.52409	.46528	.41831	.38582
.85	.60049	.53888	.48739	.44820	.42403
.95	.60936	.55395	.51011	.47927	.46325

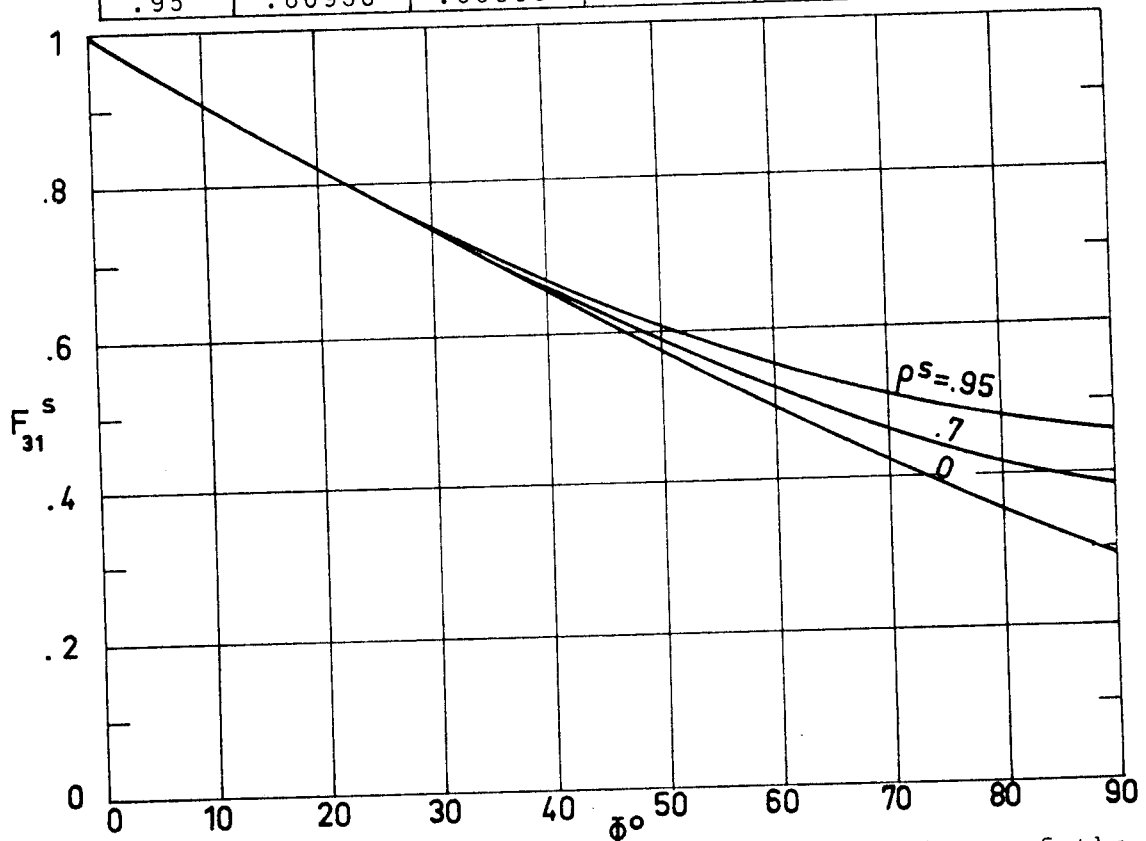


Fig 2-21. Values of F_{31}^s vs. ϕ for different values of the specular reflectance, ρ^s . Calculated by the compiler.

SPECULAR SURFACES

Planar Specular and Planar Diffuse Surfaces

$\rho^s \backslash \phi^\circ$	5	10	20	30	40
.00	.04267	.08335	.15846	.22474	.28171
.10	.04328	.08494	.16301	.23357	.29604
.20	.04475	.08817	.17059	.24643	.31493
.30	.04707	.09306	.18121	.26334	.33841
.40	.05024	.09959	.19487	.28433	.36654
.50	.05426	.10778	.21160	.30944	.39944
.60	.05913	.11763	.23139	.33873	.43724
.70	.06486	.12913	.25429	.37228	.48013
.85	.07505	.14951	.29452	.43087	.55461
.95	.08291	.16518	.32536	.47570	.61168

$\rho^s \backslash \phi^\circ$	50	60	70	80	90
.00	.32893	.36603	.39273	.40883	.41421
.10	.34991	.39471	.42852	.44913	.45606
.20	.37539	.42723	.46727	.49191	.50022
.30	.40546	.46369	.50917	.53741	.54698
.40	.44024	.50432	.55450	.58596	.59667
.50	.47993	.54942	.60369	.63799	.64974
.60	.52477	.59945	.65731	.69407	.70676
.70	.57515	.65501	.71616	.75501	.76851
.85	.66222	.75065	.81688	.85837	.87279
.95	.72921	.82474	.89536	.93884	.95368

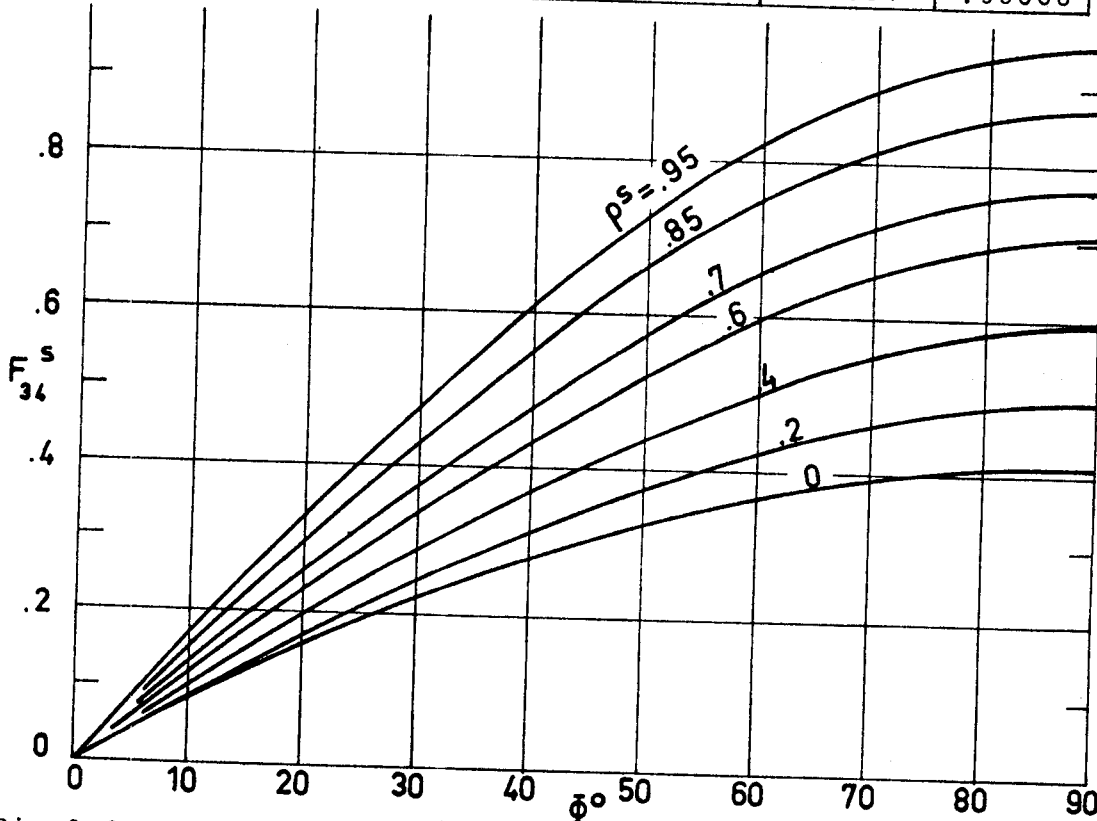


Fig 2-24. Values of F_{34}^s vs. ϕ for different values of the specular reflectance, ρ^s . Calculated by the compiler.

SPECULAR SURFACES

Planar Specular and Planar Diffuse Surfaces

$\rho^s \backslash \phi^\circ$	5	10	20	30	40
.05	.04564	.04132	.03290	.02500	.01786
.20	.18257	.16527	.13160	.10000	.07144
.30	.27385	.24791	.19739	.15000	.10716
.40	.36514	.33054	.26319	.20000	.14288
.50	.45642	.41318	.32899	.25000	.17861
.60	.54771	.49581	.39479	.30000	.21433
.70	.63899	.57845	.46059	.35000	.25005
.80	.73028	.66108	.52638	.40000	.28577
.90	.82156	.74372	.59218	.45000	.32149
.95	.86720	.78503	.62508	.47500	.33935

$\rho^s \backslash \phi^\circ$	50	60	70	80	85
.05	.01170	.00670	.00302	.00076	.00019
.20	.04679	.02679	.01206	.00304	.00076
.30	.07919	.04019	.01809	.00456	.00114
.40	.09358	.05359	.02412	.00608	.00152
.50	.11698	.06699	.03015	.00760	.00190
.60	.14037	.08038	.03618	.00912	.00228
.70	.16377	.09378	.04222	.01063	.00266
.80	.18716	.10718	.04825	.01215	.00304
.90	.21056	.12058	.05428	.01367	.00342
.95	.22226	.12728	.05729	.01443	.00362

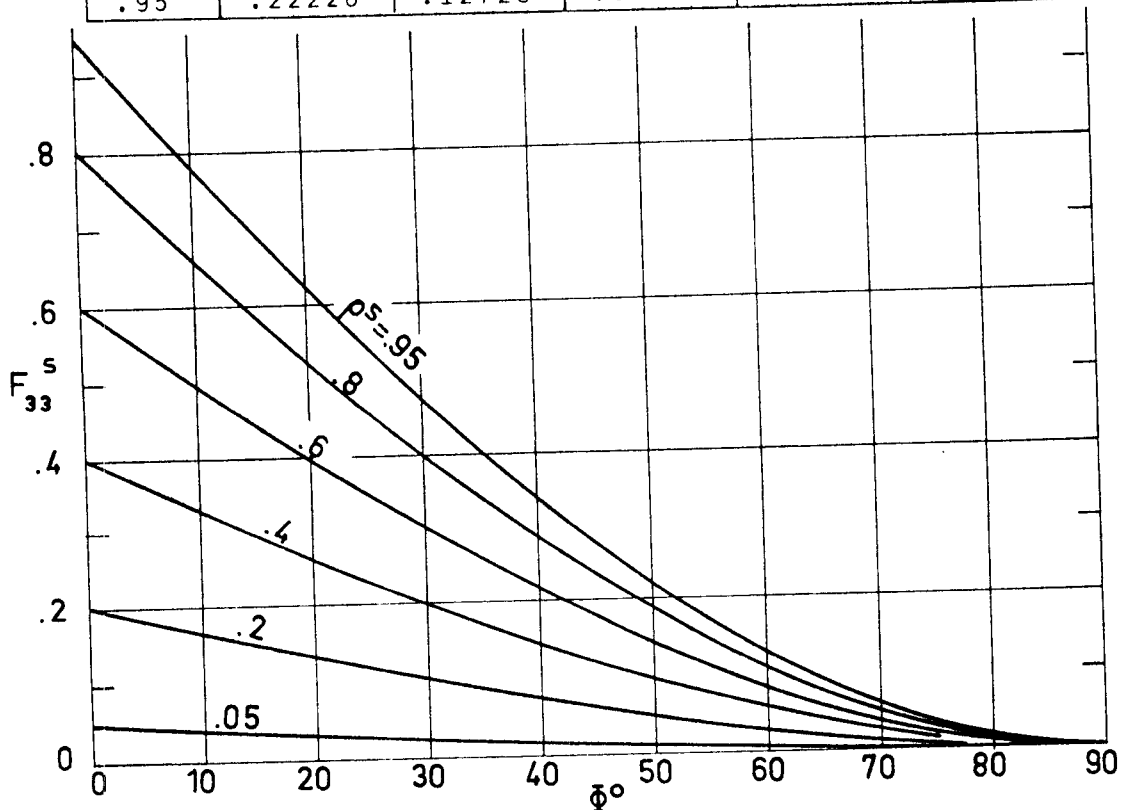


Fig 2-23. Values of F_{33}^s vs. ϕ for different values of the specular reflectance, ρ^s . Calculated by the compiler.

INTENTIONALLY BLANK PAGE

SPECULAR SURFACES
Non-Planar Specular Surfaces

2.4. NON-PLANAR SPECULAR SURFACES

2.4.1. CONCENTRIC CYLINDER OR CONCENTRIC SPHERES

Concentric cylinders of infinite length,
or concentric spheres.

Formulae:

$$F_{11}^s = \frac{\rho_2^s}{1 - \rho_1^s \rho_2^s}$$

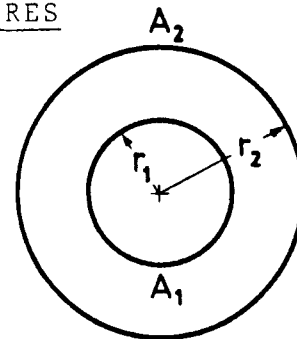
$$F_{12}^s = \frac{1}{1 - \rho_1^s \rho_2^s}$$

$$F_{21}^s = \frac{A_1/A_2}{1 - \rho_1^s \rho_2^s}$$

$$F_{22}^s = \left(1 - \frac{A_1}{A_2}\right) \frac{1}{1 - \rho_2^s} + \rho_1^s F_{21}^s$$

where $A_1/A_2 = \frac{r_1}{r_2}$ for concentric cylinders,

and $A_1/A_2 = \left(\frac{r_1}{r_2}\right)^2$ for concentric spheres.



Reference: These expressions have been obtained by the compiler.

VIEW FACTORS

References

- Cunningham, F.G. 1961 "Power Input to a Small Flat Plate from a Diffusely Radiating Sphere, with Application to Earth Satellites", NASA TN D-710, 1961.
- Eckert, E.R.G., Sparrow, E.M. 1961 "Radiative Heat Exchange Between Surfaces with Specular Reflection", International Journal of Heat and Mass Transfer, Vol. 3, 1961, pp. 42-54.
- Moon, P. 1961 "The Scientific Basic of Illuminating Engineering", Dover Publications, Inc., New York, 1961, p. 338.
- Kreith, F. 1962 "Radiation Heat Transfer for Spacecraft and Solar Power Plant Design", 1st Ed., International Textbook Company, Scranton, Pennsylvania, 1962, pp. 204-229.
- Sparrow, E.M., Eckert, E.R.G., Jonsson, V.K. 1962 "An Enclosure Theory for Radiative Exchange Between Specularly and Diffusely Reflecting Surfaces", Journal of Heat Transfer, Vol. 84c, No. 4, Nov. 1962, pp. 294-300.
- Sparrow, E.M., Miller, G.B., Jonsson, V.K. 1962 "Radiating Effectiveness of Annular-Finned Space Radiators, Including Mutual Irradiation between Radiator Elements", Journal of the Aerospace Sciences, Vol. 29, No. 11, Nov. 1972, pp. 1291-1299.

VIEW FACTORS

References

- Hamilton, D.C.,
Morgan, W.R. 1952 "Radiant-Interchange Configuration
Factors",
NACA TN 2836, 1952.
- Hottel, H.C. 1954 "Radiant-Heat Transmission",
in "Heat Transmission",
Chemical Engineering Series, 3rd Ed.,
McGraw-Hill Book Company, New York,
1954, pp. 55-125.
- Leuenberger, H.,
Person, R.A. 1956 "Compilation of Radiation Shape Factors
for Cylindrical Assemblies",
ASME paper No. 56-A-144, Nov. 1956.
- Jakob, M. 1957 "Heat Transfer",
Vol. 2, 1st Ed.,
John Wiley and Sons, Inc., New York,
1957, pp. 10-21.
- Eckert, E.R.G.,
Drake, Jr., R.M. 1959 "Heat and Mass Transfer",
2nd Ed.,
McGraw-Hill Book Company, Inc., New
York, 1959, p. 398.
- Buschman, Jr., A.J., 1961 "Configuration Factors for Exchange of
Pittman, C.M. Radiant Energy between Axisymmetrical
Sections of Cylinders, Cones, and Hem-
ispheres and Their Bases",
NASA TN D-944, 1961.

VIEW FACTORS

References

- J.P. Hartnett & T.F. Irvine Jr. Eds., Academic Press, New York, 1965, pp. 445-450.
- Sparrow, E.M., 1965 "Radiation Heat Transfer at a Surface Having
Lin, S.L. Both Specular and Diffuse Reflectance Components",
International Journal of Heat and Mass Transfer, Vol. 8, No. 5, May 1965, pp. 769-779.
- Watts, R.G. 1965 "Radiation Heat Transfer to Earth Satellites",
Journal of Heat Transfer, Vol. 87c, No. 3, Aug. 1965, pp. 369-373.
- Bien, D.D. 1966 "Configuration Factors for Thermal Radiation from Isothermal Inner Walls of Cones and Cylinders",
Journal of Spacecraft and Rockets, Vol. 3, No. 1, Jan. 1966, pp. 155-156.
- Feingold, A. 1966 "Radiant-Interchange Configuration Factors between Various Selected Plane Surfaces",
Proceedings of the Royal Society, Series A, Vol. 292, No. 1428, pp. 51-60.
- Kutateladze, S.S., 1966 "A Concise Encyclopedia of Heat Transfer",
Borishanskii, V.M. Translated from the Russian by J.B. Arthur, Pergamon Press, Oxford, 1966, pp. 242-254.
- Sarofim, A.I., 1966 "Radiative Exchange among Non-Lambert Surfaces",
Hottel, H.C. Journal of Heat Transfer, Vol. 88c, No. 1, Feb. 1966, pp. 37-44.

VIEW FACTORS

References

- Perlmutter, M., Siegel, R. 1963 "Effect of Specularly Reflecting Gray Surface on Thermal Radiation through a Tube and from Its Heated Wall",
Journal of Heat Transfer, Vol. 85c, No. 1, Feb. 1963, pp. 55-62.
- Sparrow, E.M., Jonsson, V.K. 1963 "Thermal Radiation Absorption in Rectangular Groove Cavities",
Journal of Applied Mechanics, Vol. 30e, No. 2, Jun. 1963, pp. 237-244.
- Bannister, T.C. 1965 "Radiation Geometry Factor between the Earth and a Satellite",
NASA TN D-2750, 1965.
- Clark, L.G., Anderson, E.C. 1965 "Geometric Shape Factors for Planetary-Thermal and Planetary-Reflected Radiation Incident upon Spinning and Nonspinning Spacecraft",
NASA TN D-2835, 1965.
- Jones, L.R. 1965 "Diffuse Radiation View Factors between Two Spheres",
Journal of Heat Transfer, Vol. 87c, No. 3, Aug. 1965, pp. 421-422.
- Lin, S.H., Sparrow, E.M. 1965 "Radiant Interchange among Curved Specularly Reflecting Surfaces - Application to Cylindrical and Conical Cavities",
Journal of Heat Transfer, Vol. 87c, No. 2, May 1965, pp. 299-307.
- Sparrow, E.M. 1965 "Radiation Heat Transfer between Surfaces" in "Advances in Heat Transfer", Vol. 2,

VIEW FACTORS

References

- Redor, J.F. 1973 "Introduction to Spacecraft Thermal Control",
Working Paper No. 768, ESTEC, Noordwijk,
July 1973.

VIEW FACTORS

References

- Hsu, C.J. 1967 "Shape Factor Equation for Radiant Heat Transfer between Two Arbitrary Sizes of Rectangular Planes",
The Canadian Journal of Chemical Engineering, Vol. 45, No. 1, Feb. 1967, pp. 58-60.
- Plamondon, J.A., 1967 "On the Determination of the View Function to the Images of a Surface in a Nonplanar Specular Reflector",
Horton, T.E. International Journal of Heat and Mass Transfer, Vol. 10, No. 5, May 1967, pp. 665-679.
- Campbell, J.P., 1968 "Radiant-Interchange Configuration Factors for Spherical and Conical Surfaces to Spheres",
McConnell, D.G. NASA TN D-4457, 1968.
- Feingold, A., 1970 "New Analytical Approach to the Evaluation of Configuration Factors in Radiation from Spheres and Infinitely Long Cylinders",
Gupta, K.G. Journal of Heat Transfer, Vol. 92c, No.1, Feb. 1970, pp. 69-76.
- Siegel, R., 1972 "Thermal Radiation Heat Transfer",
Howell, J.R. McGraw-Hill Book Company, New York, 1972, pp. 277-312 and pp. 748-791.
- Özisik, M.N. 1973 "Radiative Transfer and Interactions with Conduction and Convection",
John Wiley & Sons, Inc., New York, N.Y., 1973, pp. 146-152, 173-175.

HOLES, GROOVES AND CAVITIES

1 GRAY DIFFUSE SURFACES

D

HOLES, GROOVES
CAVITIES

HOLES, GROOVES, AND CAVITIES

Table of Contents

	Page
TABLE OF CONTENTS	0-1
LIST OF SYMBOLS	0-3
1. GRAY DIFFUSE SURFACES	1-1
1.1. General	1-1
1.2. Diffuse Incident Radiation	1-7
1.2.1. V-Groove	1-7
1.2.2. Parallel-Walled Groove	1-9
1.2.3. Circular-Arc Groove	1-11
1.2.4. Axisymmetrical Conical Cavity	1-13
1.2.5. Circular Cylindrical Cavity	1-15
1.2.6. Spherical Cavity	1-17
REFERENCES	2-1

INTENTIONALLY BLANK PAGE

HOLES, GROOVES, AND CAVITIES

List of Symbols

LIST OF SYMBOLS

- A_c , Surface Area of the Cavity. [m^2].
- A_h , Area of the Surface Tightly Stretched over the Cavity Opening. [m^2].
- T_w , Cavity Wall Temperature. [K].
- T_i , Surrounding Temperature Facing the i th Opening. [K].
- α , Hemispherical Total Absorptance of a Surface.
- ϵ , Hemispherical Total Emittance of a Surface. The surface is assumed to be diffuse-gray, unless otherwise stated.

Subscript

- a , Apparent Radiation Property of the Cavity.

Other symbols, mainly used to define the geometry of the configuration, are introduced when required.

D 0-4

INTENTIONALLY BLANK PAGE

GRAY DIFFUSE SURFACES

General

1. GRAY DIFFUSE SURFACES1.1. GENERAL

The radiant heat transfer properties of cavities which do not contain an absorbing-emitting medium are analyzed in this item.

When radiant energy arrives to a cavity, having one or more openings, it suffers several reflections and the corresponding absorptions at the walls of the cavity. Hence, the following effects can be observed:

1) The absorption within a single-opening cavity will exceed that of a surface, of the same absorptance, tightly stretched over the cavity opening.

2) The emission from a heated single-opening cavity will exceed that of the surface, of identical emittance and temperature, tightly stretched over the cavity opening.

3) The net radiant heat transfer rate through a passage, open at both ends, and connecting two isothermal media at different temperatures, is smaller than the net radiant heat transfer rate between the same media when separated by a non absorbing-non emitting intermediate layer.

In most cases the cavity surfaces are regarded as gray and diffuse emitters and reflectors. Nondiffuse and/or nongray conditions have been considered in several instances; particularly relevant is the case of specular reflection (Siegel & Howell (1972)).

Concerning the characteristics of the incoming radiation, either of the following two extreme alternatives are normally considered: diffuse distribution of radiation across the cavity openings,

GRAY DIFFUSE SURFACES

General

or parallel radiation.

The analysis of the radiant interchange between cavities and their environment can be achieved in a unified fashion when attention is paid to the following characteristics of the problem:

1) Openings can be treated as walls of the whole enclosure which have the property of absorbing all of the radiant energy incident upon them, and of emitting all the radiant energy streaming into the enclosure through them.

2) The cavity is normally isothermal over all its material surfaces. The enclosure representing a cavity with n openings exhibits the following distribution of temperatures: $T=T_W$ for the material surfaces; $T=T_i$ ($i=1,2,\dots,n$) for the opening facing the surrounding at temperature T_i .

3) When it is assumed that the optical characteristics of the surfaces are temperature invariant, the equations expressing the radiant interchange at any elemental surface are linear in T_W^4 and T_i^4 ($i=1,2,\dots,n$), thence a linear superposition of elemental solutions is justified.

The solution of the whole problem is expressed as the superposition of $n+1$ different solutions; all of them concern the same geometrical enclosure, having n temperatures equal to zero and the remaining one equal to that of the whole problem at the corresponding surface.

Simple examples, which will illustrate the usefulness of this superposition, are given in the following.

GRAY DIFFUSE SURFACES

General

To introduce the concept of apparent absorptance of a cavity, which to simplify the presentation is assumed to have only one opening, this opening is assimilated to a black-body surface at the temperature T_1 , while the cavity walls are at absolute zero.

The apparent absorptance, α_a , of the cavity is defined as the ratio of the energy absorbed by the cavity to the incoming radiant energy. Obviously, the radiant energy emitted by the cavity wall is zero and in no case should be taken into account for computing the apparent absorptance, α_a , of the cavity.

Conversely, for computing the apparent emittance of the cavity it is assumed that the walls are at temperature T_W , while the surroundings are at absolute zero. The radiant energy which could reach the cavity opening from an external source is not taken into account in the computation of the emittance of the cavity.

The apparent emittance, ϵ_a , of a cavity is the ratio of the radiative flux from the cavity to the radiative flux from an identically shaped, black-walled cavity at the same temperature.

For gray-walled cavities irradiated by a diffusely distributed incoming radiation, the apparent emittance, ϵ_a , equals the apparent absorptance, α_a , provided that any of the following conditions applies (Sparrow (1965)):

- 1) The cavity walls are diffuse emitters and diffuse reflectors.
- 2) The cavity walls are diffuse emitters and specular reflectors.

GRAY DIFFUSE SURFACES

General

3) The radiant flux leaving a surface element is black and diffusely distributed when the incident radiation upon the element has the same characteristics, whichever the directional characteristics of surface emittance and reflectance.

The first two cases are particularly useful since they allow to deduce absorptance data from emittance data or conversely.

The details of the proof of the above statements, which have been given by Sparrow (1965), can be outlined as follows:

1) An isothermal enclosure is defined by roofing the cavity opening with a black surface at the temperature, T_w , of the cavity.

2) The net heat transfer at any elemental wall surface of the enclosure will be zero, and the radiation within the enclosure will be black and diffusely distributed.

3) The net heat transfer at an element of wall surface can be considered as the superposition of two contributions: the heat transfer of the undisturbed cavity at temperature, T_w , and the heat transfer of an enclosure whose walls are at absolute zero, except the roof which is at temperature T_w . Since both terms cancel each other it follows that $\alpha_a = \epsilon_a$.

The transmission of radiation through isothermal passages, which are open at both ends, and which connect two isothermal environments at different temperatures, can be also calculated by means of the superposition method. In this case three elemental solutions must be superposed. The first solution corresponds to the passage,

GRAY DIFFUSE SURFACES

General

at temperature T_w , radiating through both ends to the outer space at absolute zero. In the second solution a cavity at absolute zero, formed by the passage closed at one end with a black surface, receives the energy coming from the surrounding and entering through the open end. Finally, in the third solution the passage is closed at the last mentioned end, while the radiation enters through the opposite one.

Finally it is interesting to indicate that the apparent emittance of differently shaped isothermal cavities, all of them having gray and diffuse emitting and reflecting surfaces of emittance ϵ , is quite insensitive to the cavity shape provided that the ratio A_h/A_c of the opening to cavity areas is larger than .5. Some of the results which will be presented extensively later are shown in Fig 1-1. It can be seen that the spherical and conical cavities bound above and below, respectively, the values of the apparent emittance, ϵ_a , and that the influence of the shape practically disappears for values of the ratio A_h/A_c above .5.

GRAY DIFFUSE SURFACES
General

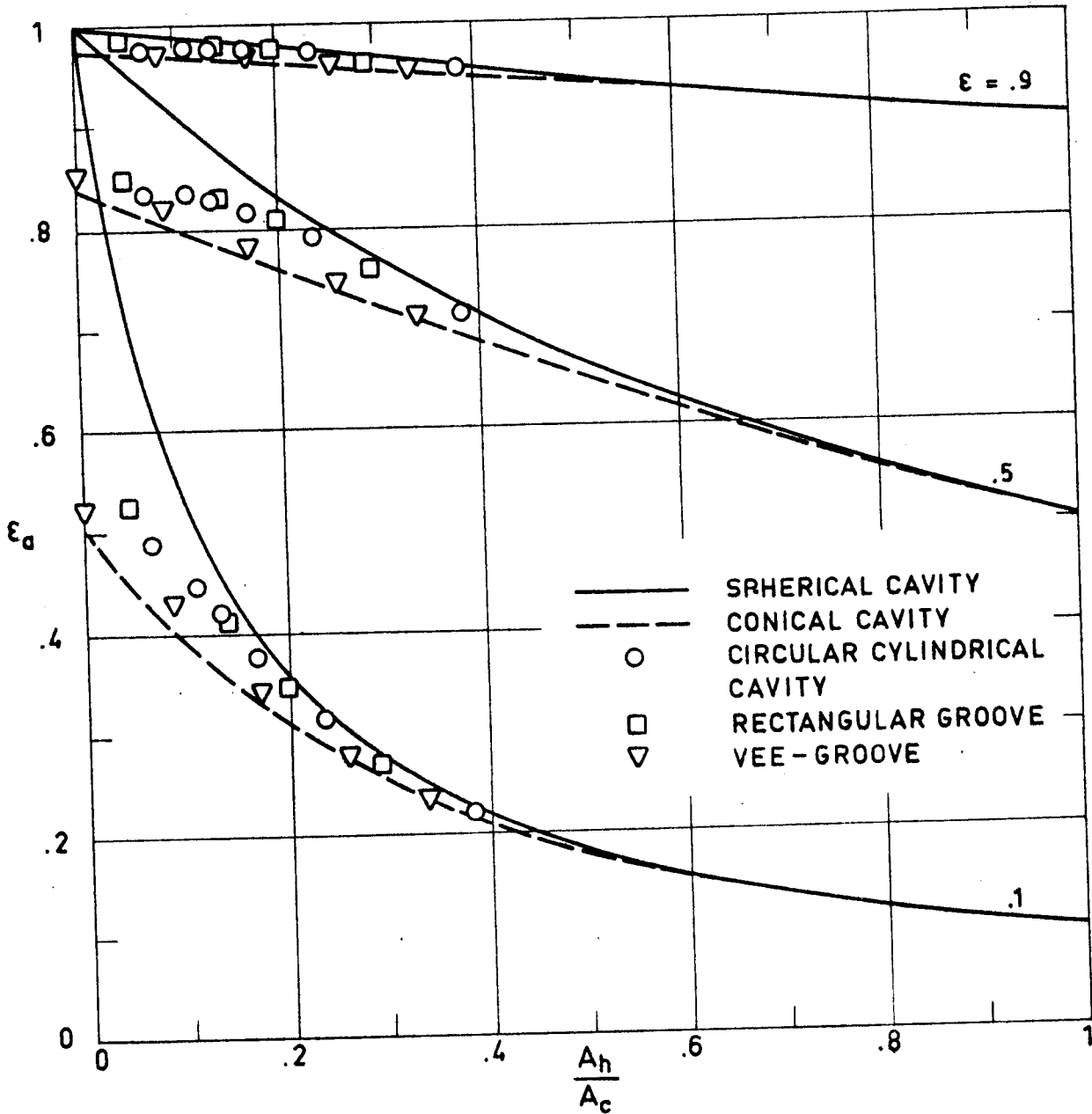


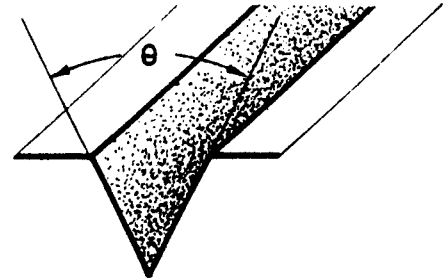
Fig 1-1. Apparent emittance, ϵ_a , of differently shaped isothermal cavities, all of them having gray diffuse emitting and reflecting surfaces, as a function of the opening to cavity area ratio, A_h/A_c , for several values of the surface emittance, ϵ . Calculated by the compiler.

GRAY DIFFUSE SURFACES
Diffuse Incident Radiation

1.2. DIFFUSE INCIDENT RADIATION

1.2.1. V-GROOVE

Symmetrical V-groove allowing emission and absorption of radiation through its opening.



All results presented in the literature have been obtained numerically.

Comments:

The reciprocity theorem for cavities applies, so that $\alpha_a = \epsilon_a$.

References: Sparrow & Lin (1962), Sparrow (1965).

GRAY DIFFUSE SURFACES
Diffuse Incident Radiation

θ°	0	10	20	30	40	50
ϵ \ A_h/A_c	0	.08716	.17365	.25882	.34202	.42262
.1	.52650	.43026	.34376	.28123	.23651	.20394
.2	.66070	.58800	.51545	.45336	.40226	.36084
.3	.74309	.68792	.63004	.57642	.52878	.48747
.4	.80316	.76115	.71572	.67163	.63049	.59311
.5	.85050	.81885	.78390	.74892	.71513	.68337
.6	.88956	.86636	.84036	.81375	.78738	.76192
.7	.92277	.90669	.88842	.86942	.85022	.83128
.8	.95165	.94165	.93019	.91810	.90570	.89325
.9	.97716	.97247	.96705	.96128	.95527	.94915

θ°	70	90	110	130	150	170
ϵ \ A_h/A_c	.57358	.70711	.81915	.90631	.96593	.99619
.1	.16115	.13548	.11936	.10919	.10316	.10034
.2	.30023	.26019	.23355	.21615	.20560	.20061
.3	.42217	.37558	.34297	.32094	.30732	.30080
.4	.53043	.48281	.44794	.42366	.40833	.40091
.5	.62757	.58286	.54879	.52436	.50864	.50095
.6	.71548	.67655	.64579	.62312	.60826	.60091
.7	.79563	.76457	.73919	.72001	.70720	.70080
.8	.86919	.84749	.82922	.81508	.80546	.80061
.9	.93706	.92582	.91609	.90839	.90306	.90034

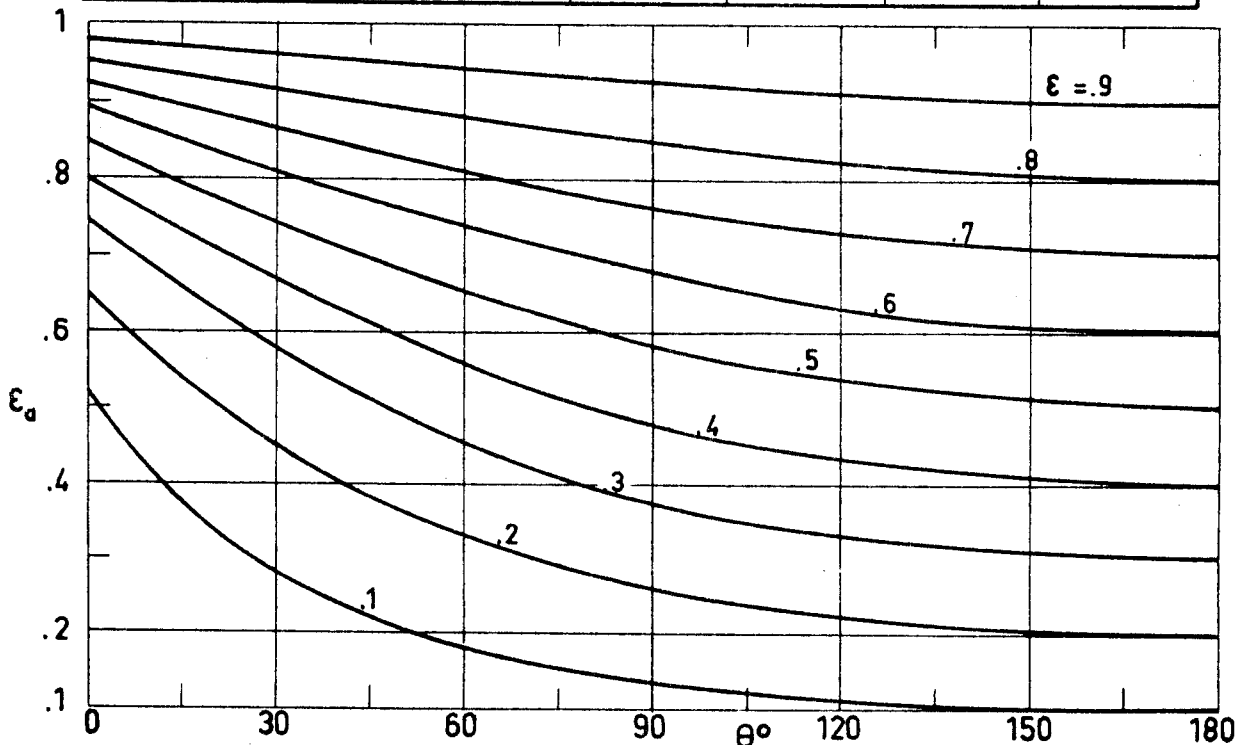
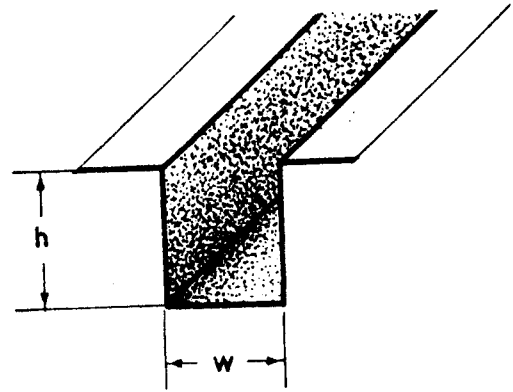


Fig 1-2. Apparent emittance, ϵ_a , of a V-groove vs. angle θ , for different values of the surface emittance, ϵ . Calculated by the compiler.

GRAY DIFFUSE SURFACES
Diffuse Incident Radiation

1.2.2. PARALLEL-WALLED GROOVE

Symmetrical parallel-walled groove allowing emission and absorption of radiation through its opening.



$$H = \frac{h}{w}$$

All results presented in the literature have been obtained numerically.

Comments:

The reciprocity theorem for cavities applies, so that $\alpha_a = \epsilon_a$.

References: Sparrow & Gregg (1962), Sparrow & Jonsson (1963a),
Sparrow (1965).

GRAY DIFFUSE SURFACES
Diffuse Incident Radiation

H	.4	.8	1.2	1.6	2	2.5
$\epsilon \backslash A_h/A_c$.55556	.38462	.29412	.23810	.20000	.16667
.1	.16556	.22285	.27160	.31278	.34741	.38296
.2	.30697	.39040	.45306	.50012	.53562	.56826
.3	.42971	.52148	.58379	.62661	.65654	.68214
.4	.53770	.62725	.68311	.71890	.74253	.76173
.5	.63389	.71473	.76165	.79002	.80794	.82195
.6	.72047	.78859	.82571	.84711	.86013	.87004
.7	.79915	.85204	.87930	.89438	.90329	.90992
.8	.87128	.90738	.92508	.93452	.93997	.94396
.9	.93794	.95627	.96487	.96932	.97183	.97365
H	3	3.5	4	4.8	5.6	≥ 10
$\epsilon \backslash A_h/A_c$.14286	.12500	.11111	.09434	.08197	.04762
.1	.41146	.43431	.45267	.47494	.49084	.52650
.2	.59167	.60867	.62119	.63496	.64384	.66070
.3	.69929	.71106	.71933	.72802	.73338	.74309
.4	.77401	.78216	.78773	.79344	.79690	.80316
.5	.83065	.83628	.84007	.84393	.84625	.85050
.6	.87605	.87989	.88246	.88506	.88663	.88956
.7	.91389	.91641	.91808	.91978	.92081	.92277
.8	.94632	.94782	.94881	.94983	.95045	.95165
.9	.97472	.97540	.97585	.97631	.97660	.97716

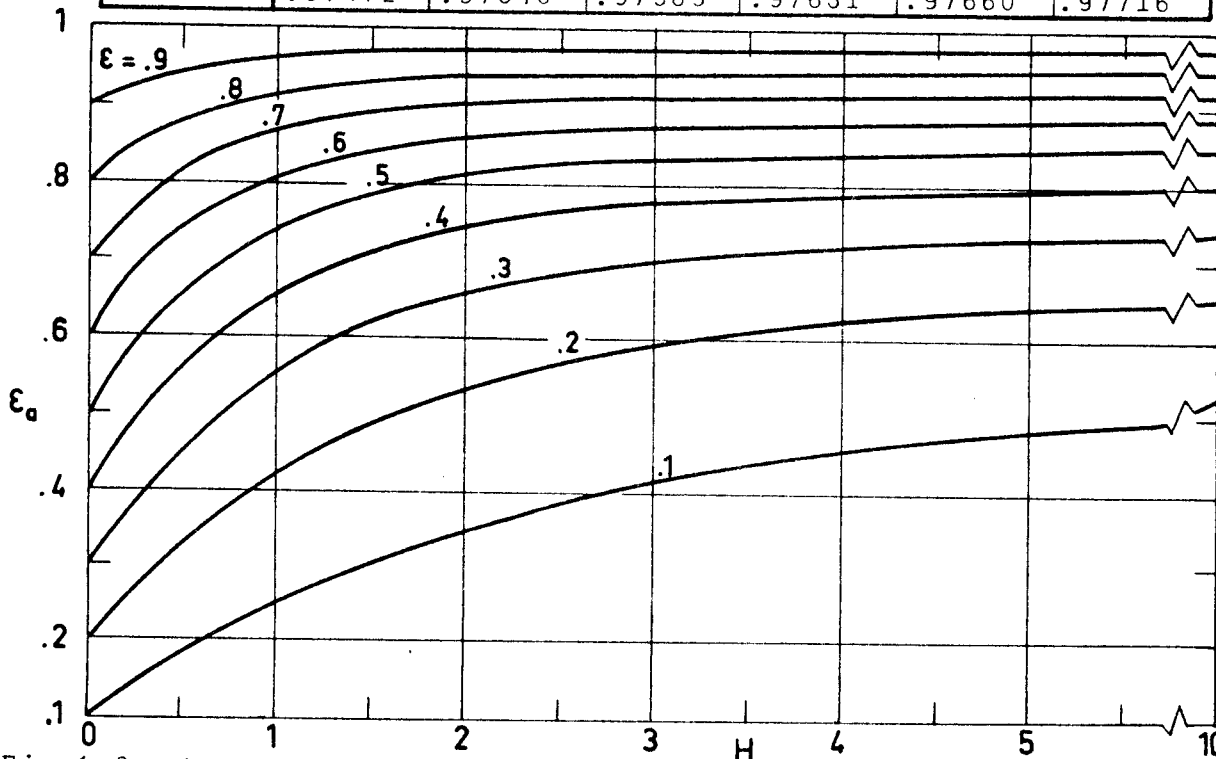
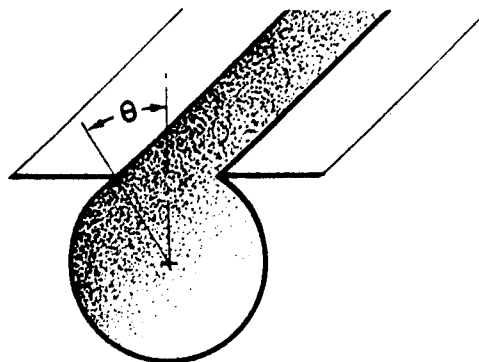


Fig 1-3. Apparent emittance, ϵ_a , of a parallel-walled groove vs. dimensionless depth, H , for different values of the surface emittance, ϵ . Calculated by the compiler.

GRAY DIFFUSE SURFACES
Diffuse Incident Radiation

1.2.3. CIRCULAR-ARC GROOVE

Inner surface of an infinitely long circular cylinder emitting and absorbing radiation through a slot which forms the cavity opening. The slot is limited by two generatrices of the cylinder.



Formula:

$$\epsilon_a = \frac{2\sqrt{\epsilon} (1 - \cos\sqrt{\epsilon}(\pi - \theta))}{\sqrt{\epsilon} (1 - \cos\sqrt{\epsilon}(\pi - \theta))(1 + \cos\theta) + \sin\sqrt{\epsilon}(\pi - \theta)\sin\theta}$$

Comments:

The reciprocity theorem for cavities applies, so that $\alpha_a = \epsilon_a$.

Reference: Obtained by the compiler after Sparrow (1965).

GRAY DIFFUSE SURFACES
Diffuse Incident Radiation

θ°	10	20	30	40	50	60
ϵ A_h/A_c	.05852	.12248	.19099	.26306	.33762	.41350
.1	.65186	.47304	.36596	.29573	.24682	.21130
.2	.80594	.66645	.56297	.48431	.42335	.37536
.3	.87525	.77207	.68652	.61541	.55614	.50665
.4	.91489	.83894	.77157	.71211	.65990	.61426
.5	.94073	.88534	.83395	.78663	.74340	.70422
.6	.95906	.91963	.88188	.84600	.81221	.78068
.7	.97286	.94617	.92004	.89460	.87006	.84659
.8	.98371	.96748	.95131	.93528	.91950	.90410
.9	.99256	.98508	.97754	.96995	.96236	.95483
θ°	70	90	110	130	150	170
ϵ A_h/A_c	.48946	.63662	.76915	.87782	.95493	.99493
.1	.18470	.14848	.12619	.11235	.10423	.10046
.2	.33715	.28160	.24518	.22164	.20748	.20082
.3	.46526	.40168	.35760	.32800	.30977	.30108
.4	.57455	.51061	.46399	.43156	.41111	.40122
.5	.66901	.60992	.56484	.53243	.51151	.50126
.6	.75155	.70088	.66060	.63071	.61100	.60122
.7	.82440	.78454	.75166	.72652	.70958	.70107
.8	.88925	.86180	.83837	.81994	.80726	.80081
.9	.94743	.93341	.92105	.91107	.90407	.90045

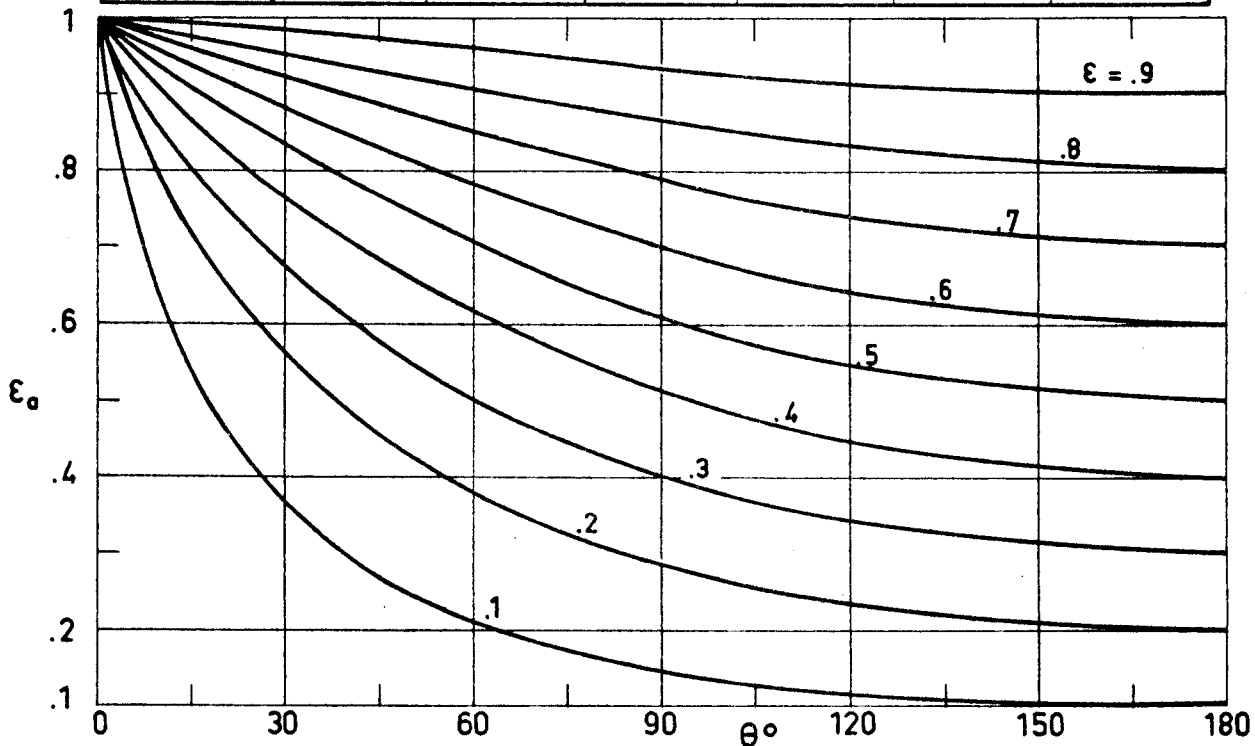
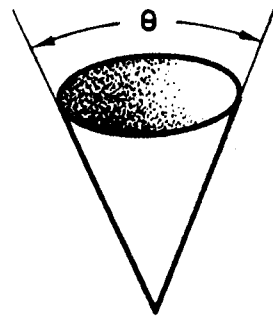


Fig 1-4. Apparent emittance, ϵ_a , of a circular-arc groove vs. opening semiangle, θ , for different values of the surface emittance, ϵ . Calculated by the compiler.

GRAY DIFFUSE SURFACES
Diffuse Incident Radiation

1.2.4. AXISYMMETRICAL CONICAL CAVITY

Inner surface of an axisymmetrical cone emitting and absorbing radiation through the base of the cone.



All results presented in the literature have been obtained numerically.

Comments:

The reciprocity theorem for cavities applies, so that $\alpha_a = \epsilon_a$.

References: Sparrow & Jonsson (1963b), Sparrow (1965).

GRAY DIFFUSE SURFACES
Diffuse Incident Radiation

θ°	0	10	20	30	40	50
ϵ \ / A_h/A_c	0	.08716	.17365	.25882	.34202	.42262
.1	.50086	.40818	.33308	.27622	.23411	.20275
.2	.63525	.56540	.50110	.44484	.39736	.35804
.3	.72182	.66798	.61571	.56680	.52260	.48361
.4	.78609	.74446	.70281	.66227	.62401	.58878
.5	.83720	.80541	.77298	.74056	.70903	.67908
.6	.87959	.85603	.83165	.80680	.78209	.75805
.7	.91575	.89923	.88197	.86411	.84604	.82812
.8	.94723	.93687	.92596	.91454	.90281	.89101
.9	.97507	.97018	.96498	.95949	.95379	.94798
θ°	70	90	110	130	150	170
ϵ \ / A_h/A_c	.57358	.70711	.81915	.90631	.96593	.99619
.1	.16083	.13539	.11933	.10919	.10316	.10034
.2	.29934	.25992	.23348	.21613	.20560	.20061
.3	.42075	.37510	.34283	.32091	.30731	.30080
.4	.52867	.48217	.44775	.42361	.40832	.40091
.5	.62565	.58212	.54855	.52430	.50863	.50095
.6	.71362	.67579	.64553	.62306	.60825	.60091
.7	.79402	.76386	.73894	.71994	.70719	.70080
.8	.86798	.84693	.82902	.81502	.80546	.80061
.9	.93640	.92550	.91597	.90836	.90306	.90034

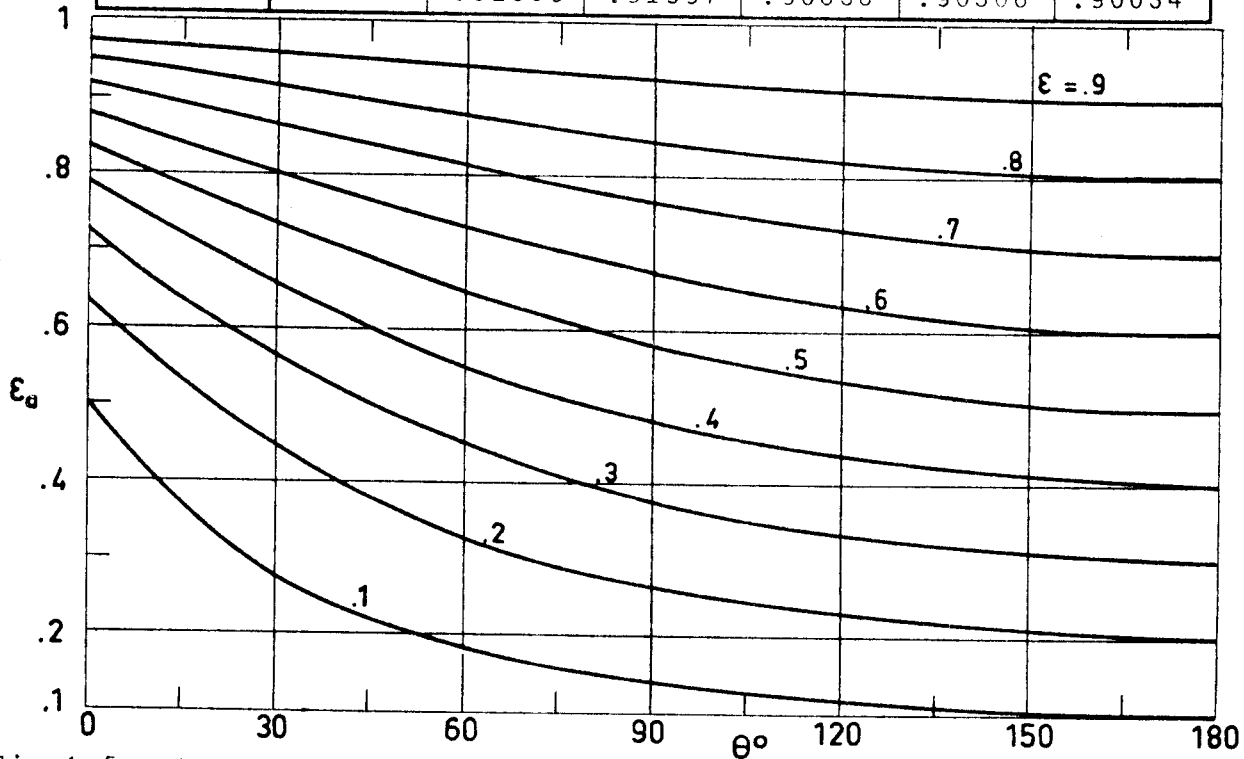
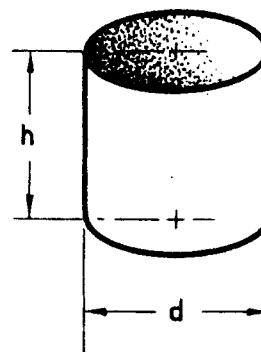


Fig 1-5. Apparent emittance, ϵ_a , of a conical cavity vs. cone angle, θ , for different values of the surface emittance, ϵ . Calculated by the compiler.

GRAY DIFFUSE SURFACES
Diffuse Incident Radiation

1.2.5. CIRCULAR CYLINDRICAL CAVITY

Inner surface of a circular cylinder plus one of its bases, emitting and absorbing radiation through the other base.



$$H = \frac{h}{d}$$

All results presented in the literature have been obtained numerically.

Comments:

The reciprocity theorem for cavities applies, so that $\alpha_a = \epsilon_a$.

References: Sparrow & Albers (1960), Sparrow, Albers & Eckert (1962), Sparrow (1965).

GRAY DIFFUSE SURFACES
Diffuse Incident Radiation

H	.4	.8	1.2	1.6	2	2.5
$\epsilon \backslash A_h/A_c$.38462	.23810	.17241	.13514	.11111	.09091
.1	.22279	.31306	.37554	.41762	.44556	.46750
.2	.39031	.50086	.56101	.59357	.61135	.62288
.3	.52144	.62774	.67613	.69870	.70957	.71587
.4	.62730	.72030	.75704	.77235	.77910	.78274
.5	.71490	.79155	.81846	.82872	.83296	.83514
.6	.78887	.84862	.86757	.87430	.87695	.87827
.7	.85238	.89573	.90831	.91252	.91412	.91491
.8	.90770	.93557	.94304	.94542	.94631	.94674
.9	.95649	.96991	.97327	.97429	.97467	.97485

H	3	3.5	4	4.8	5.6	≥ 10
$\epsilon \backslash A_h/A_c$.07692	.06667	.05882	.04950	.04273	.02439
.1	.48053	.48830	.49297	.49695	.49881	.50086
.2	.62854	.63141	.63291	.63403	.63450	.63525
.3	.71866	.71996	.72061	.72108	.72130	.72182
.4	.78426	.78494	.78528	.78554	.78567	.78609
.5	.83602	.83642	.83661	.83677	.83686	.83720
.6	.87879	.87903	.87915	.87926	.87932	.87959
.7	.91522	.91536	.91544	.91550	.91555	.91575
.8	.94691	.94699	.94703	.94707	.94710	.94723
.9	.97492	.97496	.97498	.97499	.97501	.97507

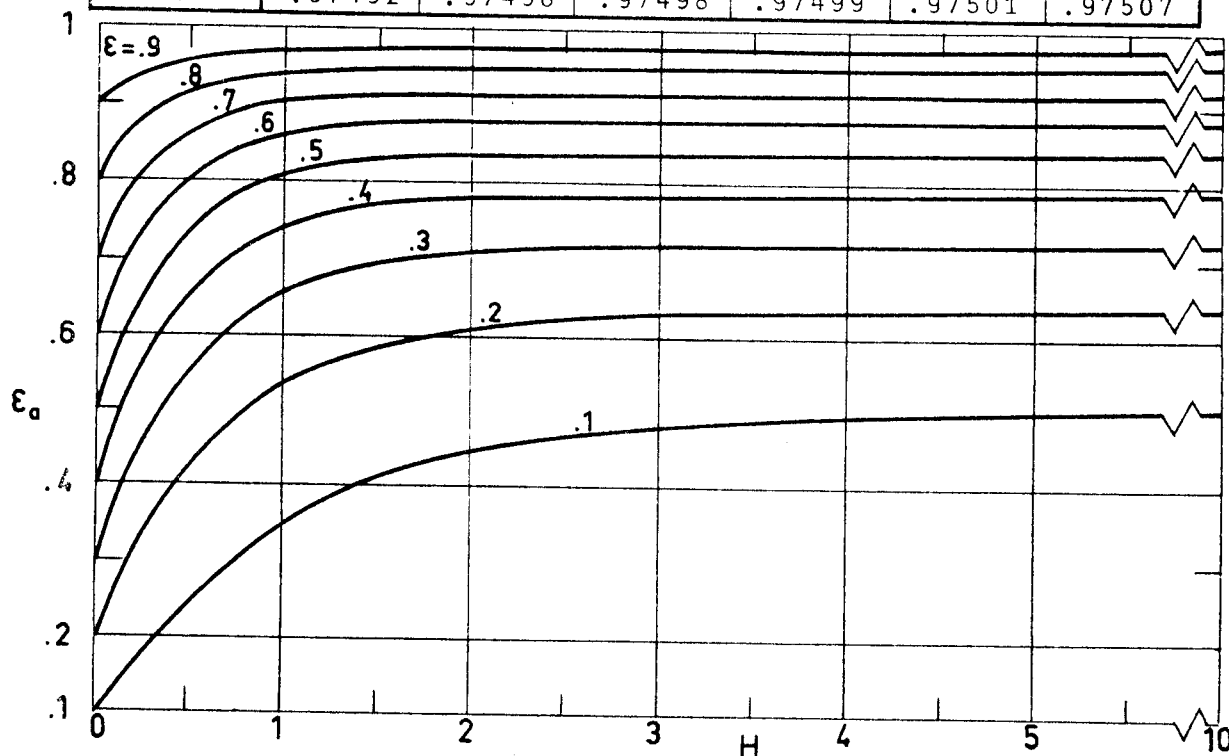


Fig 1-6. Apparent emittance, ϵ_a , of a cylindrical cavity vs. dimensionless depth, H , for different values of the surface emittance, ϵ . Calculated by the compiler.

VIEW FACTORS

- 1 DIFFUSE SURFACES
- 2 SPECULAR SURFACES

VIEW FACTORS
Table of Contents

	Page
TABLE OF CONTENTS	0-1
LIST OF SYMBOLS	0-5
1. DIFFUSE SURFACES	1-1
1.1. General	1-1
1.2. Infinitesimal to Finite Surfaces	1-3
1.2.1. Planar to Planar	1-3
1.2.1.1. Two-Dimensional Configurations	1-3
1.2.1.2. Point Source to Rectangle	1-5
1.2.1.3. Line Source to Rectangle	1-7
1.2.2. Planar to Spherical	1-9
1.2.3. Cylindrical to Spherical	1-11
1.2.4. Conical to Spherical	1-13
1.2.5. Spherical to Spherical	1-19
1.2.5.1. Sphere to Outer Sphere	1-19
1.2.5.2. Convex Hemispherical Surface to Outer Sphere	1-21
1.2.6. Ellipsoidal to Spherical	1-23
1.3. Finite to Finite Surfaces	1-27
1.3.1. Planar to Planar. Two-Dimensional Configura- tions	1-27
1.3.1.1. Two Strips of Equal Width at any Angle	1-27
1.3.1.2. Two Strips of Unequal Width Normal to Each Other	1-27
1.3.1.3. Two Parallel Strips	1-29
1.3.2. Planar to Planar. Three-Dimensional Configu- rations	1-35
1.3.2.1. Parallel Rectangles of the Same Di- mensions	1-35
1.3.2.2. Parallel Rectangles of Unequal Di- mensions	1-37
1.3.2.3. Rectangles with One Common Edge	1-39
1.3.2.4. Rectangles Placed in Intersecting Planes	1-45
1.3.2.5. Regular Polygons Forming the Bases of a Prism	1-47
1.3.2.6. Several Areas of a Prismatic Con- figuration	1-49
1.3.2.7. Parallel Coaxial Discs	1-51
1.3.2.8. Rings at Opposite Ends of a Circular Cylinder	1-53
1.3.3. Planar to Cylindrical. Two-Dimensional Con- figurations	1-55
1.3.3.1. Plane to Circular Cylinder	1-55
1.3.3.2. Plane to Rows of Circular Cylinders.	1-57

VIEW FACTORS

Table of Contents

	Page
1.3.4. Planar to Cylindrical. Three-Dimensional Configurations	1-59
1.3.4.1. Finite Length Cylinder to Outer Rectangle	1-59
1.3.4.2. Inner Rectangle to Finite-Length Cylinder	1-63
1.3.4.3. Disc to Inner Surface of a Coaxial Cylinder	1-65
1.3.4.4. Ring to Inner Surface of a Coaxial Cylinder	1-66
1.3.4.5. Finite-Length Coaxial Cylinders to Enclosed Base	1-67
1.3.5. Planar to Conical	1-69
1.3.6. Spherical to Planar	1-71
1.3.6.1. Sphere to Sector of a Coaxial Disc .	1-71
1.3.6.2. Sphere to Segment of a Coaxial Disc.	1-73
1.3.6.3. Sphere to Non-Coaxial Disc	1-75
1.3.6.4. Sphere to Arbitrary Polygon	1-77
1.3.6.5. Axisymmetrical Configurations	1-79
1.3.7. Cylindrical to Cylindrical. Two-Dimensional Configurations	1-81
1.3.7.1. Concentric Circular Cylinders	1-81
1.3.7.2. Parallel Cylinders of the Same Diameter	1-83
1.3.8. Cylindrical to Cylindrical. Axisymmetrical Configurations	1-85
1.3.8.1. Concentric Circular Cylinders of the Same Length	1-85
1.3.8.2. Concentric Circular Cylinders of Unequal Length	1-90
1.3.8.3. Finite Areas in the Same Circular Cylinder	1-91
1.3.9. Spherical to Cylindrical	1-93
1.3.10. Conical to Conical	1-95
1.3.11. Conical to Spherical	1-97
1.3.12. Spherical to Spherical	1-103
1.3.12.1. Concentric Spheres	1-103
1.3.12.2. Finite Areas in the Same Spherical Surface	1-105
1.3.12.3. Sphere to Outer Sphere	1-107
1.3.12.4. Sphere to Cap on Another Sphere of Equal Radius	1-109
1.4. Additional Sources of Data	1-111
2. SPECULAR SURFACES	2-1
2.1. General	2-1
2.2. Two Planar Specular Surfaces	2-5

VIEW FACTORS

Table of Contents

	Page
2.2.1. Two-Dimensional Configurations	2-5
2.2.1.1. Parallel Strips of Equal Width	2-5
2.2.1.2. Strips of Equal Width at Any Angle .	2-9
2.2.3. Parallel Rectangles of Same Width and Length.	2-13
2.2.4. Rectangles of Same Width and Length with One Common Edge	2-25
2.3. Planar Specular and Planar Diffuse Surfaces	2-31
2.3.1. Two-Dimensional Cavities. Cylinders of Quadrangular Cross Section	2-31
2.4. Non-Planar Specular Surfaces	2-39
2.4.1. Concentric Cylinders and Concentric Spheres .	2-39
REFERENCES	3-1

INTENTIONALLY BLANK PAGE

VIEW FACTORS
List of Symbols

LIST OF SYMBOLS

- A_i , Surface Area of the i th surface. [m^2].
- B_i , Energy Flux Leaving Surface i . Often called Radiosity.
[$W \cdot m^{-2}$].
- F_{ij} , View Factor from Diffuse Surface A_i to Diffuse Surface A_j .
- $F_{(i_1, i_2, \dots, i_n)(j_1, j_2, \dots, j_n)}$, View Factor from the Ensemble of
Diffuse Surfaces $A_{i_1}, A_{i_2}, \dots, A_{i_n}$ to
the Ensemble of Diffuse Surfaces
 $A_{j_1}, A_{j_2}, \dots, A_{j_n}$.
- F_{ij}^S , View Factor from Specular Surface A_i to Specular Surface A_j .
- H_i , Energy Flux Incident on Surface i . [$W \cdot m^{-2}$].
- $K_{i,2}$, Term which Appears in the Expression for the View Factor
between Elements of Parallel Plates. $K_{i,2} = A_i F_{ii}$.
- $K_{mn}(i, j, k, p, q, \dots)$, Fraction of the Radiative Energy Leaving A_m which
Reaches A_n after i Perfectly Specular Reflections
from Surface A_i , j from Surface A_j , k from Sur-
face A_k, \dots .
- S , Distance between Two Differential Elements. [m].
- T , Temperature. [K].
- β_i , Angle from Normal to Surface i . [Angular Degrees].
- ϵ , Hemispherical Emittance of a (diffuse-gray) Surface.
- ρ^d , Hemispherical Diffuse Reflectance of a (diffuse-gray) Sur-
face.
- ρ^S , Specular Reflectance of a (gray) Surface. It is assumed to
be independent of incident angle.

VIEW FACTORS

List of Symbols

σ , Stefan-Boltzmann Constant. $\sigma=5.6697 \times 10^{-8} \text{ W.m}^{-2}.\text{K}^{-4}$.

Other symbols, mainly used to define the geometry of the configuration, are introduced when required.

DIFFUSE SURFACES

General

1. DIFFUSE SURFACES

1.1. GENERAL

The view factor, F_{12} , between the diffuse surfaces A_1 and A_2 , is the fraction of the energy leaving the isothermal surface A_1 that arrives at A_2 .

If the receiver surface is infinitesimal, the view factor is infinitesimal for both infinitesimal and finite emitting surfaces, and is given by the expression

$$d F_{12} = \frac{\cos\beta_1 \cos\beta_2}{\pi S^2} d A_2 \quad ,$$

when both surfaces are infinitesimal, and by

$$d F_{12} = \frac{d A_2}{A_1} \int_{A_1} \frac{\cos\beta_1 \cos\beta_2}{\pi S^2} d A_1 \quad ,$$

when A_1 is finite.

If the receiver surface is finite, the view factor is finite for both infinitesimal and finite emitting surfaces, and is given by the expression

$$F_{12} = \int_{A_2} \frac{\cos\beta_1 \cos\beta_2}{\pi S^2} d A_2 \quad ,$$

when A_1 is infinitesimal, and by

$$F_{12} = \frac{1}{A_1} \int_{A_1} \int_{A_2} \frac{\cos\beta_1 \cos\beta_2}{\pi S^2} d A_2 d A_1 \quad ,$$

when A_1 is finite.

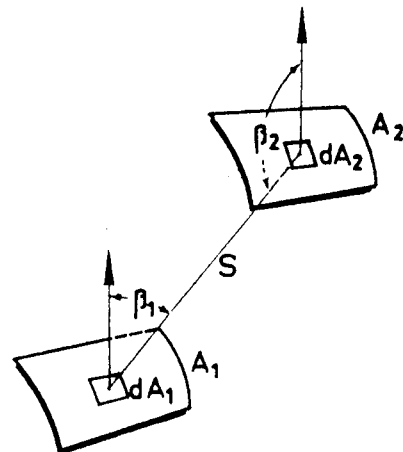


Fig 1-1. Geometric notation for view factors between diffuse surfaces.

DIFFUSE SURFACES

General

Regardless of which surfaces are considered, their view factors satisfy the following reciprocity relation:

$$A_1 F_{12} = A_2 F_{21}$$

If we consider the diffuse surfaces A_1 , A_2 and A_3 , the view factor between the surfaces A_1 and $A_2 + A_3$ is

$$F_{1(2,3)} = F_{12} + F_{13} \quad ,$$

when the receiver surface is formed by two surfaces, and

$$F_{(2,3)1} = \frac{A_2 F_{21} + A_3 F_{31}}{A_2 + A_3} \quad ,$$

when the emitting surface is formed by two surfaces. Notice that the notation $F_{1(2,3)}$ and $F_{(2,3)1}$ will be used in the following data sheets.

When an enclosure of N surfaces A_1, A_2, \dots, A_N is considered, their view factors satisfy the relation

$$\sum_{j=1}^N F_{ij} = 1 \quad ,$$

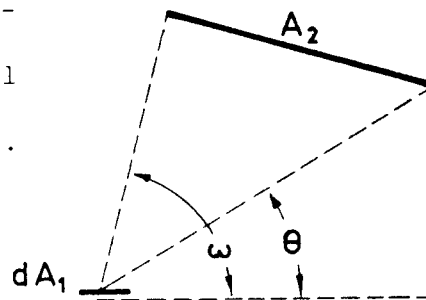
for any surface A_i . This relationship results from the fact that the overall heat transfer in the enclosure must be zero.

DIFFUSE SURFACES

Infinitesimal to Finite Surfaces

1.2. INFINITESIMAL TO FINITE SURFACES1.2.1. PLANAR TO PLANAR1.2.1.1. TWO-DIMENSIONAL CONFIGURATIONS

A plane point source dA_1 and any surface A_2 generated by an infinitely long line moving parallel to itself and to the plane of dA_1 .



Formula:

$$F_{12} = \frac{1}{2} (\cos \theta - \cos \omega)$$

References: Hamilton & Morgan (1952), Moon (1961), Kreith (1962).

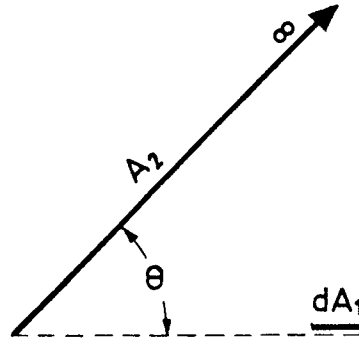
Comments:

Notice that F_{12} is independent of the shape of A_2 for given values of θ and ω .

View factors for several configurations may be obtained as a particular case of this one. An example is shown in the next page.

DIFFUSE SURFACES
Infinitesimal to Finite Surfaces

A plane point source dA_1
and any infinite plane A_2 with
the planes of dA_1 and A_2 inter-
secting at an angle θ .



Formula:

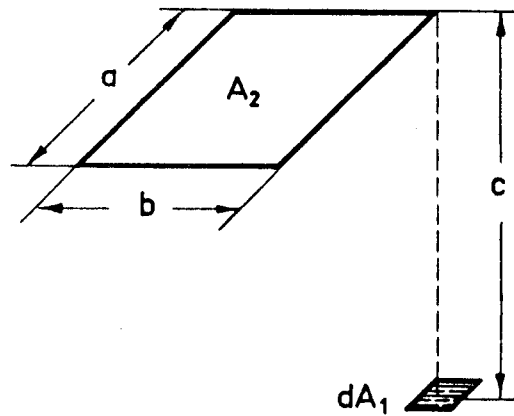
$$F_{12} = \frac{1}{2} (1 + \cos \theta)$$

References: Hamilton & Morgan (1952), Kreith (1962).

DIFFUSE SURFACE
 Infinitesimal to Finite Surfaces

1.2.1.2. POINT SOURCE TO RECTANGLE

A plane point source dA_1 and a plane rectangle A_2 parallel to the plane of dA_1 (see sketch). The normal to dA_1 passes through one corner of A_2 .



$$x = \frac{a}{c}$$

$$y = \frac{b}{c}$$

Formulae:

$$F_{12} = \frac{1}{2\pi} \left[\frac{x}{\sqrt{1+x^2}} \tan^{-1} \frac{y}{\sqrt{1+x^2}} + \frac{y}{\sqrt{1+y^2}} \tan^{-1} \frac{x}{\sqrt{1+y^2}} \right]$$

$$\lim_{y \rightarrow \infty} F_{12} = \frac{x}{4\sqrt{1+x^2}}$$

$$\lim_{x \rightarrow \infty} F_{12} = \frac{y}{4\sqrt{1+y^2}}$$

References: Hamilton & Morgan (1952), Hottel (1954), Jakob (1957), Moon (1961), Kreith (1962).

DIFUSSE SURFACES

Infinitesimal to Finite Surfaces

x \ y	.1	.2	.4	.6	1.0	2.0	4.0	∞
.1	.00314	.00616	.01147	.01553	.02034	.02386	.02472	.02488
.2	.00616	.01209	.02252	.03051	.04002	.04701	.04872	.04903
.4	.01147	.02252	.04204	.05710	.07525	.08885	.09223	.09285
.6	.01553	.03051	.05710	.07782	.10320	.12272	.12771	.12862
1.0	.02034	.04002	.07525	.10320	.13853	.16738	.17527	.17678
2.0	.02386	.04701	.08885	.12272	.16738	.20776	.22078	.22361
4.0	.02472	.04872	.09223	.12771	.17527	.22078	.23786	.24254
∞	.02488	.04903	.09285	.12862	.17678	.22361	.24254	.25000

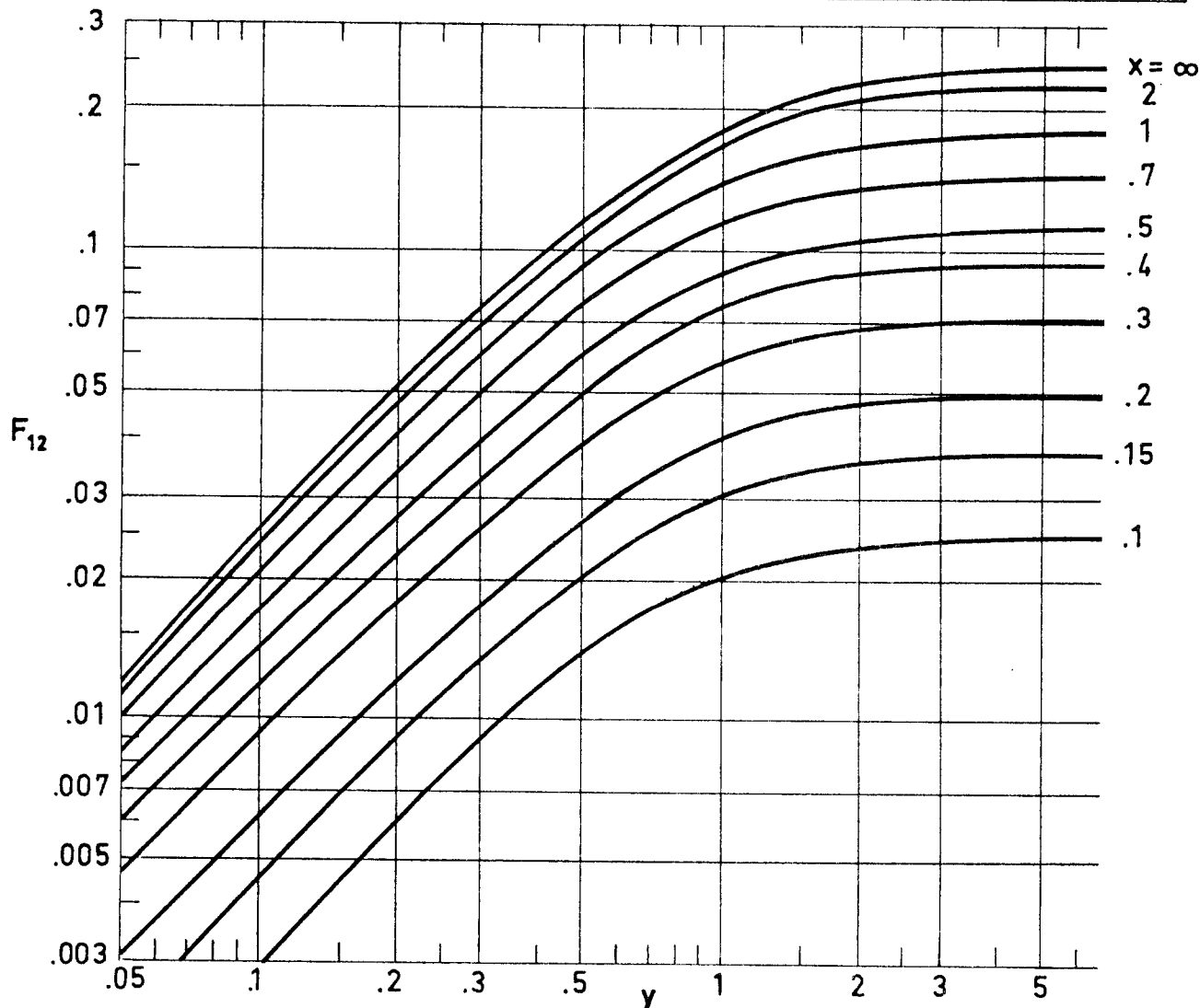
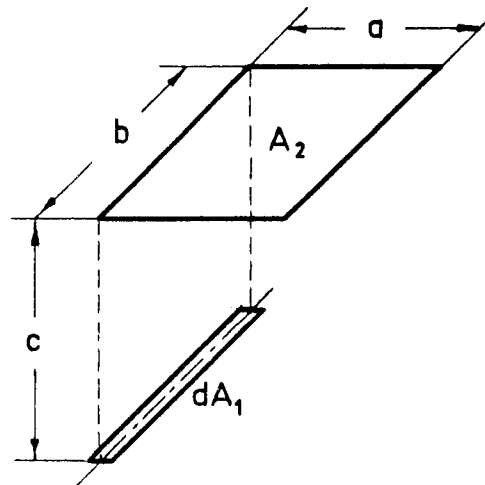


Fig 1-2. Values of F_{12} as a function of x and y . From Hamilton & Morgan (1952).

DIFFUSE SURFACES
Infinitesimal to Finite Surfaces

1.2.1.3. LINE SOURCE TO RECTANGLE

A line source dA_1 and a plane rectangle A_2 parallel to the plane of dA_1 with dA_1 opposite one edge of A_2 .



$$x = \frac{b}{c}$$

$$y = \frac{a}{c}$$

Formulae:

$$F_{12} = \frac{1}{\pi x} \left[\sqrt{1+x^2} \tan^{-1} \frac{y}{\sqrt{1+x^2}} - \tan^{-1} y + \frac{xy}{\sqrt{1+y^2}} \tan^{-1} \frac{x}{\sqrt{1+y^2}} \right]$$

$$\lim_{x \rightarrow \infty} F_{12} = \frac{y}{2\sqrt{1+y^2}}$$

$$\lim_{y \rightarrow \infty} F_{12} = \frac{1}{2} \left(\sqrt{1 + \frac{1}{x^2}} - \frac{1}{x} \right)$$

References: Hamilton & Morgan (1952), Kreith (1962).

DIFFUSE SURFACES

Infinite to Finite Surfaces

x \ y	.1	.2	.4	.6	1.0	2.0	10.0	∞
.10	.0031	.0061	.0115	.0155	.0203	.0239	.0249	.0249
.15	.0047	.0092	.0172	.0233	.0305	.0358	.0373	.0373
.20	.0062	.0122	.0228	.0309	.0405	.0475	.0495	.0495
.30	.0092	.0181	.0337	.0456	.0599	.0704	.0734	.0734
.40	.0120	.0236	.0440	.0597	.0784	.0923	.0962	.0963
.60	.0171	.0336	.0626	.0851	.1122	.1325	.1384	.1385
.80	.0213	.0419	.0784	.1067	.1412	.1675	.1753	.1754
1.00	.0284	.0488	.0914	.1247	.1656	.1974	.2070	.2071
2.00	.0350	.0690	.1297	.1781	.2397	.2912	.3088	.3090
∞	.0498	.0981	.1857	.2572	.3536	.4472	.4975	.5000

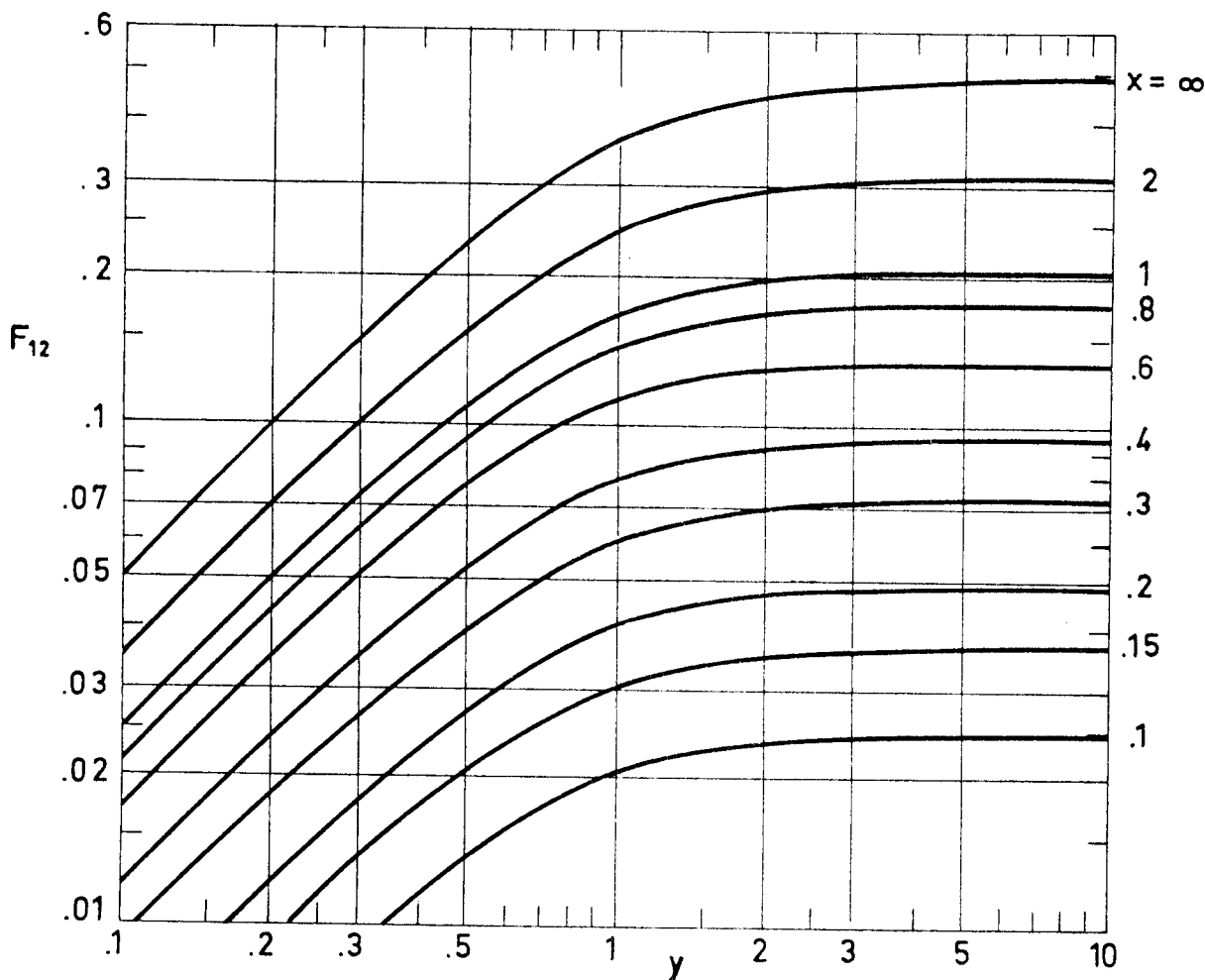


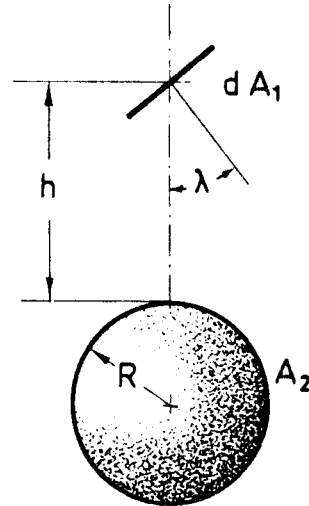
Fig 1-3. Values of F_{12} as a function of x and y . From Hamilton & Morgan (1952).

DIFFUSE SURFACES
Infinitesimal to Finite Surfaces

1.2.2. PLANAR TO SPHERICAL

One face of an elemental plate to sphere.

$$H = \frac{h}{R}$$



Formula:

The analytical expression for the view factor is only known when $\lambda + \sin^{-1} \frac{1}{1+H} < \pi/2$. In such a case:

$$F_{12} = \frac{\cos \lambda}{(1+H)^2}$$

References: Cunningham (1961), Kreith (1962), Bannister (1965), Clark & Anderson (1965).

DIFFUSE SURFACES

Infinitesimal to Finite Surfaces

H \ λ°	0	20	40	50	60	70	80
.001	.9946	.9594	.8636	.7986	.7246	.6438	.5585
.01	.9752	.9303	.8174	.7460	.6676	.5839	.4973
.05	.9062	.8523	.7215	.6428	.5600	.4752	.3906
.1	.8282	.7755	.6438	.5638	.4809	.3983	.3182
.2	.6962	.6521	.5332	.4575	.3792	.3030	.2318
.3	.5922	.5560	.4526	.3840	.3122	.2427	.1790
.5	.4432	.4177	.3398	.2853	.2267	.1692	.1173
1.	.2490	.2346	.1917	.1604	.1248	.0881	.0547
2.	.1110	.1040	.0854	.0718	.0554	.0375	.0209
5.	.0279	.0260	.0214	.0181	.0139	.0092	.0047

H \ λ°	90	100	110	120	130	140	160
.001	.4713	.3852	.3025	.2256	.1570	.0991	.0216
.01	.4107	.3271	.2487	.1774	.1158	.0665	.0091
.05	.3090	.2331	.1650	.1065	.0597	.0267	.0
.1	.2430	.1747	.1156	.0677	.0326	.0107	.0
.2	.1673	.1112	.0654	.0320	.0112	.0012	.0
.3	.1230	.0762	.0403	.0163	.0036	.0	.0
.5	.0737	.0401	.0172	.0045	.0	.0	.0
1.	.0285	.0113	.0026	.0	.0	.0	.0
2.	.0085	.0016	.0	.0	.0	.0	.0
5.	.0015	.0	.0	.0	.0	.0	.0

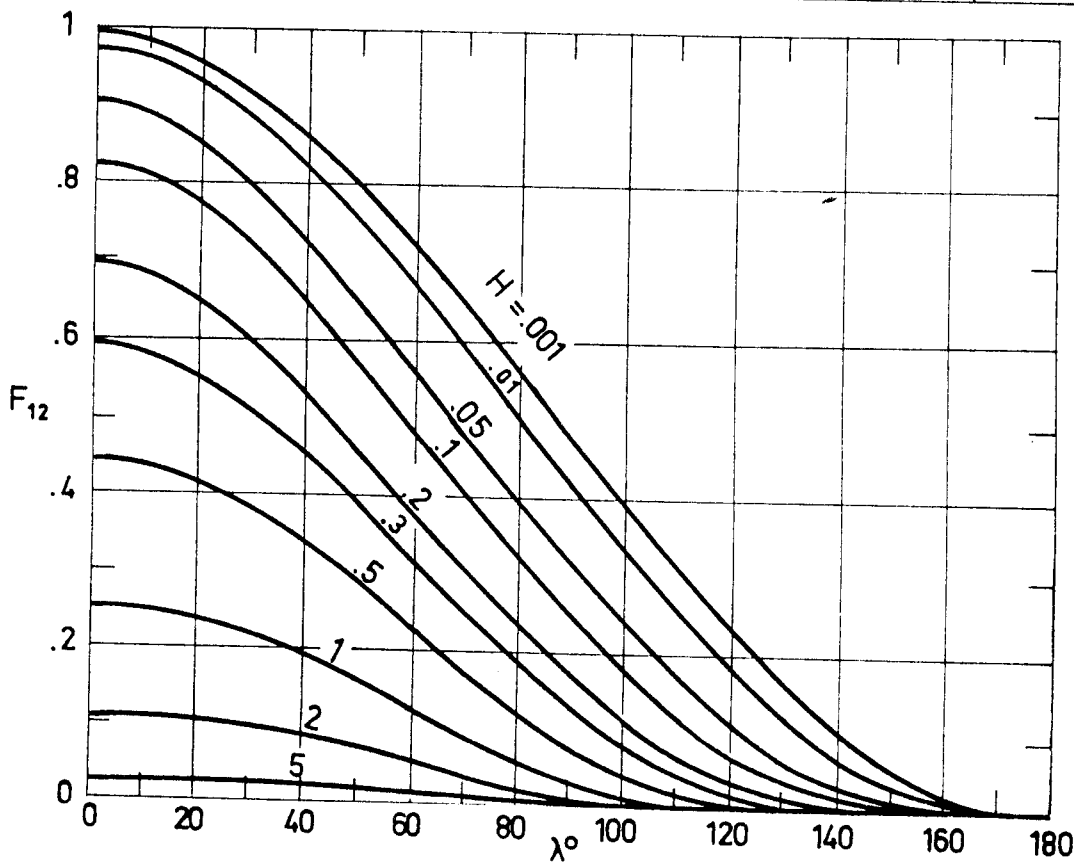


Fig 1-4. Values of F_{12} as a function of λ for different values of H . Calculated by the compiler.

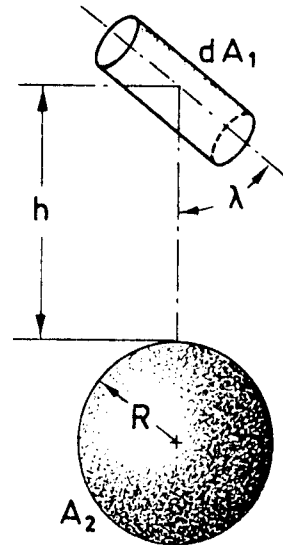
DIFFUSE SURFACES

Infinitesimal to Finite Surfaces

1.2.3. CYLINDRICAL TO SPHERICAL

Outer area of an infinitesimal cylindrical surface to sphere.

$$H = \frac{h}{R}$$



Formula:

$$F_{12} = \frac{1}{\pi^2} \int_0^{2\pi} d\phi \int_0^{\theta_0} \sqrt{1 - (\cos\theta \cos\lambda + \sin\theta \sin\lambda \cos\phi)^2} \sin\theta d\theta$$

where

$$\sin\theta_0 = \frac{1}{1 + H}$$

References: Watts (1965), Clark & Anderson (1965).

DIFFUSE SURFACES

Infinitesimal to Finite Surfaces

H \ λ°	0	10	20	30	40
.001	.4713	.4716	.4722	.4732	.4745
.01	.4107	.4115	.4135	.4166	.4206
.05	.3090	.3104	.3145	.3210	.3295
.1	.2430	.2447	.2499	.2583	.2695
.2	.1673	.1694	.1756	.1859	.1996
.3	.1230	.1253	.1321	.1432	.1577
.5	.0737	.0772	.0835	.0946	.1082
1.	.0285	.0307	.0370	.0459	.0556
2.	.0085	.0099	.0136	.0186	.0236
5.	.0015	.0019	.0030	.0044	.0058

H \ λ°	50	60	70	80	90
.001	.4761	.4778	.4796	.4810	.4815
.01	.4255	.4310	.4364	.4404	.4420
.05	.3397	.3507	.3611	.3687	.3715
.1	.2828	.2965	.3089	.3175	.3206
.2	.2151	.2303	.2431	.2514	.2543
.3	.1732	.1880	.1998	.2072	.2098
.5	.1222	.1347	.1442	.1499	.1518
1.	.0648	.0723	.0779	.0812	.0823
2.	.0279	.0331	.0337	.0353	.0358
5.	.0069	.0077	.0083	.0087	.0089

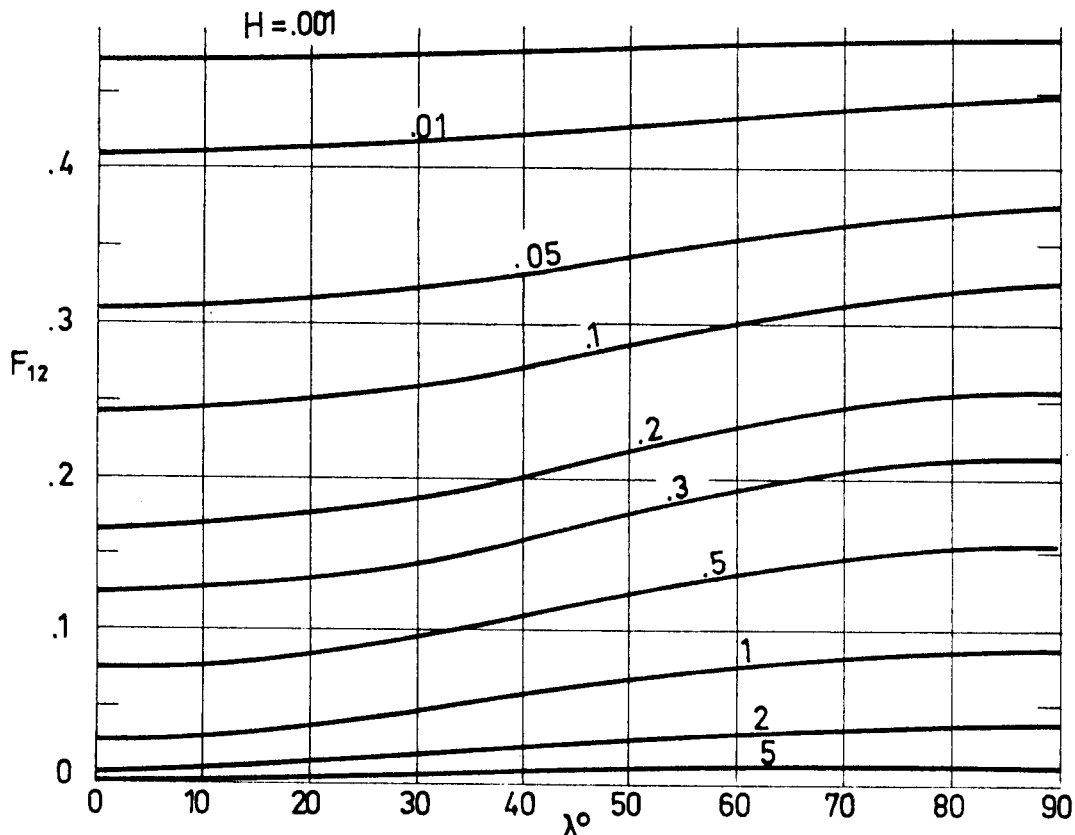


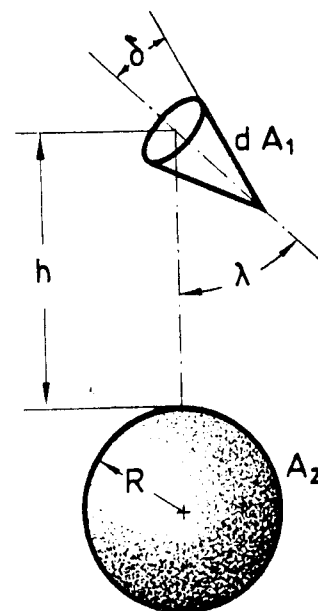
Fig 1-5. Values of F_{12} as a function of H and λ . Calculated by the compiler.

DIFFUSE SURFACES
Infinitesimal to Finite Surfaces

1.2.4. CONICAL TO SPHERICAL

Outer area of an infinitesimal conical surface to sphere.

$$H = \frac{h}{R}$$



All results presented in the literature are obtained numerically.

Reference: Clark & Anderson (1965).

DIFFUSE SURFACES

Infinitesimal to Finite Surfaces

H \ λ°	0	20	40	50	60	70	80
.001	.5585	.5540	.5412	.5320	.5213	.5091	.4956
.01	.4973	.4947	.4866	.4807	.4736	.4649	.4540
.05	.3906	.3910	.3915	.3913	.3901	.3868	.3800
.1	.3182	.3206	.3267	.3301	.3323	.3319	.3273
.2	.2318	.2363	.2483	.2550	.2600	.2619	.2593
.3	.1790	.1847	.1993	.2071	.2130	.2156	.2138
.5	.1173	.1239	.1395	.1474	.1532	.1558	.1548
1.	.0547	.0606	.0729	.0785	.0824	.0843	.0839
2.	.0209	.0243	.0310	.0338	.0357	.0366	.0365
5.	.0047	.0057	.0076	.0083	.0088	.0090	.0090

H \ λ°	90	100	110	120	140	160	180
.001	.4810	.4655	.4498	.4346	.4084	.3912	.3852
.01	.4404	.4244	.4066	.3885	.3562	.3347	.3271
.05	.3687	.3527	.3330	.3114	.2709	.2430	.2331
.1	.3175	.3024	.2828	.2605	.2168	.1857	.1747
.2	.2514	.2383	.2207	.1998	.1559	.1230	.1112
.3	.2072	.1960	.1805	.1617	.1206	.0882	.0762
.5	.1499	.1414	.1295	.1146	.0804	.0514	.0401
1.	.0812	.0763	.0694	.0607	.0397	.0198	.0113
2.	.0353	.0331	.0300	.0260	.0162	.0062	.0016
5.	.0087	.0082	.0074	.0064	.0039	.0012	.0

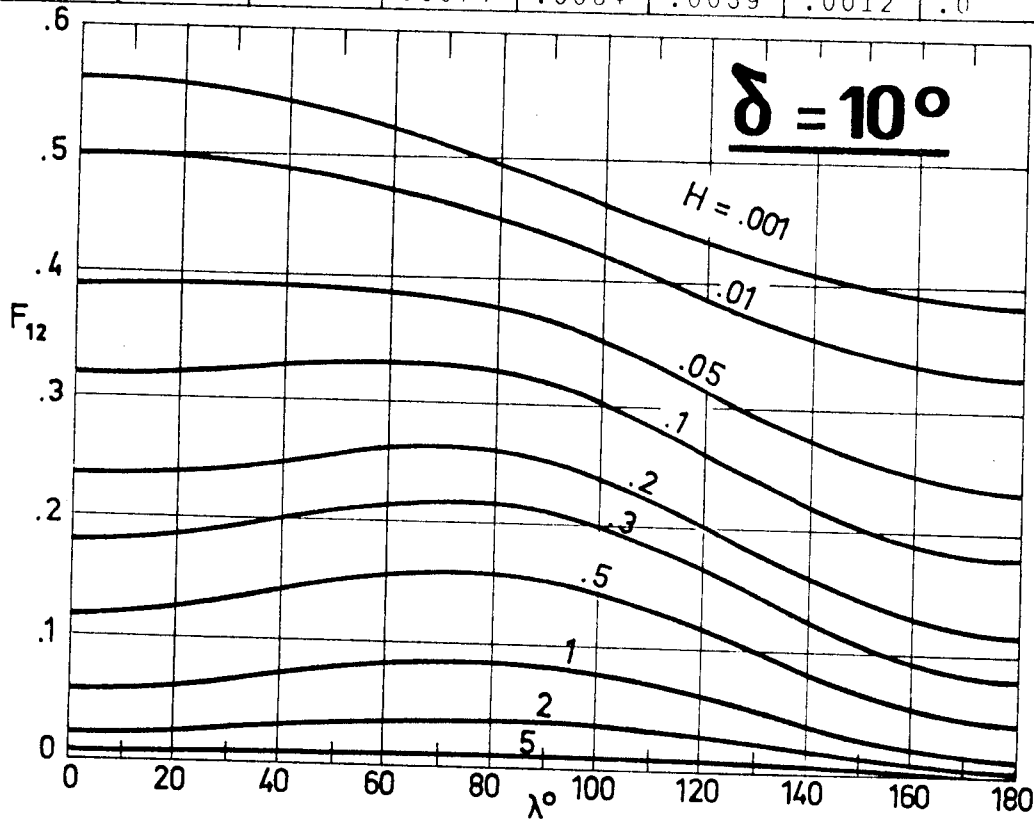


Fig 1-6. Values of F_{12} as a function of H and λ for $\delta = 10^\circ$. Calculated by the compiler.

DIFFUSE SURFACES
 Infinitesimal to Finite Surfaces

H \ λ°	0	20	40	50	60	70	80
.001	.7246	.7100	.6681	.6380	.6028	.5634	.5213
.01	.6676	.6542	.6153	.5870	.5532	.5149	.4736
.05	.5600	.5494	.5175	.4930	.4629	.4282	.3901
.1	.4809	.4726	.4457	.4243	.3976	.3665	.3323
.2	.3792	.3732	.3521	.3348	.3131	.2879	.2600
.3	.3122	.3071	.2892	.2747	.2568	.2361	.2130
.5	.2267	.2220	.2075	.1968	.1842	.1697	.1532
1.	.1248	.1203	.1102	.1044	.0981	.0910	.0824
2.	.0554	.0524	.0469	.0444	.0420	.0392	.0357
5.	.0139	.0130	.0114	.0108	.0103	.0096	.0088

H \ λ°	90	100	110	120	140	160	180
.001	.4778	.4346	.3927	.3533	.2858	.2411	.2256
.01	.4310	.3885	.3473	.3081	.2399	.1936	.1774
.05	.3507	.3114	.2730	.2362	.1701	.1233	.1065
.1	.2965	.2605	.2252	.1910	.1292	.0843	.0677
.2	.2303	.1998	.1692	.1395	.0861	.0469	.0320
.3	.1880	.1617	.1349	.1089	.0625	.0291	.0163
.5	.1347	.1146	.0937	.0731	.0373	.0132	.0045
1.	.0723	.0607	.0482	.0356	.0145	.0029	.0
2.	.0313	.0260	.0202	.0142	.0044	.0002	.0
5.	.0077	.0064	.0049	.0033	.0008	.0	.0

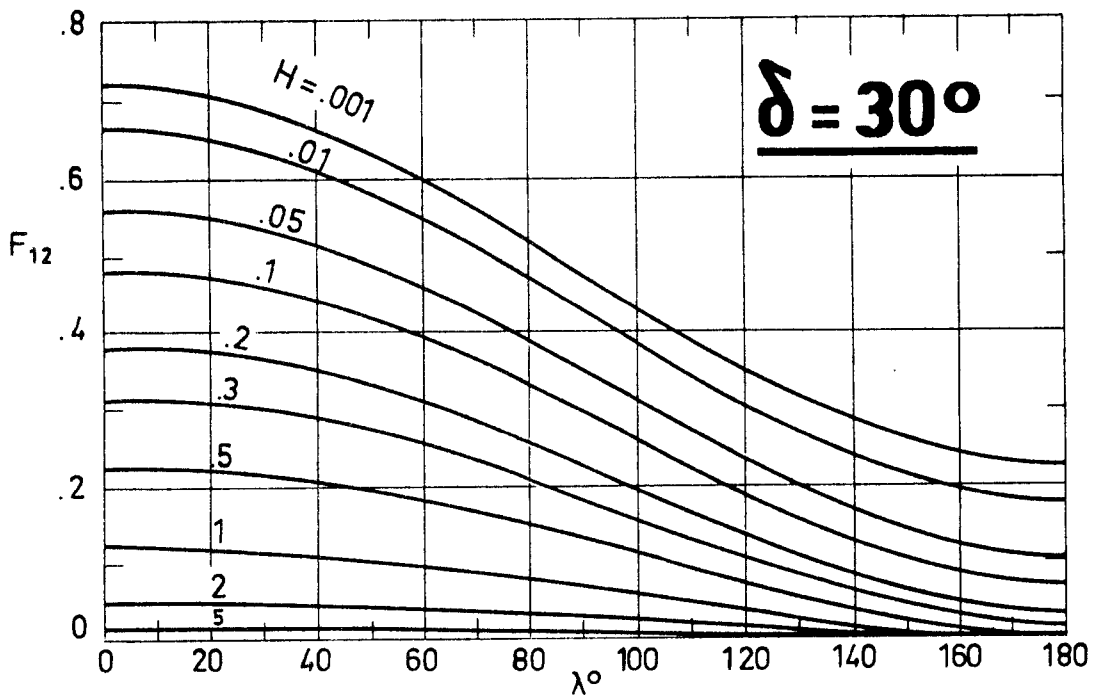


Fig 1-7. Values of F_{12} as a function of H and λ , for $\delta = 30^\circ$. Calculated by the compiler.

DIFFUSE SURFACES

Infinitesimal to Finite Surfaces

H \ λ°	0	20	40	50	60	70	80
.001	.8636	.8405	.7727	.7242	.6681	.6064	.5412
.01	.8174	.7944	.7244	.6736	.6153	.5522	.4866
.05	.7215	.6984	.6275	.5761	.5175	.4550	.3915
.1	.6438	.6204	.5511	.5017	.4457	.3864	.3267
.2	.5332	.5099	.4454	.4014	.3521	.3001	.2483
.3	.4526	.4303	.3713	.3323	.2892	.2440	.1993
.5	.3398	.3208	.2719	.2409	.2075	.1732	.1395
1.	.1917	.1798	.1489	.1298	.1102	.0912	.0729
2.	.0854	.0799	.0650	.0559	.0469	.0387	.0310
5.	.0214	.0200	.0161	.0137	.0114	.0094	.0076

H \ λ°	90	100	110	120	140	160	180
.001	.4745	.4084	.3449	.2858	.1871	.1221	.0991
.01	.4206	.3562	.2954	.2399	.1491	.0887	.0665
.05	.3295	.2709	.2173	.1701	.0952	.0455	.0267
.1	.2695	.2168	.1698	.1292	.0661	.0255	.0107
.2	.1996	.1559	.1182	.0861	.0379	.0100	.0012
.3	.1575	.1206	.0890	.0625	.0240	.0044	.0
.5	.1082	.0804	.0567	.0373	.0111	.0008	.0
1.	.0556	.0397	.0257	.0145	.0022	.0	.0
2.	.0236	.0162	.0096	.0044	.0	.0	.0
5.	.0058	.0039	.0021	.0008	.0	.0	.0

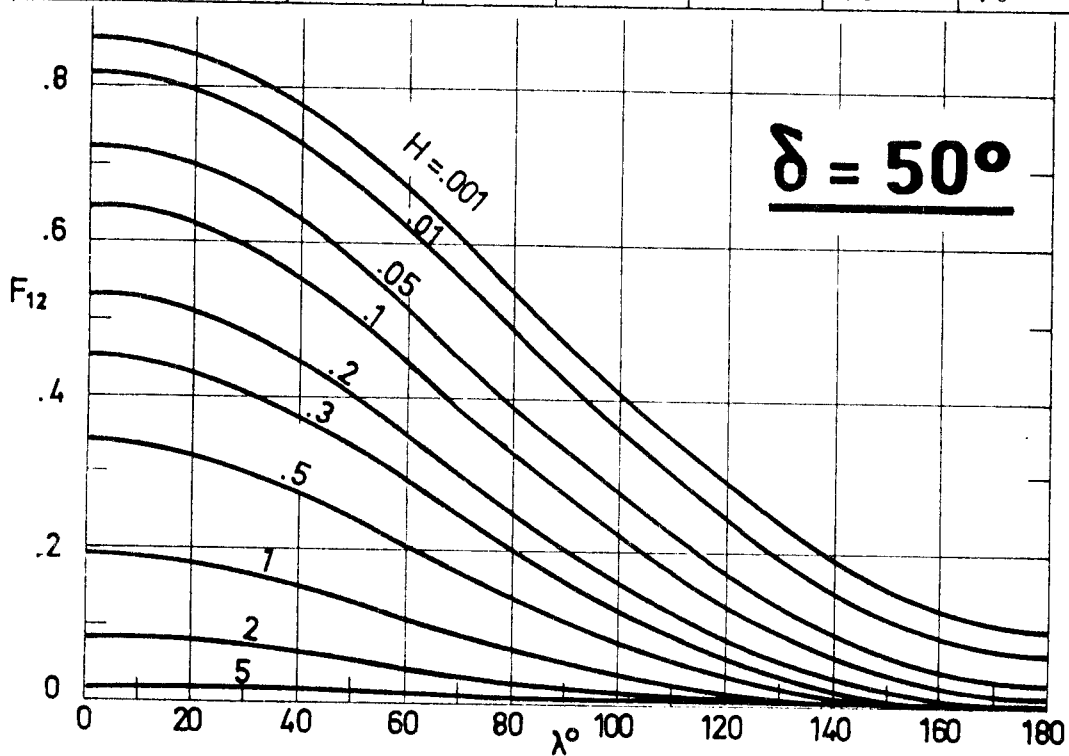


Fig 1-8. Values of F_{12} as a function of H and λ , for $\delta = 50^\circ$. Calculated by the compiler.

DIFFUSE SURFACES

Infinitesimal to Finite Surfaces

H \ λ°	0	20	40	50	60	70	80
.001	.9856	.9575	.8578	.7938	.7210	.6414	.5574
.01	.9635	.9210	.8117	.7415	.6642	.5818	.4967
.05	.8921	.8414	.7158	.6388	.5574	.4739	.3907
.1	.8145	.7645	.6380	.5601	.4789	.3976	.3188
.2	.6850	.6422	.5272	.4540	.3778	.3030	.2329
.3	.5831	.5474	.4468	.3806	.3110	.2431	.1804
.5	.4370	.4112	.3349	.2822	.2255	.1698	.1190
1.	.2454	.2311	.1887	.1581	.1236	.0884	.0563
2.	.1092	.1025	.0840	.0705	.0546	.0375	.0218
5.	.0274	.0256	.0210	.0177	.0136	.0092	.0050

H \ λ°	90	100	110	120	140	160	180
.001	.4716	.3867	.3052	.2295	.1049	.0279	.0028
.01	.4115	.3290	.2516	.1815	.0722	.0138	.0
.05	.3104	.2356	.1684	.1107	.0315	.0021	.0
.1	.2447	.1775	.1193	.0720	.0145	.0	.0
.2	.1694	.1142	.0691	.0358	.0033	.0	.0
.3	.1253	.0793	.0438	.0196	.0005	.0	.0
.5	.0762	.0430	.0201	.0067	.0	.0	.0
1.	.0307	.0135	.0041	.0005	.0	.0	.0
2.	.0099	.0028	.0001	.0	.0	.0	.0
5.	.0019	.0002	.0	.0	.0	.0	.0

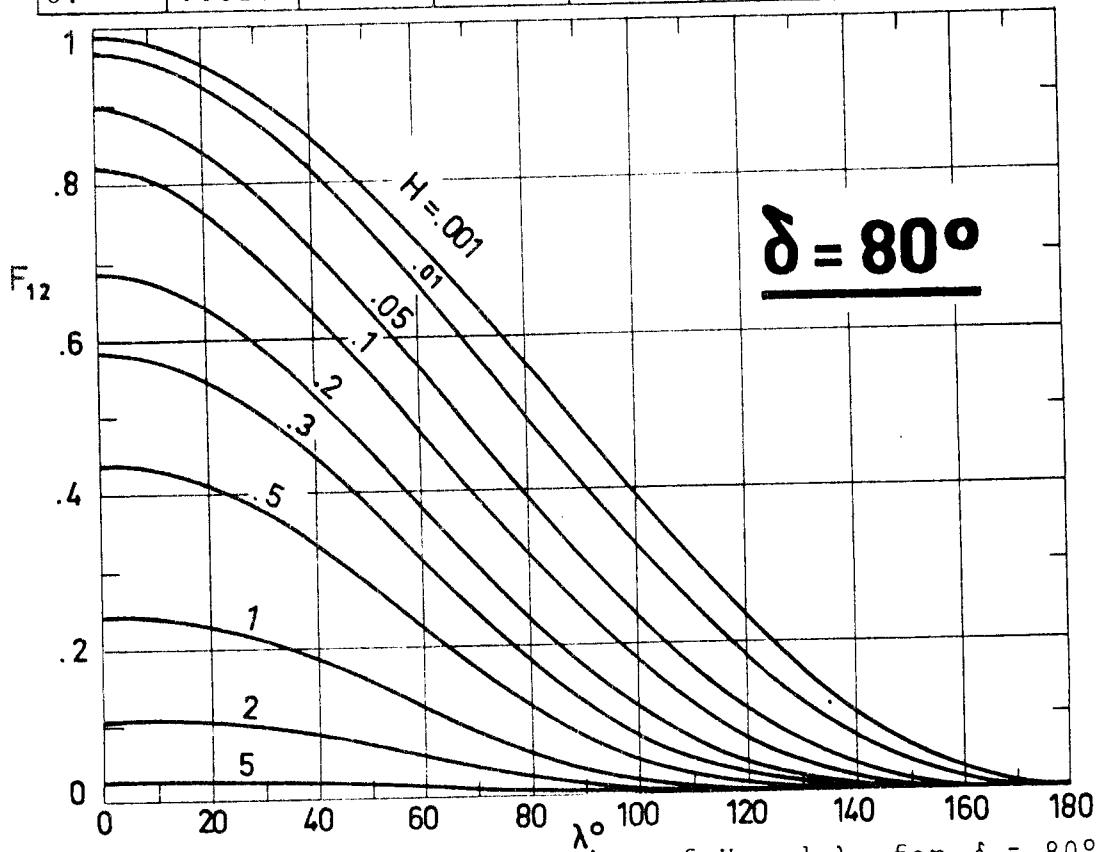


Fig 1-9. Values of F_{12} as a function of H and λ , for $\delta = 80^\circ$. Calculated by the compiler.

INTENTIONALLY BLANK PAGE

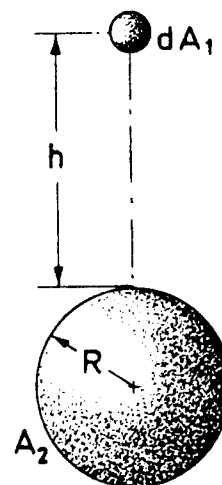
DIFFUSE SURFACES
 Infinitesimal to Finite Surfaces

1.2.5. SPHERICAL TO SPHERICAL

1.2.5.1. SPHERE TO OUTER SPHERE

Infinitesimal sphere to finite
 sphere.

$$H = \frac{h}{R}$$



Formula:

$$F_{12} = \frac{1}{2} \left[1 - \frac{\sqrt{H^2 + 2H}}{1 + H} \right]$$

Reference: Watts (1965).

DIFFUSE SURFACES
Infinitesimal to Finite Surfaces

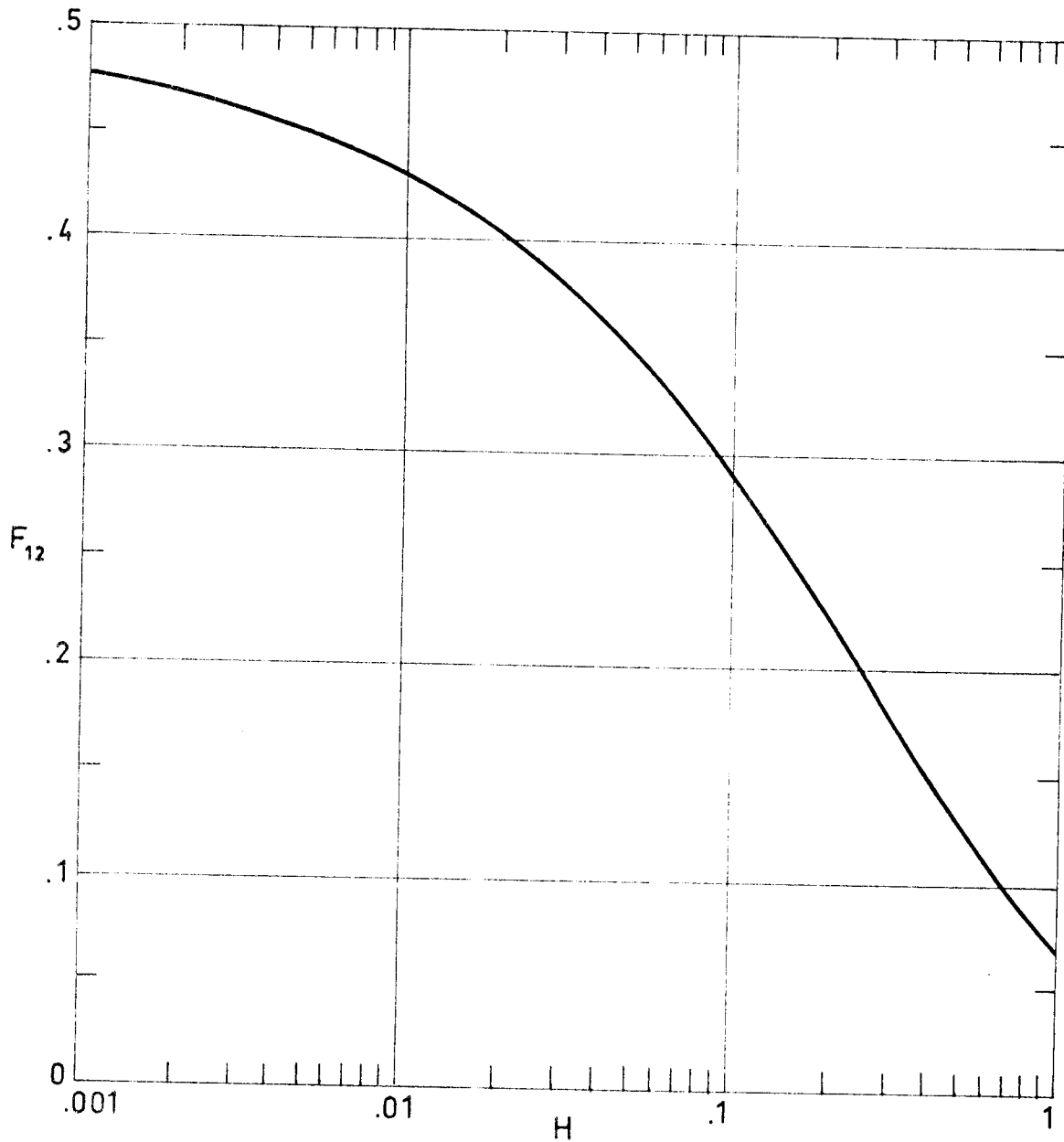


Fig 1-10. F_{12} as a function of H in the case of an infinitesimal sphere viewing a finite sphere. Calculated by the compiler.

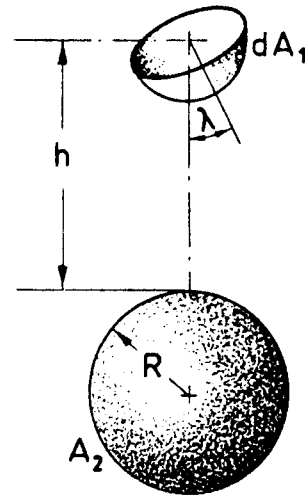
DIFFUSE SURFACES

Infinitesimal to Finite Surfaces

1.2.5.2. CONVEX HEMISPHERICAL SURFACE TO OUTER SPHERE

Convex surface of an infinitesimal hemisphere to sphere.

$$H = \frac{h}{R}$$



Formula:

$$F_{12} = \frac{1}{2} \left[1 - \frac{\sqrt{H^2 + 2H}}{1+H} + \frac{\cos \lambda}{2} \left(\frac{1}{1+H} \right)^2 \right]$$

Reference: Watts (1965).

DIFFUSE SURFACES

Infinitesimal to Finite Surfaces

λ°	0	20	40	50	60	70	80
H							
.001	.7272	.7121	.6688	.6380	.6024	.5630	.5210
.01	.6749	.6601	.6176	.5873	.5524	.5136	.4724
.05	.5743	.5606	.5213	.4933	.4609	.4251	.3869
.1	.4983	.4859	.4500	.4245	.3950	.3624	.3276
.2	.3972	.3868	.3566	.3352	.3104	.2830	.2538
.3	.3284	.3195	.2938	.2756	.2545	.2311	.2062
.5	.2384	.2317	.2124	.1987	.1829	.1653	.1466
1.0	.1295	.1257	.1149	.1072	.0982	.0884	.0778
2.0	.0564	.0547	.0499	.0465	.0425	.0381	.0334
5.0	.0139	.0135	.0123	.0115	.0105	.0094	.0082

λ°	90	100	110	120	140	160	180
H							
.001	.4777	.4343	.3923	.3529	.2865	.2432	.2282
.01	.4298	.3873	.3460	.3073	.2421	.1995	.1847
.05	.3475	.3082	.2700	.2342	.1738	.1345	.1208
.1	.2917	.2558	.2210	.1884	.1334	.0975	.0851
.2	.2236	.1935	.1642	.1368	.0906	.0605	.0500
.3	.1805	.1548	.1299	.1065	.0672	.0415	.0326
.5	.1273	.1080	.0893	.0718	.0422	.0229	.0162
1.0	.0670	.0561	.0456	.0357	.0191	.0083	.0045
2.0	.0286	.0238	.0191	.0147	.0073	.0025	.0008
5.0	.0070	.0058	.0046	.0035	.0017	.0005	.0

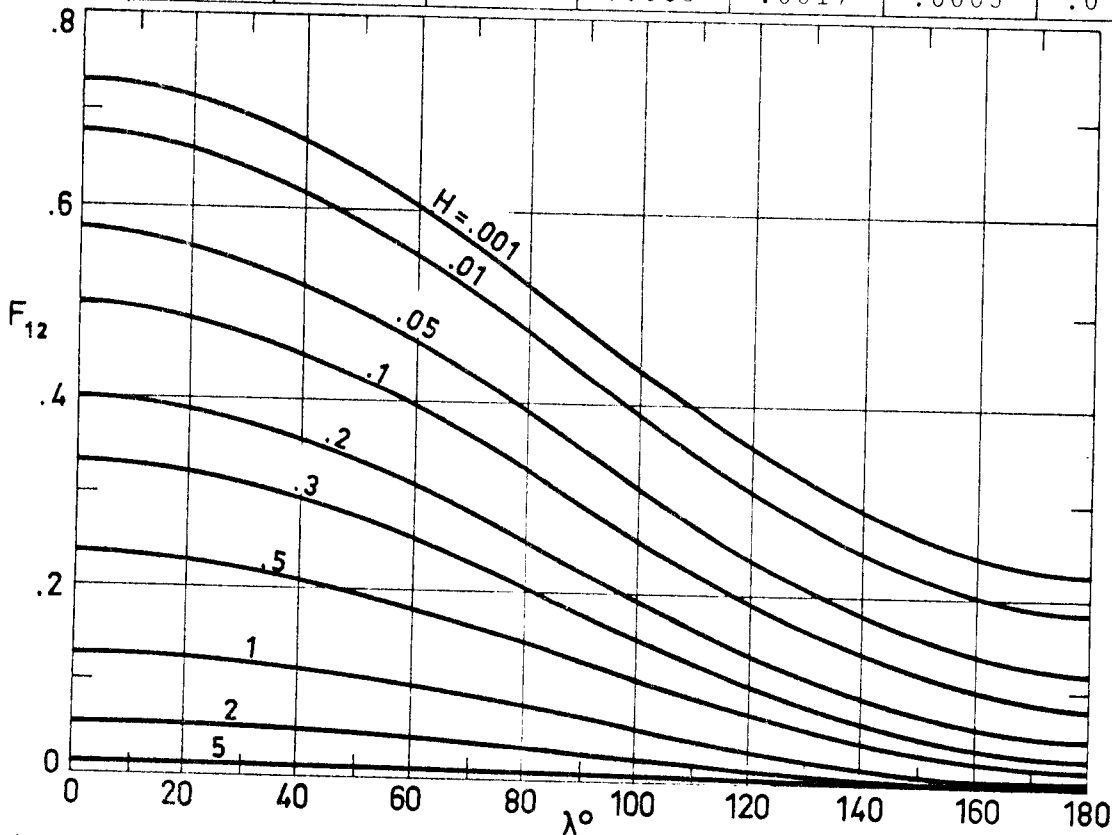


Fig 1-11. F_{12} as a function of angle λ for different values of the dimensionless distance H . Calculated by the compiler.

DIFFUSE SURFACES

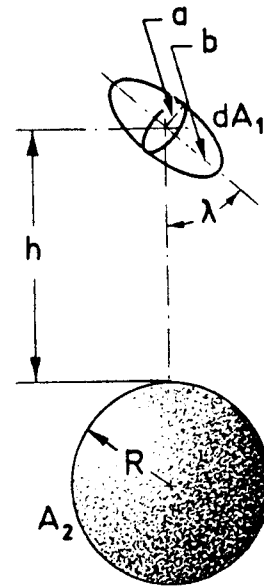
Infinitesimal to Finite Surfaces

1.2.6. ELLIPSOIDAL TO SPHERICAL

Infinitesimal ellipsoid of revolution to sphere.

$$H = \frac{h}{R}$$

$$A = \frac{a}{b}$$



Formula:

$$F_{12} = \frac{1}{S} \int_0^{2\pi} d\phi \int_0^{\theta_0} \sqrt{\frac{A^4 + \tan^2 \Delta}{A^2 + \tan^2 \Delta}} \sin\{\Delta + \tan^{-1}(A^2 \cot \Delta)\} \sin \theta d\theta$$

where:

$$\sin \theta_0 = \frac{1}{1 + H}$$

$$\cos \Delta = \cos \theta \cos \lambda + \sin \theta \sin \lambda \cos \phi$$

$$S = 2\pi \left(A + \frac{\sin^{-1} \sqrt{1-A^2}}{\sqrt{1-A^2}} \right) \quad \text{if } A < 1 \quad (\text{prolate ellipsoid})$$

$$S = 2\pi \left(A + \frac{\ln (A + \sqrt{A^2-1})}{\sqrt{A^2-1}} \right) \quad \text{if } A > 1 \quad (\text{oblate ellipsoid})$$

Reference: Watts (1965).

DIFFUSE SURFACES

Infinitesimal to Finite Surfaces

H \ λ°	0	10	20	30	40
.001	.47386	.47401	.47444	.47513	.47602
.01	.41808	.41854	.41989	.42202	.42477
.05	.32370	.32465	.32744	.33184	.33748
.1	.26166	.26288	.26646	.27209	.27927
.2	.18941	.19086	.19508	.20167	.20997
.3	.14623	.14773	.15209	.15886	.16728
.5	.09645	.09788	.10201	.10833	.11600
1.0	.04596	.04704	.05009	.05461	.05986
2.0	.01807	.01866	.02030	.02264	.02525
5.0	.00435	.00435	.00481	.00544	.00614

H \ λ°	50	60	70	80	90
.001	.47702	.47803	.47893	.47956	.47980
.01	.42788	.43104	.43383	.43578	.43649
.05	.34382	.35018	.35569	.35947	.36082
.1	.28727	.29517	.30189	.30642	.30801
.2	.21906	.22780	.23503	.23978	.24142
.3	.17632	.18485	.19176	.19625	.19780
.5	.12401	.13135	.13717	.14089	.14216
1.0	.06513	.06979	.07340	.07537	.07646
2.0	.02779	.03000	.03169	.03275	.03310
5.0	.00680	.00737	.00780	.00807	.00816

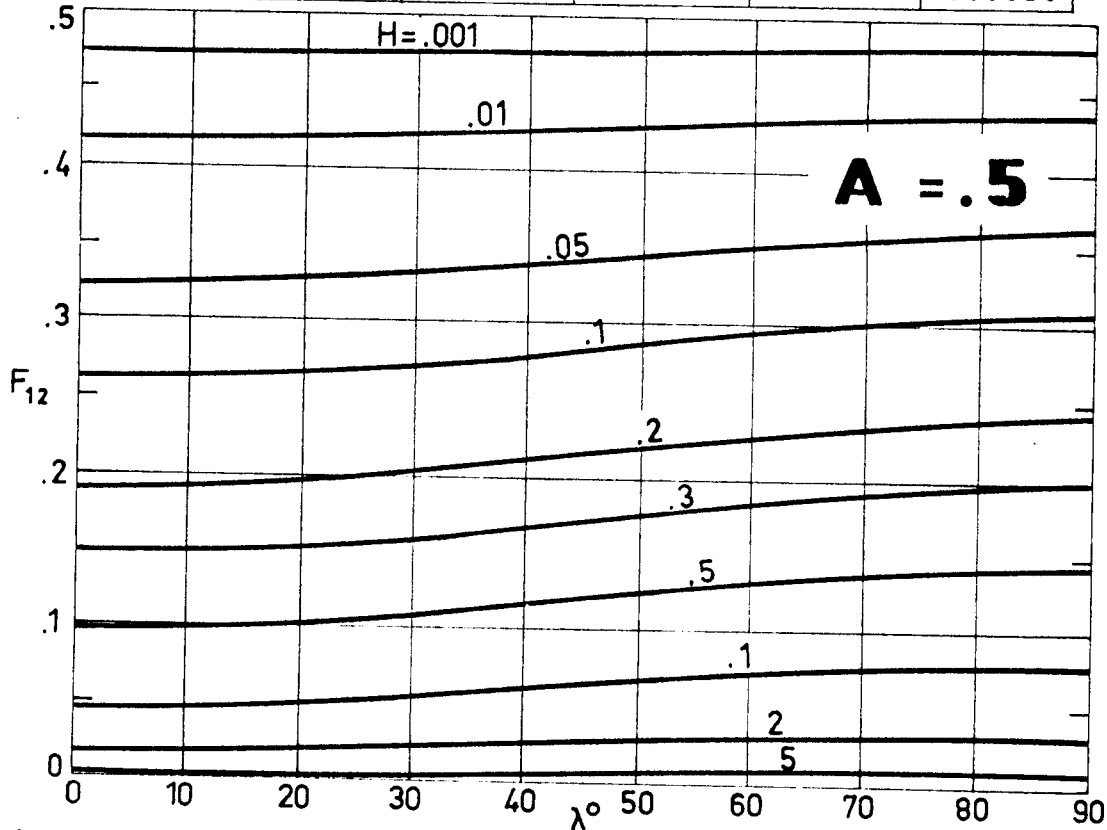


Fig 1-12. F_{12} as a function of λ and H , for $A=0.5$. Calculated by the compiler.

DIFFUSE SURFACES
 Infinitesimal to Finite Surfaces

H \ λ°	0	10	20	30	40
.001	.48106	.48089	.48039	.47967	.47884
.01	.44030	.43976	.43825	.43602	.43343
.05	.36839	.36734	.36440	.36002	.35486
.1	.31735	.31610	.31257	.30725	.30090
.2	.25171	.25040	.24666	.24096	.23403
.3	.20782	.20660	.20305	.19760	.19089
.5	.15083	.14981	.14686	.14227	.13655
1.0	.08202	.08140	.07958	.07673	.07312
2.0	.03577	.03548	.03463	.03330	.03160
5.0	.00885	.00878	.00856	.00822	.00778

H \ λ°	50	60	70	80	90
.001	.47801	.47729	.47676	.47644	.47633
.01	.43082	.42851	.42671	.42558	.42520
.05	.34960	.34486	.34113	.33887	.33796
.1	.29435	.28839	.28367	.28066	.27963
.2	.22675	.22003	.21463	.21115	.20996
.3	.18375	.17707	.17165	.16814	.16693
.5	.13034	.12443	.11956	.11636	.11524
1.0	.06912	.06522	.06192	.05971	.05974
2.0	.02969	.02778	.02617	.02504	.02464
5.0	.00729	.00679	.00636	.00606	.00595

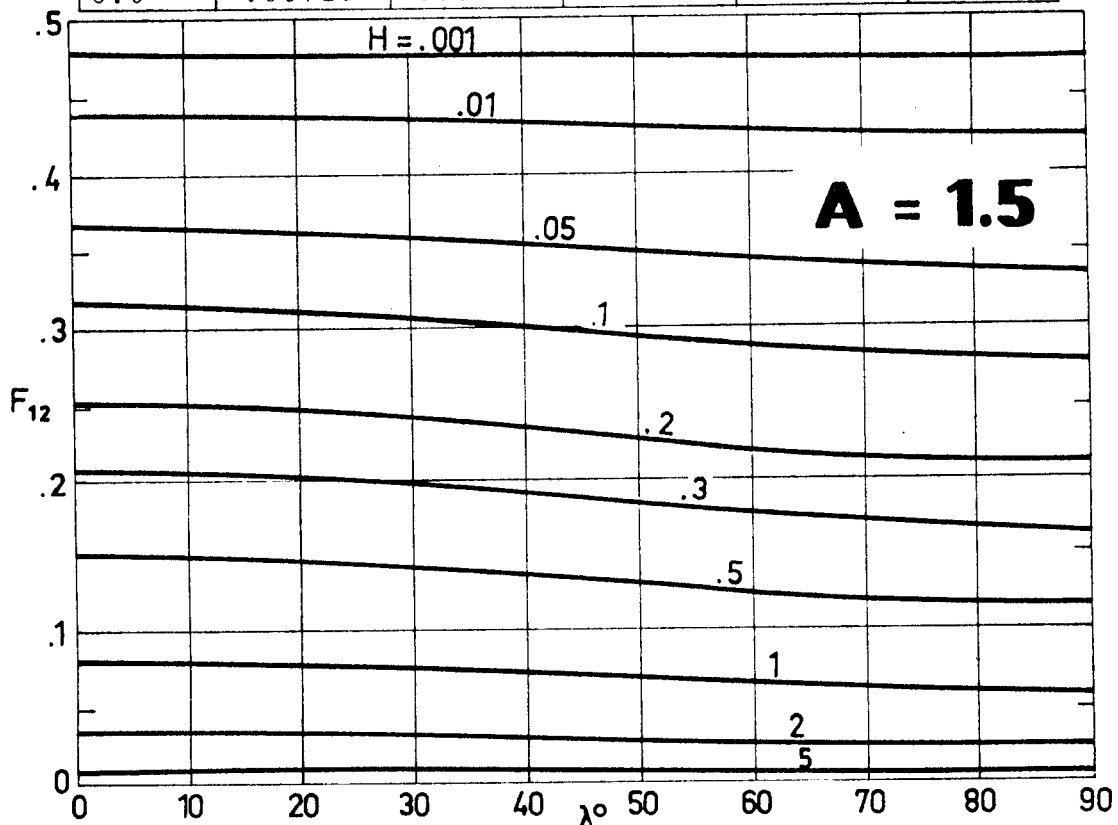


Fig 1-13. F_{12} as a function of λ and H , for $A=1.5$. Calculated by the compiler.

DIFFUSE SURFACES

Infinitesimal to Finite Surfaces

H \ λ°	0	10	20	30	40
.001	.48379	.48343	.48246	.48111	.47963
.01	.44865	.44757	.44462	.44045	.43581
.05	.38460	.38261	.37705	.36900	.35978
.1	.33685	.33457	.32810	.31850	.30722
.2	.27239	.27011	.26357	.25357	.24143
.3	.22750	.22542	.21938	.21002	.19842
.5	.16732	.16565	.16078	.15312	.14340
1.0	.09225	.09126	.08836	.08375	.07777
2.0	.04055	.04010	.03878	.03666	.03389
5.0	.01008	.00997	.00963	.00909	.00839

H \ λ°	50	60	70	80	90
.001	.47824	.47715	.47648	.47620	.47614
.01	.43133	.42752	.42474	.42313	.42262
.05	.35066	.34268	.33663	.33294	.33171
.1	.29585	.28573	.27792	.27308	.27146
.2	.22878	.21723	.20811	.20236	.20041
.3	.18604	.17448	.16520	.15927	.15724
.5	.13271	.12241	.11390	.10834	.10641
1.0	.07098	.06416	.05826	.05426	.05284
2.0	.03068	.02738	.02441	.02232	.02156
5.0	.00756	.00670	.00591	.00533	.00512

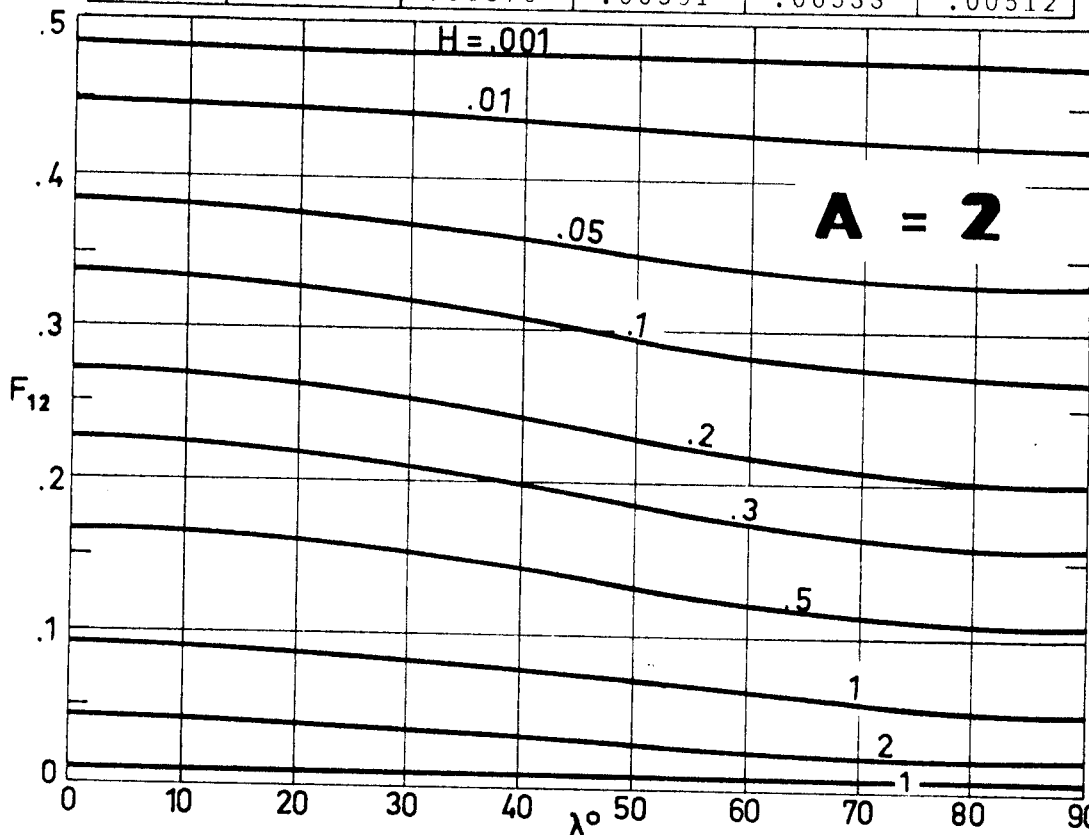


Fig 1-14. F_{12} as a function of λ and H , for $A=2$. Calculated by the compiler.

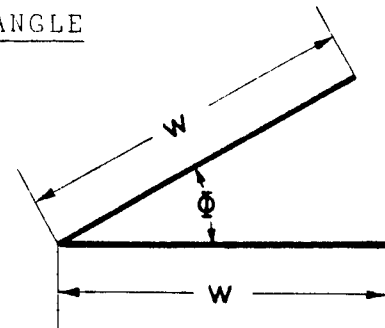
DIFFUSE SURFACES
Finite to Finite Surfaces

1.3. FINITE TO FINITE SURFACE

1.3.1. PLANAR TO PLANAR. TWO-DIMENSIONAL CONFIGURATIONS

1.3.1.1. TWO STRIPS OF EQUAL WIDTH AT ANY ANGLE

Two infinitely long plates of equal finite width w , having one common edge, and at an included angle ϕ to each other.



Formula:

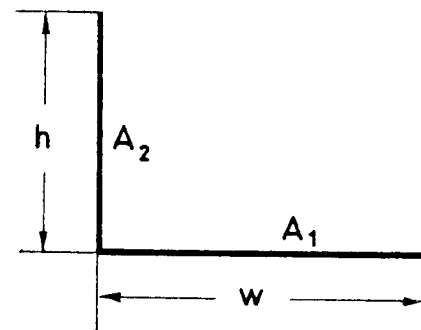
$$F_{12} = F_{21} = 1 - \sin \frac{\phi}{2}$$

Reference: Siegel & Howell (1972).

1.3.1.2. TWO STRIPS OF UNEQUAL WIDTH NORMAL TO EACH OTHER

Two infinitely long plates of unequal finite width, having one common edge, and at an included angle $\phi = 90^\circ$ to each other.

$$H = \frac{h}{w}$$



Formula:

$$F_{12} = HF_{21} = \frac{1}{2} \left[1 + H - \sqrt{1+H^2} \right]$$

References: Kreith (1962), Siegel & Howell (1972).

INTENTIONALLY BLANK PAGE

DIFFUSE SURFACES
Finite to Finite Surfaces

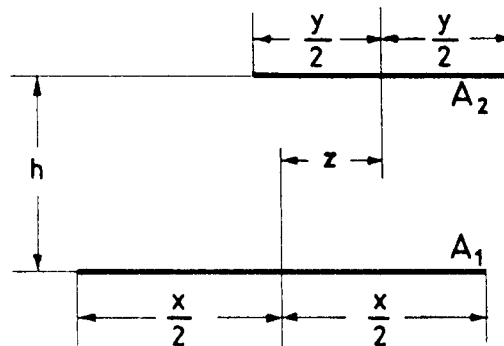
1.3.1.3. TWO PARALLEL STRIPS

Two infinitely long parallel strips of unequal width.

$$X = \frac{x}{h}$$

$$Y = \frac{y}{h}$$

$$Z = \frac{z}{h}$$



Formula:

$$F_{12} = \frac{Y}{X} \quad F_{21} = \frac{1}{2X} \left[\sqrt{1 + \left(\frac{Y+X-2Z}{2}\right)^2} + \sqrt{1 + \left(\frac{Y+X+2Z}{2}\right)^2} - \sqrt{1 + \left(\frac{X-Y-2Z}{2}\right)^2} - \sqrt{1 + \left(\frac{X-Y+2Z}{2}\right)^2} \right]$$

Reference: Kutateladze & Borishanskii (1966).

When $X=Y$ and $Z=0$, one obtains:

$$F_{12} = F_{21} = \frac{1}{X} \left[\sqrt{1 + X^2} - 1 \right]$$

References: Kreith (1962), Siegel & Howell (1972).

DIFFUSE SURFACES
Finite to Finite Surfaces

Y \ X	.1	.2	.4	.6	.8	1
.1	.04988	.04969	.04897	.04784	.04638	.04469
.2	.09938	.09902	.09761	.09538	.09250	.08916
.3	.14816	.14764	.14558	.14233	.13812	.13321
.4	.19589	.19522	.19258	.18841	.18298	.17662
.6	.28705	.28615	.28262	.27698	.26958	.26082
1.0	.44686	.44579	.44156	.43470	.42547	.41421
2.0	.70689	.70622	.70356	.69911	.69284	.68474
4.0	.89438	.89425	.89371	.89280	.89150	.88981
6.0	.94867	.94864	.94849	.94825	.94791	.94747
10.0	.98058	.98057	.98055	.98052	.98046	.98040

Y \ X	2	4	6	8	10	15
.1	.03534	.02236	.01581	.01213	.00981	.00661
.2	.07062	.04471	.03162	.02425	.01961	.01322
.3	.10577	.06705	.04743	.03638	.02942	.01982
.4	.14071	.08937	.06323	.04850	.03922	.02643
.6	.20973	.13392	.09483	.07275	.05883	.03965
1.0	.34237	.22245	.17791	.12121	.09804	.06608
2.0	.61803	.43702	.31451	.24209	.19597	.13214
4.0	.87403	.78078	.61413	.48084	.39088	.26415
6.0	.94352	.92120	.84713	.70711	.58262	.39585
10.0	.97983	.97720	.97103	.95515	.90499	.65649

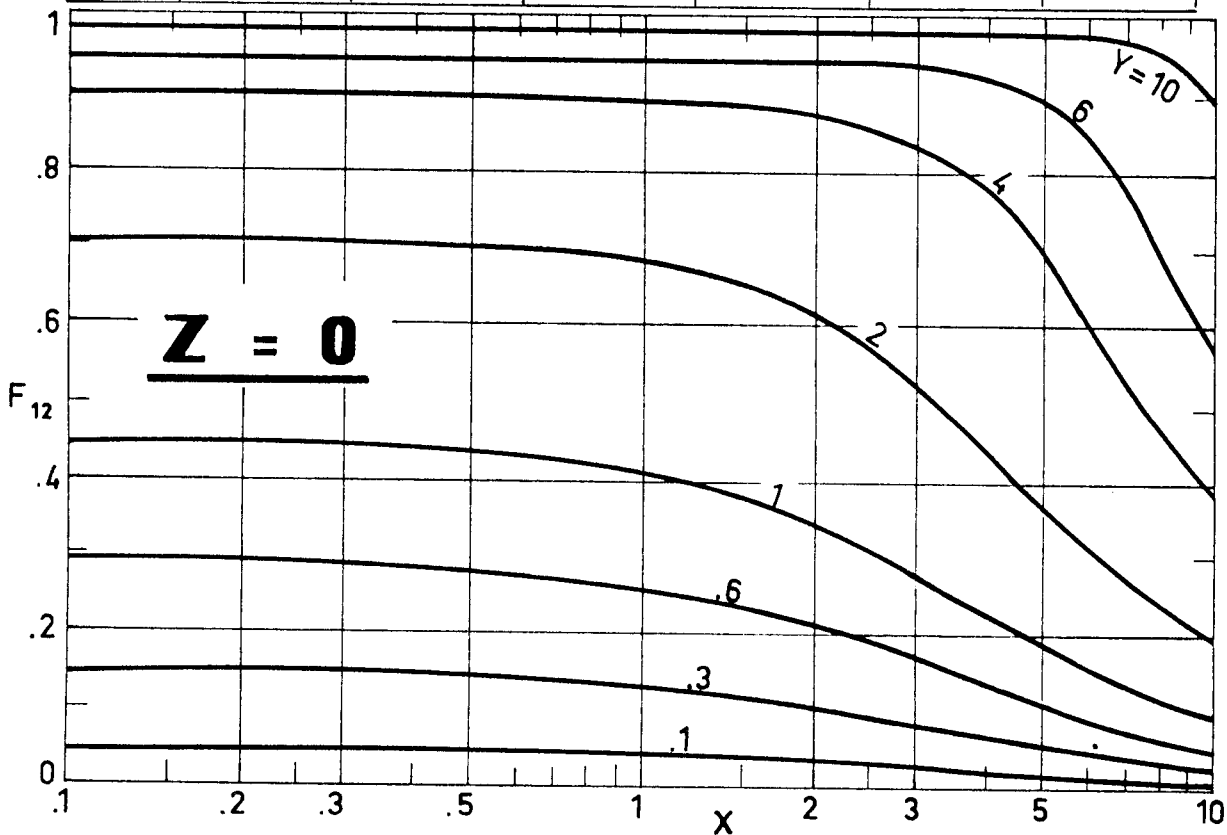


Fig 1-15. Values of F_{12} as a function of X and Y , for $Z=0$. Calculated by the compiler.

DIFFUSE SURFACES
Finite to Finite Surfaces

X \ Y	.1	.2	.4	.6	.8	1
.1	.03578	.03578	.03576	.03571	.03558	.03534
.2	.07155	.07155	.07151	.07139	.07112	.07062
.3	.10731	.10730	.10721	.10699	.10655	.10577
.4	.14305	.14301	.14285	.14249	.14182	.14071
.6	.21426	.21416	.21374	.21294	.21164	.20973
1.0	.35344	.35311	.35178	.34956	.34642	.34237
2.0	.63940	.63872	.63601	.63158	.62554	.61803
4.0	.88020	.88002	.87929	.87807	.87632	.87403
6.0	.94499	.94494	.94477	.94448	.94406	.94352
10.0	.98003	.98002	.98000	.97996	.97990	.97983

X \ Y	2	4	6	8	10	15
.1	.03197	.02201	.01575	.01211	.00980	.00661
.2	.06387	.04400	.03150	.02422	.01960	.01321
.3	.09564	.06598	.04724	.03633	.02940	.01982
.4	.12720	.08793	.06298	.04844	.03920	.02643
.6	.18947	.13171	.09445	.07265	.05880	.03964
1.0	.30902	.21851	.15725	.12105	.09798	.06607
2.0	.56482	.42648	.31287	.24171	.19584	.13213
4.0	.85296	.75172	.60659	.47946	.39051	.26412
6.0	.93862	.90989	.82755	.70138	.58148	.39577
10.0	.97920	.97628	.96914	.94939	.89320	.65606

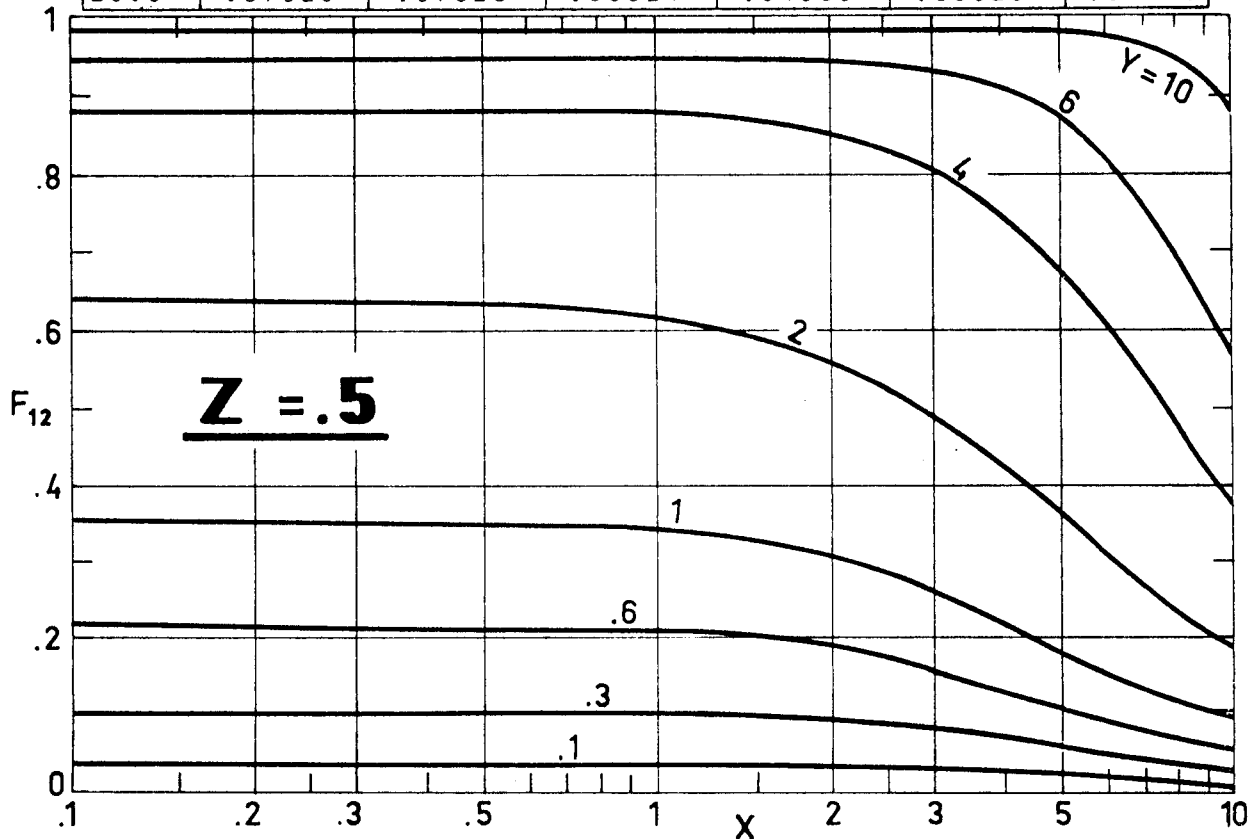


Fig 1-16. Values of F_{12} as a function of X and Y, for $Z=.5$. Calculated by the compiler.

DIFFUSE SURFACES
Finite to Finite Surfaces

X \ Y	.1	.2	.4	.6	.8	1
.1	.01771	.01776	.01796	.01828	.01872	.01925
.2	.03552	.03562	.03601	.03665	.03752	.03859
.3	.05353	.05367	.05426	.05521	.05649	.05807
.4	.07183	.07202	.07279	.07403	.07572	.07778
.6	.10967	.10995	.11105	.11284	.11523	.11813
1.0	.19255	.19293	.19445	.19688	.20007	.20382
2.0	.44719	.44712	.44685	.44640	.44575	.44490
4.0	.82778	.82743	.82603	.82368	.82038	.81611
6.0	.93226	.93219	.93189	.93139	.93069	.92976
10.0	.97827	.97826	.97823	.97818	.97810	.97801

X \ Y	2	4	6	8	10	15
.1	.02236	.02069	.01554	.01206	.00978	.00661
.2	.04471	.04137	.03107	.02412	.01957	.01321
.3	.06705	.06201	.04660	.03617	.02935	.01982
.4	.08937	.08260	.06213	.04823	.03913	.02642
.6	.13392	.12355	.09314	.07233	.05869	.03963
1.0	.22245	.20403	.15496	.12049	.09780	.06605
2.0	.43702	.39039	.30707	.24042	.19544	.13208
4.0	.78078	.67911	.58082	.47460	.38929	.26400
6.0	.92120	.87123	.77847	.68181	.57750	.39552
10.0	.97720	.97323	.96250	.92975	.86362	.65459

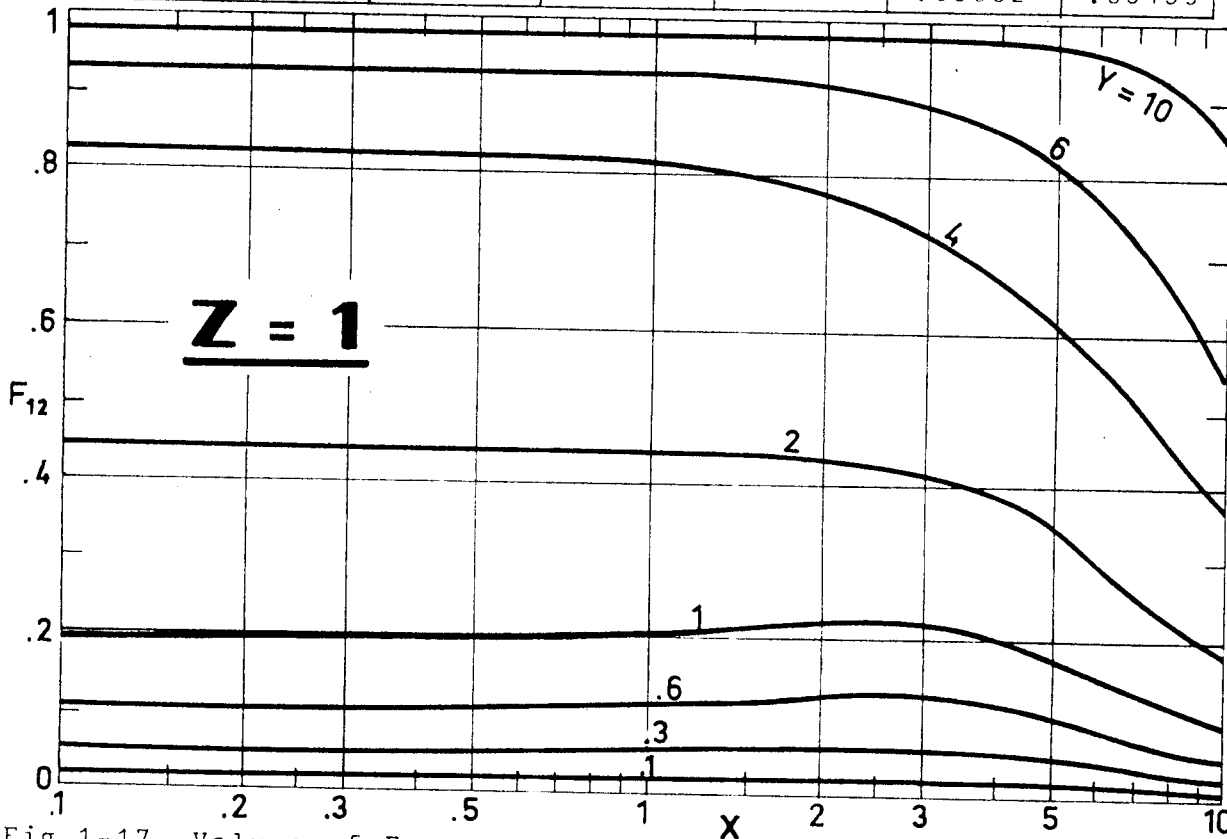


Fig 1-17. Values of F_{12} as a function of X and Y , for $Z=1$. Calculated by the compiler.

DIFFUSE SURFACES
Finite to Finite Surfaces

Y \ X	.1	.2	.4	.6	.8	1
.3	.01352	.01355	.01367	.01388	.01418	.01457
.6	.02759	.02765	.02791	.02834	.02895	.02976
1.0	.04825	.04837	.04883	.04961	.05072	.05218
2.0	.12089	.12121	.12247	.12457	.12754	.13137
3.0	.25733	.25785	.25993	.26329	.26781	.27331
4.0	.48507	.48506	.48504	.48500	.48494	.48486
5.0	.71152	.71098	.70885	.70540	.70074	.69506
6.0	.84373	.84340	.84206	.83981	.83665	.83257
8.0	.94039	.94032	.94004	.93958	.93892	.93806
10.0	.96931	.96929	.96922	.96909	.96892	.96869

Y \ X	2	4	6	8	10	15
.3	.01826	.03638	.04214	.03526	.02908	.01978
.6	.03737	.07275	.08398	.07047	.05815	.03957
1.0	.06568	.12121	.13876	.11726	.09687	.06594
2.0	.16274	.24209	.26631	.23251	.19333	.13185
3.0	.30811	.36220	.37591	.34241	.28877	.19770
4.0	.48419	.48084	.47140	.44139	.38206	.26344
5.0	.65871	.59671	.55926	.52564	.47074	.32902
6.0	.79893	.70711	.64277	.59862	.55048	.39432
8.0	.93003	.88278	.79816	.72878	.67700	.52322
10.0	.96663	.95515	.91746	.84625	.78159	.64514

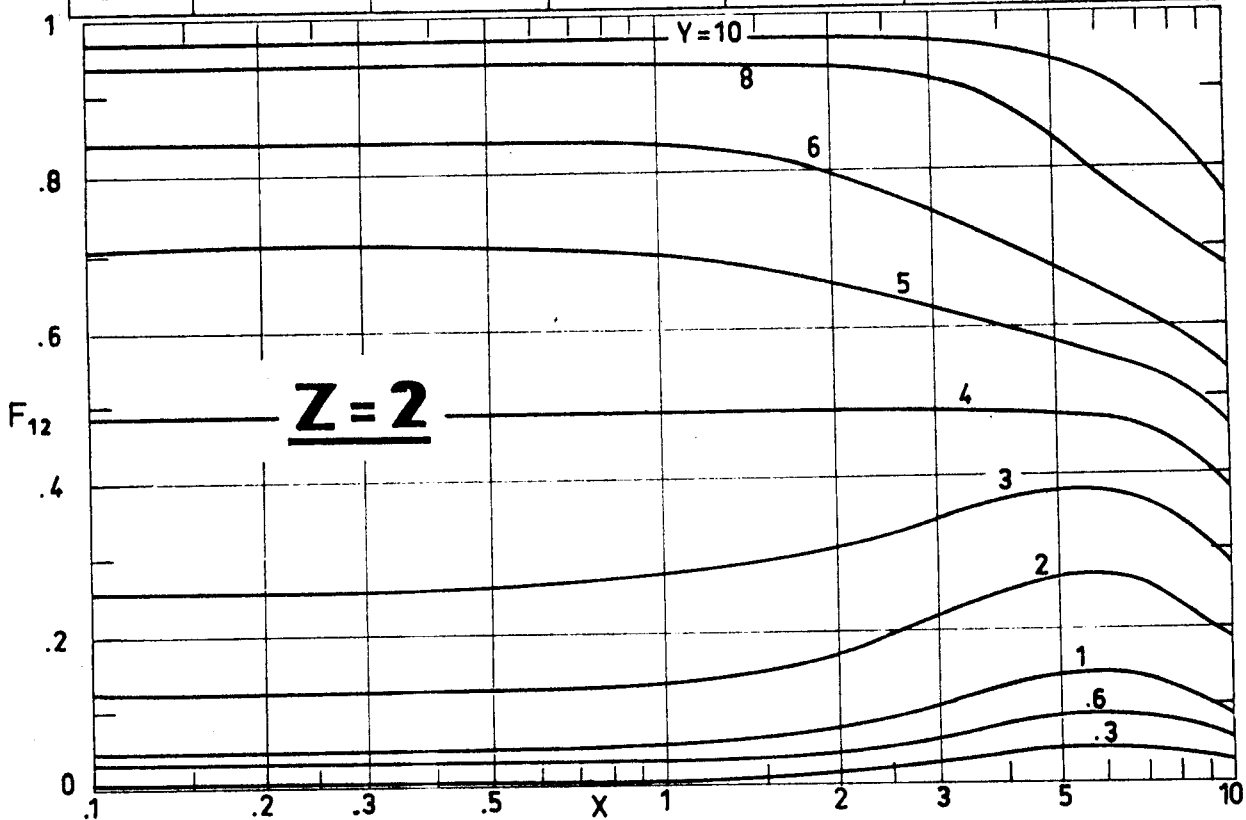


Fig 1-18. Values of F_{12} as a function of X and Y, for $Z=2$. Calculated by the compiler.

DIFFUSE SURFACES
Finite to Finite Surfaces

Y \ X	.1	.2	.4	.6	.8	1
.4	.00151	.00151	.00152	.00152	.00153	.00154
.6	.00228	.00228	.00228	.00229	.00231	.00232
1.0	.00384	.00384	.00385	.00387	.00389	.00391
2.0	.00813	.00813	.00815	.00819	.00823	.00829
4.0	.02064	.02066	.02072	.02084	.02100	.02121
6.0	.04895	.04901	.04928	.04973	.05038	.05122
8.0	.14350	.14383	.14516	.14738	.15051	.15456
9.0	.27382	.27436	.27647	.27990	.28451	.29014
9.5	.37626	.37666	.37822	.38070	.38395	.38777
10.0	.49752	.49752	.49752	.49752	.49751	.49751

Y \ X	2	4	6	8	10	15
.4	.00163	.00207	.00329	.00726	.01990	.02567
.6	.00246	.00313	.00497	.01105	.02985	.03849
1.0	.00415	.00530	.00854	.01932	.04975	.06410
2.0	.00883	.01156	.01969	.04697	.09950	.12770
4.0	.02311	.03394	.07033	.13914	.19897	.24929
6.0	.05906	.10550	.18846	.25449	.29387	.34840
8.0	.18789	.27828	.33932	.37517	.39765	.42485
9.0	.32604	.38590	.41800	.43607	.44721	.46007
9.5	.40967	.44145	.45761	.46656	.47197	.47737
10.0	.49749	.49742	.49728	.49706	.49671	.49453

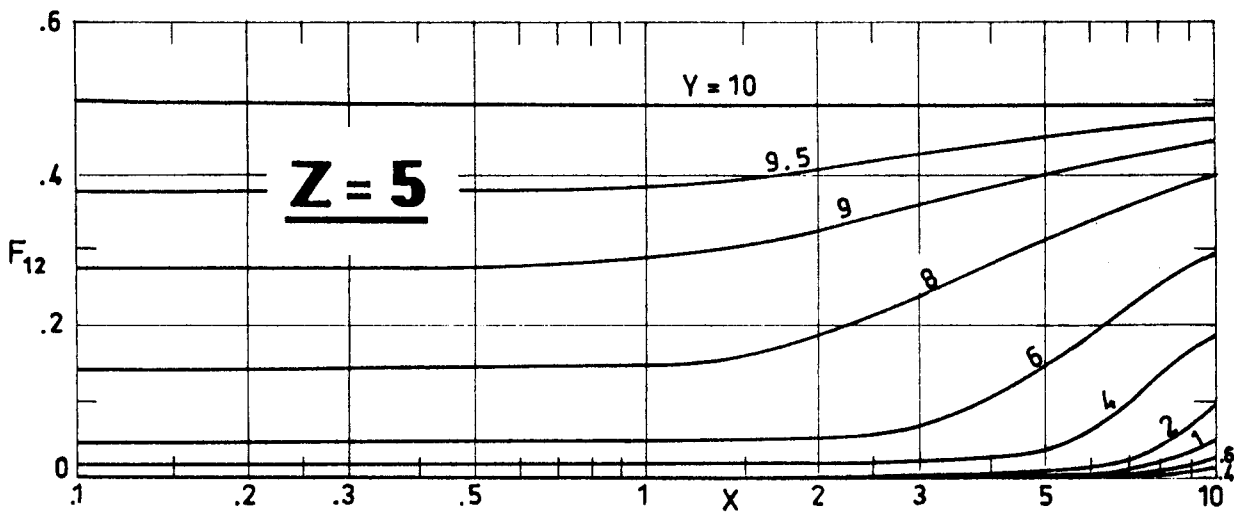


Fig 1-19. Values of F_{12} as a function of X and Y , for $Z=5$. Calculated by the compiler.

DIFFUSE SURFACES

Finite to Finite Surfaces

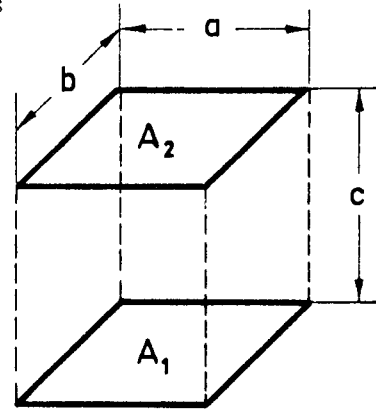
1.3.2. PLANAR TO PLANAR. THREE-DIMENSIONAL CONFIGURATIONS

1.3.2.1. PARALLEL RECTANGLES OF THE SAME DIMENSIONS

Parallel, directly opposed rectangles of same width and length.

$$X = \frac{a}{c}$$

$$Y = \frac{b}{c}$$



Formulae:

$$F_{12} = \frac{2}{\pi XY} \left\{ \ln \left[\frac{(1+X^2)(1+Y^2)}{1+X^2+Y^2} \right]^{1/2} + X\sqrt{1+Y^2} \tan^{-1} \frac{X}{\sqrt{1+Y^2}} + \right. \\ \left. + Y\sqrt{1+X^2} \tan^{-1} \frac{Y}{\sqrt{1+X^2}} - X \tan^{-1} X - Y \tan^{-1} Y \right\}$$

When $X \sim Y \ll 1$, $F_{12} = \frac{XY}{\pi}$.

References: Hamilton & Morgan (1952), Jakob (1957), Kreith (1962), Hsu (1967), Siegel & Howell (1972).

DIFFUSE SURFACES
Finite to Finite Surfaces

X \ Y	.1	.2	.4	.6	.8	1.0
.1	.00316	.00626	.01207	.01715	.02141	.02492
.2	.00626	.01240	.02392	.03398	.04243	.04941
.3	.00925	.01832	.03532	.05020	.06272	.07305
.4	.01207	.02392	.04614	.06560	.08199	.09554
.6	.01715	.03398	.06560	.09336	.11683	.13627
1.0	.02492	.04941	.09554	.13627	.17092	.19982
2.0	.03514	.06971	.13513	.19342	.24356	.28588
4.0	.04209	.08353	.16219	.23271	.29387	.34596
10.0	.04671	.09272	.18021	.25896	.32759	.38638
∞	.04988	.09902	.19258	.27698	.35078	.41421

X \ Y	2	4	6	8	10	∞
.1	.03514	.04209	.04463	.04592	.04671	.04988
.2	.06971	.08353	.08858	.09116	.09272	.09902
.3	.10318	.12372	.13123	.13507	.13739	.14677
.4	.13530	.16219	.17209	.17715	.18021	.19258
.6	.19342	.23271	.24712	.25449	.25896	.27698
1.0	.28588	.34596	.36813	.37950	.38638	.39982
2.0	.41525	.50899	.54421	.56236	.57338	.61803
4.0	.50899	.63204	.67954	.70426	.71933	.78078
10.0	.57338	.71933	.77741	.80811	.82699	.90499
∞	.61803	.78078	.84713	.88278	.90499	1

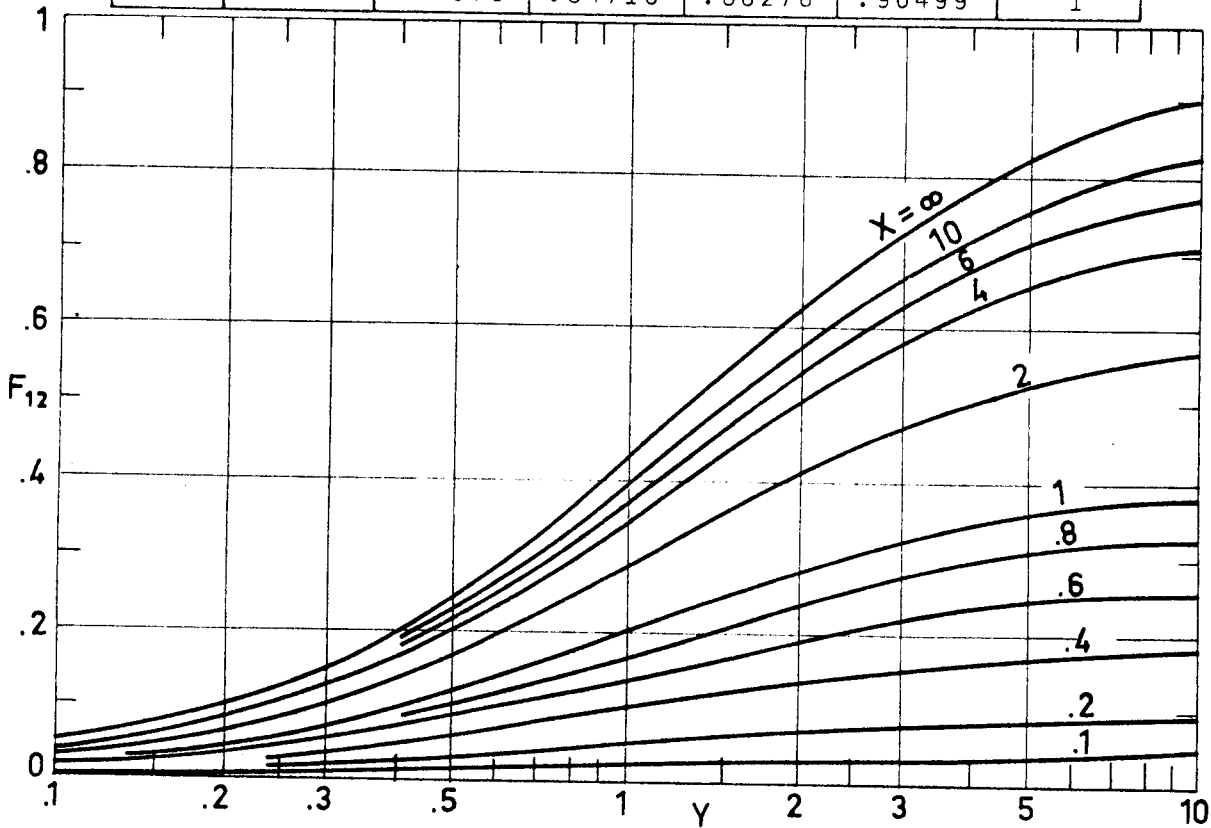


Fig 1-20. Values of F_{12} as a function of X and Y . Calculated by the compiler.

DIFFUSE SURFACES
Finite to Finite Surfaces

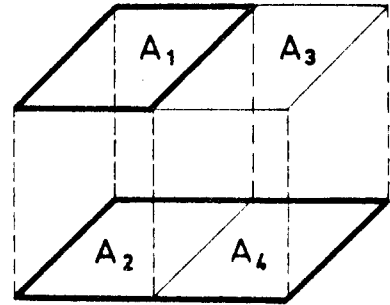
1.3.2.2. PARALLEL RECTANGLES OF UNEQUAL DIMENSIONS

The following view factors can be deduced by using the results for two parallel directly opposed rectangles.

Two rectangles in parallel planes with one rectangle directly opposite to portion of the other. View Factor is:

$$F_{1(2,4)} = \frac{1}{2A_1} (A_{(1,3)} F_{(1,3)(2,4)} + A_1 F_{12} - A_3 F_{34})$$

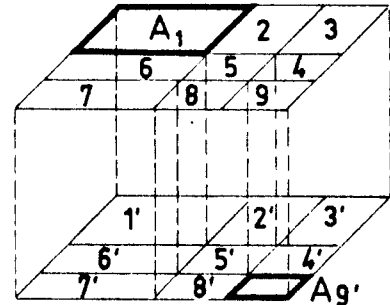
References: Moon (1961), Kreith (1962), Hsu (1967).



Two rectangles of arbitrary size in parallel planes with one edge of a rectangle parallel to one of the other. View Factor is:

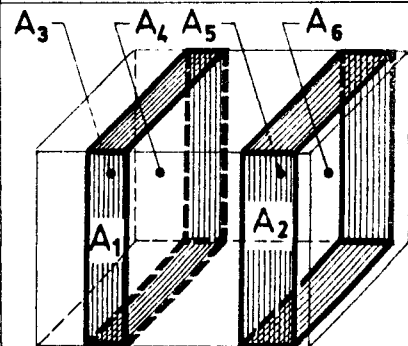
$$A_1 F_{19'} = \frac{1}{4} [K_{(1,2,3,4,5,6,7,8,9)}^2 - K_{(1,2,5,6,7,8)}^2 - K_{(2,3,4,5,8,9)}^2 - K_{(1,2,3,4,5,6)}^2 + K_{(1,2,5,6)}^2 + K_{(2,3,4,5)}^2 + K_{(4,5,8,9)}^2 - K_{(4,5)}^2 - K_{(5,8)}^2 - K_{(5,6)}^2 - K_{(4,5,6,7,8,9)}^2 + K_{(5,6,7,8)}^2 + K_{(4,5,6)}^2 + K_{(2,5,8)}^2 - K_{(2,5)}^2 + K_5^2], \text{ where } K_m^2 = A_m F_{mm}$$

Reference: Hsu (1967).



Finite area on interior of a rectangular channel. View Factor is:

$$F_{12} = \frac{A_4}{A_1} [F_{45} + F_{36} - F_{46} - F_{35}]$$

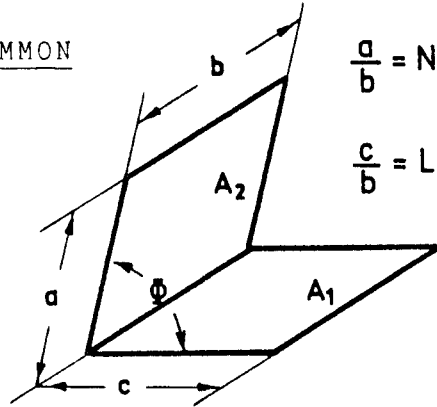


INTENTIONALLY BLANK PAGE

DIFFUSE SURFACES
Finite to Finite Surfaces

1.3.2.3. RECTANGLES WITH ONE COMMON EDGE

Two rectangles A_1 and A_2 with one common edge and included angle ϕ between the two planes.



Formulae:

$$F_{12} = \frac{1}{\pi L} \left(-\frac{\sin 2\phi}{4} \left[NL \sin \phi + \left(\frac{\pi}{2} - \phi \right) (N^2 + L^2) + L^2 \tan^{-1} \left(\frac{N - L \cos \phi}{L \sin \phi} \right) + N^2 \tan^{-1} \left(\frac{L - N \cos \phi}{N \sin \phi} \right) \right] + \right. \\ \left. + \frac{\sin^2 \phi}{4} \log_e \left\{ \left[\frac{(1 + N^2)(1 + L^2)}{1 + N^2 + L^2 - 2NL \cos \phi} \right]^{\csc^2 \phi + \cot^2 \phi} \left[\frac{L^2(1 + N^2 + L^2 - 2NL \cos \phi)}{(1 + L^2)(N^2 + L^2 - 2NL \cos \phi)} \right]^{L^2} \right\} + \right. \\ \left. + \frac{N^2 \sin^2 \phi}{4} \log_e \left[\left(\frac{N^2}{N^2 + L^2 - 2NL \cos \phi} \right) \left(\frac{1 + N^2}{1 + N^2 + L^2 - 2NL \cos \phi} \right)^{\cos 2\phi} \right] + L \tan^{-1} \left(\frac{1}{L} \right) + \right. \\ \left. + N \tan^{-1} \left(\frac{1}{N} \right) - \sqrt{N^2 + L^2 - 2NL \cos \phi} \cot^{-1} \sqrt{N^2 + L^2 - 2NL \cos \phi} + \right. \\ \left. + \frac{N \sin \phi \sin 2\phi}{2} \sqrt{1 + N^2 \sin^2 \phi} \left[\tan^{-1} \left(\frac{N \cos \phi}{\sqrt{1 + N^2 \sin^2 \phi}} \right) + \tan^{-1} \left(\frac{L - N \cos \phi}{\sqrt{1 + N^2 \sin^2 \phi}} \right) \right] + \right. \\ \left. + \cos \phi \int_0^L \sqrt{1 + z^2 \sin^2 \phi} \left[\tan^{-1} \left(\frac{N - z \cos \phi}{\sqrt{1 + z^2 \sin^2 \phi}} \right) + \tan^{-1} \left(\frac{z \cos \phi}{\sqrt{1 + z^2 \sin^2 \phi}} \right) \right] dz \right)$$

FOR $\phi = 90^\circ$,

$$F_{12} = \frac{1}{\pi L} \left(L \tan^{-1} \left(\frac{1}{L} \right) + N \tan^{-1} \left(\frac{1}{N} \right) - \sqrt{N^2 + L^2} \tan^{-1} \left(\frac{1}{\sqrt{N^2 + L^2}} \right) + \right. \\ \left. + \frac{1}{4} \log_e \left\{ \left[\frac{(1 + L^2)(1 + N^2)}{1 + N^2 + L^2} \right] \left[\frac{L^2(1 + L^2 + N^2)}{(1 + L^2)(L^2 + N^2)} \right]^{L^2} \left[\frac{N^2(1 + L^2 + N^2)}{(1 + N^2)(L^2 + N^2)} \right]^{N^2} \right\} \right)$$

$$\lim_{L \rightarrow \infty} F_{12} = 0 \quad \lim_{N \rightarrow \infty} F_{12} = \frac{1}{\pi} \left[\tan^{-1} \left(\frac{1}{L} \right) + \frac{1}{4L} \log_e (1 + L^2) - \frac{L}{4} \log_e \left(\frac{1 + L^2}{L^2} \right) \right]$$

References: Hamilton & Morgan (1952), Hottel (1954), Jakob (1957), Kreith (1962), Feingold (1966), Redor (1973).

DIFFUSE SURFACES
Finite to Finite Surfaces

$\phi = 30^\circ$

L \ N	.05	.1	.2	.4	.6	1
.1	.43521	.72838	.86050	.88904	.89475	.89800
.2	.22527	.43025	.71563	.84082	.85934	.86820
.4	.11381	.22226	.42041	.69039	.77761	.81211
.6	.07606	.14912	.28645	.51841	.66573	.75470
1.0	.04571	.08980	.17364	.32484	.45282	.61903
2.0	.02287	.04497	.08718	.16454	.23363	.35005
4.0	.01144	.02250	.04363	.08248	.11738	.17746
6.0	.00763	.01500	.02909	.05501	.07831	.11850
10.0	.00457	.00900	.01746	.03301	.04700	.07115
20.0	.00229	.00450	.00873	.01651	.02350	.03558

L \ N	2	4	6	10	20	∞
.1	.89950	.89989	.89996	.90000	.90001	.90002
.2	.87180	.87265	.87280	.87288	.87290	.87292
.4	.82272	.82478	.82511	.82527	.82534	.82536
.6	.77877	.78256	.78311	.78337	.78347	.78350
1.0	.70010	.70985	.71099	.71148	.71166	.71172
2.0	.52131	.57343	.57761	.57902	.57945	.57957
4.0	.28671	.39454	.41866	.42497	.42631	.42659
6.0	.19253	.27911	.31977	.33788	.34111	.34161
10.0	.11580	.16999	.20273	.23596	.24796	.24922
20.0	.05794	.08526	.10233	.12398	.14831	.15498

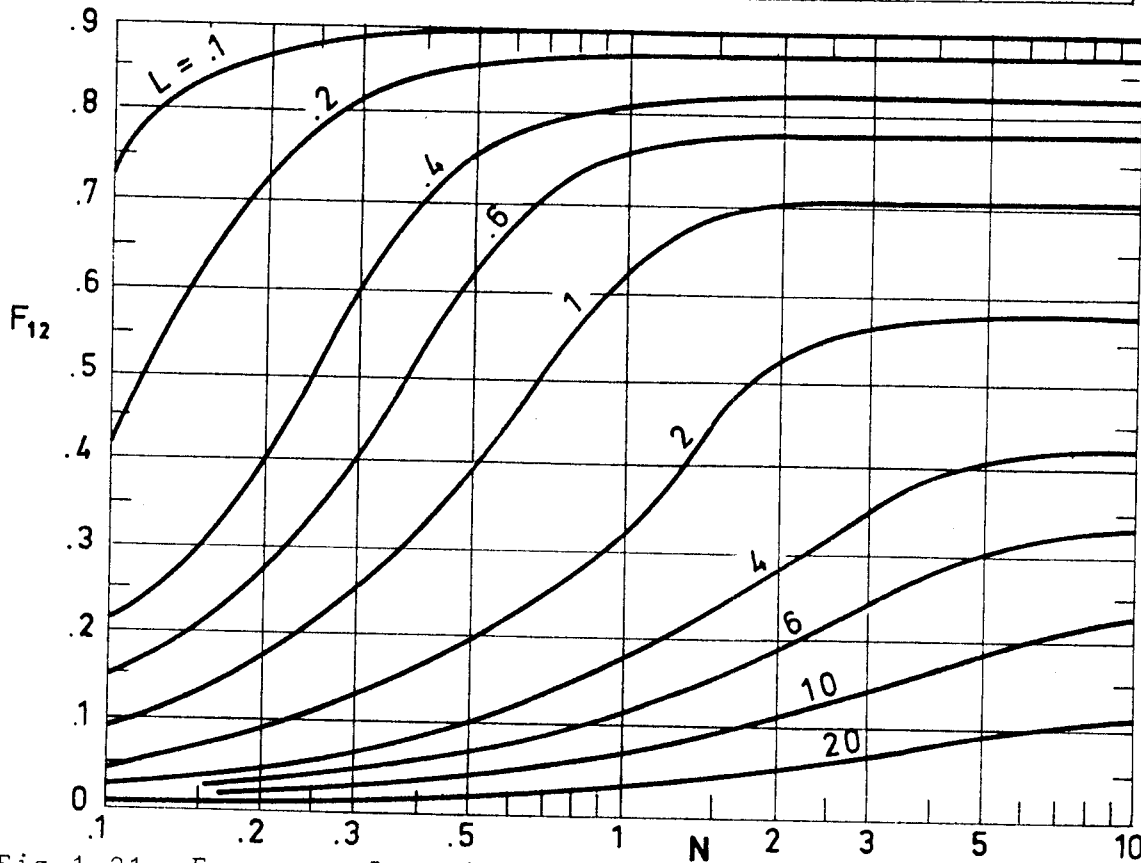


Fig 1-21. F_{12} as a function of L and N for $\phi = 30^\circ$. Table from Feingold (1966), figure from Hamilton & Morgan (1952).

DIFFUSE SURFACES
Finite to Finite Surfaces

$\phi = 60^\circ$

L \ N	.05	.1	.2	.4	.6	1
.1	.31075	.48559	.60910	.66254	.67630	.68481
.2	.16994	.30455	.47129	.58469	.61658	.63588
.4	.08789	.16564	.29235	.44348	.50900	.55369
.6	.05911	.11272	.20553	.33934	.41725	.48358
1.0	.03567	.06848	.12718	.22148	.29015	.37091
2.0	.01788	.03445	.06450	.11495	.15548	.21499
4.0	.00895	.01725	.03237	.05799	.07900	.11147
6.0	.00597	.01151	.02159	.03872	.05281	.07475
10.0	.00358	.00690	.01296	.02325	.03173	.04498
20.0	.00179	.00345	.00648	.01163	.01587	.02251

L \ N	2	4	6	10	20	∞
.1	.68898	.69011	.69031	.69042	.69046	.69048
.2	.64498	.64733	.64776	.64798	.64807	.64810
.4	.57473	.57988	.58080	.58125	.58143	.58149
.6	.51825	.52665	.52809	.52879	.52908	.52917
1.0	.42997	.44587	.44850	.44976	.45025	.45041
2.0	.28827	.32209	.32838	.33127	.33236	.33269
4.0	.16105	.20204	.21496	.22180	.22434	.22505
6.0	.10946	.14330	.15805	.16814	.17236	.17350
10.0	.06626	.08872	.10088	.11266	.11982	.12197
20.0	.03324	.04487	.05171	.05991	.06849	.07315

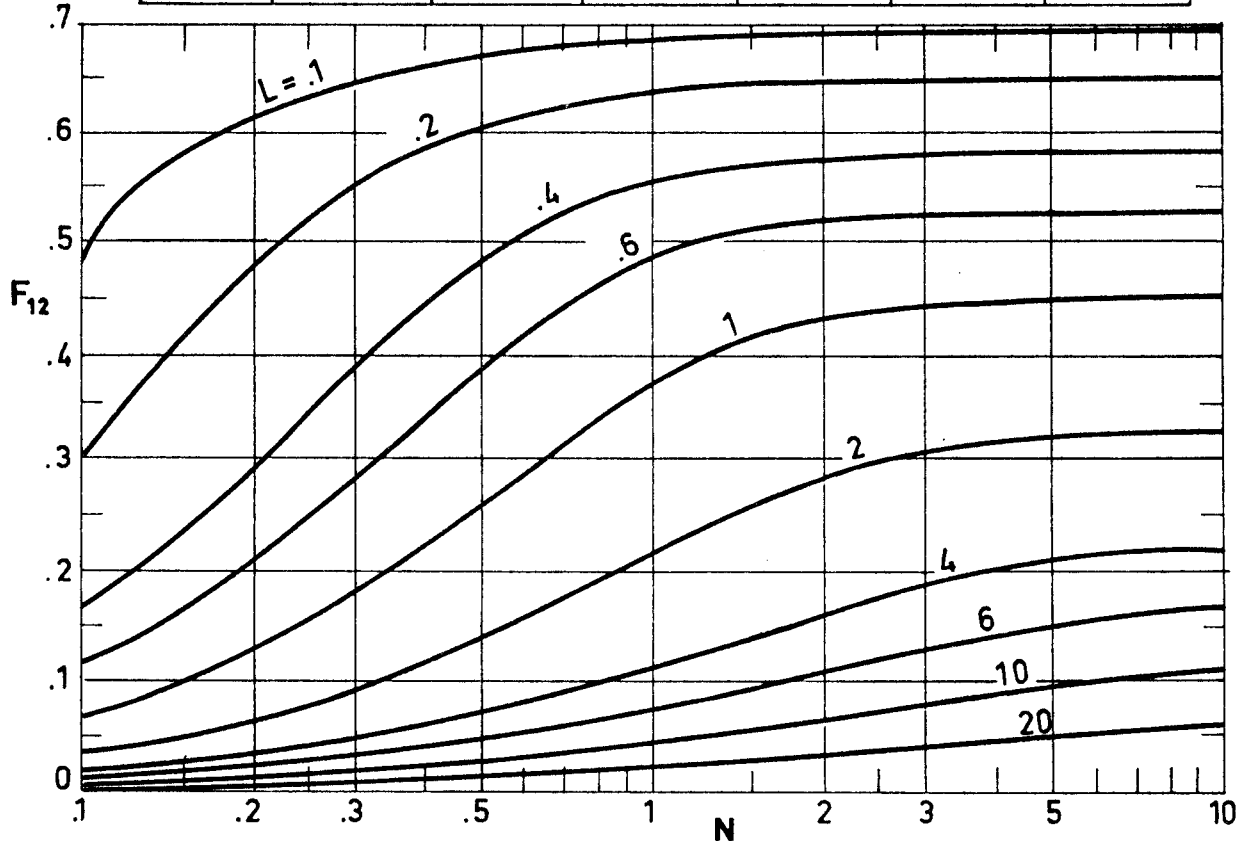


Fig 1-22. F_{12} as a function of L and N for $\phi = 60^\circ$. Table from Feingold (1966), figure from Hamilton & Morgan (1952).

DIFFUSE SURFACES
Finite to Finite Surfaces

$\phi = 90^\circ$

L \ N	.05	.1	.2	.4	.6	1
.1	.18601	.28189	.36216	.40859	.42290	.43251
.2	.10584	.18108	.27104	.34295	.36884	.38719
.4	.05607	.10215	.17147	.25032	.28809	.31924
.6	.03799	.07048	.12295	.19206	.23147	.26896
1.0	.02304	.04325	.07744	.12770	.16138	.20004
2.0	.01158	.02188	.03971	.06757	.08829	.11643
4.0	.00580	.01097	.02000	.03434	.04536	.06131
6.0	.00387	.00732	.01335	.02297	.03040	.04131
10.0	.00232	.00439	.00802	.01380	.01829	.02492
20.0	.00116	.00220	.00401	.00691	.00916	.01249

L \ N	2	4	6	10	20	∞
.1	.43755	.43898	.43925	.43939	.43945	.43947
.2	.39711	.39994	.40048	.40076	.40088	.40092
.4	.33784	.34339	.34447	.34503	.34527	.34535
.6	.29429	.30238	.30399	.30482	.30518	.30530
1.0	.23285	.24522	.24783	.24921	.24980	.25000
2.0	.14930	.16731	.17193	.17455	.17571	.17611
4.0	.08366	.10136	.10776	.11210	.11427	.11505
6.0	.05731	.07184	.07822	.08331	.08624	.08738
10.0	.03491	.04484	.04998	.05502	.05876	.06053
20.0	.01757	.02285	.02587	.02938	.03302	.03578

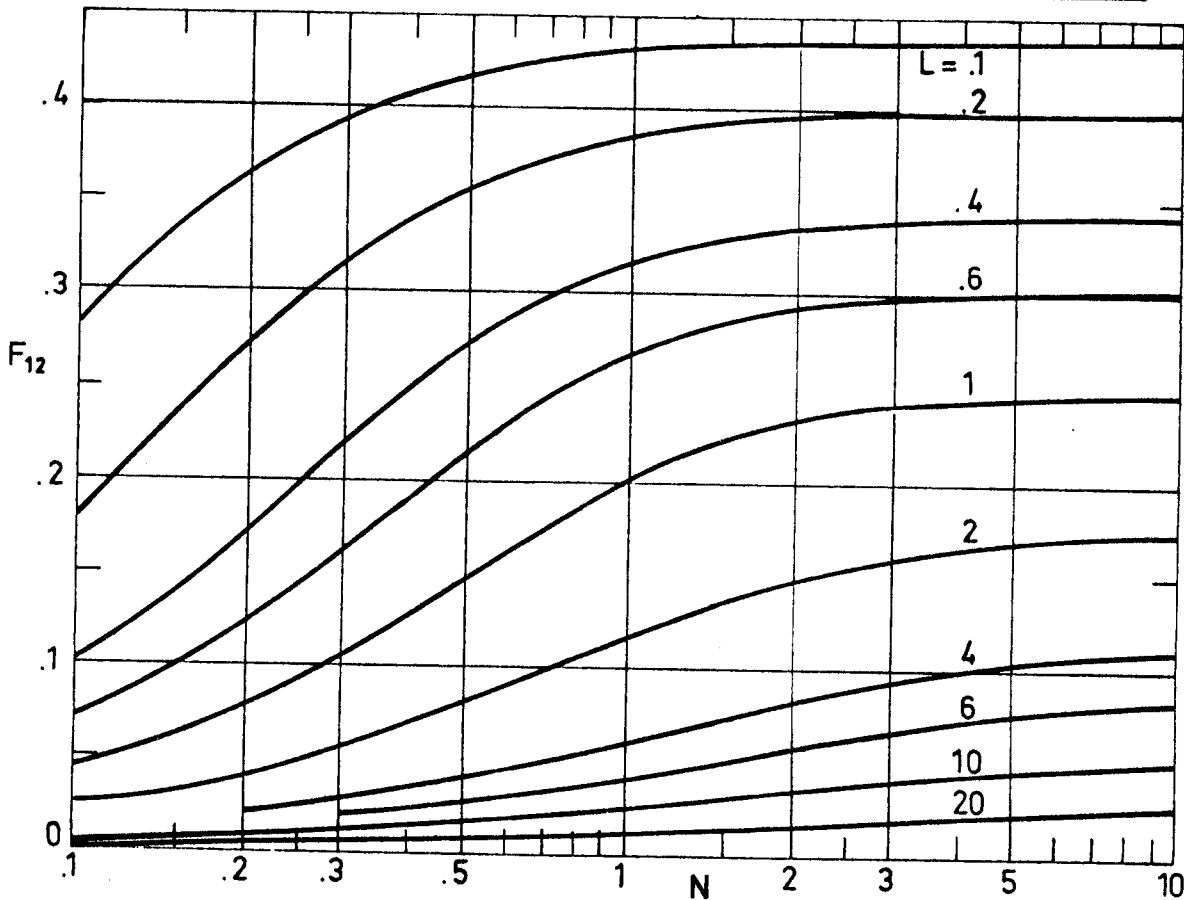


Fig 1-23. F_{12} as a function of L and N for $\phi = 90^\circ$. Table from Feingold (1966), figure from Hamilton & Morgan (1952).

DIFFUSE SURFACES
Finite to Finite Surfaces

$\phi = 120^\circ$

L \ N	.05	.1	.2	.4	.6	1
.1	.08585	.12810	.16634	.19174	.20046	.20669
.2	.05003	.08317	.12233	.15599	.16954	.18005
.4	.02698	.04794	.07799	.11151	.12827	.14328
.6	.01840	.03341	.05651	.08551	.10194	.11833
1.0	.01121	.02067	.03601	.05731	.07100	.08661
2.0	.00565	.01051	.01863	.03069	.03924	.05040
4.0	.00283	.00528	.00941	.01569	.02032	.02677
6.0	.00189	.00352	.00629	.01051	.01365	.01810
10.0	.00113	.00211	.00378	.00632	.00822	.01095
20.0	.00057	.00106	.00189	.00316	.00412	.00549

L \ N	2	4	6	10	20	∞
.1	.21013	.21115	.21135	.21145	.21150	.21151
.2	.18629	.18821	.18860	.18880	.18889	.18891
.4	.15346	.15692	.15765	.15804	.15821	.15827
.6	.13080	.13547	.13650	.13707	.13732	.13740
1.0	.10081	.10710	.10863	.10950	.10990	.11005
2.0	.06325	.07090	.07317	.07462	.07534	.07561
4.0	.03545	.04226	.04489	.04688	.04804	.04854
6.0	.02439	.02993	.03239	.03450	.03591	.03659
10.0	.01492	.01875	.02070	.02264	.02421	.02516
20.0	.00753	.00961	.01077	.01211	.01350	.01476

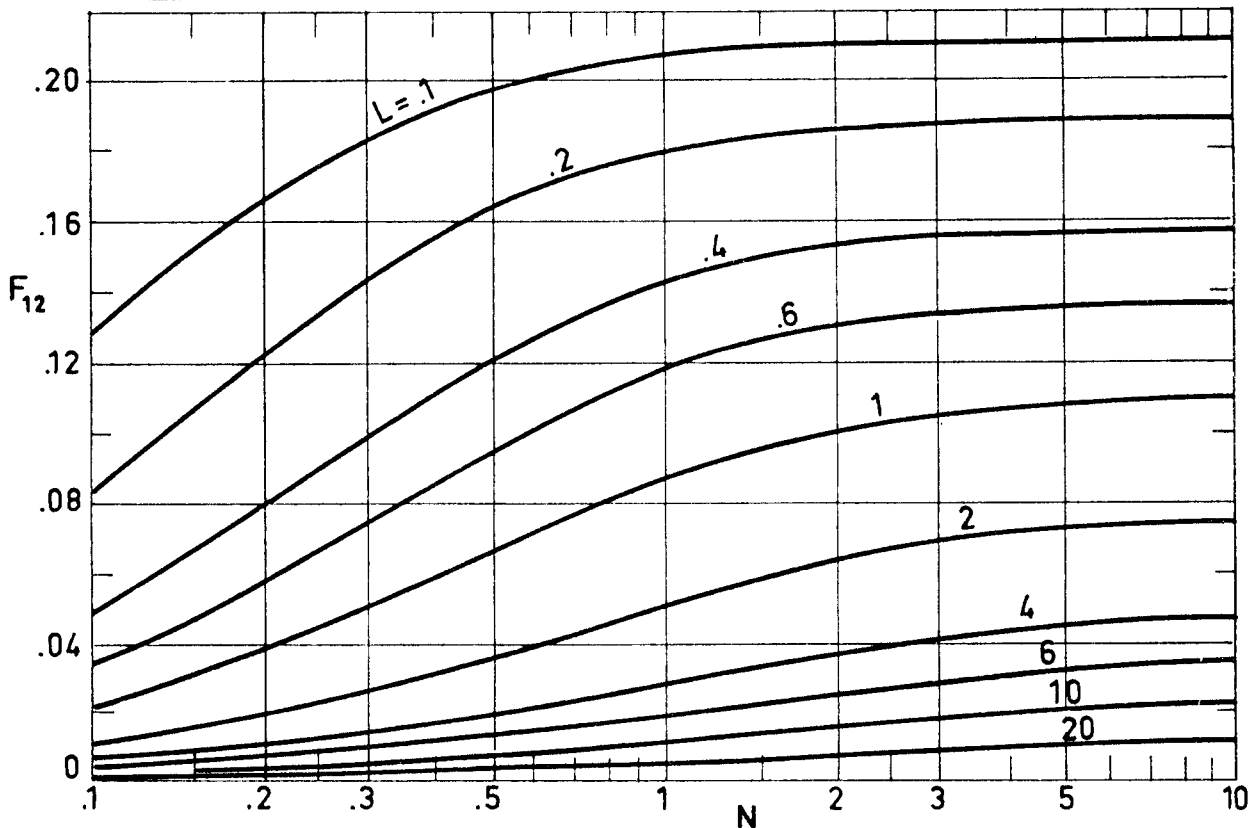


Fig 1-24. F_{12} as a function of L and N for $\phi = 120^\circ$. Table from Feingold (1966), figure from Hamilton & Morgan (1952).

DIFFUSE SURFACES
Finite to Finite Surfaces

$\phi = 150^\circ$

L \ N	.05	.1	.2	.4	.6	1
.1	.02191	.03245	.04233	.04934	.05188	.05376
.2	.01293	.02117	.03086	.03947	.04311	.04607
.4	.00705	.01234	.01973	.02791	.03208	.03596
.6	.00483	.00865	.01437	.02139	.02535	.02939
1.0	.00295	.00538	.00921	.01438	.01764	.02135
2.0	.00149	.00274	.00479	.00775	.00979	.01241
4.0	.00075	.00138	.00243	.00398	.00509	.00662
6.0	.00050	.00092	.00162	.00267	.00343	.00449
10.0	.00030	.00055	.00097	.00160	.00207	.00272
20.0	.00015	.00028	.00049	.00080	.00104	.00137

L \ N	2	4	6	10	20	∞
.1	.05484	.05517	.05523	.05527	.05529	.05529
.2	.04792	.04852	.04865	.04871	.04875	.04875
.4	.03875	.03977	.04000	.04012	.04018	.04020
.6	.03264	.03396	.03427	.03445	.03453	.03456
1.0	.02483	.02649	.02693	.02719	.02731	.02736
2.0	.01541	.01728	.01787	.01827	.01848	.01856
4.0	.00864	.01022	.01085	.01135	.01167	.01181
6.0	.00596	.00723	.00781	.00831	.00868	.00887
10.0	.00365	.00454	.00499	.00544	.00582	.00608
20.0	.00185	.00233	.00260	.00291	.00323	.00355

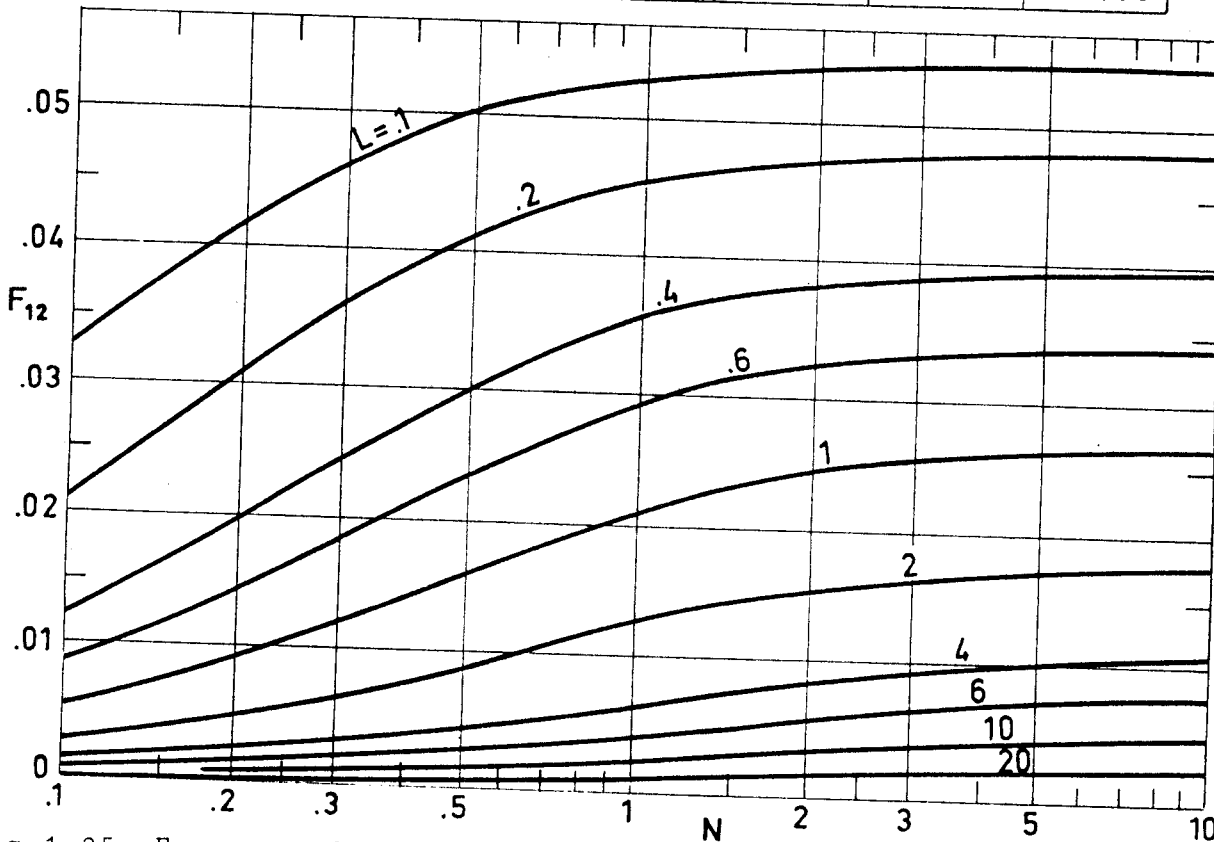


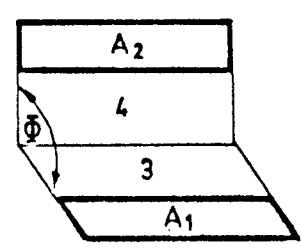
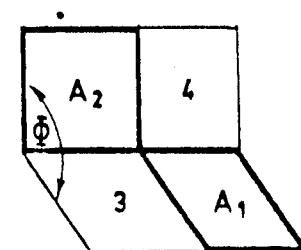
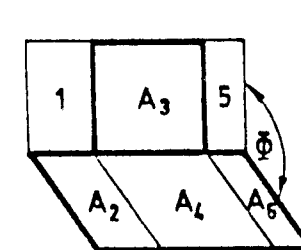
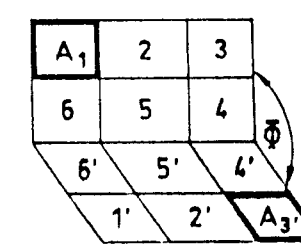
Fig 1-25. F_{12} as a function of L and N for $\phi = 150^\circ$. Table from Feingold (1966), figure from Hamilton & Morgan (1952).

DIFFUSE SURFACES

Finite to Finite Surfaces

1.3.2.4. RECTANGLES PLACED IN INTERSECTING PLANES

The following view factors can be deduced by using the results for two rectangles with one common edge.

<p>Two rectangles A_1 and A_2, with one side of A_1 parallel to one side of A_2 in planes intersecting at angle Φ. View Factor is:</p> $F_{12} = \frac{A(1,3)F(1,3)(2,4) + A_3 F_{34} - A_3 F_3(2,4) - A(1,3)F(1,3)4}{A_1}$ <p>References: Kreith (1962).</p>	
<p>Two rectangles A_1 and A_2. One side of A_1 is parallel to one side of A_2, and one corner of A_1 touches a corner of A_2. Both planes intersect at an angle Φ. View Factor is:</p> $F_{12} = \frac{1}{2A_1} [A(1,3)F(1,3)(2,4) - A_1 F_{14} - A_3 F_{32}]$ <p>References: Kreith (1962).</p>	
<p>Two rectangles, A_3 and $A(2,4,6)$, with one common edge and included angle Φ between the two planes. View Factor is:</p> $F_{3(2,4,6)} = \frac{1}{2A_3} [A(1,3)F(1,3)(2,4) + A(3,5)F(3,5)(4,6) - A_1 F_{12} - A_5 F_{56}]$ <p>References: Kreith (1962).</p>	
<p>Two rectangles A_1 and A_3'. One side of A_1 is parallel to one side of A_3'. Both planes intersect at angle Φ. View Factor is:</p> $A_1 F_{13'} = \frac{1}{2} [K_{(1,2,3,4,5,6)}^2 - K_{(2,3,4,5)}^2 - K_{(1,2,5,6)}^2 + K_{(4,5,6)}^2 - K_{(1,2,3,4,5,6)}(4',5',6') - K_{(4,5,6)}(1',2',3',4',5',6') + K_{(1,2,5,6)}(5',6') + K_{(2,3,4,5)}(4',5') + K_{(5,6)}(1',2',5',6') + K_{(4,5)}(2',3',4',5') + K_{(2,5)}^2 - K_{(2,5)5'} - K_{(5,6)6'} - K_{(4,5)2'} - K_{(5,6)5'} + K_{(5,6)5'}^2]$ <p>where $K_{(m)(n)} = A_m F_{mn}$ and $K_m^2 = A_m F_{mm}$.</p> <p>References: Hamilton & Morgan (1952), Kreith (1962).</p>	

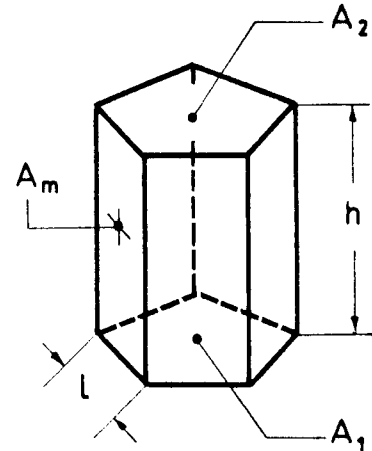
INTENTIONALLY BLANK PAGE

DIFFUSE SURFACES
Finite to Finite Surfaces

1.3.2.5. REGULAR POLYGONS FORMING THE BASES OF A PRISM

Two parallel regular polygons forming the bases of a right prism.

$$L = \frac{l}{h}$$



Formula:

$$F_{12} = 1 - \sum_{m=3}^{n+2} F_{1m}$$

where n is the number of sides of the polygon.

The values of F_{1m} can be deduced by using the results corresponding to two rectangles with one common edge, by applying simple view factor algebra.

Reference: Feingold (1966).

DIFFUSE SURFACES
Finite to Finite Surfaces

L \ n	3	4	5	6	8
.1	.00137	.00316	.00542	.00813	.01509
.2	.00544	.01240	.02098	.03104	.05498
.4	.02095	.04614	.07481	.10566	.16952
.6	.04448	.09336	.14380	.19319	.28359
1.0	.10560	.19983	.28047	.34685	.45502
2.0	.26656	.41525	.51075	.57837	.66880
4.0	.48391	.63204	.70848	.75693	.81628
6.0	.60515	.73258	.79284	.82949	.87297
10.0	.73165	.82699	.86871	.89318	.92143
20.0	.85052	.90785	.93132	.94468	.95974

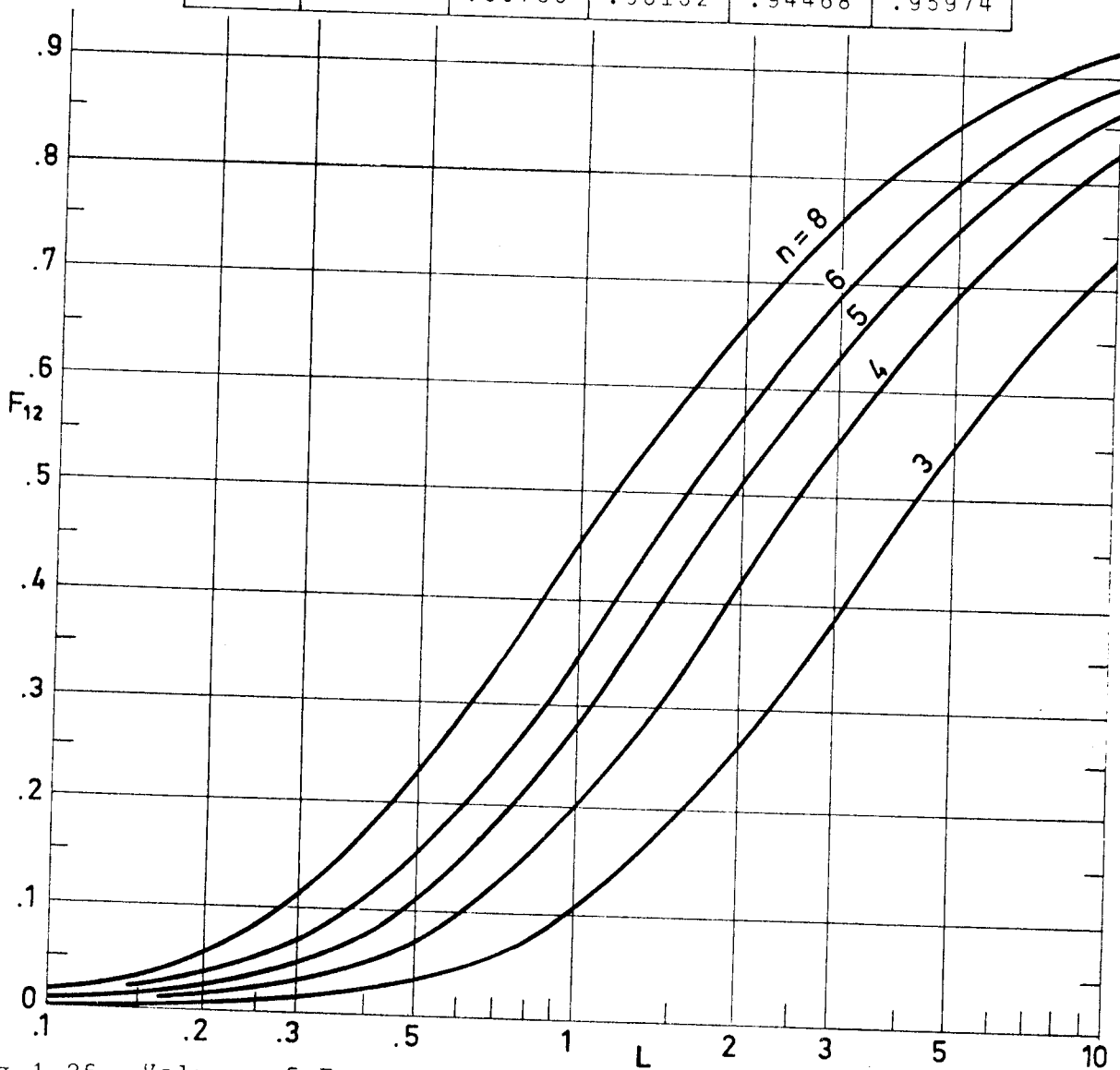


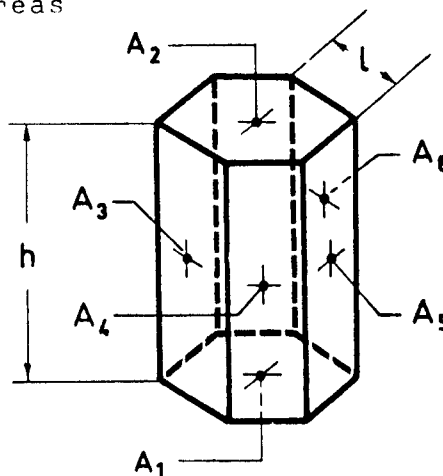
Fig 1-26. Values of F_{12} as a function of L for different regular polygons. n is the number of sides of the polygon. From Feingold (1966).

DIFFUSE SURFACES
Finite to Finite Surfaces

1.3.2.6. SEVERAL AREAS OF A PRISMATIC CONFIGURATION

View factors between various areas in a honeycomb structure.

$$L = \frac{l}{h}$$



The results being presented have been obtained by combination of the data on two parallel regular polygons with those concerning two rectangles with one common edge.

Reference: Feingold (1966).

DIFFUSE SURFACES
Finite to Finite Surfaces

L	F ₃₄	F ₃₅	F ₃₆	F ₁₃	F ₃₁	F ₁₂
.05	.13103	.22094	.25286	.16632	.02161	.00206
.1	.12810	.20995	.23800	.16531	.04295	.00813
.2	.12234	.18886	.20979	.16149	.08391	.03104
.3	.11678	.16949	.18453	.15583	.12146	.06500
.4	.11151	.15224	.16269	.14906	.15490	.10566
.5	.10656	.13715	.14420	.14179	.18419	.14928
.6	.10194	.12410	.12869	.13447	.20962	.19319
.7	.09766	.11285	.11568	.12738	.23165	.23574
.8	.09369	.10316	.10474	.12066	.25079	.27605
.9	.09001	.09478	.09549	.11439	.26746	.31369
1.0	.08662	.08676	.08760	.10886	.28282	.34685
1.5	.07296	.06248	.06135	.08567	.33388	.48596
2.0	.06325	.04817	.04689	.07027	.36514	.57837
3.0	.05041	.03279	.03170	.05144	.40095	.69135
4.0	.04226	.02479	.02390	.04051	.42101	.75693
5.0	.03659	.01990	.01916	.03340	.43393	.79958
8.0	.02655	.01249	.01201	.02189	.45496	.86866
10.0	.02264	.01000	.00961	.01780	.46256	.89318
15.0	.01679	.00667	.00641	.01215	.47333	.92713
20.0	.01350	.00501	.00481	.00922	.47909	.94468

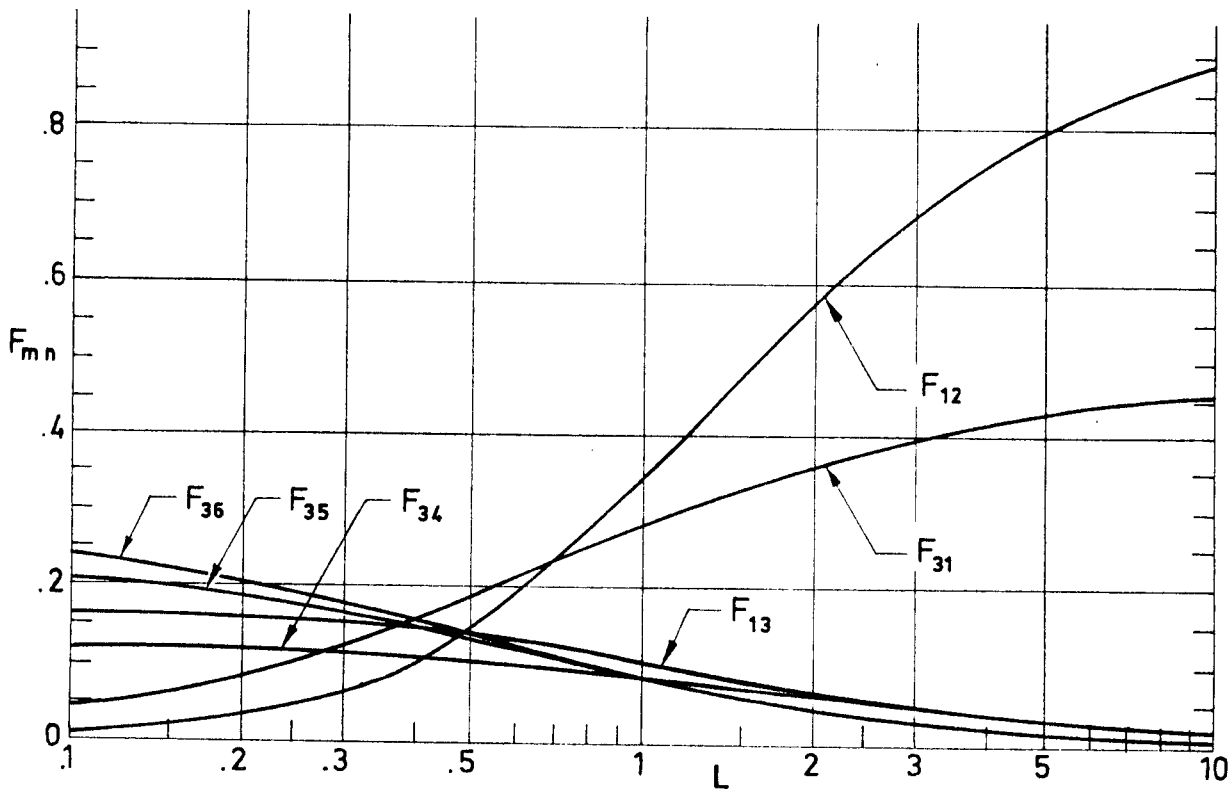


Fig 1-27. View factors between different faces of a honeycomb cell as a function of the cell length, L. From Feingold (1966).

DIFFUSE SURFACES
Finite to Finite Surfaces

1.3.2.7. PARALLEL COAXIAL DISCS

Parallel circular discs with centers along the same normal.

Formula:

$$F_{12} = \frac{1}{2} \left[x - \sqrt{x^2 - 4 \left(\frac{R_2}{R_1} \right)^2} \right]$$

with

$$x = 1 + \frac{1 + R_2^2}{R_1^2}$$

References: Hamilton & Morgan (1952), Leuenberger & Person (1956), Jakob (1957), Eckert & Drake (1959), Kreith (1962), Siegel & Howell (1972).

Comments: The following view factors may be deduced from the previous one.

Directly opposed ring to disc of arbitrary radii.

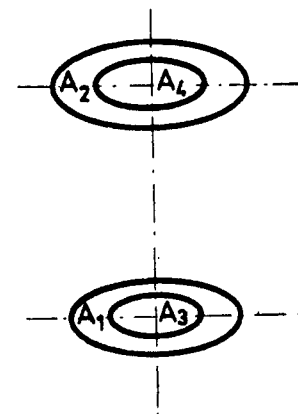
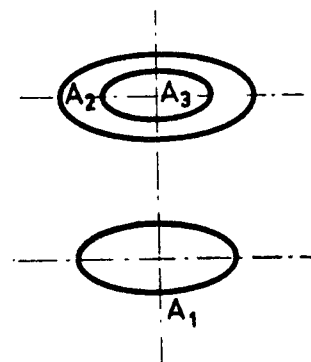
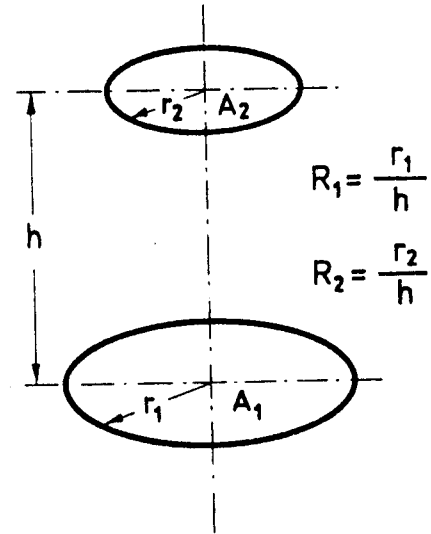
$$F_{12} = F_{1(2,3)} - F_{13}$$

Reference: Leuenberger & Person (1956).

Parallel, directly opposed plane ring areas

$$F_{12} = \left[1 + \frac{A_3}{A_1} \right] \left[F_{(1,3)(2,4)} - F_{(1,3)4} \right] - \frac{A_3}{A_1} \left[F_{3(2,4)} - F_{34} \right]$$

References: Hamilton & Morgan (1952), Leuenberger & Person (1956), Siegel & Howell (1972).



DIFFUSE SURFACES
Finite to Finite Surfaces

$R_1 \backslash R_2$.1	.2	.3	.4	.6	.8	1.
.1	.0098	.0381	.0819	.1369	.2633	.3888	.4988
.5	.0080	.0312	.0680	.1159	.2320	.3553	.4689
1.0	.0050	.0198	.0440	.0768	.1639	.2701	.3820
2.0	.0020	.0080	.0179	.0318	.0709	.1245	.1910
3.0	.0010	.0040	.0090	.0160	.0359	.0636	.0989
4.0	.0006	.0024	.0053	.0094	.0212	.0376	.0586
5.0	.0004	.0015	.0035	.0062	.0138	.0246	.0384
6.0	.0003	.0011	.0024	.0043	.0097	.0173	.0270
8.0	.0002	.0006	.0014	.0025	.0055	.0098	.0154
10.0	.0001	.0004	.0009	.0016	.0036	.0063	.0099
$R_1 \backslash R_2$	1.5	2.	3.	4.	6.	8.	10.
.1	.6917	.7997	.8999	.9411	.9730	.9846	.9901
.5	.6754	.7918	.8977	.9404	.9728	.9846	.9901
1.0	.6198	.7639	.8902	.9377	.9722	.9844	.9900
2.0	.3975	.6096	.8486	.9248	.9698	.9836	.9897
3.0	.2189	.3772	.7176	.8889	.9647	.9822	.9891
4.0	.1312	.2312	.5000	.7793	.9540	.9797	.9883
5.0	.0862	.1528	.3394	.5839	.9276	.9754	.9869
6.0	.0607	.1078	.2412	.4240	.8466	.9669	.9847
8.0	.0346	.0615	.1381	.2449	.5439	.8826	.9741
10.0	.0223	.0396	.0890	.1581	.3545	.6234	.9049

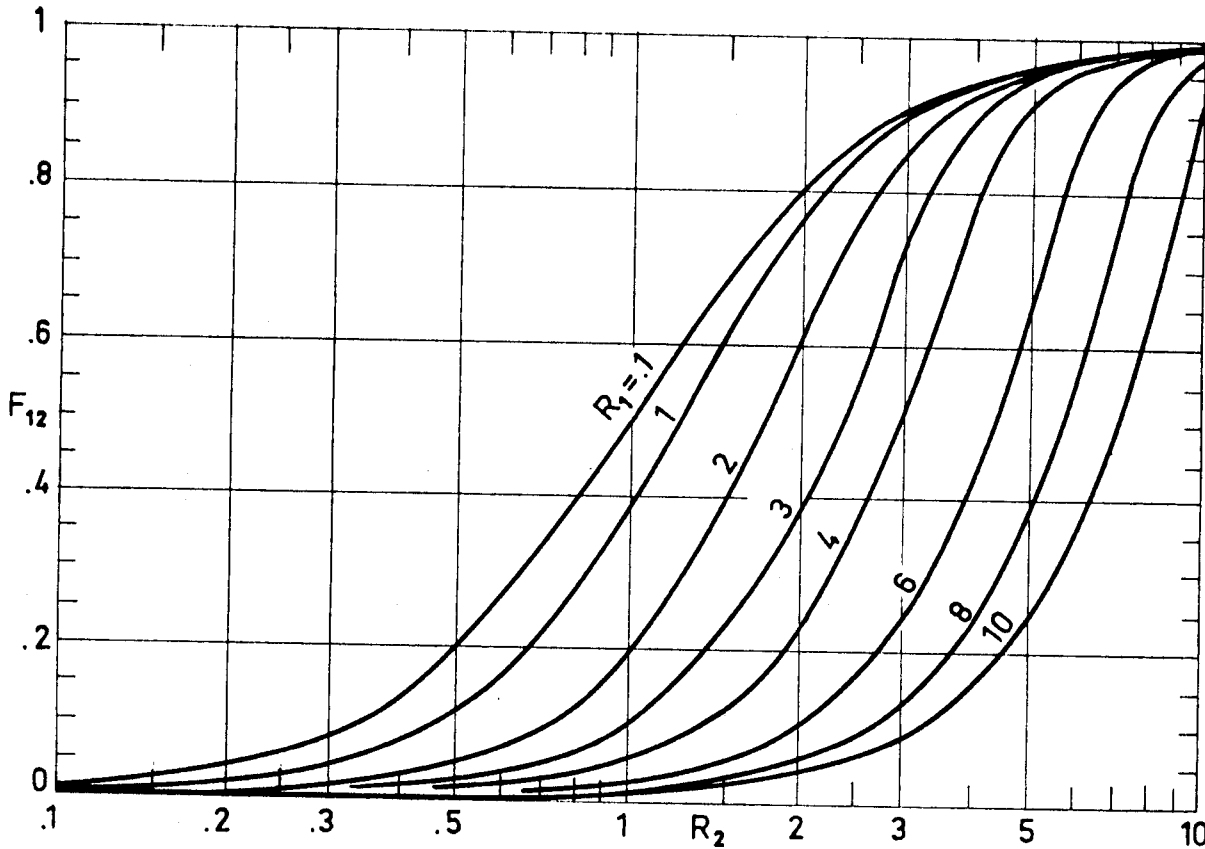


Fig 1-28. Values of F_{12} as a function of R_1 and R_2 in the case of two parallel coaxial discs. Calculated by the compiler.

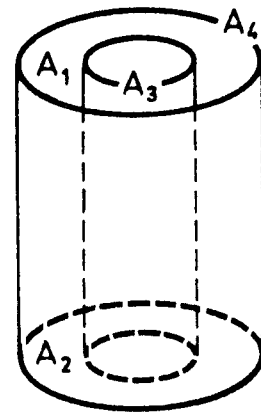
DIFFUSE SURFACES
Finite to Finite Surfaces

1.3.2.8. RINGS AT OPPOSITE ENDS OF A CIRCULAR CYLINDER

The following view factor may be obtained from those corresponding to two coaxial cylinders of equal length.

Annular ring to an equal annular ring placed at the opposite end of the cylinder. The view factor is:

$$F_{12} = 1 - \frac{A_3}{2A_1} \left[1 - \frac{A_4}{A_3} (F_{44} + 2F_{43} - 1) \right]$$



For F_{43} and F_{44} see § 1.3.8.1.

References: Leuenberger & Person (1956); Sparrow, Miller & Jonsson (1962).

INTENTIONALLY BLANK PAGE

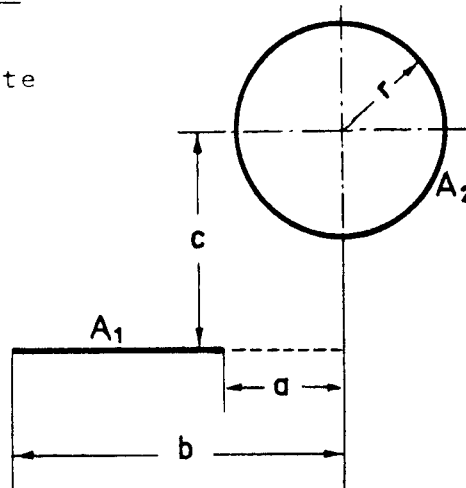
DIFFUSE SURFACES
Finite to Finite Surfaces

1.3.3. PLANAR TO CYLINDRICAL. TWO-DIMENSIONAL CONFIGURATIONS

1.3.3.1. PLANE TO CIRCULAR CYLINDER

Infinitely long plane of finite width, to parallel infinitely long cylinder.

$$c \geq r$$



Formula:

$$F_{12} = \frac{r}{b-a} \left[\tan^{-1} \frac{b}{c} - \tan^{-1} \frac{a}{c} \right]$$

where the range of $\tan^{-1} x$ is $-\pi/2$ to $\pi/2$.

References: Hamilton & Morgan (1952), Kreith (1962), Feingold & Gupta (1970), Siegel & Howell (1972).

Comments:

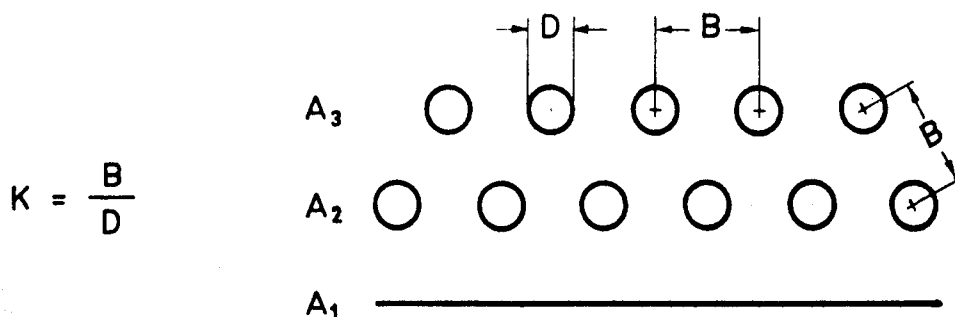
The expressions given by Hamilton & Morgan (1952) and Kreith (1962) are in error as has been pointed out both by Feingold & Gupta (1970), and Siegel & Howell (1972).

INTENTIONALLY BLANK PAGE

DIFFUSE SURFACES
Finite to Finite Surfaces

1.3.3.2. PLANE TO ROWS OF CIRCULAR CYLINDERS

Infinite plane to first row and second row of an infinite number of parallel staggered tubes having equal diameters.



Formula:

$$F_{12} = \frac{K + \tan^{-1} \sqrt{K^2 - 1} - \sqrt{K^2 - 1}}{K}$$

F_{13} has been obtained graphically. No analytical expression is available.

References: Hottel (1954), Jakob (1957).

DIFFUSE SURFACES
Finite to Finite Surfaces

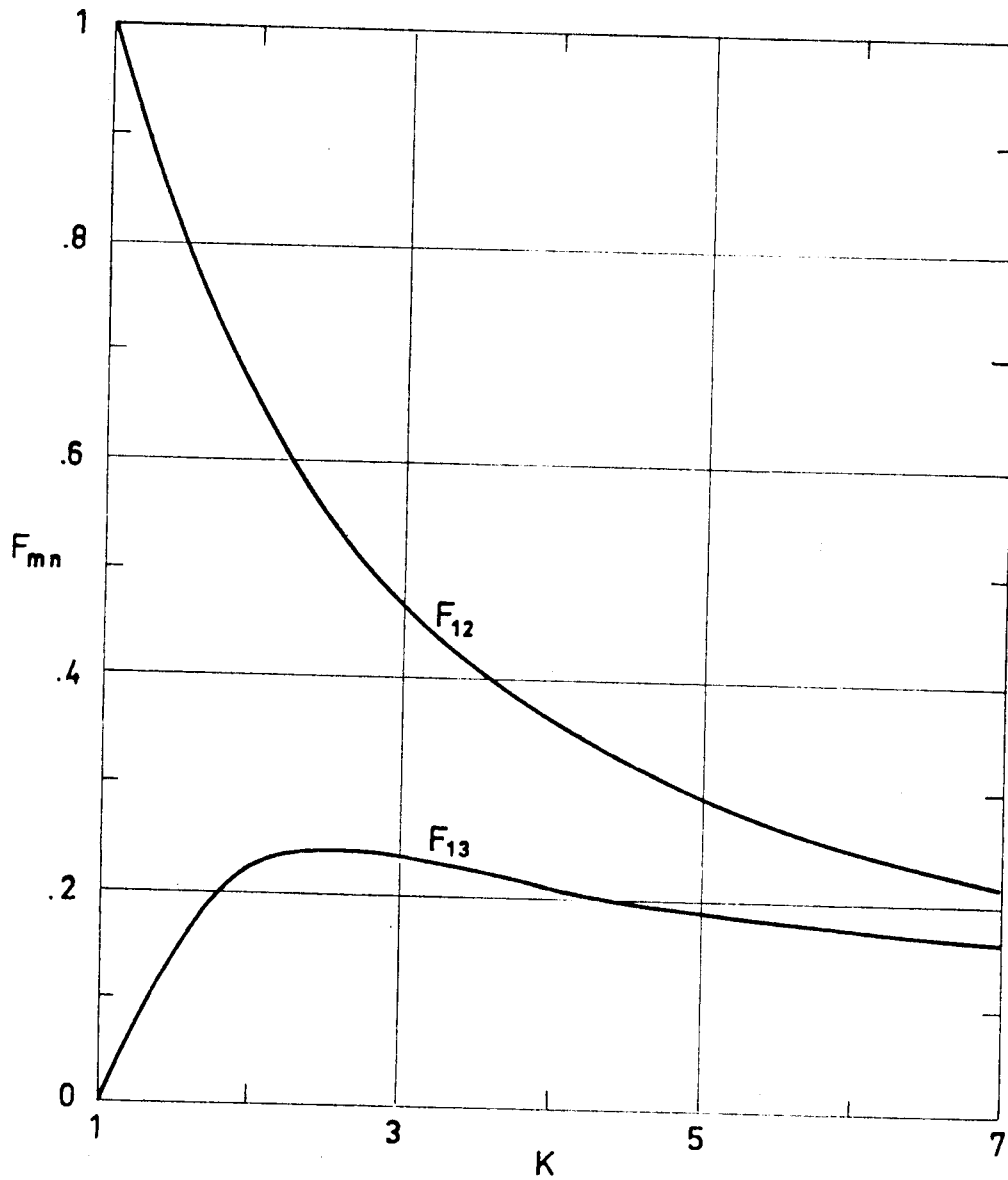


Fig 1-29. Values of F_{12} and F_{13} as a function of the parameter K . From Jakob (1957).

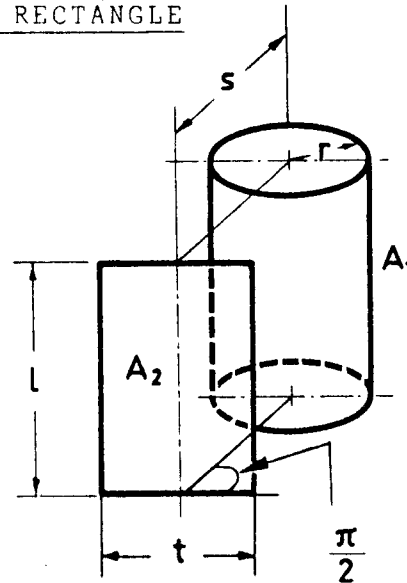
DIFFUSE SURFACES

Finite to Finite Surfaces

1.3.4. PLANAR TO CYLINDRICAL. THREE-DIMENSIONAL CONFIGURATIONS

1.3.4.1. FINITE LENGTH CYLINDER TO OUTER RECTANGLE

Finite length cylinder to rectangle with two edges parallel to cylinder axis and of length equal cylinder.



$$R = \frac{r}{l}$$

$$Z = \frac{s}{r}$$

$$T = \frac{t}{r}$$

Formula:

$$F_{12} = \frac{T}{2\pi} \int_0^1 Z v^2 \left\{ 1 - \frac{1}{\pi} \left[\cos^{-1} \frac{1+y}{1-y} - \frac{1}{2R} \left[\sqrt{(1-y)^2 + 4R^2} \cos^{-1} \left(v \frac{1+y}{1-y} \right) + (1+y) \sin^{-1} v - \frac{\pi}{2} (1-y) \right] \right] \right\} dx$$

where:

$$y = R^2 \left(1 - Z^2 - \frac{T^2 x^2}{4} \right)$$

$$v = \frac{1}{\sqrt{Z^2 + \frac{T^2 x^2}{4}}}$$

Reference: Leuenberger & Person (1956).

DIFFUSE SURFACES
Finite to Finite Surfaces

T \ R	.01	.1	.15	.2	.3	.5	.8
.5	.0780	.0779	.0779	.0778	.0778	.0776	.0774
1.0	.1475	.1471	.1468	.1466	.1461	.1451	.1437
1.5	.2047	.2035	.2028	.2022	.2009	.1982	.1943
2.0	.2498	.2475	.2463	.2450	.2426	.2377	.2306
3.0	.3123	.3076	.3050	.3024	.2973	.2874	.2736
5.0	.3778	.3682	.3629	.3577	.3476	.3293	.3061
8.0	.4203	.4047	.3963	.3883	.3734	.3482	.3193
10.0	.4351	.4164	.4065	.3973	.3805	.3530	.3224
15.0	.4550	.4306	.4183	.4072	.3879	.3578	.3254
20.0	.4649	.4366	.4230	.4110	.3905	.3594	.3265
T \ R	1	1.5	2	3	5	8	10
.5	.0772	.0769	.0765	.0758	.0744	.0723	.0710
1.0	.1427	.1403	.1380	.1335	.1253	.1151	.1095
1.5	.1918	.1856	.1799	.1694	.1526	.1346	.1257
2.0	.2261	.2155	.2059	.1899	.1665	.1438	.1331
3.0	.2651	.2468	.2318	.2086	.1783	.1513	.1392
5.0	.2931	.2673	.2477	.2196	.1850	.1555	.1426
8.0	.3040	.2747	.2534	.2234	.1873	.1570	.1437
10.0	.3065	.2764	.2546	.2242	.1878	.1573	.1440
15.0	.3090	.2781	.2560	.2251	.1883	.1576	.1442
20.0	.3098	.2786	.2563	.2254	.1885	.1577	.1443

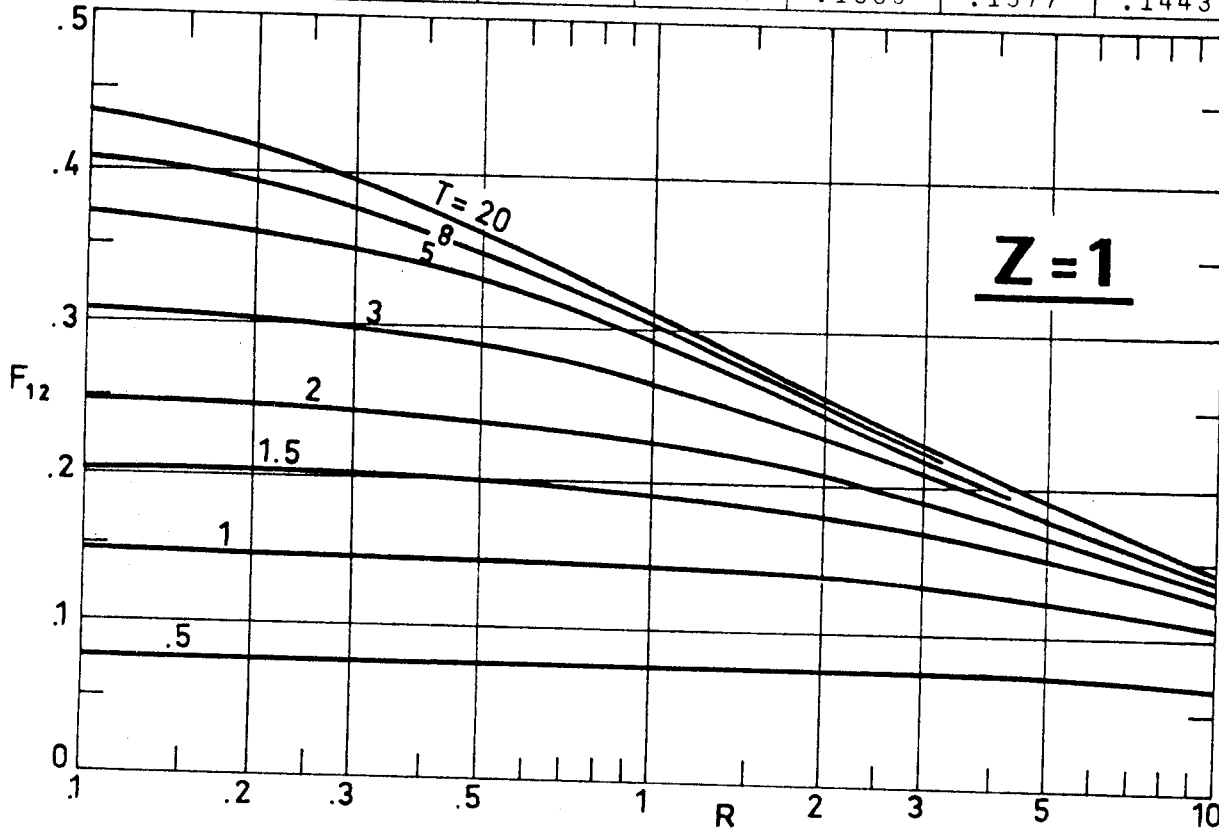


Fig 1-30. F_{12} as a function of T and R . Calculated by the compiler.

DIFFUSE SURFACES
Finite to Finite Surfaces

T \ R	.01	.1	.15	.2	.3	.5	.8
.5	.0261	.0229	.0212	.0196	.0168	.0126	.0089
1.0	.0518	.0454	.0420	.0389	.0333	.0250	.0175
1.5	.0769	.0673	.0622	.0575	.0492	.0368	.0259
2.0	.1010	.0882	.0815	.0753	.0643	.0480	.0337
3.0	.1454	.1266	.1167	.1075	.0915	.0680	.0475
5.0	.2177	.1875	.1719	.1575	.1326	.0974	.0674
8.0	.2901	.2454	.2228	.2024	.1682	.1217	.0835
10.0	.3219	.2693	.2431	.2197	.1814	.1303	.0891
15.0	.3709	.3027	.2703	.2423	.1979	.1408	.0958
20.0	.3977	.3185	.2825	.2521	.2048	.1451	.0985

T \ R	1	1.5	2	3	5	8	10
.5	.0073	.0051	.0039	.0026	.0016	.0010	.0008
1.0	.0145	.0100	.0076	.0051	.0031	.0019	.0015
1.5	.0214	.0148	.0112	.0075	.0045	.0028	.0023
2.0	.0278	.0192	.0146	.0098	.0059	.0037	.0030
3.0	.0392	.0270	.0205	.0138	.0083	.0052	.0042
5.0	.0555	.0381	.0289	.0194	.0117	.0073	.0059
8.0	.0685	.0469	.0355	.0239	.0144	.0090	.0072
10.0	.0730	.0500	.0378	.0254	.0153	.0096	.0077
15.0	.0784	.0536	.0406	.0272	.0164	.0103	.0082
20.0	.0806	.0550	.0416	.0279	.0168	.0105	.0084

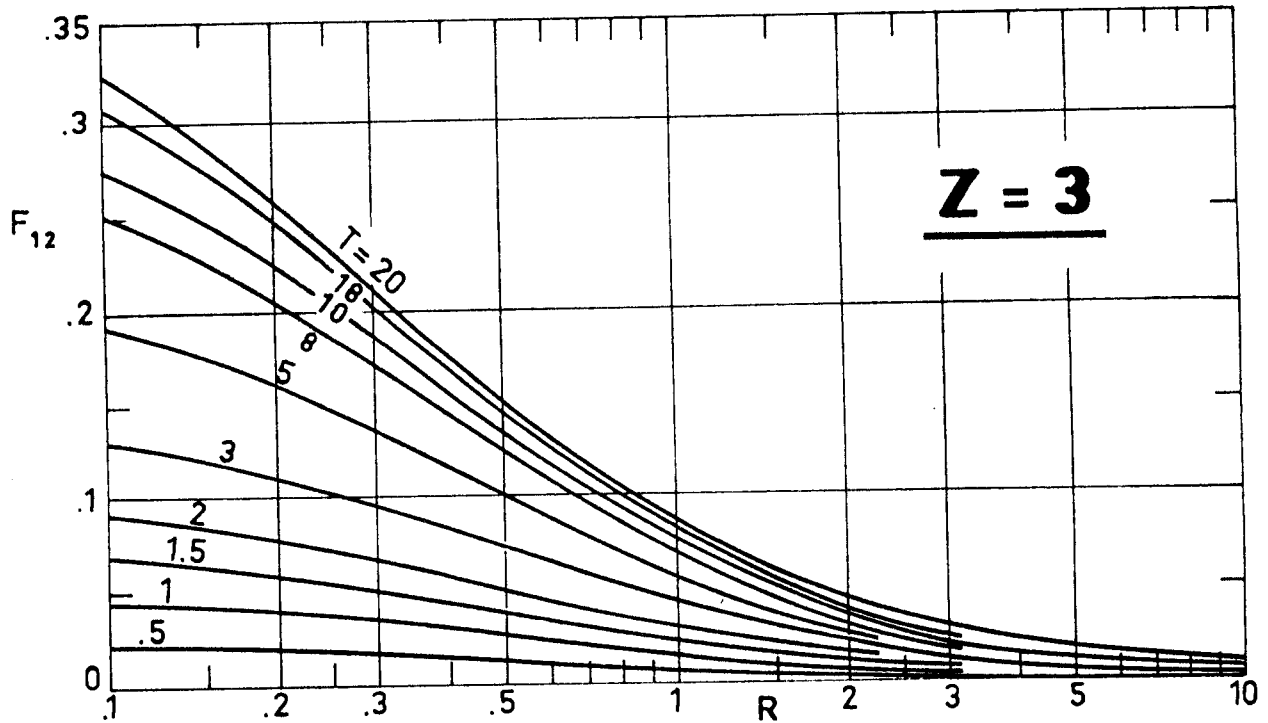


Fig 1-31. F_{12} as a function of T and R . Calculated by the compiler.

DIFFUSE SURFACES
Finite to Finite Surfaces

T \ R	.01	.1	.15	.2	.3	.5	.8
.5	.0155	.0119	.0102	.0089	.0068	.0045	.0029
1.0	.0309	.0237	.0204	.0176	.0136	.0090	.0059
1.5	.0461	.0354	.0304	.0263	.0203	.0134	.0087
2.0	.0611	.0469	.0403	.0348	.0268	.0178	.0116
3.0	.0903	.0690	.0592	.0512	.0393	.0260	.0169
5.0	.1435	.1089	.0931	.0802	.0613	.0404	.0262
8.0	.2085	.1558	.1322	.1132	.0860	.0563	.0365
10.0	.2424	.1790	.1512	.1289	.0975	.0637	.0412
15.0	.3024	.2171	.1813	.1535	.1151	.0747	.0481
20.0	.3396	.2380	.1972	.1661	.1239	.0801	.0516

T \ R	1	1.5	2	3	5	8	10
.5	.0024	.0016	.0012	.0008	.0005	.0003	.0002
1.0	.0047	.0032	.0024	.0016	.0010	.0006	.0005
1.5	.0071	.0048	.0036	.0024	.0014	.0009	.0007
2.0	.0093	.0063	.0047	.0032	.0019	.0012	.0010
3.0	.0137	.0092	.0069	.0046	.0028	.0017	.0014
5.0	.0212	.0143	.0107	.0072	.0043	.0027	.0022
8.0	.0294	.0198	.0149	.0100	.0060	.0037	.0030
10.0	.0332	.0223	.0168	.0112	.0067	.0042	.0034
15.0	.0388	.0261	.0196	.0131	.0079	.0049	.0039
20.0	.0416	.0279	.0210	.0140	.0084	.0053	.0042

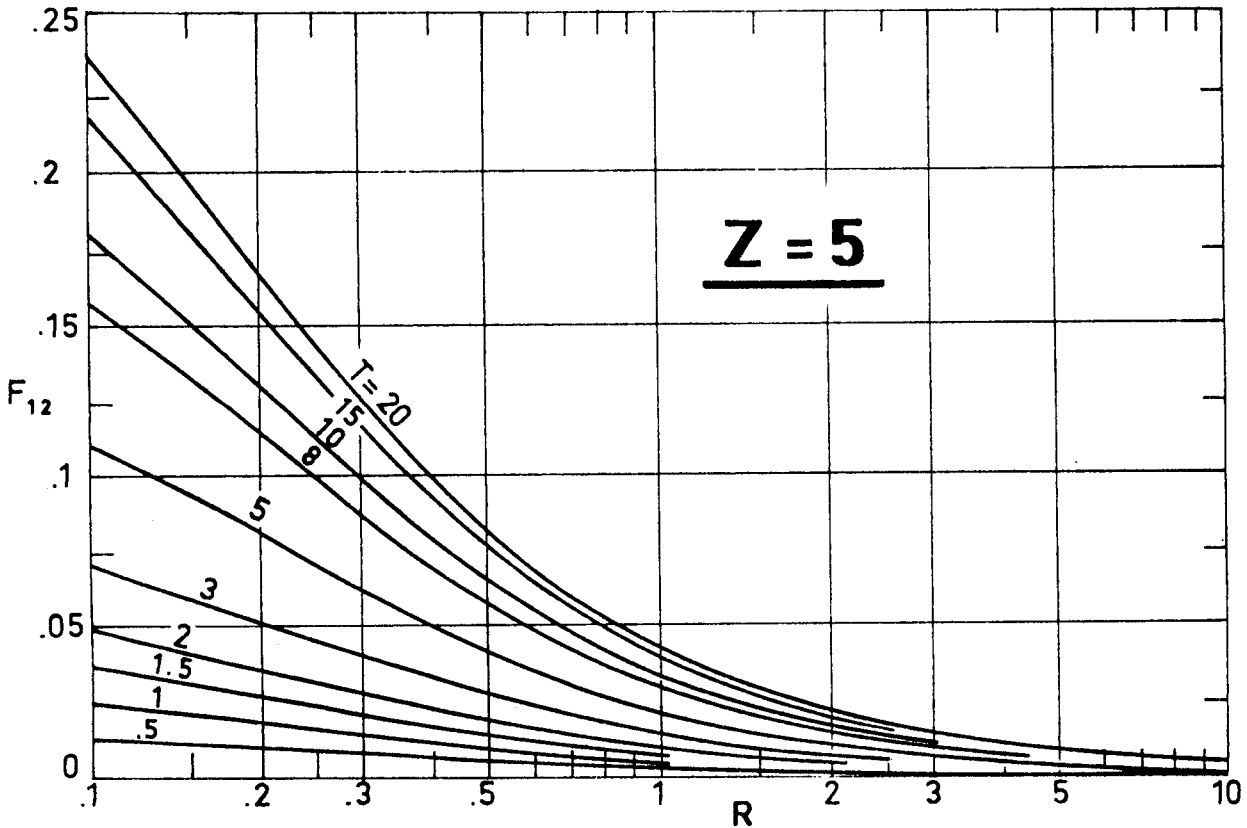
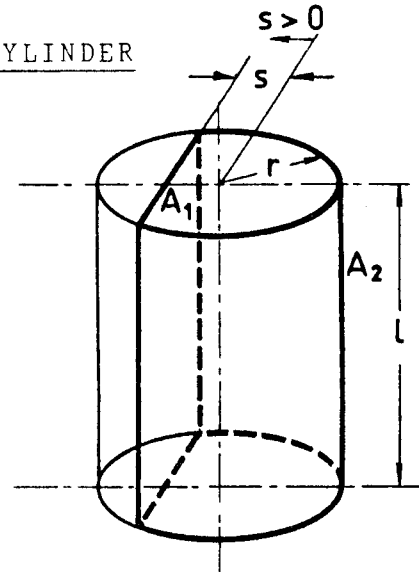


Fig 1-32. F_{12} as a function of T and R . Calculated by the compiler.

DIFFUSE SURFACES
Finite to Finite Surfaces

1.3.4.2. INNER RECTANGLE TO FINITE-LENGTH CYLINDER

Cylinder and plane of equal length parallel to cylinder axis, plane inside cylinder.



$$R = \frac{r}{l}$$

$$Z = \frac{s}{r}$$

Formulae:

$$F_{12} = 1 - \frac{1}{\pi} \left[2 \tan^{-1} 2A - \frac{1}{2A} \ln(1 + 4A^2) \right] -$$

$$- \frac{1}{4\pi A} \int_0^A \left\{ x \left[2(A^2 - x^2) \ln \frac{A+x}{A-x} + (1 + A^2 - x^2) \ln \frac{(A-x)^2 + 1}{(A+x)^2 + 1} \right] + RZ \left[2 \left[(1 - A^2 + x^2) \cos^{-1} Z - \pi \right] + \right. \right.$$

$$+ \sqrt{\left[1 + R^2(1 + Z^2) + x^2 \right]^2 - 4R^2(R^2 Z^2 + x^2)} \left[\cos^{-1} \left(\frac{Z}{|Z|} \frac{(R^2 Z^2 + xA)(A+x)^2 - R^2 Z^2 + xA}{R \sqrt{R^2 Z^2 + x^2} [(A+x)^2 + 1]} \right) + \right.$$

$$\left. \left. + \cos^{-1} \left(\frac{Z}{|Z|} \frac{(R^2 Z^2 - xA)(A-x)^2 - R^2 Z^2 - xA}{R \sqrt{R^2 Z^2 + x^2} [(A-x)^2 + 1]} \right) \right] \right\} (R^2 Z^2 + x^2)^{-1} dx$$

where:

$$A = R \sqrt{1 - Z^2}$$

and, for any argument ξ :

$$-\frac{\pi}{2} < \tan^{-1} \xi < \frac{\pi}{2}$$

$$0 < \cos^{-1} \xi < \pi$$

$$\lim_{Z \rightarrow 1} F_{12} = 1 - \frac{1}{2R} (\sqrt{1 + 4R^2} - 1)$$

$$\lim_{Z \rightarrow -1} F_{12} = 1$$

Reference: These expressions have been obtained by the compiler after Leuenberger & Person (1956).

DIFFUSE SURFACES
Finite to Finite Surfaces

R \ Z	-.95	-.9	-.8	-.7	-.6	-.4
.1	.99682	.99376	.98782	.98206	.97644	.96557
.2	.99364	.98751	.97565	.96418	.95302	.93150
.4	.98729	.97506	.95150	.92888	.90708	.86571
.6	.98095	.96268	.92771	.89453	.86298	.80447
1.0	.96833	.93823	.88172	.82973	.78201	.69826
2.0	.93732	.87975	.77845	.69387	.62351	.51536
4.0	.87856	.77651	.62153	.51432	.43768	.33661
10.0	.73093	.56272	.38272	.29102	.23542	.17065
20.0	.56279	.38385	.23815	.17445	.13815	.09759
100.0	.20468	.11950	.06730	.04728	.03649	.02490

R \ Z	-.2	0	.2	.4	.7	1
.1	.95511	.94502	.93531	.92596	.91274	.90098
.2	.91094	.89127	.87246	.85453	.82944	.80742
.4	.82713	.79116	.75771	.72669	.68467	.64922
.6	.75168	.70414	.66138	.62295	.57263	.53162
1.0	.62812	.56919	.51933	.47677	.42369	.38197
2.0	.43742	.37895	.33344	.29686	.25330	.21922
4.0	.27298	.22893	.19634	.17098	.14134	.11722
10.0	.13350	.10903	.09146	.07803	.06243	.04875
20.0	.07507	.06050	.05014	.04227	.03313	.02469
100.0	.01868	.01474	.01196	.00987	.00744	.00499

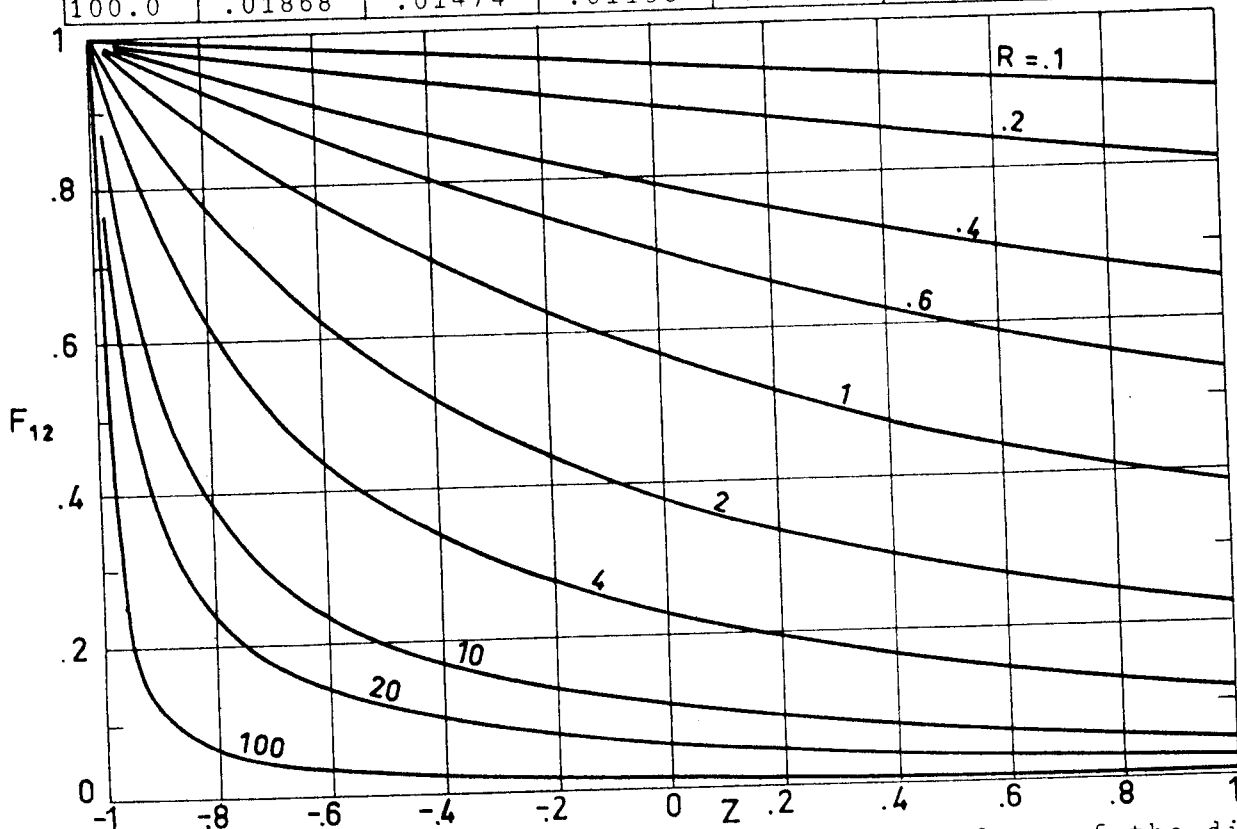


Fig 1-33. F_{12} as a function of Z , for different values of the dimensionless radius R . Calculated by the compiler.

DIFFUSE SURFACES
Finite to Finite Surfaces

1.3.4.3. DISC TO INNER SURFACE OF A COAXIAL CYLINDER

The following view factors may be obtained by use of those for two parallel circular discs with centers along the same normal.

Disk to the interior surface of a coaxial cylinder of larger or equal radius. The view factor is given by

$$F_{12} = F_{13} - F_{14}$$

For F_{13} and F_{14} see § 1.3.2.7.

Reference: Siegel & Howell (1972).

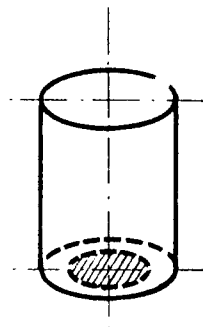
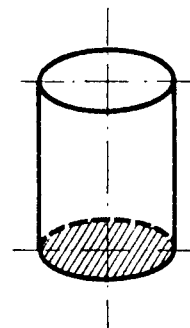
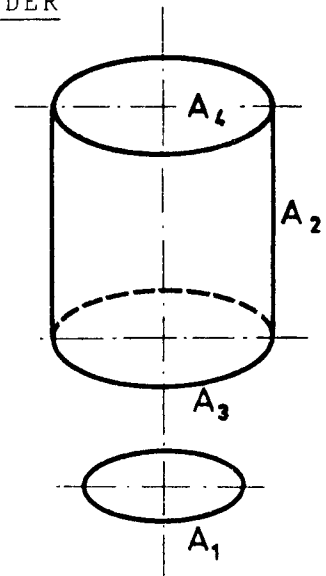
Particular cases of the previous configuration are.

Entire inner wall of finite cylinder to ends.

Reference: Bien (1966).

Inner surface of cylinder to disc at one end.

Reference: Leuenberger & Person (1956).



DIFFUSE SURFACES

Finite to Finite Surfaces

1.3.4.4. RING TO INNER SURFACE OF A COAXIAL CYLINDER

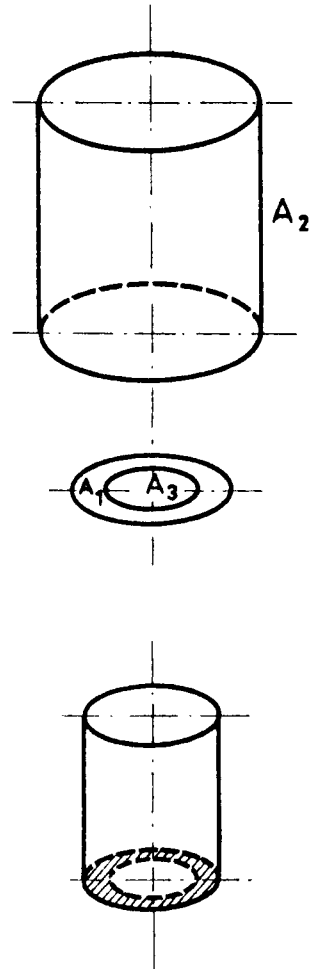
The following view factors may be obtained by use of that for a disc viewing the inner surface of a coaxial cylinder of larger or equal radius.

Ring to the inner surface of a coaxial cylinder of larger or equal radius. The view factor is given by

$$F_{12} = \left[1 + \frac{A_3}{A_1} \right] F_{(1,3)2} - \frac{A_3}{A_1} F_{32}$$

A particular case of the previous configuration is

Inner surface of cylinder to annulus on one end.



Reference: Leuenberger & Person (1956).

DIFFUSE SURFACES
Finite to Finite Surfaces

1.3.4.5. FINITE-LENGTH COAXIAL CYLINDER TO ENCLOSED BASE

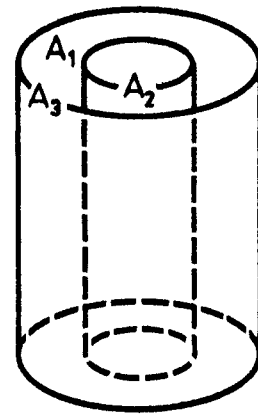
The following view factors may be obtained from those for two coaxial cylinders of equal length.

Inner or outer coaxial cylinders of the same length to annular ring placed at one end of the cylinders. The view factors are:

$$F_{21} = \frac{1}{2} (1 - F_{23})$$

$$F_{31} = \frac{1}{2} (1 - F_{32} - F_{33})$$

For F_{32} and F_{33} see § 1.3.8.1.



References: Leuenberger & Person (1956); Sparrow, Miller & Jonsson (1962).

INTENTIONALLY BLANK PAGE

DIFFUSE SURFACES
Finite to Finite Surfaces

1.3.5. PLANAR TO CONICAL

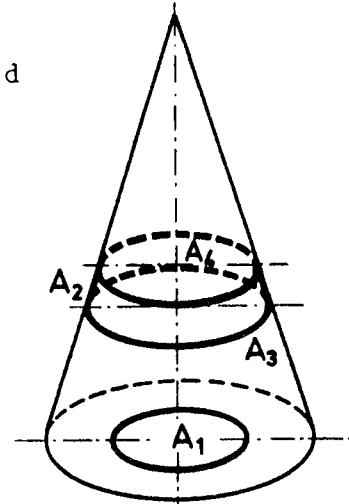
The following view factors may be obtained by use of those for two parallel circular discs.

Disc on the base of a right circular cone to an axisymmetrical portion of the conical surface.

$$F_{12} = F_{13} - F_{14}$$

For F_{13} and F_{14} see § 1.3.2.7.

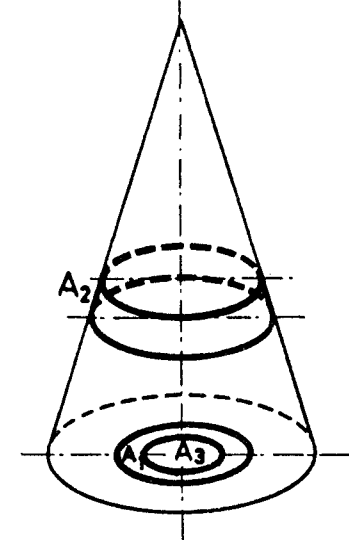
Reference: Buschman & Pittman (1961).



Ring on the base of a right circular cone to an axisymmetrical portion of the conical surface.

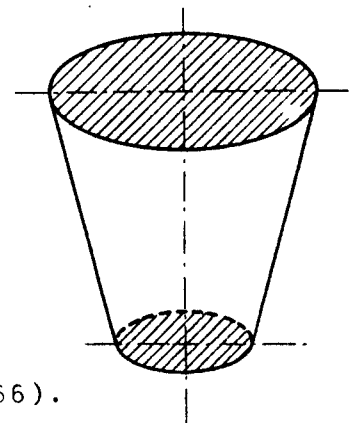
$$F_{12} = \left[1 + \frac{A_3}{A_1} \right] F_{(1,3)2} - \frac{A_3}{A_1} F_{32}$$

Reference: Buschman & Pittman (1961).



The following particular view factor can be obtained from the first one.

Inner surface of frustum of cone to ends.



References: Buschman & Pittman (1961), Bien (1966).

INTENTIONALLY BLANK PAGE

DIFFUSE SURFACES
Finite to Finite Surfaces

1.3.6. SPHERICAL TO PLANAR

1.3.6.1. SPHERE TO SECTOR OF A COAXIAL DISC

Sphere to sector of disc; normal to center of disc passes through center of sphere.

$$R_2 = \frac{r_2}{h}$$

$$h \geq r_1$$

Formulae:

$$F_{12} = \frac{\alpha}{4\pi} \left[1 - \frac{1}{\sqrt{1+R_2^2}} \right]$$

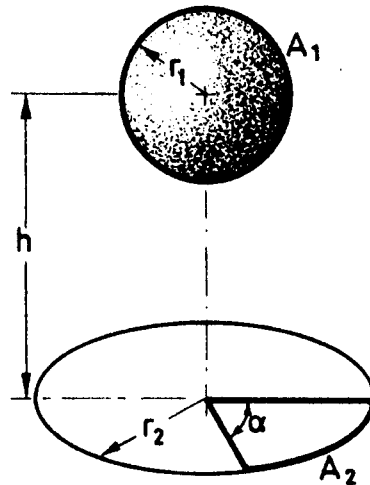
For $\alpha = 2\pi$

$$F_{12} = \frac{1}{2} \left[1 - \frac{1}{\sqrt{1+R_2^2}} \right]$$

Comments:

In the first of these two expressions α is measured in radians, although it is given in degrees in table and figure of the next page.

References: Feingold & Gupta (1970), Siegel & Howell (1972).



DIFFUSE SURFACES
Finite to Finite Surfaces

$R_2 \backslash \alpha^\circ$	30	60	90	120	150	180
.5	.00440	.00880	.01320	.01760	.02199	.02639
1.0	.01220	.02441	.03661	.04882	.06102	.07322
1.5	.01855	.03711	.05566	.07422	.09277	.11132
2.0	.02303	.04607	.06910	.09213	.11516	.13820
3.0	.02849	.05698	.08547	.11396	.14245	.17094
5.0	.03350	.06699	.10049	.13398	.16748	.20097
8.0	.03650	.07300	.10950	.14599	.18249	.21899
10.0	.03752	.07504	.11256	.15008	.18760	.22512
50.0	.04083	.08167	.12250	.16333	.20417	.24500
100.0	.04125	.08250	.12375	.16500	.20625	.24750

$R_2 \backslash \alpha^\circ$	210	240	270	300	330	360
.5	.03079	.03519	.03959	.04399	.04839	.05279
1.0	.08543	.09763	.10983	.12204	.13424	.14645
1.5	.12988	.14843	.16699	.18554	.20410	.22265
2.0	.16123	.18426	.20729	.23033	.25336	.27639
3.0	.19943	.22792	.25641	.28491	.31340	.34189
5.0	.23447	.26796	.30146	.33495	.36845	.40194
8.0	.25549	.29199	.32849	.36499	.40148	.43798
10.0	.26264	.30017	.33769	.37521	.41273	.45025
50.0	.28583	.32667	.36750	.40833	.44917	.49000
100.0	.28875	.33000	.37125	.41250	.45375	.49500

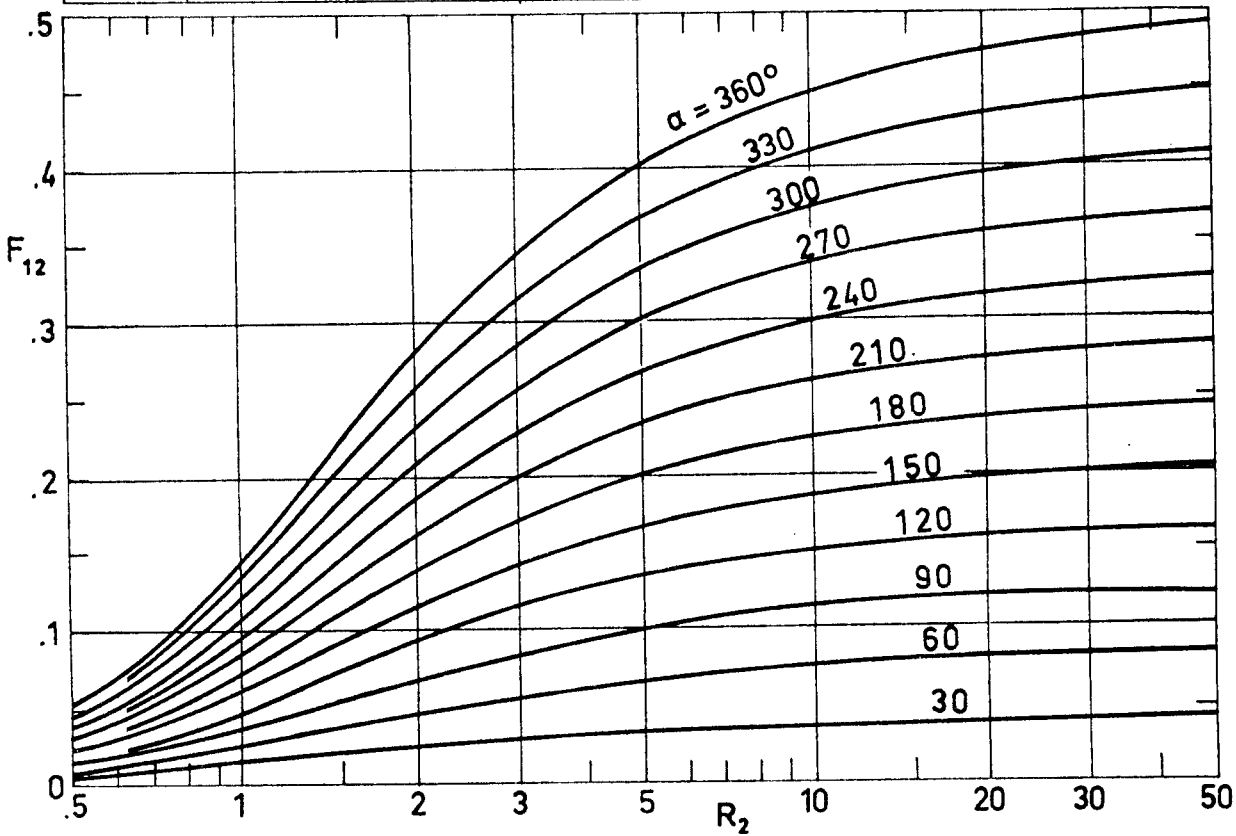


Fig 1-34. F_{12} as a function of R_2 for different values of the sector central angle α . Calculated by the compiler.

DIFFUSE SURFACES
Finite to Finite Surfaces

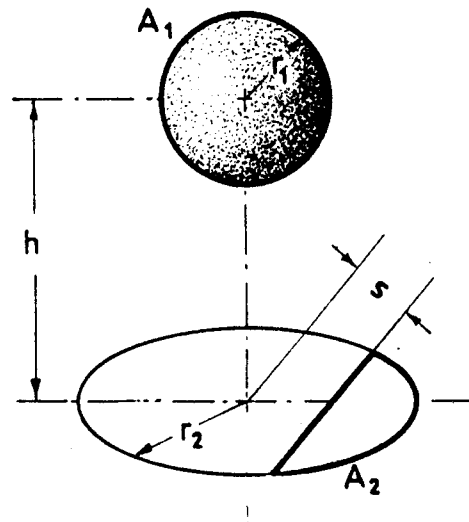
1.3.6.2. SPHERE TO SEGMENT OF A COAXIAL DISC

Sphere to segment of disc; normal to center of disc passes through center of sphere.

$$R_2 = \frac{r_2}{h}$$

$$Z = \frac{s}{r_2}$$

$$h \geq r_1$$



Formula:

$$F_{12} = \frac{1}{8} - \frac{\cos^{-1} Z}{2\pi\sqrt{1+R_2^2}} + \frac{1}{4\pi} \sin^{-1} \frac{1 - R_2^2 Z^2 - 2Z^2}{1 + R_2^2 Z^2}$$

References: Feingold & Gupta (1970), Siegel & Howell (1972).

DIFFUSE SURFACES
Finite to Finite Surfaces

Z \ R ₂	.5	1	1.5	2	3	5	8
-1.0	.0528	.1464	.2226	.2764	.3419	.4019	.4380
-.8	.0504	.1413	.2167	.2707	.3372	.3988	.4359
-.6	.0458	.1305	.2032	.2568	.3251	.3902	.4302
-.4	.0401	.1149	.1811	.2320	.3004	.3709	.4168
-.2	.0334	.0953	.1497	.1920	.2520	.3229	.3781
.0	.0264	.0732	.1113	.1382	.1709	.2010	.2190
.2	.0193	.0512	.0730	.0844	.0898	.0791	.0599
.4	.0127	.0315	.0416	.0444	.0414	.0310	.0212
.6	.0069	.0160	.0195	.0196	.0168	.0118	.0078
.8	.0024	.0052	.0059	.0057	.0047	.0032	.0021

Z \ R ₂	10	15	20	30	50	80	100
-1.0	.4502	.4667	.4750	.4833	.4900	.4938	.4950
-.8	.4486	.4656	.4742	.4828	.4897	.4935	.4948
-.6	.4439	.4625	.4718	.4812	.4887	.4929	.4944
-.4	.4329	.4549	.4661	.4774	.4864	.4915	.4932
-.2	.3997	.4311	.4427	.4649	.4788	.4867	.4894
.0	.2251	.2334	.2375	.2417	.2450	.2469	.2475
.2	.0505	.0356	.0273	.0185	.0112	.0070	.0056
.4	.0173	.0118	.0089	.0060	.0036	.0023	.0018
.6	.0063	.0043	.0032	.0021	.0013	.0008	.0006
.8	.0017	.0011	.0008	.0006	.0003	.0002	.0002

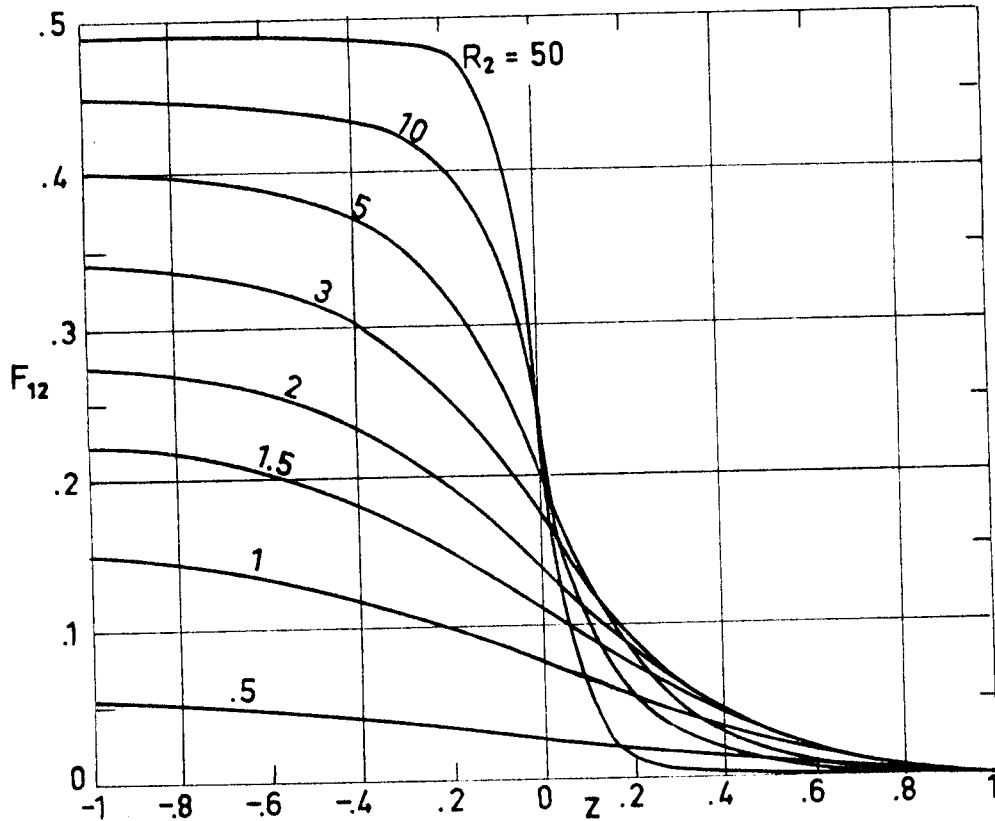


Fig 1-35. F_{12} as a function of Z for different values of R_2 .
Calculated by the compiler.

DIFFUSE SURFACES
Finite to Finite Surfaces

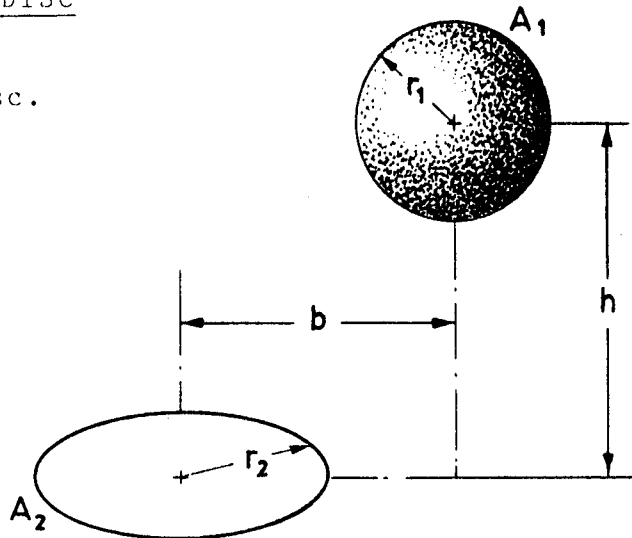
1.3.6.3. SPHERE TO NON-COAXIAL DISC

Sphere to a noncoaxial disc.

$$R = \frac{r_2}{h}$$

$$Z = \frac{b}{r_2}$$

$$h \geq r_1$$



Formula:

a) When $Z \geq 1$

$$F_{12} = \frac{1}{2\pi} \int_{Z-1}^{1+Z} \cos^{-1} \left[\frac{x^2 + Z^2 - 1}{2xZ} \right] xR^2 (1+R^2x^2)^{-3/2} dx$$

b) When $Z < 1$

$$F_{12} = \frac{1}{2\pi} \int_{1-Z}^{1+Z} \cos^{-1} \left[\frac{x^2 + Z^2 - 1}{2xZ} \right] xR^2 (1+R^2x^2)^{-3/2} dx +$$

$$+ \frac{1}{2} \left(1 - \frac{1}{\sqrt{1+R^2(1-Z)^2}} \right)$$

Reference: Feingold & Gupta (1970).

DIFFUSE SURFACES
Finite to Finite Surfaces

R \ Z	0	.2	.4	.6	.8	.9	1.
.5	.0528	.0523	.0507	.0482	.0450	.0432	.0413
1.0	.1464	.1436	.1360	.1235	.1074	.0984	.0893
1.5	.2226	.2186	.2063	.1850	.1551	.1379	.1202
2.0	.2764	.2720	.2581	.2323	.1920	.1671	.1407
3.0	.3419	.3379	.3248	.2976	.2465	.2089	.1661
5.0	.4019	.3991	.3894	.3675	.3152	.2637	.1914
8.0	.4380	.4361	.4296	.4141	.3717	.3165	.2087
10.0	.4502	.4487	.4434	.4307	.3942	.3414	.2152
50.0	.4900	.4897	.4886	.4849	.4775	.4615	.2351
100.0	.4950	.4948	.4943	.4929	.4888	.4806	.1843
R \ Z	1.1	1.2	1.4	1.6	1.8	2.	3.
.5	.0394	.0374	.0333	.0294	.0258	.0225	.0111
1.0	.0803	.0716	.0560	.0432	.0334	.0259	.0087
1.5	.1030	.0871	.0609	.0426	.0304	.0222	.0064
2.0	.1153	.0927	.0591	.0385	.0261	.0185	.0050
3.0	.1250	.0917	.0505	.0302	.0195	.0134	.0034
5.0	.1222	.0770	.0358	.0199	.0124	.0084	.0021
8.0	.1054	.0572	.0239	.0129	.0080	.0053	.0013
10.0	.0941	.0480	.0194	.0104	.0064	.0043	.0011
50.0	.0245	.0106	.0040	.0021	.0013	.0009	.0002
100.0	.0124	.0053	.0020	.0011	.0007	.0004	.0001

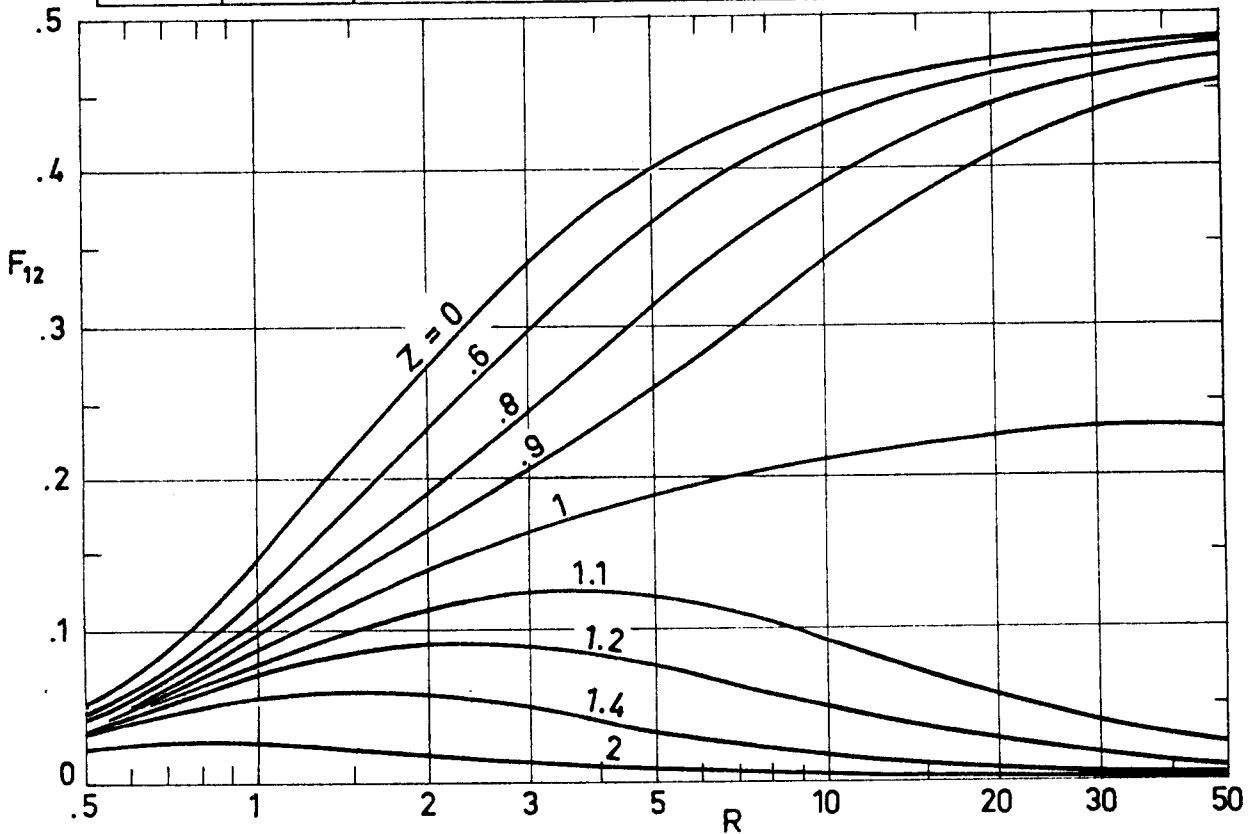


Fig 1-36. Values of F_{12} as a function of Z and R . Calculated by the compiler.

DIFFUSE SURFACES
Finite to Finite Surfaces

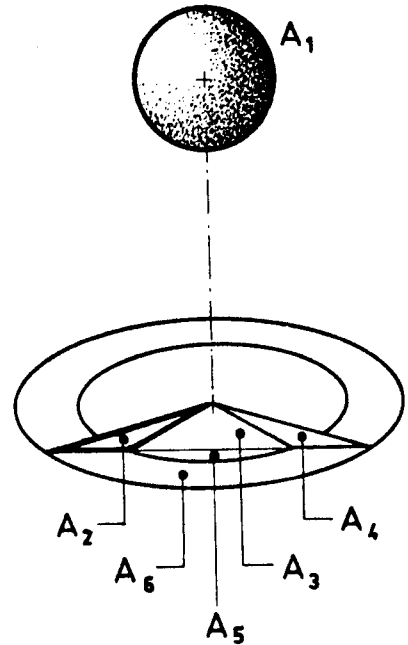
1.3.6.4. SPHERE TO ARBITRARY POLYGON

The following view factors may be obtained from those for a sphere viewing either a segment or a sector of a coaxial disc.

Sphere to general triangle with one vertex at the projection of the center of sphere on the plane of triangle. View factors is:

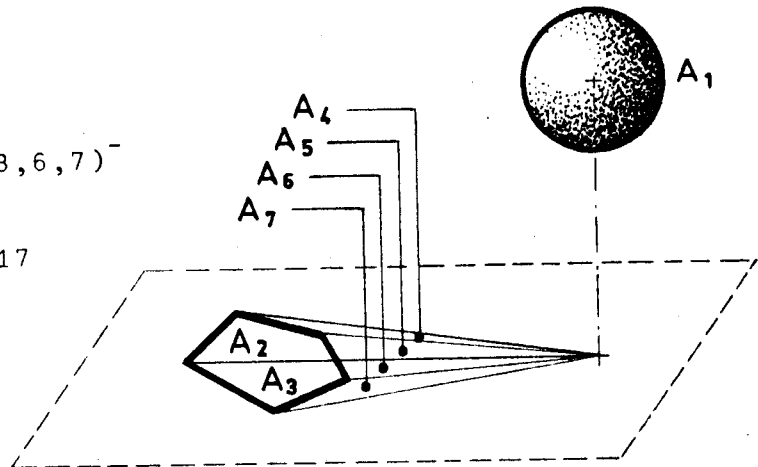
$$F_{12} = \frac{1}{2} \left[F_{1(2,3,4,5,6)} + F_{15} - F_{1(5,6)} - F_{1(3,5)} \right]$$

Reference: Feingold & Gupta (1970).



The view factor between a sphere and an arbitrary polygon may be obtained from the previous result.

$$F_{1(2,3)} = F_{1(2,4,5)} + F_{1(3,6,7)} - F_{14} - F_{15} - F_{16} - F_{17}$$



Reference: Feingold & Gupta (1970).

INTENTIONALLY BLANK PAGE

DIFFUSE SURFACES
Finite to Finite Surfaces

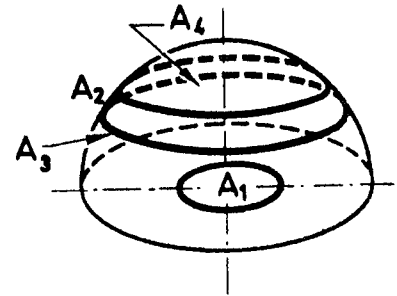
1.3.6.5. AXISYMMETRICAL CONFIGURATIONS

The following view factors may be obtained by use of those for two parallel circular discs.

Disc on the base of a hemisphere to an axisymmetrical portion of the spherical surface.

$$F_{12} = F_{13} - F_{14}$$

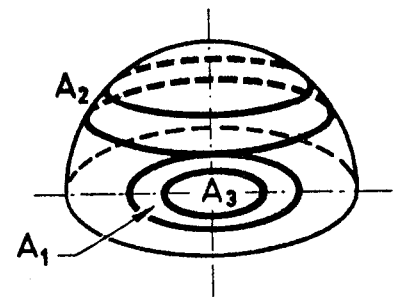
Reference: Buschman & Pittman (1961).



Ring on base of a hemisphere to an axisymmetrical portion of the spherical surface.

$$F_{12} = \left[1 + \frac{A_3}{A_1} \right] F_{(1,3)2} - \frac{A_3}{A_1} F_{32}$$

Reference: Buschman & Pittman (1961).

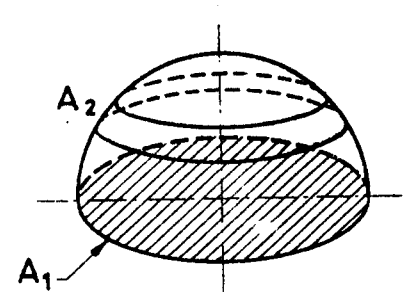


The following particular view factor can be obtained from the first one.

Axisymmetrical section of hemisphere to the base.

$$F_{12} = \frac{1}{2}$$

Reference: Buschman & Pittman (1961).



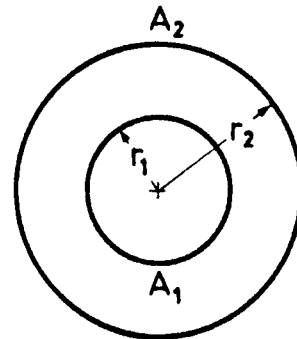
INTENTIONALLY BLANK PAGE

DIFFUSE SURFACES
Finite to Finite Surfaces

1.3.7. CYLINDRICAL TO CYLINDRICAL. TWO-DIMENSIONAL CONFIGURATIONS

1.3.7.1. CONCENTRIC CIRCULAR CYLINDERS

Two-dimensional concentric circular cylinders.



Formulae:

$$F_{12} = 1$$

$$F_{21} = \frac{r_1}{r_2}$$

$$F_{22} = 1 - \frac{r_1}{r_2}$$

References: Hamilton & Morgan (1952), Siegel & Howell (1972).

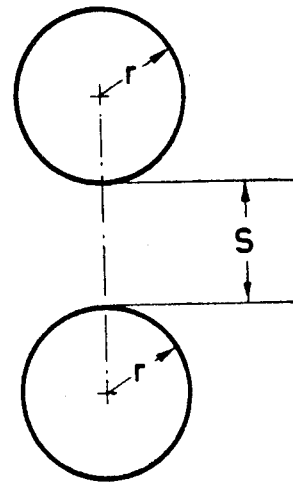
INTENTIONALLY BLANK PAGE

DIFFUSE SURFACES
Finite to Finite Surfaces

1.3.7.2. PARALLEL CYLINDERS OF THE SAME DIAMETER

Infinitely long parallel cylinders having the same diameter.

$$x = 1 + \frac{S}{2r}$$



Formula:

$$F_{12} = F_{21} = \frac{1}{\pi} \left[\sqrt{x^2 - 1} + \sin^{-1}(1/x) - x \right]$$

Reference : Siegel & Howell (1972).

DIFFUSE SURFACES
Finite to Finite Surfaces

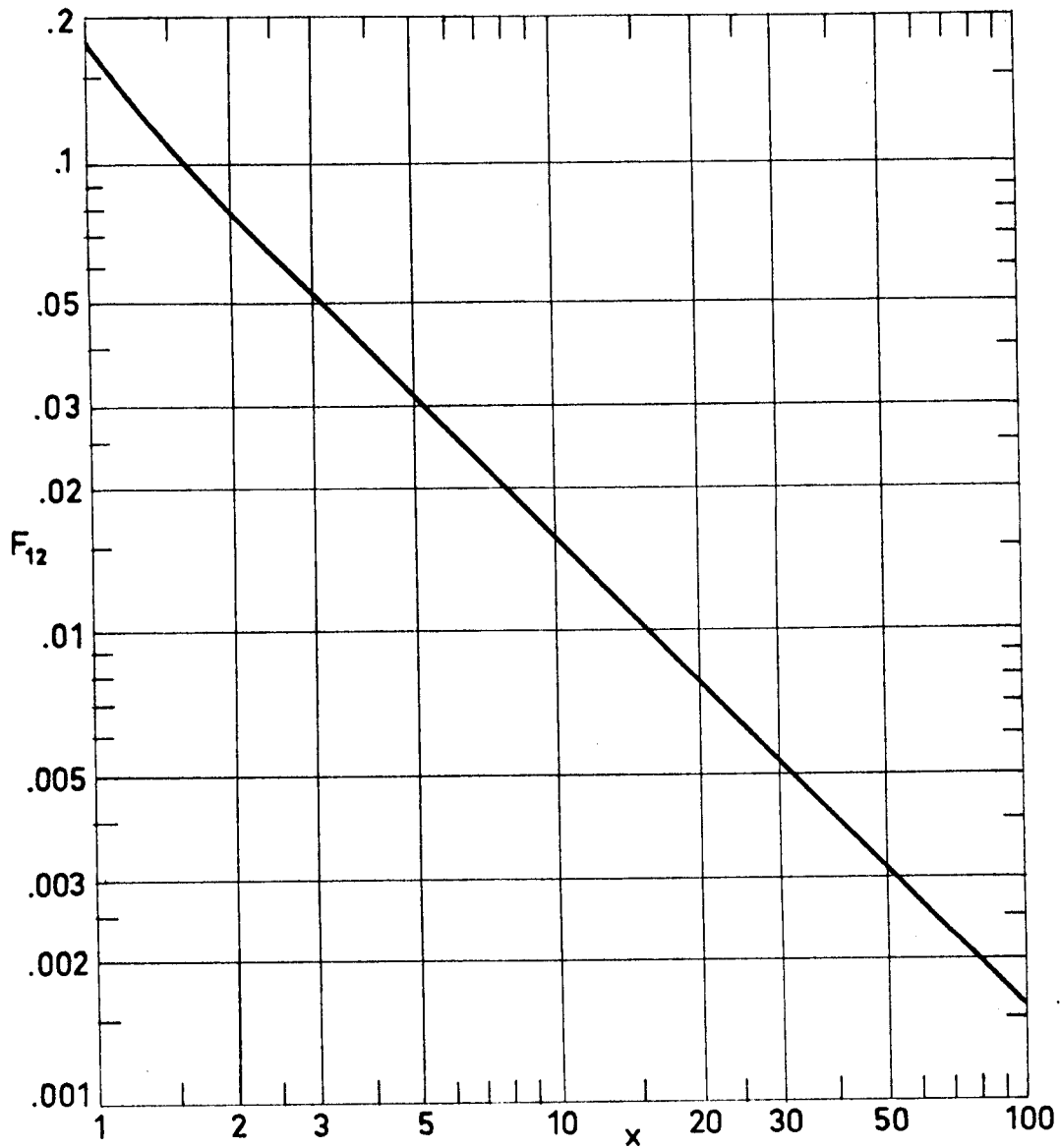


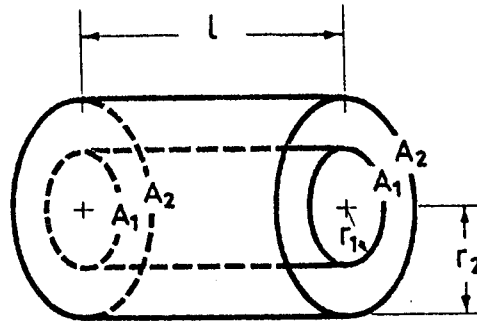
Fig 1-37. F_{12} as a function of x in the case of two infinitely long parallel cylinders of the same diameter. Calculated by the compiler.

DIFFUSE SURFACES
Finite to Finite Surfaces

1.3.8. CYLINDRICAL TO CYLINDRICAL. AXISYMMETRICAL CONFIGURATIONS

1.3.8.1. CONCENTRIC CIRCULAR
CYLINDERS OF THE
SAME LENGTH

Two concentric cylinders of same finite length.



$$R = \frac{r_2}{r_1}$$

$$L = \frac{L}{r_1}$$

Formulae:

$$F_{21} = \frac{1}{R} - \frac{1}{\pi R} \left\{ \cos^{-1} \left(\frac{B}{A} \right) - \frac{1}{2L} \left[\sqrt{(A+2)^2 - (2R)^2} \cos^{-1} \left(\frac{B}{RA} \right) + B \sin^{-1} \left(\frac{1}{R} \right) - \frac{\pi A}{2} \right] \right\}$$

$$F_{22} = 1 - \frac{1}{R} + \frac{2}{\pi R} \tan^{-1} \left(\frac{2\sqrt{R^2-1}}{L} \right) -$$

$$- \frac{L}{2\pi R} \left\{ \frac{\sqrt{4R^2+L^2}}{L} \sin^{-1} \left[\frac{4(R^2-1) + (L^2/R^2)(R^2-2)}{L^2 + 4(R^2-1)} \right] - \right.$$

$$\left. - \sin^{-1} \left(\frac{R^2-2}{R^2} \right) + \frac{\pi}{2} \left(\frac{\sqrt{4R^2+L^2}}{L} - 1 \right) \right\}$$

where for any argument ξ :

$$-\frac{\pi}{2} \leq \sin^{-1} \xi \leq \frac{\pi}{2}$$

$$0 \leq \cos^{-1} \xi \leq \pi$$

with

$$A = L^2 + R^2 - 1$$

$$B = L^2 - R^2 + 1$$

$$\lim_{L \rightarrow \infty} F_{21} = \frac{1}{R} \quad ; \quad \lim_{L \rightarrow \infty} F_{22} = 1 - \frac{1}{R}$$

References: Hamilton & Morgan (1952), Leuenberger & Person (1956), Siegel & Howell (1972).

DIFFUSE SURFACES
Finite to Finite Surfaces

L \ R	1.1	1.2	1.3	1.4	1.5	1.6	1.7	1.8	2.0	2.5
.2	.579	.365	.250	.183	.141	.113	.092	.077	.057	.031
.4	.726	.538	.409	.318	.256	.209	.174	.148	.110	.061
.6	.783	.623	.501	.408	.339	.284	.241	.207	.157	.090
.8	.814	.671	.558	.469	.398	.341	.294	.256	.198	.116
1.0	.833	.702	.596	.510	.441	.383	.335	.295	.232	.140
1.2	.845	.723	.623	.541	.473	.415	.367	.326	.261	.161
1.4	.854	.738	.643	.563	.497	.441	.393	.351	.285	.180
1.6	.861	.750	.658	.581	.516	.461	.413	.372	.305	.197
1.8	.866	.759	.670	.595	.532	.477	.430	.390	.322	.212
2.0	.871	.766	.680	.606	.544	.491	.444	.404	.337	.225
3.0	.883	.788	.709	.641	.584	.534	.490	.451	.386	.272
4.0	.890	.800	.724	.659	.604	.556	.513	.476	.413	.301
6.0	.896	.811	.739	.678	.625	.578	.538	.502	.440	.331
8.0	.899	.816	.747	.687	.635	.590	.550	.515	.455	.348
10.0	.901	.820	.751	.692	.641	.597	.558	.523	.464	.358
∞	.909	.833	.769	.714	.667	.625	.588	.556	.500	.400

L \ R	3.0	4.0	5.0	6.0	7.0	8.0	10.0	20.0	30.0	40.0
.2	.020	.010	.006	.004	.003	.002	.001	.0	.0	.0
.4	.039	.020	.012	.008	.006	.004	.003	.001	.0	.0
.6	.058	.030	.018	.012	.009	.007	.004	.001	.0	.0
.8	.076	.039	.024	.016	.012	.009	.006	.001	.001	.0
1.0	.092	.049	.030	.020	.015	.011	.007	.002	.001	.0
1.2	.108	.058	.036	.024	.017	.013	.008	.002	.001	.0
1.4	.123	.066	.041	.028	.020	.015	.010	.002	.001	.001
1.6	.136	.075	.047	.032	.023	.017	.011	.003	.001	.001
1.8	.148	.082	.052	.035	.026	.020	.012	.003	.001	.001
2.0	.159	.090	.057	.039	.028	.022	.014	.003	.001	.001
3.0	.201	.121	.079	.056	.041	.031	.020	.005	.002	.001
4.0	.228	.143	.097	.070	.052	.040	.026	.007	.003	.002
6.0	.260	.172	.122	.091	.070	.055	.037	.010	.004	.002
8.0	.277	.190	.139	.106	.083	.067	.046	.013	.006	.003
10.0	.288	.201	.150	.116	.092	.075	.053	.015	.007	.004
∞	.333	.250	.200	.167	.143	.125	.100	.050	.033	.025

These values are plotted in Fig 1-38.

DIFUSSE SURFACES
Finite to Finite Surfaces

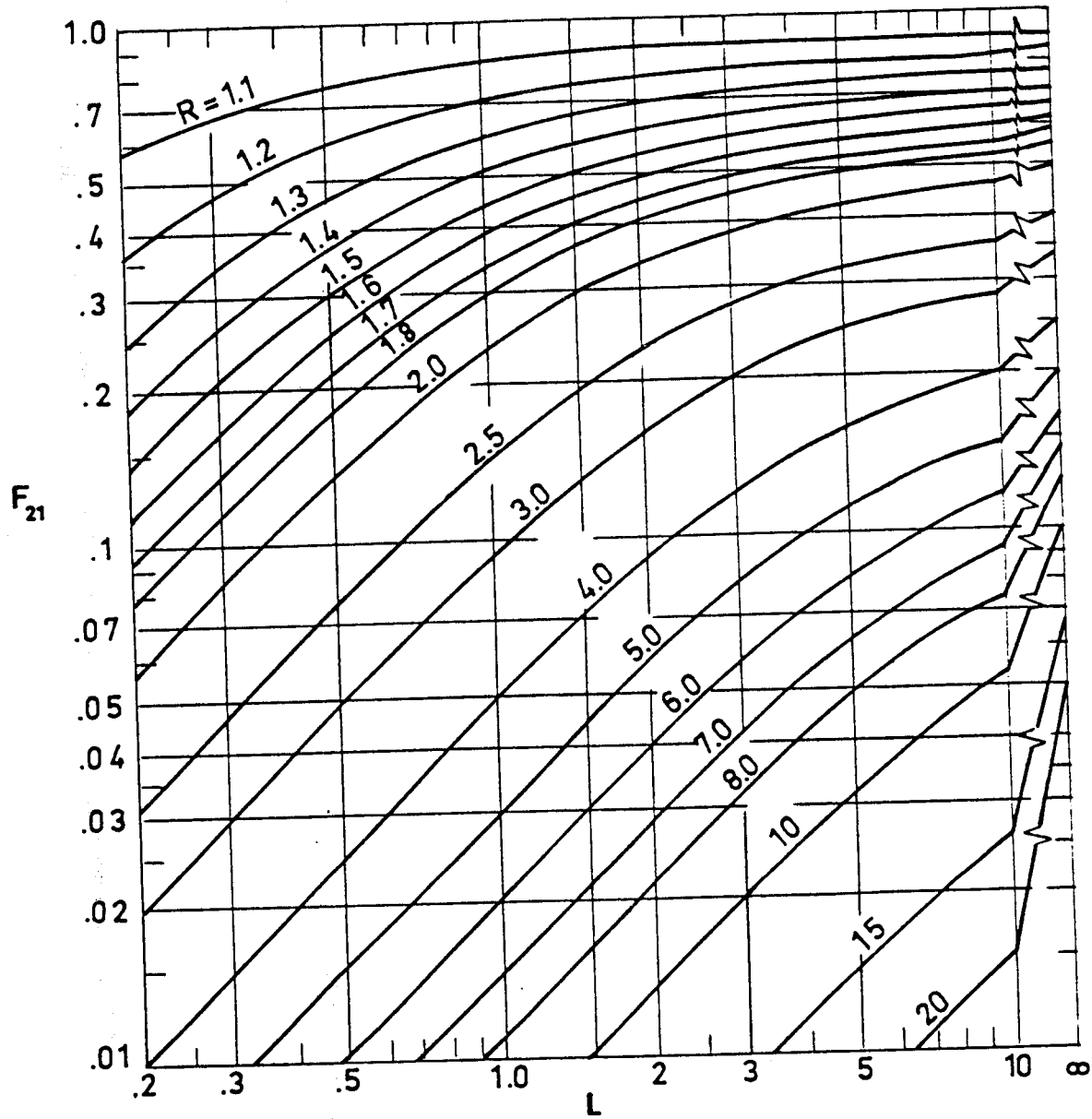


Fig 1-38. Plot of F_{21} vs. L for different values of R .
From Hamilton & Morgan (1952).

DIFFUSE SURFACES
Finite to Finite Surfaces

L \ R	1.1	1.2	1.3	1.4	1.5	1.6	1.7	1.8	2.0	2.5
.2	.021	.028	.031	.033	.034	.034	.034	.033	.032	.029
.4	.036	.050	.057	.061	.063	.064	.064	.063	.062	.056
.6	.047	.067	.079	.085	.089	.091	.091	.091	.089	.082
.8	.054	.081	.096	.106	.111	.114	.116	.116	.114	.106
1.0	.060	.091	.111	.123	.131	.135	.138	.139	.138	.129
1.2	.064	.101	.124	.138	.148	.154	.157	.159	.159	.150
1.4	.067	.108	.134	.151	.163	.170	.175	.178	.179	.170
1.6	.070	.114	.143	.163	.176	.185	.191	.194	.197	.189
1.8	.072	.118	.150	.172	.188	.198	.205	.210	.213	.207
2.0	.074	.123	.157	.181	.198	.210	.218	.223	.228	.224
3.0	.079	.136	.178	.210	.234	.252	.266	.276	.288	.293
4.0	.082	.143	.190	.227	.256	.279	.296	.310	.329	.344
6.0	.085	.151	.203	.245	.281	.308	.331	.349	.377	.411
8.0	.086	.155	.210	.255	.293	.324	.350	.372	.406	.452
10.0	.087	.157	.214	.261	.302	.334	.362	.386	.423	.479
∞	.091	.167	.231	.296	.333	.375	.412	.444	.500	.600

L \ R	3.0	4.0	5.0	6.0	7.0	8.0	10.0	20.0	30.0	40.0
.2	.026	.021	.017	.015	.013	.011	.009	.005	.003	.002
.4	.050	.041	.034	.029	.026	.023	.019	.010	.007	.005
.6	.073	.061	.051	.043	.038	.034	.028	.014	.010	.007
.8	.096	.079	.067	.057	.050	.045	.037	.019	.013	.010
1.0	.117	.097	.082	.071	.062	.056	.046	.024	.016	.012
1.2	.138	.115	.098	.084	.074	.066	.054	.029	.020	.015
1.4	.157	.132	.112	.098	.086	.077	.063	.033	.023	.017
1.6	.175	.148	.127	.110	.097	.087	.072	.038	.026	.019
1.8	.193	.164	.141	.123	.109	.097	.080	.043	.029	.022
2.0	.210	.180	.155	.135	.120	.107	.089	.047	.032	.024
3.0	.282	.249	.219	.193	.172	.155	.129	.070	.048	.036
4.0	.338	.307	.274	.245	.220	.200	.168	.092	.063	.048
6.0	.417	.397	.365	.333	.304	.278	.237	.134	.093	.071
8.0	.468	.460	.433	.402	.372	.345	.299	.174	.122	.093
10.0	.502	.506	.485	.458	.429	.401	.352	.211	.149	.115
∞	.667	.750	.800	.833	.857	.874	.900	.950	.967	.975

These values are plotted in Fig 1-39.

DIFFUSE SURFACES
Finite to Finite Surfaces

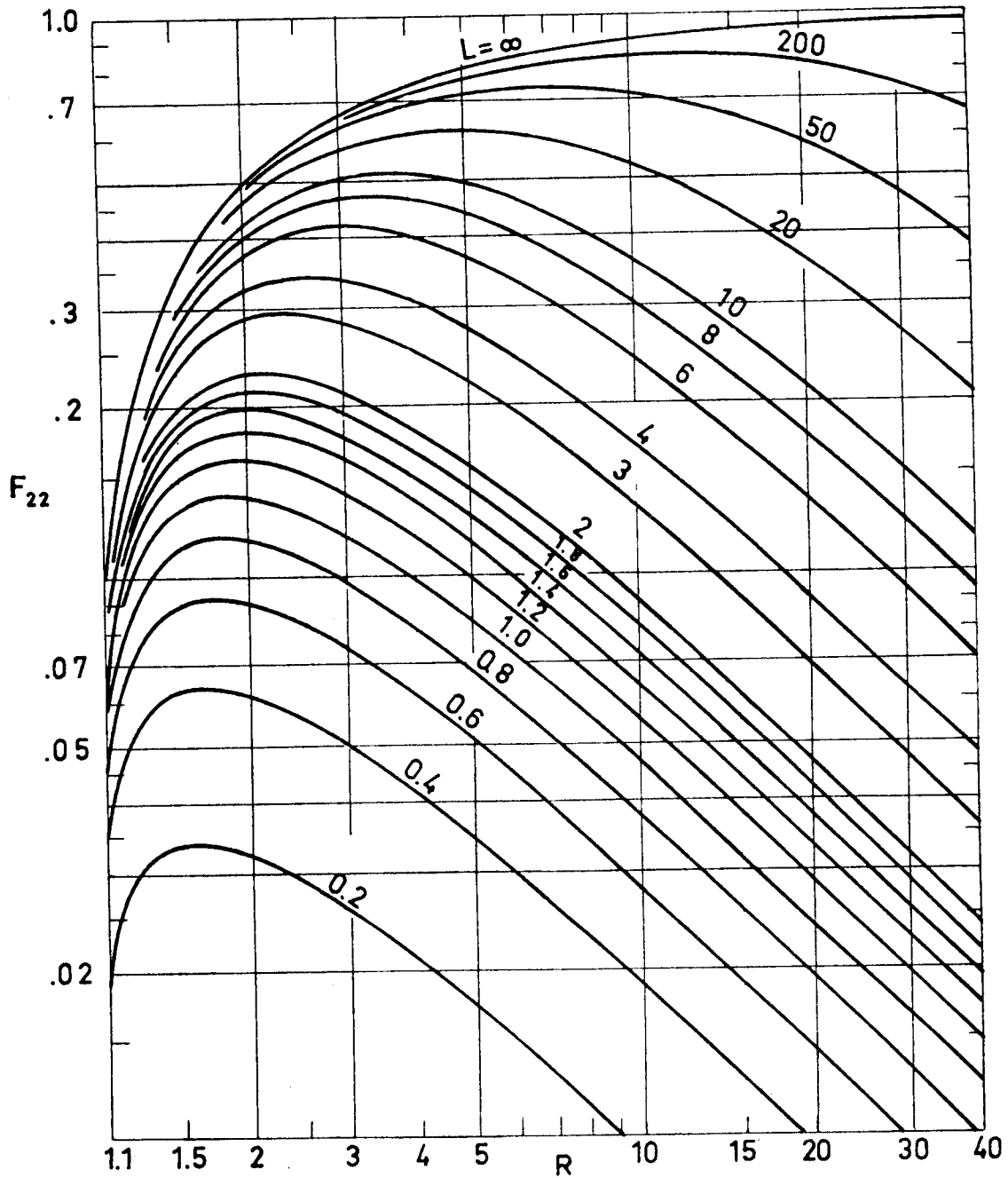


Fig 1-39. Plot of F_{22} , vs. R for different values of L .
From Hamilton & Morgan (1952).

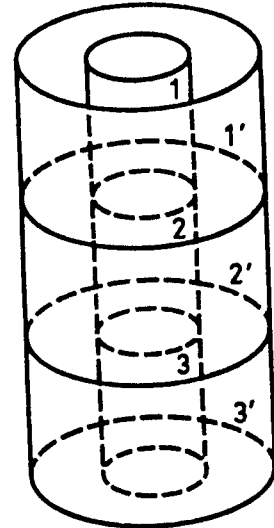
Rev. 2. 1984

DIFFUSE SURFACES
Finite to Finite Surfaces

1.3.8.2. CONCENTRIC CIRCULAR CYLINDERS OF UNEQUAL LENGTH

The following view factors can be deduced by use of the results for two concentric cylinders of the same finite length.

Concentric cylinders of different finite length. The view factors are given by the following expressions:



$$A_2 F_{2(1',2',3')} = A_{2'} F_{2'(1,2,3)} =$$

$$= \frac{1}{2} \left[K_{(1,2)2} + K_{(2,3)2} - K_{12} - K_{32} \right]$$

$$A_1 F_{13'} = A_3 F_{31'} = \frac{1}{2} \left[K_{(1,2,3)2} - K_{(1,2)2} - K_{(2,3)2} + K_{22} \right]$$

where $K_{m2} = A_m F_{mm'}$

Reference: Leuenberger & Person (1956).

DIFFUSE SURFACES
Finite to Finite Surfaces

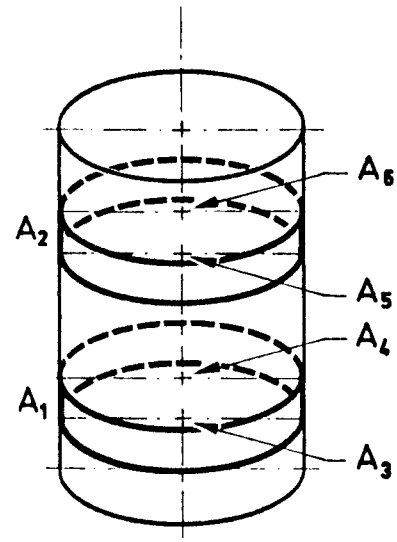
1.3.8.3. FINITE AREAS IN THE SAME CIRCULAR CYLINDER

The following view factor may be obtained from those for two parallel circular discs.

Finite ring area on interior of right circular cylinder to separate similar area

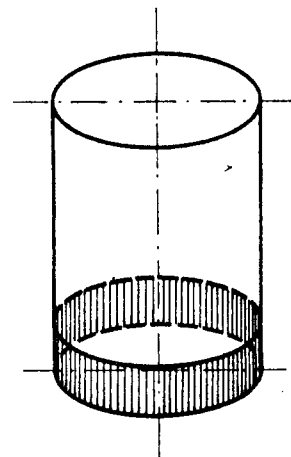
$$F_{12} = \frac{A_4}{A_1} \left[F_{45} - F_{46} - F_{35} + F_{36} \right]$$

Reference: Buschman & Pittman (1961).



The following view factor can be deduced as a particular case of the previous one.

Portion of inner surface of cylinder to remainder of inner surface.



References: Leuenberger & Person (1956), Buschman & Pittman (1961).

INTENTIONALLY BLANK PAGE

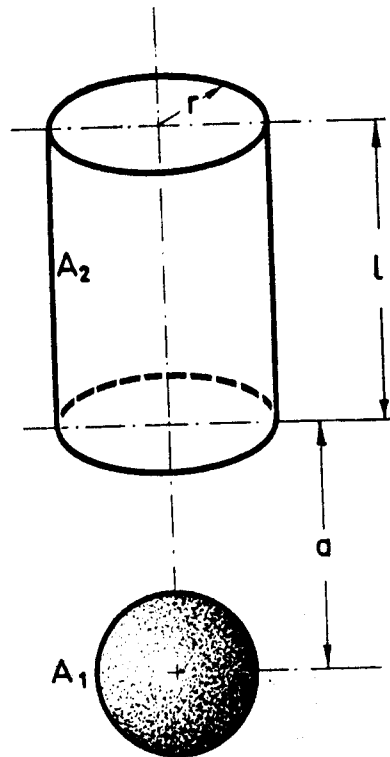
DIFFUSE SURFACES
Finite to Finite Surfaces

1.3.9. SPHERICAL TO CYLINDRICAL

Sphere to the inner surface of a coaxial cylinder having equal or larger radius.

$$R = \frac{r}{a}$$

$$Z = \frac{l}{r}$$



Formula:

$$F_{12} = \frac{1}{2} \left[\frac{1+RZ}{\sqrt{(RZ+1)^2+R^2}} - \frac{1}{\sqrt{1+R^2}} \right]$$

Reference : Feingold & Gupta (1970).

DIFFUSE SURFACES

Finite to Finite Surfaces

R \ Z	.05	.1	.15	.2	.3	.5	.8
.5	.0022	.0042	.0061	.0080	.0113	.0170	.0237
1.0	.0085	.0164	.0237	.0306	.0428	.0625	.0835
1.5	.0139	.0269	.0389	.0501	.0702	.1023	.1358
2.0	.0174	.0336	.0489	.0631	.0887	.1299	.1727
3.0	.0209	.0407	.0595	.0772	.1094	.1620	.2168
5.0	.0232	.0456	.0671	.0876	.1255	.1887	.2555
8.0	.0242	.0477	.0706	.0925	.1336	.2030	.2775
10.0	.0244	.0483	.0715	.0939	.1359	.2075	.2847
50.0	.0249	.0496	.0738	.0974	.1424	.2207	.3070
100.0	.0249	.0497	.0740	.0978	.1430	.2222	.3097

R \ Z	1	1.5	2	3	5	8	10
.5	.0271	.0335	.0379	.0431	.0478	.0503	.0511
1.0	.0937	.1107	.1208	.1315	.1396	.1434	.1444
1.5	.1514	.1766	.1908	.2050	.2150	.2194	.2205
2.0	.1924	.2236	.2406	.2572	.2683	.2730	.2741
3.0	.2419	.2808	.3015	.3208	.3333	.3383	.3396
5.0	.2861	.3329	.3571	.3792	.3929	.3983	.3996
8.0	.3117	.3638	.3904	.4142	.4287	.4342	.4356
10.0	.3202	.3742	.4017	.4261	.4409	.4465	.4478
50.0	.3470	.4077	.4381	.4647	.4804	.4862	.4875
100.0	.3503	.4119	.4427	.4695	.4853	.4911	.4925

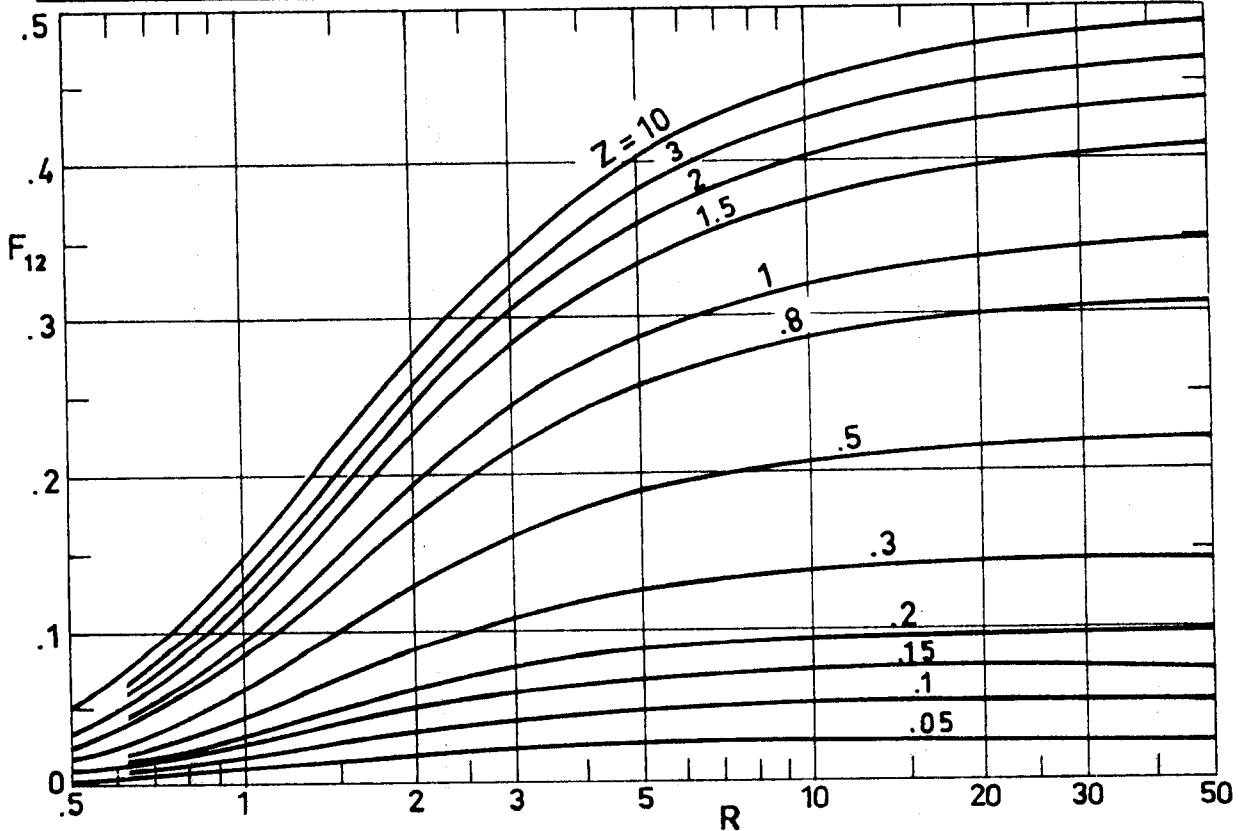


Fig 1-40. F_{12} as a function of R for different values of Z. Calculated by the compiler.

DIFFUSE SURFACES
Finite to Finite Surfaces

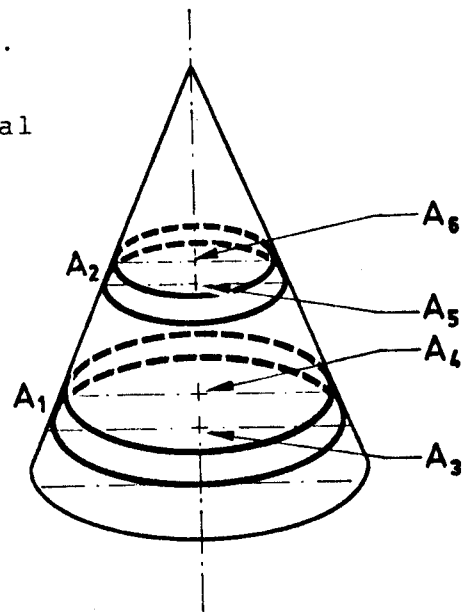
1.3.10. CONICAL TO CONICAL

The following view factor may be obtained from those corresponding to two parallel circular discs.

View factor between axisymmetrical sections of right circular cone

$$F_{12} = \frac{A_4}{A_1} (F_{45} - F_{46}) - \frac{A_3}{A_1} (F_{35} - F_{36})$$

For F_{35} , F_{36} , F_{45} and F_{46} see § 1.3.2.7.



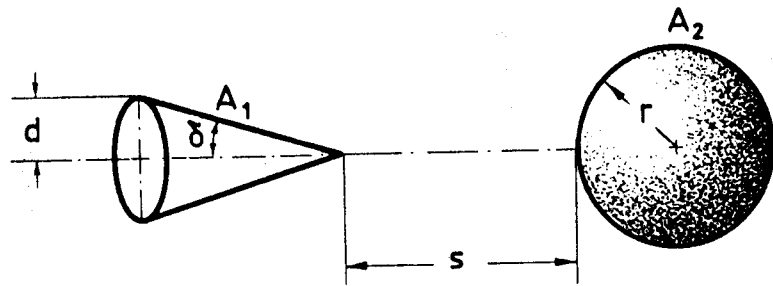
Reference: Buschman & Pittman (1961).

INTENTIONALLY BLANK PAGE

DIFFUSE SURFACES
Finite to Finite Surfaces

1.3.11. CONICAL TO SPHERICAL

Cone to sphere; axis of cone passes through center of sphere.



$$S = \frac{s}{r}$$

$$D = \frac{d}{r}$$

All results presented in the literature are obtained numerically.

Reference: Campbell & McConnell (1968).

DIFFUSE SURFACES
Finite to Finite Surfaces

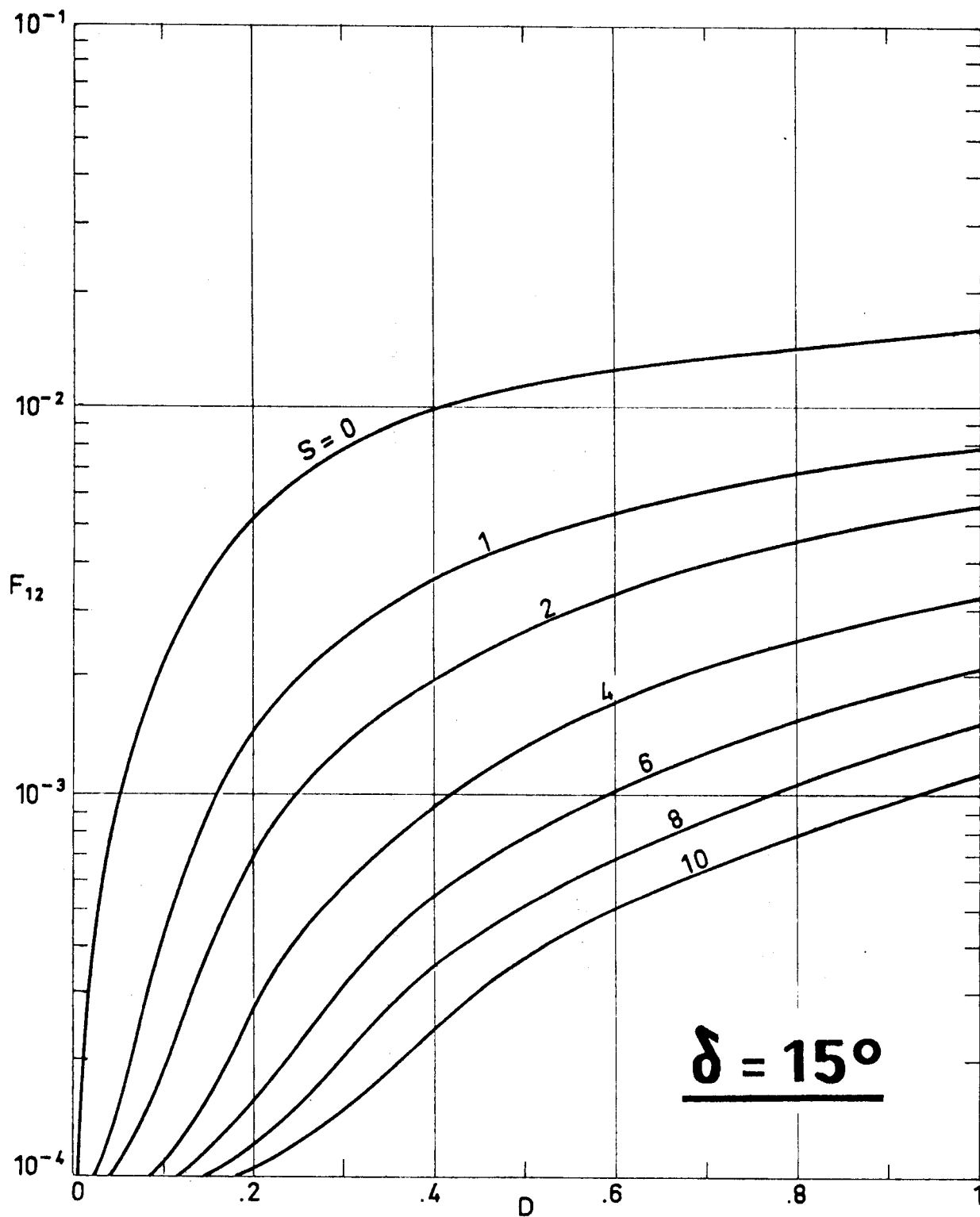


Fig 1-41. Values of F_{12} as a function of S and D , for $\delta = 15^\circ$.

From Campbell & McConnell (1968).

DIFFUSE SURFACES
Finite to Finite Surfaces

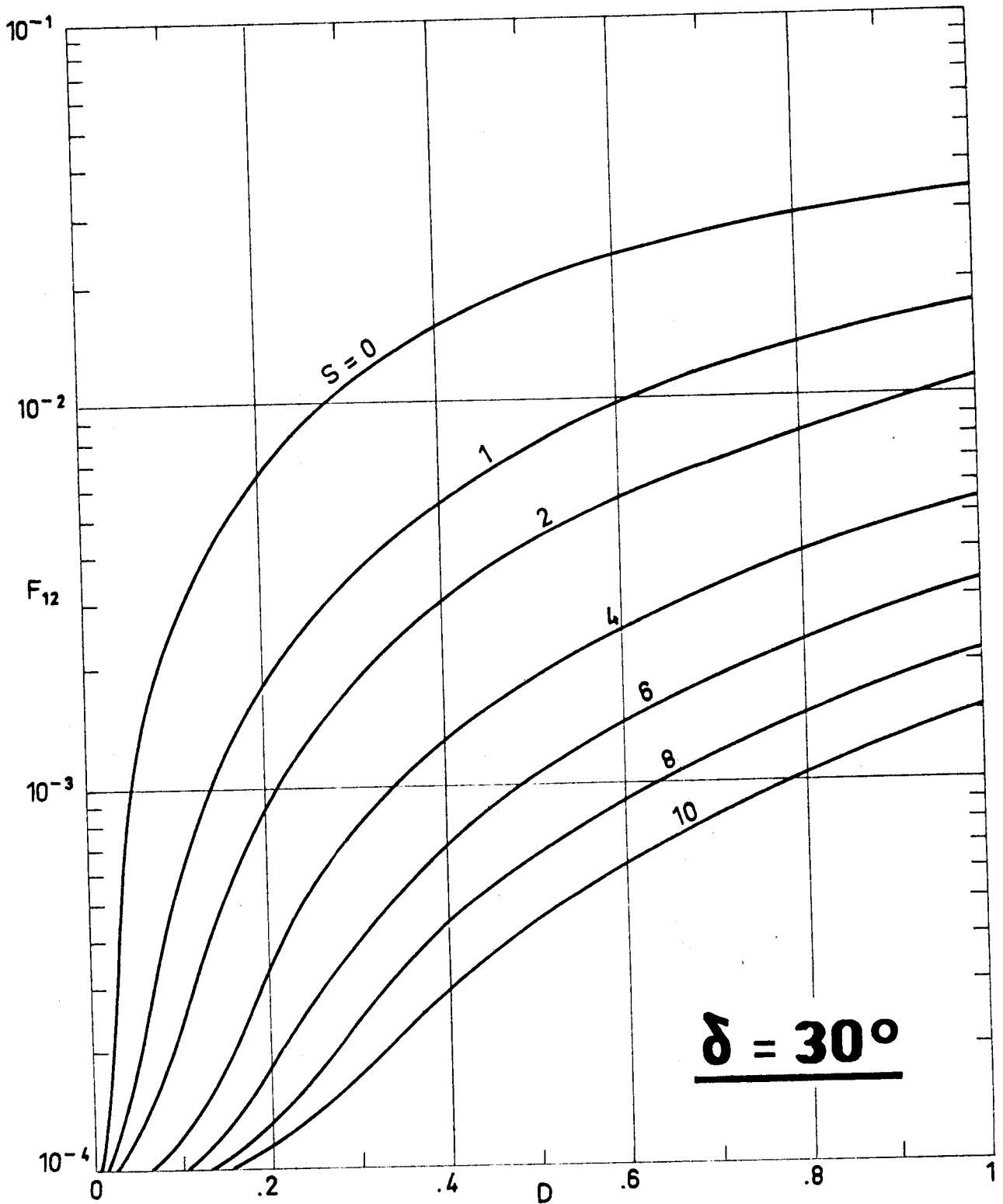


Fig 1-42. Values of F_{12} as a function of S and D , for $\delta = 30^\circ$.
From Campbell & McConnell (1968).

DIFFUSE SURFACES
Finite to Finite Surfaces

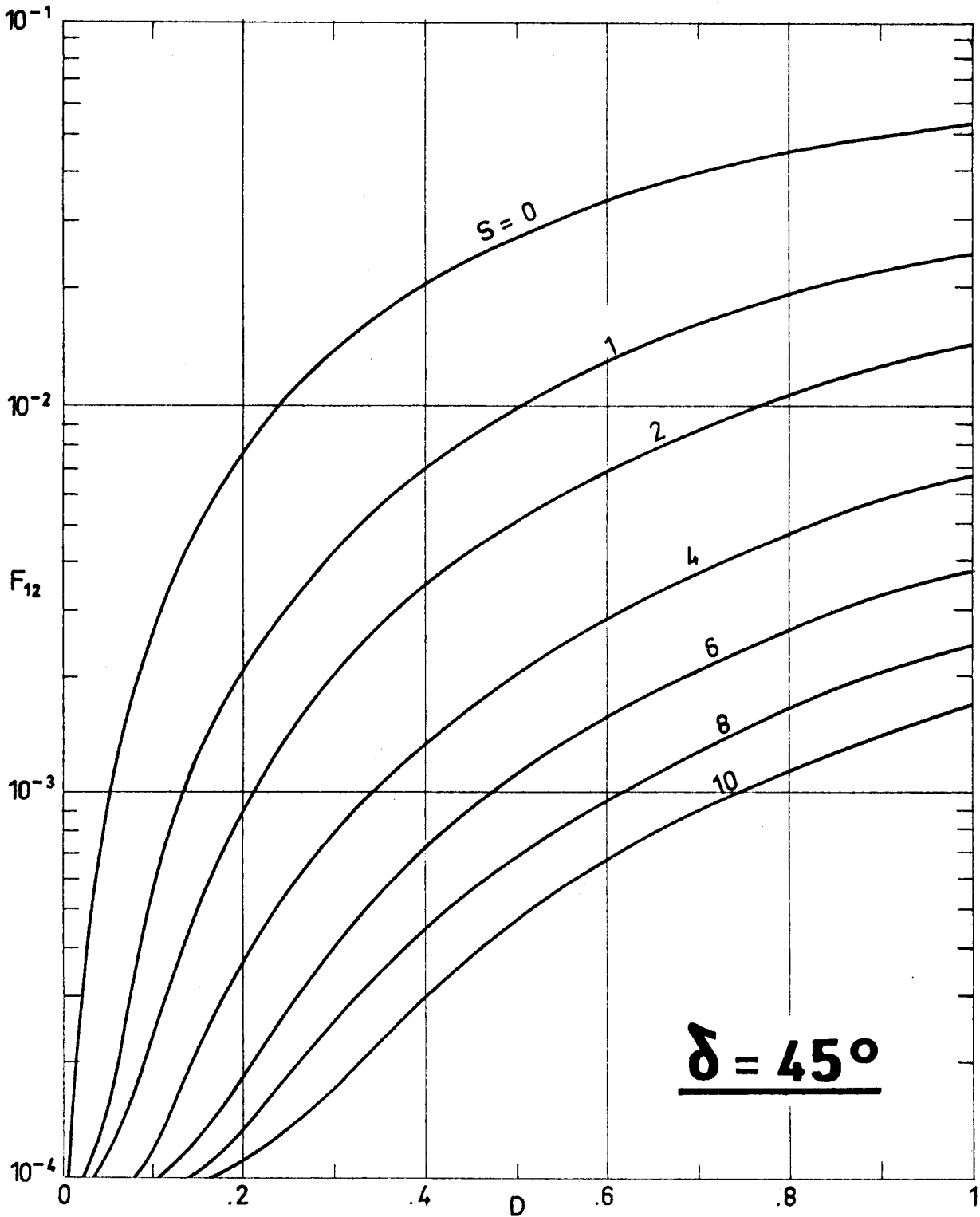


Fig 1-43. Values of F_{12} as a function of S and D , for $\delta = 45^\circ$.
From Campbell & McConnell (1968).

DIFFUSE SURFACES
Finite to Finite Surfaces

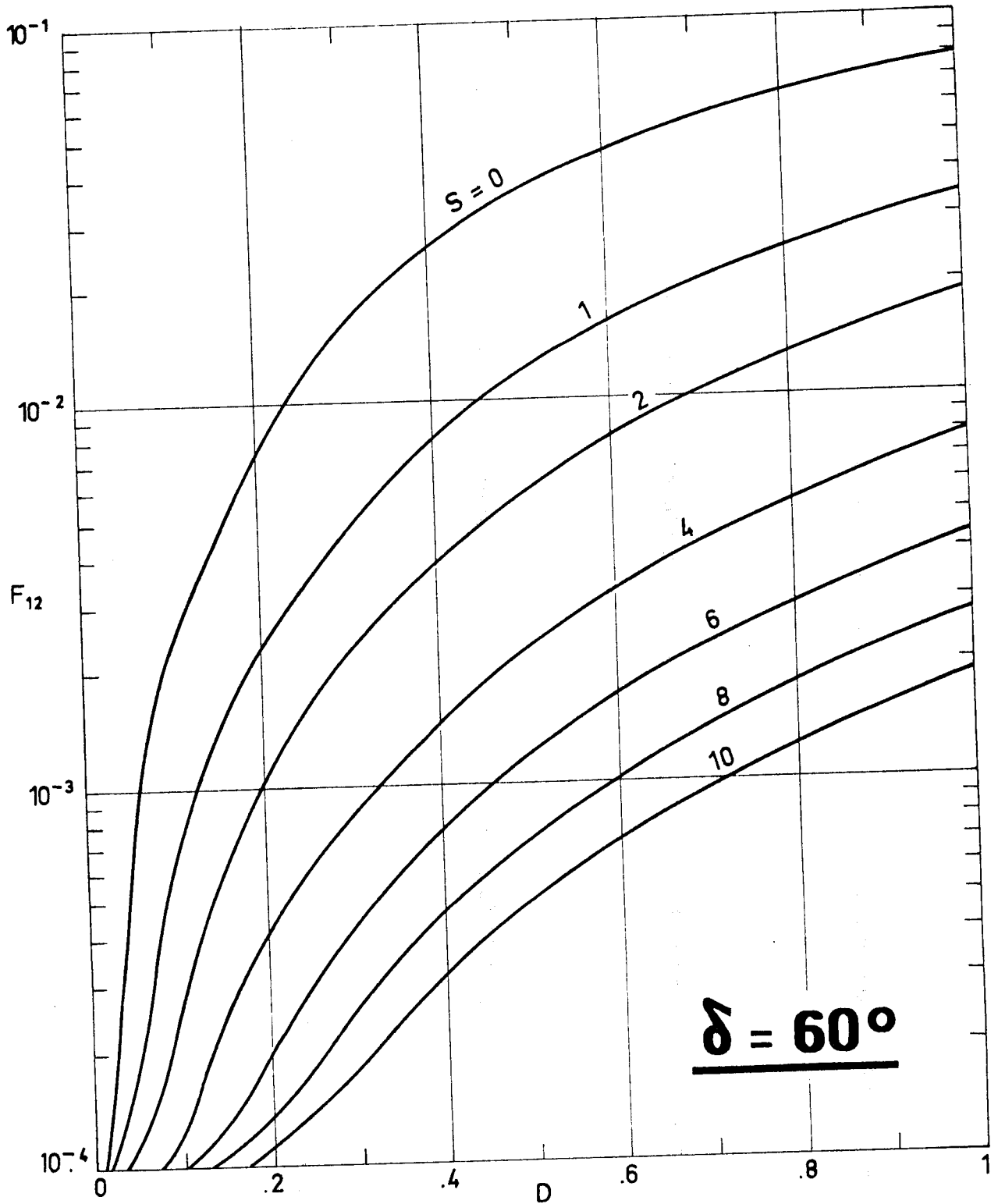


Fig 1-44. Values of F_{12} as a function of S and D , for $\delta = 60^\circ$.
From Campbell & McConnell (1968).

INTENTIONALLY BLANK PAGE

DIFFUSE SURFACES
Finite to Finite Surfaces

1.3.12. SPHERICAL TO SPHERICAL1.3.12.1. CONCENTRIC SPHERES

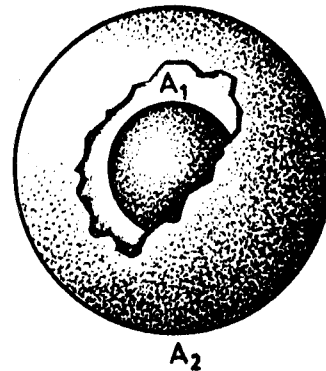
Concentric spheres; inner to outer sphere; outer to inner sphere; outer sphere to itself.

Formulae:

$$F_{12} = 1$$

$$F_{21} = \left(\frac{r_1}{r_2}\right)^2$$

$$F_{22} = 1 - \left(\frac{r_1}{r_2}\right)^2$$



where r_1 and r_2 are the radii of spheres A_1 and A_2 , respectively.

References: Hamilton & Morgan (1952), Kreith (1962), Siegel & Howell (1972).

INTENTIONALLY BLANK PAGE

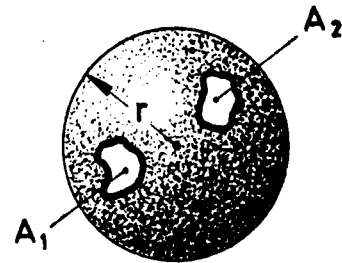
DIFFUSE SURFACES
Finite to Finite Surfaces

1.3.12.2. FINITE AREAS IN THE SAME SPHERICAL SURFACE

Finite areas on interior of spherical cavity.

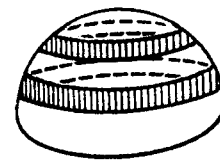
Formula:

$$F_{12} = \frac{A_2}{4\pi r^2}$$



References: Jakob (1957), Siegel & Howell (1972).

View factors between axisymmetrical sections of hemisphere can be deduced as a particular case of the previous one.



Reference: Buschman & Pittman (1961).

INTENTIONALLY BLANK PAGE

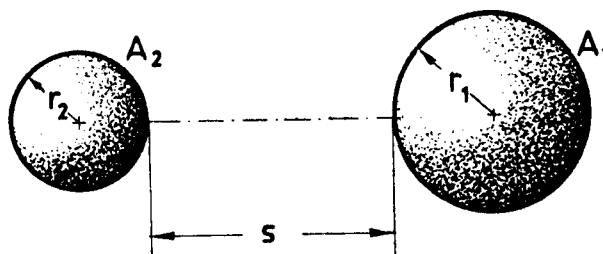
DIFFUSE SURFACES
Finite to Finite Surfaces

1.3.12.3. SPHERE TO OUTER SPHERE

Sphere to sphere.

$$S = \frac{s}{r_1}$$

$$R = \frac{r_2}{r_1}$$



All results presented in the literature are obtained numerically.

References: Jones (1965), Campbell & McConnell (1968).

DIFFUSE SURFACES
Finite to Finite Surfaces

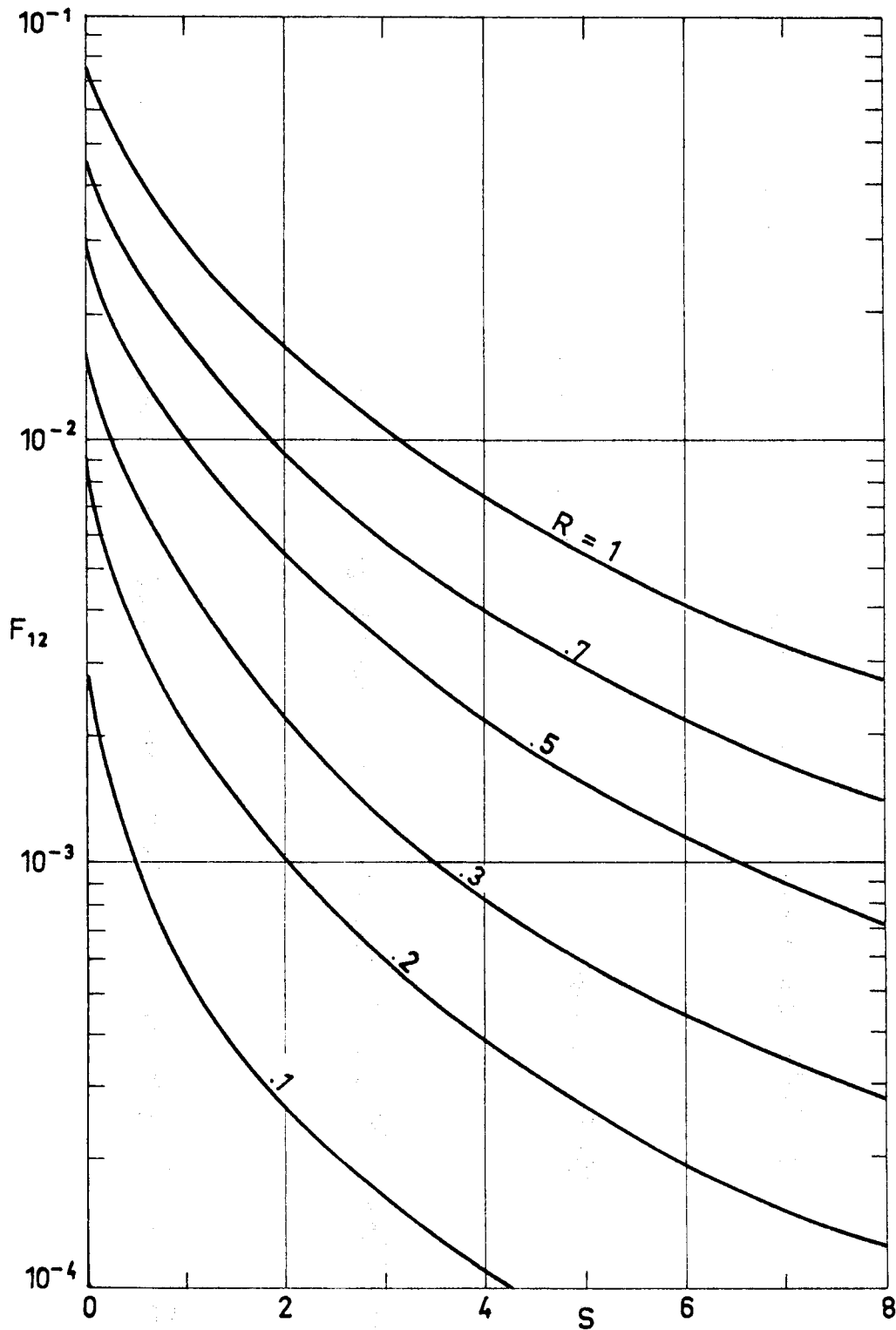


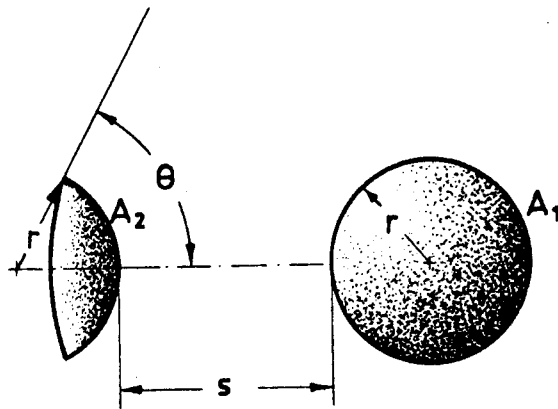
Fig 1-45. Values of F_{12} as a function of S and R . From Jones (1965).

DIFFUSE SURFACES
Finite to Finite Surfaces

1.3.12.4. SPHERE TO CAP ON ANOTHER SPHERE OF EQUAL RADIUS

Sphere to cap on another sphere having equal radius and placed in an axisymmetrical fashion.

$$S = \frac{s}{r}$$



All results presented in the literature have been obtained numerically.

Reference: Campbell & McConnell (1968).

DIFFUSE SURFACES
Finite to Finite Surfaces

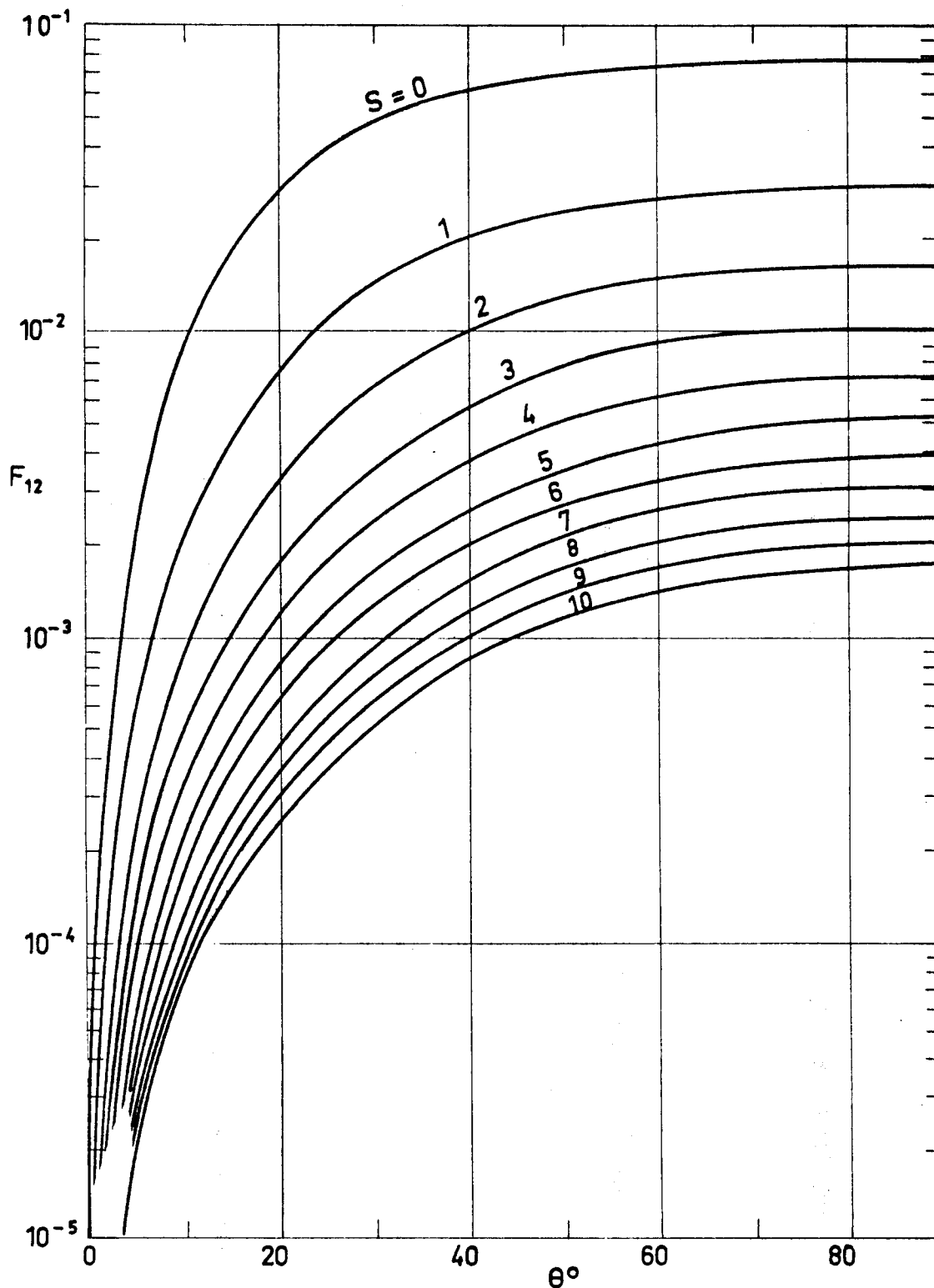


Fig 1-46. Values of F_{12} as a function of S and θ . From Campbell & McConnell (1968).

DIFFUSE SURFACES
Additional Sources of Data

1.4. ADDITIONAL SOURCES OF DATA

This Section contains information on view factors of several diffuse surface configurations not explicitly included in the previous data sheets.

The reader is referred to the previously listed references. Whenever possible, only when a new source is required the reference is given with some detail the first time it appears on each page.

The tables presented below have been borrowed from Siegel & Howell (1972). No attempt has been made to include information which has been published subsequently.

Data enclosed in pp 1-113 to 1-124 concern view factors from infinitesimal to finite diffuse surfaces. Those in pp 1-125 to 1-130 are for view factors from finite to finite diffuse surfaces.

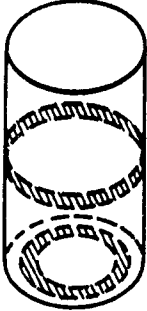
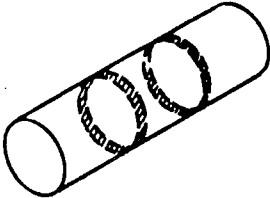
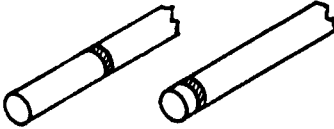
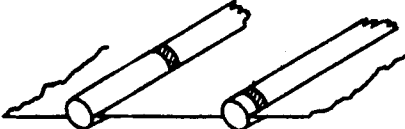

INTENTIONALLY BLANK PAGE

DIFFUSE SURFACES
Additional Sources of Data

Definition	Sketch	Sources
Elemental area to infinitely long strip of differential width lying on parallel generating line	<p>A perspective sketch showing a small rectangular shaded area on a thin, elongated rectangular strip. The strip is oriented diagonally, and a dashed line indicates its extension into the distance, representing a parallel generating line.</p>	Jakob (1957), Siegel & Howell (1972).
Infinitely long strip of differential width to similar strip on parallel generating line	<p>A perspective sketch showing two parallel, elongated rectangular strips, each with a shaded surface. They are oriented diagonally, and dashed lines indicate they extend infinitely in both directions along their length.</p>	Jakob (1957), Siegel & Howell (1972).
Strip of finite length and differential width to strip of same length on parallel generating line	<p>A perspective sketch showing two parallel, elongated rectangular strips, each with a shaded surface. They are oriented diagonally and have clearly defined, finite lengths.</p>	Siegel & Howell (1972).
Corner element of end of square channel to sectional wall element on channel	<p>A perspective sketch of a square channel. A small shaded rectangular area is shown at one of the corners of the channel's end, representing a corner element.</p>	Siegel & Howell (1972).
Ring element on fin to ring element on adjacent fin	<p>A perspective sketch showing a central cylindrical shaft with two circular fins attached to its ends. Each fin has a shaded ring-like area on its outer surface, representing ring elements on adjacent fins.</p>	Sparrow, Miller & Jonsson (1962).
Reference: Siegel & Howell (1972).		

DIFFUSE SURFACES

Additional Sources of Data

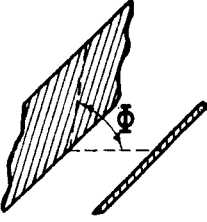
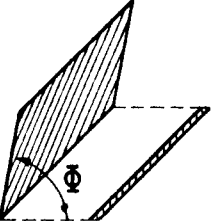

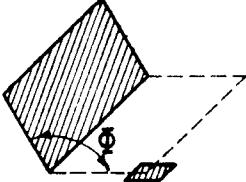
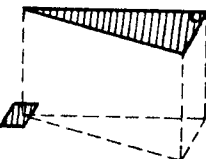
Definition	Sketch	Sources
Band of differential length on inside of cylinder to differential ring on cylinder base		Sparrow, Albers & Eckert (1962). Journal of Heat Transfer vol. 84c, No. 1, 1962, pp. 73-81.
Two ring elements on interior of right circular cylinder		Siegel & Howell (1972).
Exterior element on tube surface to exterior element on adjacent parallel tube of same diameter		Sparrow & Jonsson (1963 a). Journal of Heat Transfer vol. 85, No. 4, 1963, pp. 382-384.
Exterior element on partitioned tube to similar element on adjacent parallel tube of same diameter		Sparrow & Jonsson (1963 a).
Two elements on interior of right circular cone		Sparrow & Jonsson (1963 b). Journal of the Optical Society of America, vol. 53, No. 7, 1963, pp. 816-821.
Reference: Siegel & Howell (1972).		

DIFFUSE SURFACES
Additional Sources of Data

Definition	Sketch	Sources
Band on outside of sphere to band on another sphere		<p>($R_1=R_2$), Campbell & McConnell (1968); ($R_1 \neq R_2$), Grier (1969). NASA SP-3050, 1969.</p>
Two differential elements on exterior of toroid		<p>Grier & Sommers (1969). NASA TN D-5006, 1969.</p>
Element on exterior of toroid to ring element on exterior of toroid		<p>Grier & Sommers (1969).</p>
Element on exterior of toroid to hoop element on exterior of toroid		<p>Grier & Sommers (1969).</p>
<p>Reference: Siegel & Howell (1972).</p>		

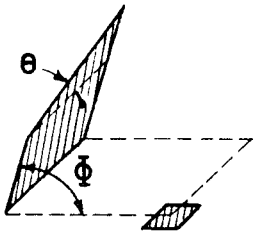
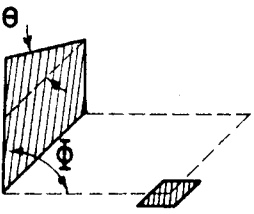
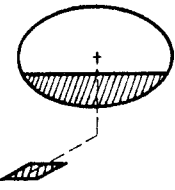
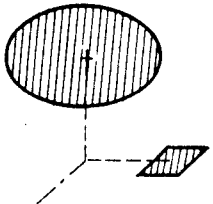
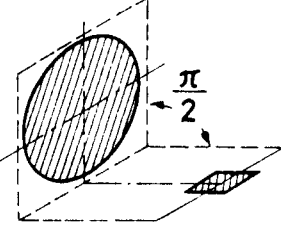
DIFFUSE SURFACES

Additional Sources of Data

Definition	Sketch	Sources
Plane strip element of any length to plane of finite width and infinite length		Siegel & Howell (1972).
Strip element of finite length to plane rectangle that intercepts plane of strip at angle ϕ and with one edge parallel to strip		Hamilton & Morgan (1952), Kreith (1962).
Area element to any parallel rectangle		Jakob (1957).
Plane element to plane rectangle; planes containing two surfaces intersect at angle ϕ		Hamilton & Morgan (1952), Kreith (1962).
Plane element to right triangle in plane parallel to plane of element; normal to element passes through vertex of triangle		Siegel & Howell (1972).
Reference: Siegel & Howell (1972).		

DIFFUSE SURFACES

Additional Sources of Data

Definition	Sketch	Sources
<p>Plane element to plane area with added triangular area; element is on corner of rectangle with one side in common with plane at angle ϕ</p>		<p>Hamilton & Morgan (1952), Kreith (1962).</p>
<p>Same geometry as preceding with triangle reversed relative to plane element</p>		<p>Hamilton & Morgan (1952), Kreith (1962).</p>
<p>Plane element to segment of disc in plane parallel to element</p>		<p>Sparrow & Cess (1966). "Radiation Heat Transfer", Brooks/Cole Publishing Company, Belmont, California, 1966.</p>
<p>Plane element to circular disc on plane parallel to that of element</p>		<p>Hamilton & Morgan (1952), Jakob (1957), Kreith (1962), Siegel & Howell (1972).</p>
<p>Plane element to circular disc; planes containing element and disc intersect at 90°, and centers of element and disc lie in plane perpendicular to those containing areas</p>		<p>Hamilton & Morgan (1952), Leuenberger & Person (1956), Kreith (1962), Siegel & Howell (1972).</p>
<p>Reference: Siegel & Howell (1972).</p>		

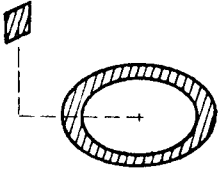
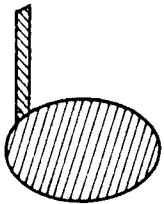
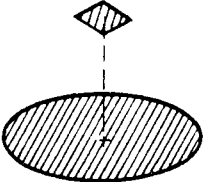
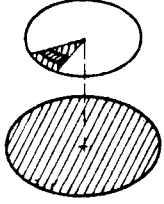
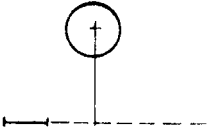
DIFFUSE SURFACES

Additional Sources of Data

Definition

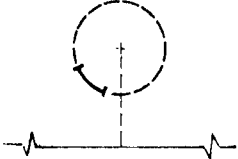
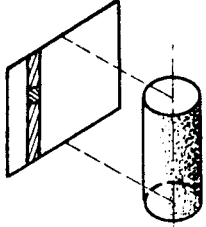
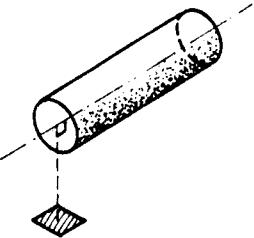
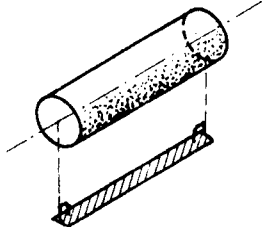

Sketch

Sources

Plane element to ring area in plane perpendicular to element		Siegel & Howell (1972).
Strip element of finite length to perpendicular circular disc located at one end of strip		Leuenberger & Person (1956).
Area element to parallel elliptical plate		Moon (1961), Siegel & Howell (1972).
Radial and wedge elements on circular disc to disc in parallel plane		Leuenberger & Person (1956).
Infinite cylinder to parallel infinitely long strip element		Feingold & Gupta (1970), Siegel & Howell (1972).
Reference: Siegel & Howell (1972).		

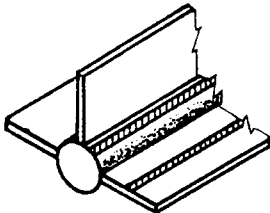
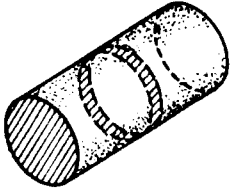
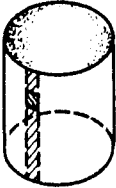
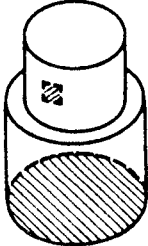
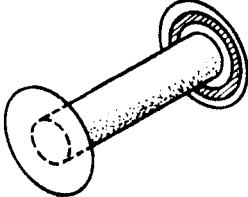
DIFFUSE SURFACES

Additional Sources of Data

Definition	Sketch	Sources
Plane of infinite width and infinite length to infinitely long strip on the surface of a parallel cylinder		Hamilton & Morgan (1952), Kreith (1962), Siegel & Howell (1972).
Strip or element on plane parallel to cylinder axis to cylinder of finite length		Leuenberger & Person (1956).
Plane element to right circular cylinder of finite length; normal to element passes through center of one end of cylinder and is perpendicular to cylinder axis		Hamilton & Morgan (1952), Kreith (1962), Siegel & Howell (1972).
Elemental strip of finite length to parallel cylinder of same length; normals at ends of strip pass through cylinder axis		Hamilton & Morgan (1952), Leuenberger & Person (1956), Kreith (1962).
Infinitely long strip of differential width to parallel semi-cylinder		Sparrow & Eckert (1962). Journal of Heat Transfer, vol. 84, No. 1, 1968, pp. 12-18.
Reference: Siegel & Howell (1972).		

DIFFUSE SURFACES

Additional Sources of Data

Definition	Sketch	Sources
Infinite strip on any side of any of three fins to tube or environment, and infinite strip on tube to fin or environment		Holcomb & Lynch (1967). Report ORNL-TM-1613, Oak Ridge National Laboratory, 1967.
Ring element on interior of right circular cylinder to end of cylinder		Siegel & Howell (1972).
Element and strip element on interior of finite cylinder to interior of cylindrical surface		Leuenberger & Person (1956).
Area element on interior of cylinder to base of second concentric cylinder; cylinders are one atop other		Leuenberger & Person (1956).
Ring element on fin to tube		Sparrow, Miller & Jonsson (1962).
Reference: Siegel & Howell (1972).		